R-04-74

Hydrogeochemical evaluation for Simpevarp model version 1.2

Preliminary site description of the Simpevarp area

Svensk Kärnbränslehantering AB

December 2004

Svensk Kärnbränslehantering AB
Swedish Nuclear Fuel
and Waste Management Co
Box 5864
SE-102 40 Stockholm Sweden
Tel 08-459 84 00
+46 8 459 84 00
Fax 08-661 57 19
+46 8 661 57 19

ISSN 1402-3091
SKB Rapport R-04-74

Hydrogeochemical evaluation for Simpevarp model version 1.2

Preliminary site description of the Simpevarp area

Svensk Kärnbränslehantering AB

December 2004

Preface

This work forms part of the Initial Site Investigation (ISI) stage of the hydrogeochemical evaluation carried out at the Simpevarp area leading to a Hydrogeochemical Site Descriptive Model (v. 1.2). SKB's HAG (Hydrogeochemical Analysis Group) personnel consisting of independent consultants and university personnel, carried out the modelling during the period April 2004 to November 2004. The INSITE and SIERG review comments on the Forsmark 1.1 version were considered where possible in this work. Several groups within HAG were involved and the evaluation was conducted independently using different approaches ranging from expert knowledge to geochemical and mathematical modelling including also transport modelling. During regular HAG meetings the results were presented and discussed. The HAG members contributing to this report where (in alphabetic order):

Luis Auqué, University of Zaragoza , Appendix#4

Gunnar Buckau, Research Center, Karlsruhe, Appendix#2

María Gimeno, University of Zaragoza , Appendix #4

Javier Gómez, University of Zaragoza , Appendix#4

Ioana Gurban, 3D-Terra, Montreal, Appenix#5

Lotta Hallbeck, Vita vegrandis, Göteborg, Appendix#3

Marcus Laaksoharju, Geopoint AB, Stockholm, Appendix#5

Jorge Molinero, University of Santiago de Compostela, Appendix#6

Juan Raposo, University of Santiago de Compostela, Appendix#6

John Smellie, Conterra AB, Stockholm, Appendix#1

Eva-Lena Tullborg, Terralogica AB, Gråbo, Appendix#1

The different modelling approaches applied on the same data set and the similarities in the results gave added confidence to the modelling results presented in this report.

Marcus Laaksoharju

HAG project leader and editor

Summary

Siting studies for SKB's programme of deep geological disposal of nuclear fuel waste currently involves the investigation of two locations, Simpevarp and Forsmark, on the eastern coast of Sweden to determine their geological, hydrogeochemical and hydrogeological characteristics. Present work completed has resulted in Model version 1.2 which represents the second evaluation of the available Simpevarp groundwater analytical data collected up to April, 2004 (i.e. the second "data freeze" of the site). The Hydrochemical Analytical Group (HAG) had access to data from Simpevarp, Ävrö, Äspö and Laxemar where a total of 822 water samples had been collected from the surface and sub-surface environment (e.g. soil pipes in the overburden, streams and lakes); 696 samples were collected from drilled boreholes. The deepest fracture groundwater samples with sufficient analytical data reflected depths down to 1.7 km. Most of the waters sampled (79%) lacked crucial analytical information that restricted the evaluation. Model version 1.2 focusses on geochemical and mixing processes affecting the groundwater composition in the uppermost part of the bedrock, down to repository levels, and eventually extending to 1000 m depth.

The complex groundwater evolution and patterns at Simpevarp are a result of many factors such as: a) the present-day topography and proximity to the Baltic Sea, b) past changes in hydrogeology related to glaciation/deglaciation, land uplift and repeated marine/lake water regressions/transgressions, and c) organic or inorganic alteration of the groundwater composition caused by microbial processes or water/rock interactions. The sampled groundwaters reflect to various degrees processes relating to modern or ancient water/rock interactions and mixing.

The groundwater flow regimes at Laxemar/Simpevarp are considered local and extend down to depths of around 600-1000 m depending on local topography. Close to the Baltic Sea coastline where topographical variation is small, groundwater flow penetration to depth will subsequently be less marked. In contrast, Laxemar is characterised by higher topography resulting in a much more dynamic groundwater circulation which appears to extend to 1000 m depth in the vicinity of borehole KLX02. The marked differences in the groundwater flow regimes between Laxemar and Simpevarp are reflected in the groundwater chemistry where four major hydrochemical groups of groundwaters (types A-D) have been identified:

TYPE A: This type comprises dilute groundwaters (< 1000 mg/L Cl; 0.5-2.0 g/L TDS) of Na-HCO_3 type present at shallow (<200 m) depths at Simpevarp, but at greater depths (0-900 m) at Laxemar. At both localities the groundwaters are marginally oxidising close to the surface, but otherwise reducing. Main reactions involve weathering, ion exchange (Ca, Mg), surface complexation, and dissolution of calcite. Redox reactions include precipitation of Fe-oxyhydroxides and some microbially-mediated reactions (SRB). Meteoric recharge water is mainly present at Laxemar whilst at Simpevarp potential mixing of recharge meteoric water and a modern sea component is observed. Localised mixing of meteoric water with deeper saline groundwaters is indicated at both Laxemar and Simpevarp.

TYPE B: This type comprises brackish groundwaters (1000-6000 mg/L Cl; 5-10 g/L TDS) present at shallow to intermediate (150-300 m) depths at Simpevarp, but at greater depths (approx. 900-1100 m) at Laxemar. At Simpevarp the groundwaters are mainly Na-Ca-Cl in type but some Na-Ca(Mg)-Cl(Br) types also occur. At Laxemar there is a

transition to more Ca-Na-Cl types with depth. Main reactions involve weathering, ion exchange (Ca, Mg) and dissolution/precipitation of calcite. Redox reactions include precipitation of pyrite and some microbially-mediated reactions (SRB). At Simpevarp there is potentially some residual Littorina Sea (old marine) component, commonly in fracture zones close to or under the Baltic Sea. At both the Simpevarp and Laxemar sites there is a glacial component and also a deep saline (non-marine) component.

TYPE C: This type comprises reducing saline groundwaters (6000-20 000 mg/L Cl; 25-30 g/L TDS) present at intermediate to deep (>300 m) levels at Simpevarp, and at even greater depths (approx. 1200 m) at Laxemar. At Simpevarp the groundwaters are mainly Na-Ca-Cl with increasingly enhanced Br and SO_4 with depth. At Laxemar they are mainly Ca-Na-Cl also with increasing enhancements of Br and SO_4 with depth. Main reactions involve ion exchange (Ca). At both sites a glacial component and a deep saline component are present. At Simpevarp the saline component may be potentially non-marine and/or non-marine/old Littorina marine in origin; at Laxemar it is more likely to be non-marine in origin.

TYPE D: This type comprises reducing highly saline groundwaters (> 20 000 mg/L Cl; to a maximum of ~70 g/L TDS) and only has been identified at Laxemar at depths exceeding 1200 m. It is mainly Ca-Na-Cl with higher Br but lower SO_4 compared to Type C groundwaters. Main reactions involve water/rock interaction for long residence times. Groundwater mixing at these depths probably involves long term mixing of deep non-marine brines driven by diffusion.

The redox state of groundwaters appears to be well described by sulphur redox pairs in agreement with some previous studies in this area and in other sites from the Fennoscandian Shield. Furthermore, the CH_4/CO_2 is another important redox pair in determining the redox state.

A modelling approach was used to simulate the composition of the highly saline or brine groundwaters and, in the Simpevarp area, concluded that mixing is the main irreversible process. It controls chloride concentration that, in turn, determines the re-equilibrium path (water-rock interaction) triggered by mixing.

Coupled transport modelling was used to model the groundwater age, tritium content and calcite dissolution/precipitation processes at shallow groundwater depths at both Laxemar and Simpevarp. The modelled results provide additional support to hydrogeological models by using independent hydrochemical information and added support to the general hydrogeochemical understanding of the site.

The modelling indicates also that the groundwater composition at repository depths is such that the representative samples from KSH01A:548-565 m and KSH02:575-580 m can meet the SKB chemical stability criteria for Eh, pH, TDS, DOC and Ca+Mg.

In this evaluation the groundwater model has been updated, the salinity distribution, mixing processes and the major reactions altering the groundwaters have been modelled down to a depth of 1000m, and an updated Hydrogeochemical Site Descriptive Model version 1.2 has been produced. More groundwater and isotopic data, together with microbial information, colloids and gases, provided additional site descriptive information. Finally, the introduction of coupled modelling provided additional possibilities to address independently the various processes in question.

Contents

1 Introduction

1.1 Background

SKB is conducting thorough investigations at two candidate sites for the eventual disposal of spent nuclear fuel. These sites are located in the municipalities of Simpevarp/Laxemar and Forsmark and the main objective is aimed at providing detailed proposals of how a deep repository can be constructed and operated. The investigations at Simpevarp -Laxemar commenced in 2002 and will take between four and eight years to complete.

The site selection and investigation phases encompass a sufficiently large scale in terms of time, space and content to make a breakdown into different stages necessary. During the initial selection phase the site that is considered most suitable for a deep repository is chosen. A few boreholes are drilled as part of an Initial Site Investigation (ISI) stage and the data they generate enables a decision to be made as to whether the site is still deemed suitable. The site and its immediate surroundings should cover an area of 5-10 km^2 in areal extent.

Provided that the preconditions established are still good, a Complete Site Investigation (CSI) stage follows. The main aim is to collect sufficient knowledge about the rock and its properties to enable SKB to produce both a site description and a construction plant description, and also to conduct a safety analysis.

The surface/near-surface hydrological and groundwater chemistry studies include charting water courses, measuring the discharge and taking water samples. Drilling is the most extensive activity conducted where some 10–20 percussion boreholes will be made to a maximum depth of 200 m and an equal number of cored boreholes to depths of 500-1000 m in depth. An extensive hydrochemistry programme together with other investigation programmes will be conducted during and after the drilling work.

1.2 Scope and Objectives

The aim of the site modelling is to develop a Hydrogeochemical Site Descriptive Model according to the Strategy for the Development of a Hydrogeochemical Site Descriptive Model (Smellie et al., 2002). The first such model for Simpevarp was the “version 0” model (SKB, 2000) followed by the 1.1 version of Simpevarp (Laaksoharju et al., 2004b).

The model presented in this report is model version 1.2 which represents the second evaluation of the available Simpevarp groundwater analytical data collected up to April 8th, 2004 (i.e. the so called “data freeze”). The Hydrochemical Analytical Group (HAG) had access to water samples collected from the surface and sub-surface environment (e.g. soil pipes in the overburden, streams and lakes); together with samples collected from drilled boreholes. The deepest samples from Simpevarp reflected conditions down to about 1000m. When modelled, many of the samples either lacked important analytical information that restricted their evaluation or the sampling or analytical

quality was in question. Model version 1.2 focuses on the processes taking place in the deeper part of the bedrock down to 1000m and with a first evaluation of the conditions at the repository level.

The work presented here forms part of the Initial Site Investigation (ISI) stage and the derived model represents the second and final ISI model based on measured data from the site investigation programme. As the investigations progress over the next years, several updated models (version 2.1 and 2.2 within the CSI program) will be derived based on supplementary analytical data and groundwater samples from new boreholes at Laxemar site and repeated sampling from existing boreholes.

1.3 Setting

The Simpevarp area is situated about 350 km south of Stockholm and is located within the confines of the Oskarshamn nuclear power plant facility. The candidate area selected for the site investigations is divided in the so-called Simpevarp area (regional area) and Simpevarp sub area (local area) and Laxemar sub area. The Simpevarp sub area is shown in Figure 1-1 and the Simpevarp area in *Figure 4-2*.

Figure 1-1: *Overview of the Simpevarp sub area showing the area for detailed site investigation (dashed line).*

1.4 Methodology and organisation of work

1.4.1 Methodology

The main objectives of the Hydrogeochemical Site Descriptive Model for the Simpevarp area are to describe the chemistry and distribution of the groundwater in the bedrock and overburden and the processes involved in its origin and evolution. The SKB hydrogeochemistry programme (Smellie et al., 2002) is intended to fulfil two basic requirements: 1) to provide representative and quality assured data for use as input parameter values in calculating long-term repository safety, and 2) to understand the present undisturbed hydrogeochemical conditions and how these conditions will change in the future. Parameter values for safety analysis include pH, Eh, S, SO_4, HCO_3, PO_4

and TDS (mainly cations), together with colloids, fulvic and humic acids, other organics, bacteria and dissolved gases. These values will be used to characterise the groundwater environment at, above and below repository depths. When the hydrogeochemical environment has been fully characterised, this knowledge, together with an understanding of the past and present groundwater evolution, should provide the basis for predicting future changes. The site investigations will therefore provide important source material for safety analyses and the environmental impact assessment of the Simpevarp area.

1.5 This report

Chapters 1-6 of this report summarise the hydrogeochemical results collated and interpreted by HAG. These results will serve as input for the final Site Descriptive Model report which will integrate collectively the results from all the geoscientific disciplines. The format and structure of this present report follows that established for the final report.

The main aim of this report is to attempt to integrate the different approaches of the HAG groups to arrive at an overall interpretation of the presently available Simpevarp hydrogeochemical data. Chapter 2 presents an overview of available information used in the modelling. Chapter 3 describes the present ideas concerning the palaeoevolution of the Simpevarp area. Chapter 4 covers the integrated evaluation of the primary hydrogeochemical data and the quantitative modelling covering the different modelling approaches attempted, the assumptions made, an evaluation of the uncertainties involved, and how such modelled results can best be visually presented. Chapter 5 summarises the hydrogeochemical description of the Simpevarp area and Chapter 6 presents the main conclusions.

The detailed contributions of the three HAG modelling groups are presented in *Appendices 1-6. Appendix 7* lists all the groundwater analytical data available at the 'data freeze' point. *Appendix 8* lists the Nordic data used as background information for the modelling. *Appendix 9* shows how the HAG modelling groups utilised the Simpevarp data.

2 Investigations, available data and other prerequisites for the modelling

2.1 Overview

The evaluation of the hydrogeochemical data has been carried out by considering not only the samples from Simpevarp, but also including data from the nearby boreholes in Ävrö, Äspö and Laxemar and in some cases also to the whole Fennoscandian hydrochemical dataset. An example of this is selecting the water end members describing other Fennoscandian sites in order to see how well they compare with the general Simpevarp trend and whether or not Simpevarp can be interpreted as part of the regional hydrogeochemical system. Consequently, information from hydrogeochemical model versions based on previously investigated sites in Sweden and elsewhere, and information from ongoing geological and hydrogeological modelling at Simpevarp, where included in the evaluation when possible.

2.1.1 Investigations and primary data aquired up to data freeze 1.1

The dataset available for the 1.1 version consisted in total of 535 water samples (Laaksoharju et al., 2004b). Samples reflecting the surface/near-surface conditions (precipitation, streams, lakes, sea water and shallow soil pipe waters) comprised a total of 419 samples. Of the remainder, 11 samples were from percussion drilled boreholes and 105 samples from core drilled boreholes; some of these borehole samples represent repeated sampling from the same isolated location or sample of the water column in an open borehole (tube sampler). In conclusion, there was a heavy bias at this stage in the site characterisation of water samples from the surface and near-surface environments. Consequently, hydrochemical evaluation at greater depths was restricted to only a few borehole sampling points.

In the total dataset only 86 surface samples, 4 percussion borehole samples and 21 core-drilled samples were analysed for all the major elements, stable isotopes and tritium at the time of the "data freeze". This meant that 21% of the total samples could be used for more detailed evaluation concerning the origin of the water.

2.1.2 Data freeze 1.2 – investigations performed and data acuired

In Table 2-1 and Table 2-2 the data collected for the data freeze 1.2 of Simpevarp (Simpevarp and Ävrö) are listed. The data used for comparison from the nearby locations of Äspö and Laxemar including the Nordic sites are listed in *Appendices 4, 7 and 8*.

Table 2-1: Samples included in the data freeze 1.2 from Simpevarp.

Subarea	Type of Water	Type of sampling	ID code	Sampling Dates	Depths	Number of Samples				
						New samples after Data Freeze 1.1	With Major Elements (ME)	With ME & Stable isotopes	With ME, Sl & Tritium	Representative
Simpevarp	Ground Water	Packered	HSH02	2003	0-200	3	3	3	3	0
			HSH03	2002,03,04	0-200	2	1	1	1	1
		Tube	KSH01A	2003	1-1000					
		Packered section		2003	156-167					
				2003	245-261					
				2002	197-313					
				2003	548-565	19	2	2	2	1
		Tube	KSH02	2003	0-991					
		Packered section		2003	419-424	2	2	1	1	1
				2003	411-467					
		Tube		2003	575-580	2	2	2	1	1
		Packered section		2004	957-958	3	1	0	0	0
				2004	958-975	1	0	0	0	0
			KSH03	2003/04	0-100	4	3	3	3	1
		Tube		2003/04	40-990	29	10	1	1	0
			KSH03A B							
	Shallow GW		PSM	2004		8	0	0	0	0
			SSMxxx	2003/04		12	0	0	0	0
	Sea W		PSMxxx	2003/04		94	72	22	16	75
	Lake W		PSMxxx	2003/04		74	56	6	6	30
	Running W		PSMxxx	2003/04		160	118	21	17	63
	Precipit		PSMxxx	2002/03		1	7	7	6	2
TOTAL new samples	Ground Waters (including shallow GW)					85	24	13	12	5
	Surface Waters (Sea, Lake, Running, Precipitation)					329	247	50	39	169
	Total					414	271	63	51	174

POM (TOTAL new samples)	Ground Waters (including shallow GW)	130	27	15	14	7
	Surface Waters (Sea, Lake, Running, Precipitation)	329	247	50	39	169
	Total	459	274	65	53	176

Table 2-2: Samples included in the data freeze 1.2 for Ävrö.

Subarea	Type of Water	Type of sampling	ID code	Sampling Dates	Depths	Number of Samples			
						New samples after Data Freeze 1.1	With Major Elements (ME)	With ME, Stable isotopes & Tritium	Representative
Ävrö	Ground Water	Packered sec.	HAV04	1987	35-100				
			HAV05	1987	50-100				
			HAV06	1987	73-100				
			HAV07	1987	69-100				
			HAV09	2003	15-131	1	0	0	0
			HAV10	2003	12-100	2	0	0	0
		Tube (50 m)	KAV01	2003	33-733	14	0	0	0
		Packered sec.		1987	420-425				
				1987	522-532				
				1987	558-563				
				1987	635-743				
			KAV04	2003, 2004	47-50	1	1	0	0
				2003, 2004	0-100	1	1	1	1
				2003, 2004	¿?	21	0	0	0
Total New Ävrö samples						40	2	1	1

2.2 Geographical data

The co-ordinates used and made available for the data freeze are listed in *Appendix 7*. These data were used in the visualisation work.

2.3 Surface investigations

Available QA data describing the composition of the surface water sampled from lakes, streams, Baltic Sea and soil pipes are listed in *Appendix 7*.

2.4 Borehole investigations

Available QA data describing the composition of the groundwater sampled from percussion and core drilled boreholes are listed in *Appendix 7*.

2.5 Other data sources

Available QA data were used as background information in the modelling (*cf. Appendix 8)* from the SICADA database describing the composition of the groundwater conditions at nearby locations such as Äspö and Laxemar and other Swedish sites including data from Finland (e.g. Pitkänen et al. 1999).

2.6 Databases

The use of the data in the different modelling work is listed in *Appendix 9*.

2.7 Model volumes

2.7.1 Regional model volume

The Simpevarp area is located at the Baltic coast some 2-3 kilometres SSE of Äspö island and 3-4 kilometres ESE from Laxemar *(Figure 4-2)*. The Simpevarp area includes Simpevarp, Ävrö, Äspö and Laxemar. A geological description of the Simpevarp area can be found in *Appendix 1*.

It is recognised that there are little groundwater chemistry information outside the modelled area and that there may be regional influences, particularly on the hydrogeology and hydrogeochemistry, of deep groundwater flow from higher ground further to the west and north-west. This possibility is being monitored at present by data from the deeper Laxemar boreholes and evidence of such flows may be included in future models under the CSI program.

2.7.2 Local model volume

The Simpevarp sub area is shown in *Figure 4-2*. The motivation for selection of the local model area is described by Anderson (2002).

2.7.3 Model areas

For the 1.2 work the focus was on data from Simpevarp but data from Laxemar and Äspö were also included in the evaluation.

3 Evolutionary aspects of the Simpevarp area

3.1 Premises for surface and groundwater evolution

The first step in the groundwater evaluation is to construct a conceptual postglacial scenario model for the site (*Figure 3-1*) based largely on known palaeohydrogeological events from Quaternary geological investigations. This model can be helpful when evaluating data since it provides constraints on the possible groundwater types that may occur. Interpretation of the glacial/postglacial events that might have affected the Simpevarp area is based on information from various sources including Fredén (2002), T. Påsse (pers. comm., 2003), Westman et al. (1999) and SKB (2002). This recent literature provides background information which is combined with more than 10 years of studies of groundwater chemical and isotopic information from sites in Sweden and Finland in combination with various hydrogeological modelling exercises of the postglacial hydrogeological events (Laaksoharju and Wallin (eds), 1997; Luukonen , 2001; Pitkänen et al., 1998 and Svensson, 1996). The presented model is therefore based on Quaternary geological facts, fracture mineralogical investigations and groundwater observations. These facts have been used to describe possible palaeo events that may have affected the groundwater composition in the bedrock.

3.1.1 Development of permafrost and saline water

When the continental ice sheet was formed at about 100 000 BP permafrost formation ahead of the advancing ice sheet probably extended to depths of several hundred metres. According to Bein and Arad (1992) the formation of permafrost in a brackish lake or sea environment (e.g. similar to the Baltic Sea) produced a layer of highly concentrated salinity ahead of the advancing freezing front. Since this saline water would be of high density, it would subsequently sink to lower depths and potentially penetrate into the bedrock where it would eventually mix with formational groundwaters of similar density. Where the bedrock was not covered by brackish lake or sea water similar freeze-out processes would occur on a smaller scale within the hydraulically active fractures and fracture zones, again resulting in formation of a higher density saline component which would gradually sink and eventually mix with existing saline groundwaters. Whether the volume of high salinity water produced from brackish waters by this freeze-out process would be adequate to produce such widespread effects is presently under debate.

With continued evolution and movement of the ice sheet, areas previously subject to permafrost would be eventually covered by ice accompanied by a rise in temperature and slow decay of the underlying permafrost layer. Hydrogeochemically, this decay may have resulted in distinctive signatures being imparted to the groundwater and fracture minerals.

3.1.2 Deglaciation and flushing by meltwater

During subsequent melting and retreat of the ice sheet the following sequence of events is thought to have influenced the Simpevarp area (see, *Figure 3-1*):

During the recession and melting of the continental ice sheet, glacial meltwater was hydraulically injected into the bedrock (> 14 000 BP) under considerable head pressure close to the ice margin. The exact penetration depth is still unknown, but depths exceeding several hundred metres are possible according to hydrodynamic modelling (e.g. Svensson, 1996). Some of the permafrost decay groundwater signatures may have been disturbed or destroyed during this stage.

Different non-saline and brackish lake/sea stages then transgressed the Simpevarp area during the period ca. 14 000-4 000 BP. Of these, two periods with brackish water can be recognised; Yoldia Sea (11 500 to 10 800 BP) and Littorina Sea starting at 9 500 and continuing to the present. The Yoldia period has probably resulted in only minor contributions to the subsurface groundwater since the water was very dilute to brackish from the large volumes of glacial meltwater it contained. Furthermore this period lasted only for 700 years. The Littorina Sea period in contrast had a maximum salinity of about twice the present Baltic Sea and this maximum prevailed at least from 6 500 to 5 000 BP; during the last 2000 years the salinity has remained almost equal to the present Baltic Sea values (Westman et al., 1999 and references therein). Because of increased density, the Littorina Sea water was able to penetrate the bedrock resulting in a density turnover which affected the groundwater in the more conductive parts of the bedrock. The density of the intruding seawater in relation to the density of the groundwater determined the final penetration depth. As the Littorina Sea stage contained the most saline groundwater, it is assumed to have had the deepest penetration depth eventually mixing with the glacial /brine groundwater mixtures already present in the bedrock.

When the Simpevarp region was subsequently raised above sea level 5 000 to 4 000 years ago, fresh meteoric recharge water formed a lens on top of the saline water because of its low density. However, local hydraulic gradients resulting from higher topography to the west of the Simpevarp area may have flushed out varying amounts of these older waters, at least to 100-150 m, with the freshwater lens mostly occupying these depths today depending on local hydraulic conditions.

Many of the natural events described above may be repeated several times during the lifespan of a repository (thousands to hundreds of thousands of years). As a result of these events, brine, glacial, marine and meteoric waters are expected to be mixed in a complex manner at various levels in the bedrock, depending on the hydraulic character of the fracture zones, groundwater density variations and borehole activities prior to groundwater sampling. For the modelling exercise which is based on the conceptual model of the site, groundwater end members reflecting, for example, Glacial meltwater and Littorina Sea water composition, were added to the data set *(cf. Appendix 5)*.

The uncertainty of the updated conceptual model increases with modelled time. The largest uncertainties are therefore associated with the stage showing the flushing of glacial melt water. The driving mechanism behind the flow lines in *Figure 3-1* is the shore level displacement due to the land uplift.

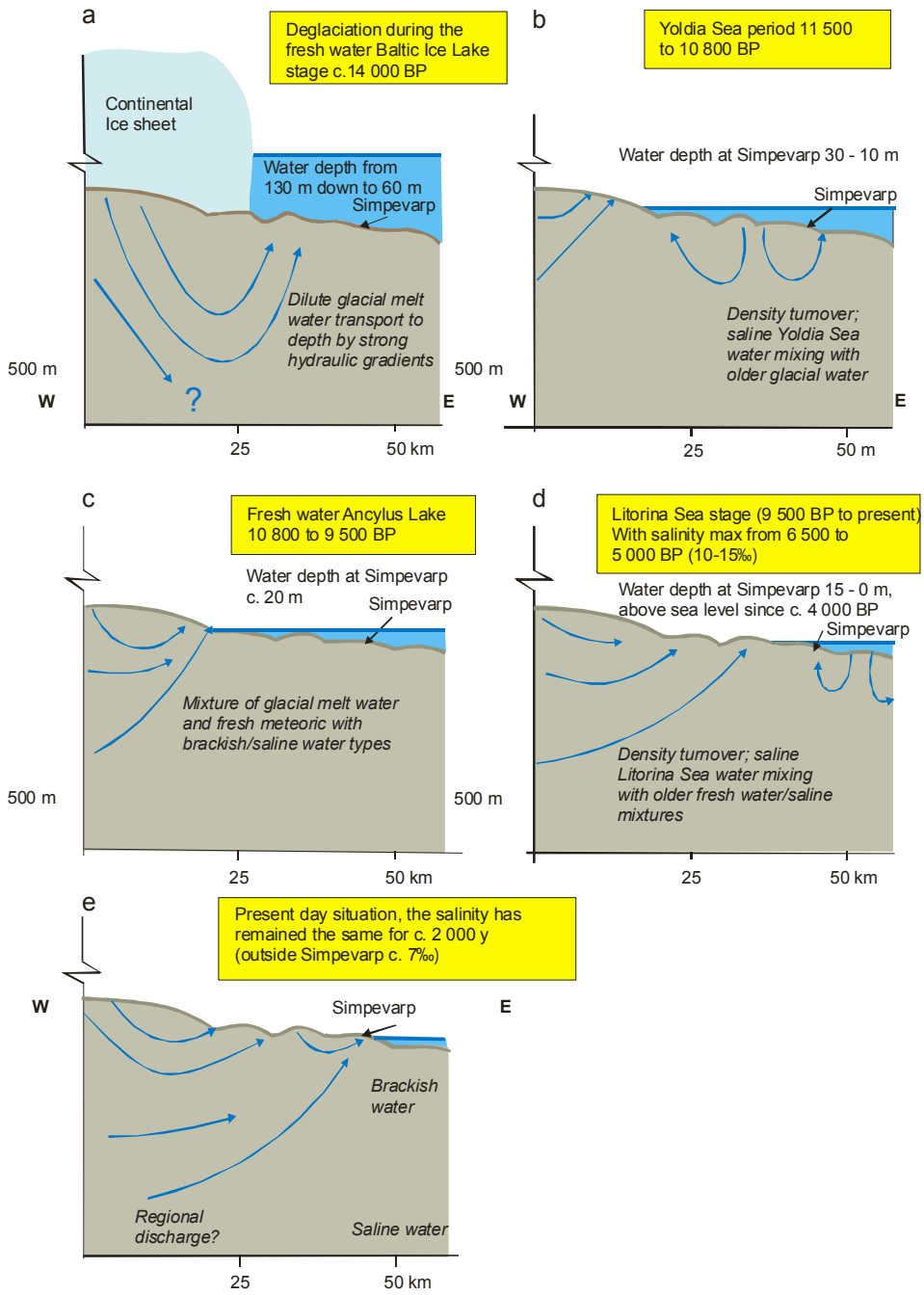

Figure 3-1: *Conceptual postglacial scenario model for the Simpevarp area. The figures show possible flow lines, density driven turnover events and non-saline, brackish and saline water interfaces. Possible relation to different known postglacial stages such as land uplift which may have affected the hydrochemical evolution of the site is shown: a) deglaciation of the continental ice, b) Yoldia Sea stage, c) Ancylus Lake stage, d) Littorina Sea stage, and e) present day Baltic Sea stage. From this conceptual model it is expected that glacial meltwater and deep and marine water of various salinities have affected the present groundwater. Based on the shoreline displacement curve compiled by T. Påsse (per. comm., 2003) and information from Fredén (2002), Westman et al. (1999) and SKB (2002).*

4 Bedrock hydrogeochemistry

4.1 State of knowledge at previous model version

The first model of the Simpevarp area was the Site Descriptive Hydrogeochemical Model version 0 (SKB, 2002). Although there were few data from the Simpevarp regional modelled area to support a detailed hydrogeochemical site descriptive model, postglacial events believed to have affected the groundwater evolution and chemistry at Simpevarp were described in a conceptual model.

The model version 1.1 (Laaksoharju et al., 2004b) represented the first evaluation of the available Simpevarp groundwater analytical data. The complex groundwater evolution and patterns at Simpevarp were modelled to be a result of many factors such as: a) the flat topography and proximity to the Baltic Sea, b) past changes in hydrogeology related to glaciation/deglaciation and land uplift associated with repeated marine/lake water regressions/transgressions, and c) organic or inorganic alteration of the groundwater composition caused by microbial processes or water/rock interactions. The sampled groundwaters reflected various degrees of modern or ancient water/rock interactions and mixing processes. Higher topography to the west of Simpevarp had resulted in hydraulic gradients which had partially flushed out old water types.

Except for seawater, most surface waters and some groundwaters from percussion boreholes represented fresh, non-saline waters according to the classification used for Äspö groundwaters. The rest of the groundwaters were brackish (Cl <5 000mg/L), except for three samples from KSH01A (at 253m and 439m depth) which were saline. Most surface waters were of Ca-HCO_3 or Na-Ca-HCO_3 type and naturally the seawater was of Na-Cl type. The deeper groundwaters were mainly of Na-Ca-Cl type (*see Figure 4-1*).

The modelling indicated three water types, one dominated by meteoric water, another affected by marine water and the third affected by glacial water. The surface meteoric type shows seasonal variations. Closer to the coast the influence of marine water is detected. With depth, the saline groundwater has been affected by glacial melt water and meteoric water.

The 1.1 version knowledge of the reactive system was that the main water-rock interaction processes that affect the chemistry in the fresh meteoric waters were: a) decomposition of organic matter, b) calcite, plagioclase, biotite and sulphide dissolution, c) Na-Ca ion exchange, and d) phyllosilicate precipitation probably extremely slow in the present low temperature environment. In contrast, for the brackish–saline groundwaters, the water/rock interaction processes seemed to be less evident although this could not be confirmed because of a lack of data. Multiple end-member mixing between marine water, glacial meltwater and deeper saline water seemed to play a significant role.

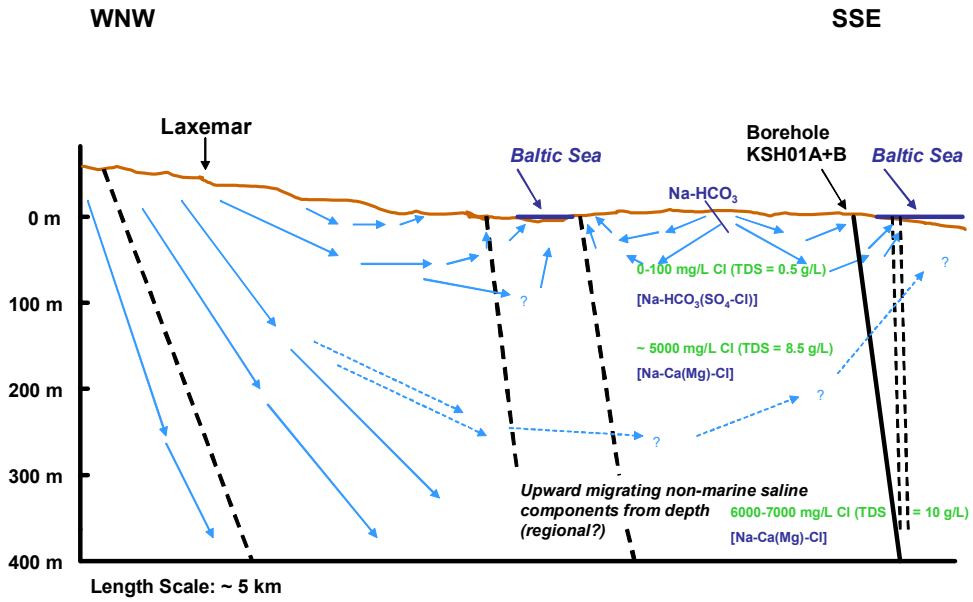

Figure 4-1: *Conceptual model version 1.1 of the Simpevarp area. Steep dashed lines refer to sub-vertical fracture zones; blue arrows indicate potential groundwater flow directions (Laaksoharju et al., 2004b).*

4.2 Evaluation of primary data

This section describes the evaluation of the primary hydrogeochemical data. Most of these data are from waters sampled at various surface locations and in a few boreholes. The evaluation essentially aims at identifying representative datasets which are used for further analysis and providing a first conceptualisation of the origin and evolution of the Simpevarp groundwaters.

4.2.1 Hydrogeochemical data evaluation

Evaluation of the Simpevarp hydrogeochemical data in Model v. 1.2 entails comparison with other geographically located sites in its near-vicinity, i.e. the so-called Simpevarp area, namely Äspö (before tunnel construction, Laxemar and Ävrö (*cf. Appendix 7*). Also data from other Fennoscandian sites such as Forsmark and Olkiluoto were compiled in the 'Nordic Table' and these data also have been evaluated with respect to properties and representativeness (*cf. Appendix 8*).

The dataset consists of 1518 water samples: 964 from Simpevarp, 302 from Laxemar, 152 from Äspö, and 100 from Ävrö. Samples reflecting surface conditions (precipitation, streams, lakes and sea water) comprise a total of 822 samples (766 from Simpevarp and 56 from Laxemar). Of the remaining 696 samples from the four subareas, 63 samples are from percussion-drilled boreholes and 633 from core-drilled boreholes; some of these borehole samples represent repeated sampling from the same isolated location or samples in a non-sealed, open borehole (tube sampling = 168 samples) and shallow soil pipe waters (23 samples).

From the total dataset only 174 surface samples and 144 groundwater samples were analysed for all the major elements, stable isotopes and tritium at the time of Data Freeze 1.2. There are some samples with additional information, mainly on colloids, dissolved gasses and microbes, which are also listed in Appendix 7. This means that 21% of the samples could be used for a detailed evaluation concerning the origin of the waters.

The detailed representativity check of the samples (*Appendix 1*) show that only 81 out of 144 samples with complete chemical data have been considered representative. The representative data are labelled in *Appendix 7*. How this dataset has been used in the different models is listed in Appendix 9.

Analysed data include the same set of parameters as in the previous stages (*c.f. Appendix 7*). The pH and electrical conductivity values used in the evaluation were ones determined in the laboratory. There are no data for Eh and temperature for the surface waters but there are data from some continuous logging of Eh, pH and temperature data from several boreholes at different depths. The selected Eh, pH and temperature values are included in the table of the chemical analysis.

Groundwater chemistry data sampled in boreholes

Three cored boreholes have been sampled, KSH01, KSH02 and KSH03. With respect to nomenclature in the report text, the first 100 m of each borehole (the initial percussion drilled portion) is referred to as 'B' (i.e. KSH01B) and from 100 m to the hole bottom (by core drilling) is referred to as 'A' (i.e. KSH01A).

The borehole sampling locations at the Simpevarp area are shown in *Figure 4-2* and the sampling and analytical data have been reported for the groundwaters by Wacker (2003a); Berg (2003a,b) and draft versions of a P-report (Wacker et al., 2004) were available at the time for the data freeze. The analytical programme included: major cations and anions (Na, K, Ca, Mg, Si, Cl, HCO_3^- SO_4^{2-}, S^{2-}), trace elements (Br, F, Fe, Mn, Li, Sr, DOC, N, PO_4^{3-}, U, Th, Sc, Rb, In, Cs, Ba, Tl, Y and REEs) and stable (^{18}O, ^{2}H, ^{13}C, ^{37}Cl, ^{10}B, ^{34}S) and radioactive-radiogenic (^{3}H, ^{226}Ra, ^{228}Ra, ^{222}Rn, ^{238}U, ^{235}U, ^{234}U, ^{232}Th, ^{230}Th and ^{228}Th) isotopes, microbes, gases and colloids. *(cf. Appendix 7).*

The different analytical results obtained with contrasting analytical techniques for Fe and S have been confirmed with speciation-solubility calculations and checking their effects on the charge balance. The values selected for modelling were those obtained by ion chromatography (SO_4^{2-}) and spectrophotometry (Fe) assuming no colloidal contribution. The selected pH and Eh values correspond to available downhole data *(cf. Appendix 7).*

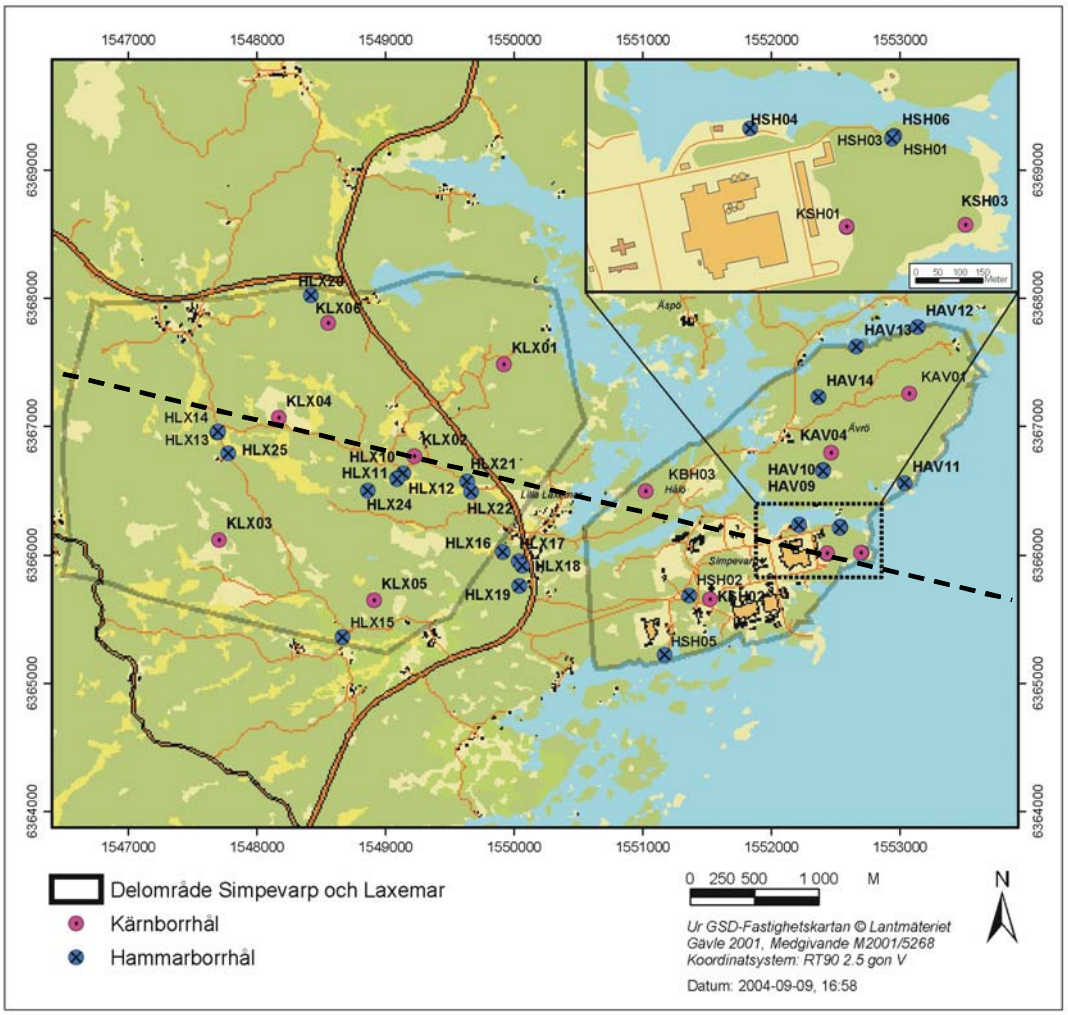

Figure 4-2: *The groundwater sampling locations at the Simpevarp sub area (right hand area). Laxemar sub area (left hand area) and Äspö data were included in the evaluation in the so-called groundwater data from Simpevarp area. The dotted line indicates the orientation of cutting plane used for the visualisations.*

Representativeness of the data

By definition, a high quality sample is considered to be that which best reflects the undisturbed hydrological and geochemical *in-situ* conditions for the sampled section. A low quality sample may contain *in-situ*, on-line, at-line, on-site or off-site errors such as contamination from tubes of varying compositions, air contamination, losses or uptake of CO_2, long storage times prior to analysis, analytical errors etc. The quality may also be influenced by the rationale in locating the borehole and selecting the sampling points. Some errors are easily avoided, others are difficult or impossible to avoid. Furthermore, chemical responses to these influences are sometimes, but not always, apparent.

Simpevarp area

Included in the Simpevarp v. 1.2 evaluation are data representing surface and near-surface waters collected from the Baltic Sea, Lakes, Streams, and also from shallow Soil Pipes placed in the overburden. These data, because of the complex nature of the sampling locations (i.e. subject to annual and seasonal trends, potential recharge/discharge areas etc.) have been evaluated based only on charge balance (Lake and Stream waters), charge balance and observed contamination during sampling (Soil Pipe waters) and charge balance and salinity (Baltic Sea waters). Some precipitation values are also included but have not undergone any representativity check because of unpredictable annual and seasonal trends and possible evaporation (for details see *Appendix 1*).

The Simpevarp groundwater analytical data are compiled in the SICADA database, and form the basis of the hydrochemical evaluation. The data have already undergone an initial screening process by field and laboratory personnel based on sampling, sample preparation and analytical criteria (Wacker 2003a). The next stage in the hydrogeochemical site descriptive process, is to assess these screened data in more detail to derive a standard set of representative groundwater data for hydrogeochemical modelling purposes.

For this assessment the initial most important stage is to check for groundwater contamination. To accomplish this stage an intimate knowledge of the borehole site is required which entails borehole geology and hydrogeology and a detailed log of borehole activities. These latter activities are a major source of groundwater contamination and include:

- drilling and borehole cleaning;
- open hole effects;
- downhole geophysical/geochemical logging;
- downhole hydraulic logging/testing/pumping, and
- downhole sampling of groundwaters.

In *Appendix 1* in this report these potential sources of contamination have been addressed and documented systematically for each borehole drilled and for each borehole section sampled. The degree of contamination has been judged, for example, by plotting tritium against percentage drilling water and using measured values with specifically defined limits, i.e. charge balance (±5%) and drilling water component (<1%), and supported qualitatively by expert judgement based on detailed studies of the distribution and behaviour of the major ions and isotopes. The final selection of data which best represents the sampled borehole section is based on:

- The final selection of data which best represents the sampled borehole section is based on identifying as near as possible a complete set of major ion and isotope (particularly tritium, ^{18}O and deuterium) analytical data. This is not always the case, however, and a degree of flexibility is necessary in order to achieve an adequate dataset to work with. For example:

- A charge balance of ±5% was considered acceptable. In some cases groundwaters exceeding this range were chosen to provide a more representative selection of groundwaters. These groundwaters should therefore be treated with some caution when used in the modelling exercises.

- In many cases the drilling water content was either not recorded or not measured. Less than 1% drilling water was considered acceptable. In some cases groundwaters were chosen when exceeding this range to provide a more representative selection of groundwaters. These groundwaters also should be treated with some caution when used in the modelling exercises.

- Some of the older tritium data were analysed with a higher detection limit of 8TU; the detection limit lies around 0.02TU for recent analyses. For some groundwaters an approximate tritium value is suggested where no recorded value is available. This value is selected normally from the same borehole section but representing an earlier or later sample.

Appendix 1 shows a summary of the Simpevarp data, together with the POM sites, indicating the use of selected criteria (charge balance; drilling water content; tritium content) to identify the samples considered representative. Resulting from this assessment, two groundwater sample types are highlighted in the *Appendix 7*: one type considered representative, the other type less representative but suitable when used with caution[1].

The drilling event is considered to be the major source for contamination of the formation groundwater. During drilling large hydraulic pressure differences can occur due to uplifting/lowering of the equipment, pumping and injection of drilling fluids. These events can facilitate unwanted mixing and contamination of the groundwater in the fractures, or the cutting at the drilling head itself can change the hydraulic properties of the borehole fractures. It is therefore of major importance to analyse the drilling events in detail. From this information not only the uranine spiked drilling water can be traced, but also the major risk of contamination and disturbances from foreign water volumes can be directly identified. Insufficient or excessive extraction of water from a fracture zone prior to sampling can be calculated by applying the DIS (Drilling Impact Study) modelling (Gurban and Laaksoharju, 2002).

A hydraulically active fracture zone in one isolated section in borehole KSH01A:548-565m was the subject of the DIS modelling (156.5-167m and 245-261.5m were investigated in the 1.1 version). The modelling carried out for this fracture zone was based on the DIFF (differential flow meter logging) measurements and the main aim was to model the amount of the contamination (*Figure 4-3*) for this particular fracture zone *(cf. Appendix 5)*. The DIS calculations show that the section was contaminated with 22.4m^3 of foreign water during the drilling of this section of which a maximum of 23.61% consisted of drilling water. The maximum uranine lost to the fracture during drilling was 0.04 mg/L, which represents 23.6% drilling water. Later drilling activities could have increased the amount of contamination. The result from the sampling shows 18.7% remaining drilling water in the first chemical sample after pumping 336 hours, and 10.7% remaining drilling water in the last sample after pumping 1675 hours. The average flow rate was 200 mL/min (Wacker et al, 2004). The volume removed was

[1] The quality of the tritium analyses has varied over the years and it is sometimes difficult to separate realiable tritum data from less reliable in the older data set from Äspö/Laxemar. Consequently, and these older data should be used carefully.

calculated to be 20 m^3. This can be compared with the maximum 22.4 m^3 volume of water that contaminated the fracture. The average amount of drilling water remaining in the fracture is 2.4 m^3. The DIS calculations show that pumping should have continued further in order to remove the additional 2.4m^3.

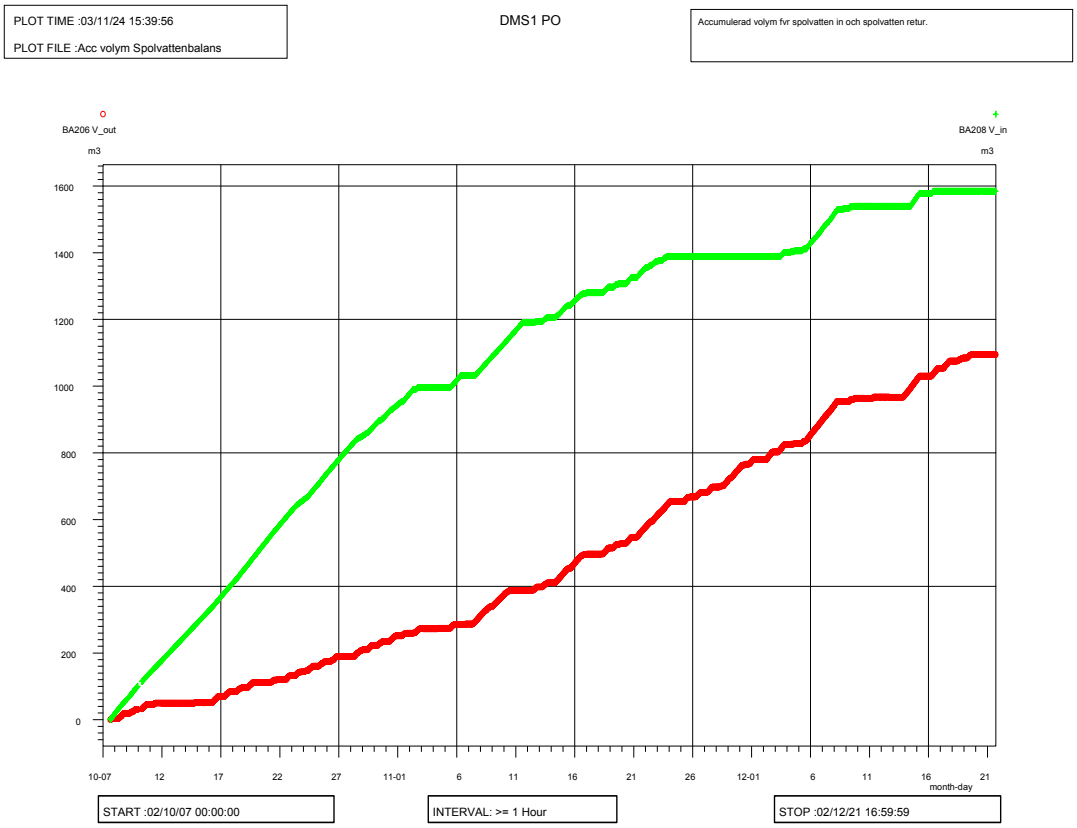

Figure 4-3: *Accumulated drilling water volume pumped in (in green) and drilling water volume pumped out (in red) in borehole KSH01A+B with time. The monitoring of the amount of drilling water pumped into the borehole is of varying quality indicated by 2 or 3 plateaus with no inflow. During the "plateau period" drilling was conducted and water is still pumped in. The error is due to a sensor problem.*

One fundamental question in modelling is whether the uncertainties lead to a risk of misunderstanding the information in the data. Generally the uncertainties from the analytical measurements are lower than the uncertainties caused by the modelling but the variability during sampling is generally higher than the model uncertainties.

Nordic sites

The Nordic sites, in addition to Simpevarp area, comprise Forsmark and all remaining Swedish sites studied over the last 20-25 years; Olkiluoto in Finland is also included (for more information see, *Appendix 1*). Most of these sites have

undergone earlier detailed assessments as to groundwater quality and representativeness, e.g. Gideå, Kamlunge, Klipperås, Fjällveden, Svartboberget, Finnsjön (Smellie et al., 1985, 1987; Smellie and Wikberg, 1989), Lansjärv (Bäckblom and Stanfors, 1989) and Olkiluoto (Pitkänen et al., 1999, 2004). Based on this information the Nordic Table has been highlighted with respect to representative and less representative groundwater samples (*Appendix 8*) The 'less' representative groundwaters do not meet all of the criteria for representativeness but are sufficiently important to be included. The importance of early or 'First Strike' samples is emphasised in the evaluation discussed in *Appendix 1* and listed in *Appendix 8*. These are coloured green in the Nordic Table and involve one or more of the following deviations from being considered 'representative':

- lack of important ions – especially Br;
- lack of ^{18}O and deuterium data;
- variation in salinity during the time-series measurements; and
- few or an absence of time-series measurements.

The representative groundwaters are highlighted in the Nordic Table in orange (Appendix 8).

Explorative analysis

A commonly used approach in groundwater modelling is to start the evaluation by explorative analysis of different groundwater variables and properties. The degree of mixing, the type of reactions and the origin and evolution of the groundwater can be indicated by applying such analyses. Also of major importance is to relate, as much as possible, the groundwaters sampled to the near-vicinity geology and hydrogeology.

Borehole properties

Figure 4-4, *Figure 4-5* and *Figure 4-6* represents a schematic representation of boreholes KSH01A+B, KSH02+B and KSH03A+B and the intercepted structures and their hydraulic conductivities; groundwater sampling locations are indicated and the sampled chloride contents are shown. The results from drillcore mapping, BIPS measurements, differential flow measurements and electric conductivities together with groundwater quality and representativeness of the samples are discussed in great detail for all investigated boreholes in *Appendix 1*.

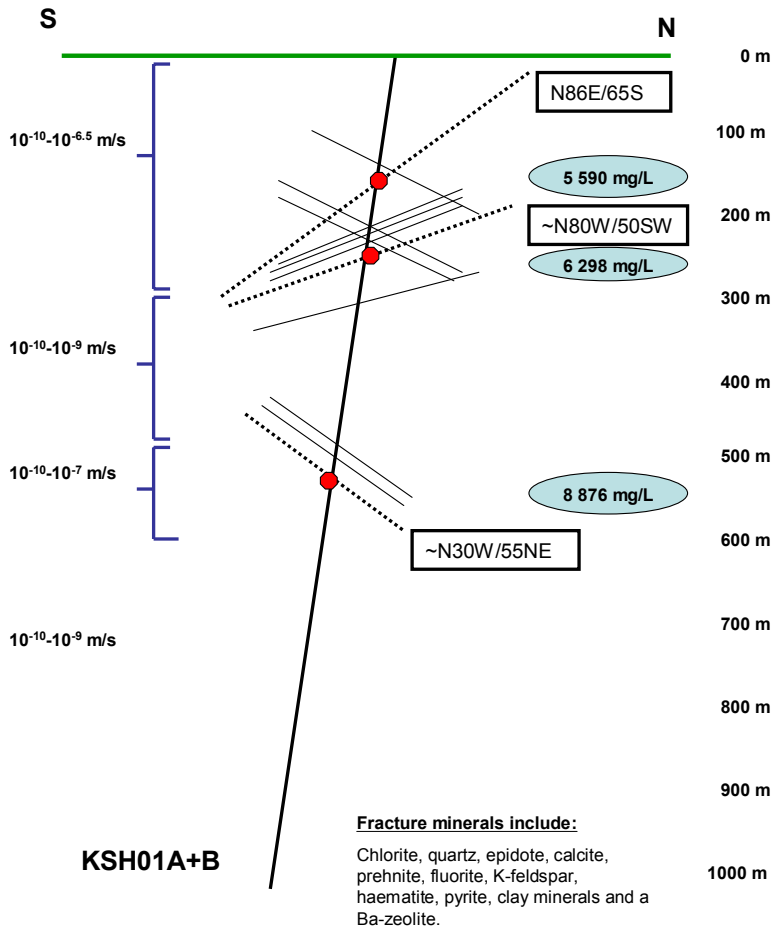

Figure 4-4: *Borehole KSH01A+B showing intercepted structures and their hydraulic conductivities; groundwater sampling locations are indicated in red with the mg/L chloride content in blue. Dotted lines represent sampled structures.*

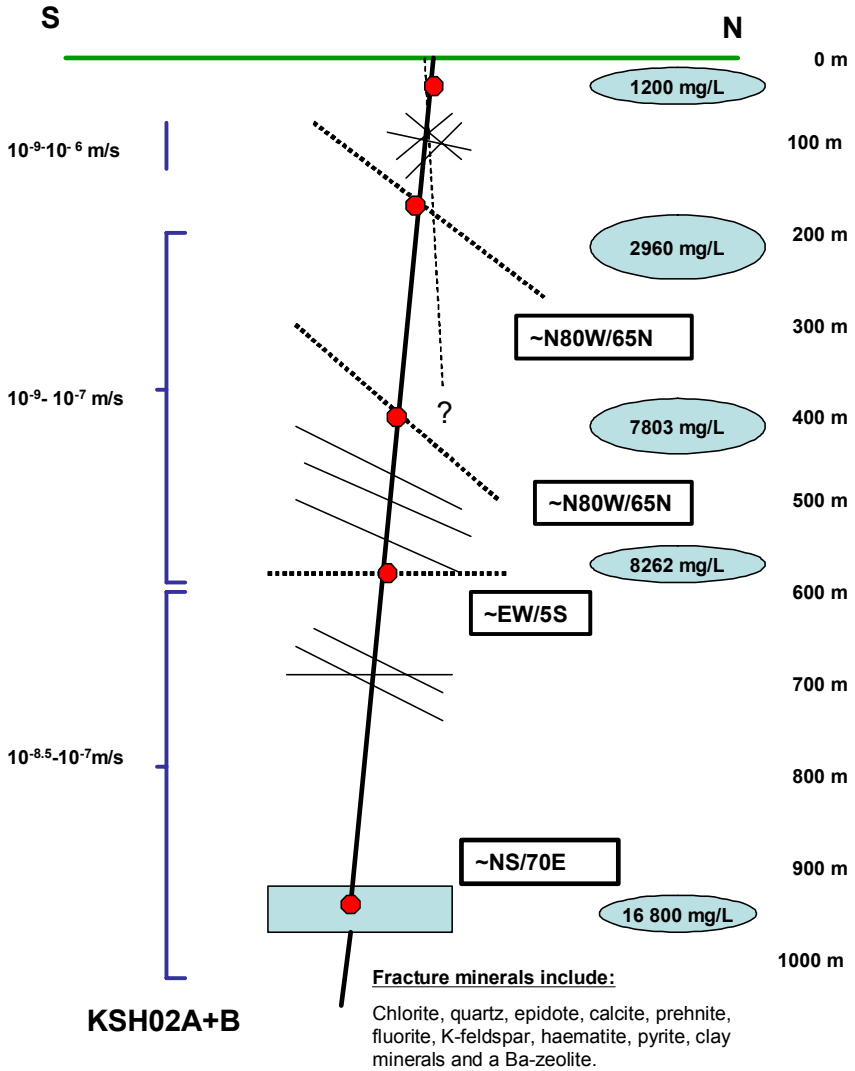

Figure 4-5: *Borehole KSH02+B showing intercepted structures and their hydraulic conductivities; groundwater sampling locations are indicated in red with the mg/L chloride content in blue. Dotted lines represent sampled structures.*

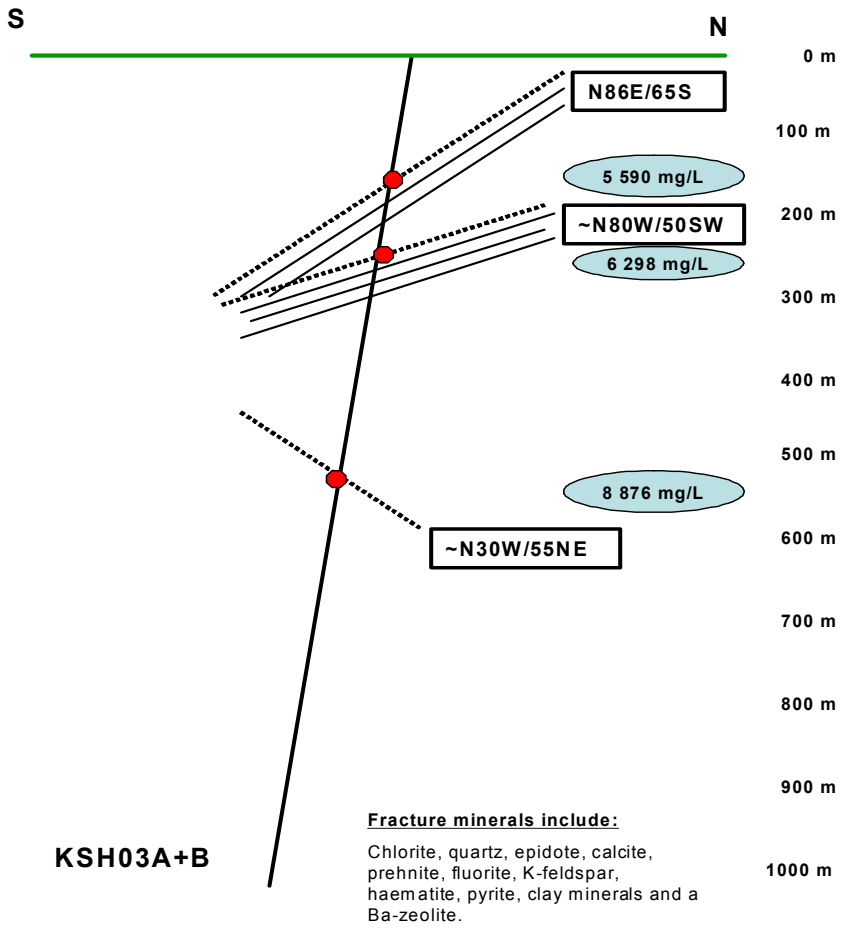

Figure 4-6: *Borehole KSH03A+B showing intercepted structures and their hydraulic conductivities; groundwater sampling locations are indicated in red with the mg/L chloride content in blue. Dotted lines represent sampled structures.*

Evaluation of scatter plots

The hydrochemical data have been expressed in several X-Y plots to derive trends that may facilitate interpretation. Since chloride is generally conservative in normal groundwater systems its use is appropriate to study hydrochemical evolution trends when coupled to ions, ranging from conservative and non-conservative, to provide information on mixing, dilution, sources/sinks etc. Many of the X-Y plots therefore involve chloride as one of the variables.

The hydrogeochemical evaluation presented below follows a systematic approach (see, Smellie et al., 2002) commencing with traditional plots (e.g. Piper Plots) to group the main groundwater types characterising the Simpevarp area and to identify general evolutionary or reaction trends. Comparisons are made with hydrochemical information from the POM sites geographically located close to Simpevarp and previously investigated (i.e. Äspö, Laxemar, Ävrö, Oskarshamn and Bockholmen). Importantly, the hydrogeochemistry is related also to the regional and local geology and hydrogeology in

order to understand the overall (i.e. large- and small-scale) dynamics and evolution of the groundwater systems which characterise the Simpevarp sub area. A more detailed evaluation of the major components and isotopes can be found in *Appendicies 1 and 4*. Discussion of many reactive elements is presented in the modelling part of this report and also in *Appendix 4*.

Piper Plot

Water classification is presented in *Appendicies 1 and 5*. The main groundwater groups characterising Simpevarp area are: a) shallow (<200 m) Na-HCO_3 to Na-Cl-HCO_3 to Na-Ca-Cl- HCO_3 to Na-Ca-Cl types, b) intermediate (approx. 200-600 m) Na-Ca-Cl (with some enhanced SO_4 and Br) types, and c) deep (>600 m) with increasingly enhanced Na-Ca-Cl(Br, SO_4). The variation in compositions, especially in the upper 200 m of the bedrock, is due to local hydrodynamic flow conditions leading to mixing of varying proportions. Microbially mediated reactions are also important influencing both HCO_3 and SO_4, especially in the 200-600 m interval.

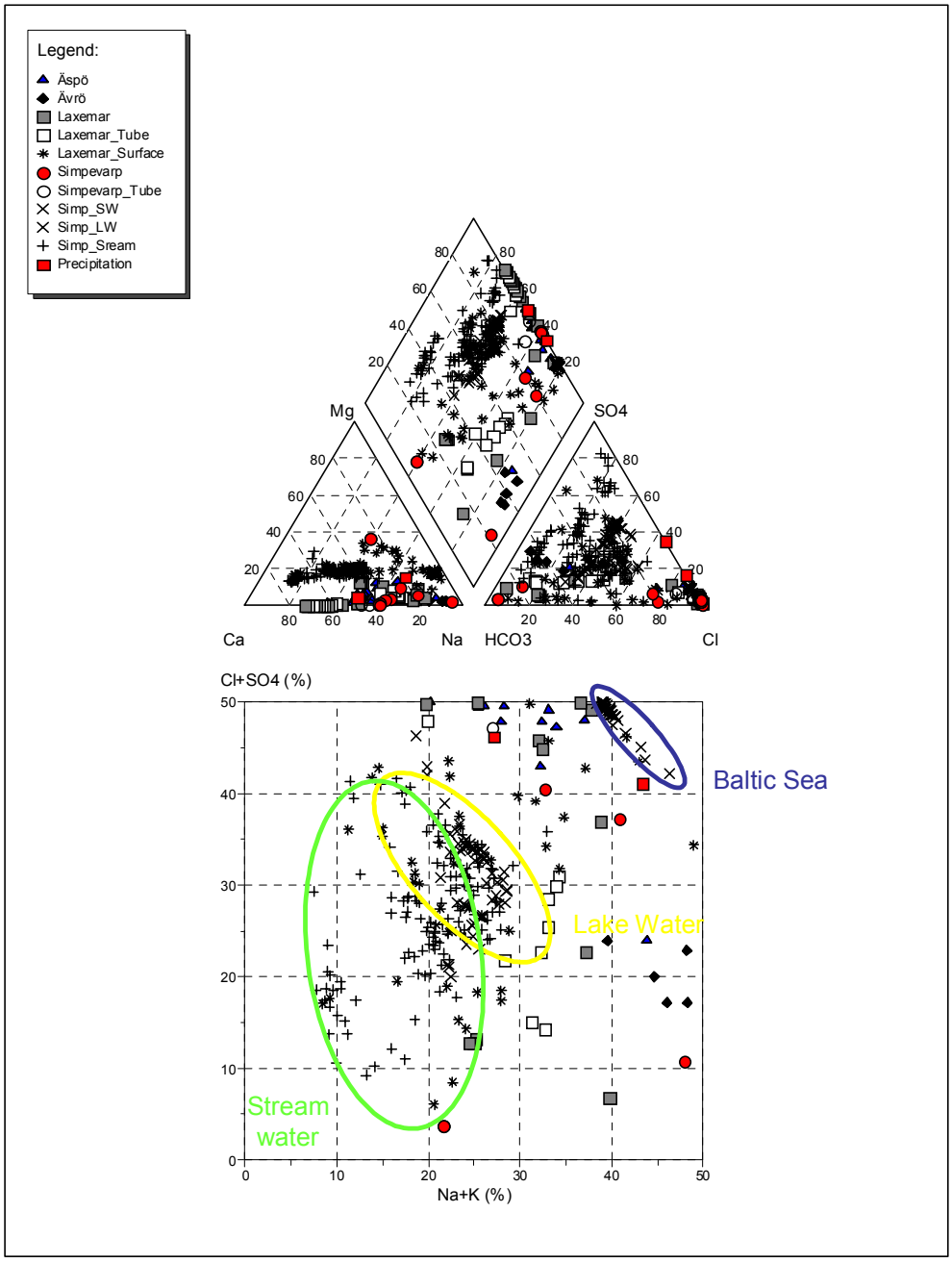

Figure 4-7: *Piper and Ludwig-Langelier plots of surface, near-surface and groundwaters from Simpevarp sub area compared with other groundwater data in the Simpevarp region. Indicated on the diagram are surface water groupings involving Baltic Sea, Stream and Lake waters.*

Set in a more regional context (*Figure 4-7*), the Simpevarp sub area groundwaters (red infilled circles) generally conform in chemistry to similar depth-related groupings representing the Simpevarp area data. The deep highly saline Laxemar groundwaters show a clear differentiation from all the other sites.

Comparison of Simpevarp waters, representing the Baltic Sea (SW), Lakes (LW) and Streams with the Laxemar surface waters, show some degree of grouping. This is suggested in many of the following diagrams. Here the Baltic Sea is clearly

differentiated with a concentrated cluster at high $Cl+SO_4$ which reflects a representative Baltic Sea composition for the Simpevarp latitude. The plot also separates the Simpevarp Lake waters from the Stream waters, the latter clearly indicating a lower Na+K content, and the main Lake water cluster suggesting a slightly higher $Cl+SO_4$ content. There is a wide distribution of Stream waters and, as would be expected, some degree of overlap between the Lake waters, which occurs particularly at higher $Cl+SO_4$ contents. The Laxemar surface waters are scattered throughout the diagram although with a more dense clustering close to the Simpevarp Lake waters but with a significant overlap with the Stream waters.

General comparison of Cl vs depth with other sites

Comparison of the Simpevarp sub area chloride data with some of the Simpevarp areas, together with Forsmark and Olkiluoto, is shown in *Figure 4-8*. It may be argued that such a comparison should be treated with caution since Forsmark and Olkiluoto are geographically distant, have a differing palaeo-evolution and represent different hydrogeological regimes. Furthermore, Laxemar, although close by, represents more a mainland environment and involves greater depths. However, since the Fennoscandian basement hydrogeochemistry probably shares general similarities irrespective of geographic location, *Figure 4-8* may serve a useful purpose particularly with respect to establishing whether a Littorina component is present in the Simpevarp sub area groundwaters.

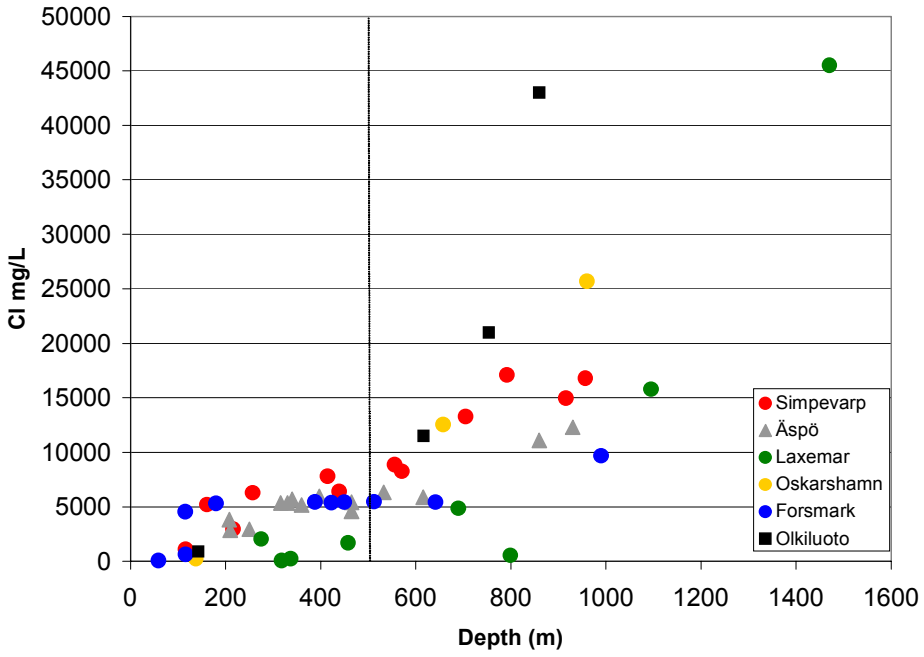

Figure 4-8: *Depth comparison of chloride between different Swedish and Fennoscandian sites.*

The Laxemar data show mostly dilute groundwaters (< 2000 mg/L Cl) extending to approx. 600 m for KLXO1 and to around 1000 m for KLX02 before a rapid increase in salinity to maximum values of around 47 g/L Cl at 1500m. Olkiluoto shows an initial

sharp increase in chloride at around 150 m to a levelling off at 5000 mg/L Cl which continues to 450 m; here there is a relatively steady increase to maximum values of around 20 g/L Cl at 900 m depth (one maximum value of 45.5 g/L Cl was recorded). The available Forsmark data so far show a close similarity to the initial Olkiluoto trends, although the levelling off at approx. 5000 mg/L Cl continues to around 650 m where a small increase to 10 000 mg/L Cl is achieved at 1000 m; there are no deeper groundwater data to compare ultimate salinity contents. In addition the Äspö trends generally are close to those of Forsmark.

The Simpevarp data fall along the general plateau characterised to approx. 500 m depth by chloride ranging from around 5.100-6.300 mg/L Cl (*Figure 4-8*). In addition the Simpevarp profile so far shares a close similarity with Oskarshamn and shares with Äspö and Forsmark similar trends over the first approx. 600 m.

Tracing the Littorina Sea signature with Mg, Br, and $\delta^{18}O$

The Littorina stage in the postglacial evolution of the Baltic Sea commenced when the passage to the Atlantic Ocean opened through Öresund in the southern part of the Baltic Sea. The relatively high sea level together with the early stages of isostatic land uplift led to a successively increasing inflow of marine water into the Baltic Sea. Salinities twice as high as modern Baltic Sea have been estimated for a time period of about 2000 years starting some 7000 years ago (cf. description of the post glacial scenario). From shore displacement curves it is clear that Simpevarp and Laxemar in part were covered by the Littorina Sea. Due to the topography of the area and the on-going isotstatic land uplift, the Laxemar area was probably influenced only to a small degree, whereas the Simpevarp peninsula was covered for several thousands of years until eventual emergence during uplift initiated a recharge meteoric water system some 4000 to 5000 years ago. This recharge system effectively flushed out much of the Littorina Sea water that had penetrated the bedrock.

The Forsmark area, in contrast, has been covered by the Littorina Sea for a much longer period of time and the low topography implies that it reached several tens of kilometres further inland. Furthermore, the present meteoric recharge stage following uplift and emergence has only prevailed for less than 1000 years such that any flushing out of the Littorina Sea component is less pronounced. Stronger evidence of a Littorina Sea water signature can therefore be expected in groundwaters at Forsmark.

Comparison of Forsmark data with the Simpevarp-Äspö-Laxemar-Oskarshamn (KOV01, is one of the characterised boreholes from the Oskarshamn site, situated within the village Oskarshamn near the harbour) data indicates large differences in the character and origin of the groundwaters, especially for brackish groundwaters with chloride contents of around 4000-6000 mg/L Cl. This is exemplified in three plots showing chloride versus magnesium, bromide and $\delta^{18}O$ (*Figure 4-9*, *Figure 4-10* and *Figure 4-11*). For a more detailed discussion and plots showing individual boreholes see *Appendix 1*. The magnesium versus chloride plot (*Figure 4-9*) clearly shows the difference between the Forsmark and Simpevarp groundwaters characterised by chloride contents up to 5500 ppm Cl; characteristically the Forsmark samples closely follow the modern marine (Baltic Sea) trend. Those few groundwaters that plot within the Simpevarp group are from greater depths in the bedrock and, as such, have been influenced by mixing with deeper non-marine saline groundwaters. A few samples from Äspö (KAS06 and HAS02; *Figure 4-9*) also show relatively high Mg contents, although not as high as in the Forsmark groundwaters with similar chloride contents. Most of the

Simpevarp area groundwaters show low Mg values although small increases are observed for samples in the chloride interval 4000-6300 mg/L.

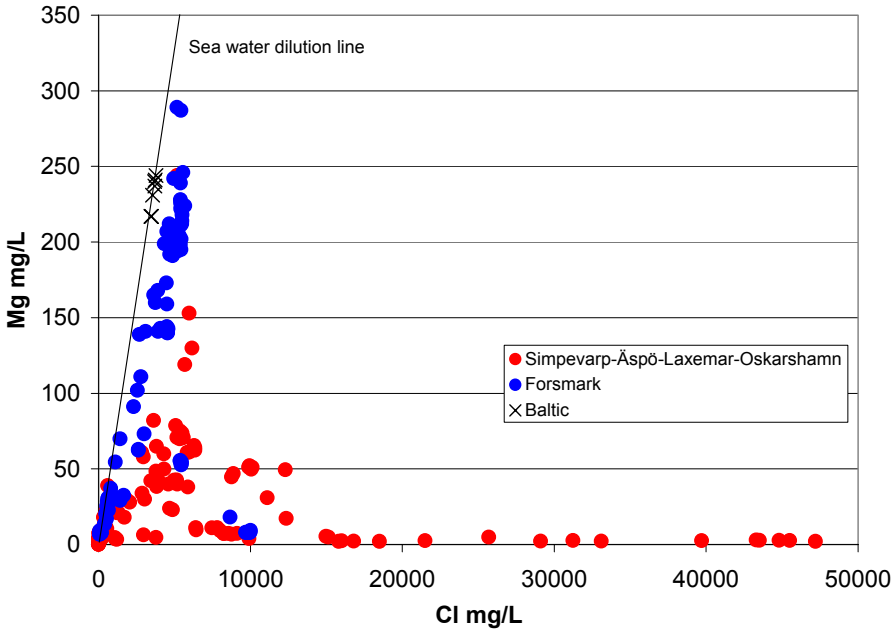

Figure 4-9: *Mg versus Cl for groundwaters from Forsmark and other sites (Simpevarp-Äspö-Laxemar-Oskarshamn (KOV01)). Baltic Sea waters from Simpevarp area and Forsmark are included for reference.*

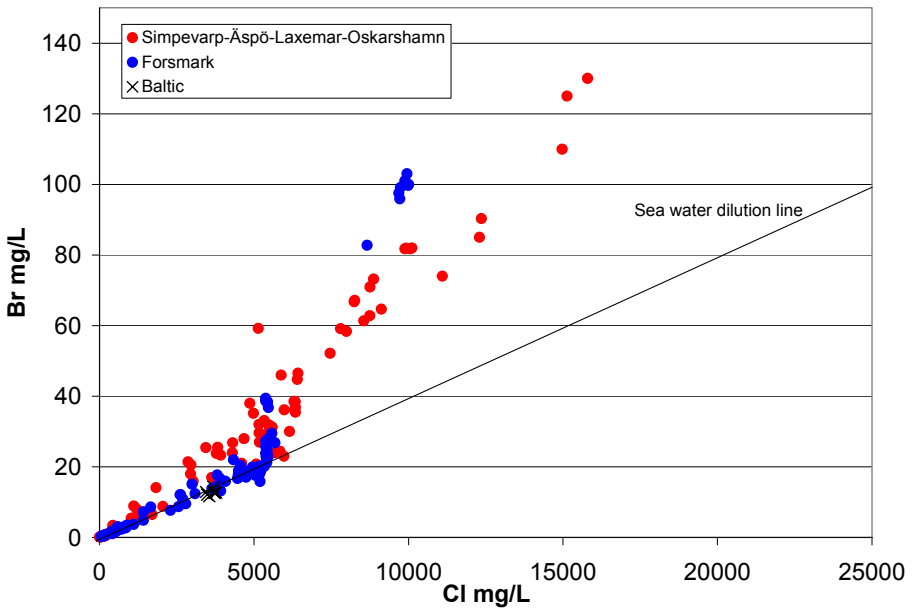

Figure 4-10: *Br versus Cl for groundwater samples from Forsmark and other sites (Simpevarp-Äspö-Laxemar-Oskarshamn (KOV01)). Baltic Sea waters from Forsmark and Simpevarp areas are included for reference.*

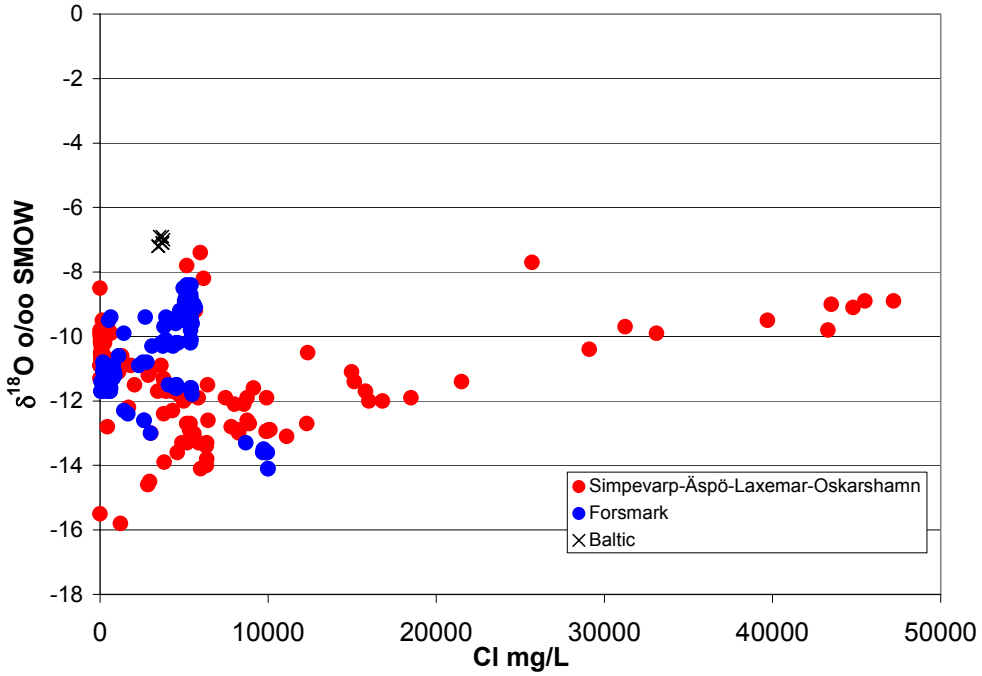

Figure 4-11: *$\delta^{18}O$ versus Cl for groundwaters from Forsmark and other sites (Simpevarp-Äspö-Laxemar-Oskarshamn (KOV01)). Baltic Sea waters from Simpevarp area are included for reference.*

The bromide versus chloride plot (*Figure 4-10*) underlines the marine signature for most of the Forsmark groundwaters up to contents of 5500 mg/L Cl, whereas marine signatures only are obtained in a few of the Simpevarp area groundwaters. This observation is strengthened in the $\delta^{18}O$ versus chloride plot (*Figure 4-11*) which shows deviating groundwater trends for Forsmark and Simpevarp.

Generally, with a few exceptions, the brackish to saline groundwaters up to 5500 mg/L Cl at Forsmark show indications of a marine origin in terms of: a) Br/Cl ratios, b) Mg values ≥100 mg/L, and c) $\delta^{18}O$ values higher than meteoric waters (due to in-mixing of marine waters). In contrast, for the Äspö-Simpevarp/Laxemar samples these criteria are only fulfilled in samples from KAS06 and one sample in KSH03A. In both cases the groundwater samples have been collected from fracture zones outcropping close to the shoreline or under the Baltic Sea.

The chloride content and $\delta^{18}O$ value for the Littorina Sea at maximum salinity is difficult to determine precisely. Interpretations of salinities based on fossil fauna together with $\delta^{18}O$ analyses of the fossils has resulted in suggested salinities around 6500 mg/L Cl and $\delta^{18}O$ values ~ -4.5‰ SMOW (Donner, 1994; Pitkänen et al., 2003). In *Figure 4-12* (Cl versus $\delta^{18}O$) groundwaters from the Simpevarp area show Br/Cl ratio < 0.0045 and magnesium values > 100 mg/L. For comparison are included a small set of samples from Forsmark and the values for selected groundwaters at Olkiluoto considered to contain the largest proportion of Littorina Sea water (Pitkänen et al., 2003). As can be seen in the figure these values cluster along a mixing line from the suggested Littorina Sea composition to a typical glacial meltwater. Notably, none of the Simpevarp bedrock groundwaters sampled so far show values in total agreement with a Littorina Sea component. At least two explanations can be suggested: 1) the cluster represents the Littorina Sea at the time when the water intruded, and 2) the Littorina Sea water was mixed with glacial meltwater in the bedrock.

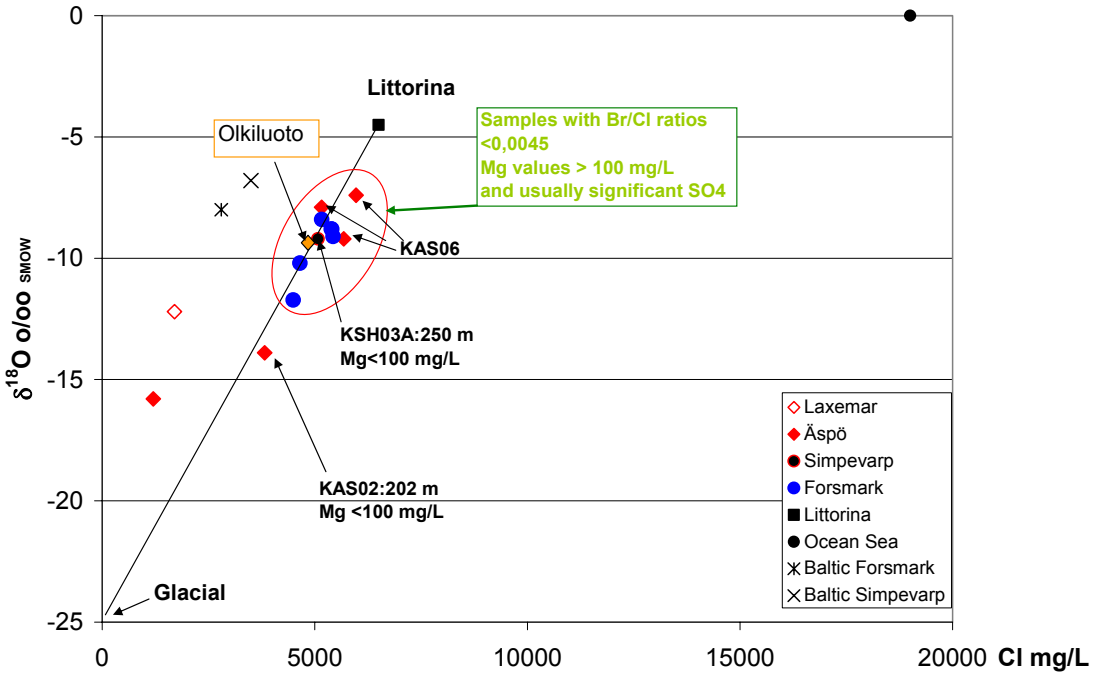

Figure 4-12: *$\delta^{18}O$ versus chloride content for potential marine groundwaters from Simpevarp area, Äspö, Forsmark and Olkiluoto, the latter from Pitkänen et al. (2003).*

In conclusion, groundwaters from the Äspö, Laxemar and Simpevarp sites at best only show a weak presence of a Littorina Sea water component. However, based on the post glacial scenario for the region, it is reasonable to assume that Littorina Sea water penetrated into the bedrock but has been flushed out subsequently by later recharge meteoric waters during early uplift. This has been facilitated by the fact that the maximum penetration of these Littorina waters appear to have been restricted to shallow depths (approx. 150-300 m). Greater penetration depths may have occurred along some of the sub-vertical structures in the area, but to date there is an absence of data to support this.

Some contributions of ion exchange processes to enhanced magnesium contents in a number of the Simpevarp area groundwaters must also be considered. The nature of such magnesium sources are presently uncertain, but water/rock interaction through weathering processes and/or removal by ion exchange processes of earlier marine sources from near-surface sediments to subsequent recharging meteoric waters could be invoked.

Plot of oxygen-18 versus deuterium

Figure 4-13 details the stable isotope data which plot on or close to the Global Meteoric Water Line (GMWL) indicating a meteoric origin. In accordance with many of the other plots, two main groundwater groups are indicated: a) shallow dilute groundwaters ranging from $\delta^{18}O$ = -11.3 to -9.8 ‰ SMOW, δD = -80.4 to 74.3 ‰ SMOW, and b) brackish to saline groundwaters ranging from $\delta^{18}O$ = -14.0 to -12.7 ‰ SMOW, δD = -

100.0 to -93.8 ‰ SMOW. The two tube samples plot within group (a). The heavier group (a) isotopic values suggest a modern meteoric recharge component. The lighter isotopic values of group (b) indicate the presence of a cold recharge meteoric component (glacial melt water?). The limited data suggest there is no major Baltic Sea influence on the sampled Simpevarp groundwaters.

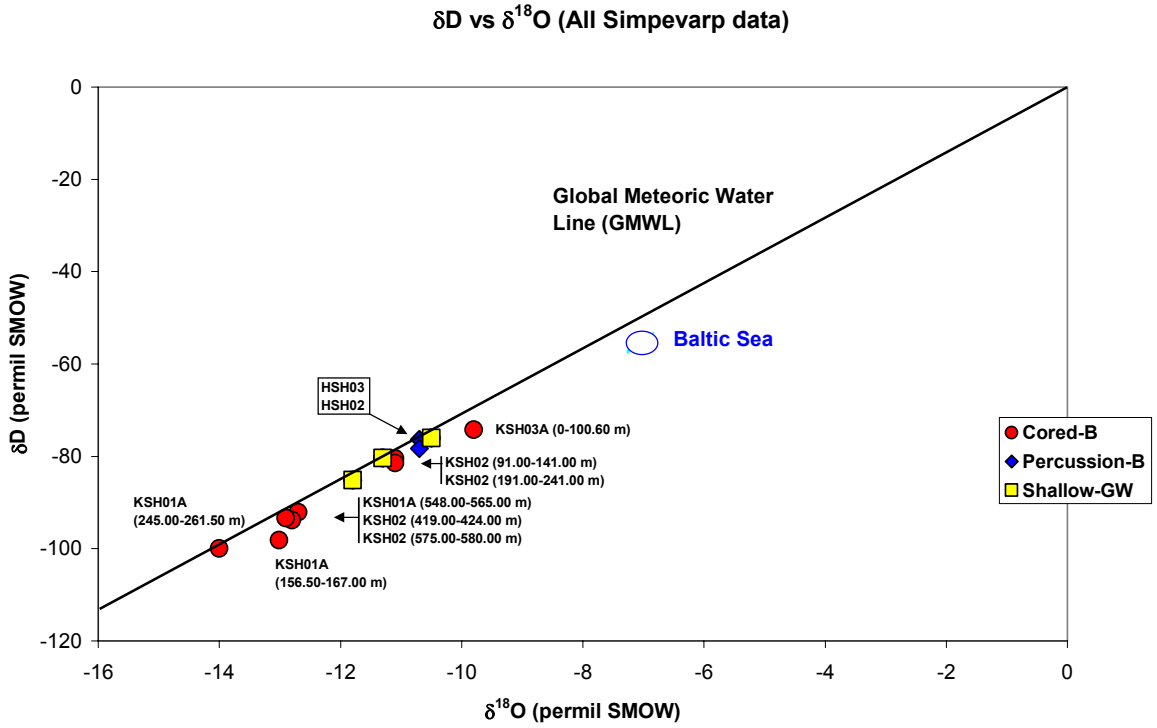

Figure 4-13: *Plot of $\delta^{18}O$ versus δD for all Simpevarp area data.*

Plot of calcium/magnesium versus bromide/chloride

By plotting Ca/Mg versus Br/Cl, *Figure 4-14* provides an opportunity to differentiate those groundwaters of modern marine origin (e.g. Baltic Sea) from non-marine or non-marine/old marine mixing origin. The figure clearly shows the Baltic Sea group of modern marine waters and also the deepest non-marine saline groundwaters from Laxemar and Oskarshamn (KOV01). Between these two extreme end-members lie most of the groundwater data. The red arrow shows the direction towards the deep saline non-marine types, and much of the data plotting along this pathway represent groundwaters which contain an increasing component of the deep saline non-marine end-member. Likewise, at the other extreme, some of the plotted data closest to the modern marine end-member may well comprise groundwaters with a modern marine water signature, although in this case there is not a clear transition zone as might be expected if mixing processes were occurring. The other possibility is the presence of an older marine component (e.g. Littorina Sea) in the shallower brackish groundwaters which persist from 100-500 m depth, depending on local conditions. These groundwaters are circled in blue and indicate enhancements of, for example, Mg and Br.

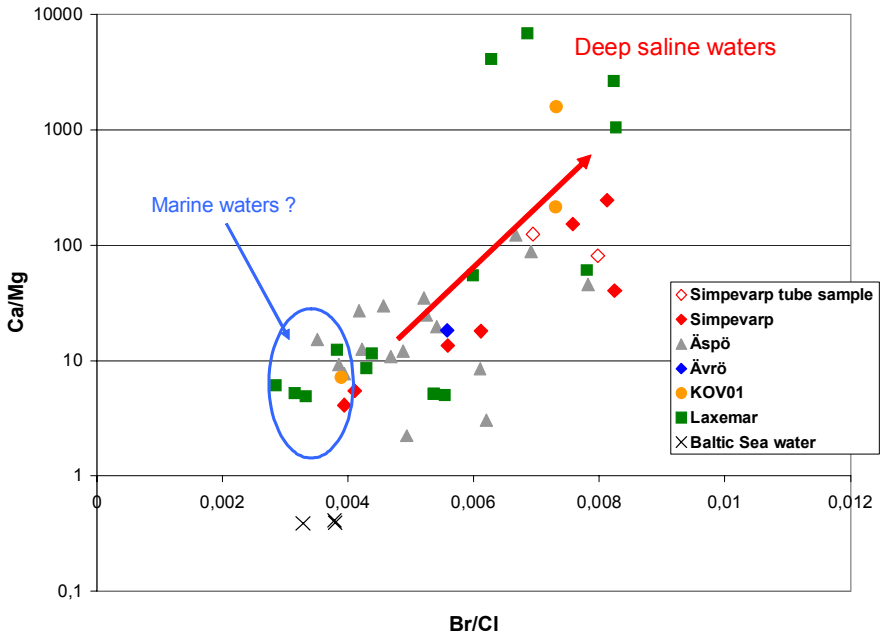

Figure 4-14: *Plot comparing all Simpevarp area Ca/Mg vs Br/ Cl data.*

Plot of oxygen-18 versus chloride

Figure 4-15 shows the decrease in $\delta^{18}O$ with increasing salinity (i.e. depth).

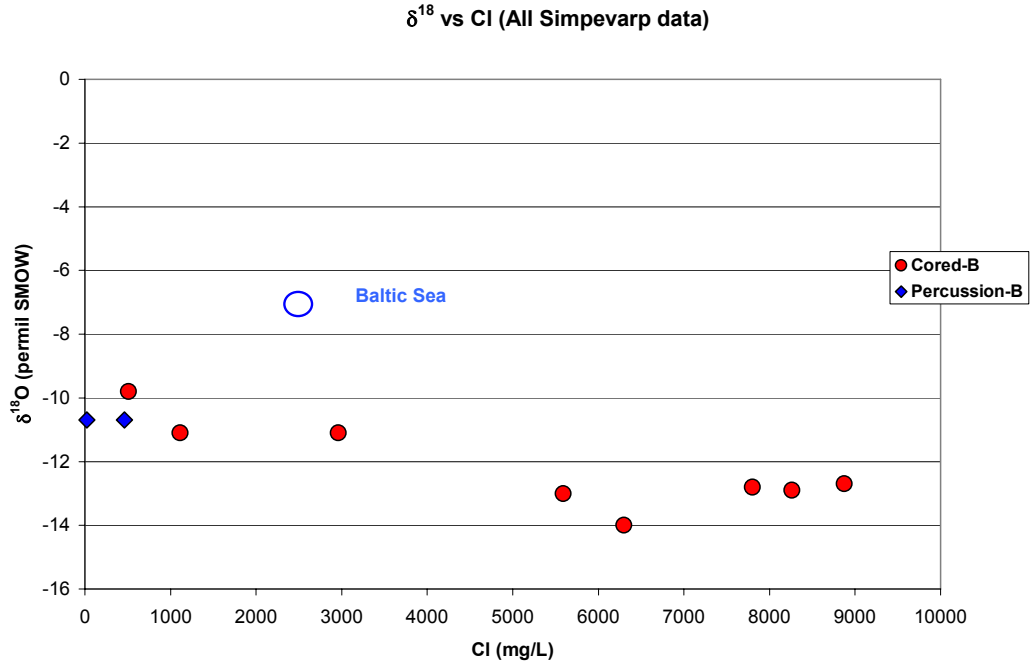

Figure 4-15: *Plot of $\delta^{18}O$ versus Cl for all Simpevarp data.*

Figure 4-16 compares the Simpevarp data with the POM sites. The light group (b) Simpevarp groundwaters from the deeper cored boreholes fall within the same range of many of the Äspö groundwaters known for their cold climate recharge signatures.

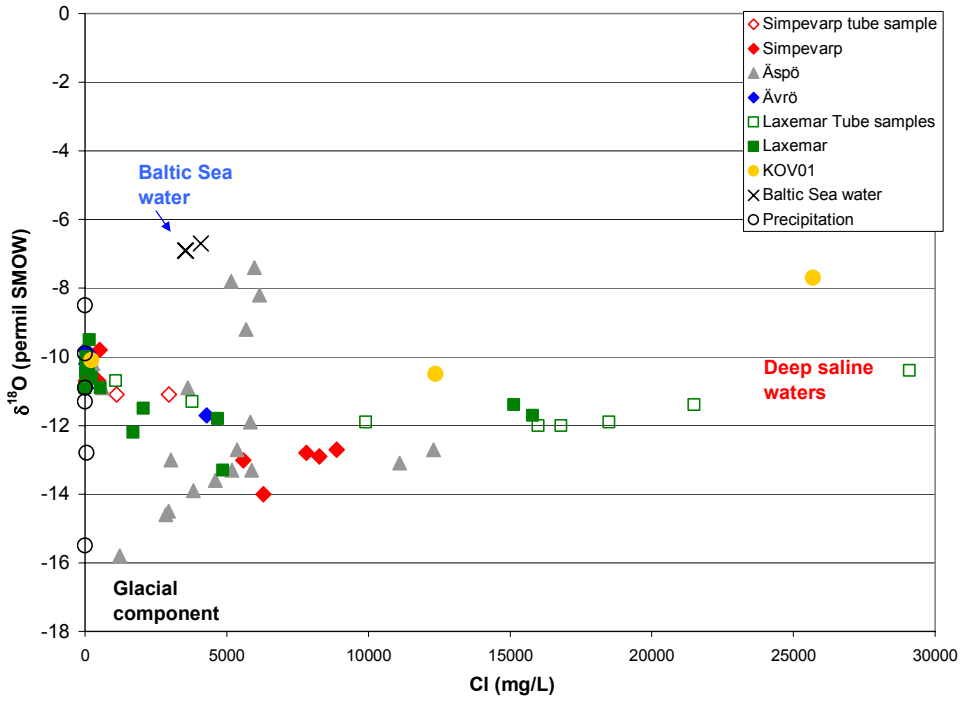

Figure 4-16: *Plot comparing all Simpevarp $\delta^{18}O$ versus Cl data with the other sites.*

Tritium

Tritium produced by the bomb tests during the early 1960´s is a good tracer for waters recharged within the past four decades. As part of an international monitoring campaign, peak values between 1000 and 4300 TU were recorded at Huddinge near Stockholm in the years 1963-1964 and values reaching almost 6000 TU were recorded at Arjeplog and Kiruna in northern Sweden (IAEA database). Due to decay (half life of 12 years) and dispersion, in addition to a cessation of the nuclear bomb tests, precipitation tritium values decreased so that the measurements carried out at Huddinge during 1969 showed that values had dropped to between 74 and 240 TU.

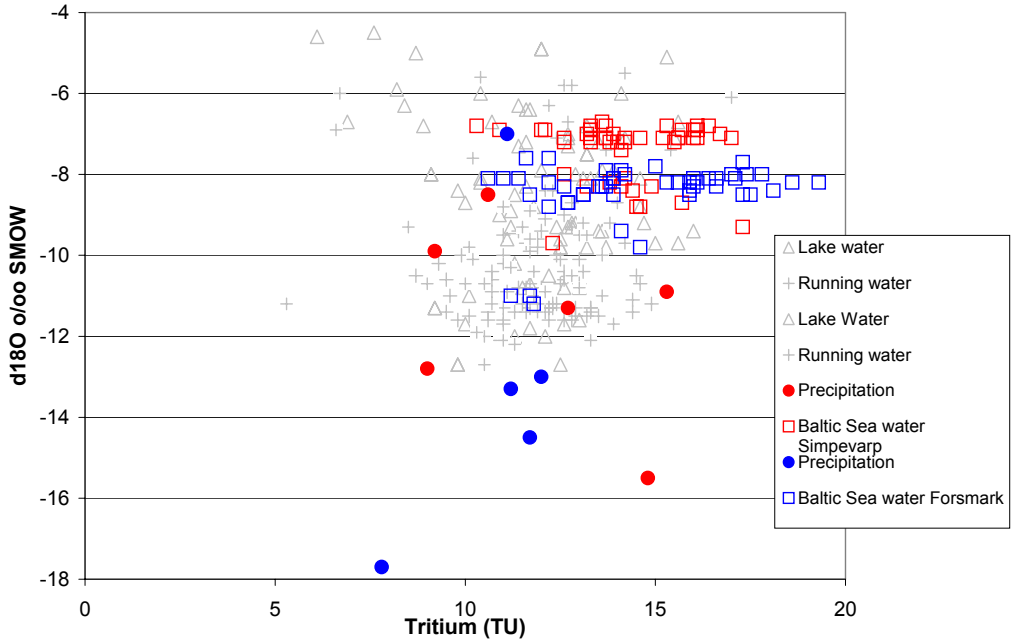

Figure 4-17: *Plot of $\delta^{18}O$ versus tritium in surface water samples from the Simpevarp and Forsmark sites.*

Present day surface waters from the Simpevarp and Forsmarks sites show values of 7-20 TU with exceptions of a few Lake and Stream water samples from Forsmark (*Figure 4-17*). Generally, the Baltic Sea samples (10.3-19.3 TU) show somewhat higher values compared to the meteoric surface waters (7.8-15 TU) for precipitation. The Forsmark Baltic Sea samples show some values that are higher than the Simpevarp Baltic Sea samples but the spread is large for both sites. The successive lowering of tritium contents versus time elapsed since the bomb tests may explain the higher values in the Baltic Sea (due to reservoir effects) compared with precipitation. The difference between the Simpevarp and Forsmark Baltic Sea samples can be a north-south effect, with higher tritium values in the north compared to the south. However this is not demonstrated by the precipitation values (*Figure 4-17*). Moreover, the ^{14}C content in the Baltic Sea water is relatively similar between the two sites (*Figure 4-18*). It should be emphasised that the precipitation values are very few, show a large variation in tritium and therefore are not considered very conclusive. Continued systematic sampling of precipitation for tritium analyses is encouraged. One problem in using tritium for the interpretation of near-surface recharge/discharge is, as mentioned above, the variation in content in the recharge water over time, which implies that near-surface groundwaters with values around 15 TU can be 100% recent or a mixture of old meteoric (tritium free) and a small portion (10%) of water from the sixties at the height of the atmospheric nuclear bomb tests.

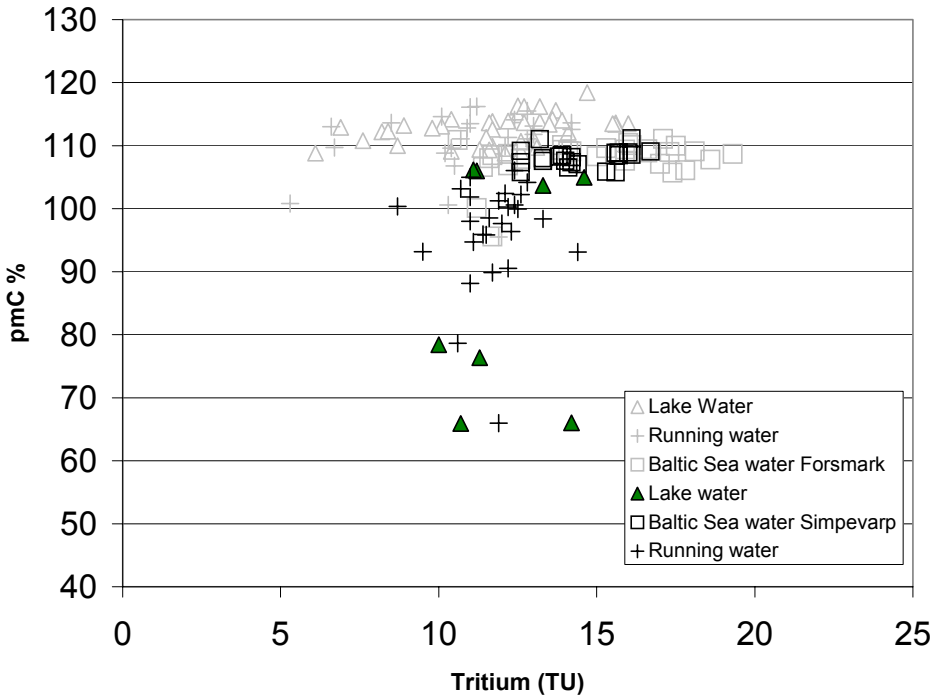

Figure 4-18: *Plot of ^{14}C (pmC) versus tritium in surface waters from Simpevarp (shown in black and green) and Forsmark (in grey).*

The plot of tritium versus ^{14}C for surface waters from Forsmark and Simpevarp show large differences concerning the Lake and running Stream waters of the two sites. At Simpevarp the Lake and Stream waters show a distinct decrease in ^{14}C content whereas the tritium values remain the same or show a small decrease. They can be explained by HCO_3 added to the waters originating either from calcites devoid of ^{14}C or due to microbial oxidation of organic material with lower (or no) ^{14}C. This is the pattern expected for near-surface waters. At Forsmark, in contrast, most Lake and running Stream waters have higher ^{14}C values compared with Baltic Sea waters whereas the tritium values range from 5-15 TU. The reason for this is not clear and several explanations are possible.

An additional problem in using tritium for groundwater modelling for the Simpevarp site is shown in *Figure 4-19* where percentage drilling water content is plotted against tritium content. The drilling water used from percussion borehole HSH03 has tritium values in the range of 4.7 to 9.4 TU. Since the subsurface production of tritium is expected to be very low in the granitoids of the Simpevarp area, a linear relation between drilling fluid portion and tritium would be expected for the deeper samples. As can be seen, the tube samples from borehole KSH01A+B (750-1000 m) deviate from this trend. Two different explanations are possible: 1) surface waters of other sources than the drilling fluid have entered and mixed within the borehole, or 2) the uranine tracer used to spike the drilling fluid has not been added uniformly throughout the drilling phase resulting in erroneous determinations of drilling water content in the sampled groundwaters. High tritium values compared to drilling fluid portion are also obtained in some groundwaters from the upper 200 m of the bedrock and are probably explained by inmixing (artificially or natural) of young meteoric recharge waters.

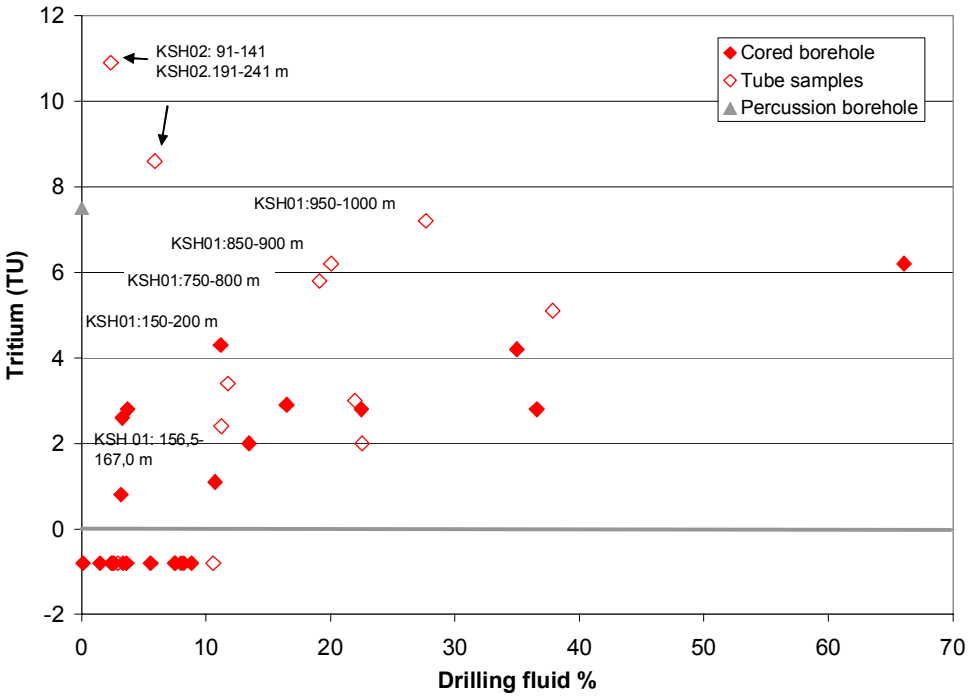

Figure 4-19: *Plot of tritium versus drilling fluid for boreholes HSH03, KSH01A+B, KSH02 and KSH03A.*

The extreme deviation from a linear trend shown by the borehole KSH02 tube samples (91-141 m and 191-241 m) is significant as these two samples have been included in the ion-ion plots described in *Appendix 1*. One of the criteria for their selection as being of 'limited suitability' was a relatively low drilling water content. However, in retrospect, they should have been avoided because of contamination from shallower near-surface groundwaters with significant tritium. Contamination from near-surface groundwaters is clear from some of the ion-ion plots.

Carbon and carbon isotopes

Review of existing data from Äspö and Ävrö

Interpretation of the carbon inventory (see *Appendix 2)* and how this inventory has evolved contributes to understanding of the nature of the principle groundwater contributors, key geochemical processes and possibly in some cases to the origin and age of the contributors. The work thus aims at contributing to provision of trust in the hydrological interpretation and determination of key geochemical processes.

The objectives were: (i) to provide a methodology for interpretation of the groundwater carbon inventory, (ii) to provide tools for extending the database by relevant carbon inventory descriptors, and (iii) to outline future activities.

The approach used is a very simple and straightforward one. It makes use of simple assumptions such as the DIC biogenic inventory having a ^{13}C value of –27 ‰, the same

as in the source material for recharge under C-3 plant material soil and vegetation. If there are recharge contributions from lakes or wetlands with standing water with DIC exchange/isotopic fractionation with the atmosphere, such simple approaches are not valid. The same is true if there is microbial activity in the subsurface producing methane or carbon dioxide or considerable precipitation of DIC. Another problem is the heterogeneous carbon isotope composition of the frqacture calcites that are partly dissolved in the upper part of the flowpaths. The main idea, however, is that by using this simple approach, systems/samples can be identified that basically follow this simple route in the development of the DIC inventory and deviations can be identified for further clarification. However, because the available carbon isotope data from the Simpevarp 1.2.data freeze are still very limited, especially concerning groundwaters, no tests therefore have been performed within this model version.

Carbon and carbon isotope data from Simpevarp

The stable carbon isotope ratios, expressed as $\delta^{13}C$ ‰ PDB, and radiocarbon contents (^{14}C) expressed as pmC (percentage modern carbon), and HCO_3^-, have been analysed from surface waters and groundwaters (see *Appendix 1)*. The tritium versus ^{14}C for surface waters has been discussed already in the previous section. *Figure 4-20* shows $\delta^{13}C$ versus tritium for the Simpevarp waters.

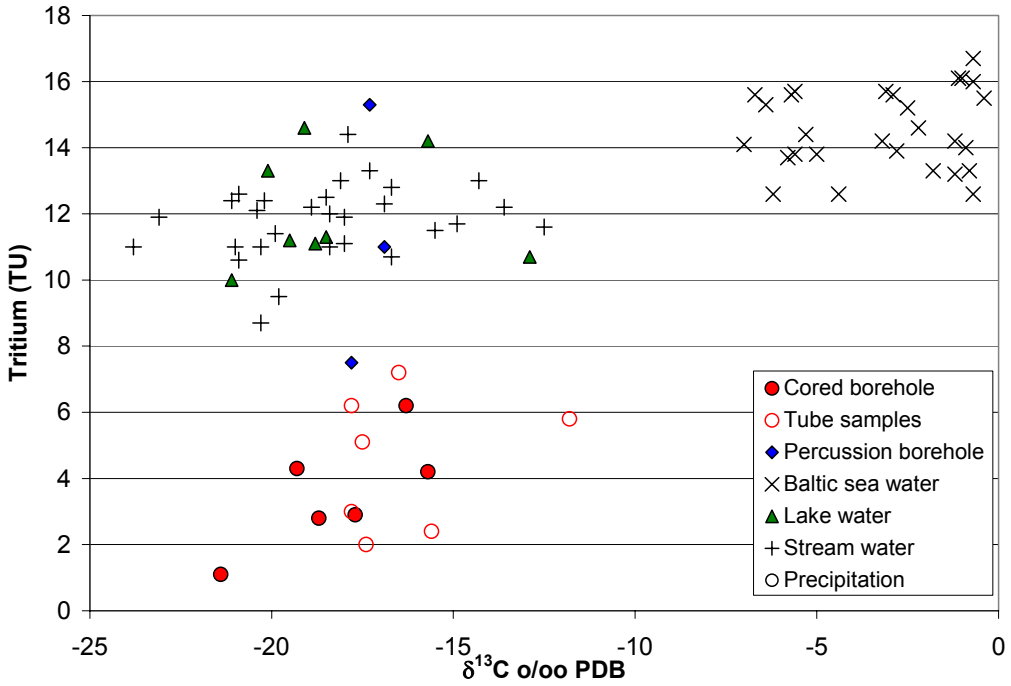

Figure 4-20: *Plot of tritium versus $\delta^{13}C$ in surface waters and groundwaters from Simpevarp.*

The Baltic Sea water has high carbon isotope values produced by equilibria with atmospheric CO_2; this contrasts with all the other waters, both surface and groundwaters, which significantly show lower values. CO_2 produced in the soil cover

due to breakdown and oxidation of organic material usually results in $\delta^{13}C$ values of around -20 ‰ PDB which can partly explain the dissolved $\delta^{13}C$ (HCO_3^-). However, the lowering in $\delta^{14}C$ accompanying the decrease in $\delta^{13}C$ in some lake and stream waters indicate that calcite dissolution may have taken place as well, and/or breakdown of old organic material.

The fracture calcites show no homogeneous $\delta^{13}C$-values and it is therefore not possible to model calcite dissolution as a two end member mixing. Since to date only six ^{14}C analyses of groundwaters from packed-off sections are available from the Simpevarp area, existing data from Laxemar, Äspö and Ävrö have been included in two plots showing $\delta^{13}C$ (HCO_3^-) versus ^{14}C (*Figure 4-21*) and $\delta^{13}C$ (HCO_3^-) versus HCO_3^- (*Figure 4-22*). The plots show that there is no real correlation between ^{14}C and $\delta^{13}C$, i.e. there is no indication of a change in $\delta^{13}C$ with age. Instead, most groundwater samples show values in the range of -15 to -22 ‰ $\delta^{13}C$ indicating that breakdown of organic material plays a major role and has occurred either in the near-surface (being transported downwards) or that *in situ* production has taken place. An organic origin is also supported by the $\delta^{13}C$ versus HCO_3^- plot where the groundwater samples with the highest HCO_3^- content show relatively homogeneous $\delta^{13}C$ values clustering at -16 to -20‰ $\delta^{13}C$.

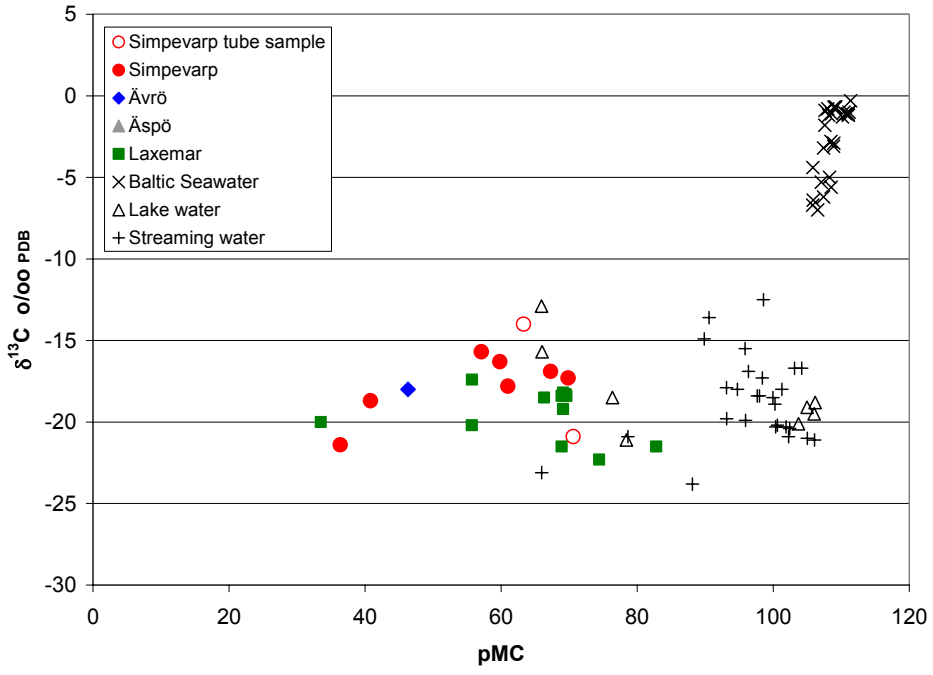

Figure 4-21: *$\delta^{13}C$ (HCO3-) versus ^{14}C in surface waters and groundwaters from Simpevarp, Laxemar and Ävrö.*

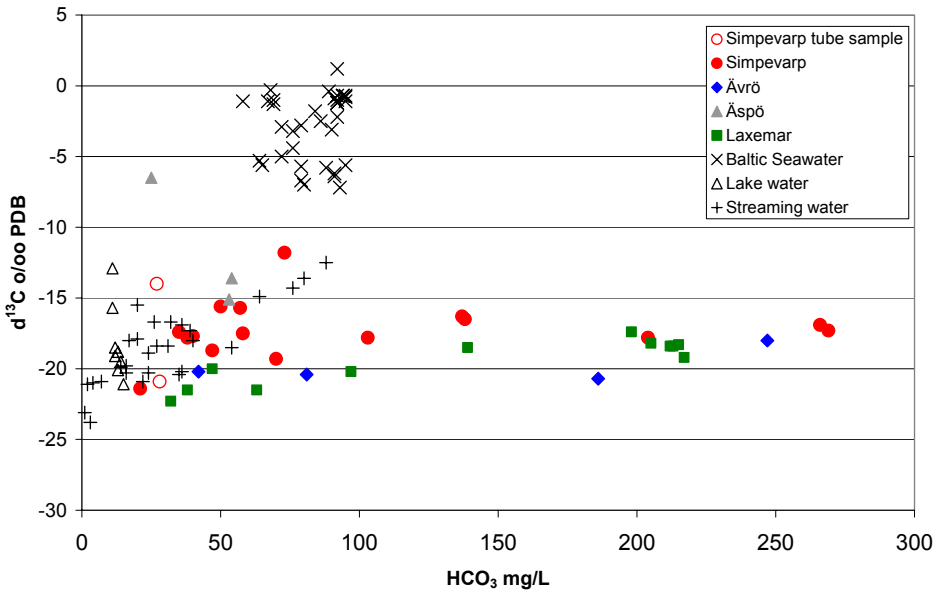

Figure 4-22: *$\delta^{13}C$ (HCO_3) versus HCO_3 in surface waters and groundwaters from Simpevarp, Laxemar Äspö and Ävrö.*

Groundwater age distribution was modelled in *Appendix 6* by taking both 100 pmC and 85 pmC as initial values for the recharge water. Based on (1) geochemical evidence of calcite dissolution, (2) ^{13}C values of fresh groundwater, and (3) previous experience and published data of other granitic aquifers, it is believed that an initial value of 100 pmC for recharge water in Simpevarp is highly unlikely The modelling shown in *Figure 4-23* indicates that the age of fresh groundwater at Simpevarp (at a depth of 100–200 m) could be in the order of magnitude of some decades to hundreds of years, instead of thousands of years as estimated from measurements.

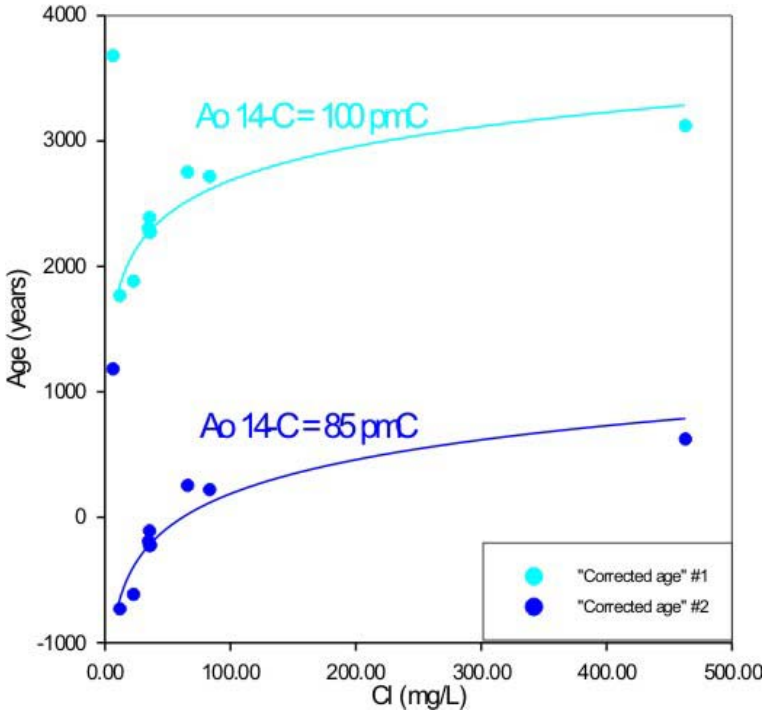

Figure 4-23: *^{14}C-derived ages of fresh groundwater samples of Simpevarp area assuming initial values of 100 pmC and 85 pmC.*

Sulphur isotopes

Sulphur isotope ratios, expressed as δ^{34}S ‰ CDT, have been measured in dissolved sulphate in Baltic Sea waters, surface waters and groundwaters from the Simpevarp area. Over 200 analyses have been performed of which 30 are groundwaters from boreholes KSH01A+B and KSH02 at Simpevarp with two exceptions; one from Laxemar (HLX10) and one from Ävrö (KAV04). The isotope results are plotted versus SO_4^{2-} contents (*Figure 4-24*) and versus Cl contents (*Figure 4-25*). Unfortunately, neither SO_4^{2-} nor Cl contents were measured in 10 of the groundwater samples analysed for δ^{34}S. Better coordination of these measurements is considered essential for continued sampling and analyses in the area.

The recorded values vary within a wide range (-1 to +24 ‰ CDT) indicating different sulphur sources for the dissolved SO_4^{2-}. For the surface waters (Lake and Stream waters) the SO_4^{2-} content is usually below 50 mg/L and the δ^{34}S relatively low but variable (-1 to +15 ‰ CDT) with most of the samples in the range 2-9 ‰ CDT. These relatively low values indicate that atmospheric deposition and oxidation of sulphides in the overburden is the origin for the SO_4^{2-}. The Baltic Sea waters cluster around the 20 ‰ CDT marine line but show a relatively large spread (16-23 ‰ CDT). The reason for this is not fully understood but suggestions include: a) contribution from land discharge sources (e.g. streams) to various degrees (low values), and b) potential bacterial modification creating high values in the remaining SO_4^{2-}.

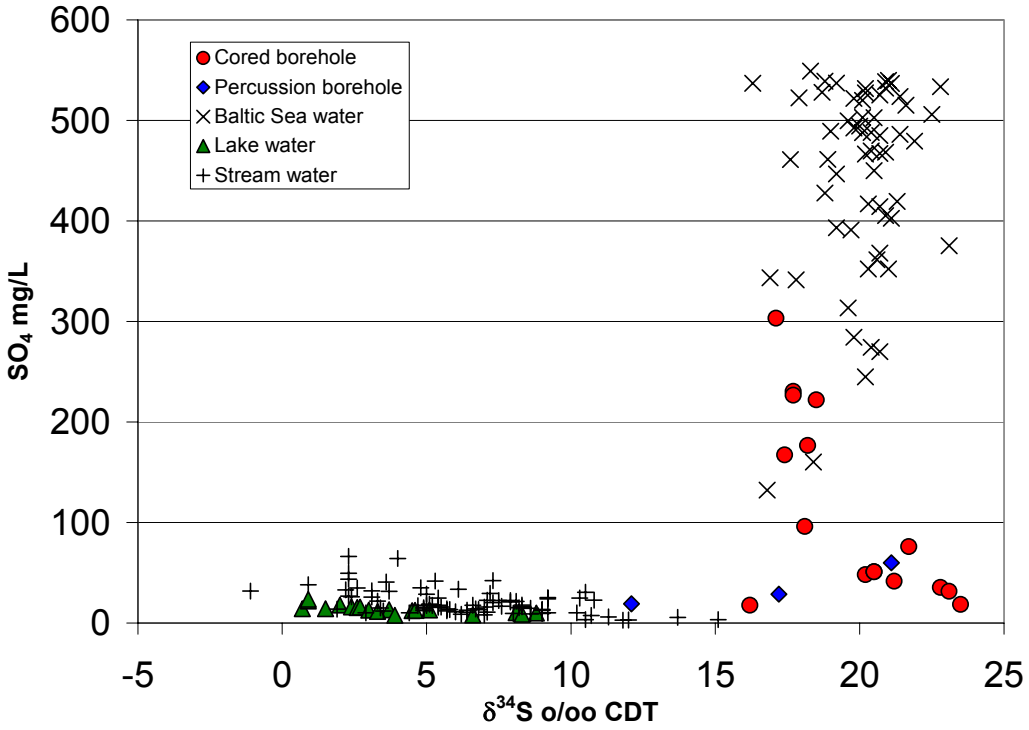

Figure 4-24: *Plot of $\delta^{34}S$ versus SO_4^{2-} in surface waters and groundwaters. The grey line indicates the marine value at around 20 ‰ CDT.*

The borehole groundwaters (*Figure 4-25*) show $\delta^{34}S$ values in the same range as the Baltic Sea waters but with a clear indication of $\delta^{34}S$ values greater than +21 ‰ CDT in samples with low SO_4^{2-}. These latter values are interpreted as a product of sulphate reduction taking place in groundwaters identified in *Figure 4-25* with a chloride content between 5000 and 6300 mg/L. The five groundwaters with higher salinities share lower $\delta^{34}S$ but higher SO_4 contents. The $\delta^{34}S$ values of these groundwaters are, however, still within the range for the analysed Baltic Sea waters. The SO_4^{2-} contents are still not high enough to invoke dissolution or leaching as a mechanism, more likely processes are in-mixing of marine waters although in-mixing of SO_4^{2-} from deep brine waters cannot be excluded. Deep saline SO_4^{2-} sources may have resulted from the leaching of sediments and/or dissolution of gypsum previously present in fractures. Lowering of the $\delta^{34}S$ signature by oxidation of sulphides seems to be less probable for the groundwater samples and is not supported by fracture mineral investigations (Drake and Tullborg, 2004; P-report in press).

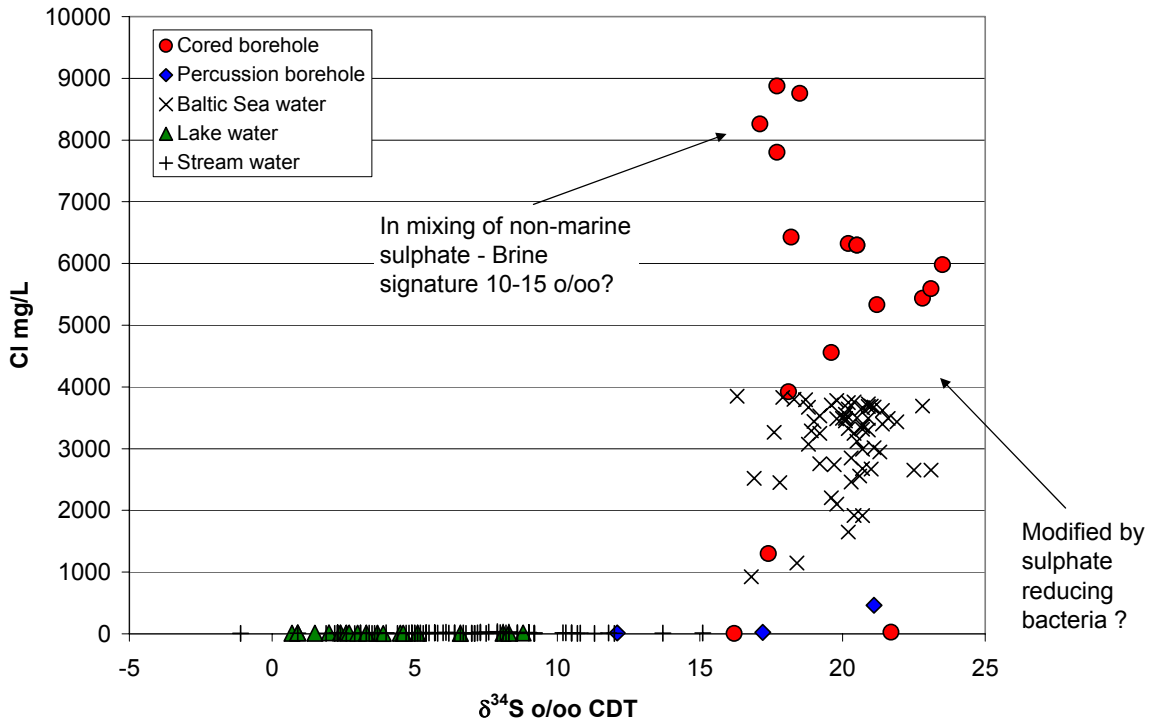

Figure 4-25: *Plot of $\delta^{34}S$ versus Cl in surface waters and groundwaters. The grey line indicates the marine value at around 20 ‰ CDT.*

As discussed in *Appendix 1*, the SO_4 content in deep groundwaters from the Oskarshamn area show different trends versus Cl content. The Laxemar samples show relatively high SO_4 content in the saline waters, whereas the KOV01 samples show extremely low values. The most saline water at Simpevarp (16800 mg/L Cl) has a SO_4 content of around 600 mg/L. Geochemical modelling (*Appendix 4*) indicates dissolution of gypsum as a possible source for SO_4 in the groundwaters. A few observations of fracture gypsum in the lower part of borehole KSH03A have been documented. Unfortunately, no $\delta^{34}S$ measurements are so far available from this gypsum or from the waters at Simpevarp with chloride contents greater than 9000 mg/L.

Strontium isotopes

Strontium isotope ratios ($^{87}Sr/^{86}Sr$) have been measured in groundwater samples and Baltic Sea waters from the Simpevarp area and these are plotted versus strontium content in *Figure 4-26*. Also included in this diagram are groundwater analyses from Forsmark and a few analyses from Laxemar and Ävrö.

^{87}Sr is a radiogenic isotope produced by the decay of ^{87}Rb (half-life $5x10^{10}$a). Marine waters show a distinct Sr isotope signature (0.7092) which is very close to the measured values in the Baltic Sea waters, whereas groundwaters from the different sites (*Figure 4-26*) show values significantly more enriched in radiogenic Sr. Water/rock interaction processes involving Rb-containing minerals are the reason for this. The relatively small variation in Sr isotope ratios within each area, particularly at the Simpevarp, Ävrö and Laxemar sites, is probably an indication that ion exchange reactions with clay minerals

along the groundwater flow paths is an important process. For the Simpevarp/Laxemar area there is a tendency towards higher contents of radiogenic Sr in the groundwaters with greatest salinity (and thus the highest Sr contents measured). Because of the limited data it is not possible to explain this observation, but in the absence of any mineralogical reasons, it is likely that greater residence times for these deep saline groundwaters result in more extensive mineral/water interactions. The higher $^{87}Sr/^{86}Sr$ ratios in the Forsmark samples are most probably due to differences in the composition of the bedrock and fracture minerals compared to Simpevarp.

The possibility of tracing marine components by the use of Sr isotopes is often debated. Clay minerals in the fractures may, however, make such interpretations difficult. For example, the strong present-day major ion Littorina Sea signature in the Forsmark groundwaters is not reflected by any marine Sr isotope imprint. Instead, modification of the Sr isotope values is probably attributable to ion exchange processes.

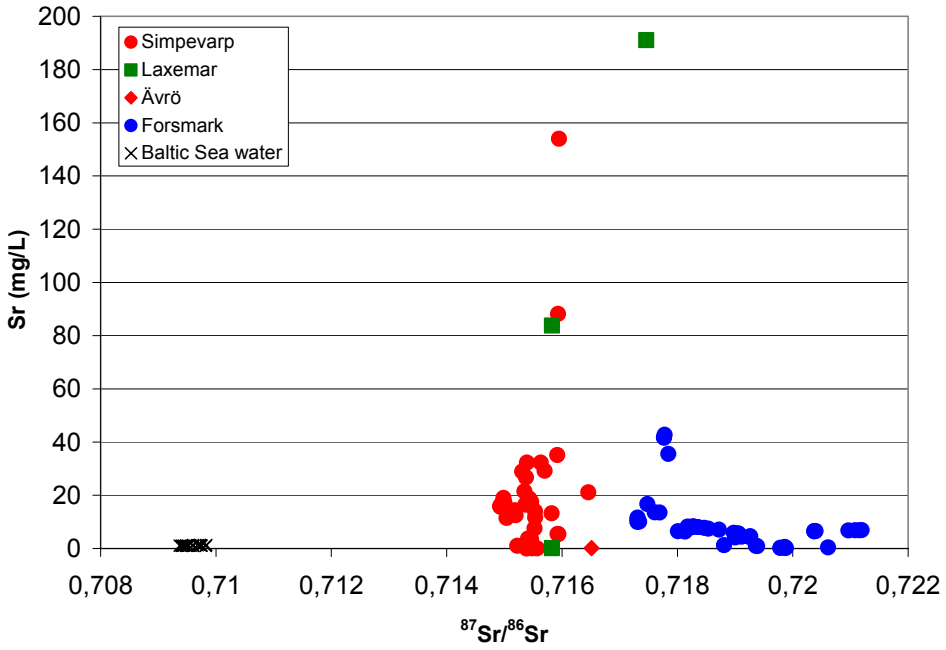

Figure 4-26: *Plot of $^{87}Sr/^{86}Sr$ ratios versus Sr in groundwaters from Simpevarp, Laxemar, Ävrö and Forsmark. Also included are Baltic Sea waters from Simpevarp and Forsmark.*

Chlorine isotopes

Stable chlorine isotopes have been analysed on waters from the Simpevarp area. *Figure 4-27* plots $\delta^{37}Cl$ vs Cl for the Simpevarp, Laxemar, Ävrö and Forsmark sites, including Baltic Sea and surface Lake and Stream waters from Simpevarp. According to Frape et al. (1996) modern Baltic and possibly palaeo-Baltic waters may be recognised by negative $\delta^{37}Cl$ signatures related to salt leachates from Palaeozoic salt deposits south of the Baltic Sea; influence by water-rock interaction tends to result in positive $\delta^{37}Cl$

signatures. Clark and Fritz (1997) also show a clear distinction between the Fennoscndian and Canadian Shield crystalline rock groundwaters and groundwaters from sedimentary aquifers.

Taking into consideration the analytical uncertainty of around ±0.2 ‰, *Figure 4-27* shows that the Simpevarp cored borehole groundwaters are characterised by positive values (+0.14 to +0.75 ‰ SMOC). The Baltic Sea waters fall within the range of -0.28 to +0.27 ‰ SMOC and the surface Stream waters and the percussion borehole groundwaters with very low Cl contents show the largest spread in δ^{37}Cl values (-0.03 to +0.44 ‰ SMOC). These data suggest that the deeper cored borehole groundwaters are characterised by water/rock interaction processes, whilst the near-surface percussion borehole groundwaters are mainly marine derived. The distribution of Baltic Sea and surface Lake and Stream waters suggest some mixing components of marine-derived and deeper groundwater sources.

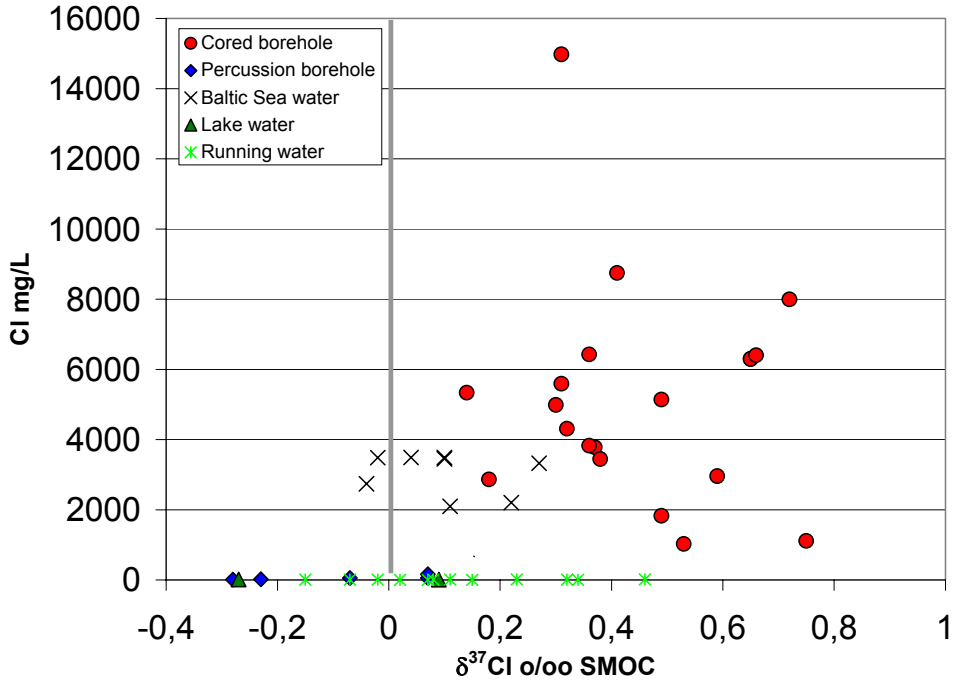

Figure 4-27: *Plot of δ^{37}Cl versus Cl in surface and near-surface waters, groundwaters, and Baltic Sea waters from Simpevarp.*

For comparison δ^{37}Cl values for groundwaters from Laxemar and Forsmark have been plotted together with the Simpevarp data (*Figure 4-28*); additional Baltic Sea samples from the Forsmark area have been included also. For the groundwaters with Cl contents around 5000 mg/L there is a large variation in δ^{37}Cl values; most of the Forsmark samples show slightly negative values whereas the Simpevarp samples show values on the positive side. For groundwaters with higher Cl contents (>6000 mg/L) the Simpevarp and Laxemar samples show values greater than 0.3 ‰ SMOC. The Forsmark sample (only one available so far) shows 0.09 ‰ SMOC. This plot therefore suggests that for groundwaters containing around 5000 mg/L Cl, the Forsmark data indicate a greater marine signature involved (Littorina Sea?).

This is further emphasised by plotting the Br/Cl ratios against δ^{37}Cl (*Figure 4-29*). This plot shows that groundwaters significantly enriched in Br (i.e. Simpevarp and Laxemar), compared to marine waters (i.e. Baltic Sea) and those groundwaters with a marine

signature (i.e. Forsmark), display positive $\delta^{37}Cl$ values. The Forsmark groundwaters characterised by more marine-derived Br/Cl ratios cluster closer to 0 ‰ SMOC with a similarly large spread of values as for the Baltic Sea samples. At Forsmark the more positive values reflect deeper groundwaters from the cored boreholes where mixing with marine waters is less marked.

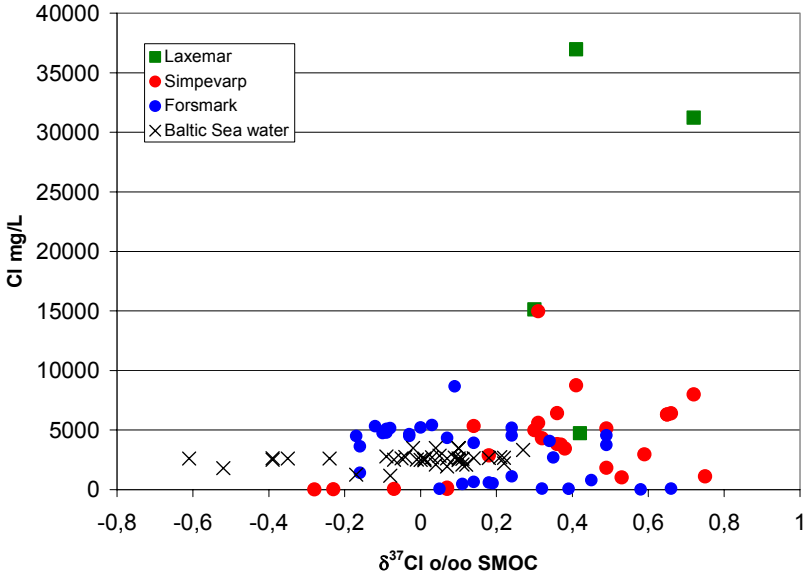

Figure 4-28: *Plot of $\delta^{37}Cl$ versus Cl in groundwaters from Simpevarp, Laxemar and Forsmark, and Baltic Sea waters from Simpevarp area and Forsmark.*

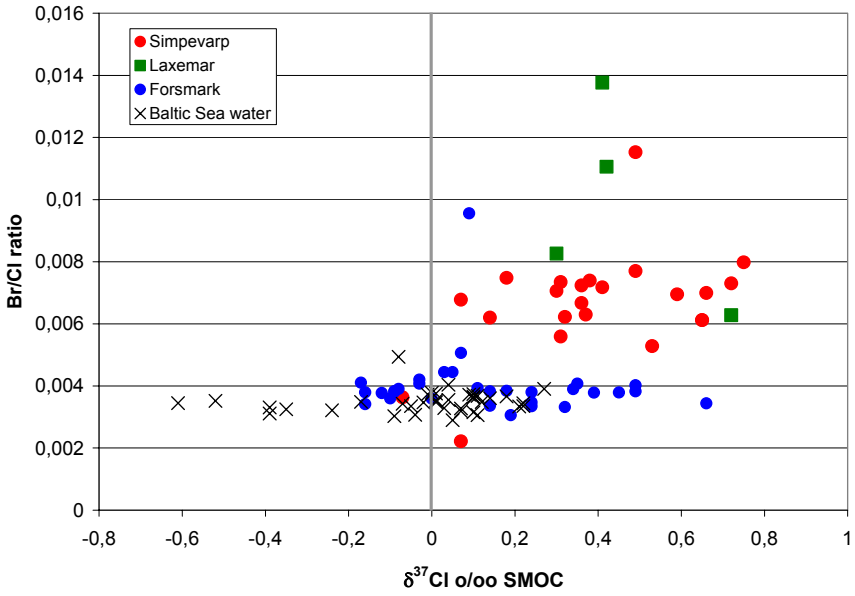

Figure 4-29: *Plot of $\delta^{37}Cl$ versus Br/Cl ratio in groundwaters from Simpevarp, Laxemar and Forsmark, and Baltic Sea waters from Simpevarp area and Forsmark.*

Trace elements

Only a few data exist for the majority of groundwaters and even some of these are incomplete (*c.f. Appendix 1*). The following was concluded from the evaluation:

- Sr, Cs and Rb show a positive correlation with depth (and therefore Cl).
- Ba varies considerably but a negative correlation with SO_4^{2-} is indicated, possibly explained by the solubility control of barite.
- Mn contents show large variations in near-surface waters, usually uniform or slightly decreased values in groundwaters down to 600 metres depth, and decreasing values at greater depths.
- The uranium contents are below 2 µg/L in all the analysed waters. The surface waters show values between 0.16 and 1.9 µg/L whereas the Baltic Sea waters all display values around 0.8 µg/L; most of the groundwater samples are low in uranium (≤ 0,2 µg/L). Higher uranium in surface and near-surface waters is usually observed and is caused by oxidising conditions at the surface. The mobility of the oxidised and dissolved uranium is highly dependent on access to complexing agents, mostly in form of HCO_3^- which is produced in the soil cover and the near-surface environment.

Calcites

Isotopic evidence from calcites sampled from borehole KSH01A+B supports the results from the hydrogeological and hydrochemical studies which show that the upper part of the bedrock at Simpevarp is much more hydraulically conductive and dynamic than the deeper part (>300 m) and have probably been so for a very long time. The number of open fractures and the amounts of calcite in the deeper fractured bedrock is limited. Furthermore, the stable isotope ratios support the decreased interaction with biogenic carbonate at depths greater than 300 metres in KSH01A+B. The morphology of the calcites formed in open fractures show crystal shapes typical for brackish or saline groundwater carbonates with one exception. This is in agreement with the present groundwater chemistry where saline groundwaters (>5000 mg/L Cl) are sampled already at a depth of 150 m. For further information see *Appendix 1*.

Microbes

Figure 4-30 shows the distribution of the different microbial groups found at the three sampled levels in KSH01A and the measured redox potentials. The right part of the *Figure 4-30* shows a so-called redox ladder with different microbial respiration redox couples placed at their respective E_0'. The red line in this figure marks the redox interval measured in KSH01A. These redox values coincide where sulphate reducers and methanogens can be found and correlates very well with the Most Probable Number (MPN) results for this borehole. If iron- and manganese reducers were to be found, the measured redox values had to be at least 50 mV higher. Redox calculations show that the redox pairs $SO4^{2-}/S^{2-}$ and CH_4/CO_2 give values that agree with the measured redox

potentials and by that also with the microorganisms found. A detailed description of the results are found in *Appendix 3*.

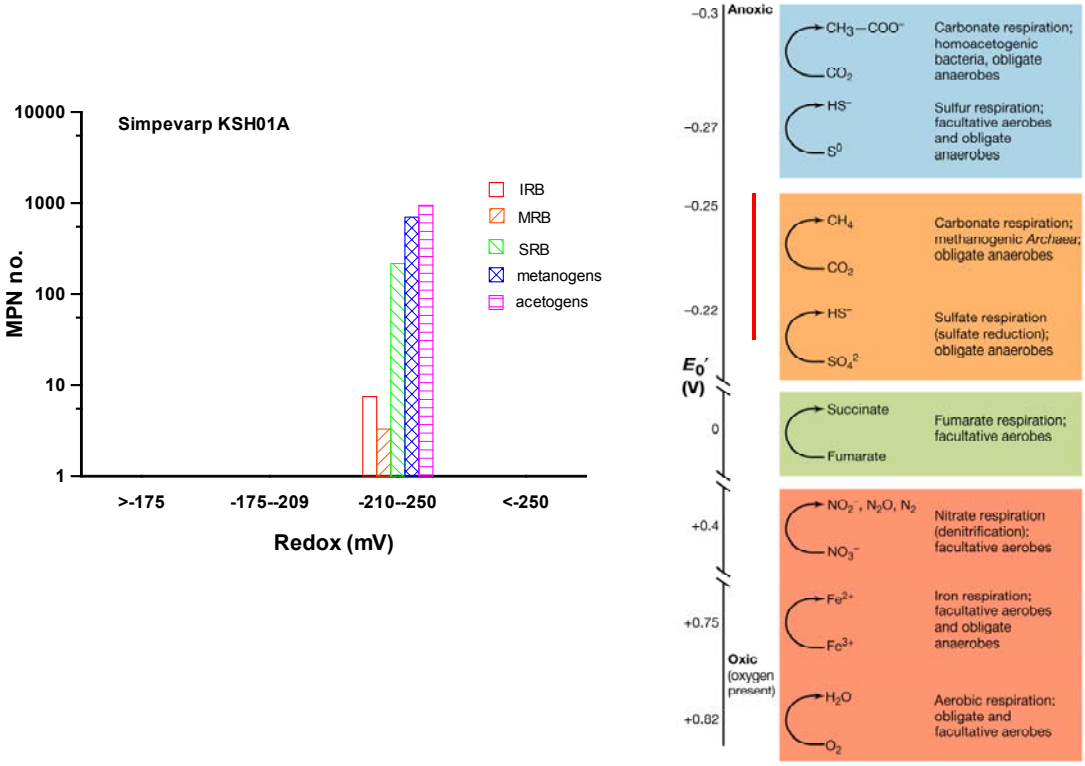

Figure 4-30: *The sum of the most probable number of microorganisms plotted versus redox intervals. The data are from sampling of ground water in borehole KSH01A in the Simpevarp area.*

In *Figure 4-31* the MPN data are plotted versus depth. Here it can be seen that a higher number of microorganisms were found in the depth interval 101 –300 m, that is the two shallowest sampling points than at the deepest, 548-565.5 m section. Since there are two sampled depths at the 101-300 interval, the sum of MPN values was divided by 2. This finding indicates that the activity of microorganisms is higher in the groundwater from the shallower sites.

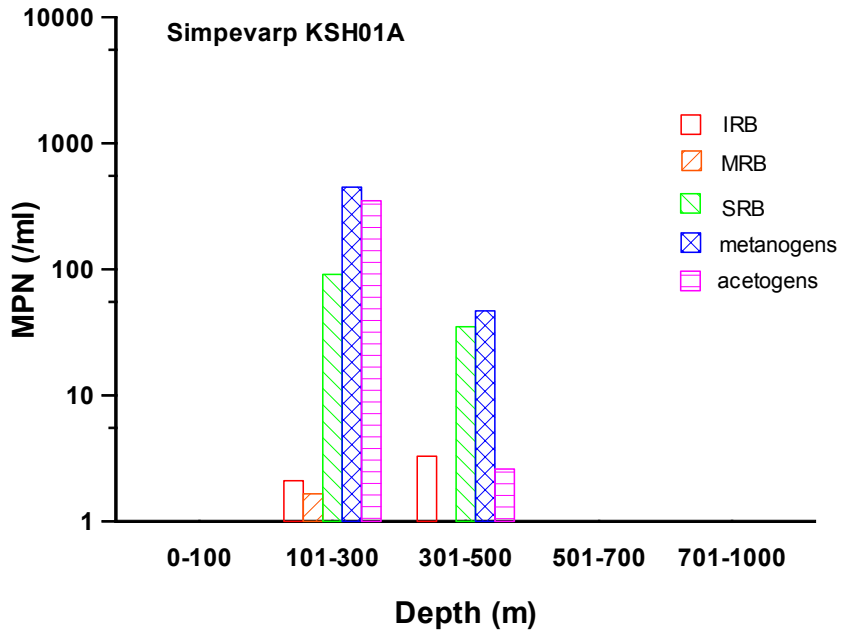

Figure 4-31: *The sums of most probable number of microorganisms plotted versus depth intervals. The data are from sampling of groundwater in borehole KSH01A in the Simpevarp area.*

Figure 4-32 shows a one-dimensional redox model of borehole KSH01A including the 3 sampling depths and intercepting structures. Flow measurements showed that the fracture zone at 245-261.6 m covers a large area but each fracture had a low flow. The low flow velocity was probably due to clay formation in the fractures (Laaksoharju et al. 2004b). *Figure 4-32* shows that in the shallowest part of the borehole, 156.5 – 167 m, the sulphate reducing bacteria were dominant. The measured and the calculated redox redox values with the redox pair SO_4^{2-}/S^{2-} support this finding. In version Simpevarp 1.1, pryrite was reported as one of the minerals found in fracture fillings and this too supports the microbiological data and gives an explanation to why the measured sulphide data at this depth were very low.

At the next sampling depth, 245 –261.6 m, heterotrophic methanogens and acetogens dominated. The measured and calculated redox values this time with CO_2/CH_4 as redox pair corresponds with the redox interval where these types of microorganisms can be found.

Finally, the deepest section has in general very low activity. The flow at this location was lower than that at the depth above and the redox value was low. The lowest measured redox value at this depth was –265 mV. The E_0' where autotrophic acetogenesis takes place is around -300 mV and the measured low redox strengthens the suggestion that acetogens would be the most active at this depth even though MPN numbers were very low. The reason for this might be that the MPN method is difficult to apply to autotrophic organisms and that the MPN method therefore gave lower values than in realty.

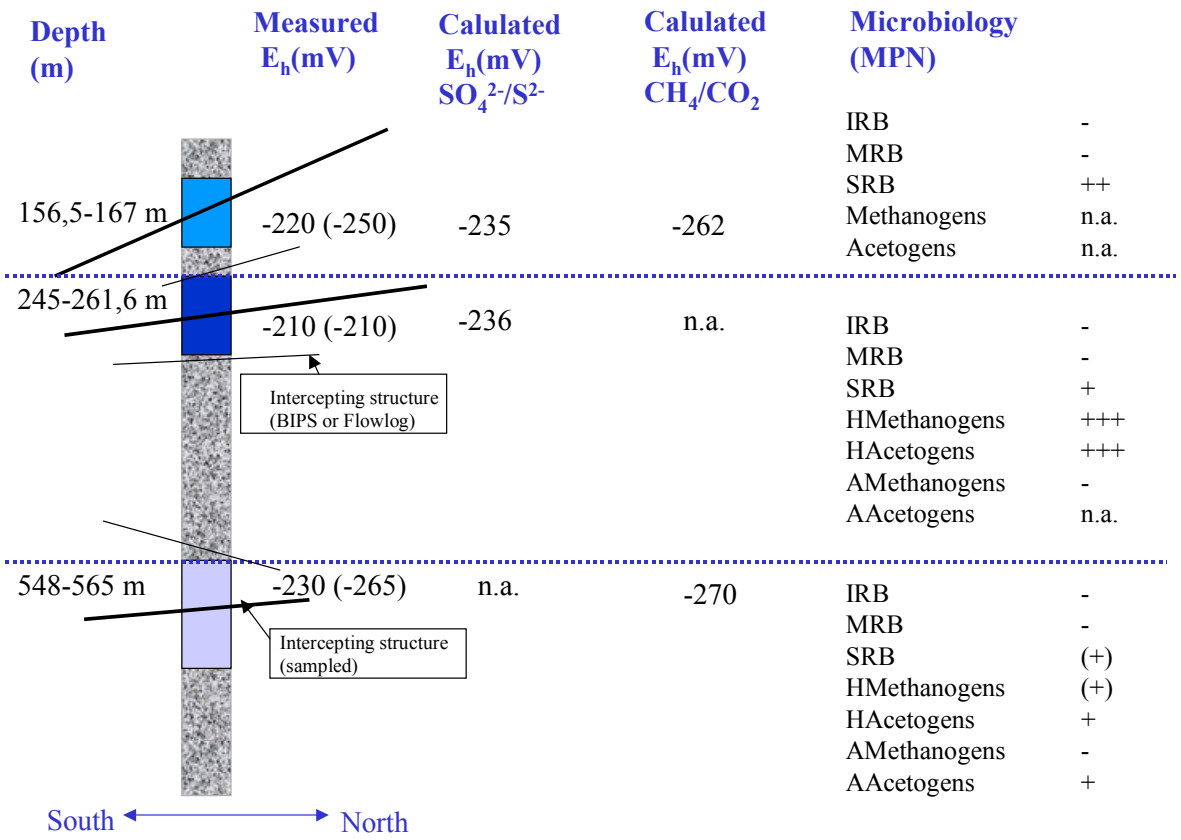

Figure 4-32: *Biogeochemical model of borehole KSH01A in Simpevarp (n.a.=not analysed). Bracketed numbers inidcate redox measurements conducted at different time than the microbial sampling.*

Colloids

The colloid data have been evaluated from the Simpevarp site (*Appendix 3*). The data represent mostly old data sampled during the last 10 years, since few new data were available at the time for the data freeze 1.2.

It was detected that the amount of colloids decreases with depth in KLX01 but not in KAV01. Furthermore, the amount does not vary much at the different depth. The sampled depths were 422.5 m, 525.5 m and 560.5 m and they differ only 140 m in depth, which is not large in relation to the total depth explored (*Figure 4-33*). The average concentration of colloids in this study is 63±49 μgL^{-1} and is in agreement with colloid studies from Switzerland (30±10 and 10±5 μgL^{-1}) and Canada (300±300 μgL^{-1}) where they used the same approach as at Simpevarp (Laaksoharju, 1995).

However, because of the few data available it is difficult to draw far-reaching conclusions from this analysis. In particular, the lack of data for numbers of particles

makes it difficult to make calculations of possible binding sites for radionuclides in the different colloid fractions.

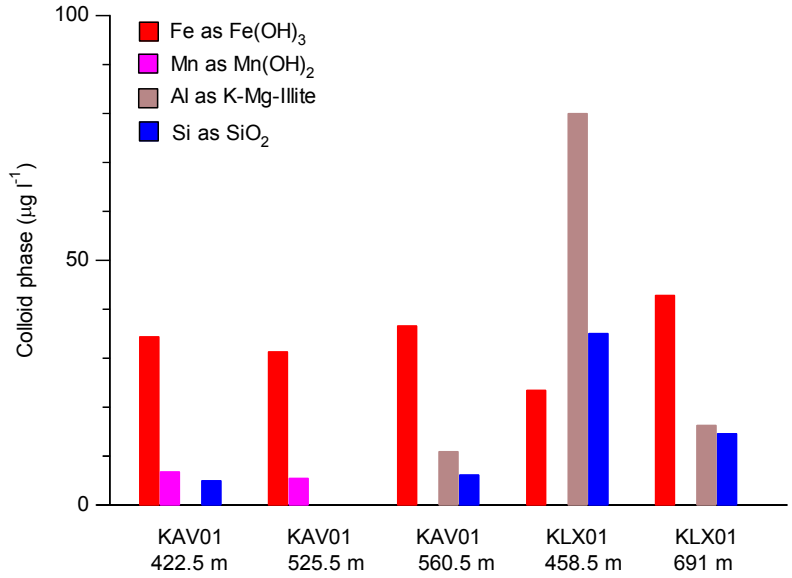

Figure 4-33: *The composition of colloids sampled from 2 boreholes, KAV01 and KLX01, in the Simpevarp area. Calcite and sulphur values are omitted in this figure.*

Gas

In the study reported in *Appendix 3* up to 12 gases were analysed: helium, argon, nitrogen, carbon dioxide, methane, carbon monoxide, oxygen, hydrogen, ethyne, ethene, ethane and propane. Borehole KSH01A is the only one that was complete regarding analysed gas components. Data for the total volume of gas were available only for five depths in two of the boreholes. They contain between 44 and 80 mL L^{-1} and this is in accordance with volumes found at other locations in the Fennoscandian shield. The highest amounts of gas have been found in deep groundwater in Olkiluoto in Finland with volumes up to above 1000 mL L^{-1} (Pitkänen, 2004). The gas volume data from KLX01 does not include propane (C_3H_8), oxygen, argon or hydrogen and therefore the volume from this borehole should, therefore, not be compared to the volumes from KSH01A.

Figure 4-34 shows that the amount of nitrogen decreases with depth in KLX01 but in KSH01A it is the opposite trend. It has to be noticed that the data from KSH01A are from shallower water and from KLX01 below 600 m. The nitrogen concentration in groundwater from Olkiluoto, Finland showed an increasing trend with depth down to 1100 m (Pitkänen, 2004).

Helium concentration in both boreholes in the Simpevarp area showed a slight decrease with depth but there is little variation among the data. Helium concentrations in Olkiluoto increased with depth following the nitrogen concentration.

The origin of nitrogen and helium in groundwater is considered to be crustal degassing of the bedrock. Another source for helium can be radioactive decay, also from the bedrock.

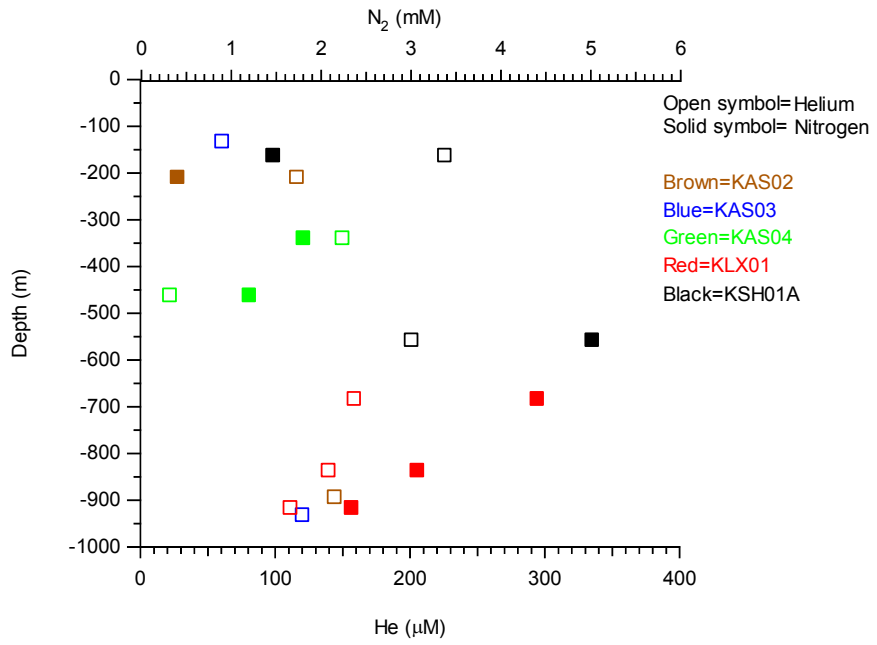

Figure 4-34: *The concentrations of nitrogen and helium plotted versus depth in samples from boreholes in the Äspö, Laxemar and Simpevarp.*

Carbon dioxide in groundwater is a dissociation product of dissolved carbonates in fractures in the bedrock. The carbon dioxide concentrations in samples from the Simpevarp area are fairly constant in the different boreholes with values below 0.1 mM *(Figure 4-35)*. There is a slight tendency that the concentration decreases with depth down to 500-600 m and below that the values are more or less constant. This pattern has also been observed for carbon dioxide concentrations in groundwater from the Olkilouto Site in Finland. (Pitkänen, 2004)

Methane is found in low concentrations, 0.5 – 3 µM, in all boreholes at all depths but no trend in concentration can be seen due to the very restricted amount of available data *(Figure 4-35)*. In KSH01A, the value for the greatest depth 556.5 m sampled is lower than for 161.75 m, i.e. 1.8 µM compared to 2.7 µM, respectively.

The origin of methane in groundwater can be either biotic or abiotic. The biotic methane is produced by methanothrophic Achaea, a group of prokaryotic organisms. They can utilise either C1-compounds or acetate. They can also fixate carbon dioxide with hydrogen gas as an energy and electron source. The origin of their substrate can be biodegraded organic matter as in sea and lake sediments or composts. Carbon dioxide and hydrogen can also originate in the mantle (Apps and Van de Kamp, 1993).

Abiogenic methane is produced in, for example, hydrothermal systems during water-rock interactions (*cf. Appendix 3*).

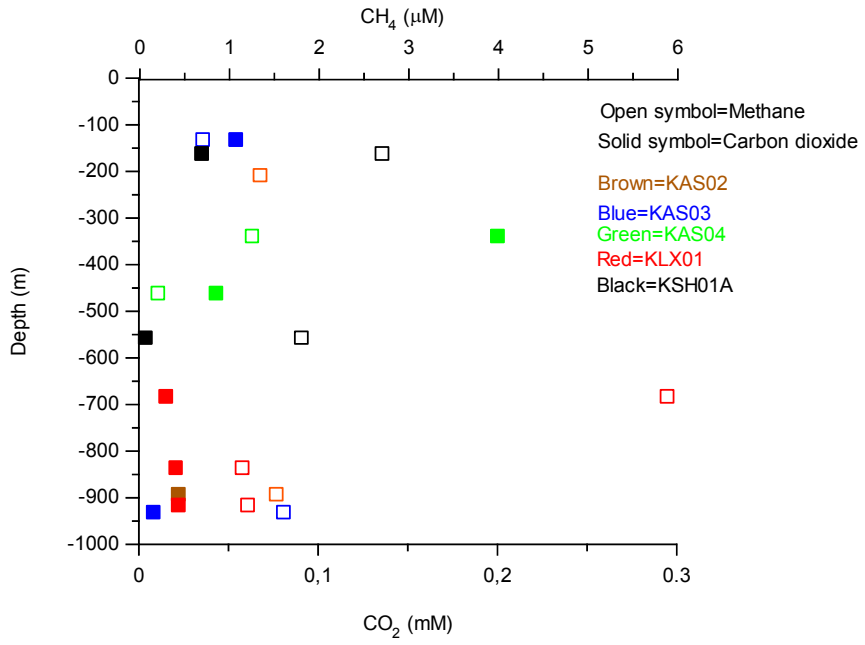

Figure 4-35: *Carbon dioxide and methane plotted versus depth in samples from boreholes in the Äspö, Laxemar and Simpevarp areas.*

4.3 Modelling assumptions and input from other disciplines

The modelling assumption is that the obtained groundwater compositions are a result of mixing and reactions including different water types. The water types are a result of palaeohydrogeology and modern hydrogeology *(see, Figure 3-1)*. A schematic presentation of how a site evaluation/modelling is performed, its components, and the interaction with other geo-scientific disciplines, is shown in *Figure 4-36*. The methodology applied in this report is described in detail by Smellie et al. (2002).

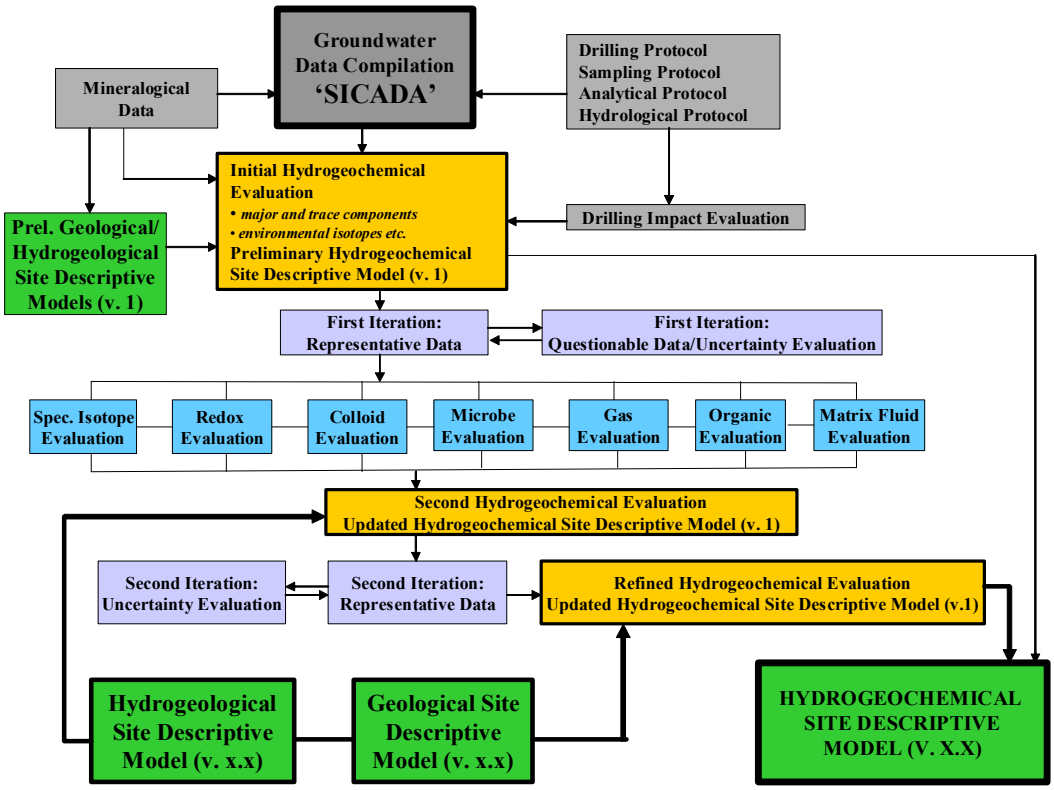

Figure 4-36: *The evaluation and modelling steps used in this report (after Smellie et al., 2002).*

For the groundwater chemical calculations and simulations the following standard tools were used:

For evaluation and explorative analyses of the groundwater:

- AquaChem: Aqueous geochemical data analysis, plotting and modelling tool (Waterloo Hydrogeologic).

Mathematical simulation tools:

- PHREEQC with the database WATEQ4F: Chemical speciation and saturation index calculations, reaction path, advective-transport and inverse modelling (Parkhurst and Appelo, 1999).
- M3: Mixing and Massbalance Modelling (Laaksoharju et al., 1999b).
- Flow and reactive transport simulations: CORE^{2D} (Samper et al., 2000).

Visualisation/animation:

- TECPLOT: 2D/3D interpolation, visualisation and animation tool (Amtec Engineering Inc.)

Hydrogeochemical modelling involves the integration of different geoscientific disciplines such as geology and hydrogeology. This information is used as background

information, supportive information or as independent information when models are constructed or compared (*c.f. Appendix 6*).

Geological information is used in hydrogeochemical modelling as direct input in mass-balance modelling but also to judge the feasibility of the results from, for example, saturation index modelling. For this particular modelling exercise geological data were summarised, the information was reviewed and the relevant rock types, fracture minerals and mineral alterations were identified *(c.f. Appendix 1 and 4)*.

The underlying geostructural model provides important information of water-conducting fractures used for the understanding and modelling of the hydrodynamics. The cross section used for visualisation of groundwater properties is generally selected with respect to the geological model and the hydrogeological simulations (*c.f. Appendix 1 and 5*). The available hydrogeological information and the results from hydrogeological modelling is directly used in the coupled flow and transport modelling (*c.f. Appendix 6*). The measured values of Cl, ^{18}O, ^{2}H, ^{14}C and the results from the M3 mixing calculations were provided to the hydrogeologists to be used in their modelling (*c.f. Appendix 5*).

4.4 Conceptual model with potential alternatives

The alternative conceptual models tested included different reference waters and local and regional models *(cf. Appendix 5)*, and various modelling tools and approaches were applied on the data set. In addition the concept where the water composition is a result of reactions rather than mixing is discussed in *Appendix 4*.

4.5 Hydrogeochemical modelling, mass-balance and coupled modelling

4.5.1 Hydrogeochemical modelling

Hydrogeochemical modelling has been carried out with PHREEQC (Parkhurst and Appelo, 1999) using the WATEQ4F thermodynamic database. The modeling focused on speciation-solubility calculations, reaction path modelling and redox system analysis. The calculations are used to investigate the processes that control water composition at Simpevarp. This chapter is divided into two main sections, the first one concerning the state of non-redox elements and phases, and the second focussed on the redox state of the system. A detailed description of the modelling performed can be found in *Appendix 4*.

Carbonate system

Superficial fresh waters show a wide range of pH values as a consequence of their multiple origins (*Figure 4-37*). The lowest values are associated with waters with a marked influence of atmospheric and biogenic CO_2; the highest values (up to 8.5 pH units) are associated with the most diluted groundwater. Overall this gives a decreasing trend with chloride when the rest of the groundwater samples are taken into consideration. Nevertheless, this trend is affected by uncertainties in pH measurements in the laboratory and there are not enough data from in-situ logging of pH to make a more careful evaluation.

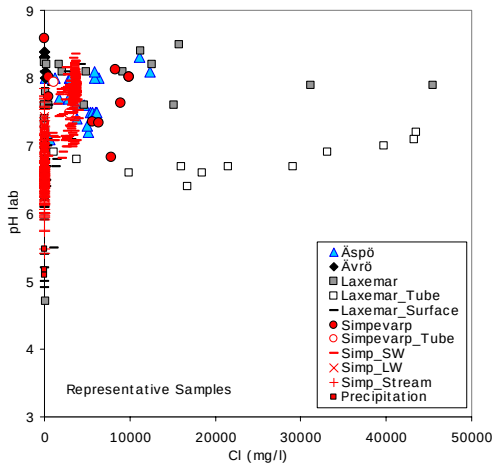

Figure 4-37: *pH vs. chloride content in mg/L (increasing with depth) in waters from the site.*

Alkalinity (HCO_3^-) is, together with chloride and sulphate, the third major anion in the system, and is the most abundant in the non-saline waters. Its concentration increases in the shallower groundwaters (*Figure 4-38a*) as a result of atmospheric and biogenic CO_2 influence and/or calcite dissolution. The alkalinity content reaches equilibrium (or super saturation) with calcite in the fresh groundwaters (*Figure 4-38a* and *Figure 4-39a*) and then decreases dramatically with depth as it is consumed by calcite precipitation, whereas calcium keeps increasing as a result of mixing (*Figure 4-38b*).

As can be seen in *Figure 4-38b*, calcium shows a good positive correlation with increasing chloride concentration in saline groundwaters, suggesting that mixing is the main process controlling this element. In spite of the extent of reequilibrium with calcite affecting Ca, the high Ca content of the mixed waters (originating from the brine end member) obliterates the effects of mass transfer with respect to this mineral. This fact justifies the quasi-conservative behaviour of calcium, at least in waters with chloride contents higher than 10000 mg/L. Simple theoretical simulations of mixing between a brine end member and a dilute water, with and without calcite equilibrium, have shown the negligible influence of reequilibrium on the final dissolved calcium contents.

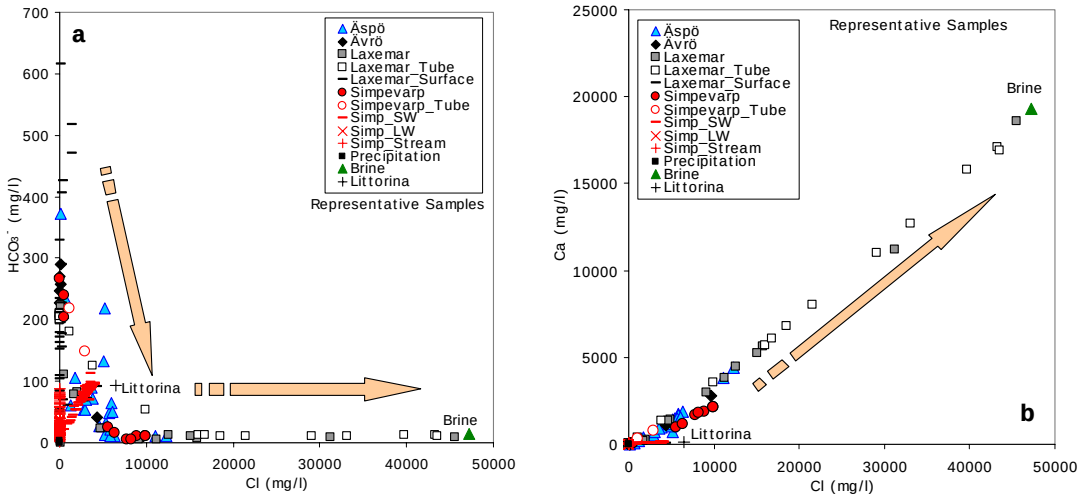

Figure 4-38: *Alkalinity(a) and calcium (b) vs. Cl in waters from the site.*

Figure 4-39 shows the calcite saturation index in the groundwaters. The alkalinity trend described above can be readily explained in this plot. The uncertainty associated with the saturation index calculation (±0.5) is higher than that usually considered (±0.3). This is due to problems during the laboratory measurements of pH (CO_2 outgassing and ingassing), as was described in the report for the 1.1 phase (Laaksoharju *et al.*, 2004a,b).

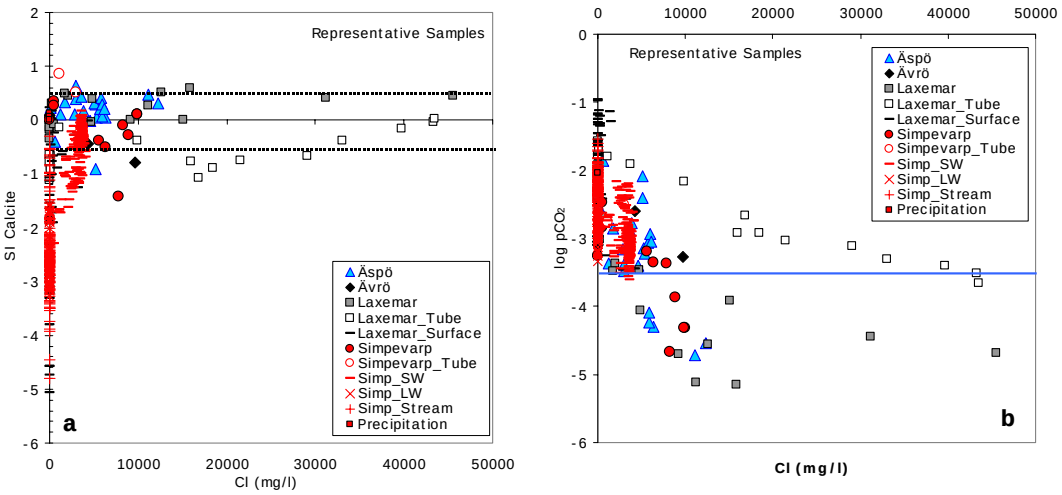

Figure 4-39: *a) Calculated calcite saturation indexes and b) partial pressure of CO_2 against chloride for waters from the Simpevarp area. The dashed lines in the figure represent the uncertainty associated with SI calculations. The blue line in Figure b represents the value in the atmosphere.*

Silica system

The content of dissolved SiO_2 in surface waters indicates a typical trend of weathering, while in groundwaters it has a narrow range of variation indicative of partial reequilibrium (*Figure 4-40a*). The general process evolves from an increase in dissolved SiO_2 by dissolution of silicates in surface waters and shallow groundwaters to a

progressive decrease related to the participation of silica polymorphs and aluminosilicates which control dissolved silica as the residence time of the waters increases. This can be seen in *Figure 4-40b*.

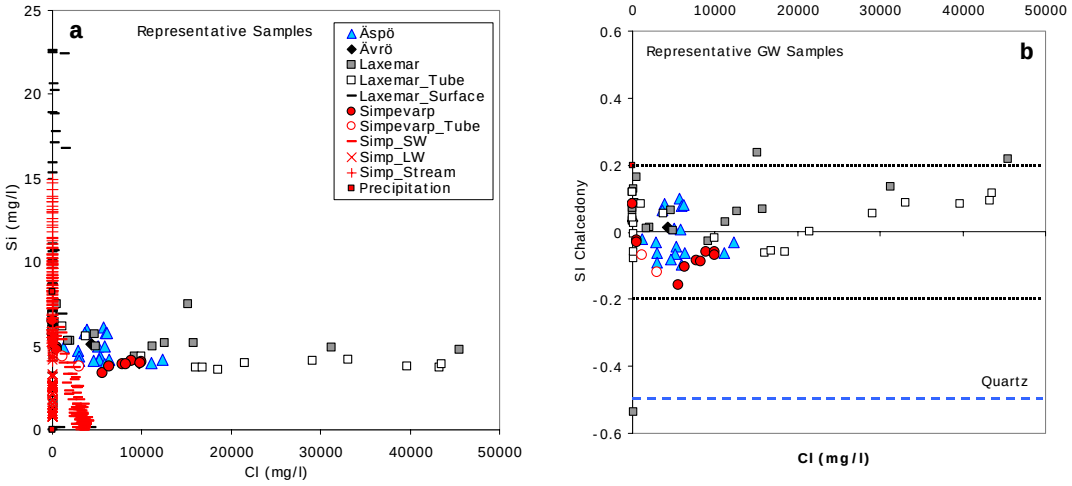

Figure 4-40: *(a) Plot of SiO_2 vs.Cl for all waters. (b) Saturation indexes of chalcedony and quartz as a function of Cl in the waters. The dashed lines represent the uncertainty associated with SI calculations (Deutsch et al., 1982).*

The weathering of rock-forming minerals is the main source of dissolved silica. Superficial waters have a variable degree of saturation with respect to silica phases (quartz and chalcedony), compatible with the weathering hypothesis, and a rather unclear control by secondary phases. This is a rough generalisation, useful for this general description but it should be noted that surface waters come from diverse systems (streams, lakes and soil zones) involving contrasting processes (evaporation, biological uptake, etc.; Laaksoharju *et al.*, 2004b) that affect silica concentrations.

Saline groundwaters are oversaturated with quartz and close to equilibrium with chalcedony (*Figure 4-40b*). Saturation indices are relatively constant and independent of the chloride content; this suggests that the groundwater has already reached, at least, an apparent equilibrium state associated with the formation of aluminosilicates or secondary siliceous phases like chalcedony, which seems to be controlling dissolved silica.

The lack of QA aluminium data for Simpevarp groundwaters precludes a speciation-solubility analysis of aluminosilicates. Therefore, activity diagrams were used to study the relationship between silicate minerals and their stability. This analysis will be discussed later in this report *(c.f Appendix 5)*.

Sulphate system

*Figure 4-41*a, showing SO_4 vs Cl, indicates an obvious modern Baltic Sea water dilution trend affecting some of the groundwater samples. In general, these groundwater data lend support to the absence of a significant postglacial marine component, suggesting instead the mixing with deeper, more saline waters of a non-marine origin. Perhaps the most interesting aspect is the different evolution shown by sulphate in all Simpevarp site waters (which increases with salinity) compared with the sulphate behaviour at other sites. *Figure 4-41b* shows the sulphate contents in Olkiluoto and

Forsmark[2] sites. In both cases, after an initial increase in sulphate (reaching the maximum values when salinity is around 5000-6000 mg/L of Cl) there is a clear decrease towards zero. For the same chloride content, sulphate concentrations of the Simpevarp site waters are clearly higher.

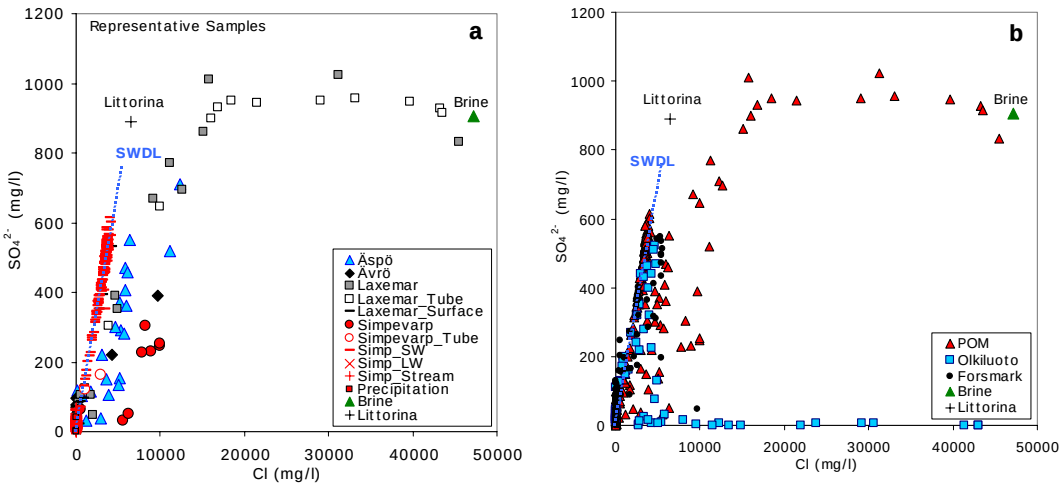

Figure 4-41: *(a)Plot of SO_4 vs Cl for all data. (b) Plot comparing Simpevarp area data with Forsmark and Olkiluoto samples.*

This contrasting behaviour must be related to the process controlling the sulphate content in these waters. Analysing the saturation state of waters with respect to gypsum (*Figure 4-42b*) some conclusions can be drawn. For the whole set of Simpevarp site groundwaters, the gypsum SI trend indicates a clear evolution towards equilibrium (*Figure 4-42a*) which is reached at chloride values of 10000 mg/L and maintained even in the most saline waters. This equilibrium, defined mainly in the most saline and deepest groundwaters from Laxemar, introduces a new controlling phase in the groundwater system. Moreover, it can help to solve the uncertainties reported in previous works (Laaksoharju and Wallin, 1997) on the unusual sulphate behaviour in Laxemar waters. In fact, Laaksoharju *et al.* (1995) reported the presence of gypsum as a fracture filling mineral in this subarea, though in small amounts. In addition, the influence of gypsum as the sulphate limiting phase has been already reported in the Canadian Shield (Gascoyne, 2004).

[2] Forsmark data shows a lower salinity than Olkiluoto data, but the trend shown by the more saline waters in Forsmark follows the same evolution as in Olkiluoto.

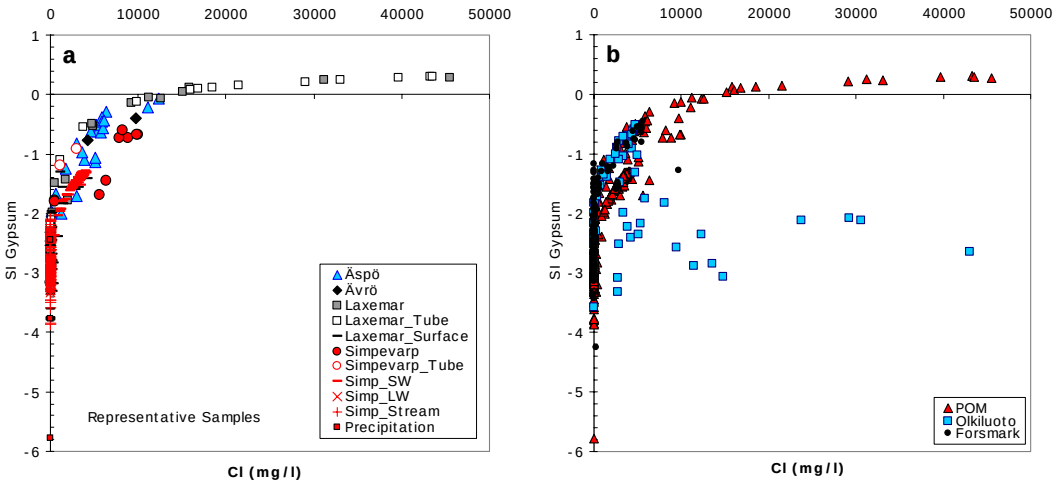

Figure 4-42: *(a)Plot of Gypsum saturation index vs Cl for all Simpevarp area data. (b) Scatter plot comparing Simpevarp area data with Forsmark and Olkiluoto data.*

The behaviour of other sulphate minerals, like celestite ($SrSO_4$), was also checked. The SI trend is similar to the one shown by gypsum and, therefore, celestite should be considered as another possible new controlling phase in this groundwater system. Celestite has not yet been identified in the bedrock. Some consequences of these new equilibrium situations with respect to other phases (Strontianite) and to the Ca/Sr ratio are discussed in Appendix 4.

Aluminosilicate system

The mineralogical results from KSH01A + B have demonstrated the presence of a complex sequence of fracture fillings. Apart from chlorite and calcite, epidote, prenhite, laumontite, Ba-zeolite, adularia, albite, haematites and pyrite have also been reported. Small amounts of outermost coatings with smectite, interstratified clay minerals and illite, with high surface area, have also been identified. This set of minerals is common to the other subareas (e.g., Äspö).

Besides the granite rock-forming minerals, some of these fracture-filling phases are aluminosilicate minerals with which groundwaters have been in contact during their geochemical evolution. Therefore they are important water-rock interaction phases. However, as already pointed out, the lack of aluminium data for the Simpevarp site groundwaters precludes a speciation-solubility analysis, limiting their analysis to stability diagrams.

The accuracy of these diagrams depends on pH and is therefore affected by uncertainties in its value. Uncertainties in the equilibrium constants of the aluminosilicates (especially the phyllosilicates) also affect the conclusions drawn from these diagrams and the results of any theoretical model performed with them (e.g. Laaksoharju and Wallin, 1997; Trotignon *et al.*, 1997, 1999). In this context the study of aluminosilicate phases has been limited to those with lower uncertainties and using thermodynamic data that have already given reasonable results in systems similar to the one studied here. That means that the aluminosilicate system studied here is limited to adularia, albite, kaolinite, (laumontite, prenhite and chlorite is studied in *Appendix 4*),

and the selected thermodynamic data are the ones calculated at 15ºC by Grimaud *et al.* (1990) for the Stripa groundwaters.

Stability diagrams

The following description includes a general evaluation of the Simpevarp area groundwaters based on their position in the stability diagrams and a discussion on the effects of mixing and reaction in the more saline, older groundwaters[3]. This discussion is illustrated with a theoretical equilibrium modelling. The question of the origin of the saline groundwaters (brine end member) is not discussed here, and the model just assumes that they are already in the system, participating in mixing processes. Nevertheless, the last part of this section deals with the potential use of this modelling approach to predict the chemical characteristics of these very old saline groundwaters.

Figure 4-43 shows the stability diagram kaolinite-albite-adularia for the Simpevarp area waters. Green and blue arrows show the main trends that can be distinguished. The first trend (green arrows) crosses the kaolinite stability field and goes towards the limit with adularia. This trend is defined by surface and shallow groundwaters. They are modern waters with low chloride contents and whose geochemical evolution is the result of water-rock interaction.

The evolution path of these waters in the kaolinite field shows a slope around 2, typical of weathering-alteration processes in granitic materials. This trend represents the effects of a progressive dissolution of the rock-forming minerals (calcite, chlorite, plagioclase, K-feldspars, etc.). Along this process, partial reequilibria with phyllosilicates (e.g. kaolinite) can be reached. Ionic exchange and, finally, calcite precipitation can also take place.

Waters close to or on the kaolinite-adularia boundary would correspond to the more evolved samples in this water-rock interaction process. A special case is certain Laxemar groundwaters, which are very diluted (30-150 mg/L Cl) but at great depths (up to 700 m in KLX02 borehole). The position of these samples in the diagram would support a meteoric origin without a mixing component with more saline waters, but with a residence (reaction) time longer than the shallower groundwaters.

Laxemar waters taken by tube sampling are placed in the kaolinite field but this is uncertain due to the possible "artificial mixing" during sampling, and, probably, to the pH measurements.

The second trend (blue arrow) evolves parallel to the adularia-albite limit indicating an equilibrium situation. Brackish and saline groundwaters from the POM area follow this second trend. This result is very similar to Stripa waters (compare the figures and scale, *cf. Appendix 4*) but there is an important difference: maximum chloride contents in Stripa only reach 700 mg/L, whereas Simpevarp area groundwaters, plotted in the same position, reach chloride values up to 45000 mg/L. Stripa groundwaters' residence time has been estimated as being approximately 100000 years (Fontes *et al.*, 1989). That means that even in that time, water-rock interaction provides only 700 mg/L of chloride. It is clear, therefore, that an additional source of salinity is needed in the Simpevarp waters to

[3] In this section different diagrams and computer simulations for Simpevarp area groundwaters are presented, in some of the cases together with other sites (Olkiluoto and Stripa).

justify much higher chloride values in much younger waters. This source is the mixing with a saline component (marine and/or non marine).

Another interesting finding is that in the trend parallel to the adularia-albite limit the range of salinity in the Simpevarp area groundwaters is very broad, including not only the most saline waters (close to brine end member composition), but also waters with around 5000 mg/L Cl. This points again to the important effects of mixing in these waters.

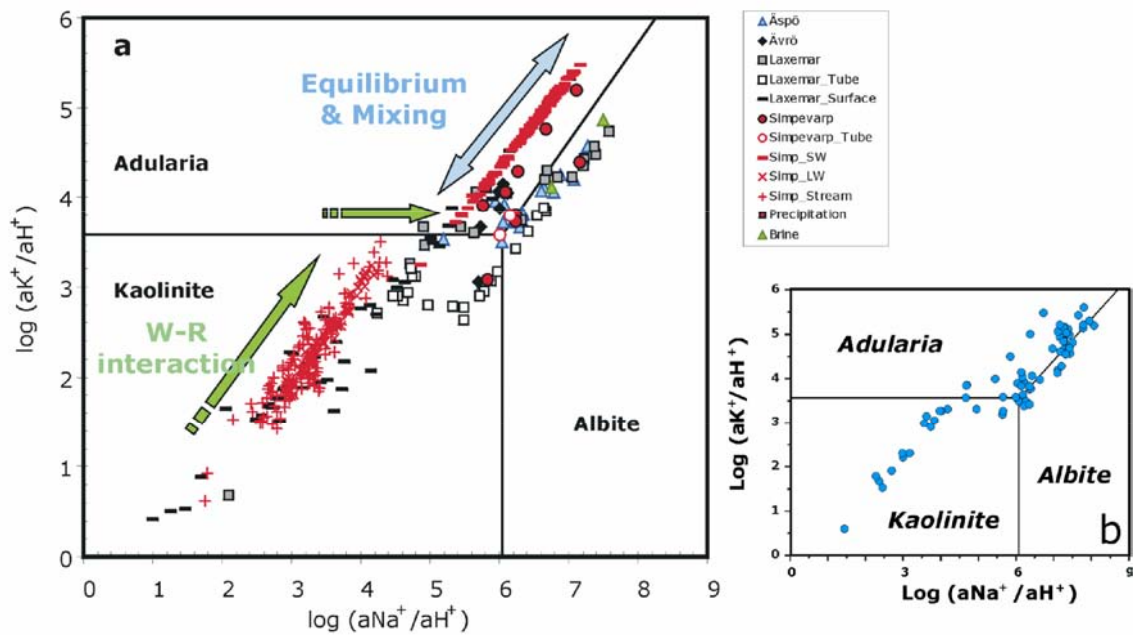

Figure 4-43: *Stability diagrams for kaolinite, adularia and albite in the Simpevarp area groundwaters (a) and in the Stripa groundwaters (b).*

In *Figure 4-44* the Simpevarp area samples have been plotted together with those of Olkiluoto (Pitkänen *et al.*, 2004). Olkiluoto waters occupy the same location as Simpevarp area waters. Olkiluoto samples in the kaolinite stability field and in the kaolinite-adularia boundary correspond to subsurface or shallow groundwaters whose chemistry is controlled by water-rock interaction. Samples located on the adularia-albite boundary correspond to brackish and saline groundwaters characterised by having undergone complex mixing processes (between Meteoric, Littorina, Glacial and Saline end members, Pitkänen *et al.*, 2004).

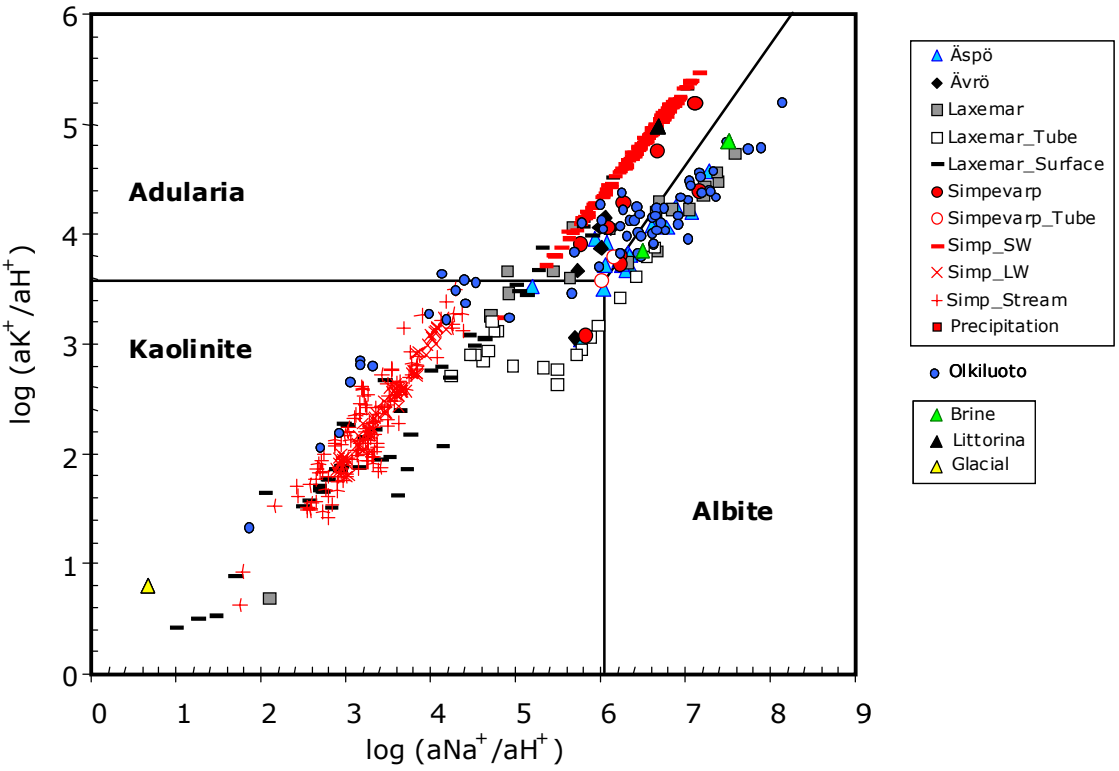

Figure 4-44: *Stability diagram for kaolinite, adularia and albite. Together with the Simpevarp area waters, the Olkiluoto groundwaters (Pitkänen et al., 2004) and the theoretical end members (Brine, Littorina and Glacial) have been plotted.*

The position of the theoretical end members is also shown in *Figure 4-44* (Brine, Littorina and Glacial; Meteoric is close to Glacial). It is fairly clear that the evolutionary path of these waters is the result of (a) reaction between diluted waters (surface and shallow groundwaters) and rock, (b) mixing in depth with more saline groundwaters in different proportions as a function of location and residence time, and (c) the simultaneous interaction of these deep waters with the rock.

Simulating the Brine water composition

The thermodynamic approach described in *Appendix 4* to assess mixing and reaction processes provides an ideal tool for predicting the composition of groundwaters with long residence times. This is the case of the "old brine end members" found in the Scandinavian Shield. These groundwaters can be considered as having reached a "global" equilibrium with calcite, chalcedony and different aluminosilicaltes. This kind of approach was used by Michard and co-workers (e.g. Michard, 1980; Michard *et al.*, 1986) to predict the composition of some granitic thermal groundwaters assuming thermodynamic equilibrium between the water and a selected mineral assemblage, as a function of chemical contents not controlled by mineral equilibria (e.g. Cl). This model was also applied by Grimaud *et al.* (1990) to the low temperature granitic groundwaters at Stripa.

More recently, Trotignon *et al.* (1997, 1999) applied the same concept to Äspö groundwaters (from KAS02 and KAS03 boreholes) and reported a high sensitivity of the predictions to the mineral equilibrium constants, mainly from laumontite. They found a reasonable fit between the predicted values and the measured concentrations for the assemblage calcedony + kaolinite + albite + adularia + laumontite with the selected equilibrium constants.

Here, the approach of Trotingon et al. was extrapolated to calculate "brine compositions" using the same assemblage (calcedony, kaolinite, albite, adularia and laumontite) plus calcite and gypsum (saline waters in Simpevarp area are in equilibrium with these minerals as explained above), and the thermodynamic data from Grimaud *et al.* (1990) except for kaolinite and laumontite. The equilibrium constants for these minerals were taken from the best fit of Trotignon et al.

The procedure consists of the following steps: pure water (Glacial end member) was equilibrated with the selected mineral assemblage imposing, simultaneously, different chloride concentrations up to "brine" values. PHREEQC was used then to simulate this process. The results obtained for the Brine end member and for the more saline water in Olkiluoto (KR12/741/1; Pitkänen *et al.*, 2004) are shown in *Table 4-1*.

Comparing the predicted values with the measured ones, it is clear that in most cases the fit is quite good (pH, Na, Ca, SiO_2). But, more interesting, the predictions are able to reproduce the main groundwater features: pH values close to 8 and very low alkalinity. Considering the thermodynamic uncertainties associated to these calculations, one can say that in general the results are fairly good.

A plot of the concentration data on *Table 4-1* as a function of chloride concentration (*Figure 4-45*) shows some other interesting facts. It makes clear that the concentration of elements controlled by equilibrium with the mineral assemblage depends on chloride content. This conclusion is not new (Michard, 1987) but it has important implications in the context of the mixing and reaction processes that affect this kind of system. For the oldest mixing event, it clearly shows that chloride is a useful conservative element to compute mixing proportions. Therefore, it could be concluded that in the Simpevarp area mixing is the main irreversible process. It controls the chloride concentration which, in turn, determines the re-equilibrium path (water-rock interaction) triggered by mixing.

Table 4-1: Predicted and observed concentrations for the brines in Simpevarp site area (Brine end member) and in Olkiluoto.

Increasing chloride concentration

	Initial water			Prediction			Prediction
	Glacial	Equilibrium with the selected mineral assemblage	Olkiluoto Brine	Olkiluoto Br (Theor)	Equilibrium with the selected mineral assemblage	Brine end member	Brine (Theor)
mCl	1.41E-05		0.8754	0.8833		1.442	1.443
pH	5.8		8.3	7.95		7-8	7.8
mNa	7.39E-06		0.366	0.375		0.400	0.490
mK	1.02E-05		0.0005	0.00145		0.00126	0.00213
mCa	4.49E-06		0.258	0.261		0.521	0.490
mH_4SiO_4	1.42E-04		9.79E-05	9.30E-05		6.67E-05	7.40E-05
mAlkalinity	1.97E-06		1.32E-04	5.39E-05		2.50E-04	4.56E-05
mSO_4	5.20E-06		5.38E-05	7.27E-03*		5.14E-03	5.36E-03

* The equilibrium with gypsum assumption is not valid in these waters as they are clearly undersaturated.

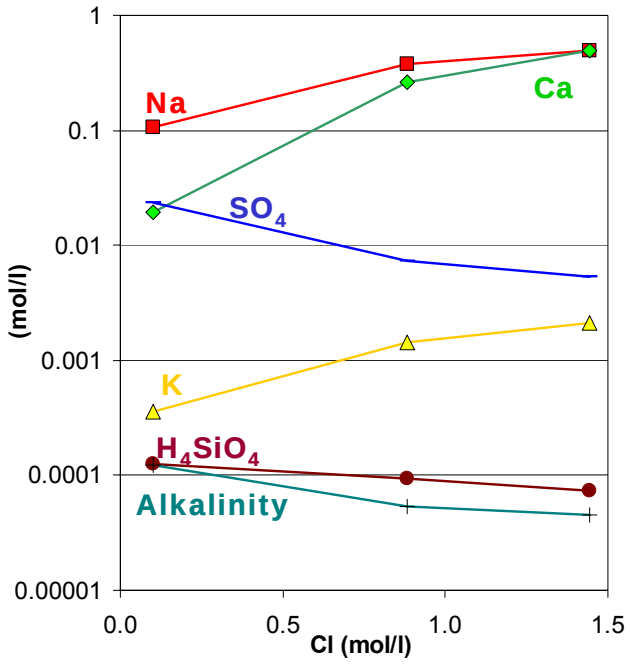

Figure 4-45: *Evolution of chemical contents as a function of chloride, maintaining the equilibrium with the selected mineral assemblage.*

Redox modelling

For Simpevarp 1.2, the amount of suitable data for a redox study is greater than for Simpevarp 1.1 and, therefore, this study is more complete. The two possibilities suggested in previous studies about the redox state of the groundwaters have been reassessed, namely: (a) the iron system controls the redox state (Grenthe *et al.*, 1992); and (b) the sulphur system controls the redox state (e.g. Nordstrom and Puigdomenech, 1986). Some of the samples supplied with data freeze 1.2 have been used previously to support both interpretations (Grenthe *et al.*, 1992; Glynn and Voss, 1999).

For this modelling exercise samples with adequate redox data were selected. This includes Eh and pH data from continuous logging (from this data freeze and from previous reports, Smellie and Laaksoharju, 1992; Laaksoharju *et al.*, 1995), analytical data[4] for Fe^{2+}, S^{2-} and CH_4, and microbiological information. The selected samples cover the four subareas (Äspö, Ävrö, Laxemar and Simpevarp) and a wide range of depths (130 to 930 m).

Redox pair calculations

The results from the redox pair calculations (*cf. Appendix 4*) are summarised in *Figure 4-46* and *Figure 4-47*. The Eh calculated with the $Fe(OH)_3/Fe^{2+}$ redox pair and Grenthe's calibration agrees reasonably well with most of the Eh values measured in Ävrö and Äspö. This good fit was expected as these samples were used by Grenthe and co-workers to perform the calibration. The Eh calculated with the same redox pair but for microcrystalline $Fe(OH)_3$ is much more oxidant. On the contrary, the microcrystalline phase gives the best results in the case of Simpevarp and some Laxemar samples, whereas Grenthe's calibration gives much more reducing Eh values (*Figure 4-46*). This observation was already made in the previous phase (Simpevarp 1.1, Laaksoharju *et al.*, 2004b; and Forsmark, Laarksoharju *et al.*, 2004a). This fact suggests that the groundwater redox state can be controlled by iron oxides and oxyhydroxides with different degrees of crystallinity.

[4] The range of analytical concentrations are: $Fe^{2+} = 8.9\cdot10^{-8}$ - $3.6\cdot10^{-4}$; $S^{2-} = 3.12\cdot10^{-7}$ - $2.3\cdot10^{-4}$; $SO4^{2-} = 9\cdot10^{-6}$ - $1.3\cdot10^{-2}$; $CH_4 = 2.5\cdot10^{-7}$ - $3.8\cdot10^{-6}$

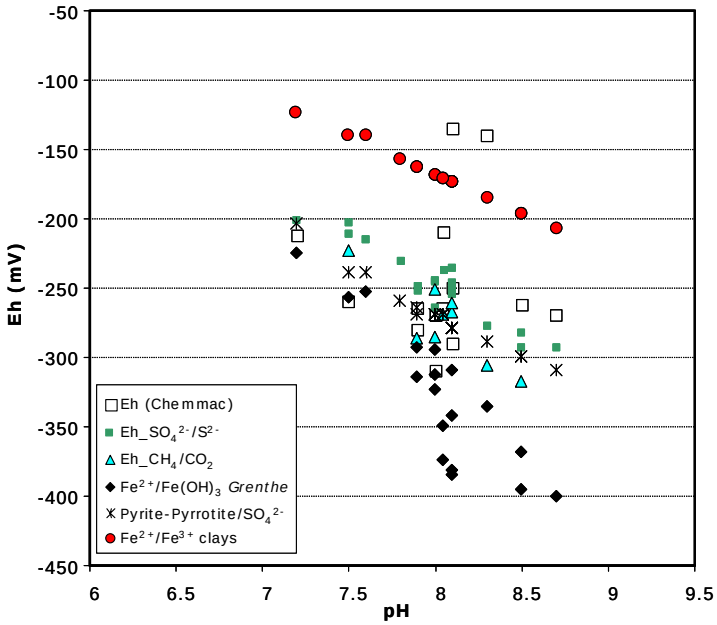

Figure 4-46: *Comparison of redox results for different redox pairs.*

Except for a few samples, the different "sulphur system" redox pairs provide Eh values coincident with the potentiometrically measured Eh. The SO_4^{2-}/S^{2-} homogeneous redox pair gives Eh values similar to the ones obtained from the heterogeneous pairs (Pyrite/SO_4^{2-} and FeS/SO_4^{2-}; *Figure 4-47*) as calculated with the WATEQ4F thermodynamic data. A sensitivity analysis carried out comparing these data to those of Bruno *et al.*'s (1999) shows only minor differences.

As expected, Eh values obtained with the CH_4/CO_2 pair are close to the ones obtained with SO_4^{2-}/S^{2-} (and also to the remaining sulphur redox pairs). Therefore, they also agree well with the potentiometrically measured Eh.

For the Äspö and Ävrö samples there is good agreement between the potentiometrically measured Eh and the value calculated from the following redox pairs: heterogeneous and homogeneous sulphur pairs, CH_4/CO_2 and Grenthe's calibration for $Fe(OH)_3/Fe^{2+}$. In Simpevarp, the redox pair results also agree very well with the measured Eh values; however, the iron system seems to be controlled by a microcrystalline hydroxide instead of by an intermediate phase (Grenthe's calibration). Finally, in Laxemar the sulphur redox pairs show good agreement with potentiometric Eh. In common with the iron hydroxide pair, the best agreement with the measured value is not always obtained with the same pair, for example, in some cases Grenthe's calibration is the one which better agrees with the measured Eh and in other cases is the microcrystalline phase which agrees better. Some samples have a potentiometric Eh considerably lower than any other calculated using the redox pairs (*cf. Appendix 4*).

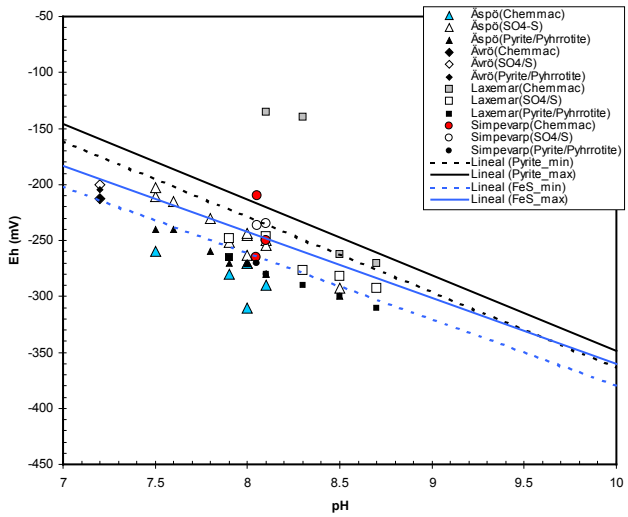

Figure 4-47: *Eh-pH diagram showing the calculated Eh values for the Simpevarp samples. The Eh values obtained from potentiometric measurements are included in the figure. The Eh values from the SO42-/S2- redox pair are represented with open symbols and the values obtained with the pyrite-pyhrrotite/SO42- pair, with a filled black symbol. "Pyrite_min" and "Pyrite max" lines represent the equilibrium situation for the range of SO42- and Fe2+ concentration found in the Simpevarp groundwaters. The same is valid for the FeS/SO42- equilibrium.*

The results given by the sulphur system are more homogeneous and in better agreement with each other than those obtained from the $Fe(OH)_3/Fe^{2+}$ redox pair. This suggests that the sulphur system is the main controller of the groundwater redox state, as reported previously (Nordstrom and Puigdomenech, 1986; Glynn and Voss, 1997; Laaksoharju *et al.*, 2004 a, b). The CH_4/CO_2 redox pair gives results in good agreement with the sulphur pairs. This conclusion is supported by the microbial measurements in KSH01A (*c.f. Appendix 3*) In summary, all these redox pairs should be used when characterizing the redox state of the groundwaters. However, the variable results obtained with the $Fe(OH)_3/Fe^{2+}$ pair do not mean that the iron system does not participate in the redox control of these waters. For more details see *Appendix 4*.

Conceptual model for the redox system

The redox state of groundwaters in the Simpevarp area appears to be well described by sulphur redox pairs in agreement with some previous studies in this area (Glynn and Voss, 1999; Laaksoharju *et al.*, 2004a,b) and in other sites from the Fennoscandian Shield (Nordstrom and Puigdomenech, 1986; Laaksoharju *et al.*, 2004b; Pitkänen *et al.*, 2004). Besides, from the analysis performed here it can be concluded that CH_4/CO_2 is another important redox pair in determining the redox state.

The presence of sulphate reducing bacteria and methanogens widely distributed in the Äspö and Simpevarp can be related to the above discussion and supports the probability that the sulphur and methane redox pairs could be the prevailing ones in controlling a microbiologically mediated redox state. High quality measurements of S^{2-} and CH_4 are needed to pursue this approach.

However, in agreement with Grenthe *et al.* (1992), the work presented here also supports the fact that the iron system contributes to the control of the redox state through different oxide-oxyhydroxides. The issue is to clearly identify the real contribution of the iron system due to the variable crystallinity of the phases involved

and their evolution by, probably fast, recrystallisation. This fact indicates that more than one iron phase could be controlling the Eh in different groundwaters, although theoretically, with enough time, they could all eventually tend to an equilibrium with goethite and therefore to lower Eh values than the measured ones.

The interaction between the iron and sulphur systems is evident through sulphate reducing bacteria and sulphide mineral precipitation. Several lines of reasoning indicate that this process is effective at different levels in the investigated Simpevarp area. For instance, recent pyrite coatings have been identified in the fracture fillings of Simpevarp, which is an additional support to the good results of sulphur redox pairs. However, the influence of iron oxyhydroxide crystallinity on sulphide precipitation has also been rated in the Simpevarp subarea as an important factor.

Therefore, although the sulphur system can be considered the best suited to characterise the redox state of the groundwaters, a better understanding of the iron system is needed to assess its particular contribution to the redox state or to the reductive capacity of these groundwater systems.

4.5.2 M3 modelling

Introduction

A further modelling approach which is useful in helping judge the origin, mixing and major reactions influencing groundwater samples is the M3 modelling concept (Multivariate Mixing and Mass-balance calculations) detailed in Laaksoharju et al., (1995) and Laaksoharju et al. (1999b) and applied on the Simpevarp 1.1 data in Laaksoharju (ed.) et al., 2004.

Model results

The M3 method consists of 4 steps where the first step is a standard principal component analysis (PCA), selection of reference waters, followed by calculations of mixing proportions, and finally mass balance calculations (for more details see *Appendix 5*).

The reference waters used in the M3 modelling have been identified from: a) previous site investigations (e.g. Äspö and Laxemar), b) evaluation of the Simpevarp primary data set, and c) selecting possible compositions of end-members which according to the post glacial conceptual model (*Figure 3-1*) may have affected the site. The selected reference waters are more extreme than actually present at Simpevarp (e.g. Rain-60 or Littorina Sea). Their function is a) to be able to compare differences/similarities of the Simpevarp groundwaters with possible end-members, b) to be available to describe all available data used in the local and regional model, and c) to facilitate comparison with the results from the hydrogeological modelling. The analytical composition of the selected reference waters are listed in *Appendix 5*. The reference waters should not be regarded as point sources of flow but rather as possible contributors to the obtained water type. The reference waters have the following features:

- **Brine water:** Represents the sampled deep brine type (Cl = 47000 mg/L) of water found in KLX02: 1631-1681m (Laaksoharju et al., 1995a). An old age for the Brine is suggested by the measured ^{36}Cl values indicating a minimum residence time of 1.5Ma for the Cl component (Laaksoharju and Wallin (eds.), 1997). The sample contains some tritium (TU 4.2) which is believed to be

contamination from borehole activities. In the modelling 0 TU were used for this sample.

- **Glacial water:** Represents a possible melt-water composition from the last glaciation >13000BP. Modern sampled glacial melt water from Norway was used for the major elements and the $\delta^{18}O$ isotope value (–21 ‰ SMOW) was based on measured values of $\delta^{18}O$ in calcite surface deposits (Tullborg and Larsson, 1984). The $\delta^{2}H$ value (–158 ‰ SMOW) is a calculated value based on the equation ($\delta H = 8 \times \delta^{18}O + 10$) for the global meteoric water line.

- **Littorina Sea:** Represents old marine water and its calculated composition has been based on Pitkänen et al. (1999). This water is used for modelling purposes to represent past Baltic Sea water composition.

- **Modified Sea water (Sea sediment):** Represents sea water affected by microbial sulphate reduction.

- **Precipitation:** Corresponds to infiltration of meteoric water (the origin can be rain or snow) from 1960. Sampled modern meteoric water with a modelled high tritium (2000 TU) content was used to represent precipitation from that period.

The results of the PCA modelling are shown at regional scale (Simpevarp area data are compared with Forsmark data and other Nordic sites data) in *Figure 4-48* and in *Figure 4-49* at local scale using only the Simpevarp area data.

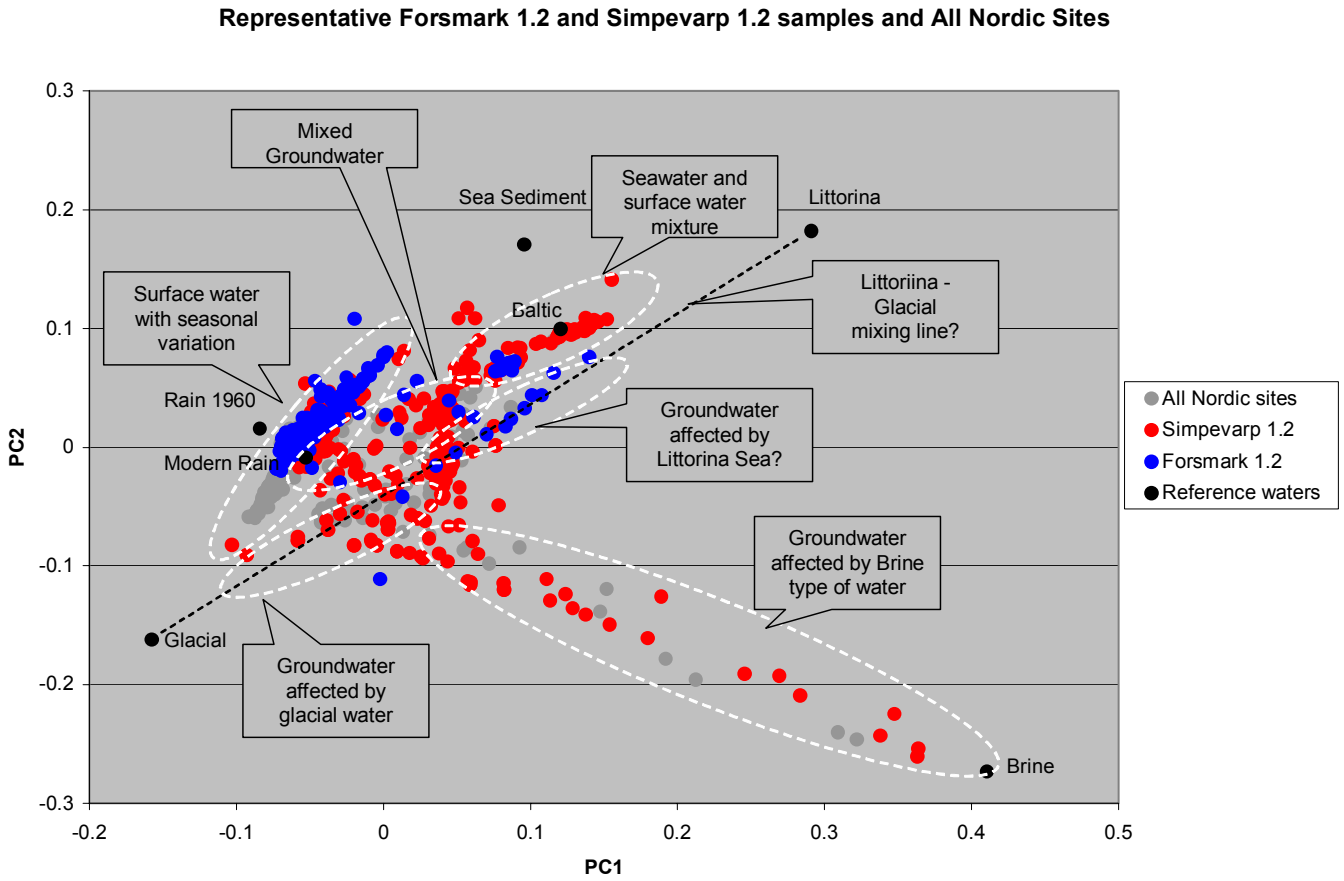

Figure 4-48: *PCA modelling of the representative Simpevarp area, Forsmark and Nordic data. The reference waters used in the modelling are indicated and the possible influenses from different end-members on the samples are indicated.*

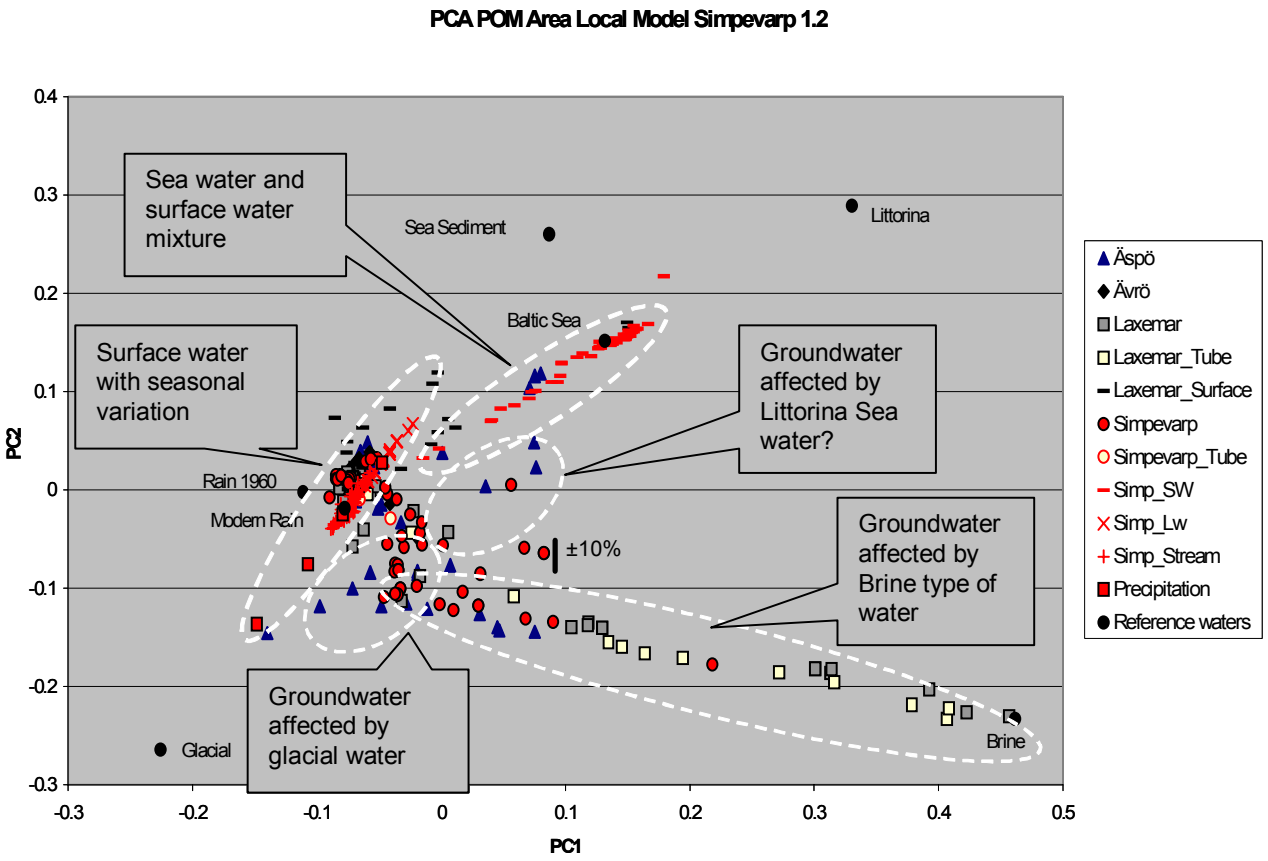

Figure 4-49: *PCA modelling of the representative Simpevarp area data. The reference waters used in the modelling are indicated and the possible influences from different end-members on the samples are indicated. The model uncertainty ±10% is shown as an black error bar and how the location of a single the sample can vary in the plot within that uncertainty limit; the analytical uncertainty is ±5% and represents therefore half of the error bar. The variance is : First principal component: 0.41, First and second principal components: 0.69, First, second and third principal components: 0.79.*

The M3 modelling shown in *Figure 4-48* indicates that the Simpevarp area samples are affected by all the reference waters: Meteoric, Marine, Glacial and Brine. Forsmark 1.2 data are lacking a clear indication of Brine component. Only a few samples from Forsmark indicate a Glacial-Brine component. The Littorina signature is much clearer at Forsmark compared with the data from the Simpevarp area. *Figure 4-49* shows that four water types occurs at the Simpevarp area, one dominated by meteoric water, the second affected by marine water, the third saline groundwater affected by glacial water, and finally a deep water affected by brine type groundwater. The surface meteoric groundwater type shows seasonal variations. Closer to the coast the influence of marine water is detected for the shallow samples. With depth the glacial, meteoric and brine type of waters have affected the saline groundwater. Only a few samples from Äspö and one from Simpevarp are showing a possible Littorina Sea water influence. The deviation calculations in the M3 mixing calculations show potential for organic decomposition/calcite dissolution in the shallow water. Indications of ion exchange and sulphate reduction have been modelled. These M3 results support the initial evaluation of primary data and general modelling results described in previous chapters.

4.5.3 Visualisation of the groundwater properties

Measured Cl content and the calculated M3 mixing proportions based on representative samples are shown for two core boreholes within the modelling domain (*Figure 4-50*). The results for all the boreholes are shown in *Appendix 5*. The purpose of the plots is to show the water type, changes with depth, and to facilitate comparison of the hydrochemical results with the hydrogeological results. Due to the fact that the hydrogeologists use only 4 reference waters, the marine components (Littorina and Sea Sediment reference waters) were combined and referred to as Marine water.

a) b)

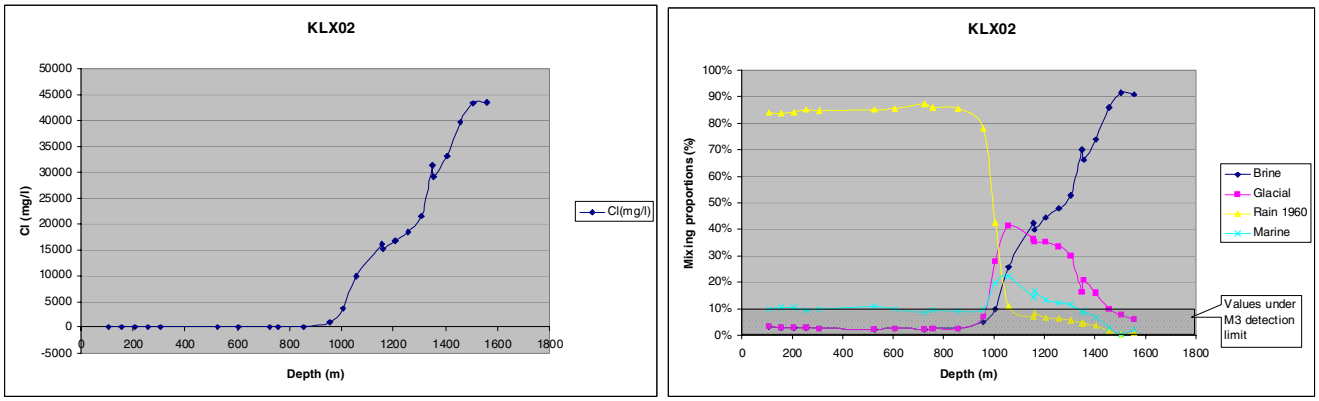

c) d)

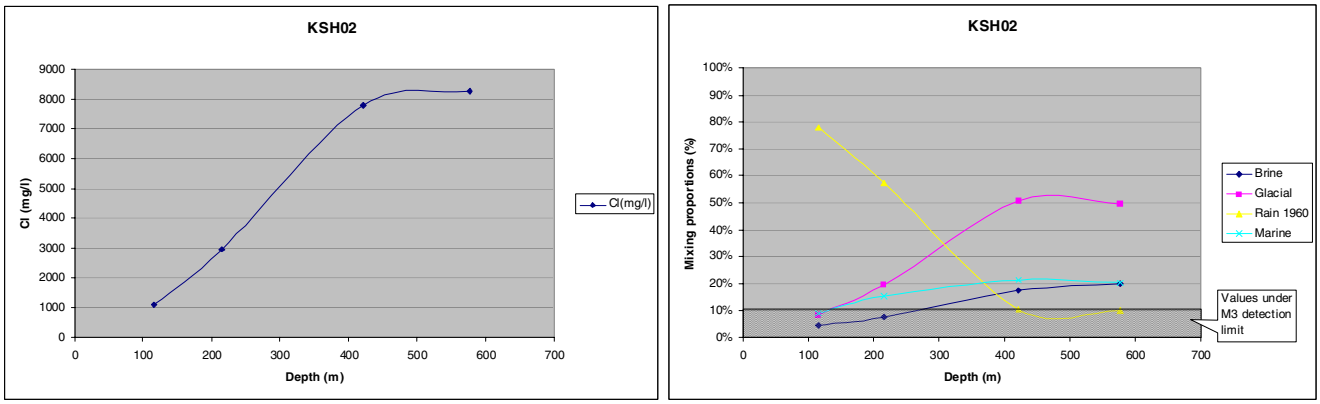

Figure 4-50: *(a) and (b) scatter plot of the Cl content and mixing proportions with depth for borehole KLX02. (c) and (d) scatter plot of the Cl content and mixing proportions with depth of borehole KSH02. A mixing proportion of less than 10% is regarded as being under the detection limit of the M3 method and is therefore shaded. The mixing proportions have an uncertainty range of ±0.1 mixing units.*

The 3D/2D visualisation of the Simpevarp Cl values was performed using the Tecplot code. *Figure 4-51* shows the 3D and the 2D visualisation of Cl in the sampling points for both representative and non-representative samples and for the M3 mixing proportions based on representative samples. The Cl figures (*Figure 4-51a, b*) reflect the possible uncertainties in the interpolations if the non-representative samples are

included but also the effect from sampling artefacts on the site description. The relatively few observations in the 3D space results in uncertainties; only in the near-vicinity of the observations are the uncertainties low. However, the interpolations can still be used to indicate the major occurrence of the different water types at the site. For example, a) Meteoric water is dominating in the west part and in the middle part of the cutting plane, b) Marine water is found towards the coast and under the sea in the east part of the cutting plane, c) Glacial water is found in the middle part of the cutting plane, and d) Brine type water is dominating at depth.

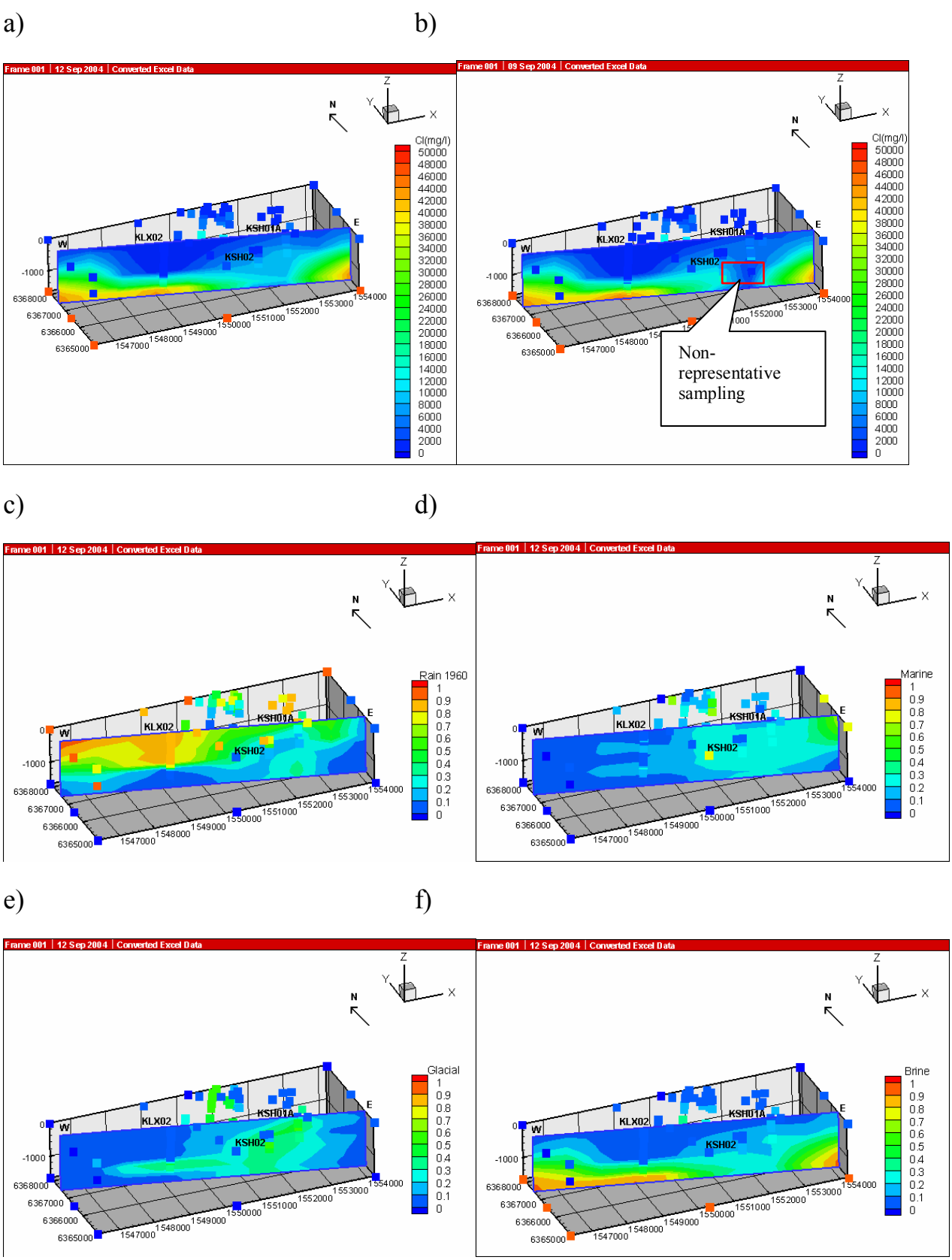

Figure 4-51: *3D interpolation and 2D visualisation of the groundwater properties along the W-E cutting plane, for orientation see Figure 4-2. (a) Cl interpolation based on representative samples (b) Cl interpolation including representative and non-representative samples. Figures c, d, e and f show the mixing proportions for the water*

types Rain 1960, Marine, Glacial and Brine. The x, y, z coordinates represent the Easting, Northing and elevation in metres.

4.5.4 Coupled modelling

A first attempt for combined hydrogeological and hydrochemical analysis of Simpevarp subarea is described in *Appendix 6*. The main objective of this exercise is to develop a framework to integrate available hydrogeological and hydrochemical information, with special emphasis on the consistency assessment between them.

Present time hydrogeological conditions of the Laxemar/Simpevarp area consist of a dynamic fresh-groundwater aquifer overlying a deeper and virtually stagnant saline groundwater system. The present work focusses on the coupling between groundwater flow, solute transport and geochemical processes actually taking place within the dynamic aquifer.

Qualitative analysis of environmental isotopes of the Simpevarp/Laxemar fresh groundwater samples suggests an average water age from several decades to 100 years. The Simpevarp subarea appears, therefore, to be the discharge area of a dynamic fresh water aquifer. Tritium activities measured at Simpevarp boreholes are consistent with mixing between recent, modern and sub-modern fresh groundwaters. The mixing is produced by the convergence of flow lines discharging on the Baltic Sea coast.

Combined analyses of isotopic and hydrochemical information of fresh groundwater samples allows identification of some trends which are consistent with the hydrogeological conceptual model of the area. The distributed recharge (resent water) of the granitic fresh aquifer is supported through the analysis of shallow groundwater samples. These recharge groundwaters are Ca-CO_3 in type, have high ^{14}C contents, tritium values are close to actual precipitation, and the waters are under-saturated with respect to calcite. On the other hand, deep fresh-groundwater samples from Simpevarp (at depths of 100–200 m) could correspond to the granitic aquifer discharge (older water). These waters are Na–HCO_3 type and show an average age of decades which may be one hundred years. Tritium values are mainly between 10–15 TU and the water is saturated in respect with calcite. Midway between recharge to discharge the deep groundwaters from Laxemar show a clear influence of recharge from the 1960's and 1970's and characterised by 'intermediate' hydrochemical signatures. However this conclusion is based on the presently available set of tritium data, the credibility of which, as pointed out in section 4.2.1, has been partly questioned. A larger set of new and dependable tritium data from the Laxemar area will be used in the forthcoming modelling where also information from the hydrogeological model version Simpevarp 1.2 can be used and the above assumptions will be tested further.

It has been detected that some lake waters show isotopic signatures very similar to Simpevarp groundwater. This could be reflecting the presence of lakes constituting local discharge areas of the granitic aquifer.

Numerical modelling of groundwater flow and solute transport has been performed in order to simulate groundwater age and tritium concentration *(Figure 4-52)*. As expected, kinematic porosity has been identified as the most sensitive parameter affecting the transport model results. Measured activities of environmental isotopes can only be reproduced numerically by using the same porosity values (order of magnitude of 10^{-3}) proposed by hydrogeological models of Simpevarp version 1.1, which were calibrated

using salinity data. Thus, the present model results provide additional support to hydrogeological models by using independent hydrochemical information.

a)

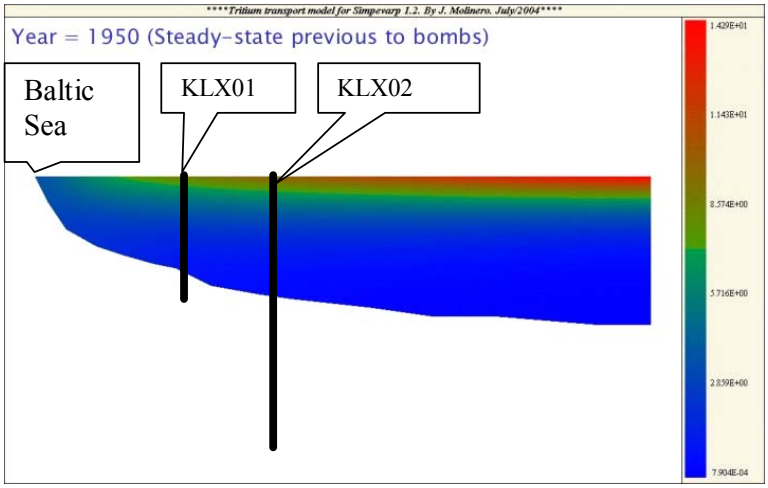

b)

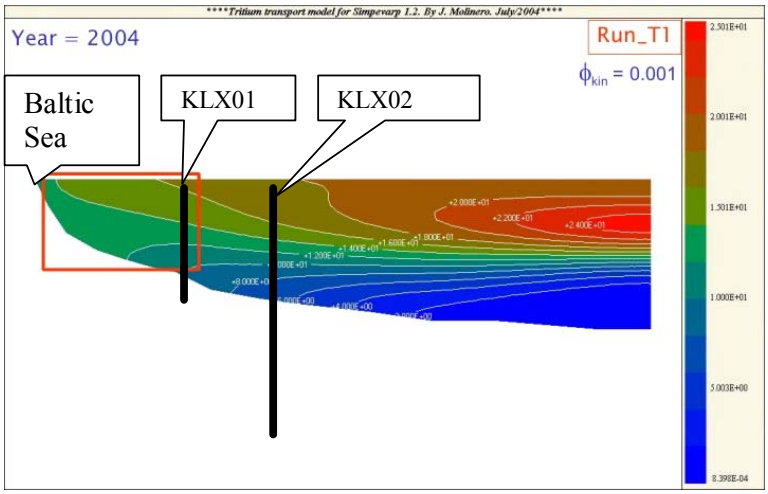

Figure 4-52: *(a) Simulated tritium contents in the Laxemar/Simpevarp fresh-water aquifer at year 1950. It can be seen that maximum tritium contents of near 15 TU are computed at the subsurface levels. The depth down to 100–200 m consists of fresh groundwater which is tritium free at year 1950. (b) Simulated tritium contents at year 2004, by using a kinematic porosity value of 0.001. The red square represents the equivalent area of fresh groundwaters at Simpevarp. The location of boreholes KLX01 and KLX02 are shown and the depth of the simulation is 1000 m. The bottom of the model domain corresponds to the saline-fresh water interface computed by Svensson (1996).*

A first attempt at coupled groundwater flow and reactive solute transport modelling has been performed. The hydrogeochemical part of the model consists of a set of 23 homogeneous reactions (aqueous complexes), calcite dissolution/precipitation and cation exchange. A calcite dissolution front (*Figure 4-53*) is computed by flushing saline water with fresh recharge (infiltrated) water, in agreement with one of the main processes described in previous hydrochemical models in this report. However, computed calcite dissolution cannot explain the measured concentrations of bicarbonate

and calcium. By including Ca-Na exchange the computed results are in good agreement with calcium and sodium concentrations measured at Simpevarp. For more details see *Appendix 6*.

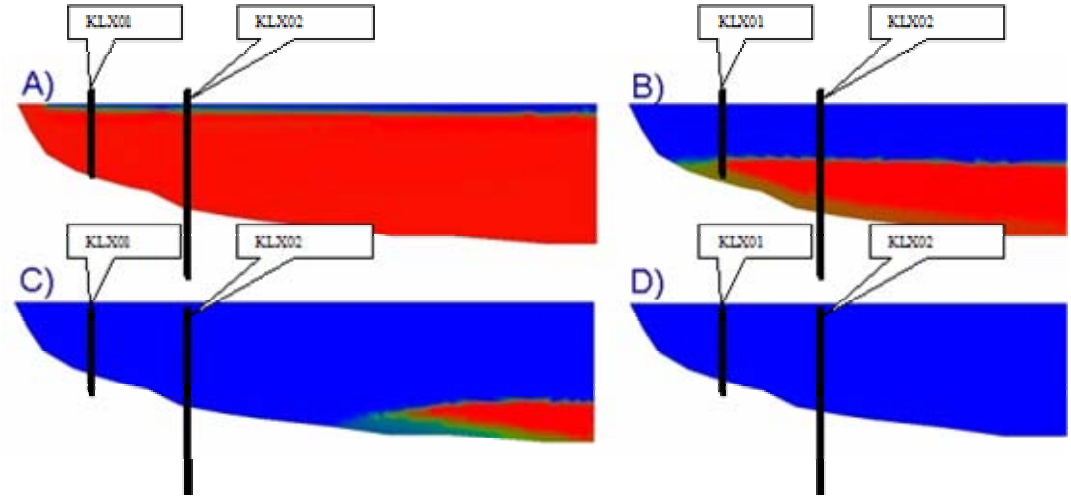

Figure 4-53: *Simulated calcite dissolution front at: A) 6 000 days; B) 56 000 days; C) 126 000 days and D) 256 000 days. The blue colour indicates the locations where dissolution of calcite occurs. The location of boreholes KLX01 and KLX02 are shown and the maximum depth of the simulation is 1200 m. For geographical orientation see Figure 4-2.*

The measured bicarbonate concentrations are higher than computed ones. A possible explanation could lie in the microbially-mediated decomposition of organic matter. This process has been described in the Äspö groundwaters (Banwart, 1999; Banwart et al., 1999), and successfully modelled by coupled hydro-bio-geochemical approaches (Molinero et al., 2004). The current version of the reactive transport model underestimates dissolved silica and sulphate, as well as overestimates dissolved iron. Most probably this is due to the occurrence of water-rock interaction processes involving silicates, pyrite, iron oxides and phyllosilicates, as already proposed by the hydrochemical model version Simpevarp 1.1 (Laaksoharju et al., 2004b). For more details see *Appendix 6*.

4.6 Evaluation of uncertainties

At every phase of the hydrogeochemical investigation programme – drilling, sampling, analysis, evaluation, modelling – uncertainties are introduced which have to be accounted for, addressed fully and clearly documented to provide confidence in the end result, whether it will be the site descriptive model or repository safety analysis and design (Smellie et al, 2002). Handling the uncertainties involved in constructing a site descriptive model has been documented in detail by Andersson et al. (2001 and 2002). The uncertainties can be conceptual uncertainties, data uncertainty, spatial variability of data, chosen scale, degree of confidence in the selected model, and error, precision, accuracy and bias in the predictions. Some of the identified uncertainties recognised during the modelling exercise are discussed below.

The following data uncertainties have been estimated, calculated or modelled for the Simpevarp data; these are based on models used for the Simpevarp 1.1 model version and

for the nearby Äspö Model Domain where similar uncertainties are believed to affect the present modelling:

- disturbances from drilling; may be ± 10-70% (c.f. DIS modelling in *Appendix 5*)
- effects from drilling during sampling; is <5%
- sampling; may be ± 10%
- influence associated with the uplifting of water; may be ± 10%
- sample handling and preparation; may be ± 5%
- analytical error associated with laboratory measurements; is ± 5% (the effects on the modelling was tested in *Appendix 1*).
- mean groundwater variability during groundwater sampling (first/last sample); is about 25%.

The M3 model uncertainty; is ±0.1units within 90% confidence interval (the effects on the modelling were tested in *Appendix 5*).

Conceptual errors can occur in, for example, the palaeohydrogeological conceptual model. The influence and occurrences of old water end members in the bedrock can only be indicated by using certain element or isotopic signatures. The uncertainty is therefore generally increasing with the age of the end member. The relevance of an end member participating in the groundwater formation can be tested by introducing alternative end member compositions or by using hydrodynamic modelling to test if old water types can reside in the bedrock during prevailing hydrogeological conditions. In this model version the validation is checked by comparison with hydrogeological simulations.

Uncertainties in the PHREEQC code depend on which code version is being used. Generally the analytical uncertainties and uncertainties concerning the thermodynamic data bases are of importance (in speciation-solubility calculations). Care also is required to select mineral phases which are realistic (even better if they have been positively identified) for the systems being modelled. These errors can be addressed by using sensitivity analyses, alternative models and descriptions. A sensitivity analysis was performed concerning the calculations of activity coefficients in waters with high ionic strength and also the uncertainties of the stability diagrams were discussed in *Appendix 4*.

The uncertainty due to 3D interpolation and visualisation depends on various issues, i.e. data quality, distribution, model uncertainties, assumptions and limitations introduced. The uncertainties are therefore often site specific and some of them can be tested such as the effect of 2D/3D interpolations. The site specific uncertainties can be tested by using quantified uncertainties, alternative models, and comparison with independent models such as hydrogeological simulations.

Uncertainties in the coupled reactive transport modelling are numerous at the present SI stage. These uncertainties can be of two main types: (a) conceptual model uncertainties and (b) parameter uncertainties. Reactive transport modelling is based on Simpevarp version 1.1 hydrogeological and current hydrochemical conceptual models. Then, possible conceptual uncertainties are directly translated into the reactive transport model results. Conceptual uncertainties are mainly related to the extent and nature of boundary

conditions (i.e. dimensions of the model, water recharge values, etc.), and the selection of physical-chemical processes included in the calculations. Parameter uncertainties are also present in the model (permeability, porosity, cation exchange capacity, amount of calcite in the granite, etc.). However, reactive transport model has been used as a tool for testing the consistency (or plausibility) of different assumptions. It is considered that parameter uncertainty is less relevant than conceptual uncertainties at the present stage.

The discrepancies between different modelling approaches can be due to differences in the boundary conditions used in the models or in the assumptions made. The discrepancies between models should be used as an important validation and confidence building opportunity to guide further modelling efforts. In this work the use of different modelling approaches starting from manual evaluation to advanced coupled modelling can be used as a tool for confidence building. The same type of process descriptions independent of the modelling tool or approach increases the confidence in the modelling.

4.7 Feedback to other disciplines

4.7.1 Comparison between the hydrogeological and hydrogeochemical models

Since hydrogeology and hydrogeochemistry deal with the same geological and hydrodynamic properties, these two disciplines should be able to complement each other when describing/modelling the groundwater system. Testing such an integrated modelling approach was the focus of a SKB project (Task 5) based on the Äspö HRL (Wikberg 1998; Rhén and Smellie (eds), 2003). The advantages with such an approach were identified as follows:

- Hydrogeological models will be constrained by a new data set. If, as an example, the hydrogeological model, which treats advection and diffusion processes in highly heterogeneous media, cannot produce any Meteoric water at a certain depth and the hydrogeochemical data indicate that there is a certain fraction of this water type at this depth, then the model parameters and/or processes has to be revised.

- Hydrogeological models are fully three dimensional and transient processes such as shoreline displacement and variable-density flow can be treated, which means that the spatial variability of flow related hydrogeochemical processes can be modeled, visualised and communicated. In particular, the role of the nearby borehole hydraulic conditions for the chemical sampling can be described.

- Hydrogeochemical models generally focus on the effects from reactions on the obtained groundwater rather than on the effects from transport. An integrated modelling approach can describe flow directions and hence help to understand the origin of the groundwater. The turn over time of the groundwater system can indicate the age of the groundwater and, knowing the flow rate, can be used to indicate the reaction rate. The obtained groundwater chemistry is a result of reactions and transport, and therefore only an integrated description can be used to correctly describe the measurements.

- By comparing two independent modelling approaches a consistency check can be made. As a result greater confidence in active processes, geometrical description and material properties can be gained.

Major recent developments in hydrogeological modelling of the Simpevarp area (I. Rhén pers. comm., 2004) represents further progress since the TASK#5 exercise (Rhén and Smellie eds., 2003). The present 1.2 modelling has further developed the comparison and integration between hydrochemistry and hydrogeology. The hydrogeological model can provide predictions of the groundwater components and isotopes such as Cl, ^{18}O and ^{2}H in the connected rock matrix, in the flowing groundwater and for dynamic predictions over time for the different water types (meteoric, marine, glacial and brine). Furthermore, the hydrodynamic model can, independently from chemistry, predict these salinity features at any point of the modelled rock volume, and the predictions can be checked by direct hydrogeochemical measurements or calculations. The mixing proportions from the hydrogeological model can, for example, be directly compared with the mixing calculations from the hydrogeochemical modelling (*Figure 4-54*) or, conversely, the hydrogeochemical model can be used to predict the chemistry which results from only transport and which, in turn, can be compared with that obtained from reactions. The modelling will increase the understanding of transport, mixing and reactions and will also provide a tool for predicting future chemical changes due to climate changes. The coupled transport modelling presented in *Appendix 6* can be used as an independent validity tool to check different processes and transport hypotheses.

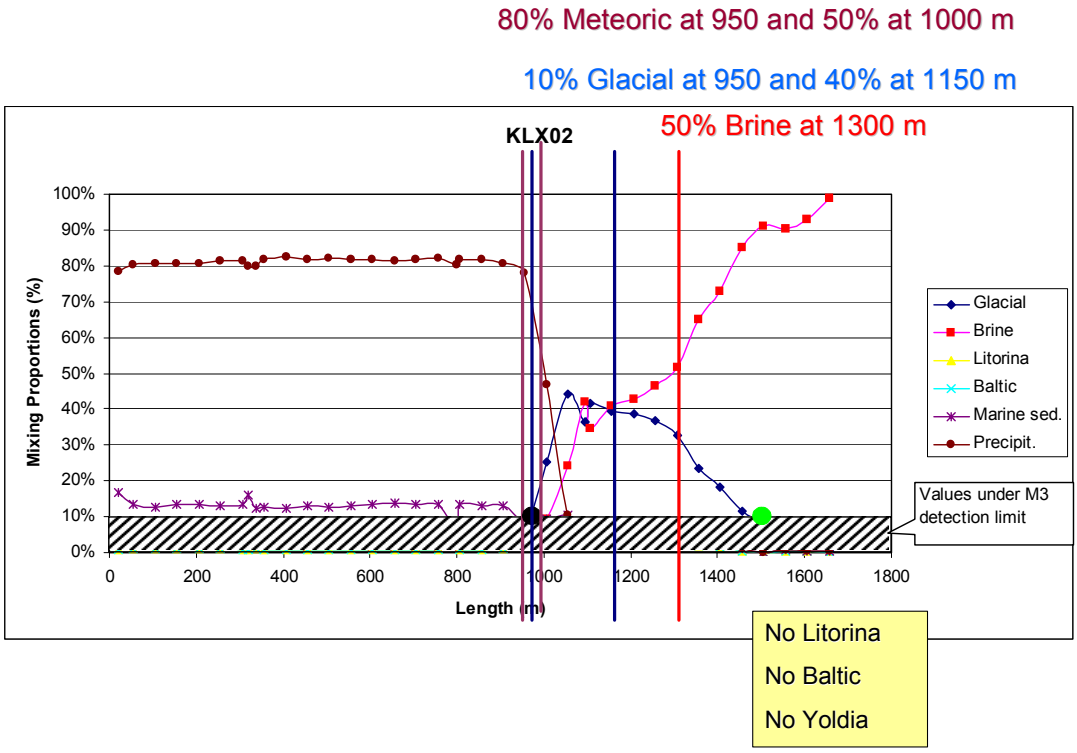

Figure 4-54: *Example of comparison between hydrogeological and hydrogeochemical modelling. The mixing proportions from the hydrogeological model (vertical lines) is compared with the M3 mixing calculations (horizontal lines) for borehole KLX02 (S. Follin, per. comm.., 2004). The mixing calculations are based on the regional M3 model.*

5 Resulting description of the Simpevarp area

5.1 Bedrock Hydrogeochemical Description

5.1.1 Groundwater composition

One of the objectives of the Initial Site Investigation (ISI) stage is to produce versions of the hydrogeochemical descriptive model on a site scale. Visualisation of the hydrogeochemical evaluation documented in this report is in the form of a vertical transect through the Laxemar and Simpevarp subareas (for orientation see *Figure 4-2*). The vertical extent of the transect is to approx. 1700 m to accommodate the deepest borehole (KLX02) in the Laxemar site. The approach to locate and construct the transect is described in Appendix 1. Based on existing geological and hydrogeological information a schematic manual version of the transect was produced to facilitate illustrating the most important structures/fault zones and their potential hydraulic impact on the groundwater flow (*Figure 5-1*). This hydraulic information was then integrated with the results of the hydrogeochemical evaluation and modelling results to produce the vertical and lateral changes in the groundwater chemistry (*Figure 5-1*).

In the Simpevarp subarea the main intersected structures have an approximate NE-SW orientation; in the Laxemar subarea the transect is mostly parallel to the main WNW-SSE structural trends. The former are considered sub-vertical whilst at Laxemar the structures tend to dip at shallower angles to the SW or NE. Combined, these structures effectively divide both the Simpevarp and Laxemar areas into structural compartments as illustrated in *Figure 5-1*. It is also believed that each major structural compartment will be characterised by its own local hydraulic groundwater flow regime (*Figure 5-1*). Most of the vertical to sub-vertical fracture zones are considered as discharging groundwater pathways.

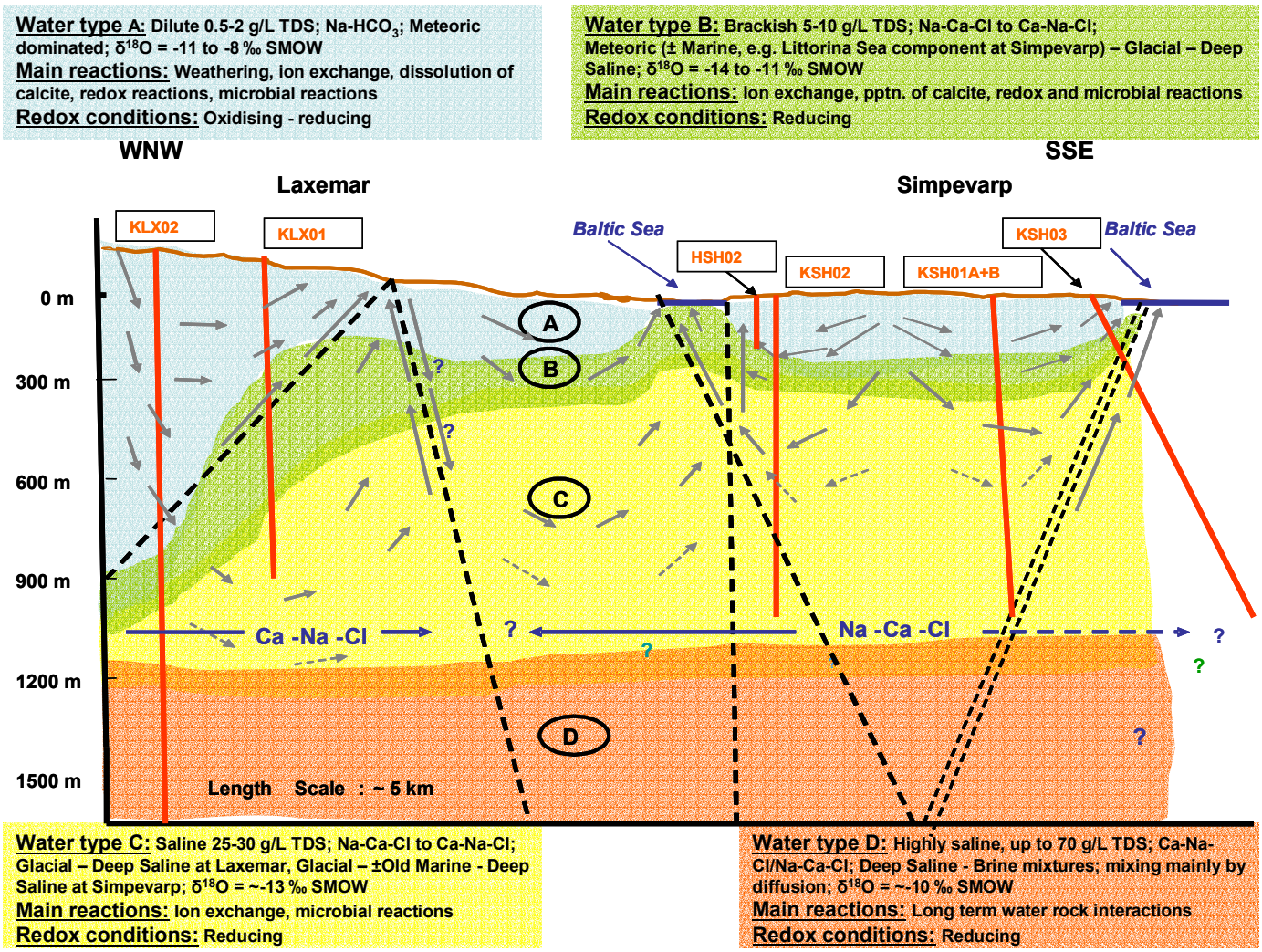

Figure 5-1: *Schematic conceptual hydrogeochemical model based on integrating the major structures, the major groundwater flow directions and the different groundwater chemistries (A-D) and properties.*

The groundwater flow regimes at Laxemar/Simpevarp are considered local and extend down to depths of around 600-1000 m depending on local topography. Close to the Baltic Sea coastline where topographical variation is small, groundwater flow penetration to depth will subsequently be less marked. In contrast, Laxemar is characterised by higher topography resulting in a much more dynamic groundwater circulation which appears to extend to 1000 m depth in the vicinity of borehole KLX02 (*Figure 5-1*).

The marked differences in the groundwater flow regimes between the Laxemar and Simpevarp areas are reflected in the groundwater chemistry. *Figure 5-1* shows four major recognised hydrochemical groups of groundwaters denoted by A-D. Question marks are inserted where there is a degree of uncertainty, i.e.:

- Between groundwater types A and B close to borehole KLX02 at Laxemar. There is some uncertainty whether dilute recharge Na-HCO_3 waters extend to

the depth indicated. Some short-circuiting of groundwater flow paths by borehole KLX02 may be occurring.

- Between types C and D within the Simpevarp site. The extent of Na-Ca-Cl groundwaters below 1000 m is unknown. In addition, it is uncertain whether there is an eventual transition to Ca-Na-Cl groundwater types at even greater depths.

- In terms of depth location, chemistry, major reactions and main mixing processes, the main features of these four groundwater types are summarised below.

TYPE A – Shallow (<200 m) at Simpevarp but deeper (0-900 m) at Laxemar

Dilute groundwater (< 1000 mg/L Cl; 0.5-2.0 g/L TDS)

Mainly Na-HCO_3 in type

Redox: Marginally oxidising close to the surface, otherwise reducing

Main reactions: Weathering; ion exchange (Ca, Mg); dissolution of calcite; redox reactions (e.g. precipitation of Fe-oxyhydroxides); microbially-mediated reactions (SRB)

Mixing processes: Mainly meteoric recharge water at Laxemar; potential mixing of recharge meteoric water and a modern sea component at Simpevarp; localised mixing of meteoric water with deeper saline groundwaters at Laxemar and Simpevarp

TYPE B – Shallow to intermediate (150-300 m) at Simpevarp but deeper (approx. 900-1100 m) at Laxemar)

Brackish groundwater (1000-6000 mg/L Cl; 5-10 g/L TDS)

Mainly Na-Ca-Cl in type but some Na-Ca(Mg)-Cl(Br) types at Simpevarp; transition to more Ca-Na-Cl types at Laxemar

Redox: Reducing

Main reactions: Ion exchange (Ca, Mg); precipitation of calcite; redox reactions (e.g. precipitation of pyrite), microbial reactions

Mixing processes: Potential residual Littorina Sea (old marine) component at Simpevarp, usually in fracture zones close to or under the Baltic Sea; meteoric and potential glacial component at Simpevarp and Laxemar; potential deep saline (non-marine) component at Simpevarp and at Laxemar

TYPE C - Intermediate to deep (>300 m) at Simpevarp but deeper (approx. 1200 m) at Laxemar

Saline (6000-20 000 mg/L Cl; 25-30 g/L TDS)

Mainly Na-Ca-Cl with increasingly enhanced Br and SO_4 with depth at Simpevarp; mainly Ca-Na-Cl with increasing enhancements of Br and SO_4 with depth at Laxemar

Redox: Reducing

Main reactions: Ion exchange (Ca), microbial reactions

Mixing processes: Potential glacial component at Simpevarp and Laxemar; potential deep saline (i.e. non-marine and/or non-marine/old Littorina marine) component at Simpevarp, deep saline (non-marine) component at Laxemar

TYPE D – Deep (> 1200 m) only at Laxemar

Highly saline (> 20 000 mg/L Cl; to a maximum of ~70 g/L TDS)

Mainly Ca-Na-Cl with higher Br but lower SO_4 compared to Type C groundwaters

Redox: Reducing

Main reactions: Water/rock reactions under long residence times, microbial reactions

Mixing processes: Probably long term mixing of deeper, non-marine saline component driven by diffusion

Deep groundwaters at Simpevarp and Äspö (1000 m) are Na-Ca-Cl in type; deep groundwaters at Oskarshamn (KOV01; 1000 m) and at Laxemar (1700 m) are Ca-Na-Cl in type. Since Laxemar is inland and Oskarshamn is close to the coast, this could be an indication of very deep discharging groundwaters at Oskarshamn. Therefore, at greater depths below Simpevarp and Äspö than presently sampled, Ca-Na-Cl groundwaters might be expected.

5.1.2 Process and boundary conditions

The detailed evaluation of the groundwater observations indicates the following features:

Descriptive observations

Main elements

- Overall depth trends show increasing TDS with increasing depth. In particular the Ca/Na and Br/Cl ratios increase markedly.
- Sulphate and Mg show an overall decrease with depth with greater dispersion from approx. 200-600 m. Bicarbonate decreases sharply with depth.
- Ca/Mg and Br/Cl ratios versus Cl content indicate a deep, non-marine source of the salinity for most of the borehole samples. This is similar to groundwaters from the Äspö, Laxemar and Oskarshamn (KOV01) boreholes.
- Deep groundwaters at Simpevarp and Äspö (1000 m) are Na-Ca-Cl in type; deep groundwaters at Oskarshamn (KOV01; 1000 m) and at Laxemar (1700 m) are Ca-Na-Cl in type. Since Laxemar is inland and Oskarshamn is close to the coast, this could be an indication of discharging very deep groundwaters at Oskarshamn. At greater depths below Simpevarp and Äspö than presently sampled, Ca-Na-Cl groundwaters therefore might be expected.

- A small set of brackish groundwaters (1000-6000 mg/L Cl), located around 150-300 m depth, show marine signatures of possible Littorina Sea origin. These are located in fracture zones close to or under the Baltic Sea.

- $\delta^{18}O$ versus Cl indicates a contribution of glacial waters to the brackish and deeper saline water samples.

- The SO_4 contents show a large variation for the brackish and saline groundwaters. In the brackish groundwaters with 5000-6300 mg/L Cl, microbially mediated sulphate reduction is taking place. The SO_4^{2-} contents in the more highly saline groundwaters are still not high enough to invoke dissolution or leaching as a mechanism. More likely processes are in-mixing of marine waters although in-mixing of SO_4^{2-} from deep brine waters cannot be excluded. Deep saline SO_4^{2-} sources (> 20 000 mg/L Cl) may have resulted from the leaching of sediments and/or dissolution of gypsum previously present in fractures.

Isotopes

- The isotope data from the boreholes are still relatively few and often do not correspond to the most representative samples. To compensate, most of the available data have been plotted with the objective of determining trends rather than far reaching conclusions.

- With respect to tritium, generally the Baltic Sea samples show somewhat higher values (10.3-19.3 TU) compared to the meteoric surface waters (7.8-15 TU). The successive lowering of the tritium contents versus time elapsed since the bomb tests may explain the higher values in the Baltic Sea (due to reservoir effects). Note that the precipitation values are very few, show a large variation in tritium and therefore are not considered very conclusive. Continued systematic sampling of precipitation for tritium analyses is recommended.

- For carbon, plots of ^{14}C versus $\delta^{13}C$ versus HCO_3^- show that there is no real correlation between ^{14}C and $\delta^{13}C$, i.e. there is no indication of a change in $\delta^{13}C$ with age. Breakdown of organic material plays a major role and has occurred either in the near-surface (being transported downwards) or that *in situ* production has taken place. An organic origin is also supported by the $\delta^{13}C$ versus HCO_3^- plot where the groundwater samples showing the highest HCO_3 contents show relatively homogeneous $\delta^{13}C$ values.

- The plot of tritium versus ^{14}C for surface waters from Simpevarp area shows a distinct decrease in ^{14}C content in the Lake and Stream waters, whereas the tritium values remain the same or show a small decrease. The explanation is that HCO_3^- added to the waters originates either from calcites devoid of ^{14}C or due to microbial oxidation of organic material with lower (or no) ^{14}C. This is the pattern expected for near-surface waters.

- Marine waters show a distinct Sr isotope signature (0.7092) which is very close to the measured values in the Baltic Sea waters, whereas groundwaters from the different sites show values significantly more enriched in radiogenic Sr. Water/rock interaction processes involving Rb-containing minerals are the reason for this. The relatively small variation in Sr isotope ratios within each area, particularly at the Simpevarp and Laxemar subareas, is probably an indication that ion exchange reactions with clay minerals along the groundwater

flow paths is an important process. For the Simpevarp/Laxemar area there is a tendency towards higher contents of radiogenic Sr in the waters with highest salinities (and thus the highest Sr contents measured). Because of the limited data it is not possible to explain this observation, but in the absence of any mineralogical reasons, it is likely that greater residence times for these deep saline groundwaters result in more extensive mineral/water interactions.

- The borehole groundwaters generally show $\delta^{34}S$ values in the same range as the Baltic Sea waters but with a clear indication in the brackish groundwaters of $\delta^{34}S$ values greater than +21 ‰ CDT in samples with low SO_4^{2-}. This may be explained by modification of the isotope ratios by sulphur-reducing bacteria. The higher saline groundwaters share lower $\delta^{34}S$ but higher SO_4^{2-} contents. The $\delta^{34}S$ values of these deeper groundwaters are, however, still within the range for the analysed Baltic Sea waters.

- The $\delta^{37}Cl$ data suggest that the deeper cored borehole groundwaters are characterised by water/rock interaction processes, whilst the near-surface percussion borehole groundwaters are mainly marine derived. The distribution of Baltic Sea and surface Lake and Stream waters suggest some mixing components of marine-derived and deeper groundwater sources.

Microbes, colloids and gases

- As there were only three sets of microbiological data available from one borehole (KSH01A), the model version produced is one-dimensional.

- Redox potentials in borehole KSH01A were in general low, below –200 mV at all sampled depths.

- Sulphate reducing bacteria dominated at the shallowest level sampled, 156.5–167 m.

- At the mid level, 245 –261.6 m, heterotrophic methanogens and acetogens were dominant.

- At the deepest level autotrophic and heterotrophic acetogens were found but only in low numbers.

- The large numbers of microorganisms at level 245–261.6 m were probably due to the large fracture area with high amounts of fracture surfaces inducing significant perturbations and favourable conditions for life.

- The abundance of microbial species and their activity in borehole KSH01A seem to be closely correlated with the redox potential.

- The numbers of colloids decrease with depth in KLX01 but not in KAV01. Furthermore, the numbers do not vary much at the different depths sampled. The sampled depths were 422.5 m, 525.5 m and 560.5 m respectively, i.e. an extent of only 140 m which is not much in relation the total depth explored. The average number of colloids in this study is 63±49 μg L^{-1} and is in agreement with colloid studies from Switzerland (30±10 and 10±5 μg L^{-1}) and Canada (300±300 μg L^{-1}) where they used the same approach as in the Simpevarp area (Laaksoharju, 1995).

- Up to 12 gases were analysed: helium, argon, nitrogen, carbon dioxide, methane, carbon monoxide, oxygen, hydrogen, ethyne, ethene, ethane and propane. KSH01A was the only borehole sampled completely regarding analysed gas components. Numbers for the total volume of gas were available only for 5 depths in two of the boreholes. They contain between 44 and 80 mL L^{-1} and this is in accordance with volumes found at other places in the Fennoscandian shield.

Modelled observations

PHREEQC modelling

Groundwater in the Simpevarp area can be divided into three groups based on their salinity:

- Saline groundwaters. Mixing with a brine end member is responsible, directly or indirectly, for most of their chemical content, especially from Cl concentrations higher than 10 000 mg/L. Their alkalinity is low, and controlled by equilibrium with calcite. pH is controlled by calcite equilibrium and, possibly, aluminosilicate reactions. In contrast to other Fennoscandian sites, sulphate is controlled by gypsum (supported by gypsum identified in fracture fillings) in high saline groundwaters. These old mixed waters tend, with time, to re-equilibrate with a relatively constant mineral assemblage, irrespective of their initial elemental contents. These reactions are slow and can be approached by equilibrium modelling (with aluminosilicates), although other alternatives can be explored (clay minerals).

- Brackish groundwaters. They have been subject to more complex mixing processes involving all possible end-members. A combination of slow and fast chemical reactions (eg. Na-K-Ca ion exchange, calcite precipitation, etc) have influenced the mixed waters

- Non saline groundwaters. These waters are the result of "pure" water-rock interaction or mixing of the previous types with recent waters. They lack a clear thermodynamic control. Control is by fast chemical reactions (ionic exchange, surface complexation reactions, calcite dissolution-precipitation, etc.) coupled with more important irreversible processes (fracture mineral dissolution, decomposition of organic matter, etc.).

The redox state of groundwaters in the Simpevarp area appears to be well described by sulphur redox pairs in agreement with some previous studies in this area and in other sites from the Fennoscandian Shield. Besides, from the analysis performed here it can be concluded that CH_4/CO_2 is another important redox pair in determining the redox state. Therefore, although the sulphur system can be considered the best suited to characterise the redox state of the groundwaters, a better understanding of the iron system is needed to assess its particular contribution to the redox state or to the reductive capacity of these groundwater systems.

A modelling approach was used to simulate the brine composition concluding that in the Simpevarp area the mixing is the main irreversible process. It controls chloride concentration that, in turn, determines the re-equilibrium path (water-rock interaction) triggered by mixing. This result emphasises the important effort made in the Swedish (and Finish) framework to characterize the mixing process. Moreover, it justifies the

selection of chloride as the main descriptive variable when studying the geochemical evolution of these systems.

M3 and DIS modelling

- M3 modelling helped to summarise and understand the data in terms of origin, mixing proportions and reactions.
- The surface meteoric type waters show seasonal variations and closer to the coast the influence of marine water is indicated. With depth the glacial, meteoric and brine type of waters have affected the groundwater salinity. Only a few samples from Äspö and one from Simpevarp show a possible Littorina Sea water influence. The deviation calculations in the M3 mixing calculations show the potential for organic decomposition/calcite dissolution in the shallow water. Indications of ion exchange and sulphate reduction have been modelled. These M3 results support the initial evaluation of primary data and general modelling results.
- The 3D/2D visualisations indicate that meteoric water is dominating in the western part and in the central part of the modelling domain. Marine water is found towards the coast and under the sea in the eastern part of the cutting plane. Glacial water is found in the central part of the cutting plane and Brine type of water is dominating at depth.
- DIS evaluation can help to judge the representativeness of the sampled data. The section 548-565m in KSH01 was investigated and the results showed that the amount of drilling water remaining in the fracture is 2.4 m^3. The calculations showed that the pumping should have continued further in order to remove the additional 2.4m^3.

Coupled transport modelling

- Qualitative analysis of environmental isotopes representing the Simpevarp/Laxemar fresh groundwater samples suggests an average water age from several decades to 100 years.
- The Simpevarp subarea appears to be the discharge area of a dynamic fresh water aquifer. Tritium activities measured are consistent with mixing between recent, modern and sub-modern fresh groundwaters. The mixing is produced by the convergence of flow lines discharging on the Baltic Sea coast.
- Combined analyses of isotopic and hydrochemical information of fresh groundwater samples allows the identification of clear trends which are consistent with the hydrogeological knowledge of the area.
- It has been detected that some lake water shows isotopic signatures very similar to Simpevarp subarea groundwater. This could be reflecting the presence of lakes constituting local discharge areas of the granitic aquifer.
- Numerical modelling of groundwater flow and solute transport has been performed in order to simulate groundwater age and tritium concentration. The

model results provide additional support to hydrogeological models by using independent hydrochemical information.

- A first attempt to coupled groundwater flow and reactive solute transport modelling has been performed. A calcite dissolution front is computed due to the flushing of saline water by fresh recharge (infiltrated) water, in agreement with one of the main processes detected by previous hydrochemical models. However, computed calcite dissolution cannot explain measured concentration of bicarbonate and calcium. By including Ca-Na exchange the computed results are in good agreement with calcium and sodium concentrations measured at Simpevarp.

- Measured bicarbonate concentrations are higher than those computed. A possible explanation could lie in microbially-mediated decomposition of organic matter. The current version of the reactive transport model underestimates dissolved silica and sulphate, as well as overestimates dissolved iron. Most probably this is due to the occurrence of water/rock interaction processes involving silicates, pyrite, iron oxides and phyllosilicates.

Hydrochemical stability criteria

The modelling indicates that the groundwater composition at the repository depth, is such that the representative sample from KSH01A:548-565m and KSH02:575-580m can meet the SKB chemical stability criteria (Table 5-1) for Eh, pH, TDS, DOC and Ca+Mg (see Anderson et al., 2000).

Table 5-1:The hydrochemical stability criteria defined by SKB are valid for the analysed values of the represenative sample KSH01A:548-565m and KSH02:575-580m.

	Eh mV	pH (units)	TDS (g/L)	DOC (mg/L)	Colloids (mg/L)	Ca+Mg (mg/L)
Criterion	<0	6-10	<100	<20	<0.5	>4
KSH01A:548-565m	-230	7.6	15.1	<1	NA	1947
KSH02:575-580m	NA	8.1	14.1	<1	NA	1797

NA = Not analysed

5.2 Consistency between bedrock disciplines

The consistency between the hydrochemical and hydrogeological description will be discussed in the integrated site description report.

5.3 Consistency in interface between the surface and bedrock system

The groundwater chemistry description data from surface to depth are used to produce a description at the interface between the surface and bedrock water systems. The coupled modelling in Appendix 6 describes this interaction. A more detailed description will be given in the integrated site description report.

6 Conclusions

6.1 Overall changes since previous model version

In this report the salinity distribution, water type occurrence, mixing processes and the major reactions altering the groundwaters have been modelled in detail to the depth of 1000m. A new Hydrogeochemical Site Descriptive Model version 1.2 has evolved. The resulting description has improved compared to the 1.1 version by producing a more detailed process modelling, redox description, and microbial description including colloids and gas. The microbial characterisation gives direct support to, for example, the redox modelling. The coupled transport modelling can address processes questions from a transport point of view which is a major improvement.

6.2 Overall understanding of the site

The overall understanding of the site describes the major processes taking place at the surface and to depth which includes the expected repository levels. The confidence in this description is relatively high since independent model approaches were utilised in the work. The origin, the postglacial evolution and the major reactions in the waters are fairly well understood. However the confidence concerning the spatial variation is low due to relatively few observations at depth. The continuation of the ongoing sampling programme at Laxemar will provide better spatial information and thus will increase confidence.

6.3 Implication for further modelling

Comparison and integration between geological and hydrogeological models was in this model version restricted to input concerning the structural model, fracture mineralogy, postglacial scenario models, chloride, TDS, oxygen-18, tritium, carbon-14 and mixing proportion calculations.

Future coupled reactive transport modelling should incorporate additional geochemical processes using the same sequential methodology adopted for calcite dissolution and cation exchange as shown in Appendix 6. Further developments could also incorporate geological heterogeneity, as well as the deeper saline groundwater system.

The use of independent modelling approaches within the HAG group provided the possibility to compare the outcome of the different models and to use discrepancies between models to guide further modelling efforts. The many similarities resulting from the HAG modelling gave confidence to the obtained results.

The correct choice of groundwater end members is important for many of the modelling exercises reported. Whilst experience from Äspö and other Fennoscandian sites has contributed to a standard set of groundwater end members, individual sites (at different depths) may lack one or more of these standard end members. This possibility will have to be taken into account. In the future versions end-member variants will be further tested and also alternative models to M3 to calculate the groundwater mixing proportions will be explored (J. Gomez, per. comm., 2004). The general application of alternative models and descriptions should be further developed in future versions together with uncertainty tests of the models applied.

6.4 Implications for the ongoing site investigation programme

From the HAG modelling work the following suggestions have been made for the ongoing site investigation programme (***the response from the site is indicated in italics***):

- All samples should have x, y, z coordinates in order to be useful in the visualisation work. These coordinates should be listed in SICADA as are the mid section coordinates. Those z coordinates not always available for the surface samples (sea, lake, streams) were estimated to be 0. However, to the depth of the model (1.6 km) this represents an error of 1-2% in the model.

  There are x, y and z coordinates for most of the samples in SICADA, and this is certainly the case for the surface samples. The z coordinates for streams and lakes were measured early this year; no z coordinates were measured for the sea locations. Samples taken from different boreholes should also have z coordinates since the coordinates for the borehole are measured in connection with drilling.

- It is necessary to know exactly the meaning of each column in the SICADA table including the detection limits (e.g. S^{2-}) of the analytical techniques and the number of significant decimals.

  A document should be produced where all these parameters (e.g. detection limits, decimals etc.) are described.

- It is not sufficient to only analyse for ^{10}B; ^{11}B and B are needed also for interpretation. Methane, aluminium, ^{36}Cl and density measurements are needed in the more saline samples.

  ^{10}B and ^{11}B are analysed as an isotopic ratio. Boron can perhaps be analysed with ICP but it is unclear just now if this is possible. This will be investigated further. Aluminium can also be investigated with ICP and in fact Al is analysed in many cases (i.e. samples with chemistry class 5). Methane might be difficult to analyse. Furthermore, it might be difficult to find a laboratory that can analyse ^{36}Cl, but this is possible if the HAG-group can come up with a suitable suggestion. With respect to density measurements, nowadays these are always performed (if there is enough water) at the Äspö laboratory.

- pH is always measured in the field but the data reported in the SICADA table are laboratory-derived pH values. It is necessary to have access to the field pH and these should be included in the SICADA extraction routines.

  The pH is very seldom measured in the field. Today it is only measured in the field during the sampling of the soil pipes and these data are included in SICADA. For surface waters the pH is measured in the field with the probe and these data are in the file archive. To extract these data properly from SICADA requires the SICADA personnel.

- Uranium series data from the IFE are probably erroneous in SICADA; they may have been wrongly reported from the IFE or measured insufficiently. Irrespective, in the way the data are now presented they would be better deleted.

  We are investigating if we should send U, Th and the Ra/Rn samples to a laboratory in Scotland instead. Forsmark already have sent some samples to Scotland and are right now evaluating the results.

- The SICADA table, following highlighting of the representative samples, should be checked by the site chemist before finally putting them on the project place.

  The site chemist can only, to a certain degree, check the SICADA table. Primarily to make sure that everything that should be in the table is there and to see if there are some obvious samples that should be ignored or changed. Also, the information put together by the site chemist, prior to both this and the last "datafreeze", contains very useful information about what to expect in the data freeze, for example, deviations, comments from the executers, comments to the QC control etc. The problem right now is that it is all in Swedish but it might be a good idea to translate that information.

- The *in-situ* Eh and pH measurements (CHEMMAC) are very useful and efforts should be made to obtain as many measurements as possible.

  Effort is made to obtain as many measurements as possible.

- Drilling data should be made available at an early stage in order to facilitate DIS modelling. Data requirements are: a) the drilling water volume pumped in and out from the borehole, b) the uranine concentration in the drilling water pumped in and out from the borehole, and c) the water pressure and drawdown along the borehole.

  With respect to points a), b) and c), these data are reported to SICADA during the drilling period and this information is available. The SICADA- personnel can provide these data if needed.

- The monitoring equipment should be more reliable concerning, for example: a) the water pressure sensor, and b) the quality of the uranine concentration in the return water. Frequent flow meter malfunctions should be avoided.

  Point a) this is a question best handled by the Activity leader for Drilling. Point b) samples are taken frequently during drilling and from the returning water during drilling. These samples are analysed at the Äspö laboratory.

- New boreholes at Laxemar will improve hydrogeological boundary conditions and their implications with respect to the relevance of possible regional groundwater flows. Inland hydrogeological and hydrochemical sampling and measurements should be planned to constrain and reduce uncertainties concerning the boundary conditions.

  It is planned that Complete Chemical Characterisation will be performed in boreholes KLX08 and KLX11 at Laxemar. In boreholes KLX05, KLX06 and KLX10 it is planned that water samples from different borehole sections will be taken in connection with the hydrological tests (PSS). In KLX07 and KLX08 water samples will be taken in connection with the swiw-measurements.

- Standard topographical maps in combination with the location of the boreholes are more useful for modelling to make cross-sections, establish hypotheses about recharge or discharge zones etc., compared to colour maps without topographic information.

  Maps of this sort can be found in the various Model version 1.1 documents.

- Future drilling will probably include intersecting large-scale (regional?) fracture zones (e.g. KLX06 at Laxemar); some have already been carried out (e.g. KSH03A at Simpevarp). When adequate volumes of water are available from these zones, analysis of $^{3}He/^{4}He$ and methane ($\delta^{13}C$) would be useful to understand the depth of origin of regional groundwater flow systems.

  The site personnel believe that these parameters are too difficult to analyse.

- Repeated sampling from old boreholes could give confidence in the obtained values but could also indicate effects from dynamic open borehole effects.

  Monitoring of existing boreholes will be performed commencing in 2005. All of the core drilled boreholes will be sampled twice a year (two sections in each borehole). About a third of the percussion drilled boreholes will also be sampled twice a year (one section in each borehole).

- Noble gases (Ar, Kr etc.) from suitable borehole locations might be considered to derive groundwater recharge temperatures and residence times etc.

  Analyses of gases from different sections in the borehole are performed within the activity Complete Chemical Characterisation.

- Surface sampling of ^{4}He (e.g. as carried out at the URL, Whiteshell, Canada) may help to locate major areas of groundwater discharge.

  The site personnel believe that this parameter is too difficult to analyse.

- If possible, the detection limits for the trace element data should be improved upon.

  This will also be investigated further at the site.

Acknowledgements

This study forms part of the SKB site investigation programme, managed and supported by the Swedish Nuclear Fuel and Waste Management Company (SKB), Stockholm. The support and advice from Anders Ström, SKB and Anders Winberg, Conterra AB are acknowledged. The helpful comments by the internal reviewers Mel Gascoyne, GGP Inc., Bill Wallin, Geokema AB and Sten Berglund, SKB improved the work. The helpful interaction with the site chemist Liselotte Ekström, Studsvik is acknowledged.

References

Andersson J., Berglund J., Follin S., Hakami E., Halvarson J., Hermanson J., Laaksoharju M., Rhén I., Wahlgren C-H., 2002. Testing the methodology for site descriptive modelling, Application for the Laxemar area. SKB TR-02-19, Svensk Kärnbränslehantering AB.

Andersson, J., Christiansson, R. and Munier, R., 2001. Djupförvarsteknik: Hantering av osäkerheter vid platsbeskrivande modeller. Tech. Doc. (TD-01-40), SKB, Stockholm, Sweden.

Apps J A. and Van de Kamp PC. 1993. Energy gases of abiogenic origin in the Earth's crust. The future of energy gases. US Geological Survey Prof. Pap. 1570, 81-132.

Banwart, S. (1999). Reduction of iron (III) minerals by natural organic matter in groundwater. Geochim. Cosmochim. Acta, 63, 2919 – 2928.

Banwart, S.; Gustafsson, E. & Laaksoharju, M. (1999): Hydrological and reactive processes during rapid recharge to fracture zones. The Äspö large scale redox experiment. App. Geoch. 14, 873-892.

Bein A, Arad A, 1992. Formation of saline groundwaters in the Baltic region through freezing of seawater during glacial periods. Journal of Hydrology, 140, Elsevier Science B.V., pp75-87.

Berg C., 2003a. Hydrochemical logging in KAV01. Oskarshamn site investigation. SKB P-03-89.

Berg C., 2003b. Hydrochemical logging in KSH02. Oskarshamn site investigation. SKB P-03-88.

Bruno, J., Cera, E., Grivé, M., Rollin, C., Ahonen, L., Kaija, J., Blomqvist, R., El Aamrani, F.Z., Casas, I., de Pablo, J. (1999). Redox Processes in the Palmottu Uranium Deposit. Redox measurements and redox controls in the Palmottu System. (Technical Report), Quantisci, Barcelona, Spain, 76 p.

Bäckblom, G and Stanfors, R., 1989. Interdisciplinary study of post-glacial faulting in the Lansjärv area, northern Sweden. SKB Tech. Rep. (TR-89-31), SKB, Stockholm, Sweden.

Clark, I. & Fritz, P. (1997): Environmental Isotopes in Hydrogeology. Lewis Publishers. Boca Raton, Florida. 328 pp.

Deutsch, W.J., Jenne, E.A. and Krupka, K.M. (1982). Solubility equilibria in basalt aquifers: The Columbia Plateau, Eastern Washington, USA. Chem. Geol., 36, 15-34.

Drake, H and Tullborg E-L., 2004. Fracture mineralogy – results from XRD, microscopy, SEM/EDS and stable isotopes analyses. SKB- P-report , in press.

Frape, S.K., Byrant, G. Blomqvist, R. and Ruskeeniemi, T., 1966. Evidence from stable chlorine isotopes for multiple sources of chloride in groundwaters from crystalline

shield environments. In: Isotopes in Water Resources Management, 1966. IAEA-SM-336/24, Vol. 1, 19-30.

Fontes, J.-Ch., Louvat, D. and Michelot, J.-L. (1989). Some constraints on geochemistry and environmental isotopes for the study of low fracture flows in crystalline rocks - The Stripa case. In: International Atomic Energy Agency (Eds.) Isotopes techniques in the study of the Hydrology of Fractured and Fissured Rocks. IAEA, Vienna, Austria.

Fredén, C., 2002. Berg och Jord, Sveriges Nationalatlas. 208 pp.

Gascoyne, M. (2004). Hydrogeochemistry, groundwater ages and sources of salts in a granitic batholith on the Canadian Shield southeastern Manitoba. Appl. Geochem., 19, 519-560.

Glynn, P.D. and Voss, C.I. (1999). *SITE-94*. Geochemical characterization of Simpevarp ground waters near the Äspö Hard Rock laboratory. (Technical Report SKI R 96-29), SKI, Stockholm, Sweden, 210 p.

Grenthe, I.; Stumm, W.; Laaksoharju, M.; Nilson, A.C. and Wikberg, P. (1992). Redox potentials and redox reactions in deep groundwater systems. Chem. Geol., 98, 131-150.

Grimaud, D.; Beaucaire, C. and Michard, G. (1990). Modeling of the evolution of ground waters in a granite system at low temperature: the Stripa ground waters, Sweden. Applied Geochemistry, 5, 515-525.

Gurban I and Laaksoharju M, 2002. Drilling Impact Study (DIS); Evaluation of the influences of drilling, in special on the changes on groundwater parameters. SKB report PIR-03-02.

Laaksoharju M (ed), Gimeno M, Smellie J, Tullborg E-L, Gurban I, Auqué L, Gómez J. (2004a). Hydrogeochemical evaluation of the Forsmark site, model version 1.1. SKB R-04-05.

Laaksoharju M (editor), Smellie J, Gimeno M, Auqué L, Gomez , Tullborg E-L and Gurban I, (2004b). Hydrochemical evaluation of the Simpevarp area, model version 1.1. SKB Report R 04-16, Stockholm, Sweden.

Laaksoharju M, Skårman C, Skårman E, 1999b. Multivariate Mixing and Mass-balance (M3) calculations, a new tool for decoding hydrogeochemical information. Applied Geochemistry Vol. 14, #7, 1999, Elsevier Science Ltd., pp861-871.

Laaksoharju M, Smellie J, Nilsson A-C, Skårman C, 1995. Groundwater sampling and chemical characterisation of the Laxemar deep borehole KLX02. SKB Technical Report TR 95-05, Stockholm, Sweden.

Laaksoharju M. Degueldre C. Skårman C. 1995. Studies of colloids and their importance for repository performance assessment SKB Technical Report TR-95-24, Stockholm, Sweden.

Laaksoharju, M. & Wallin, B. (1997): Evolution of the groundwater chemistry at the Äspö Hard Rock Laboratory. Proceedings of the second Äspö International Geochemistry Workshop, June 6-7, 1995. SKB, International Cooperation Report 97-04.

Laaksoharju M, Smellie J, Nilsson A-C, Skårman C, 1995a. Groundwater sampling and

chemical characterisation of the Laxemar deep borehole KLX02. SKB Technical Report TR 95-05, Stockholm, Sweden.

Michard, G. (1980). Contrôle des concentrations d'éléments dissous dans les eaux thermales et géothermales. J. fr. Hydrol., **11**, 7-16.

Michard, G. (1987). Controls of the chemical composition of geothermal waters. Chemical Transport in Metasomatic Processes, , 323-353.

Michard, G., Sanjuan, B., Criaud, A., Fouillac, C., Pentcheva, E., Petrov, P.S., Alexieva, R. (1986). Equilibria and geothermometry in hot alkaline waters from granites of SW Bulgaria. *Geochem. J.,* **20**, 159-171.

Molinero, J. & Samper, J. (2004): Modeling Groundwater Flow and Solute Transport in Fracture Zones: Conceptual and Numerical Models of the Redox Zone Experiment at Äspö (Sweden). Journal of Hydraulic Research, 42, 157 – 172.

Molinero, J.; Samper, J.; Zhang, G. & Yang, C.B. (2004): Biogeochemical reactive transport model of the Redox Zone Experiment of the Äspö Hard Rock Laboratory in Sweden. Nuclear Technology, 148, (to appear in Nov. 2004), in press.

Nordstrom, D.K. and Puigdomenech, I. (1986). Redox chemistry of deep ground-waters in Sweden. (Technical Report SKB TR 86-03), SKB, Stockholm, Sweden, 30 p.

Parkhurst, D. L. and Appelo, C.A.J. (1999). User's Guide to PHREEQC (Version 2), a computer program for speciation, batch-reaction, one-dimensional transport, and inverse geochemical calculations. U.S. Geological Survey Water-Resources Investigations Report 99-4259, 312 p.

Pitkänen, P., Partamies, S. and Luukkonen, A. (2004). Hydrogeochemical interpretation of baseline groundwater conditions at the Olkiluoto Site. (Technical Report POSIVA 2003-07), POSIVA, Helsinki, Finland, 159 p.

Pitkänen, P.; Luukkonen, A.; Ruotsalainen, P.; Leino-Forsman, H. and Vuorinen, U. (1998). Geochemical modelling of groundwater evolution and residence time at the Kivetty site. POSIVA Report 98-07, Helsinki, Finland, 139 p.

Pitkänen, P.; Luukkonen, A.; Ruotsalainen, P.; Leino-Forsman, H. and Vuorinen, U. (1999). Geochemical modelling of groundwater evolution and residence time at the Olkilouto site. POSIVA Report 98-10, Helsinki, Finland, 184 p.

Rhen, I. and Smellie, J., 2003. Task force modelling of groundwater flow and transport of solutes. Task 5 summary report. SKB Tech. Rep. (TR-03-01), SKB, Stockholm, Sweden. (ISSN 1404-0344).

Samper, J.; Delgado, J.; Juncosa, R. & Montenegro, L. (2000): CORE^{2D} v 2.0: A Code for non-isothermal water flow and reactive solute transport. User's manual.ENRESA Technical report 06/2000.

SKB (2002): Simpevarp – site descriptive model version 0. SKB R-02-35.

Smellie J and Laaksoharju M, 1992. The Äspö hard rock laboratory: final evaluation of the hydrogeochemical pre-investigations in relation to existing geologic and hydraulic conditions. SKB Technical Report TR 92-31, Swedish Nuclear Fuel and Waste Management Co., Stockholm, Sweden, 239 p.

Smellie, J, Laaksoharju, M and Tullborg, E-L (2002) Hydrochemical site descriptive model – a stategy for the model development during site investigation. SKB R-02-49.

Smellie, J. & Tullborg, E-L (2004): Explorative analysis, expert judgement and modelling. In: Hydrochemical evaluation of the Simpevarp area, model version 1.1. Appendix 1. SKB R-04-16.

Smellie, J.A.T. and Wikberg, P., 1989. Hydrochemical investigations at the Finnsjön site, central Sweden. J. Hydrol., 126, 147-169.

Smellie, J.A.T., Larsson, N-Å., Wikberg, P. and Carlsson, L., 1985. Hydrochemical investigations in crystalline bedrock in relation to existing hydraulic conditions: Experience from the SKB test-sites in Sweden. SKB Tech. Rep. (TR-85-11), SKB, Stockholm, Sweden.

Smellie, J.A.T., Larsson, N-Å., Wikberg, P., Puigdomenech, I. and Tullborg, E-L., 1987. Hydrochemical investigations in crystalline bedrock in relation to existing hydraulic conditions: Klipperås test-site, Småland, southern Sweden. SKB Tech. Rep. (TR-87-21), SKB, Stockholm, Sweden.

Svensson U, 1996. SKB Palaeohydrogeological programme. Regional groundwater flow due to advancing and retreating glacier-scoping calculations. In: SKB Project Report U 96-35, Stockholm, Sweden.

Tullborg E-L, and Larson S. Å. (1984). δ18O and δ13C for limestones, calcite fissure infillings and calcite precipitates from Sweden. Geologiska föreningens i Stockholm förhandlingar 106(2).

Trotignon, L., Beaucaire, C., Louvat, D. and Aranyossy, J.F. (1999). Equilibrium geochemical modelling of Äspö groundwaters: a sensitivity study of thermodynamic equilibrium constants. Appl. Geochem., 14, 907-916.

Trotignon, L., Beaucaire, C., Louvat, D. and Aranyossy, J.F. (1997). Equilibrium geochemical modelling of Äspö groundwaters: a sensitivity study to model parameters. In: Laaksoharju, M. and Wallin, B. (Eds.) Evolution of the groundwater chemistry at the Äspö Hard Rock Laboratory. (Report SKB 97-04), SKB, Stockholm, Sweden.

Wacker P., Berg C., Bergelin A., 2004. Complete hydrochemical characterisation of KSH01A. SKB P report in print.
Wacker, P. 2003a. Oskarshamn site investigation. Hydrochemical logging in KSH01A. SKB P-03-87.

Westman, P., Wastegård, S., Schoning K.and Gustafsson, B. 1999: Salinity change in the Baltic Sea during the last 8 500 yearsw: evidence causes and models. SKB TR 99-38.

Wikberg P, 1998. Äspö Task Force on modelling of groundwater flow and transport of solutes. SKB progress report HRL-98-07.

Appendix 1: Explorative analysis and expert judgement of major components and isotopes

Contribution to the model version 1.2

John Smellie [1)] Eva-Lena Tullborg [2)]

Conterra AB, Stockholm [1)]

Terralogica AB, Göteborg [2)]

November 2004

Contents

1 Geological and hydrogeological setting

1.1 Regional geology

The Simpevarp site is located at the Baltic coast some 2-3 kilometres SSE of Äspö island and 3-4 kilometres WSE from Laxemar (Fig. 1-1). The area forms part of the TransScandinavian Igneous Belt of Precambrian basement rocks (dated to around 1.8 Ga) dominated by granitoids which, at Simpevarp, comprise rocks ranging from red/grey granite (i.e. Ävrö granite) to grey quartz monzodiorite. A weak foliation is mostly observed. These rocks are usually medium-grained but with some fine-grained and porphyritic varieties. Along the south-east part of the Simpevarp peninsula a grey-coloured, fine-grained variety of quartz monzodiorite occurs and a sub-volcanic origin has been proposed. Because of its close relationship with the quartz monzodiorite and similarity in composition, the term dioritoid has been suggested. Small amounts of aplitic (named fine-grained granite), dioritic and gabbroic rock-types also occur sporadically in smaller bodies. Transecting all above-named rock-types are dykes characterised by fine- to medium-grained granite and pegmatites.

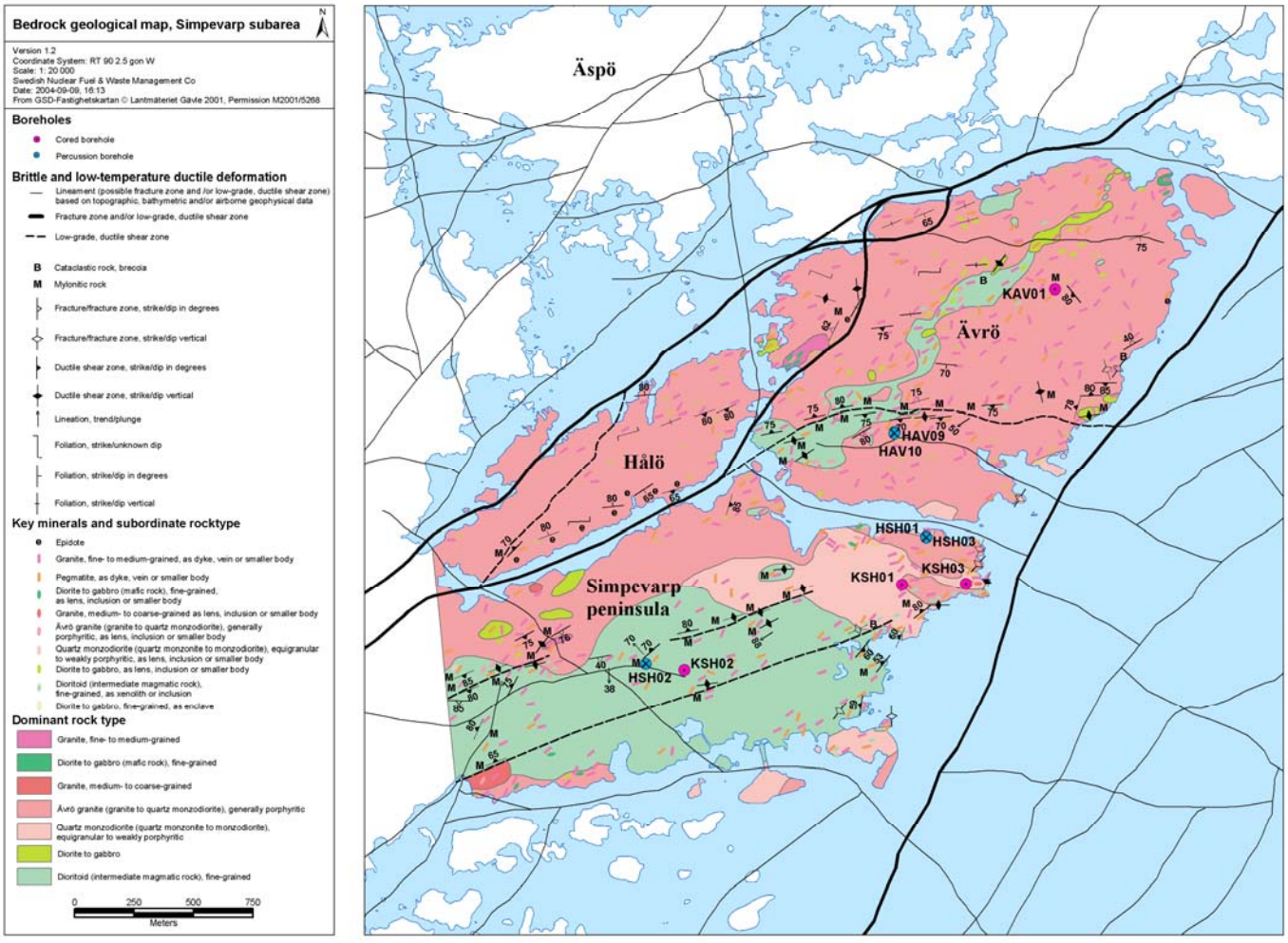

Figure 1-1: *Geological setting at the Simpevarp site.*

All rock-types have also been subjected to alteration (red staining caused by disseminated micrograins of haematite) largely due to post-crystallisation penetration of hydrothermal fluids along pre-existing zones of weakness (e.g. fractures).

On a regional scale NE-SW oriented deformation zones are dominant. Completing the structural network are mostly discontinuous E-W and NW-SE oriented regional deformation zones. At the local scale, the Simpevarp site is bounded to the west and east by the large-scale regional NE-SW deformation zones aligned sub-parallel to the coast, and to the north and south by the approximately NW-SE and NE-SW oriented deformation zones.

1.2 Regional hydrogeology

The net precipitation at Simpevarp is set to 165 mm/y (i.e. within a possible interval of 150-180 mm/y), and this water penetrates the groundsurface where most of it flows near the surface in the soil layers (and possibly in the upper most part of the rock surface if more fractured) eventually forming streams, lakes and wetlands. An estimated 1-10 mm/year is recharging into the rock near the bedrock surface; at greater depths the flux decreases (Ingvar Rhén, per. comm., 2004).

At the local site-scale, the groundwater circulation is controlled by small flow-lines to great depth (i.e. 1000 m) determined by the relatively flat but irregular topography. Regional large-scale groundwater circulation (hundreds of kilometres) is not expected to play an important role at Simpevarp.

1.3 Borehole locations and drilling

The borehole locations are shown in Figure 1-1 but in more detail in Figure 1-2. The main focus of this Simpevarp v.1.2 evaluation are boreholes KSH01A, KSH02 and KSH03A and B located at the edge of the OKG Nuclear Power Facility to the east close to the Baltic Sea coast.

The first attempt to obtain flushing water for drilling borehole KSH01A failed with percussion borehole HSH01 (insufficient capacity); a second attempt with percussion borehole HSH03 (0-201 m) was successful. For borehole KSH02, located close to the western side of the OKG complex and slightly further from the Baltic Sea, percussion borehole HSH02 (0-200 m) supplied adequate flushing water. Borehole KSH03A, B, angled to intercept the regional deformation zone parallel to the coast, was drilled also using flushing water from percussion borehole HSH03 (0-201 m).

Also shown in Figure 1-2, and included in this evaluation, are data from existing cored boreholes representing the Laxemar site (KLX01 and KLX02), and the Ävrö site (KAV01 and KAV04). These two locations form part of the POM group of investigated sites – Äspö, Laxemar, Ävrö, Oskarshamn and Bockholmen – in the vicinity of Simpevarp.

1.4 Fracture filling studies

Central issues in groundwater evaluation are the nature and influence of the fracture mineral fillings on the groundwater chemistry under equilibrium and near-equilibrium hydrogeochemical conditions, and the influence of changing groundwater chemistries (e.g. external effects such as glaciations) on the type and chemistry of the fracture fillings.

Figure 1-2: *Location of hydrogeochemically prioritised boreholes KSH01A, KSH02 and KSH03A, B together with the respective flushing water percussion boreholes HSH02 and HSH03. Also indicated are boreholes KLX01 and KLX02 (Laxemar) and KAV01 (Ävrö) which represent two of the POM sites used in the Simpevarp evaluation.*

Fracture minerals are initially documented during mapping of the drillcore which forms an integral part of the bore map system used in the site characterisation protocol. Based on this information, fracture filling phases are further selected for more detailed study which involves:

- X-ray diffractometry; especially used for identification of clay minerals and gouge material. A total of 23 samples from the Simpevarp area have been analysed by XRD.
- Microscopy of fracture fillings; around 30 fractures from KSH01A+B have been sampled and 30 thin sections and 5 fracture surfaces have been studied by SEM. (Drake and Tullborg, 2004, in press).
- Isotopic analyses ($\delta^{13}C$ and $\delta^{18}O$) of fracture calcites sampled from borehole KSH01 A+B have also been carried out (Drake and Tullborg, 2004, in press)

The most common fracture minerals at the Simpevarp site are chlorite and calcites which occur in several different varieties and are present in most of the open fractures. Other common minerals are epidote, prehnite, laumontite, quartz, adularia (low-temperature K-feldspar), fluorite, haematite and pyrite. A Ba-zeolite named harmotome has been identified in some fractures and apophyllite more rarely has been identified. Gypsum (small amounts) has been identified in two fractures from KSH03A.

Clay minerals identified, in addition to chlorite, comprise a) corrensite (mixed layer chlorite/smectite or chlorite/vermiculite clay; the smectite or vermiculite layer are characterised by swelling properties), b) illite, mixed-layer illite/smectite (swelling), and c) a few observations of smectites.

Sample selection, preparation and results from the XRD analysis and from microscopy and SEM studies are presented in Appendix 1.

The fracture mineralogy as revealed in drillcore KSH01A+B (Fig. 1-3) shows several generations of mineralisation ranging from epidote facies (epidote, albite, quartz, calcite pyrite and muscovite) in combination with ductile deformation, to brittle deformation in combination with oxidation and formation of haematite, causing extensive red staining of the wall rock along the fractures. Subsequent breccia sealing by prehnite-fluorite, calcite and Fe-Mg chlorite has occurred followed by adularia, haematite, Mg-chlorite and calcite formation. The latest hydrothermal mineralisation has resulted in, with decreasing temperature, the formation of Mg-chlorite, adularia, laumontite (Ca-zeolite), pyrite, haematite, harmotome (Ba-zeolite), Fe-chlorite (sperulitic), calcite + REE-carbonates and clay minerals.

The outermost coatings along the hydraulically conductive fractures consist mainly of clay minerals (illite and mixed layer clays; corrensite = chorite/smectite and illite/smectite) together with calcite and minor grains of pyrite (Fig. 1-4). It is assumed that especially the calcite and pyrite formation are ongoing processes although the amounts of possible recent precipitates are low.

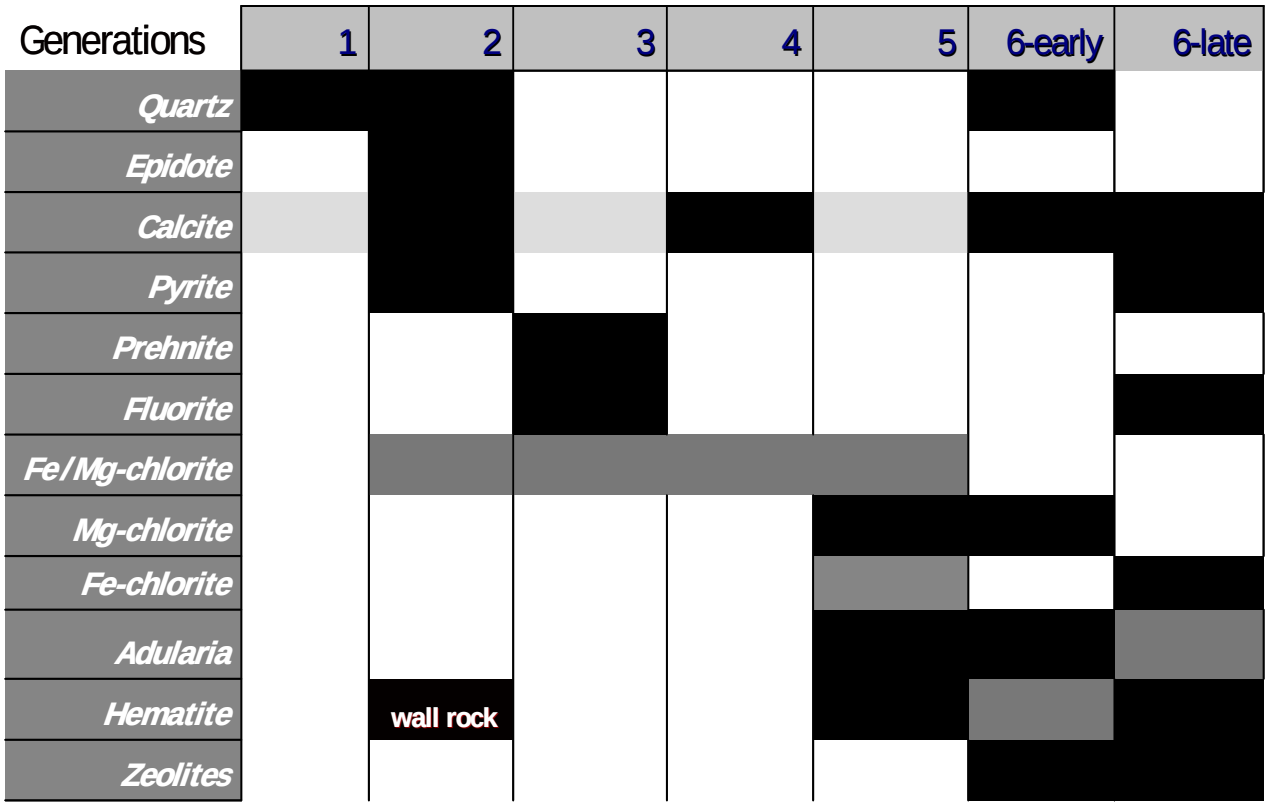

Figure 1-3. *Compiled results showing the paragenesis of different generations determined from microscopy and SEM/EDS (Drake and Tullborg, 2004, in press).*

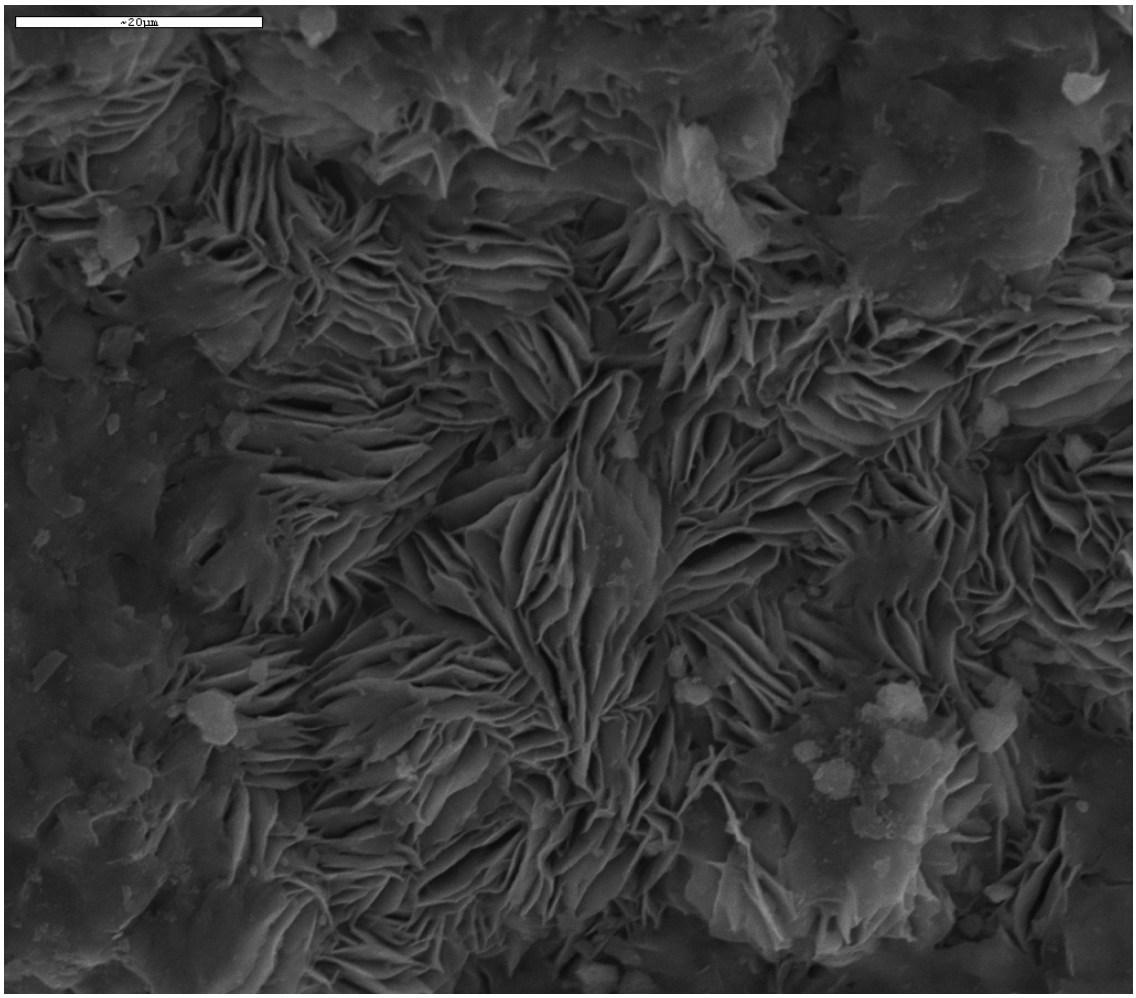

Figure 1-4. *SEM photo showing mixed layer clay on a fracture surface from KSH01A (scale bar = 20 mm); Drake and Tullborg (2004, in press).*

From the fracture filling studies it can be concluded that:

- The overall fracture mineralogy is very similar to earlier observations in the Äspö HRL (e.g. Landström and Tullborg 1995; Andersson et al., 2002).
- Drillcore KSH01A+B is well preserved (flushing and grinding have been minimised), which has facilitated sampling of relatively undisturbed clay mineral samples. Furthermore, calcite and pyrites formed on the fracture edge as well as soft or brittle zeolites minerals have been possible to study. This has, for example, resulted in the identification of the previously overlooked Ba-zeolite harmotome.
- The red staining of the wall rock around many fractures and fractures zones corresponds to hydrothermal alteration/oxidation, which has resulted in saussuritisation of plagioclase, breakdown of biotite to chlorite and oxidation of Fe(II)

to form haematite, mainly present as micrograins giving the red colour. However, there is not always a perfect agreement between the extent of hydrothermal alteration and red staining (Landström et al., 2001).

- Within the fractures several generations of haematite and pyrite are present. The identification of small pyrite grains in the outermost layers of the fracture coatings are in agreement with the present reducing groundwater in the Simpevarp area. More detailed studies of redox sensitive minerals and the timing of the hydrothermal oxidation is ongoing.

- It has so far not been possible to tie different fracture minerals to different fracture orientations. Previously this has proven difficult within the large data set from Äspö (Munier; 1993).

- The sequence of mineral paragenesis shows the transition from epidote facies in combination with ductile deformation over to brittle deformation and breccia sealing during prehnite facies and subsequent zeolite facies.A further decreasing formation temperature series indicate that the fractures were initiated relatively early in the geological history of the host rock and have been reactivated during several different periods under various physiochemical conditions.

- The locations of the hydraulically conductive fractures are mostly associated with the presence of gouge filled faults produced by brittle reactivation of earlier ductile precursors or hydrothermally sealed fractures. The outermost coatings along the hydraulically conductive fractures consist mainly of clay minerals usually illite and mixed layer clays (corrensite = chorite/smectite and illite/smectite) together with calcite and minor grains of pyrite.

2 Groundwater quality and representativeness

Prior to any hydrochemical evaluation is the necessity to judge the quality and the representativeness of the groundwater data derived from the site characterisation in question. The thoroughness of this exercise may vary depending on the eventual use of the data, for example, high quality groundwater data are required for geochemical equilibrium reaction modelling, whilst semi-quantitative data may suffice to model large-scale variations in groundwater chemistry or distinguish time-series chemical trends. The hydrogeochemical evaluation approach used at Simpevarp and the uncertainties involved are based on the methodology outlined in SKB R-02-49.

Evaluation of the Simpevarp hydrogeochemical data in Model v. 1.2 entails comparison with other geographically located sites in its near-vicinity, i.e. the so-called 'POM' sites (***P***latsundersökningar i ***O***skarsha***M***n), namely Äspö, Laxemar, Ävrö, Oskarshamn and Bockholmen, and also other Fennoscandian sites such as Forsmark and Olkiluoto. Groundwater data from all these sites are compiled in the 'Nordic Table' and these data also have been evaluated with respect to representativeness. This was carried out in parallel to the Simpevarp and Forsmark v. 1.2 data evaluations and further illustrated in Appendices 2 and 3 to this report. Details of the Forsmark v. 1.2 data evaluation will be documented in a later report.

2.1 Simpevarp site

The Simpevarp groundwater analytical data compiled in the SICADA database, which form the basis to the hydrochemical evaluation, will have already undergone an initial screening process by field and laboratory personnel based on sampling, sample preparation and analytical criteria. The next stage in the hydrogeochemical site descriptive process, the focus of this report, is to assess these screened data in more detail to derive a standard set of representative groundwater data for hydrogeochemical modelling purposes.

For this assessment the initial most important stage is to check for groundwater contamination. To accomplish this an intimate knowledge of the borehole site is required which entails borehole geology and hydrogeology and a detailed log of borehole activities. These latter activities are a major source of groundwater contamination and include:

- drilling and borehole cleaning;
- open hole effects;
- downhole geophysical/geochemical logging;
- downhole hydraulic logging/testing/pumping, and
- downhole sampling of groundwaters.

In Chapters 3-5 in this report these potential sources of contamination have been addressed and documented systematically for each borehole drilled and for each borehole section sampled. Where applicable, use has been made of results from the Drilling Impact Study (DIS) (Gurban and Laaksoharju, 2004). The degree of contamination has been judged, for example, by plotting tritium against percentage drilling water (cf. section 7.4.1; Fig. 7.4-3) and using measured values with specifically defined limits, i.e. charge balance (±5%) and

drilling water component (<1%), and supported qualitatively by expert judgement based on detailed studies of the distribution and behaviour of the major ions and isotopes.

The final selection of data which best represents the sampled borehole section is based on identifying as near as possible a complete set of major ion and isotope (particularly tritium, ^{18}O and deuterium) analytical data. This is not always the case, however, and a degree of flexibility is necessary in order to achieve an adequate dataset to work with. For example:

- A charge balance of ±5% was considered acceptable. In some cases groundwaters were chosen when exceeding this range to provide a more representative selection of groundwaters. These groundwaters should therefore be treated with some caution when used in the modelling exercises..
- In many cases the drilling water content was either not recorded or not measured. Less than 1% drilling water was considered acceptable. In some cases groundwaters were chosen when exceeding this range to provide a more representative selection of groundwaters. These groundwaters also should be treated with some caution when used in the modelling exercises.
- Some of the older tritium data were analysed with a higher detection limit of 8TU; the detection limit lies around 0.02TU for recent anlayses. For some groundwaters an approximate tritium value is suggested where no recorded value is available. This value is selected normally from the same borehole section but representing an earlier or later sample.

Appendix 2 shows a summary of the Simpevarp data, together with the POM sites, indicating the use of selected criteria (charge balance; drilling water content; tritium content) to identify the samples considered representative. Resulting from this assessment, two groundwater sample types are highlighted in the SICADA database: one type considered representative, the other type less representative but suitable when used with caution.

2.2 Nordic sites

The Nordic sites, in addition to Simpevarp and the POM sites, comprise Forsmark and all remaining Swedish sites studied over the last 20-25 years; Olkiluoto in Finland is also included. Most of these sites have undergone earlier detailed assessments as to groundwater quality and representativeness, e.g. Gideå, Kamlunge, Klipperås, Fjällveden, Svartboberget, Finnsjön (Smellie et al., 1985, 1987; Smellie and Wikberg, 1989), Lansjärv (Bäckblom and Stanfors, 1989) and Olkiluoto (Pitkänen et al., 1999, 2004). Based on this information the Nordic Table has been highlighted with respect to representative and less representative groundwater samples, similar to the POM sites referred to above in section 2.1.

The ‘less’ representative groundwaters do not meet all of the criteria for representativeness but are sufficiently important to be included (Appendix 3). The importance of early or ‘First Strike’ samples is emphasised in this evaluation. These are coloured green in the Nordic Table and involve one or more of the following deviations from being considered ‘representative’:

- lack of important ions – especially Br;
- lack of ^{18}O and deuterium data;
- variation in salinity during the time-series measurements; and
- few or an absence of time-series measurements.

The representative groundwaters are highlighted in the Nordic Table in orange. Some, however, lack bromine data, and these are highlighted in Appendix 3 also using orange font.

3 Borehole KSH01A

Borehole KSH01A was drilled to a depth of 1003 m at an inclination of 80.6° C to the horizontal and cased to 100.24 m.

3.1 Geological and hydrogeological character

Borehole KSH01A penetrates different rock units (Fig. 3.1). The main rock type in the upper part of the borehole (to 345 m) is the quartz monzodiorite with smaller volumes of dioritoid at 205-245 m and 325-340 m; larger amounts of dioritoid occur from 345-630 m. At greater depths to 1000 m are found granitic to granodioritic rocks (Ävtö granite) mixed with quartz monzodiorite. Smaller horizons of fine-grained granite occur at 360-365 m (mixed with pegmatite), 680-690 m and 720-730 m (mixed with mafic rocks) and 860-870 m. Large lengths of the drillcore show an increased fracture frequency accompanied by intense wall rock alteration/oxidation. This is most prominent in sections 250-285 m, 420-450 m and 590-630 m. Below 700 m the fracture frequency is significantly lower and only a slight alteration of the rock is observed.

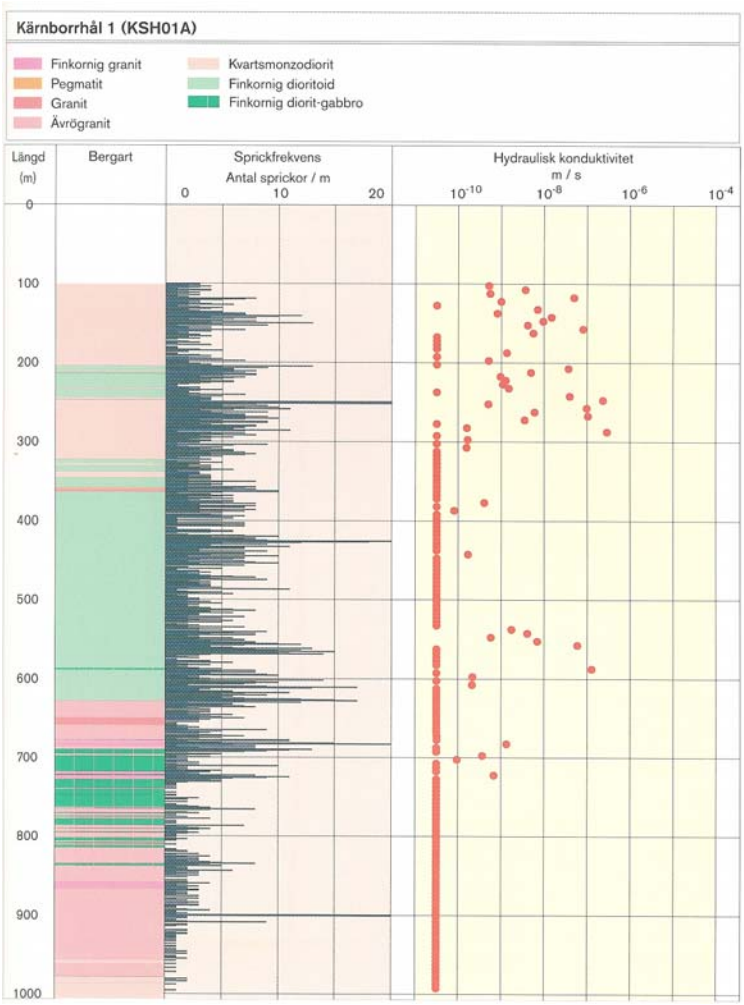

Figure 3-1: *Integrated geology, fracture frequency and hydraulic conductivity along borehole KSH01A*

The differential downhole flow measurements reveal a hydraulic conductivity of 10^{-9}-$10^{-6.5}$ ms^{-1} from 100 m (extent of the casing) to 300 m. At greater depths, to approx. 700 m depth, conductivities decrease to 10^{-10}-10^{-9} ms^{-1}; one major exception occurs from 540-600 m (10^{-10}-$10^{-6.5}$ ms^{-1}) which represents one of the groundwater sampling locations at 548-565 m.

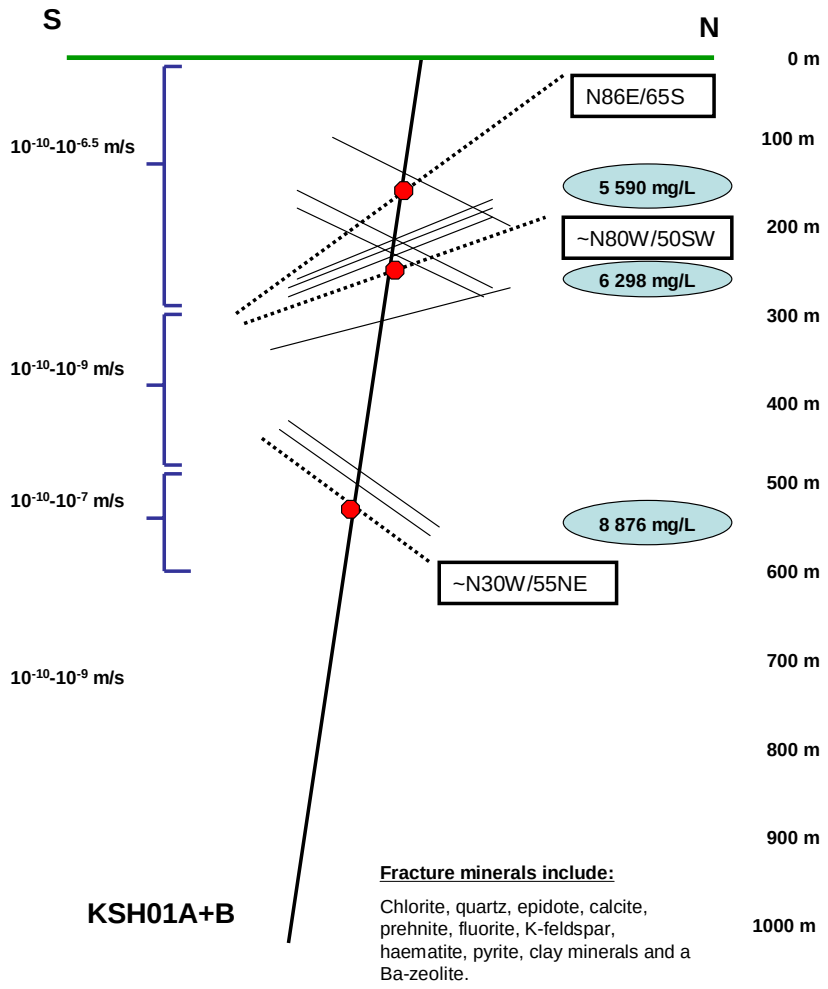

Figure 3-2: *Borehole KSH01A+B showing intercepted structures and their hydraulic conductivities; groundwater sampling locations are indicated in red with the mg/L chloride content in blue.*

Figure 3-2 represents a schematic representation of borehole KSH01A+B and the intercepted structures and their hydraulic conductivities; groundwater sampling locations are indicated in red and the sampled mg/L chloride contents are shown in blue. Drillcore mapping and available downhole BIPS measurements show that both sub-vertical and sub-horizontal fractures occur but the former structures are clearly dominant; this is partly due to the vertical orientation of the borehole.

Fractures are especially frequent in the upper 300 m of the borehole (see also Fig. 3-1) trending northwest and dipping mostly to the south and southwest. Lower intensity fracturing of similar trend but dipping to the northeast occurs between 550-600 m; at around 700 m a major isolated fracture trends northeast dipping to the west.

As presented in section 1.4, the fracture minerals identified are chlorite, calcite, epidote, quartz, low temperature K-feldspar (adularia), prehnite, laumontite, albite, fluorite, Ba-zeolite (harmotome), barite, pyrite, titanite, anatase/rutile, apatite, muscovite, hematite, apophyllite, REE-carbonate, amphibole, ilmenite and clay minerals, dominantly illite, mixed layer clays (illite-smectite), corrensite and to lesser degree smectite. Rarely, additional sulphides like chalcopyrite, galena and sphalerite have been found.

Several generations of fracture mineralisations have been identified ranging from quartz (probably associated with post-magmatic circulation) to epidote facies (epidote, albite, quartz, calcite, pyrite, Fe-Mg chlorite, titanite and muscovite) in combination with ductile deformation (leading to epidote mylonite) associated with oxidation and formation of haematite causing extensive red staining of the wall rock adjacent to the fractures. The epidote mylonite has been later reactivated by a brittle deformation phase. Subsequent breccia sealing by prehnite-fluorite, calcite and Fe-Mg chlorite has occurred followed by andularia haematite, harmontone (Ba-zeolite), Fe-chlorite (spherulite), calcite + REE-carbonates and clay minerals. The outermost coatings along the hydraulically conductive fractures consist mainly of clay minerals of mixed layer clay type (corrensite = chlorite/smectite) together with calcite and minor grains of pyrite.

Figure 3-3 shows BIPS-images from KSH01A locating the major water-conducting fractures which probably have contributed to most of the groundwaters sampled from borehole sections 156-50-167.00 m and 245.00-261.50 m. Striking is the amount of clay preserved in the fractures following triple-tube drilling; during normal core drilling this would otherwise have been flushed out and lost. Detailed mineralogical examination of these two zones revealed the following:

- One dominating fracture occurs at 159.50 m (section 156.50-167.00 m) with an orientation of N65E/65 S and with several millimetre thick fillings of chlorite and clay minerals of mixed layer clay type including layers of chlorite and smectite/vermiculite. The filling is rich in calcite and some equigranular calcite crystals were identified. Also minute pyrite crystals were found in the clay filling. One additional fracture at 161.3 m with an orientation of N86W/76N was also identified in the sampled section, this is however subordinate to the one at 159.50 m.

- The entire section (245-261.50 m) represents an altered and oxidised section of the bedrock and several open fractures were identified from the BIPS. There was also a several decimetre long zone at 251 m with intense chemical alteration and clay formation which is at the centre of the sampled fracture zone. It is difficult to exactly pinpoint the water-conducting parts from the differential flow log and very surprisingly the water flow seems to be low (because of the large clay content?). The minerals identified in the zone are chlorite, mixed layer clays with chlorite-smectite/vermiculite layers, adularia, haematite, quartz and calcite. The orientation of this structure can not be evaluated from the BIPS-images.

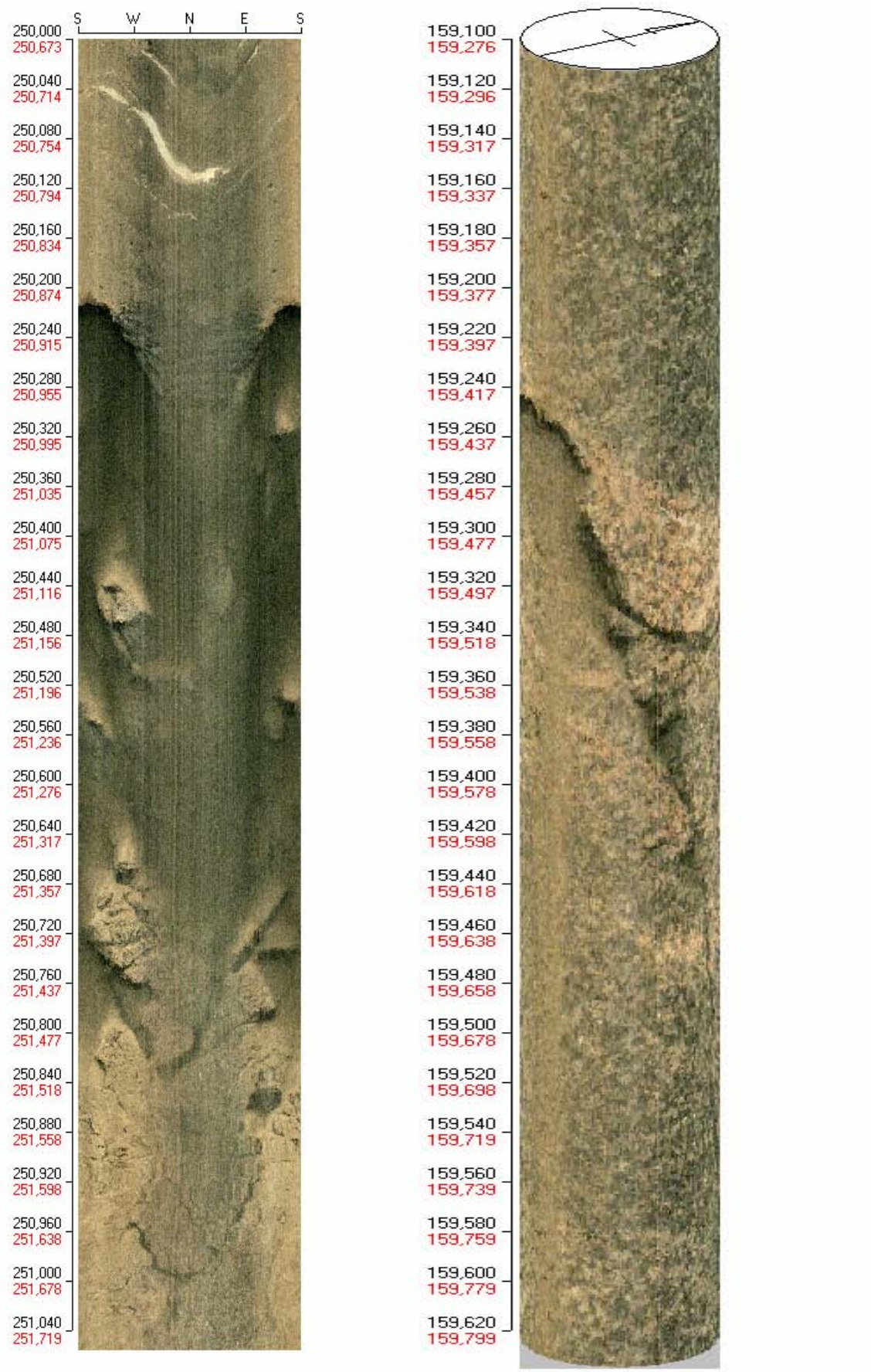

Figure 3-3a: *BIPS-images from KSH01A showing the probable main water-conducting open fractures sampled from borehole sections 156-50-167.00 m and 245.00-261.50 m.*

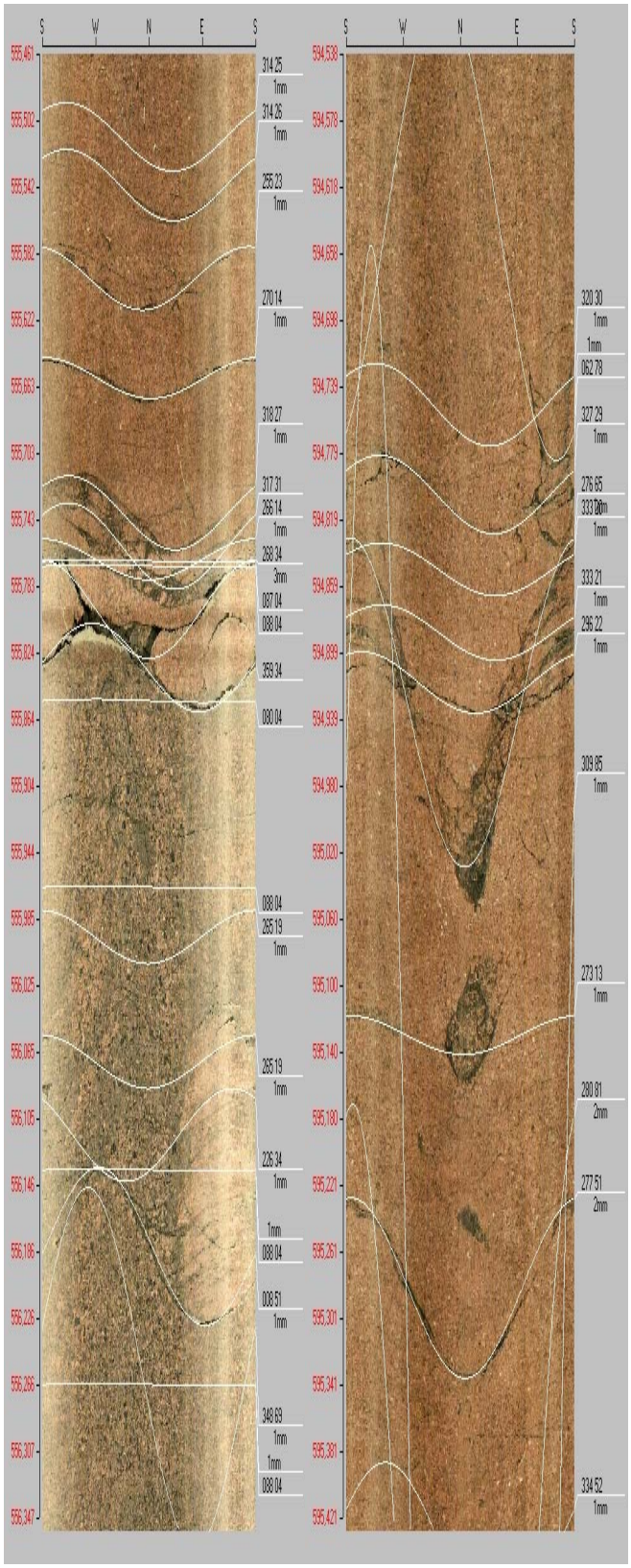

Figure 3-3b: *BIPS-images from KSH01A showing a water-conducting open fracture sampled from borehole sections between 548.00-565.00 m.*

Borehole KSH01A is cased to 100.24 m depth which excludes BIPS and differential Flow Meter data from this length. As described above for Figure 3-1, hydraulic conductivities range from 10^{-10}-$10^{-6.5}$ ms^{-1} in the upper 300 m to 10^{-10}-10^{-9} ms^{-1} from 300-500 m and increasing to 10^{-10}-10^{-7} ms^{-1} from 500-600 m; at around 700 m values decrease again to 10^{-10}-10^{-9} ms^{-1}. From 725 m to the hole bottom at 1003 m no data are available indicating very low hydraulic conductivities and a hydraulically tight bedrock. Figure 3-4a also indicates the hydraulic head values and Figure 3-4b indicates the measured groundwater flow rates (and directions relative to the borehole) during pumping and under natural flow conditions.

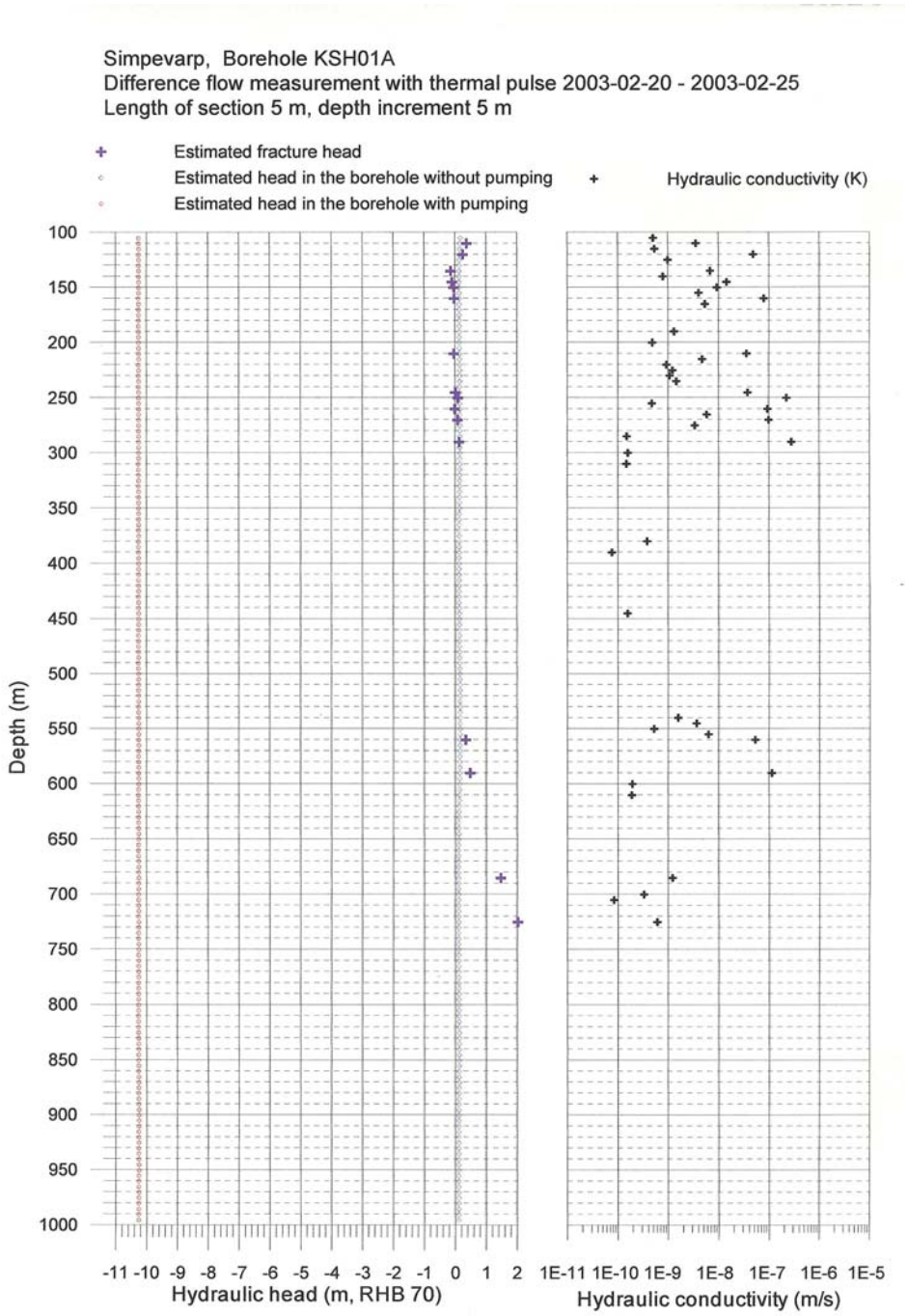

Figure 3-4a: *Differential flow meter measurements along borehole KSH01A (100.24 to 1003 m) of hydraulic head and conductivity.*

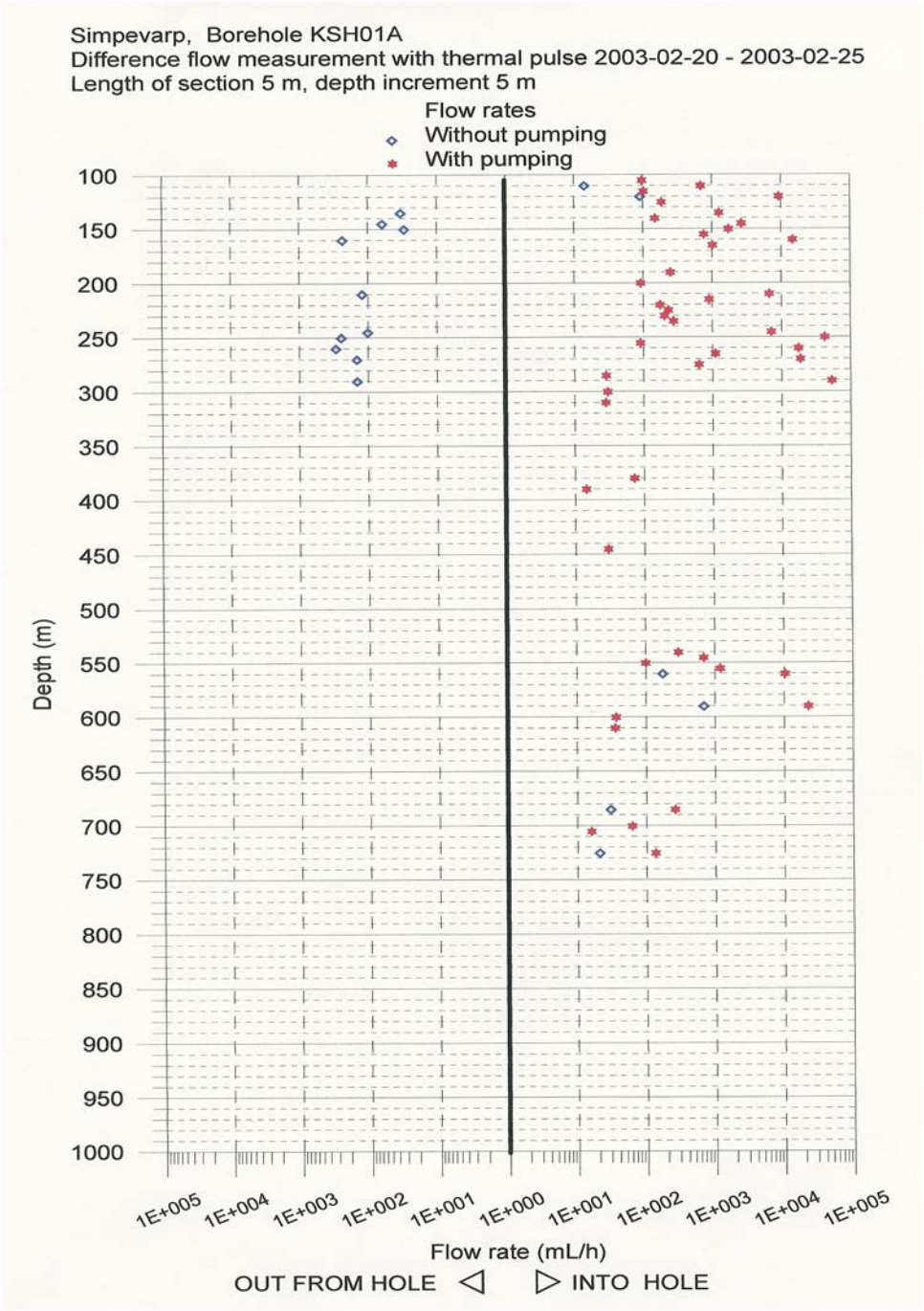

Figure 3-4b: *Differential flow meter measurements along borehole KSH01A (100.24 to 1003 m) of groundwater flow rate (mL/h) into and out of the borehole.*

The recorded rates of groundwater flow under 'natural' hydraulic conditions (i.e. no pumping) via fractures into the borehole from the surrounding bedrock, and conversely from the borehole into the bedrock, indicate that water movement is mostly out from the borehole to the surrounding bedrock in the upper 300 m and from the bedrock to the borehole from 300-750 m (Fig. 3-4b). From 750 m to the hole bottom the absence of data suggest a very tight, low transmissive bedrock. During pumping all movement of formational groundwater is into the borehole. Under open hole conditions, therefore, given strong hydraulic gradients, formation groundwater would be expected to leave the borehole at shallower depths where there is an increase in hydraulic conductivity coinciding with the location of the KSH01A sampling sections, and enter the borehole

at the 550-600 m level where the hydraulic conductivity increases to around 10^{-7} ms^{-1}. Because of the very low hydraulic conductivities at depths greater than 600 m ($<10^{-9}$ ms^{-1}) it is very doubtful that any open-hole circulation is active along this length and any drilling water would tend to be trapped.

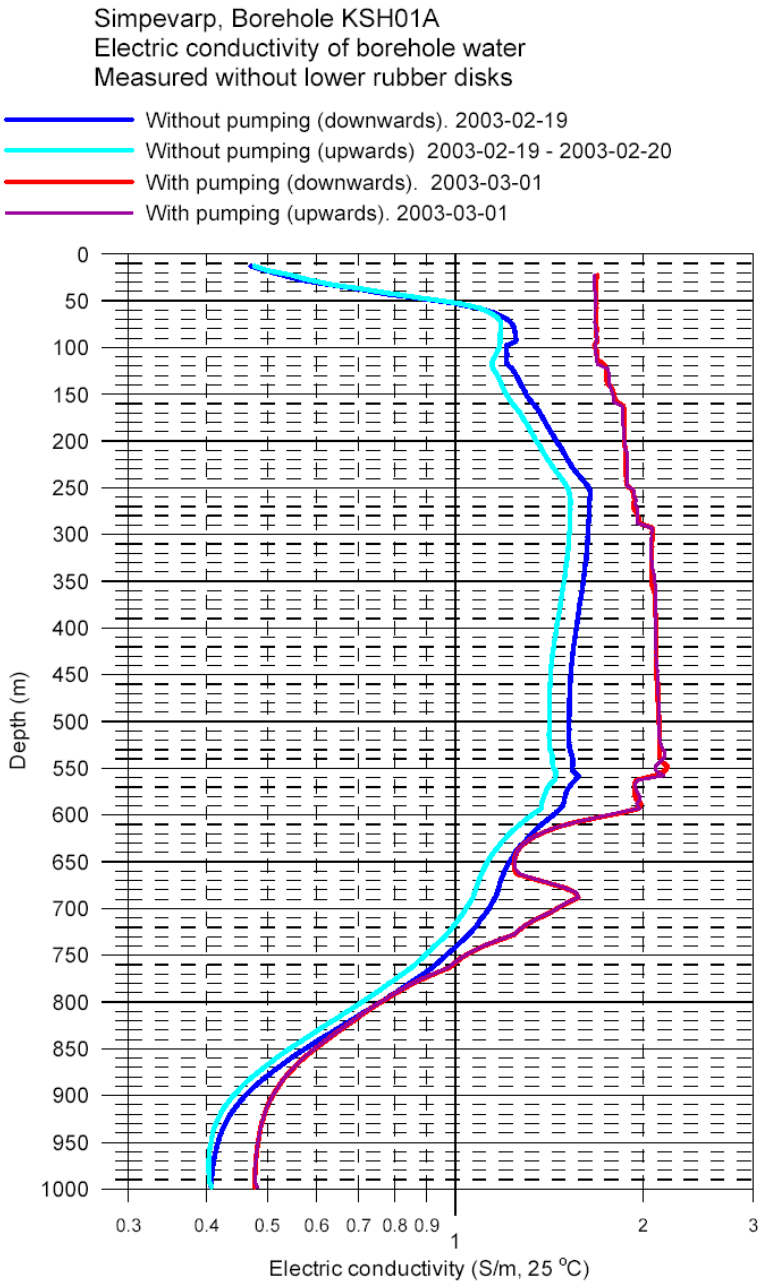

Figure 3-5: *Electrical conductivity log for borehole KSH01A during open hole conditions.*

Figure 3-5 shows downhole electrical conductivity (EC) measurements from borehole KSH01A during open hole conditions; the upper 100 m is not relevant as it relates to the cased borehole section. Considering the more natural flow conditions without pumping (blue lines), at 100 m depth the EC values are around 1.3 Sm^{-1} and this is maintained to around 550 m. At this depth there is a steady downward trend to lower salinities

ultimately achieving 0.4 Sm^{-1} at the hole bottom. These trends, closely reflected by the pumped values, emphasise the inflow (see Fig, 3-4b) and homogenisation of groundwater salinity in the upper 500 m of the borehole corresponding to generally higher hydraulic conductivities. The marked decrease in salinity in the deeper 500 m of the borehole is a result of the accumulation of flushing water from percussion borehole HSH03 during drilling activities. Following drilling, no nitrogen gas lift pumping was carried out to flush/clean the borehole. The flushing water is dilute (~ 450 mg/L Cl) and Na (Ca)-HCO_3 (Cl) in type, and was not removed.

3.2 Groundwater quality and representativeness

Borehole KSH01A was drilled to a depth of 1003 m at an inclination of 80.6^o C to the horizontal and the flushing water was obtained from percussion borehole HSH03 (0-200 m). The chemistry of this water shows it to be basically a fresh to slightly brackish Na(Ca)-HCO_3(SO_4-Cl) type with a chloride content of approx. 500 mg/L. Tritium varies from 4.7-10 TU.

3.2.1 Available data

Available data included:

- Borehole activity logs
- Chemmac on-line monitoring data of O_2, Eh, electrical conductivity and temperature
- Groundwater chemistry from open hole tube sampling
- Groundwater chemistry from isolated borehole sections

NB. Only some on-line monitored *in-situ* field pH values were measured; most recorded pH values are laboratory-derived and lie about 0.6 pH units under the *in-situ* values.

3.2.2 Borehole activity logs

The downhole activity log for borehole KSH01 relating to potential groundwater disturbances, is given below. Samples highlighted by red font were taken during drilling (i.e. using wireline techniques), open hole tube sampling is highlighted by green font, and sampling following borehole completion from pre-determined packed-off borehole sections is denoted by blue font.

Activity	Date	Comments
Core drilling (KSH01A)	2002-08-22 to 2003-01-17	100.24-1003.00 m
Water sampling	*2002-10-24*	*Wireline (197.00-313.42 m)*
Water sampling	*2002-11-16*	*Wireline (585.00-593.00 m)*
Water sampling	*2002-11-20*	*Wireline (531.00-619.42 m)*

Core drilling (KSH01B)	2003-01-17 to 2003-01-25	0-100.25 m
Tube sampling	2003-01-29	Class 3 (0-1003.00 m)
Radar logging	2003-02-06 to 2003-02-07	0-1000 m
Flow meter logging	2003-02-17 to 2003-03-03	0-1000 m
Geophysical logging	200-03-05	0-1000 m
BIPS logging	2003-03-22	0-1000 m
Water sampling	2003-03-28	Class 5 (156.50-167.00 m) Chemmac monitoring equipment failure noted during this sampling.
Water sampling	2003-04-24	Class 5 (245.00-61.500 m) Chemmac monitoring equipment failure noted during this sampling.
Water sampling	2003-06-26 to 2003-09-15	Class 5 (548.00-565.00 m)

3.2.3 Sampling during drilling

Three samples were collected during drilling: 197.00-313.42 m, 585.00-593.00 and 531.00-619.42 m. The decision to sample was based on a combination of factors: a) drilling expert judgement (e.g. fluctuations in drilling speed; changes in flushing water pressure etc.), b) variations in electrical conductivity of the flushing water that may indicate a sudden influx of brackish or saline waters etc., and c) evidence of potential water-conducting fractures from drillcore inspection. An evaluation was subsequently carried out to try and establish a reliable methodology to locate potential water-conducting fractures during the drilling process. This was unsuccessful in resolving the many problems.

Consequently there is little information to go on, but the drilling water component from two borehole sections indicates 66.09% (section 585.00-593.00 m) and 34.98% (section 531.00-619.42 m) respectively. Corresponding tritium contents are 6.2 and 4.2 TU. The percentage drilling water reported for section 197.0-313.42 m was less than 10% and only 1.1 TU was recorded. The major ion chemistry reflects the dilution effect of the drilling water component in the former two sections; in contrast, section 197.00-313.42 m (in addition to low tritium and lower flushing water content) appears to be more acceptable recording representative major ion values expected at such bedrock depths (i.e. around 6000 mg/L Cl, 2440 mg/L Na, 1020 mg/L Ca; 18.5 mg/L SO_4 etc.) when compared to the later collected Class 5 samples (see below).

3.2.4 Open hole tube sampling

Open hole tube sampling was the next major borehole activity; these data can be very useful in evaluating borehole groundwater circulation pathways and groundwater budgets (e.g. water in and water out between the borehole and surrounding bedrock). Understanding these processes helps greatly in assessing water quality and representativeness.

Hydraulically, open boreholes usually establish groundwater circulation controlled by the piezometric head and the number and hydraulic properties of intersected water-conducting fractures or fracture zones. Groundwater may therefore either flow from the borehole into the bedrock or *vice-versa* and, in addition, groundwater flow systems in the bedrock may be short-circuited, i.e. it may be easier for formation water to flow into and along the borehole rather than through the bedrock. As described above, Figure 3-4b shows the groundwater flow directions into and out from borehole KSH01A during and in the absence of pumping. For this discussion it is the absence of pumping data that are relevant. These indicate that in the upper 300 m 'natural' groundwater flow is from the borehole into the surrounding bedrock, whilst between 550-750 m groundwater flow is into the borehole. This may give rise to some degree of open hole circulation of groundwater. However, because of the very low transmissivities, low flow rates and high salinities characterising the 600-750 m level (and certainly to the bottom of the borehole), groundwater circulation will be generally weak over the period of measurement and sampling. It is more likely, therefore, that the open hole groundwater chemistry will be influenced by residual flushing water at depth (since no high pressure nitrogen clearance was carried out) and any penetration downwards of formation water from the upper 300 m to depth will be determined by salinity differentials.

Tube sampling entails lowering an array of coupled tubes each of 50 m length to the borehole bottom; this is carried out with care to avoid excessive groundwater perturbation. When the tubes have been placed down the borehole, valves at each end of the tubes are opened allowing the groundwater to rise up and fill each tube. When this is considered complete, the valves are closed and the tube array is hoisted to the surface whereupon each tube is systematically emptied and the samples prepared for transport and analysis. One completely filled 50 m long tube would amount to 2.5 dm^3 of groundwater. However, the total water volume in each tube was less than expected (SKB P-03-87) and three tubes were discarded. Precipitation or suspended material was present in most of the collected samples.

Figure 3-6 shows the percentage of flushing water (i.e. from percussion borehole HSH03) present in borehole KSH01A under open hole conditions; lower values characterise the upper 300 m (10-15%) and higher values from 400 m downwards (15-30%). This is supported by the tritium contents introduced by the flushing water (4.7-10 TU) which along the borehole increase from 5.1 TU at the 500 m level to 7.2 TU at the borehole bottom. The increasing presence of more dilute flushing water with depth is reflected in most of the chemical plots, for example δD vs $\delta^{18}O$ (Fig. 3-7) (SKB P-03-87).

Figures 3-6 and 3-7 (see SKB P-03-87 for other plots) show a clear dominance of residual near-surface derived flushing water in Borehole KSH01A from about 500 m downwards:

- decreasing Na, Ca and Cl

- decreasing K, Mg, Br and Sr
- increasingly heavy δD and $\delta^{18}O$

The distribution of HCO_3, which shows a marked increase, may be influenced by its sensitivity to microbial reactions. Other bacteria-sensitive species, for example SO_4 and Fe(II), show a slight decrease (SO_4) and strong fluctuations, eventually decreasing with respect to Fe(II). The former may indicate the presence of sulphate-reducing bacteria. Because of some problems encountered during drilling, i.e. iron contamination from abrasion of the stainless steel drilling rods drilling crown, it is uncertain whether the observed Fe(II) fluctuations are artefacts of this contamination or represent geochemically reliable data.

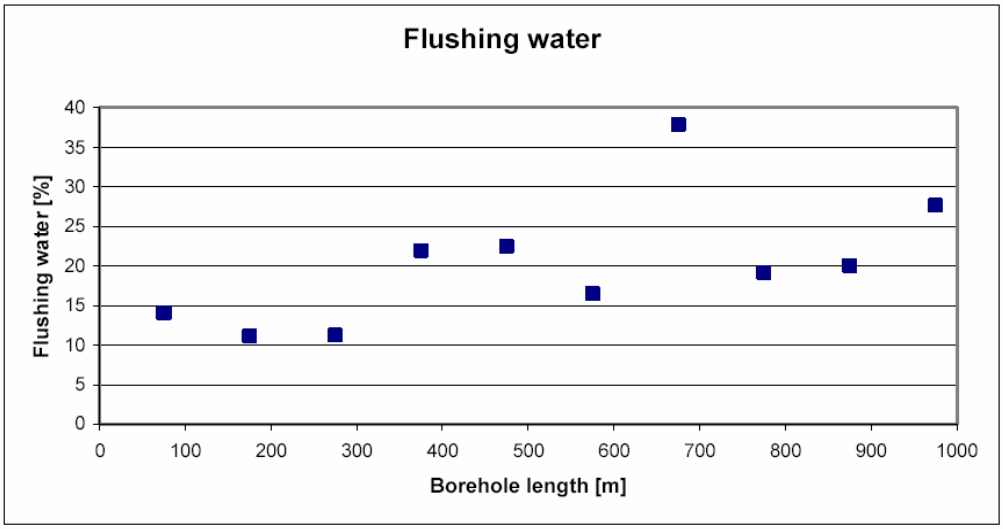

Figure 3-6: *Percentage of residual flushing water in borehole KSH01A under open hole conditions.*

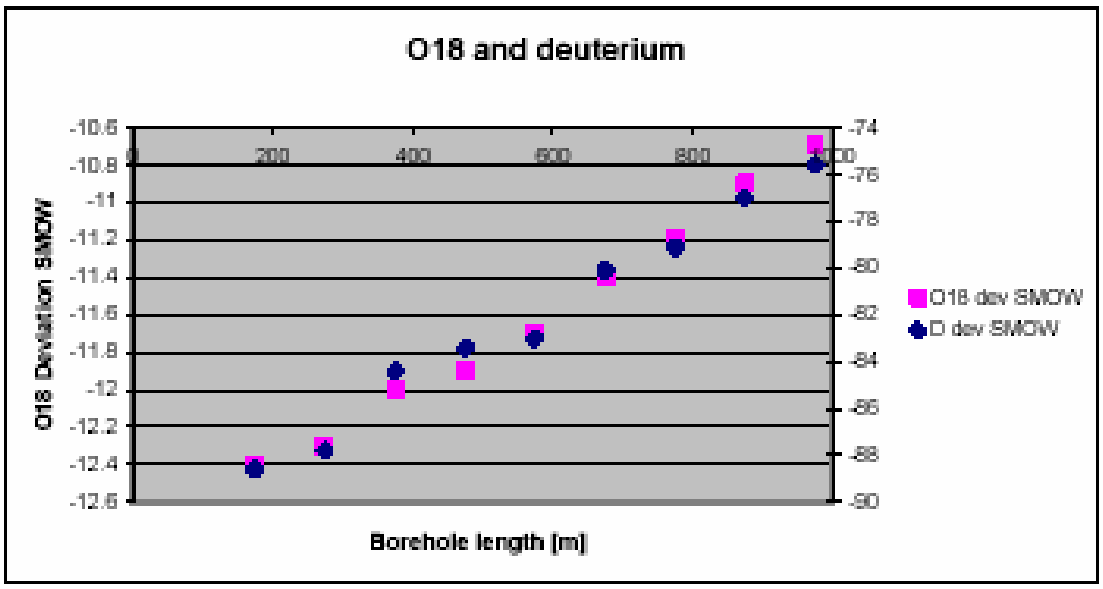

Figure 3-7: *Distribution of $\delta^{18}O$ and δD in open borehole KSH01A.*

Some of the chemical profiles from the upper approx. 400 m of the borehole may be explained also by flushing water contamination. However, the δD and $\delta^{18}O$ plot (Fig. 3-7) shows only typical values for the flushing water (i.e. $\delta^{18}O$ = -10.60‰ and δD = -77‰ SMOW for HSH03) at the deepest part of the borehole. In the upper part of the borehole the values are generally closer to fracture groundwaters later sampled from the isolated borehole sections at 156.50-167.00 m and 245.00-261.50 m (see below). Since the groundwater is less contaminated by flushing water at these shallower depths, compositions more representative of the fracture groundwater would be expected.

Representivity: As a general conclusion, these open hole tube samples are not representative for borehole KSH01A and should be discarded from the modelling exercises.

3.2.5 Sampling from packed-off borehole sections

Borehole section 156.50-167.00 m

Chemmac monitoring commenced on 2003-03-27 and was completed in 2003-04-23; sampling commenced on 2003-03-31 and continued to 2003-04-23 with eventual selection of data taken from sampled groundwaters taken on the 2003-03-31, 2003-04-07, 2003-04-14 and 2003-04-16.

The Chemmac monitoring protocol (SICADA) indicates, based on electrical conductivity and redox potential measurements, that 'stabilisation' of the extracted groundwater from the borehole section reflected electrical conductivity values of around 1540-1560 $mSm^{-1}$and redox potential measurements of around -265-275 mV; O_2 registered zero. In reality stabilisation was never really totally achieved during the monitoring period since both the electrical conductivity and redox potential continued to systematically change slowly throughout with increasing and decreasing values respectively. At one stage on 2003-04-03 there was a pause in monitoring and redox values in particular quickly increased (accompanied by O_2); it took some 5 days before the conductivity values returned to their pre-pause level.

These small monitoring trends are reflected in the chemistry of a selection of 18 groundwaters sampled and analysed through the sampling period, although not all analytical data are recorded. For example, chloride content increased only from 5166 to 5590 mg/L during the sampling period. In conclusion, since the fluctuations are small the values tabulated in the dataset can be considered representative. This supported by the low drilling water contents (2.39-3.70%) and also tritium which was below detection for the first three samples and 2.8TU for the fourth sample provided in the dataset.

As indicated above, pH measurements are mostly laboratory-derived; only a few *in-situ* values are from the Chemmac monitoring which indicated an average of 0.6 pH units lower than the laboratory values.

Representivity: This sampled level can be considered representative.

Borehole section 245.00-261.50 m

Chemmac monitoring commenced on 2003-04-25 and was completed in 2003-05-16; sampling of a series of six groundwaters was carried out during this time. The

Chemmac monitoring protocol (SICADA) indicates, based on electrical conductivity and redox potential measurements, that ‘stabilisation’ of the extracted groundwater from the borehole section reflected electrical conductivity values of around 1770-1790 mSm^{-1} and redox potential measurements of around -210-220 mV; (O_2 registered zero). In common with the shallower level discussed above there was an increase in electrical conductivity and decrease in redox potential with monitoring time, but this was very slight. This is reflected in the chemistry where all the major ions showed no significant variation. Moreover, drilling water was less than 1% and tritium was below detection.

As mentioned above, pH measurements are mostly laboratory-derived.

Representivity: This sampled level can be considered representative.

4 Borehole KSH02

Borehole KSH02 was drilled to a depth of 1001.11 m at an inclination of 85.4° C to the horizontal and cased to 80 m.

4.1 Geological and hydrogeological character

Borehole KSH02, in comparison to KSH01A, penetrates a relatively homogeneous rock mass dominated by fine-grained dioritoid (Fig. 4-1). Between approx. 500-750 m there is an increase in thin horizons of fine-grained granite and subsidiary pegmatite; only one significant horizon of fine-grained diorite-gabbro occurs close to the bottom of the borehole. Large lengths of the drillcore to 800 m show an increased fracture frequency (6-10 open fractures/metre) accompanied by intense wall rock alteration/oxidation. This is most prominent in sections 280-310 m and 450-650 m. Below 750 m the fracture frequency is significantly lower (1-4 open fractures /metre) and only a slight alteration of the rock is observed.

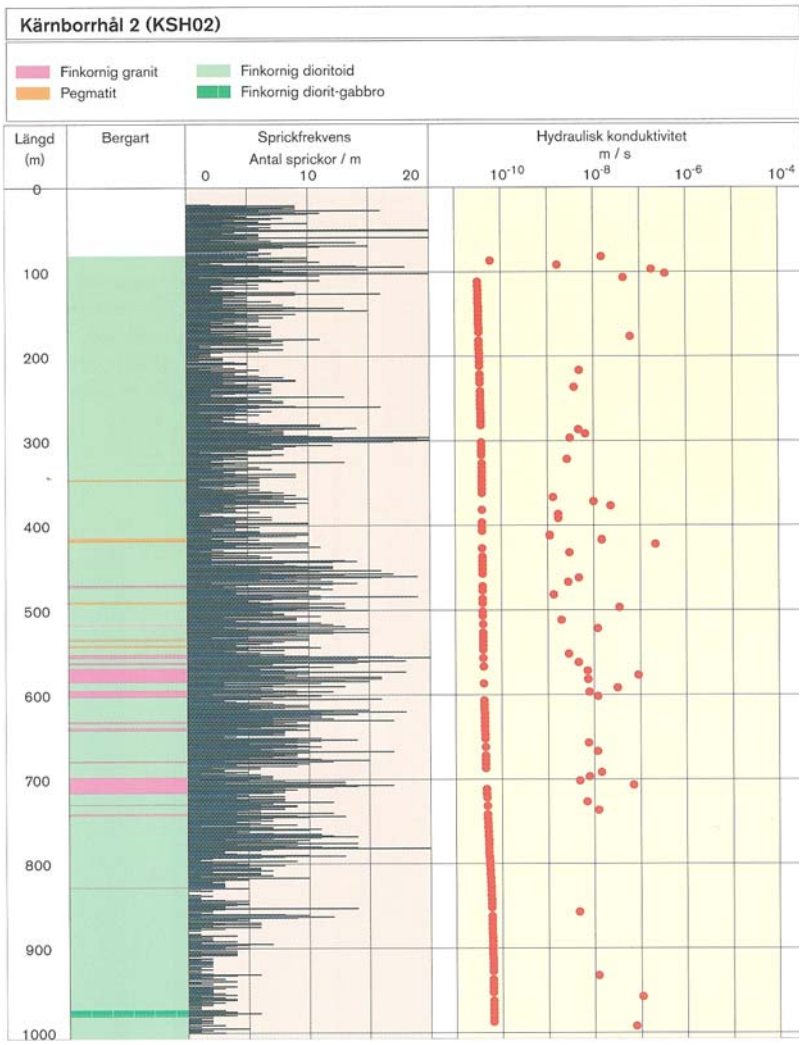

Figure 4-1: *Integrated geology, fracture frequency and hydraulic conductivity along borehole KSH02*

The differential downhole flow measurements reveal a general distribution of hydraulic conductivity ranging from 10^{-9}-10^{-7} ms^{-1} extending the full length of the borehole. From 600-1000 m there is an overall decrease in permeability. The highest hydraulic conductivities recorded where $3.7x10^{-7}$ ms^{-1} and $2.2x10^{-7}$ ms^{-1} corresponding to depths of 104.01 m and 424.06 m respectively; both were included in the groundwater sampling programme (see below).

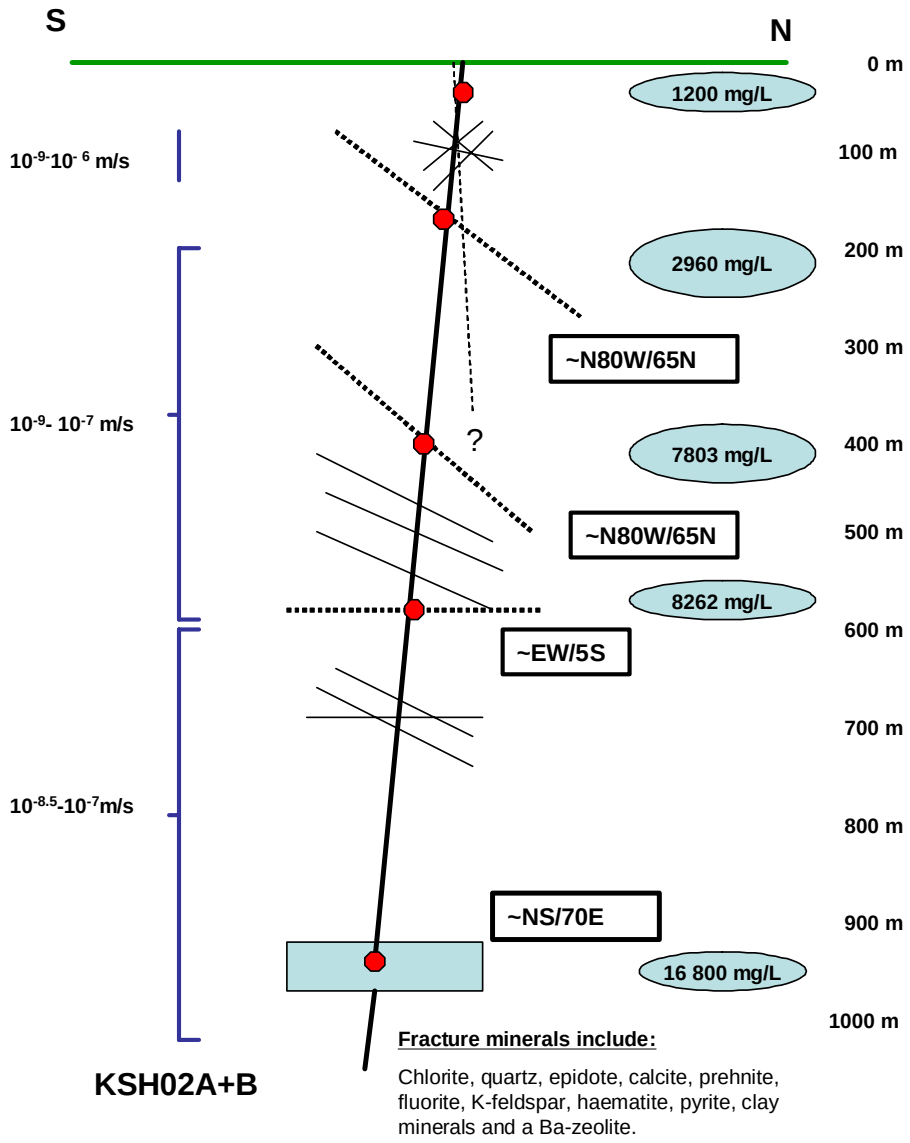

Figure 4-2: *Borehole KSH02+B showing intercepted structures and their hydraulic conductivities; groundwater sampling locations are indicated in red with the mg/L chloride content in blue.*

Figure 4-2 represents a schematic representation of borehole KSH02+B and the intercepted structures and their hydraulic conductivities; groundwater sampling locations are indicated in red and the sampled mg/L chloride contents are shown in blue. Drillcore mapping and available BIPS measurements show that both sub-vertical and

sub-horizontal fractures occur but the former structures are clearly dominant; this is partly due to the vertical orientation of the borehole.

Fractures are especially frequent to approx. 800 m (see also Fig. 4-1) trending northwest and dipping mostly to the south and southwest. Lower intensity fracturing of similar trend but dipping to the northeast occurs between 550-600 m; at around 700 m a major isolated fracture trends northeast dipping to the west.

The fracture minerals identified and their petrogenesis are similar to that already described for borehole KSH01A.

Figure 4-3 shows BIPS-images from KSH02 locating two of the major water-conducting fractures which probably have contributed to most of the groundwaters sampled from borehole sections

Figure 4-3: *BIPS-images from KSH02 showing the probable main water-conducting open fractures sampled from borehole sections 419-424 m and 575-580 m .*

Borehole KSH02 is cased to 80 m depth which excludes BIPS and differential Flow Meter data from this length. As described above for Figure 4-1 and in Figure 4-4a, hydraulic conductivities generally range from 10^{-9}-10^{-7} ms^{-1} along the borehole with slightly higher values at 104.01 m and 424.06 m. From approx. 100-200 m and 350-750 m the borehole is characterised by increased hydraulic conductivities; from 750 m to the hole bottom at 1001 m lower conductivities are typical apart from slight increases

documented from 960-1000 m. Figure 4-4b indicates the measured groundwater flow rates (and directions relative to the borehole) during pumping and under natural flow conditions (SKB P-03-110).

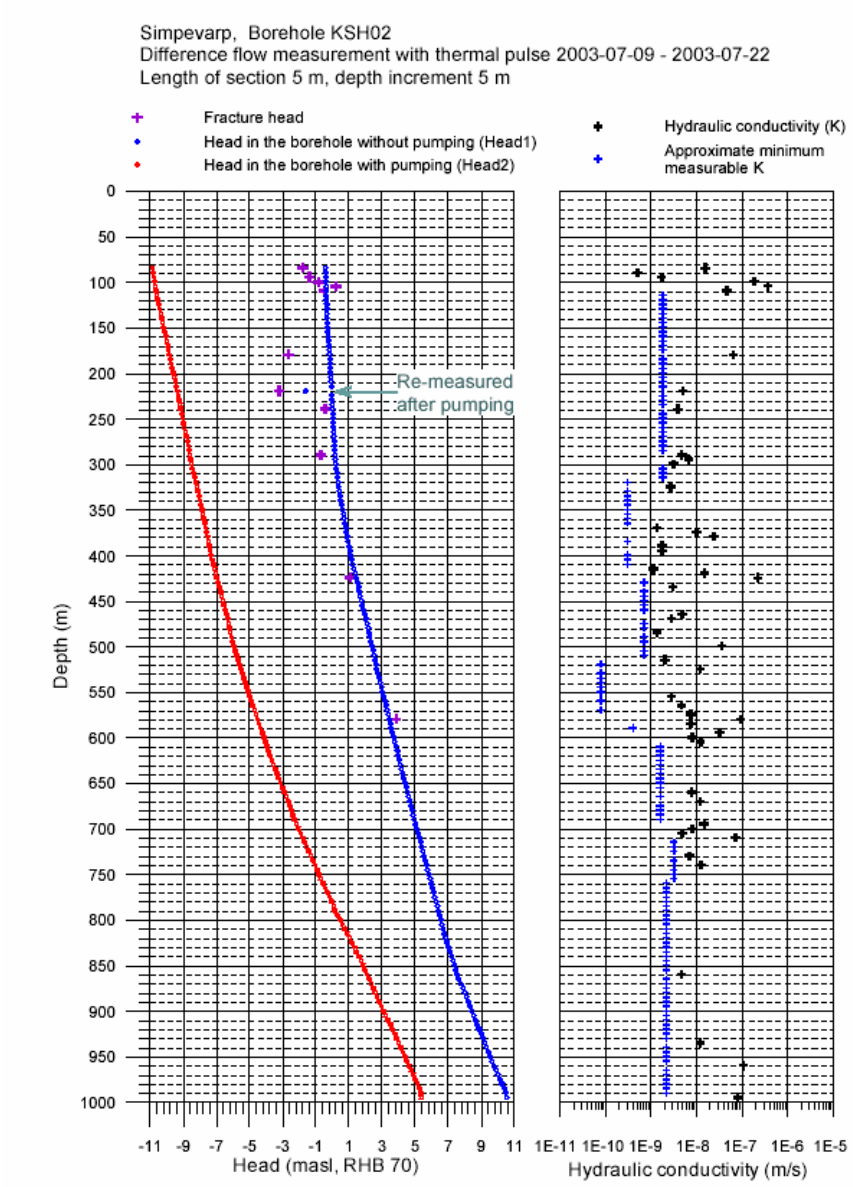

Figure 4-4a: *Differential flow meter measurements along borehole KSH02 (80-1001.1 m) recording hydraulic head and conductivity (SKB P-03-110).*

The recorded rates of groundwater flow under 'natural' hydraulic conditions (i.e. no pumping) via fractures into the borehole from the surrounding bedrock, and conversely from the borehole into the bedrock, indicate that water movement is mostly out from the borehole to the surrounding bedrock in the upper 450 m with one exception at 104.1 m where some flow is indicated from the bedrock to the borehole (Fig. 4-4b). From 450 m to the hole bottom the absence of data (apart from one measurement at approx. 580 m) suggest a very tight, low transmissive bedrock.

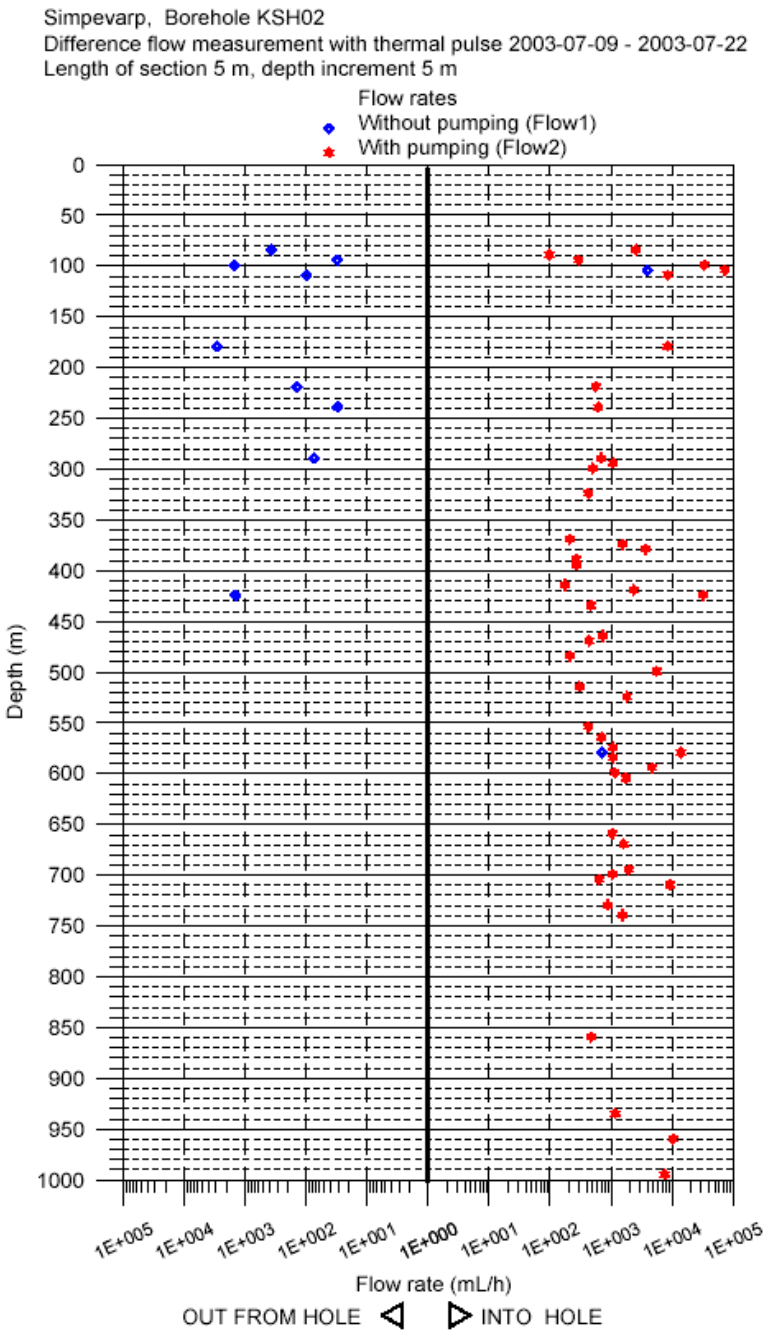

Figure 4-4b: *Differential flow meter measurements along borehole KSH02 (80 to 1001.11 m) recording groundwater flow rate (mL/h) into and out of the borehole (SKB P-03-110).*

During pumping all movement of formational groundwater is into the borehole. Under open hole conditions, therefore, formation groundwater would be expected to infiltrate from the borehole to the bedrock down to at shallower depths where there is an increase in hydraulic conductivity coinciding with the location of the KSH01A sampling sections, and enter the borehole at the 550-600 m level where the hydraulic conductivity increases to around 10^{-7} ms^{-1}. Because of the very low hydraulic conductivities at depths greater than 600 m ($<10^{-9}$ ms^{-1}) it is very doubtful that any open-hole circulation is active along this length and any drilling water would tend to be trapped.

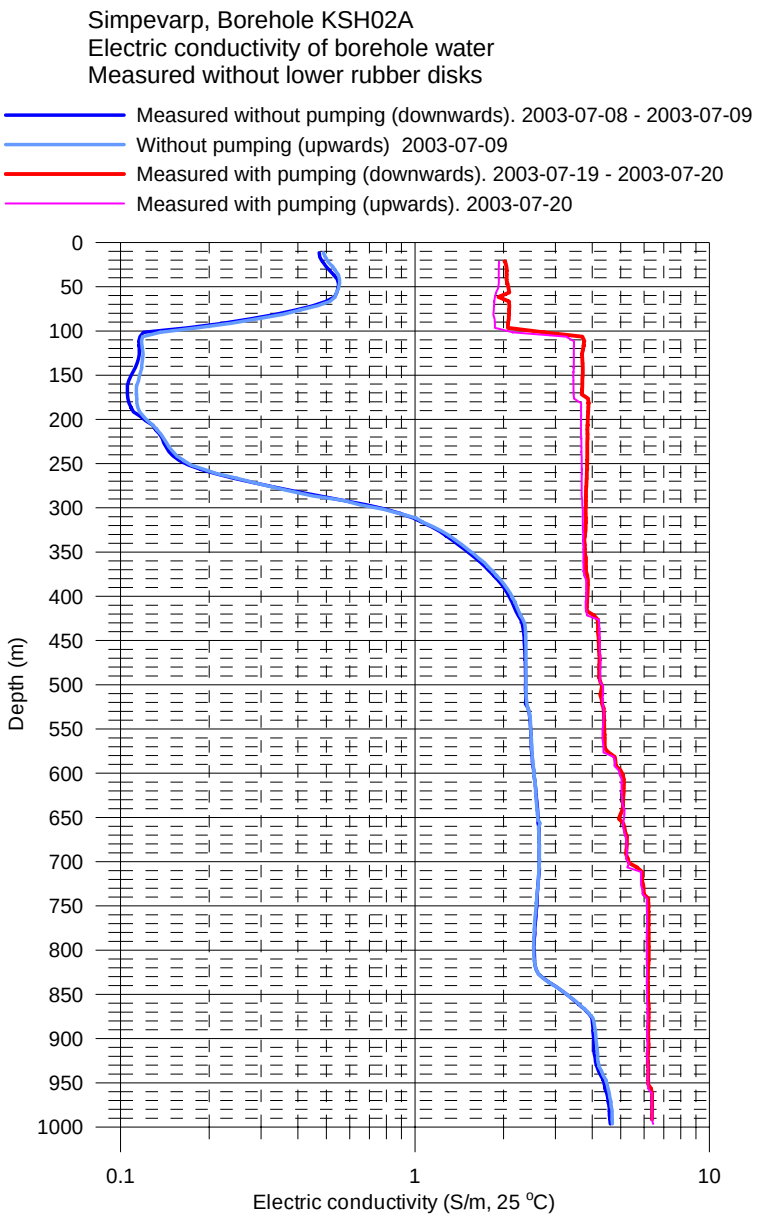

Figure 4-5: *Electrical conductivity log for borehole KAS02A during open hole conditions.*

Figure 4-5 shows downhole electrical conductivity (EC) measurements for borehole KSH02A under open hole conditions; the upper 100 m is not relevant as it relates to the cased borehole section (KSH02B). Considering the more natural flow conditions without pumping (blue line), at 100 m depth the EC values are close to 0.1 Sm^{-1} and this is maintained to around 250 m. At this depth there is a rapid increase eventually reaching 2.5 Sm^{-1} at 450 m; here it levels out until 830 m where there is a slight increase in salinity to 4 Sm^{-1} finally achieving 4.7 Sm^{-1} at the borehole bottom.

This low salinity recorded from 100-250 m probably corresponds to the equivalent level in borehole HSH02 which provided the source of the flushing water used during drilling, i.e. markedly fresh and dilute at approx. 17 mg/L Cl. The increase in salinity with depth corresponds to the sampled level at 411.85-467.07 m where the chloride content lies around 6500 mg/L.

4.2 Groundwater quality and representativeness

Borehole KSH02 was drilled to a depth of 1001.11 m at an inclination of 85.4° C to the horizontal and cased to 80 m. Flushing water was obtained from percussion borehole HSH02 (0-200 m). The chemistry of this water shows it to be dilute $NaHCO_3$ in type with a chloride content of approx. 55 mg/L. Tritium varies from 11-15 TU.

4.2.1 Available data

Available data included:

- Borehole activity logs
- Groundwater chemistry from open hole tube sampling
- Groundwater chemistry from isolated borehole sections

No Chemmac log data (pH, Eh, Temp., El. conductivity) were available.

4.2.2 Borehole activity logs

The downhole activity log for borehole KSH02 relating to potential groundwater disturbances, is given below. Samples highlighted by red font were taken during drilling (e.g. using wireline techniques), open hole tube sampling is highlighted by green font, and sampling following borehole completion from pre-determined packed-off borehole sections is denoted by blue font. Some groundwater samples are referred to as 'unclassified', i.e. presumably not falling within the range of Class 1 to 5 in the analytical protocol.

Activity	Date	Comments
Core drilling	2003-01-28 to 2003-06-11	65.85-1001.11 m
BIPS logging	2003-02-08	17.00-97.00 m
Geophysical logging	2003-02-09 to 2003-02-10	0-100 m
PLU pump test	2003-02-10	0-100.5 m
Water sampling	2003-02-10	Class 3 (6.65-100.5 m)
Geophysical logging	2003-02-11 to 2003-03-12	100-1001 m
PLU pump tests	2003-03-14 to 2003-03-15	Intervals (81.10-192.22 m)
Rock stress measurements	2003-03-18	Overcoring method
PLU pump tests	2003-03-22 to 2003-03-31	Intervals (192.00-447.74 m)
Rock stress measurements	2003-03-31 to 2003-04-07	Overcoring method
PLU pump tests	2003-03-31 to 2003-04-09	Intervals (447.74-467.07 m)

Water sampling	2003-04-08 to 2003-04-09	Wireline (411.85-467.07 m)
PLU pump tests	2003-04-08	Intervals (410.85-467.07 m)
Water sampling	2003-04-08 to 2003-04-09	Unclassified
PLU pump tests	2003-04-09	Interval (0.00-479.08 m)
Water sampling	2003-04-09	Class 3 (411.85-467.07 m)
PLU pump tests	2003-04-10 to 2003-05-07	Intervals (479.08-755.17 m)
Water sampling	2003-05-07 to 2003-05-08	Wireline (738.00-755.17 m)
PLU pump tests	2003-04-07 to 2003-05-08	Intervals (755.17-762.08 m)
Water sampling	2003-05-08	Class 3 (738.00-755.17 m)
PLU pump tests	2003-05-09 to 2003-05-14	Intervals (762.08-803.15 m)
Water sampling	2003-05-14	Class 3 (699.00-803.15 m)
PLU pump tests	2003-05-14 to 2003-06-04	Intervals (803.15-1011.11 m)
Tube sampling	2003-06-18 to 2003-06-18	Class 3 (00.00-991.00 m)
Geophysical logging	2003-06-29 to 2003-07-09	100-1001 m
Flow meter logging	2003-07-07 to 2003-07-22	100-1001 m
PLU injection test	2003-09-02	Interval 419-424 m
Water sampling	2003-09-02 to 2003-09-05	Unclassified (419-424 m)
Water sampling	2003-09-05	Class 5 (419-424 m)
PLU injection test	2003-09-09	Intervals (575-580 m)
PLU pump test	2003-09-09 to 2003-09-17	Intervals (575-580 m)
Water sampling	2003-09-09 to 2993-09-15	Unclassified (575-580 m)
Water sampling	2003-09-15	Class 5 (575-580 m)
PLU injection test	2003-09-24 to 2003-11-13	Intervals (101.50 to 701.50 m)
Water sampling	2004-02-10	Class 1 (957.20 – 958.20 m)
Water sampling	2004-02-11	Class 1 (958.20 – 975.20 m)
Water sampling	2004-02-11	Class 5 (957.20 – 958.20 m)
Radar logging	2004-02-17	80-987 m

4.2.3 Sampling during drilling

Four samples were collected during drilling: 6.65-100.50 m, 411.85-467.07 m, 738.00-755.17 m and 699-803.15 m. From each sampled level the representativeness of the samples is evaluated as being suitable, limited suitability or unsuitable.

6.65-100.50 m: High content of flushing water (26.64%), charge balance error within limit (-1.85%), incomplete analyses (no isotopes). ***Unsuitable.***

411.85-467.07 m: Moderate content of flushing water (5.56%), charge balance error within limit (-3.96%), tritium below detection, stable isotope data. ***Limited suitability.***

738.00-755.17 m: Very high content of flushing water (52.41%), no charge balance error recorded, incomplete analyses (no isotopes). ***Unsuitable.***

699-803.15 m: Very high content of flushing water (52.99%), no charge balance error recorded, incomplete analyses (no isotopes). ***Unsuitable.***

4.2.4 Open hole tube sampling

Percussion borehole HSH02 (0-200 m) is the source of flushing water for the drilling of KSH02. It is a dilute $NaHCO_3$ meteoric groundwater of high tritium content (11-15TU), high pmc (~69) and normal recharge stable isotope signatures ($\delta^{18}O$ = -10.78‰ SMOW; δD = -78‰ SMOW). In an open borehole situation, especially borehole KSH02 where hydraulic conductivities are mostly within the range of 10^{-9}-10^{-7} ms^{-1} and water-conducting fracture zones below 600 m are rare, the flushing water might be expected to dominate open hole conditions.

On retrieval of the tubes it was apparent that only a few tube sections had accumulated adequate water for analysis and archivation, a further indication of the low permeable nature of the bedrock.

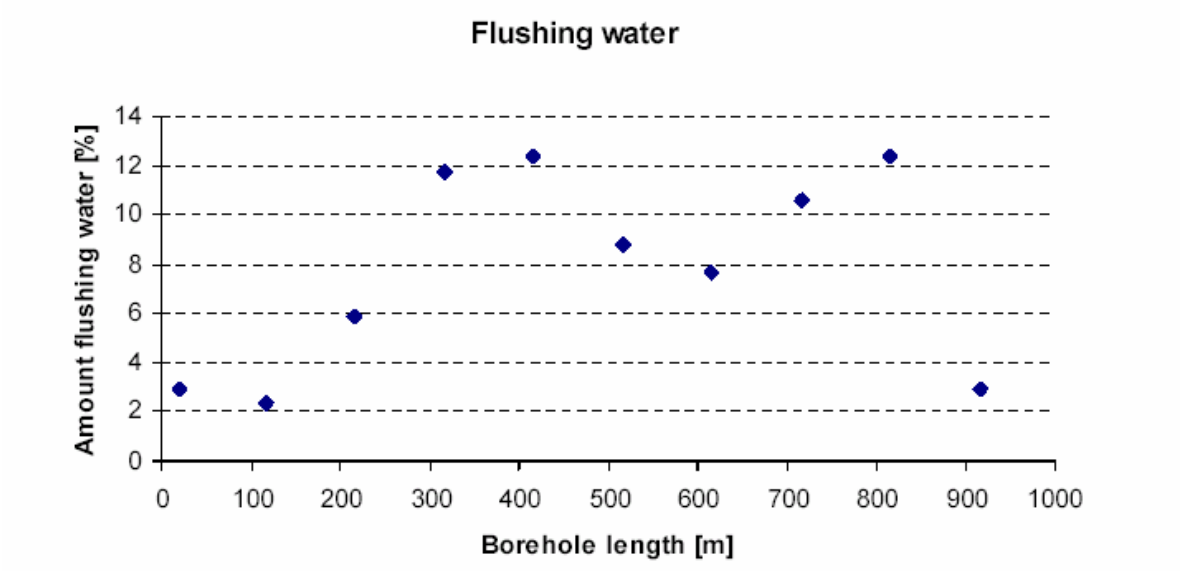

Figure 4-6: *Percentage of residual flushing water in borehole KSH02 under open hole conditions.*

Figure 4-6 (from SKB P-03-88) shows moderate to high flushing water contents (6-13%) apart from the shallowest two samples (20.5 and 116 m) and the deepest sample (916 m) with just over 2%. Flushing water (or near-surface water) contamination is also indicated by the significant tritium values, at least to around 350 m (with 3.4TU), and also reflected at 416 m and even at 816 m by high pmc values of 63.3 and 70.6 respectively.

Figure 4-7 shows dilute waters (<1000 mg/L Cl) dominating the upper 200 m and high salinities (>14000 mg/L Cl) dominating the deepest 900-1000 m of the borehole.

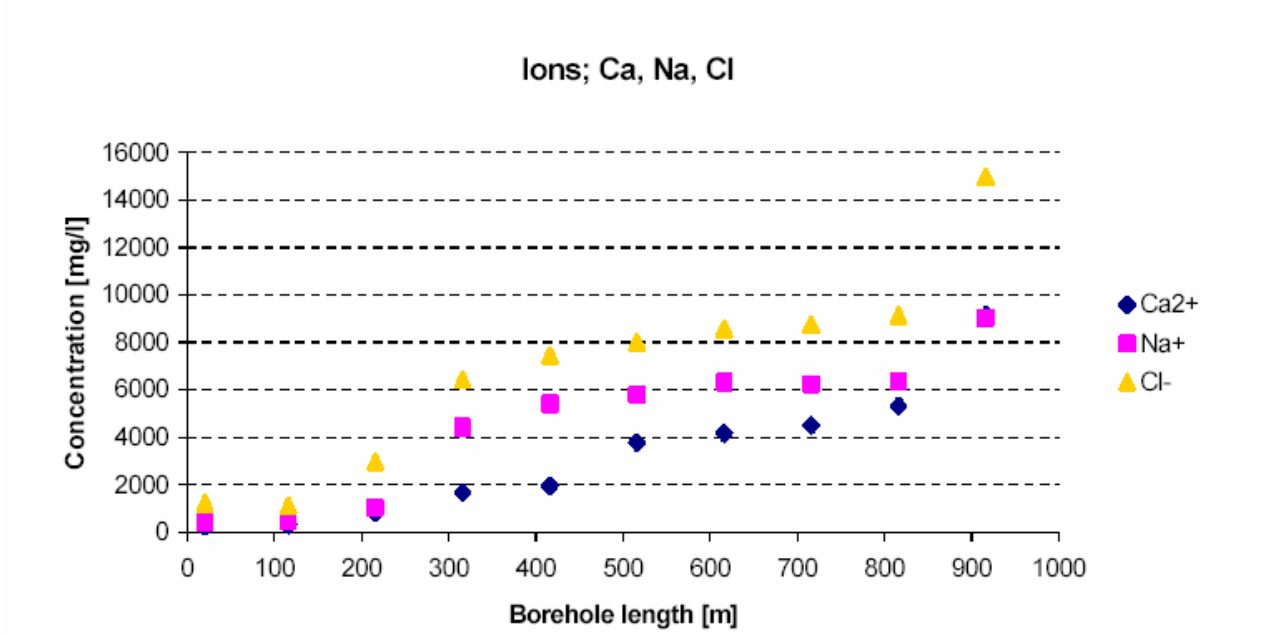

Figure 4-7: *Salinity variation in borehole KSH02 under open hole conditions.*

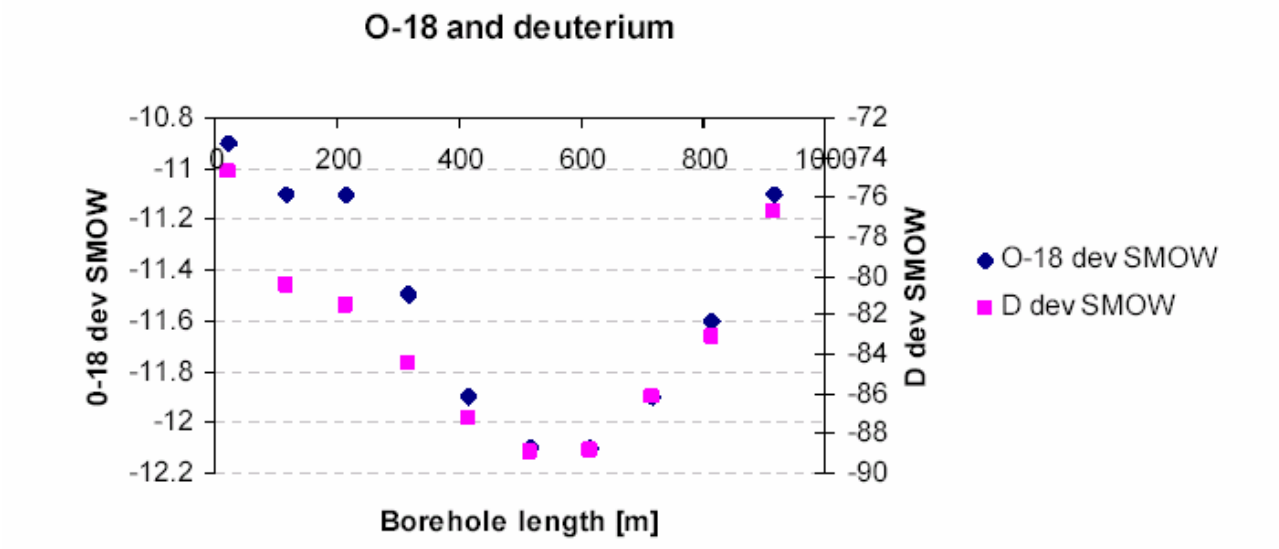

Figure 4-8: *Distribution of $\delta^{18}O$ and δD in open borehole KSH02*

Figure 4-8 shows typical near-surface modern precipitation values of $\delta^{18}O$ and δD in the shallowest sample (0-100 m). From 100-300 m there is a rapid decrease in δD which does not coincide with $\delta^{18}O$; heavier near-surface $\delta^{18}O$ values persist to 200 m and even from 200-300 m (less so at 400 m) there persists this disparity. The lightest $\delta^{18}O$ values (i.e. suggesting cold climate recharge) maximise at 12.1‰ at 550-600 m before increasing to heavier values, together with δD, to the bottom of the borehole.

For some of the other analysed ions (see SKB P-03-88 for other plots) depth trends include:

- initial decrease of pH to 300m (8-7 units) followed by a gradual increase to 850 m (7.4 units) and a sharp increase to approx. 8 units at 900 m,
- decrease of HCO_3 to 400 m (~200 – 25 mg/L) which persists to 900 m where it decreases further to ~15 mg/L), and
- K, Mg, Br and Sr commence at low values (<10 mg/L) until 200 m where they increase slightly and stabilise until 800 m. Here Br and Sr increase markedly at 900 m whilst Mg and K remain constant.

Given the overall low permeability of borehole KSH02, particularly at depth, and given the fact that the borehole was not cleared of flushing water and drilling debris following drilling, under open hole conditions the groundwater content in the borehole would be expected to contain: a) near-surface water from around 100 m, b) residual flushing water and, perhaps, c) some formation groundwater from the bottom 50 m of the borehole which is suggested from the slight rise in hydraulic conductivity at this depth (see Figs. 4-1 and 4-4b). Generally, the data suggest the upward movement (by diffusion?) of highly saline, dense groundwaters from 900-1000 m (~15 000 mg/L Cl; no tritium), the downward movement of dilute, near-surface meteoric groundwaters (<1 000 mg/L Cl; tritiated), and a central area (~150-900 m) of mixing. This central area also contains formation water as indicated by the lighter stable isotope values than the flushing water used in the drilling (e.g. 12.1 vs 10.7‰ $\delta^{18}O$).

Based on a ±5% charge balance error limit, only one sample at 241 m (-3.50%) is considered acceptable; the remaining groundwater samples range from -13.6 to +34.2%. The reason for this is not known (SKB P-03-88).

Representative: None completely representative due to charge imbalance errors; closest and of limited suitability are **s**amples from levels 0-41 m, 41-91 m, 91-141 m, 191-241 m and 891-941 m.

4.2.5 Sampling from packed-off borehole sections

Groundwater samples from five isolated borehole sections have been collected during drilling and following borehole completion: 419.00-424.00 m, 575.00-580.00 m, 957.20-958.20 m (x2) and 958.20-975.20 m. From each sampled level the representativeness of the samples is judged to be suitable, of limited suitability or unsuitable.

419.00-424.00 m: Low content of flushing water (1.53%), charge balance error outside limit (-12.88%), incomplete analyses (no isotopes). ***Unsuitable.***

575.00-580.00 m: Low content of flushing water (0.13%), charge balance error outside limit (-13.16%), no tritium value recorded, stable isotope data. ***Limited suitability.***

957.20-958.20 m: Location sampled in two consecutive days. Low content of flushing water (0.18-0.39%), charge balance on first sample within limit (-4.13%), incomplete analyses (no isotopes). ***Limited suitability.***

958.20-975.20 m: Low content of flushing water (0.40%), charge balance error not recorded, incomplete analyses (no isotopes). ***Limited suitability.***

5 Borehole KSH03A

Borehole KSH03A was drilled to a depth of 1000.70 m at an inclination of 57^{o} C to the horizontal and cased to 100.6 m.

5.1 Geological and hydrogeological character

Borehole KSH03A from approx. 100-180 m initially penetrates mostly fine-grained dioritoid and Ävrö granite containing some small pegmatite horizons (Fig. 5-1). From 200-280 m quartz monzodiorite dominates and, finally, homogeneous Ävrö granite dominates to the hole bottom containing only a few significant horizons of fine-grained dioritoid, diorite gabbro and granite. From 100-180 m the rock is characterised by 3-5 open fractures/metre increasing markedly from 180-300 m where up to 20 open fractures/metre have been recorded accompanied by intense wall rock alteration/oxidation. From 300 m to the hole bottom the average open fracture frequency is 0-3/metre; exceptions include around the 860 m and 930-975 m levels where there is an increase to 5-10 open fractures/metre and only a slight alteration of the rock is observed.

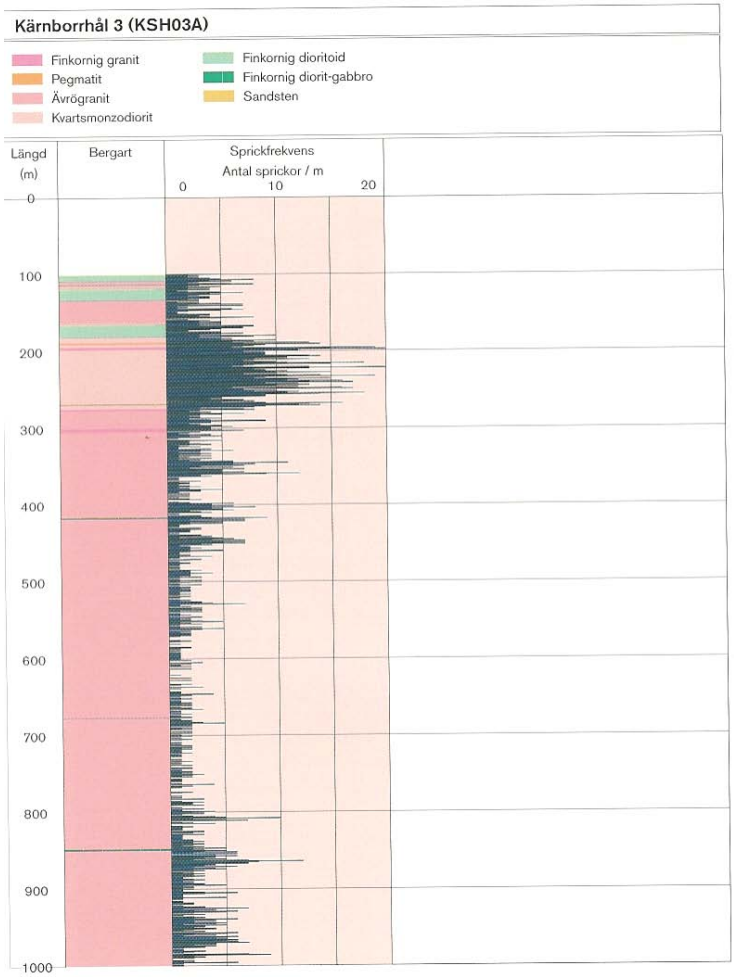

Figure 5-1: *Integrated geology, fracture frequency and hydraulic conductivity along borehole KSH03A.*

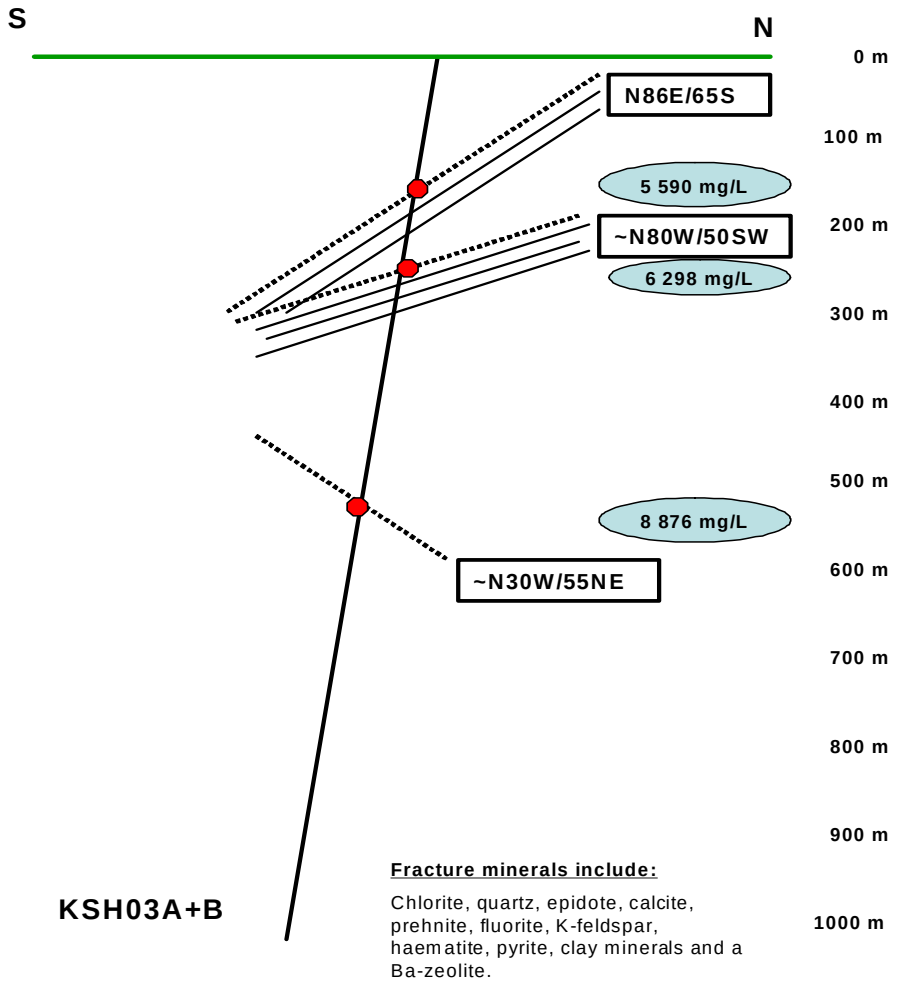

Figure 5-2: *Borehole KSH03A+B showing intercepted structures and their hydraulic conductivities; groundwater sampling locations are indicated in red with the mg/L chloride content in blue.*

Figure 5-2 is a schematic representation of borehole KSH03+B showing the major intercepted structures; no documented hydraulic conductivities were available. Locations are indicated in red and the sampled mg/L chloride contents are shown in blue. Drillcore mapping and available downhole BIPS measurements show that both sub-vertical and sub-horizontal fractures occur but the former structures are clearly dominant; this is partly due to the vertical orientation of the borehole.

Fractures are especially frequent between approx. 150-300 m (see also Fig. 5-1) trending northwest and dipping mostly to the south and southwest; this may represent a fracture zone of regional scale. Lower intensity fracturing of similar trend but dipping to the northeast occurs between 550-600 m.

The fracture minerals identified and their petrogenesis are similar to that already described for boreholes KSH01A and KSH02.

Although BIPS-imaging was carried out in borehole KSH03A+B, the quality is so poor that no examples are reproduced here for illustration purposes (SKB P-04-48).

No differential flow meter log is available for borehole KSH03A, only from 28-97 m in borehole KSH03B.

5.2 Groundwater quality and representativeness

Borehole KSH03A was drilled to a depth of 1000.70 m at an inclination of 57^{o} C to the horizontal and cased to 100.6 m. Flushing water was obtained from percussion borehole HSH03 (0-200 m). The chemistry of this water shows it to be basically a fresh to slightly brackish Na(Ca)-HCO_3(SO_4-Cl) type with a chloride content of approx. 500 mg/L. Tritium varies from 4.7-10 TU.

5.2.1 Available data

Available data included:

- Borehole activity logs
- Groundwater chemistry from open hole tube sampling
- Groundwater chemistry from isolated borehole sections

No Chemmac log data (pH, Eh, Temp., El. conductivity) were available.

5.2.2 Borehole activity logs

The downhole activity log for borehole KSH03A relating to potential groundwater disturbances, is given below. Samples highlighted by red font were taken during drilling (e.g. using wireline techniques), open hole tube sampling is highlighted by green font, and sampling following borehole completion is denoted by blue font. Some groundwater samples are referred to as ‘unclassified’, i.e. presumably not falling within the range of Class 1 to 5 in the analytical protocol.

Activity	Date	Comments
Percussion drilling	2003-08-13 to 2003-08-19	0-100.60 m
Open hole pumping	2003-08-20 to 2003-08-21	0-100.60 m
Flow meter logging	2003.08-21	28-97 m (borehole KSH03B)
Water sampling	2003-08-21	Class 3 (0-100.6 m)
Core drilling	2003-09-11 to 2003-11-07	100.06-1000.70 m
PLU pump tests	2003-09-13 to 2003-09-21	Air-lift pumping
Water sampling	2003-09-21	Class 3 (200.60-291.88 m)

PLU pump tests		Intervals (115.65-291.88 m)
Water sampling	2003-09-21	Class 3 (200.60-291.88 m)
PLU pump tests	2003-09-23 to 2003-10-01	Intervals (290.60-508.26 m
Water sampling	2003-10-01	Unclassified (409.50-508.26 m)
PLU pump tests	2003-10-02 to 2003-10-16	Intervals (410.07-697.60 m)
Water sampling	2003-10-16	Class 3 (599-698 m)
PLU pump tests	2003-10-16 to 2003 10 -23	Intervals (599.53-892.55 m)
Water sampling	2003-10-23	Class 3 (698-788 m)
PLU pump tests	2003-10-23 to 2003-10-30	Intervals (788.00-892.55 m)
Water sample	2003-10-31	Class 3 (788.00-893.00 m)
PLU pump tests	2003-10-31 to 2003-11-11	Intervals (893.00-1000.77 m)
Water sampling	2003-11-12	Class 2 (890-1000 m)
PLU pump tests	2003-11-13 to 2003-11-14	Interval (0-1000.7 m)
Water sampling	2003-11-19 to 2003-11-20	Class 1 (0.00-990.00 m)
Geophysical logging	2003-12-02 to 2003-12-13	0-100.60 m
Tube sampling	2004-01-27	Class 3 (0-940 m)
PLU injection tests	2004-02-09 to 2003-02-12	Intervals (102.50-995.00 m)

5.2.3 Sampling during drilling

Five samples were collected from approx. 100 m borehole sections at different levels: 200.60-291.88 m, 599.00-698.00 m, 698.00-788.00 m, 788.00-893.00 m, 890.00-1000.00 m. The flushing water contents are unreliable due to variable doses of uranine. From each sampled level the representativeness of the samples is evaluated as being suitable, limited suitability or unsuitable.

200.60-291.88 m: High content of flushing water (22.48%), charge balance error within limit (-2.63%), low tritium (2.8TU). ***Unsuitable.***

599.00-698.00 m: Low content of flushing water (0.56%), charge balance error not recorded, incomplete major ion analyses and no isotope data). ***Limited suitability.***

698.00-788.00 m: Very high content of flushing water (90.12%), charge balance error not recorded, incomplete major ion analyses and no isotope data. ***Unsuitable.***

788.00-893.00 m: Very high content of flushing water (92.10%), charge balance error not recorded, incomplete major ion analyses and no isotope data)

890.00-1000.00 m: High content of flushing water (29.48%), charge balance error not recorded, incomplete major ion analyses and no isotope data. ***Unsuitable***.

5.2.4 Open hole tube sampling

No documentation is available and the data provided are incomplete (e.g. no isotope analyses). Those data relating to flushing water content show high values of contamination which range from 3.68-20.90%. This partly may be the result of variable doses of added uranine which, in turn, may be due to mechanical problems regulating the addition of flushing water.

Salinities increase markedly with depth with 17 100 Cl being sampled from the 890-940 m level; this sample is also characterised with the least flushing water component (3.68%).

In contrast to Borehole KSH02, the charge balance errors all lie within the ±5% limit; one exception is a 10.91% error at the 90-140 m level.

Representative: None representative; qualitatively the deepest sample may be of use for salinity estimations and major ion plots.

5.2.5 Sampling from packed-off borehole sections

Groundwater samples from five isolated borehole sections have been collected during drilling and following borehole completion: 419.00-424.00 m, 575.00-580.00 m, 957.20-958.20 m (x2) and 958.20-975.20 m. From each sampled level the representativeness of the samples is evaluated as being suitable, of limited suitability or unsuitable.

419.00-424.00 m: Low content of flushing water (1.53%), charge balance error outside limit (-12.88%), incomplete analyses (no isotopes). ***Unsuitable.***

575.00-580.00 m: Low content of flushing water (0.13%), charge balance error outside limit (-13.16%), no tritium value recorded, stable isotope data. ***Limited suitability.***

957.20-958.20 m: Location sampled in two consecutive days. Low content of flushing water (0.18-0.39%), charge balance on first sample within limit (-4.13%), incomplete analyses (no isotopes). ***Limited suitability.***

958.20-975.20 m: Low content of flushing water (0.40%), charge balance error not recorded, incomplete analyses (no isotopes). ***Limited suitability.***

6 Additional input

Included in the Simpevarp v. 1.2 Hydrogeochemical Site Characterisation evaluation are data representing surface and near-surface waters collected from the Baltic Sea, Lakes, Streams, and also from shallow Soil Pipes placed in the overburden. These data, because of the complex nature of the sampling locations (i.e. subject to annual and seasonal trends, potential recharge/discharge areas etc.) have been evaluated based only on charge balance (Lake and Stream waters), charge balance and observed contamination during sampling (Soil Pipe waters) and charge balance and salinity (Baltic Sea waters). Some precipitation values are also included but have not undergone any representativity check because of unpredictable annual and seasonal trends and possible evaporation.

In addition, borehole groundwater data from earlier investigations centred in the Äspö area and surrounding regions also are included. Collectively these are referred to as 'POM' (***P***latsundersökningar i ***O***skarsha***M***n) and include Äspö, Laxemar, Ävrö, Oskarshamn and Bockholmen. Some of these data have already undergone a quantitative representivity judgement (e.g. Smellie and Laaksoharju, 1992; Laaksoharju et al., 1995) whilst the rest have been evaluated more qualitatively. Suggested modelling groundwater values have been highlighted in the Nordic Groundwater Table available in ProjectPlace.

7 Hydrogeochemical evaluation

The hydrogeochemical evaluation presented below follows a systematic approach (see SKB R-02-49) commencing with traditional plots (e.g. Piper Plots) to group the main groundwater types characterising the Simpevarp site and to identify general evolutionary or reaction trends. Based on this background knowledge the focus then centres on the more detailed hydrogeochemistry of the site boreholes themselves and, ultimately, on the detail of the actual borehole sections sampled. Comparisons are made with hydrochemical information from the 'POM' sites geographically located close to Simpevarp and previously investigated (i.e. Äspö, Laxemar, Ävrö, Oskarshamn and Bockholmen). Importantly, the hydrogeochemistry is related also to the regional and local geology and hydrogeology in order to understand the overall (i.e. large- and small-scale) dynamics and evolution of the groundwater systems which characterise the Simpevarp site.

The Simpevarp data have undergone a rigorous assessment of their representativeness and selected values have been judged suitable for modelling purposes (cf. Chapters 3-5). Other data not judged totally representative may still provide valuable information, for example: a) the use of some of the major ion analyses in hydrochemical plots, and b) observed compositional changes with time which may reflect groundwater mixing, either artificially induced by pumping and/or sampling or due to natural flow.

In this present evaluation the most quantitative and representative hydrogeochemical information from predetermined packed off borehole sections from the Simpevarp site provide the main focus of the study. Two Tube samples at shallow depths (borehole KSH02: 91-141 m and 191.241 m), judged to be of limited suitability, have been used with caution. The chemical data have been expressed in several X-Y plots to derive trends that may facilitate interpretation.

In addition to the borehole data, an extensive sampling of Baltic Sea, Lake, Stream and Soil Pipe waters have been collected and analysed. These have also been evaluated as to their suitability and are included in some the X-Y plots which relate mostly to surface and near-surface waters; for the deeper groundwater plots only the Soil Pipe data and an average value for the Baltic Sea is included.

7.1 General groundwater types and hydrochemical trends

The main groundwater groups characterising Simpevarp are: a) shallow (<200 m) Na-HCO_3 to Na-Cl-HCO_3 to Na-Ca-Cl- HCO_3 to Na-Ca-Cl types, b) intermediate (approx. 200-600 m) Na-Ca-Cl (with some enhanced SO_4 and Br) types, and c) deep (>600 m) with increasingly enhanced Na-Ca-Cl(Br, SO_4). The variation in compositions, especially in the upper 200 m of the bedrock, is due to local hydrodynamic flow conditions leading to mixing of varying proportions. Microbially mediated reactions are also important influencing both HCO_3 and SO_4, especially in the 200-600 m interval.

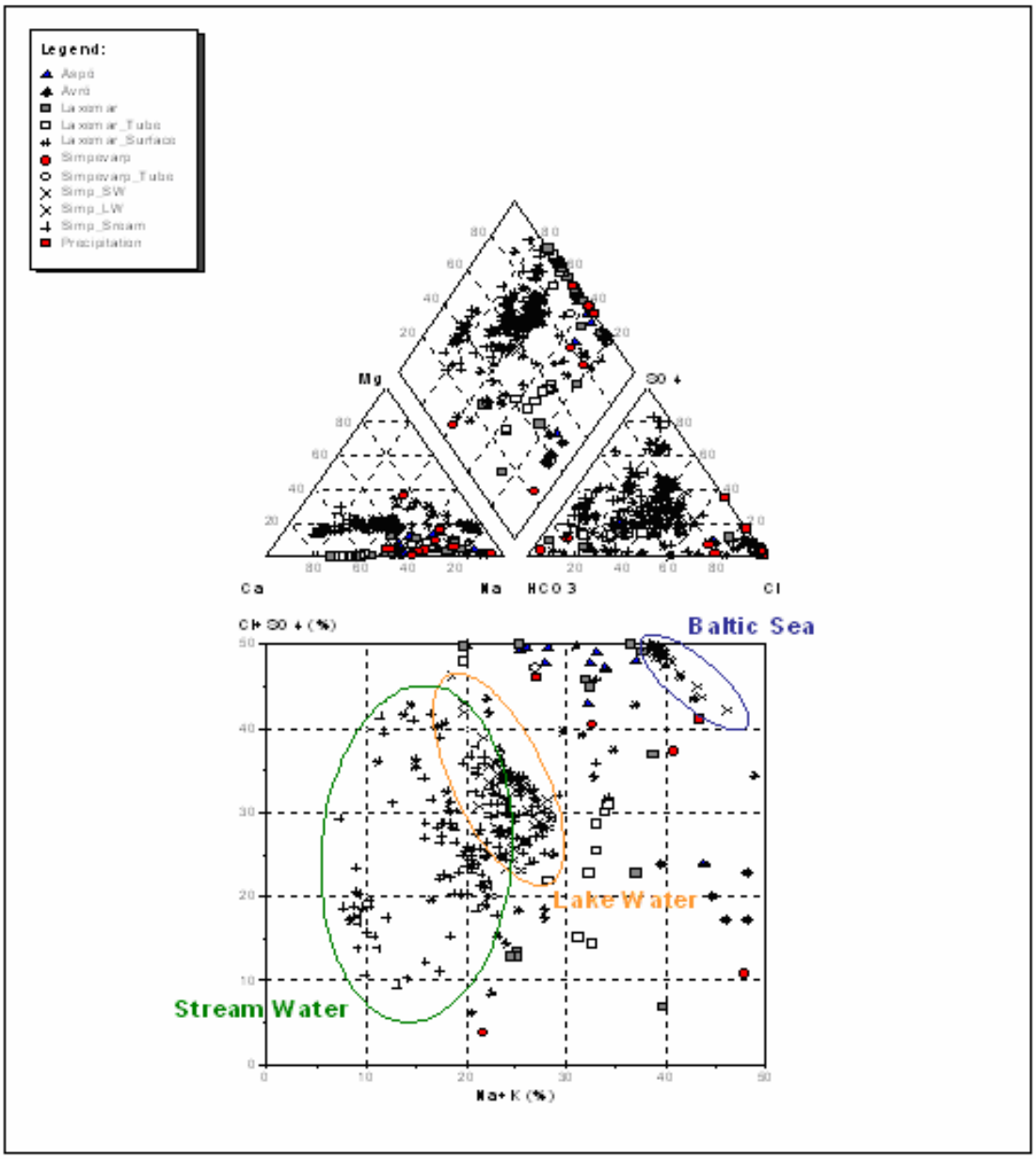

Figure 7.1-1: *Piper Plots of surface, near-surface and groundwaters from Simpevarp compared with other sites (POM sites) in the Simpevarp region. Indicated on the diagram are surface water groupings involving Baltic Sea, Stream and Lake waters.*

Set in a more regional context (Fig. 7.1-1), the Simpevarp groundwaters (red infilled circles) generally conform in chemistry to similar depth-related groupings representing the POM sites. The deep highly saline Laxemar groundwaters show a clear differentiation from all the other sites.

Comparison of Simpevarp waters, representing the Baltic Sea (SW), Lakes (LW) and Streams with the Laxemar surface waters, show some degree of grouping. This is suggested in most of the diagrams but best illustrated in the $Cl+SO_4$ vs Na+K plot. Here the Baltic Sea is clearly differentiated with a concentrated cluster at high $Cl+SO_4$ which reflects a representative Baltic Sea composition for the Simpevarp latitude. The plot also separates the Simpevarp Lake waters from the Stream waters, the latter clearly indicating a lower Na+K content, and the main Lake water cluster suggesting a slightly higher $Cl+SO_4$ content. There is a wide distribution of Stream waters and, as would be expected, some degree of overlap between the Lake waters, which occurs particularly at higher $Cl+SO_4$ contents. The Laxemar surface waters plot throughout the diagram although with a more dense clustering close to the Simpevarp Lake waters but with a significant overlap with the Stream waters.

7.2 Major ion and isotope plots for all Simpevarp data and comparison with the POM and other Fennoscandian sites

The major ion and isotope contents of the groundwaters are initially described in relation to depth to establish the general stratification trends if present. Since chloride in groundwater systems is considered be conservative, plots of chloride with selected cations and isotopes are then used to help evaluate the major geochemical reaction and mixing processes which characterise the Simpevarp site. The Simpevarp data are compared to the POM sites and, when applicable, compared to other Fennoscandian localities (i.e. Forsmark and Olkiluoto).

7.2.1 Hydrochemical depth trends

All Simpevarp data

pH

The cored boreholes show little significant pH trend with depth although a small decrease to 400 m followed by an equally small alkalinity increase levelling off from 600-1000 m is suggested (Fig. 7.2-1). Greatest acidity occurs in one of the shallow soil pipe groundwaters; near neutral groundwater is shown by one other soil pipe sample and also from one borehole section in KSH02 at 419-424 m.

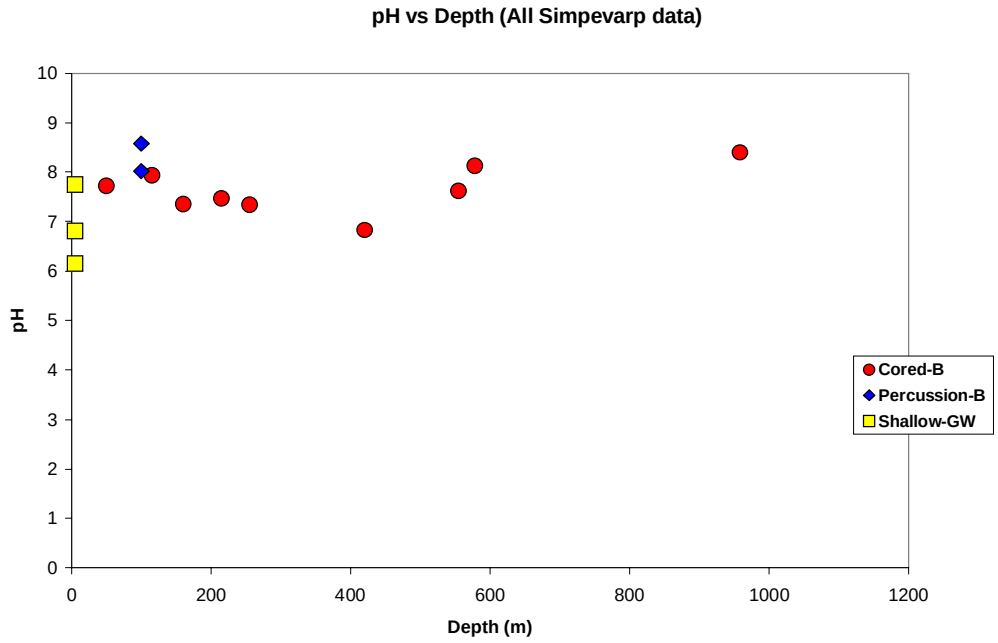

Figure 7.2-1: *Variation of pH with depth*

Sodium

Figure 7.2-2 shows that the first 100 m is characterised by dilute groundwaters with low sodium (<500 mg/L). This is followed by a sharp increase to around 2250 mg/L at 200 m; the groundwater with the lower sodium content at around 1000 mg/L at 255 m is a Tube sample and should be treated with caution. From 200 m to the deepest sample

collected at 958 m there is a steady increase in sodium content to a maximum of 4630 mg/L.

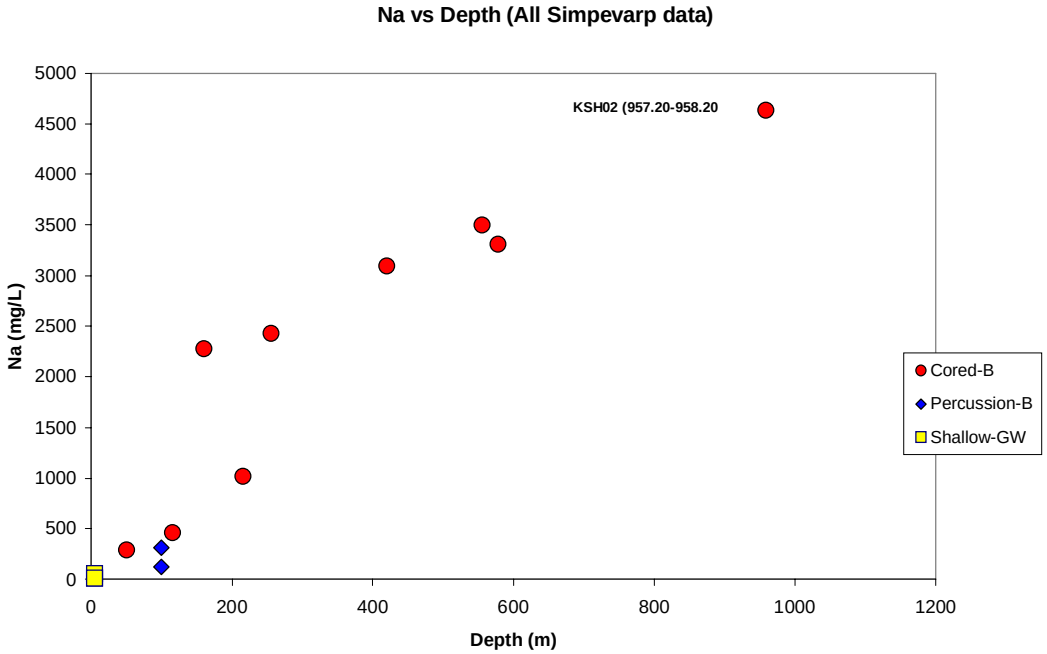

Figure 7.2-2: *Variation of Na with depth*

Potassium

Potassium (Fig. 7.2-3) shows a general pattern of consistently low values (range 2.15-14.70 mg/L) throughout the length of the borehole sampled, with the marked exception of KSH01A (548-565 m) which records 77 mg/L K. There is no obvious reason for this.

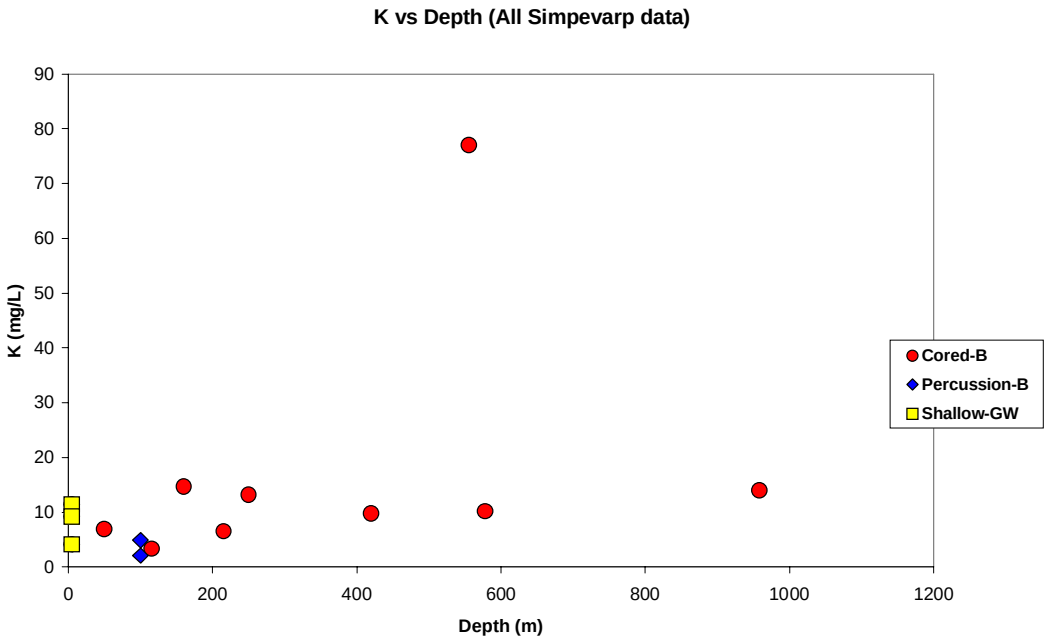

Figure 7.2-3: *Variation of K with depth*

Calcium

Calcium distribution (Fig. 7.2-4) shows similar general features to sodium apart from a greater jump in concentration between 600 m depth (~2000 mg/L) and the deepest groundwater at 957.20-958.20 m (4930 mg/L Ca).

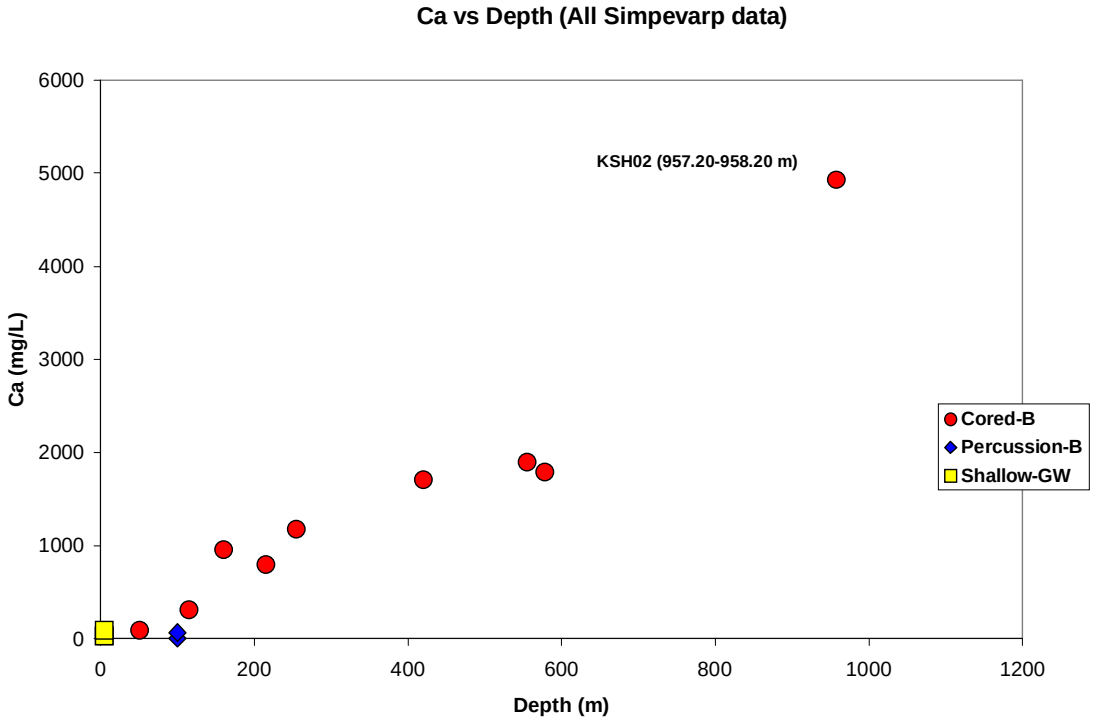

Figure 7.2-4: *Variation of Ca with depth*

Magnesium

Apart from the three highest values (> 45 mg/L Mg), the magnesium distribution shows a systematic decrease in content from the near-surface soil pipe groundwaters (10-30 mg/L), to the shallow dilute borehole groundwaters (1.4-22.8 mg/L) to eventually the deepest groundwater with 4.8 mg/L Mg (Fig. 7.2-5). The two anomalous groundwaters with the highest magnesium centre around the 200 m mark with lower concentrations at 600 m. The small increase associated with the soil pipe groundwaters and groundwater representing 0-100.60 m from borehole KSH03A may suggests an influx of marine water which could derive from Baltic Sea water or an older marine type.

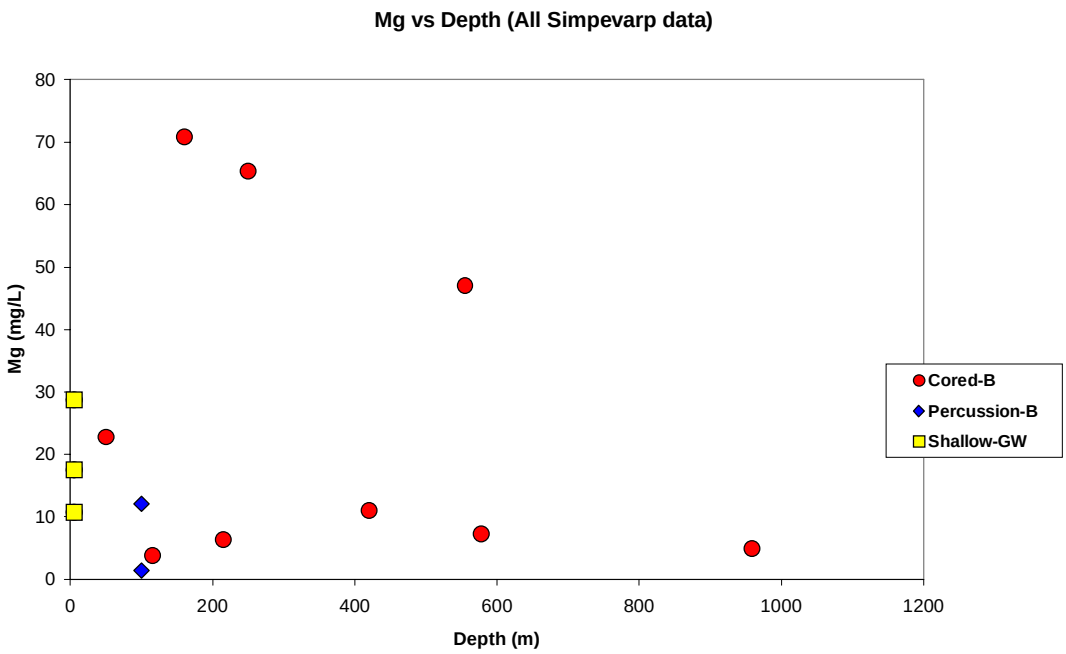

Figure 7.2-5: *Variation of Mg with depth*

Bicarbonate

Figure 7.2-6 shows high bicarbonate in groundwater prevailing at the near-surface down to around 150 m depth. At greater depths the bicarbonate content is consistently low (<25 mg/L).

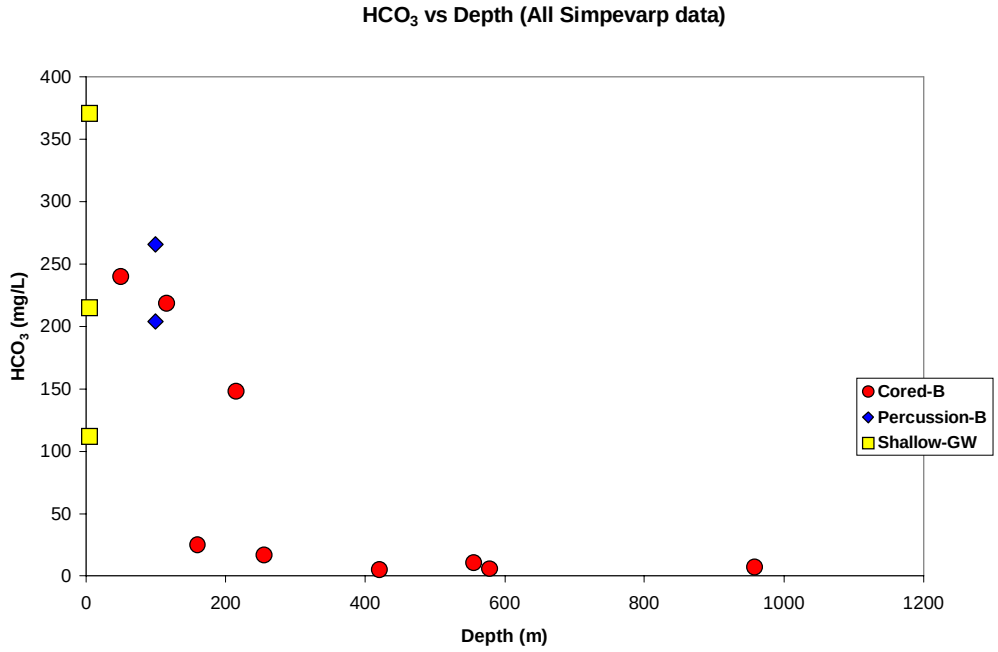

Figure 7.2-6: *Variation of HCO_3 with depth*

Chloride

In common with sodium and calcium, Figure 7.2-7 shows a similar trend for chloride including the rapid increase in content at around the 200 m depth reflecting the transition from near-surface and shallow dilute groundwaters (<1000 mg/L) to deeper more brackish types (5000-6000 mg/L). At greater depths than 600 m there is also a marked increase to a maximum of 16800 mg/L Cl.

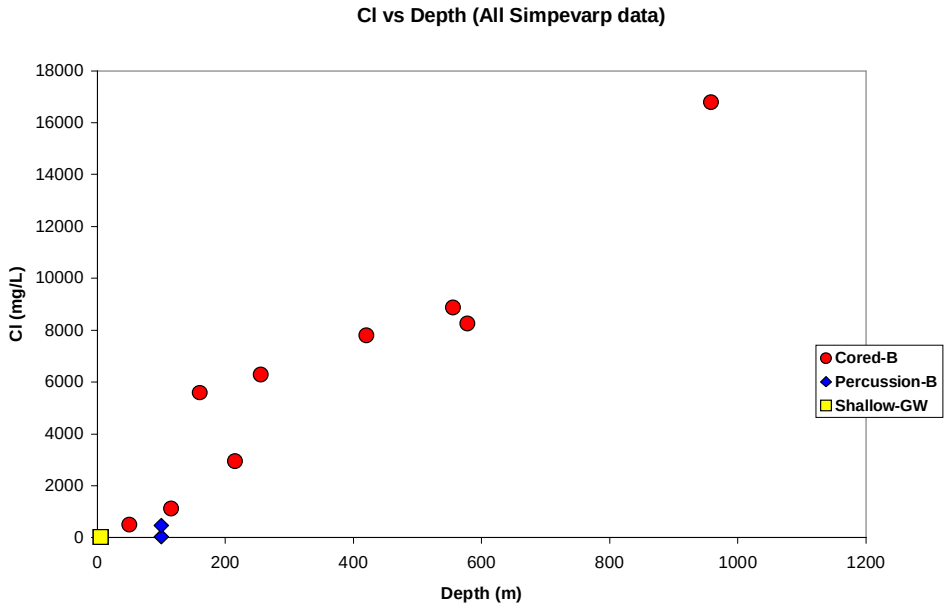

Figure 7.2-7: Variation of Cl with depth

Bromide

Bromide (Fig. 7.2-8) shows a similar behaviour to that of chloride with depth.

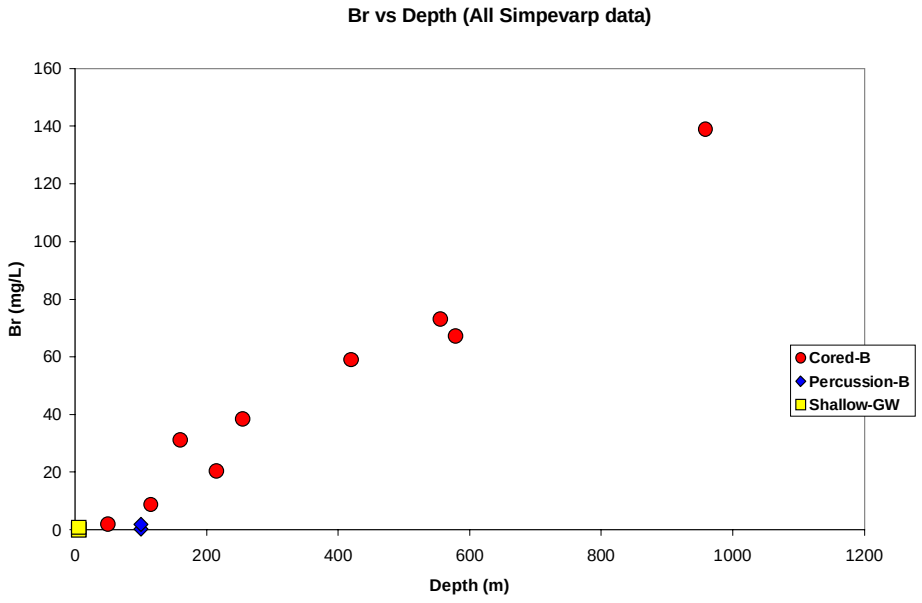

Figure 7.2-8: *Variation of Br with depth*

Sulphate

Generally, sulphate shows a systematic increase in content with increasing depth, to a maximum of 608 mg/L at approx. 960 m (Fig. 7.2-9). However, at shallow depths (0-300 m) there appears to be two trends, one of lower and one of higher concentration. However, since the two higher values correspond to Tube samples from borehole KSH02 from 91-141 m and 191-241 m, they may reflect some perturbance particularly sensitive to sulphate and should be neglected. The dominant trend therefore is low sulphate to around 300 m depth and then a steady increase to around 600 m followed by a sharp increase at greater depths.

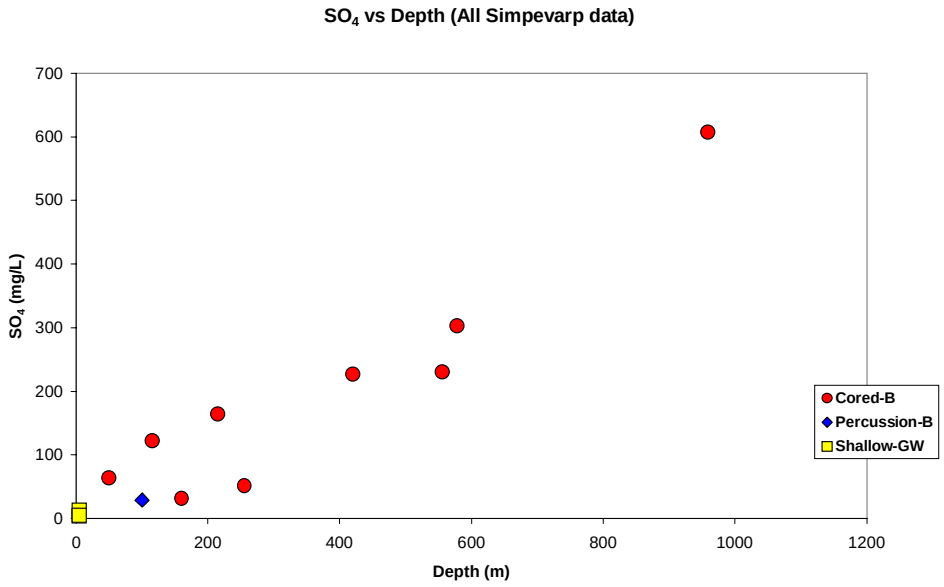

Figure 7.2-9: Variation of SO_4 with depth

Comparison with the POM sites

Chloride

Comparison of the Simpevarp chloride data with some of the POM sites, together with Forsmark and Olkiluoto, is shown in Figure 7.2-10. It may be argued that such a comparison should be treated with caution since Forsmark and Olkiluoto are geographically distant, have a differing palaeo-evolution and represent different hydrogeological regimes. Furthermore, Laxemar, although close by, represents more a mainland environment and involves greater depths. However, since the Fennoscandian basement hydrogeochemistry probably shares general similarities irrespective of geographic location, Figure 7.2-10 may serve a useful purpose particularly with respect to establishing whether a Littorina component is present in the Simpevarp groundwaters.

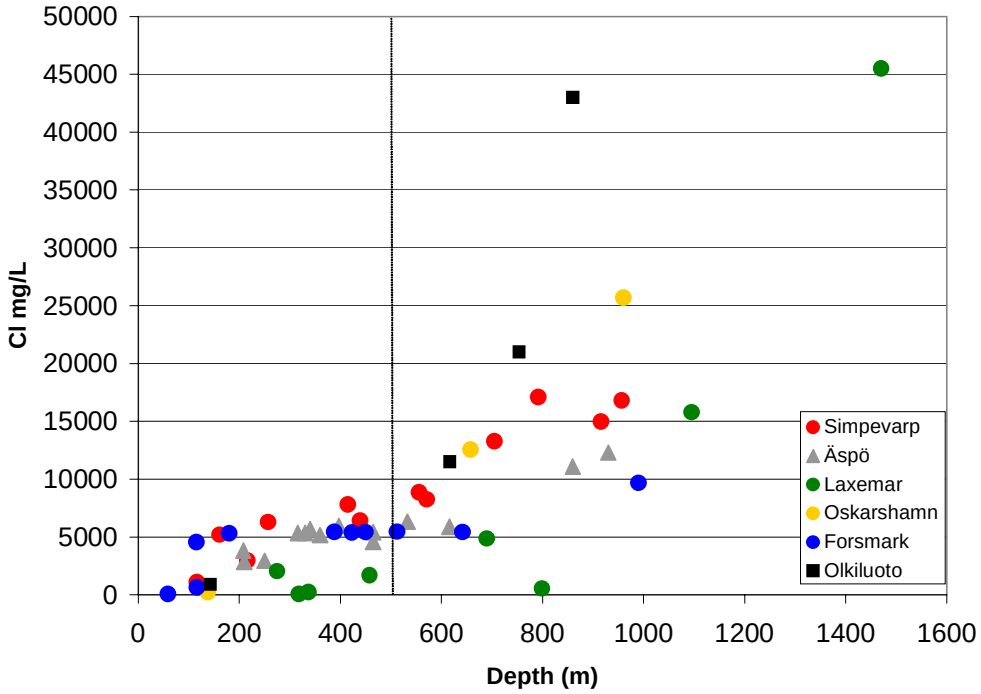

Figure 7.2-10: *Depth comparison of chloride between different POM and Fennoscandian sites.*

The Laxemar data show mostly dilute groundwaters (< 2000 mg/L Cl) extending to approx. 600 m for KLXO1 and to around 1000 m for KLX02 before a rapid increase in salinity to maximum values of around 47 g/L Cl at 1700 m. Olkiluoto shows an initial sharp increase in chloride at around 150 m to a levelling off at 5000 mg/L Cl which continues to 450 m; here there is a relatively steady increase to maximum values of around 20 g/L Cl at 900 m depth (one maximum value of 44 g/L Cl was recorded). The available Forsmark data so far show a close similarity to the initial Olkiluoto trends, although the levelling off at approx. 5000 mg/L Cl continues to around 650 m where a small increase to 10 000 mg/L Cl is achieved at 1000 m; there are no deeper groundwater data to compare ultimate salinity contents. In addition the Äspö trends generally are close to those of Forsmark.

The Simpevarp data, as described above (Fig. 7.2-7), fall along the general plateau characterised to approx. 500 m depth by chloride ranging from around 5.100-6.300 mg/L Cl (Fig. 7.2-10). In addition the Simpevarp profile so far shares a close similarity with Oskarshamn and shares with Äspö and Forsmark similar trends over the first approx. 600 m.

7.2.2 Hydrochemical evolution trends – major ions and stable isotopes

Using data judged to be representative, X-Y plots are presented for most of the analysed major ions and isotopes. Some additional data judged of limited suitability (e.g. some open hole tube samples of high salinity) have also been included when considered appropriate. Furthermore, local scale hydrochemical trends characteristic of the Simpevarp site are compared with the POM sites and sometimes with other sites in Fennoscandia to provide a more regional setting for interpretation.

The plots are presented in sequence, first excluding the most saline groundwater to help focus in on the near-surface and shallow groundwaters and their characteristics, then including the most saline groundwater, and finally to compare with the POM and Fennoscandian sites if appropriate.

Plots of sodium versus chloride

All Simpevarp data

Figure 7.2-11 shows a close correlation between Na and Cl. Two main trends are indicated: a) shallow groundwater trend (upper approx. 100 m) closely following the modern sea water dilution line and representing groundwaters from soil pipes, percussion boreholes and the upper part (0-100.60 m) of cored borehole KSH03A, and b) deep groundwater trend (cored boreholes) which progressively deviates from the modern sea water dilution line with increasing depth and salinity. This latter deviation can be explained by increased mixing with an older deep saline component of a non-marine or non-marine/old marine origin.

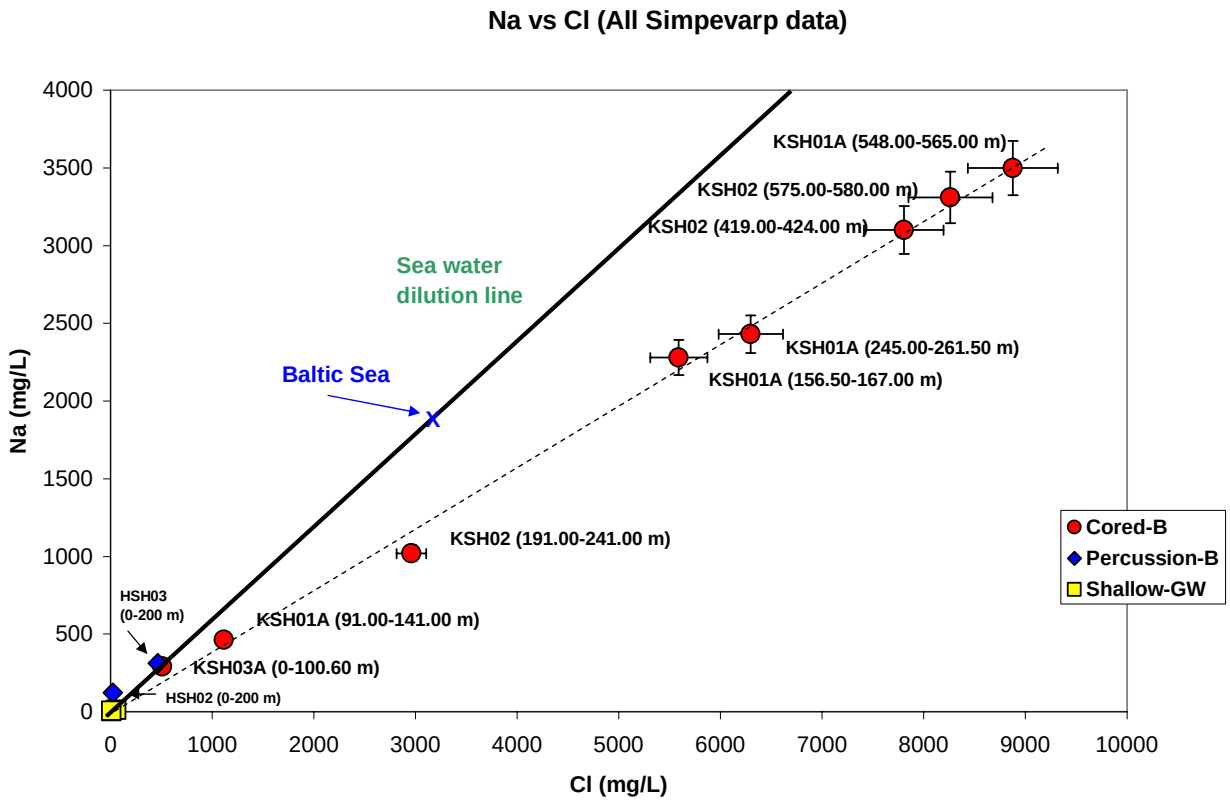

Figure 7.2-11: *Plot of Na vs Cl for all Simpevarp data (excluding the deepest groundwater) showing error bars ±5%.*

Figure 7.2-12 includes the deepest, most saline groundwater (borehole KSH02: 957.20-958.20 m), which shows a marked deviation from the rest of the cored borehole groundwaters. This strengthens the suggestion that mixing with a deep, non-marine saline component is occurring with greater probability at increased depth.

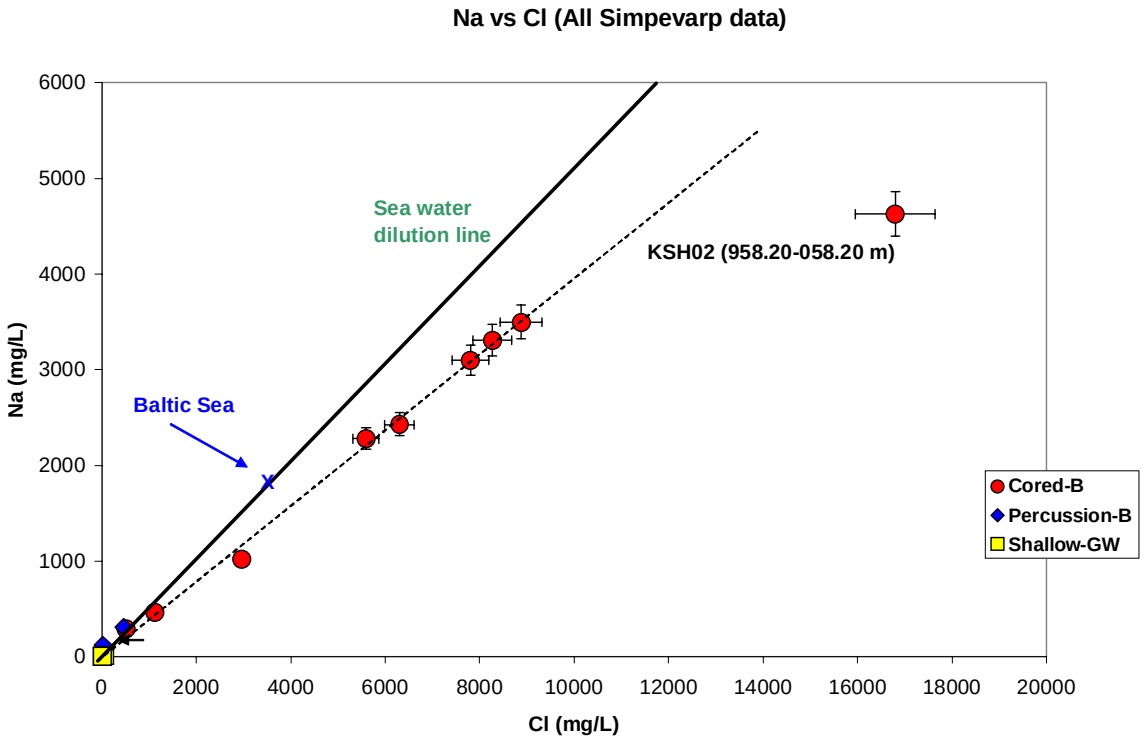

Figure 7.2-12: Plot of Na vs Cl for all Simpevarp data (including the deepest groundwater) showing error bars ±5%.

Comparison with the POM sites

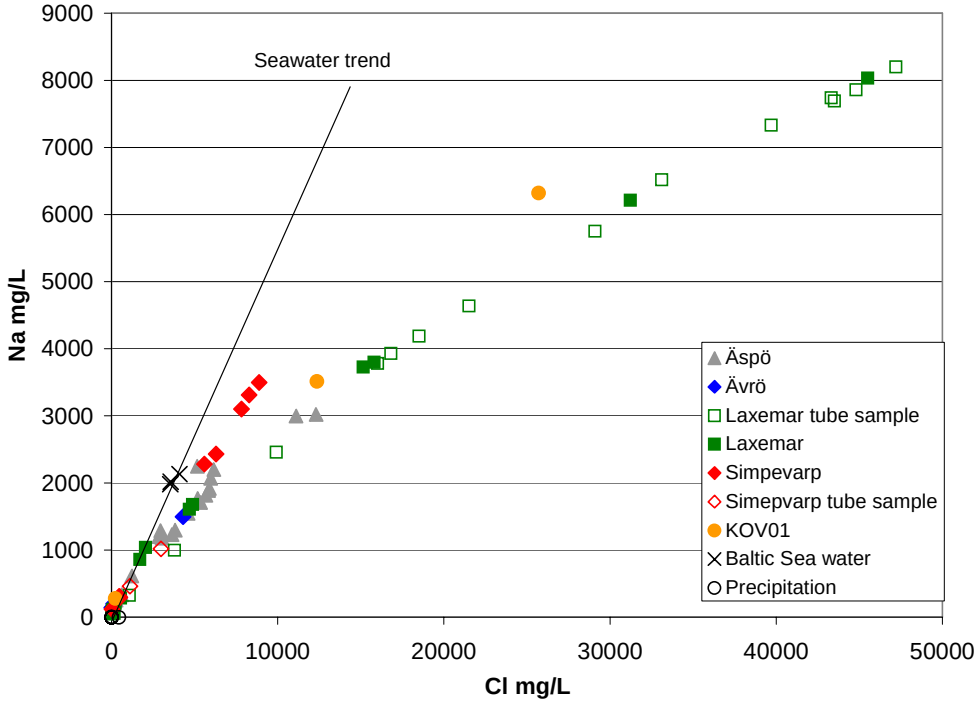

Figure 7.2-13: *Plot comparing all Simpevarp Na vs Cl data with the POM sites.*

Figure 7.2-13 compares the Simpevarp site with the POM site data; selected open hole tube samples have been included for Simpevarp and Laxemar for illustrative purposes when considered close to the representative values. Clearly illustrated is the: a) additional support for a shallow groundwater trend along the modern sea water dilution line, and b) additional support for a deviation trend towards a more non-modern marine and/or non-marine salinity source with increasing depth. A further trend towards an increased deviation is shown by the highly saline Laxemar and Oskarshamn (KOV01) groundwaters (and possibly by some of the saline Äspö samples) at approx. 10000 mg/L Cl. This marked deviation indicates a more definitive non-marine origin to the saline groundwaters. This apparent difference between Simpevarp and especially Laxemar reflects the fact that the deep Laxemar groundwaters are Ca.Na-Cl dominant, whilst the Simpevarp deep groundwaters (so far) are Na-Ca-Cl dominant. This further discussed in relation to calcium contents (Fig. 7.2-19)

Plots of magnesium versus chloride

All Simpevarp data

Figure 7.2-14 shows a close alignement of shallow groundwaters to the modern sea water dilution line. In addition, there is a marked deviation by borehole KSH02 groundwaters characterised by low Mg contents (<10 mg/L) and increasing salinity. These Mg contents result in a clear distinction between borehole KSH01A where Mg ranges from 47.0-70.8 mg/L. Furthermore, borehole KSH01A indicates a decrease in Mg with increasing depth and salinity. This suggests the possibility that borehole KSH01A groundwaters contain a component of marine water, either modern (Baltic Sea) and/or ancient (Littorina?) in origin. Borehole KSH02, in contrast, appears to have been shielded hydraulically from such a possibility. Flushing water contamination of borehole KSH01A can be ruled out as the source of this water (i.e. borehole HSH03) is characteristically very dilute (12.1 mg/L Mg).

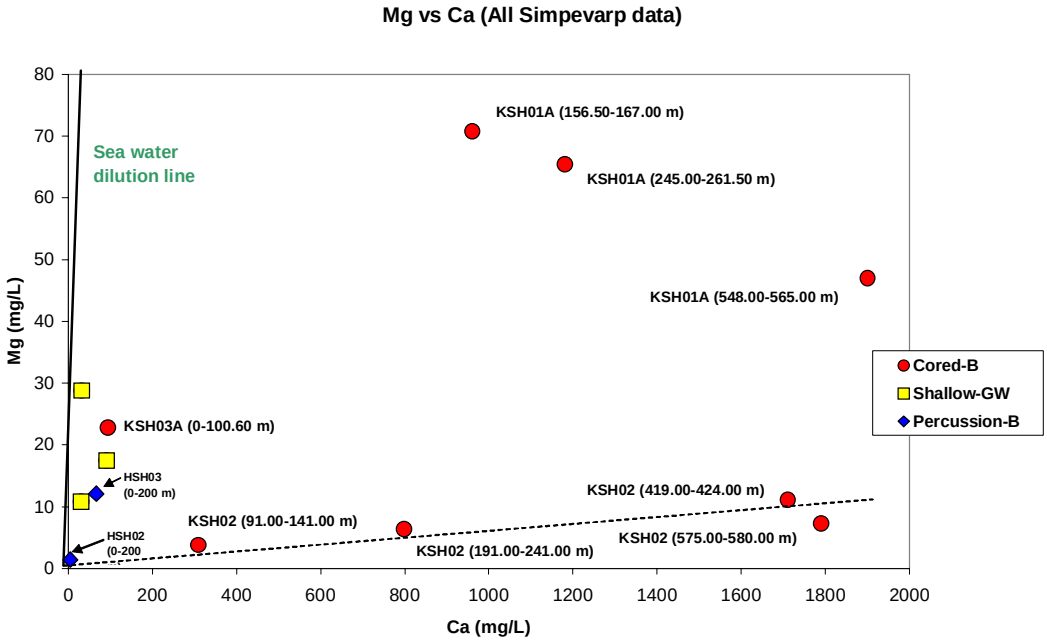

Figure 7.2-14: *Plot of Mg vs Cl for all Simpevarp data (excluding the deepest groundwater) showing error bars ±5%.*

Moreover, examination of the three sections sampled in borehole KSH01A shows a clear indication that with greater depth the influence of the marine component is decreasing with a corresponding increase in a non-marine saline component, and this trend seems to be converging towards the borehole KSH02 groundwaters. This is made even more obvious in Figure 7.2-15 which includes the deepest groundwater sample.

A further observation from Figure 7.2-14 is the spread of Mg values at low Cl contents for the Soil Pipe samples (10.8-28.8 mg/L); this may reflect: a) contact with an older marine water followed by cation exchange reactions and later flushing out of chloride, or b) simply water-rock interaction of recharge with minerals in the soil.

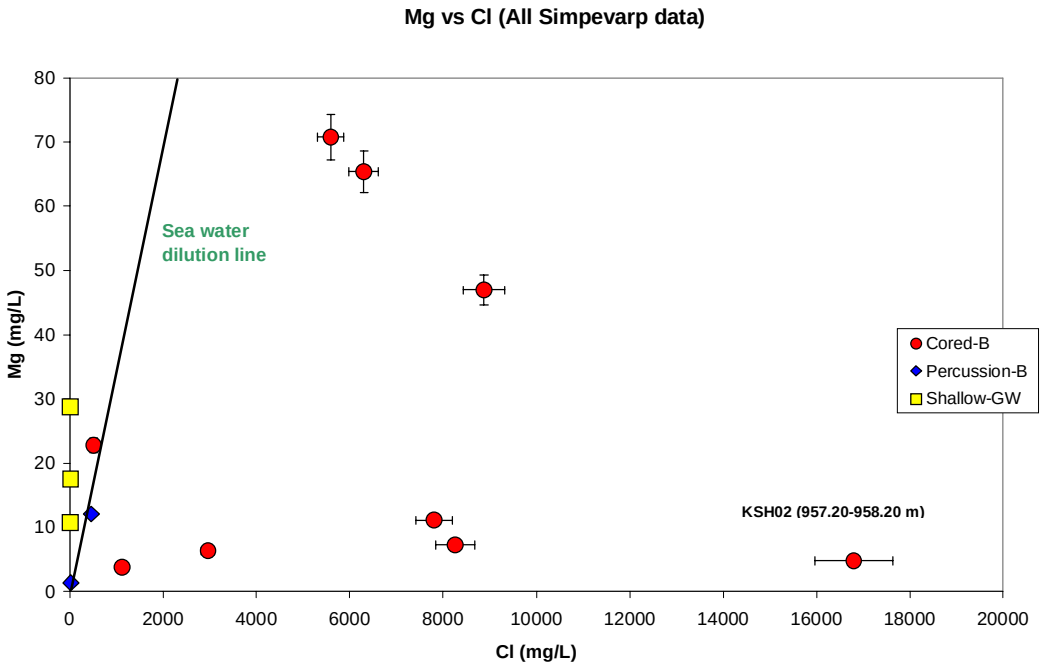

Figure 7.2-15: *Plot of Mg vs Cl for all Simpevarp data (including the deepest groundwater) showing error bars ±5%.*

Comparison with the POM sites

Comparison with the POM site data is shown in Figure 7.2-16. The association of the KSH02 groundwaters with the deep Laxemar and Oskarshamn (KOV01) data supports a non-marine origin for the measured salinity. In contrast the KSH01A groundwaters (particularly the two shallow samples) plot together with other groundwaters (mainly Äspö) characterised by higher Mg contents which may suggest some residual Littorina Sea water component .

In general there is no strong indication from the Simpevarp borehole data of any significant Littorina Sea component, in contrast to the Forsmark site. For example the Simpevarp Mg values are too low (3.80-70.80 mg/L) compared to the estimated values for the Littorina Sea composition (Mg ~448 mg/L; Cl ~6500 mg/L) as derived by Pitkänen et al (1999). However, some indications do exist and this discussed in greater detail in section 7.7.

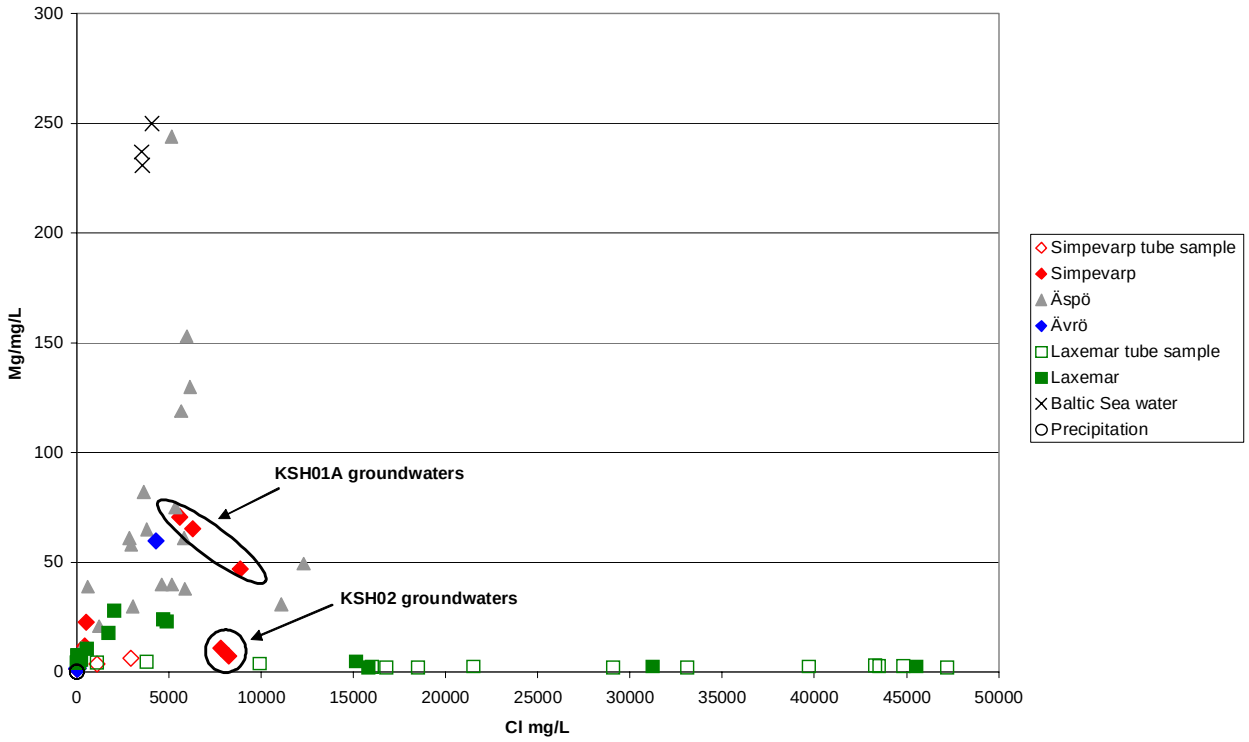

Figure 7.2-16: *Plot comparing all Simpevarp Mg vs Cl data with the POM sites.*

Plots of calcium versus chloride

All Simpevarp data

Figure 7.2-17 shows that all samples deviate from the modern sea water dilution line and two main trends are suggested demarcating a higher saline group (>7000 mg/L Cl), and a lower saline group (5500-6500 mg/L Cl). An additional trend suggested by open hole tube samples KSH01A (91-141 m) and KSH02 (191-241 m) most probably reflects some artificial mixing in the borehole and should be treated with caution. The possibility of the two salinity trends may be attributed to variations in mixing with deeper, more highly saline and calcium-rich groundwaters which have undergone extensive water/rock interaction.

Figure 7.2-18 includes the deepest, most saline groundwater (borehole KSH02: 957.20-958.20 m), which shows a marked deviation from the rest of the cored borehole groundwaters. In common with sodium (see above), this strengthens the suggestion that mixing with a deep, non-marine saline component is occurring with greater probability at increased depth.

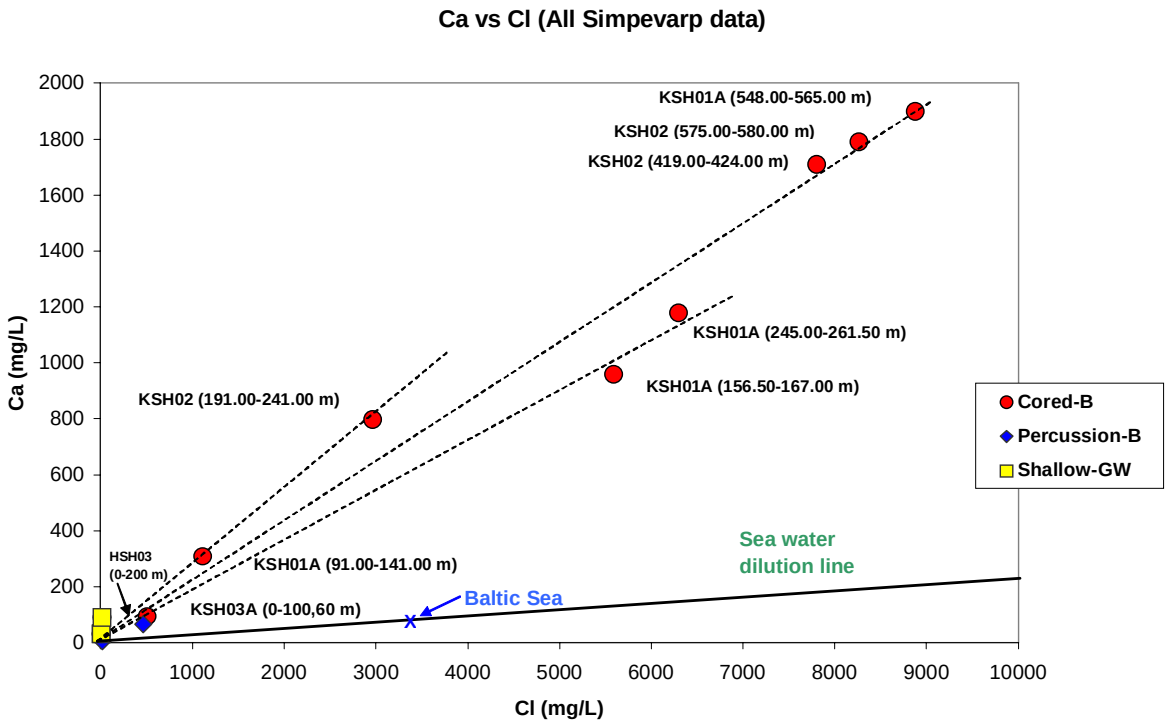

Figure 7.2-17: *Plot of Ca vs Cl for all Simpevarp data (excluding the deepest groundwater).*

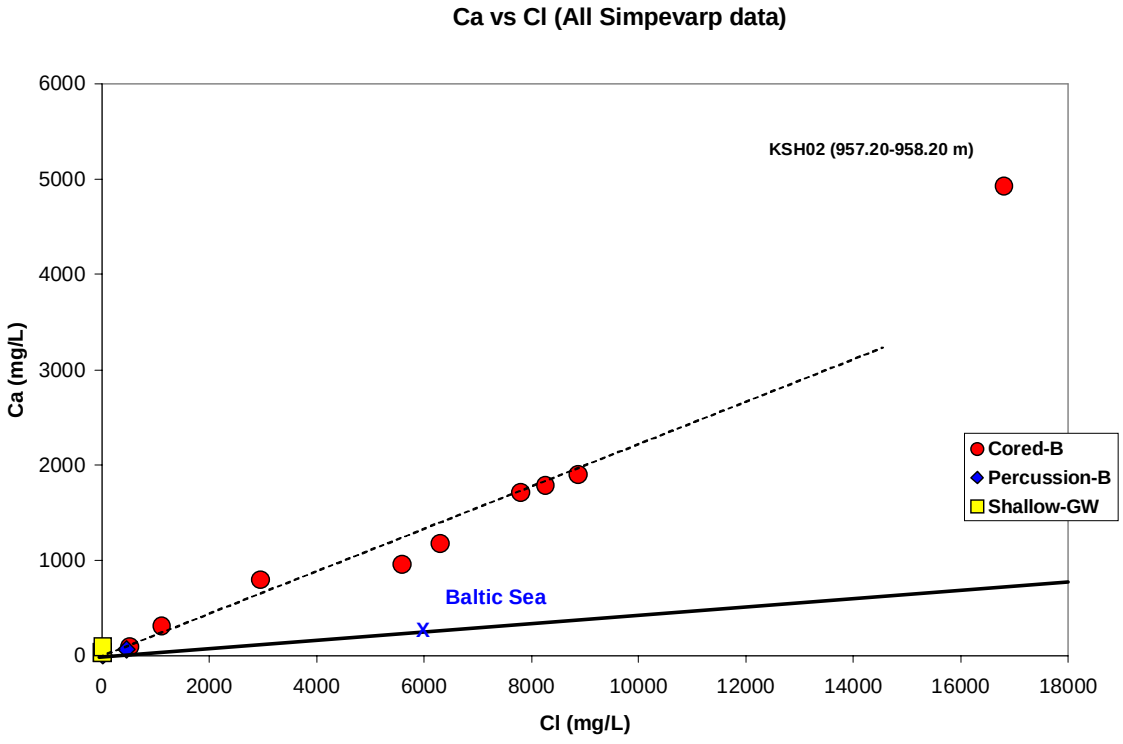

Figure 7.2-18: *Plot of Ca vs Cl for all Simpevarp data (including the deepest groundwater).*

Comparison with the POM sites

Compared to the POM sites (Fig. 7.2-19) Simpevarp follows the same general trend but it is noticeable in more detail that Simpevarp and Oskarshamn (KOV01) show a small deviation suggesting a lower calcium content. This is matched by higher sodium contents shown in Figure 7.2-13. This underlines the basic difference between the deeep Laxemar groundwaters which are Ca-Na-Cl in type, the deep Oskarshamn groundwaters which have lower calcium but still Ca-Na-Cl in type, and the deepest Simpevarp/Oskarshamn groundwaters which are Na-Ca-Cl in type (although this might represent a transitionary stage to a Ca-Na–Cl type at even greater depths).

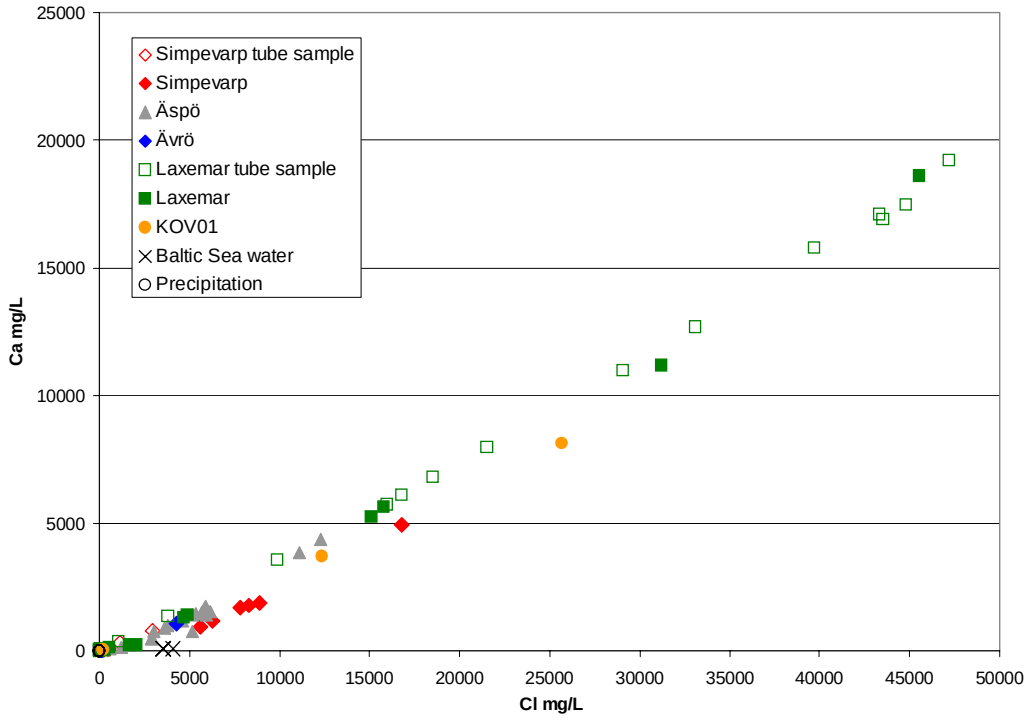

Figure 7.2-19: *Plot comparing all Simpevarp Ca vs Cl data with the POM sites.*

Plots of sulphate versus chloride

All Simpevarp data

Figure 7.2-20 shows no obvious mixing trends; the main observations are the two KSH01A outliers with low sulphate compared to the higher sulphate group of cored borehole groundwaters collected at greater depths. As pointed out earlier (section 7.2.1; Fig. 7.2-9) the two Tube samples (KSH01A: 91-141 m and 191-241 m) should be neglected in this present discussion. This essentially subdivides the groundwaters into three groups: a) shallow, dilute groundwaters (<30 mg/L SO_4) closely correlated with the sea water dilution line, b) brackish, low sulphate groundwaters (<50 mg/L SO_4) at slightly greater depths (150-260 m), and c) deeper saline, higher sulphate groundwaters (>100 mg/L SO_4). The association of high sulphate with high salinity is consistent with mixing with deep groundwaters of non-marine or non-marine/old marine mixing origin. This is supported further by the deepest and most saline groundwater containing 608 mg/L SO_4 (Fig. 7.2-21).

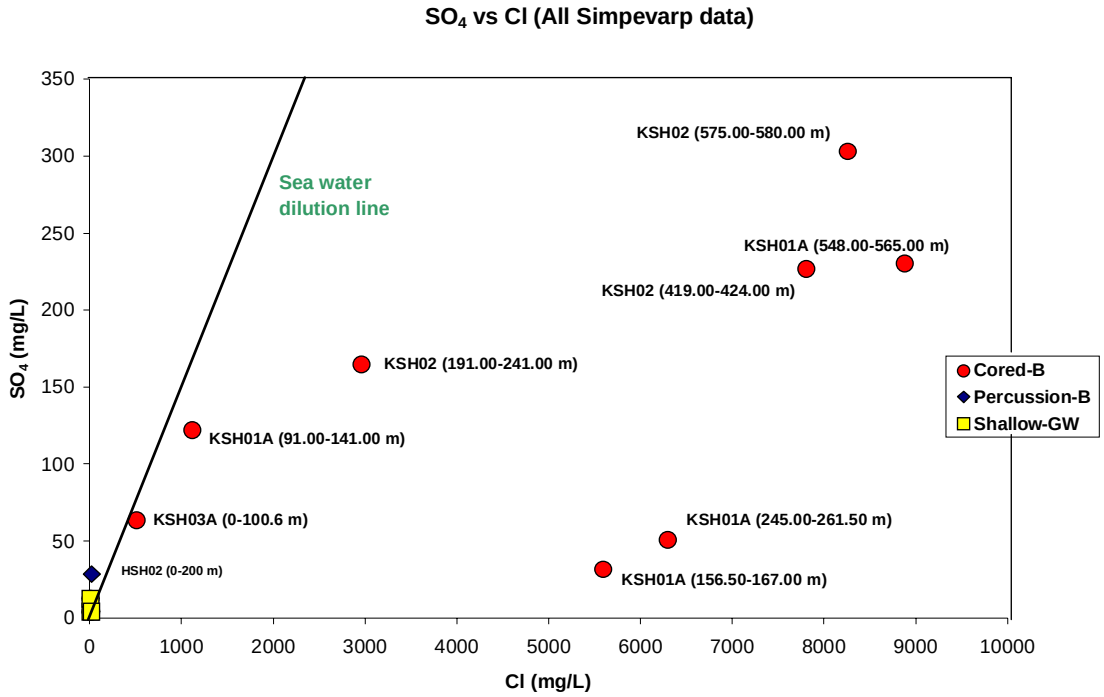

Figure 7.2-20: *Plot of SO_4 vs Cl for all Simpevarp data (excluding the deepest groundwater).*

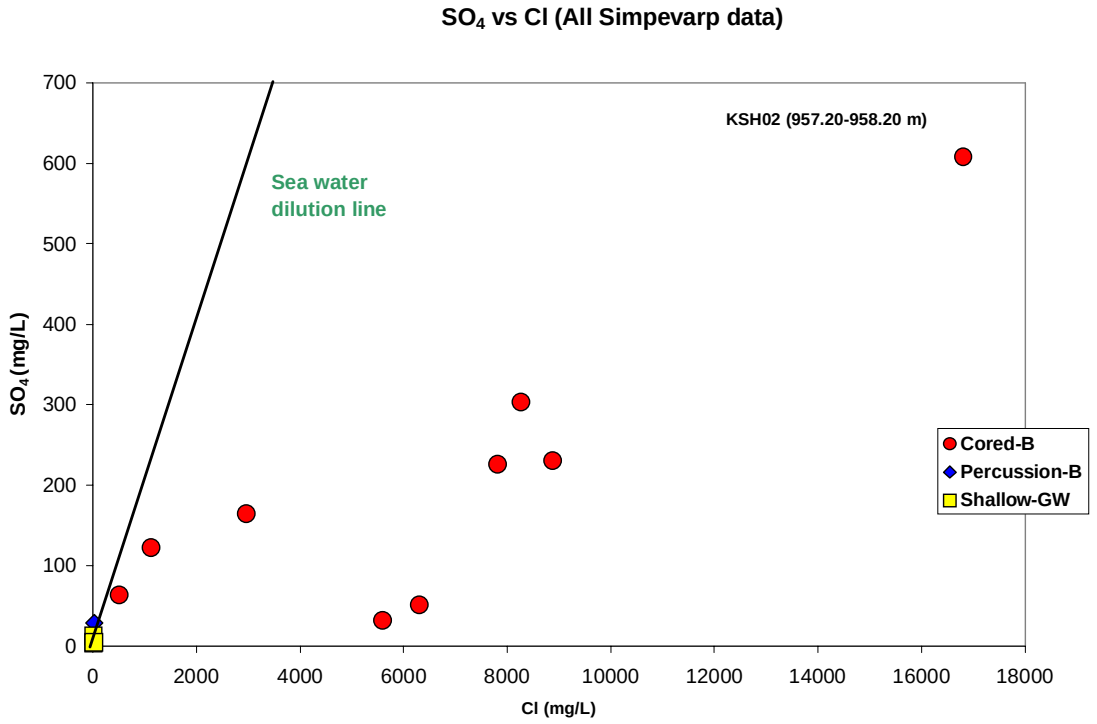

Figure 7.2-21: *Plot of SO_4 vs Cl for all Simpevarp data (including the deepest groundwater).*

Comparison with the POM sites

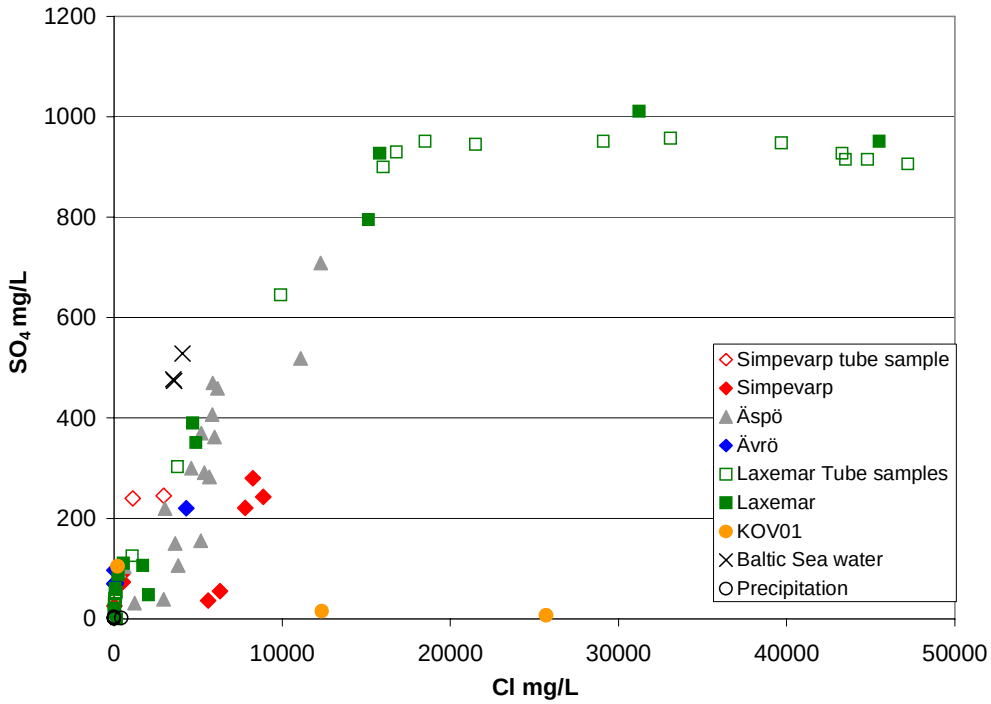

Figure 7.2-22: *Plot comparing all Simpevarp SO_4 vs Cl data with the POM sites.*

Figure 7.2-22 shows that with the notable exception of Oskarshamn (KOV01), all sites generally show a consistent increase in sulphate with increasing salinity. Several Laxemar groundwaters indicate a levelling of sulphate at around 900-1000 mg/L despite a significant increase in salinity from 15000-50000 mg/L Cl. This limitation of sulphate content in saline groundwaters was also noted by Gascoyne (2004) at the URL site in Canada; in this case it was attributed it to the solubility control exerted by gypsum which was close to saturation in the groundwaters.

Plots of bromide versus chloride

All Simpevarp data

Figure 7.2-23 shows the gradual depth-related increase in bromide with increase in chloride. The shallow dilute groundwaters plot close to the modern sea dilution line whilst the deeper samples show an increasing deviation with depth; once again the highest salinity samples suggest a distinct non-marine or non-marine/old marine mixing origin. This feature is further accentuated in Figure 7.2-24.

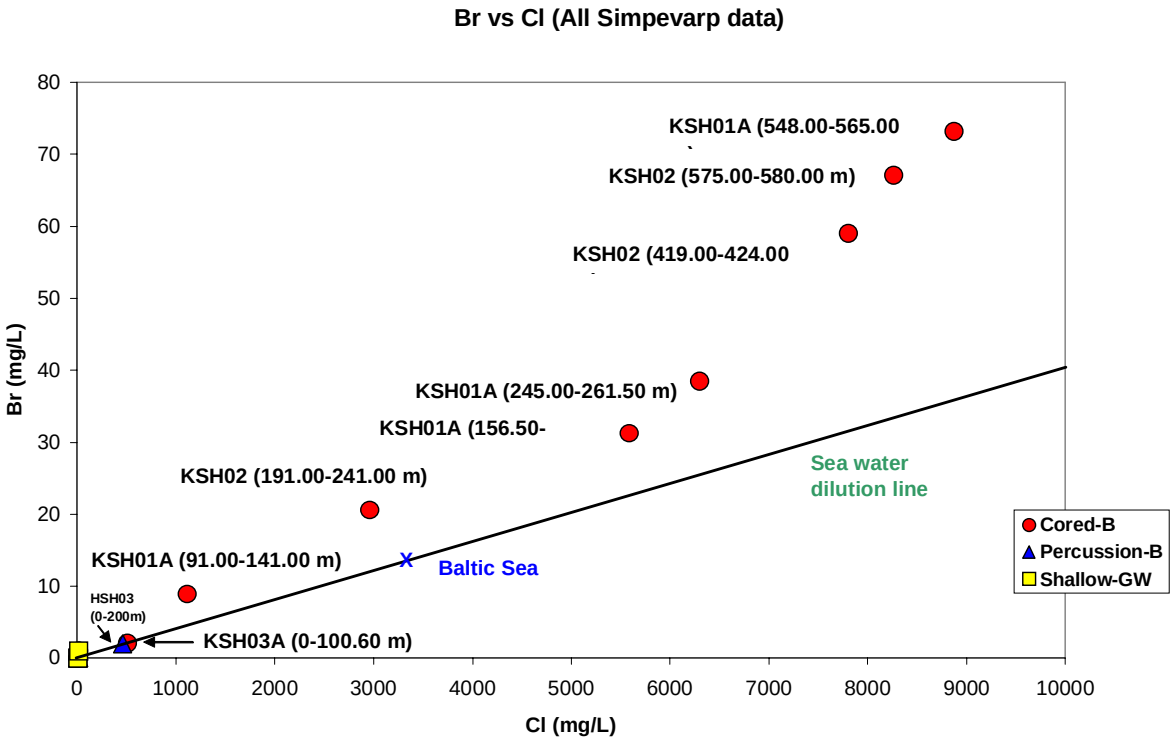

Figure 7.2-23: Plot of Br vs Cl for all Simpevarp data (excluding the deepest groundwater) .

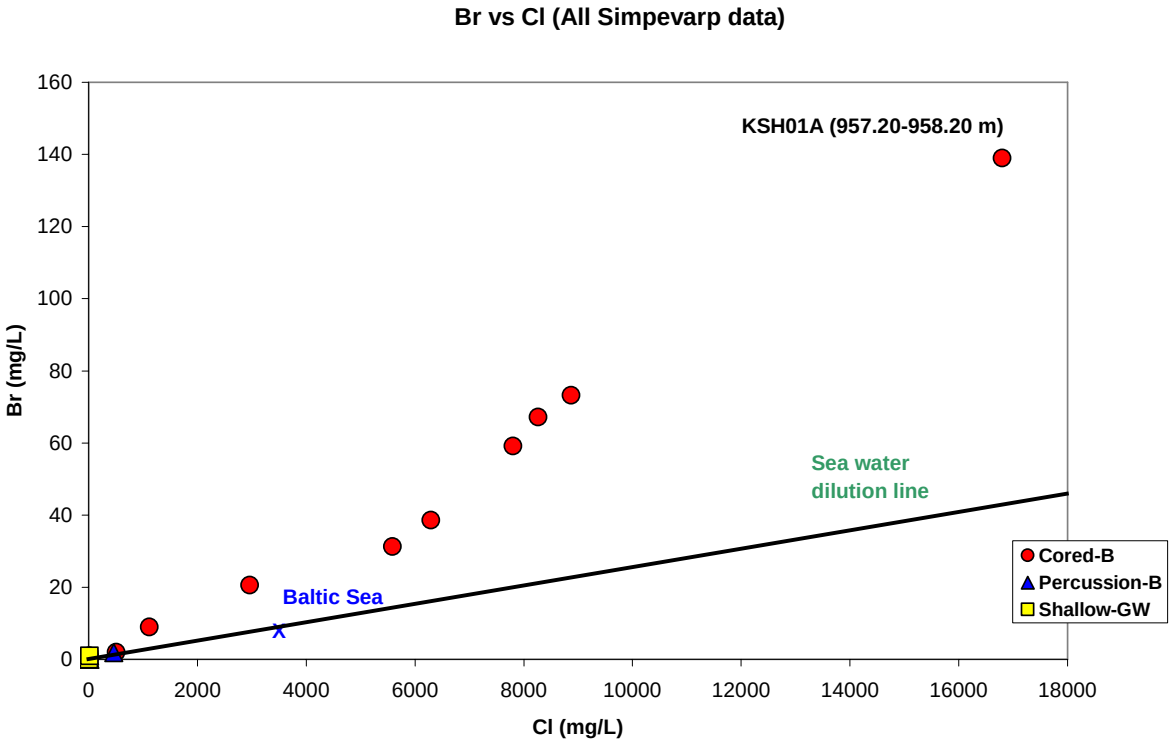

Figure 7.2-24: *Plot of Br vs Cl for all Simpevarp data (including the deepest groundwater) .*

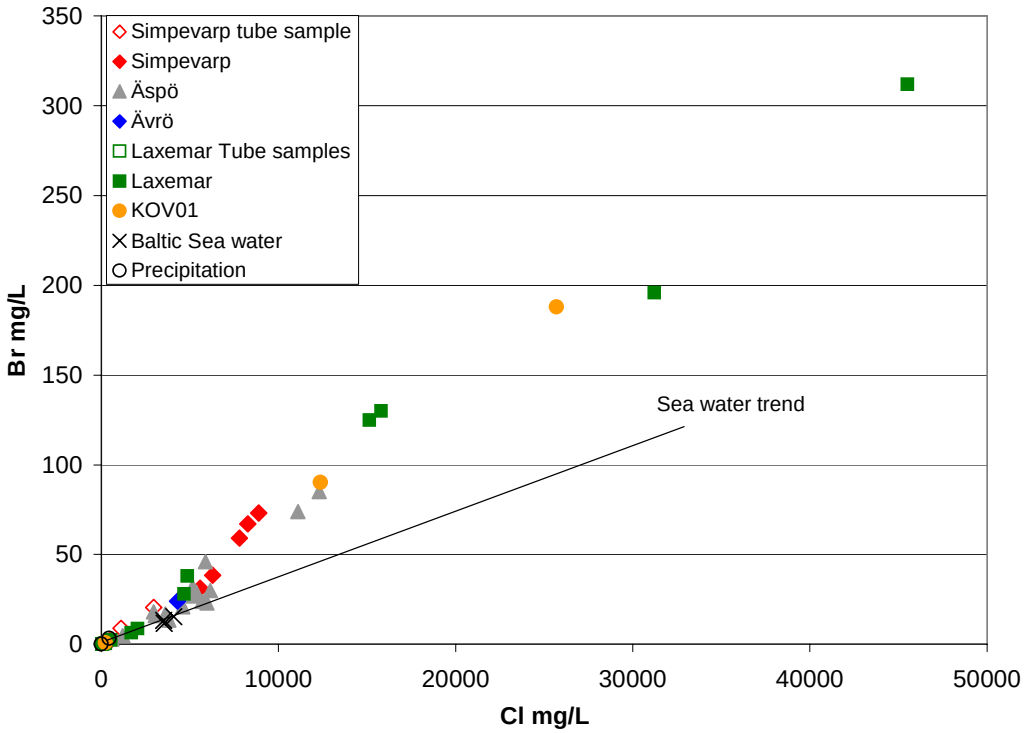

Figure 7.2-25: *Plot comparing all Simpevarp Br vs Cl data with the POM sites.*

Comparison with the POM sites

Comparison with the POM sites (Fig. 7-26) shows the Simpevarp samples plotting along the lower part of a well defined trend of increasing bromide with increasing salinity defined by the Oskarshamn and Laxemar groundwaters and to a lesser extent by the most saline Äspö groundwaters. This feature lends further support for a deep, non-marine or non-marine/old marine mixing origin for the deepest, most saline Simpevarp samples.

Plots of bicarbonate versus chloride

All Simpevarp data

Figure 7.2-26, combining all Simpevarp data, emphasis high bicarbonate contents (>100 mg/L) present in the shallow, dilute groundwaters, contrasting with low contents (> 30 mg/L) in the brackish to highly saline groundwaters. The ringed groundwaters represent the tube samples and should be neglected in this present discussion.

Comparison with the POM sites (Fig. 7.2-27) further clarifies the sharp transition from high to low bicarbonate where groundwaters are brackish in type, i.e. within the range of 5000-6000 mg/L Cl., corresponding to depths of around 150-200 m at Simpevarp.

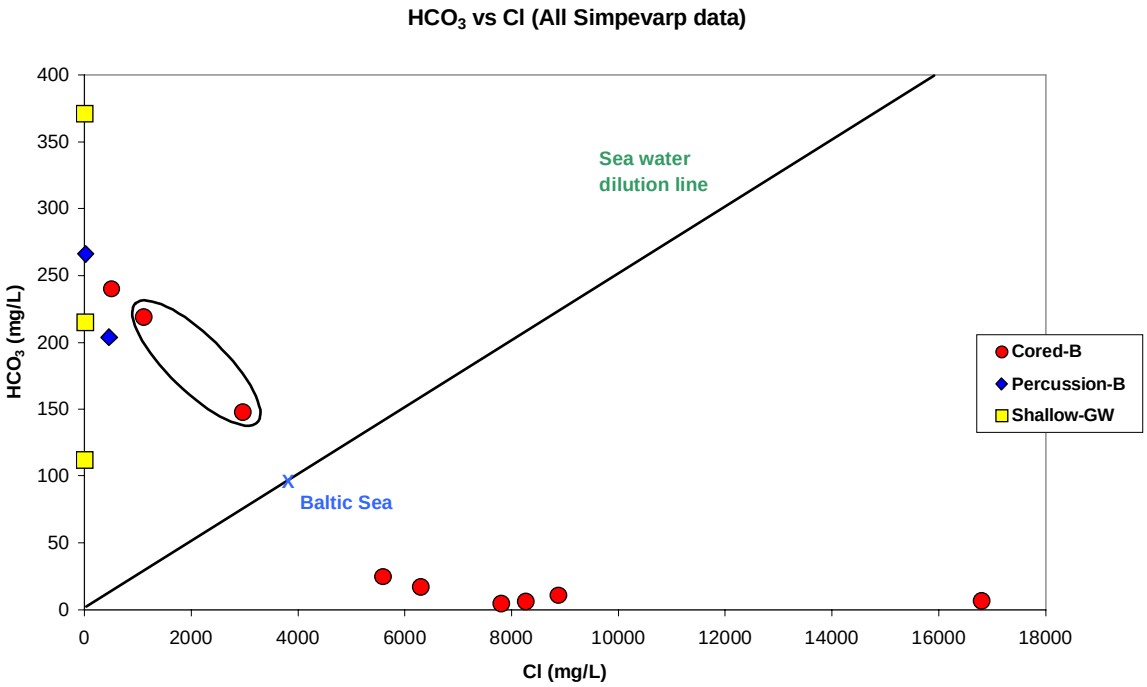

Figure 7.2-26: Plot of HCO_3 vs Cl for all Simpevarp data (KSH02 Tube samples are ringed).

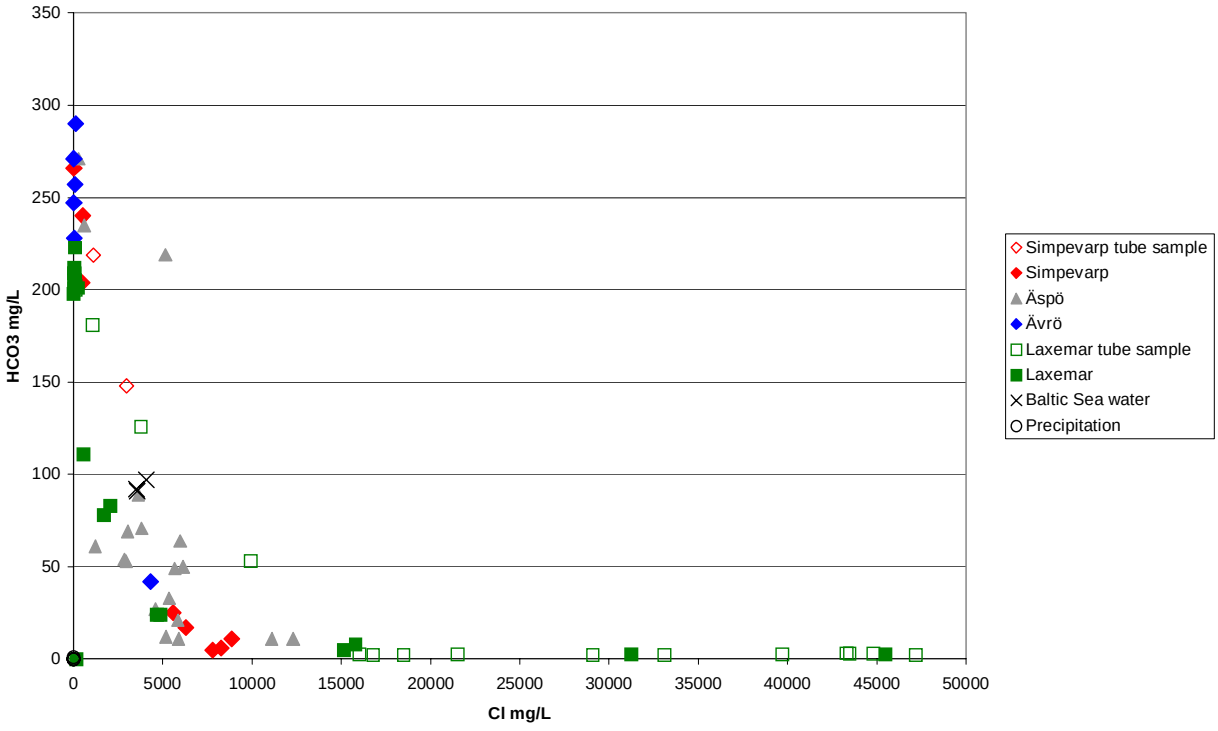

Figure 7.2-27: *Plot comparing all Simpevarp HCO_3 vs Cl data with the POM sites.*

Plot of magnesium versus calcium

All Simpevarp data

Figure 7.2-28 illustrates once again the shallow dilute groundwaters aligned close to the modern sea water dilution line and the distinct difference between groundwaters from KSH01A and KSH02. This plot basically reflects the Mg vs Cl plot (Fig. 7.2-14) which is not so surprising given the close correlation of high salinity with high calcium content (Fig. 7.2-18). However, it further supports the hypothesis that borehole KSH01A may contain a component of marine-derived water not shared by borehole KSH02.

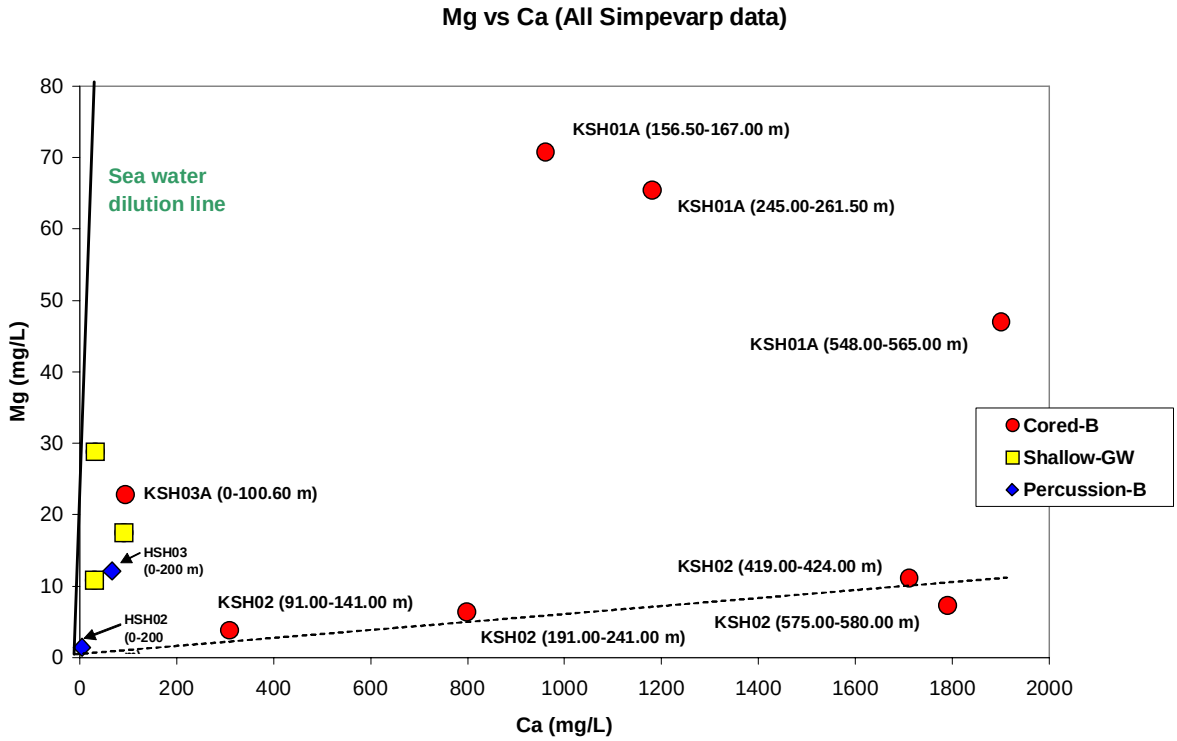

Figure 7.2-28: *Plot of Mg vs Ca for all Simpevarp data (excluding the deepest groundwater).*

Comparison with the POM sites

This is not reproduced here as it reflects the Mg vs Ca plot in Figure 7.2-10.

Plot of calcium versus sulphate

All Simpevarp data

Figures 7.2-29 and 7.2-30 show, in common with Mg vs Ca (Fig. 7.2-28), that plotting Ca versus SO_4 basically reflects the SO_4 vs Cl plot (Fig. 7.2-22) due to the close correlation of high salinity with high calcium content (Fig. 7.2-18). In addition, given the sensitivity of calcium to ion exchange processes and the fact that sulphate may be influenced by microbially mediated reactions, this may explain some of the lack of

correlation shown by the dilute to brackish groundwaters at shallower depths (Fig. 7.2-30).

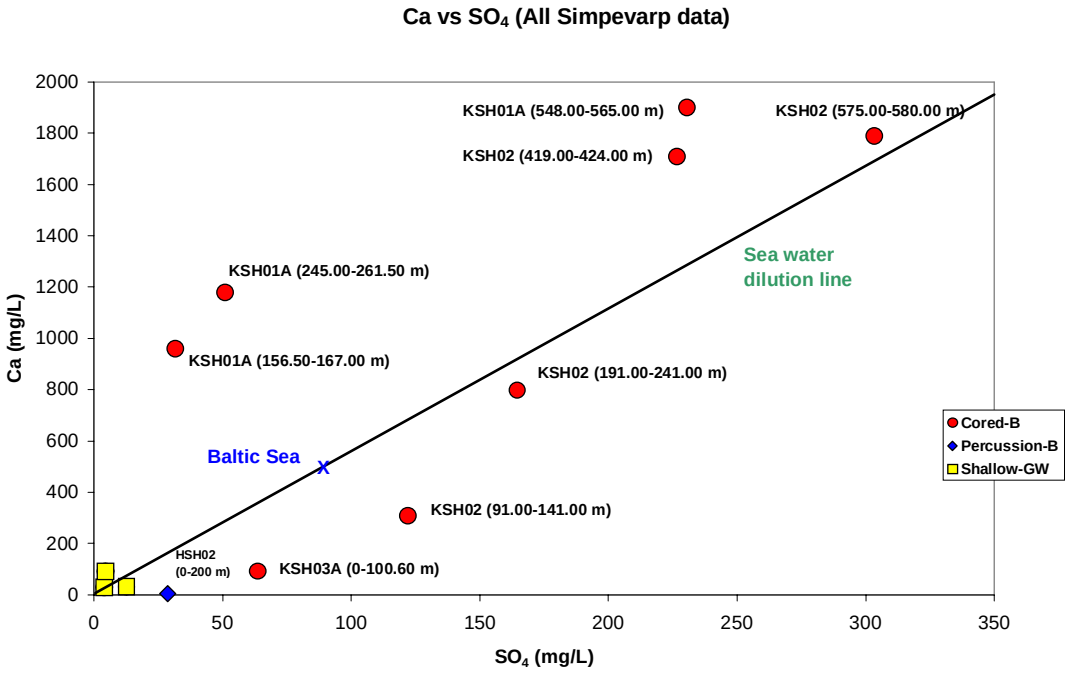

Figure 7.2-29: *Plot of Ca vs SO_4 for all Simpevarp data (excluding the deepest groundwater).*

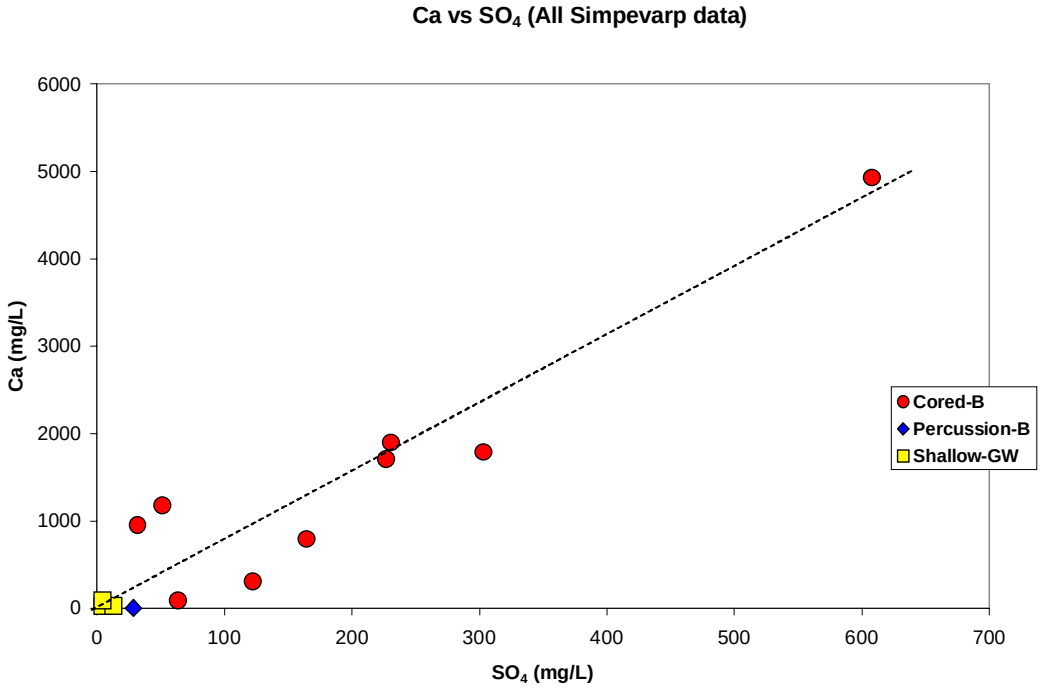

Figure 7.2-30: *Plot of Ca vs SO_4 for all Simpevarp data (including the deepest groundwater).*

Comparison with the POM sites

This is not reproduced here as it reflects the Ca v. SO_4 plot in Figure 7.2-18.

Plot of calcium/magnesium versus bromide/chloride

Comparison with the POM sites

By plotting Ca/Mg versus Br/Cl, Figure 7.2-31 provides an opportunity to differentiate those groundwaters of modern marine origin (e.g. Baltic Sea) from non-marine or non-marine/old marine mixing origin. The figure clearly shows the Baltic Sea group of modern marine waters and also the deepest non-marine saline groundwaters from Laxemar and Oskarshamn (KOV01). Between these two extreme end-members lie most of the groundwater data. The red arrow shows the direction towards the deep saline non-marine types, and much of the data plotting along this pathway represent groundwaters which contain an increasing component of the deep saline non-marine end-member. Likewise, at the other extreme, some of the plotted data closest to the modern marine end-member may well comprise groundwaters with a modern marine water signature, although in this case there is not a clear transition zone which might be expected if mixing processes were occurring. The other possibility is the presence of an older marine component (e.g. Littorina Sea) in the shallower brackish groundwaters which persist from 100-500 m depth, depending on local conditions. These groundwaters are circled in blue and indicate enhancements of, for example, Mg and Br. This topic of a possible Littorina Sea water signature is taken up in detail in section 7.7.

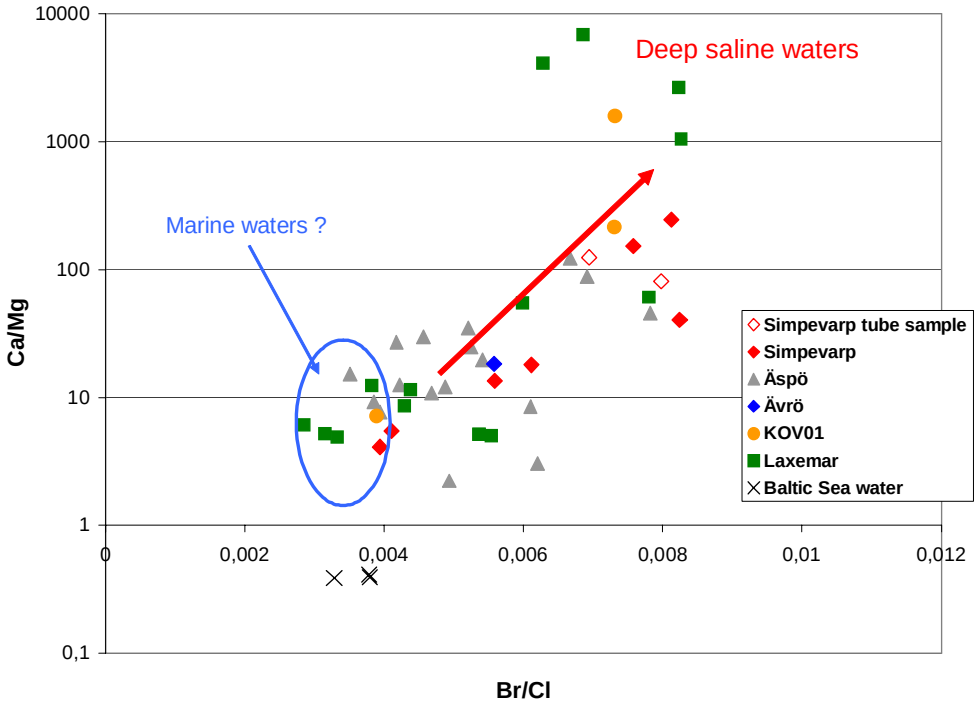

Figure 7.2-31: *Plot comparing all Simpevarp Ca/Mg vs Br/ Cl data with the POM sites.*

Plot of oxygen-18 versus deuterium

All Simpevarp data

Figure 7.2-32 details the stable isotope data which plot on or close to the Global Meteoric Water Line (GMWL) indicating a meteoric origin. In accordance with many of the other plots, two main groundwater groups are indicated: a) shallow dilute groundwaters ranging from $\delta^{18}O$ = -11.3 to -9.8 ‰ SMOW, δD = -80.4 to 74.3 ‰ SMOW, and b) brackish to saline groundwaters ranging from $\delta^{18}O$ = -14.0 to -12.7 ‰ SMOW, δD = -100.0 to -93.8 ‰ SMOW. The two tube samples plot within group (a). The heavier group (a) isotopic values suggest a modern meteoric recharge component. The lighter isotopic values of group (b) indicate the presence of a cold recharge meteoric component (glacial melt water?). The limited data suggest there is no major Baltic Sea influence on the sampled groundwaters.

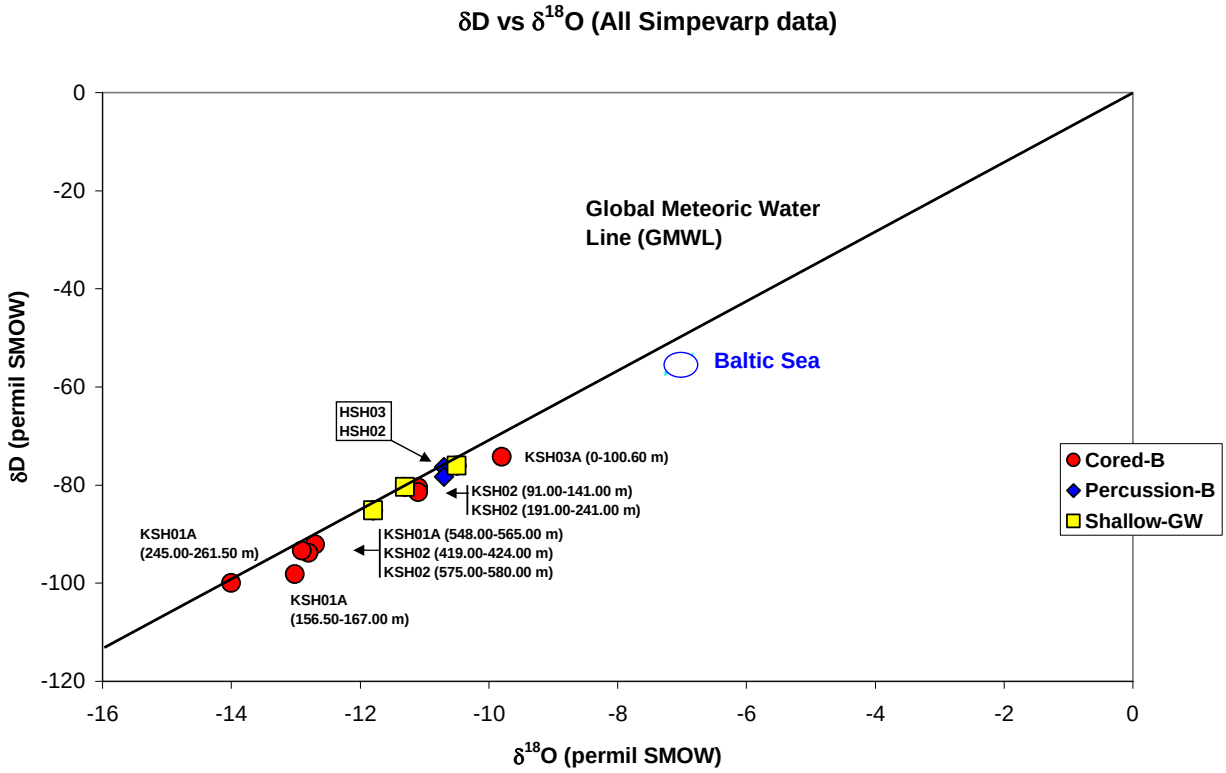

Figure 7.2-32: *Plot of $\delta^{18}O$ versus δD for all Simpevarp data.*

Plot of oxygen-18 versus chloride

All Simpevarp data

Figure 7.2-33 shows the decrease in $\delta^{18}O$ with increasing salinity (i.e. depth)

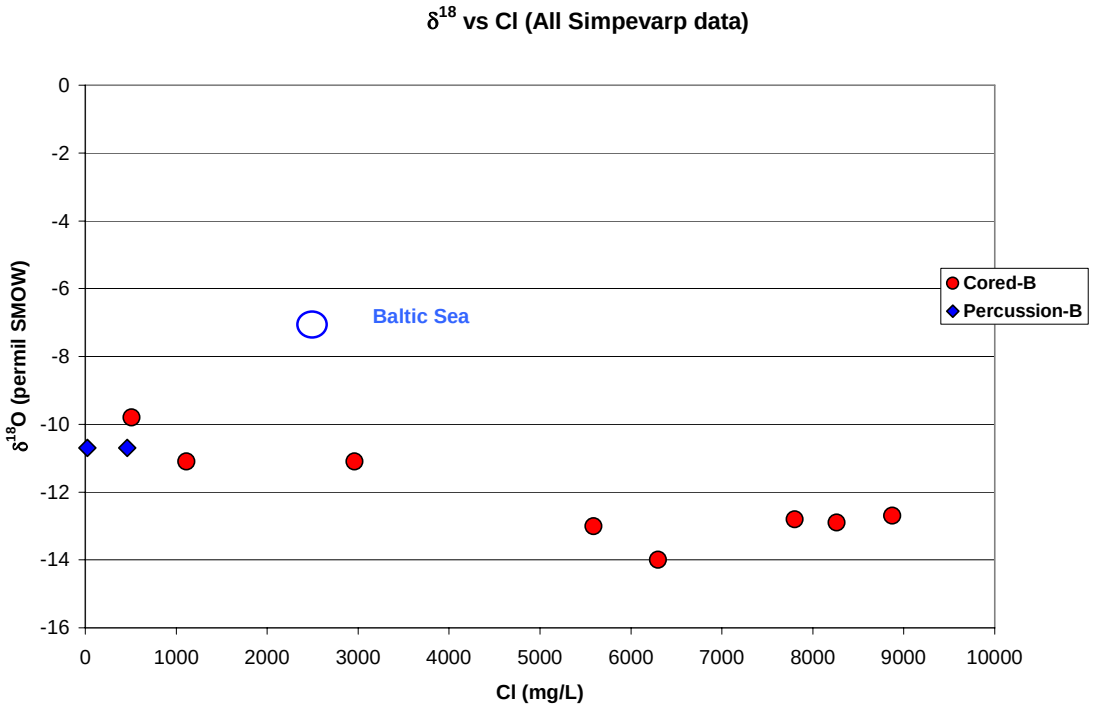

Figure 7.2-33: *Plot of $\delta^{18}O$ versus Cl for all Simpevarp data.*

Comparison with the POM sites

Figure 7.2-34 compares the Simpevarp data with the POM sites. The light Group (b) Simpevarp groundwaters from the deeper cored boreholes fall within the same range of many of the Äspö groundwaters known for their cold climate recharge signatures.

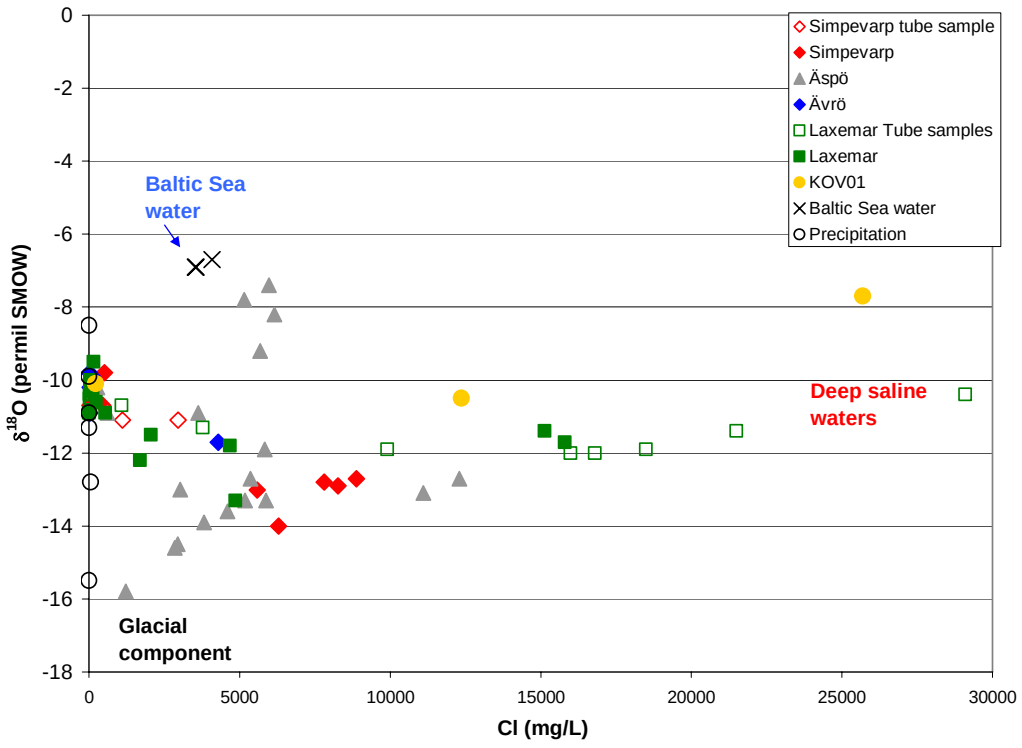

Figure 7.2-34: *Plot comparing all Simpevarp $\delta^{18}O$ versus Cl data with the POM sites.*

7.3 Trace element plots for all Simpevarp data

This section presents data of available trace element analyses from the cored boreholes. Only a few data exist for the majority of groundwaters and even some of these are incomplete. Plotted below are some examples of trace elements for which there is enough data to indicate depth trends. Cerium versus depth (Fig. 7.3-1) was chosen to illustrate the limitation of most of the available data, i.e. usually a detectable amount in the near-surface groundwaters to 200 m, and then most lie below detection for the deeper, more saline groundwaters. Lanthanum (Fig. 7.3-2) is another example where most values lie close to or under detection in the upper 600 m of the bedrock.

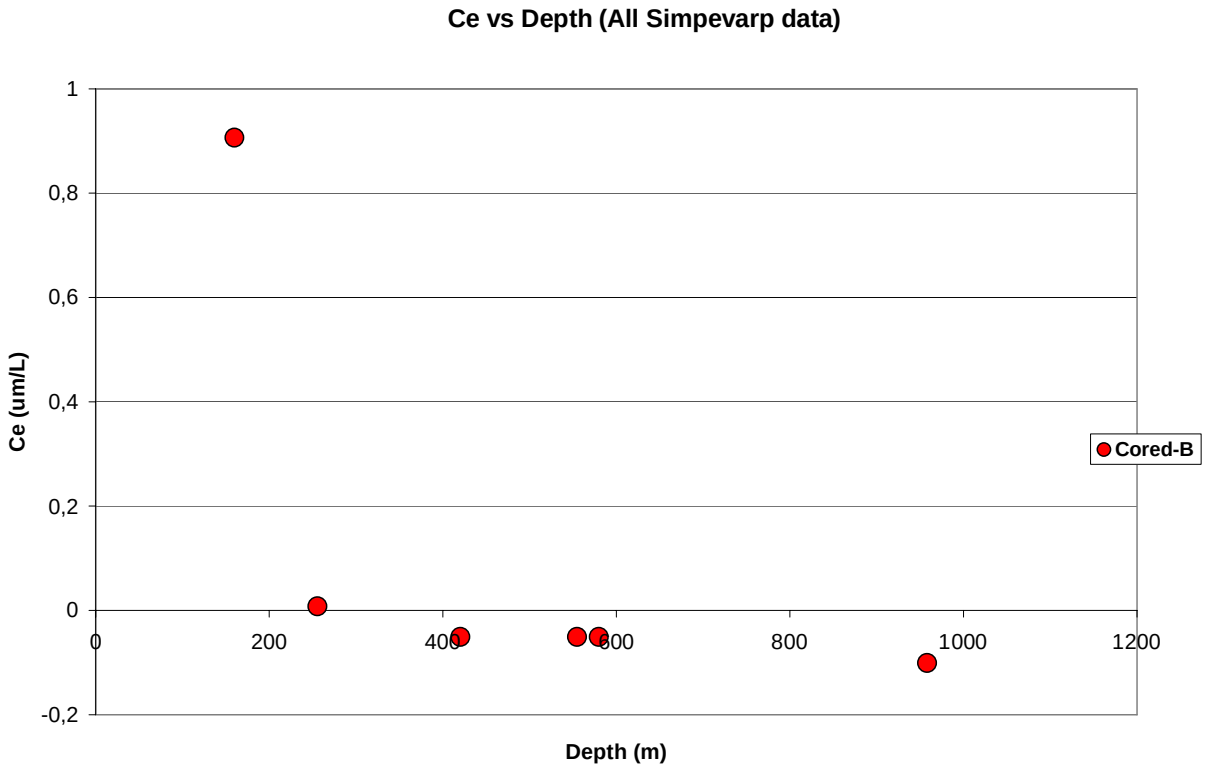

Figure 7.3-1: *Plot of cerium versus depth.*

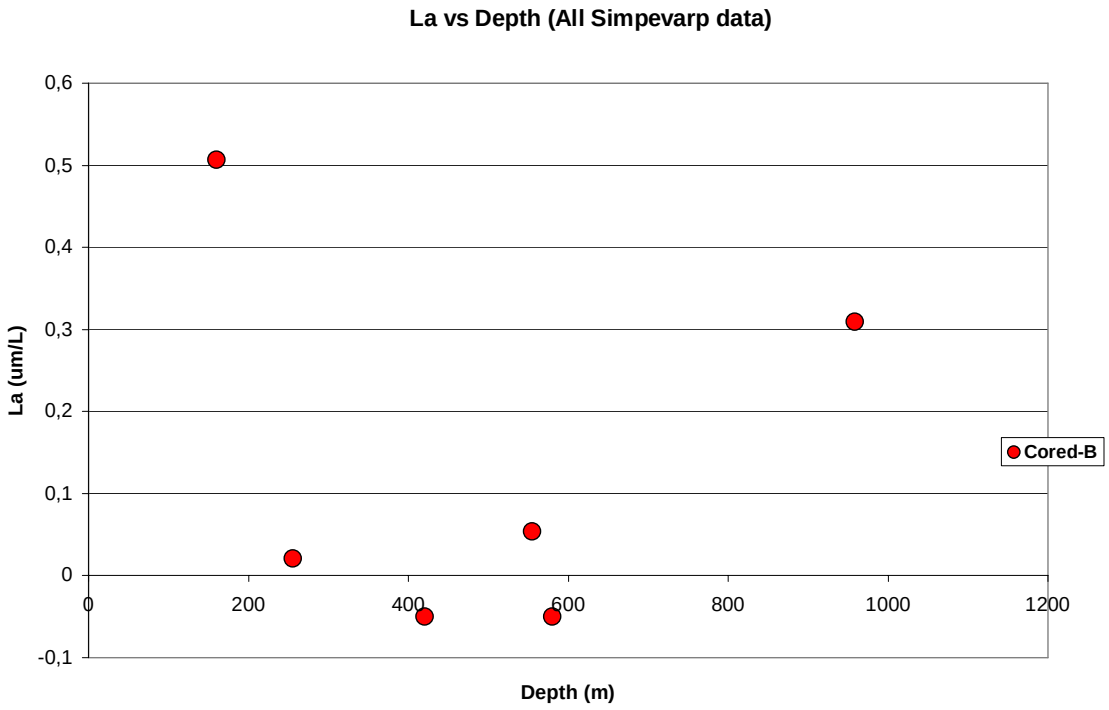

Figure 7.3-2: *Plot of lanthanum versus depth.*

Figures 7.3-3 and 7.3-4 show strontium and rubidium respectively. Strontium shows a gradual increase from the first 100 m where it is near zero, to 30 mg/L at 600m. Following there aooears to be a sharp increase achieving 88.2 mg/l close to 1000 m. Rubidium shows a fairly uniform content over the first 600 m (20-35 µg/L) before increasing to 69.2 µg/L at 600 m. Both these trends indicate increasing water/rock interaction processes with increasing depth, in line with the earlier observed the increase in salinity (chloride), calcium and sodium.

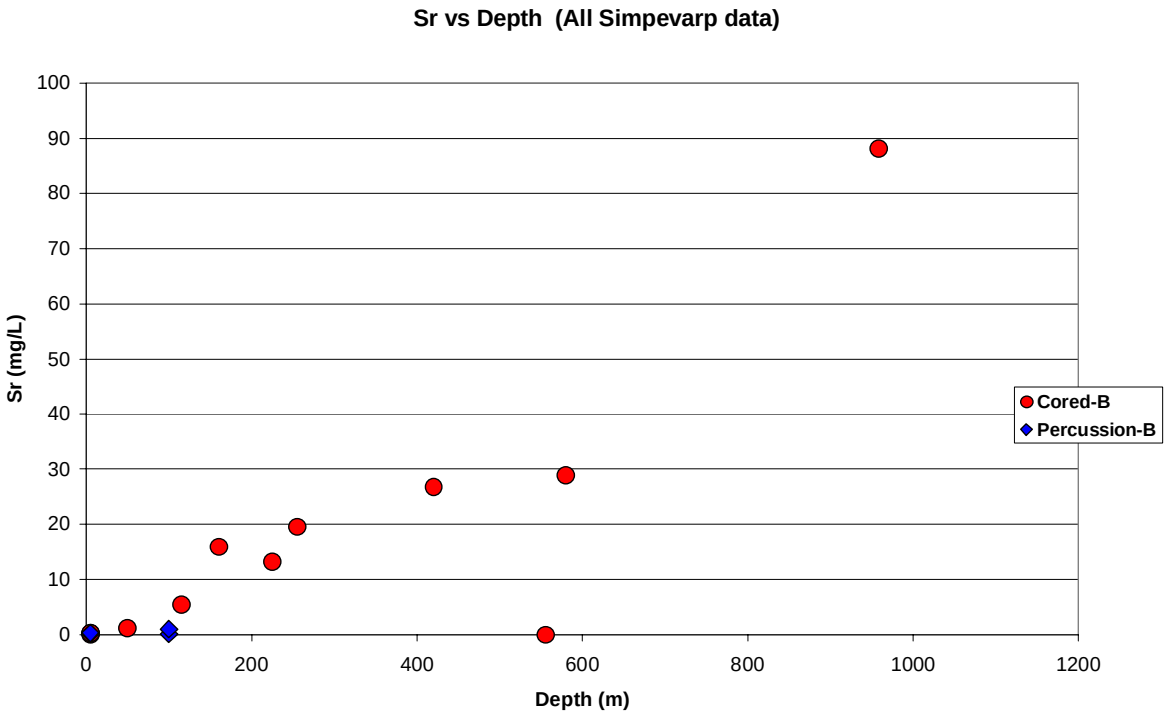

Figure 7.3-3: *Plot of strontium versus depth.*

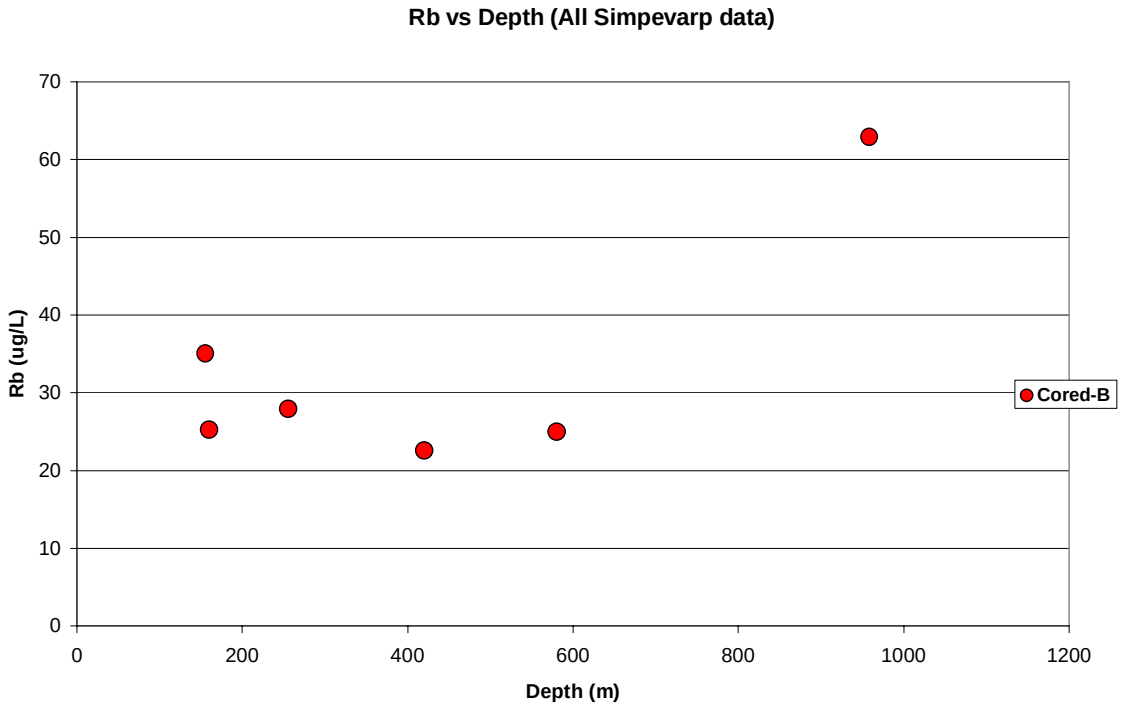

Figure 7.3-4: *Plot of rubidium versus depth.*

Caesium (Fig. 7.3-5) suggests a slight increase (1.21-2.41 µg/L) to 600 m followed by a gradual increase to 5.03 µg/L at 958 m. This approximately reflects the behaviour of yttrium (Fig. 7.3-6).

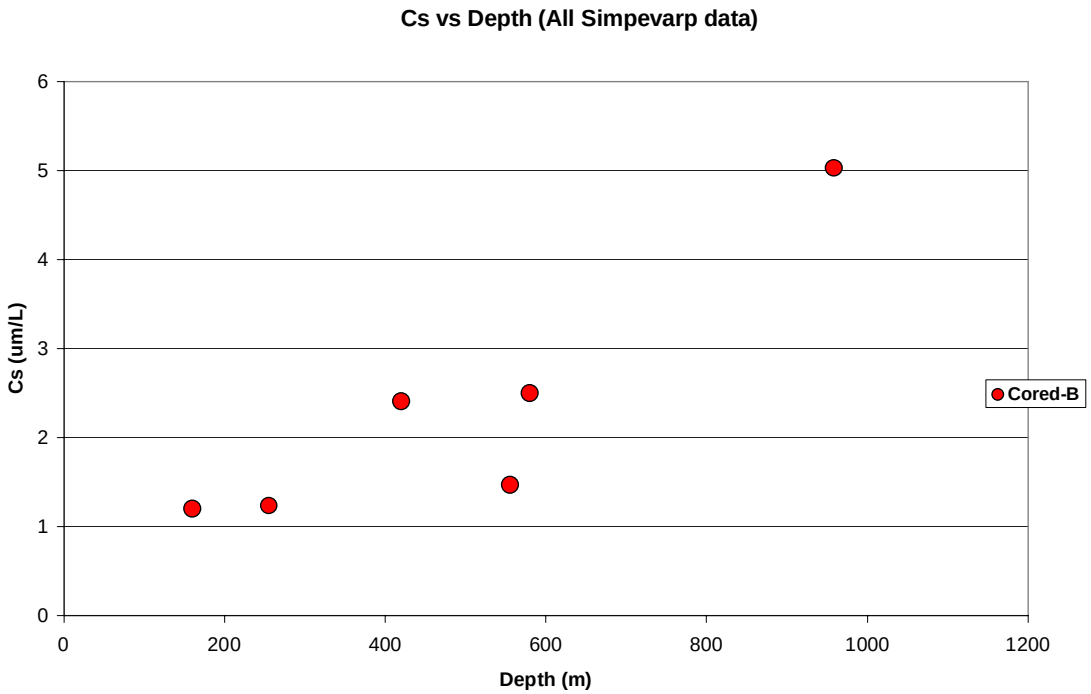

Figure 7.3-5: *Plot of ceasium versus depth.*

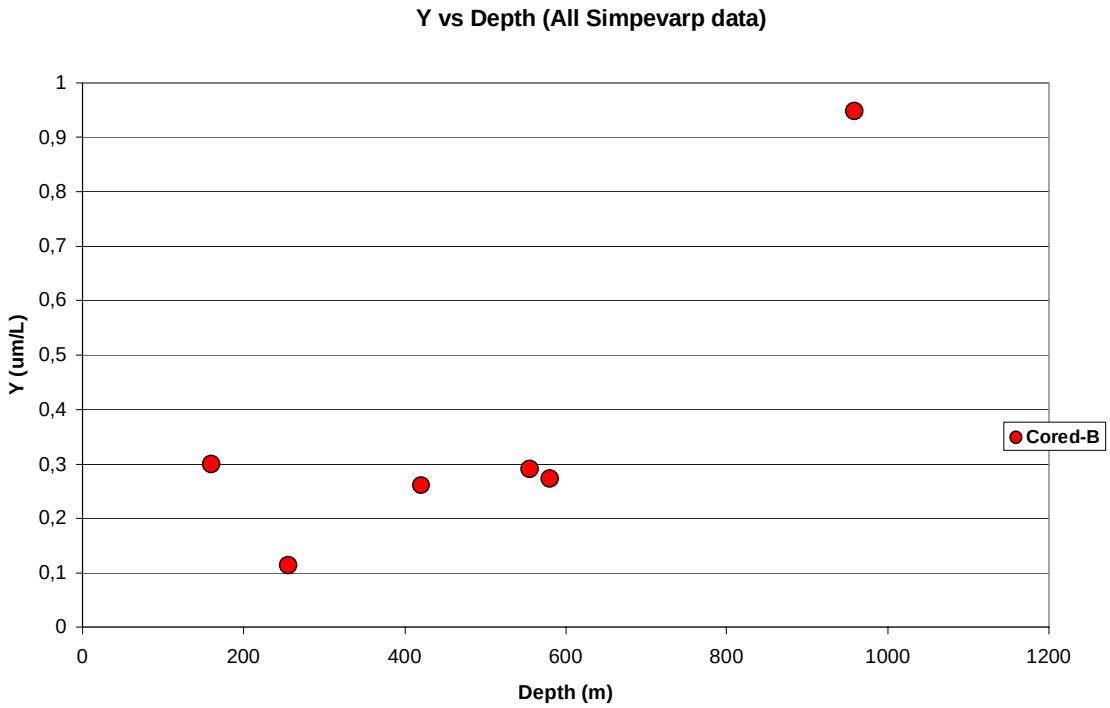

Figure 7.3-6: *Plot of yttrium versus depth.*

7.4 Isotope plots for all Simpevarp data and comparison with the POM and other Fennoscandian sites

This section presents groundwater isotope data relating to tritium, stable carbon and radiocarbon, stable sulphur ($\delta^{34}S$) and chlorine isotopes ($\delta^{37}Cl$), stable and radiogenic strontium ($^{87/86}Sr$), and boron ($^{11/10}B$).

7.4.1 Tritium

Tritium produced by the bomb tests during the early 1960´s is a good tracer for waters recharged within the past four decades. As part of an international monitoring campaign, peak values between 1000 and 4300 TU were recorded at Huddinge near Stockholm in the years 1963-1964 and values reaching almost 6000 TU were recorded at Arjeplog and Kiruna in northern Sweden (IAEA database). Due to decay (half life of 12 years) and dispersion, in addition to a cessation of the nuclear bomb tests, precipitation tritium values decreased so that the measurements carried out at Huddinge during 1969 showed that values had dropped to between 74 and 240 TU.

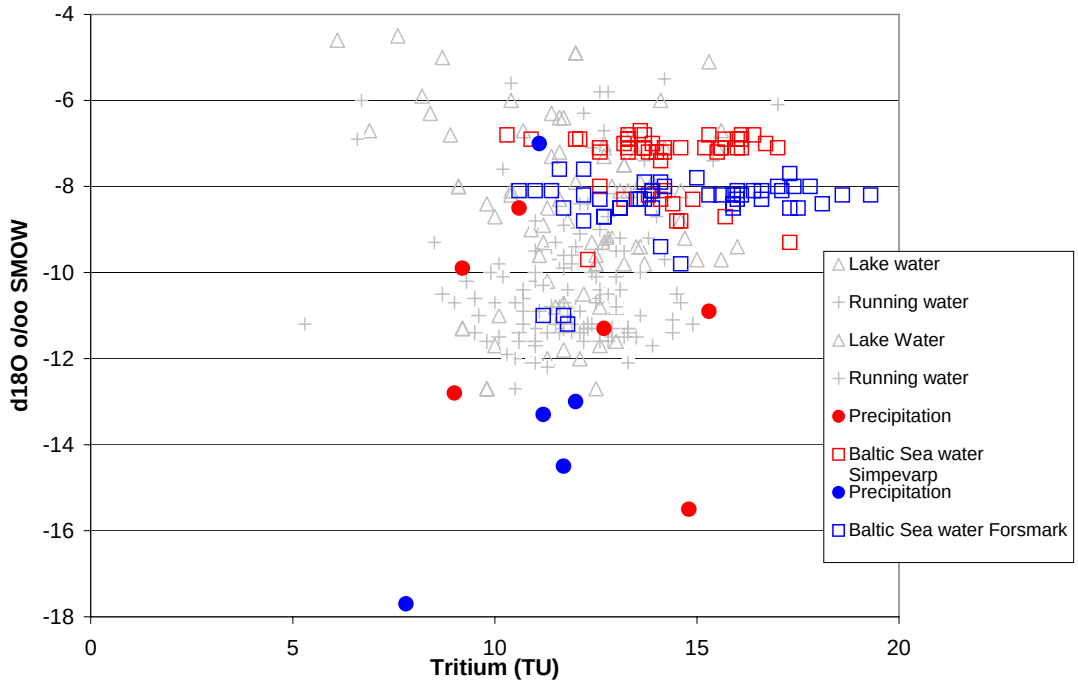

Figure 7.4-1*: Plot of $\delta^{18}O$ versus tritium in surface water samples from the Forsmark and Simpevarp sites.*

Present day surface waters from the Simpevarp and Forsmarks sites show values of 7-20 TU with exceptions of a few Lake and Stream water samples from Forsmark (Fig. 7.4-1). Generally, the Baltic Sea samples (10.3-19.3 TU) show somewhat higher values compared to the meteoric surface waters (7.8-15 TU) for precipitation. The Forsmark Baltic Sea samples show some values that are higher than the Simpevarp Baltic Sea samples but the spread is large for both sites. The successive lowering of tritium contents versus time elapsed since the bomb tests may explain the higher values in the Baltic Sea (due to reservoir effects) compared with precipitation. The difference

between the Simpevarp and Forsmark Baltic Sea samples can be a north-south effect, with higher tritium values in the north compared to the south. However this is not demonstrated by the precipitation values (Fig. 7.4-1). Moreover, the ^{14}C content in the Baltic Sea water is relatively similar between the two sites (Fig. 7.4-2). It should be emphasised that the precipitation values are very few, show a large variation in tritium and therefore are not considered very conclusive. Continued systematic sampling of precipitation for tritium analyses is encouraged. One problem in using tritium for the interpretation of near-surface recharge/discharge is, as mentioned above, the variation in content in the recharge water over time, which implies that near-surface groundwaters with values around 15 TU can be 100% recent or a mixture of old meteoric (tritium free) and a small portion (10%) of water from the sixties at the height of the atmospheric nuclear bomb tests.

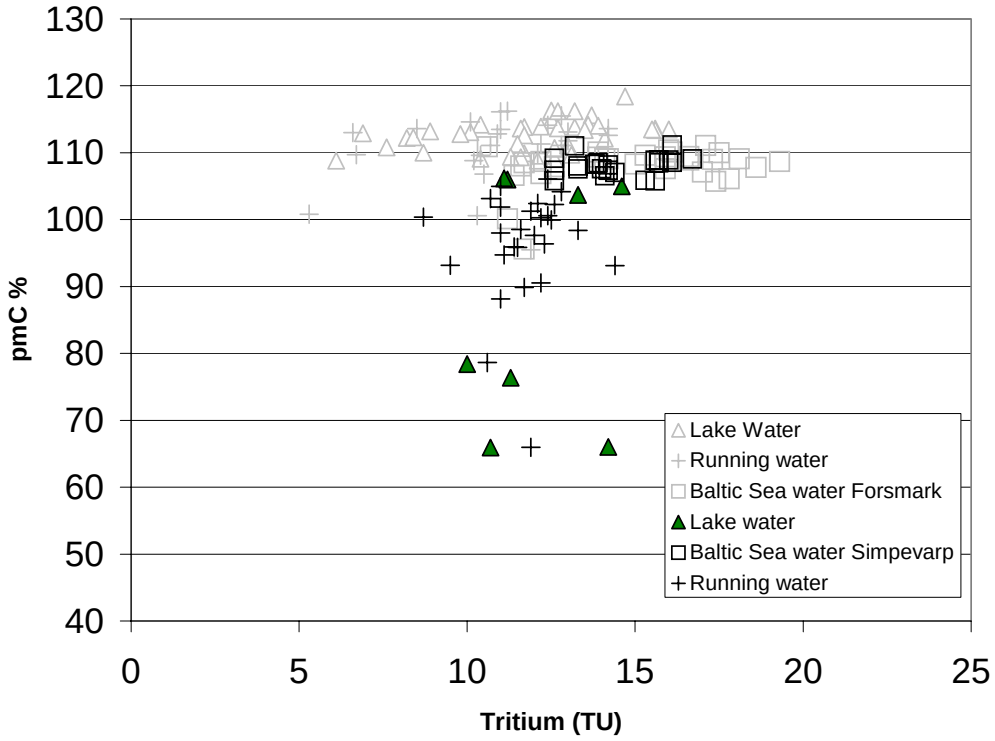

Figure 7.4-2: *Plot of ^{14}C (pmC) versus tritium in surface waters from Simpevarp (shown in black and green) and Forsmark (in grey).*

The plot of tritium versus ^{14}C for surface waters from Forsmark and Simpevarp show large differences concerning the Lake and running Stream waters of the two sites. At Simpevarp the Lake and Stream waters show a distinct decrease in ^{14}C content whereas the tritium values remain the same or show a small decrease. The can be explained by HCO_3 added to the waters originating either from calcites devoid of ^{14}C or due to microbial oxidation of organic material with lower (or no) ^{14}C. This is the pattern expected for near-surface waters. At Forsmark, in contrast, most Lake and running Stream waters have higher ^{14}C values compared with Baltic Sea waters whereas the tritium values range from 5-15 TU. The reason for this is not clear and several explanations are possible, but this will be discussed in more detail in the Forsmark model version 1.2. report scheduled for December, 2004.

An additional problem in using tritium for groundwater modelling for the Simpevarp site is shown in Figure 7.4-3 where percentage drilling water content is plotted against tritium content. The drilling water used from percussion borehole HSH03 has tritium values in the range of 4.7 to 9.4 TU. Since the subsurface production of tritium is expected to be very low in the granitoids of the Simpevarp area, a linear relation between drilling fluid portion and tritium would be expected for the deeper samples. As can be seen, the tube samples from borehole KSH01A+B (750-1000 m) deviate from this trend. Two different explanations are possible: 1) surface waters of other sources than the drilling fluid have entered and mixed within the borehole, or 2) the uranine tracer used to spike the drilling fluid has not been added uniformly throughout the drilling phase resulting in erroneous determinations of drilling water content in the sampled groundwaters. High tritium values compared to drilling fluid portion are also obtained in some groundwaters from the upper 200 m of the bedrock and are probably explained by inmixing (artificially or natural) of young meteoric recharge waters.

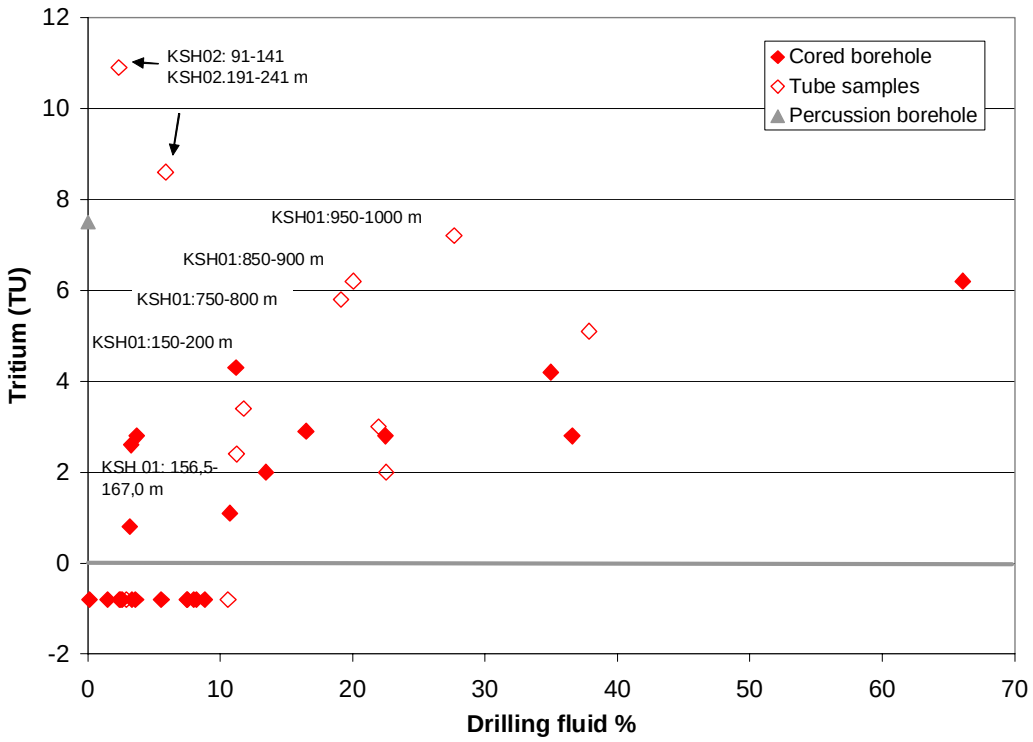

Figure 7.4-3: *Plot of tritium versus drilling fluid for boreholes HSH03, KSH01A+B, KSH02 and KSH03A.*

The extreme deviation from a linear trend shown by the borehole KSH02 tube samples (91-141 m and 191-241 m) is significant as these two samples have been included in the ion-ion plots described in section 7.2. One of the criteria for their selection as being of 'limited suitability' was a relatively low drilling water content. However, in retrospect, they should have been avoided because of contamination from shallower near-surface groundwaters with significant tritium. Contamination from near-surface groundwaters is clear from some of the ion-ion plots.

7.4.2 Carbon

The stable carbon isotope ratios, expressed as $\delta^{13}C$ ‰ PDB and radiocarbon contents (^{14}C) expressed as pmC (percentage modern carbon), and HCO_3^-, have been analysed from surface waters and groundwaters. The tritium versus ^{14}C for surface waters has been discussed already in the previous section 7.4.1. Figure 7.4-4 shows $\delta^{13}C$ for the Simpevarp waters versus tritium.

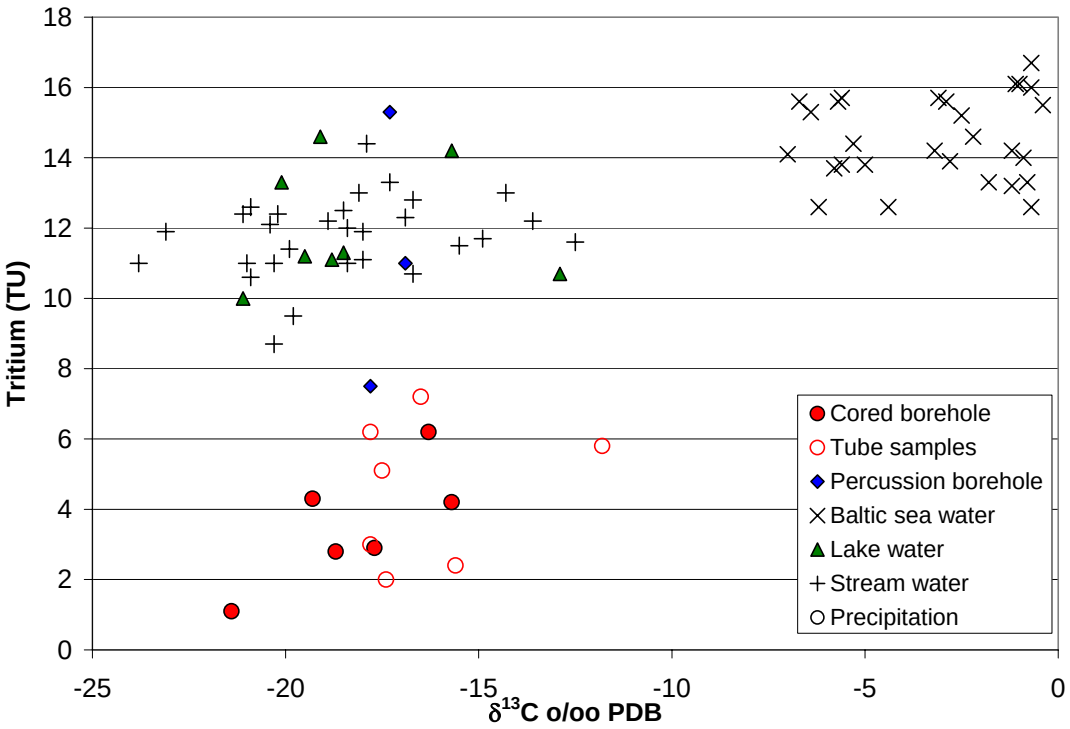

Figure 7.4-4: *Plot of tritium versus $\delta^{13}C$ in surface waters and groundwaters from Simpevarp.*

The Baltic Sea water has high carbon isotope values produced by equilibria with atmospheric CO_2; this contrasts with all the other waters, both surface and groundwaters, which show significantly lower values. CO_2 produced in the soil cover due to breakdown and oxidation of organic material usually results in $\delta^{13}C$ values of around -20 ‰ PDB which can partly explain the dissolved $\delta^{13}C$ (HCO_3^-). However, the lowering in ^{14}C accompanying the decrease in $\delta^{13}C$ (HCO_3^-) in some lake and running waters indicate that calcite dissolution have taken place as well. The fracture calcites show no homogenous $\delta^{13}C$-values (cf section 7.5) and it is therefore not possible to model calcite dissolution as a two end member mixing. Since to date only six ^{14}C analyses of groundwaters from packed-off sections are available from the Simpevarp area, existing data from Laxemar, Äspö and Ävrö have been included in two plots showing $\delta^{13}C$ (HCO_3^-) versus ^{14}C (Fig. 7.4-5) and $\delta^{13}C$ (HCO_3^-) versus HCO_3^-(Fig. 7.4-6). The plots show that there is no real correlation between ^{14}C and $\delta^{13}C$, i.e. there is no indication of a change in $\delta^{13}C$ with age. Instead, most groundwater samples show values in the range of -15 to -22 ‰ $\delta^{13}C$ indicating that breakdown of organic material plays a major role and has occurred either in the near-surface (being transported downwards) or that *in situ* production has taken place. An organic origin is also supported by the $\delta^{13}C$ versus HCO_3^- plot where the groundwater samples showing the

highest HCO_3^- content show relatively homogenous $\delta^{13}C$ values clustering at -16 to -20‰ $\delta^{13}C$.

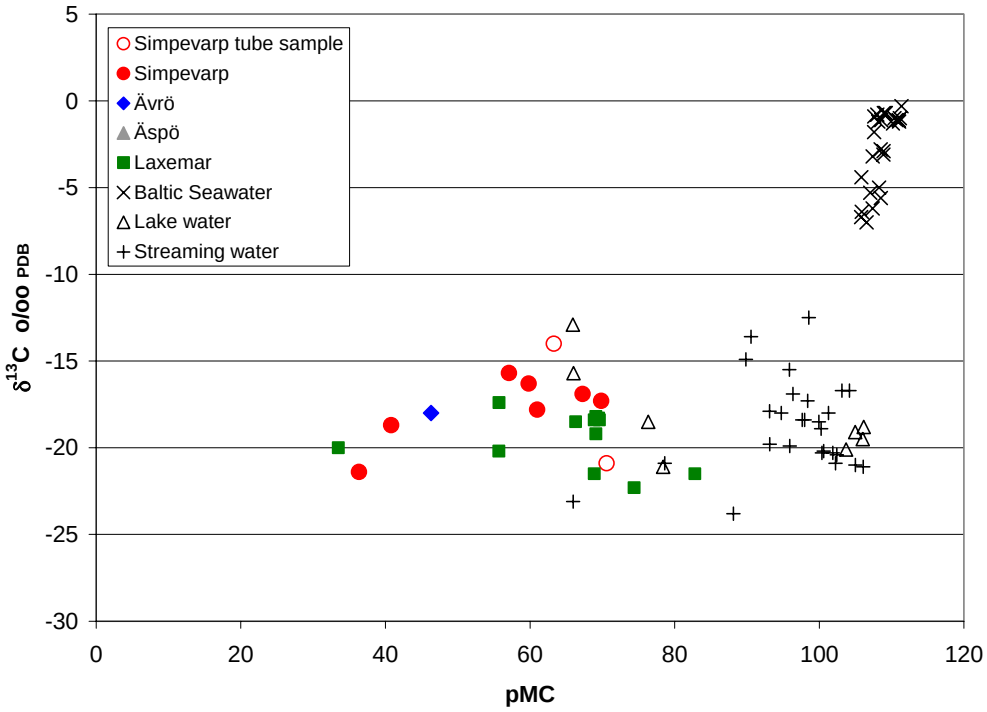

Figure 7.4-5: *$\delta^{13}C$ (HCO_3^-) versus ^{14}C in surface waters and groundwaters from Simpevarp, Laxemar and Ävrö.*

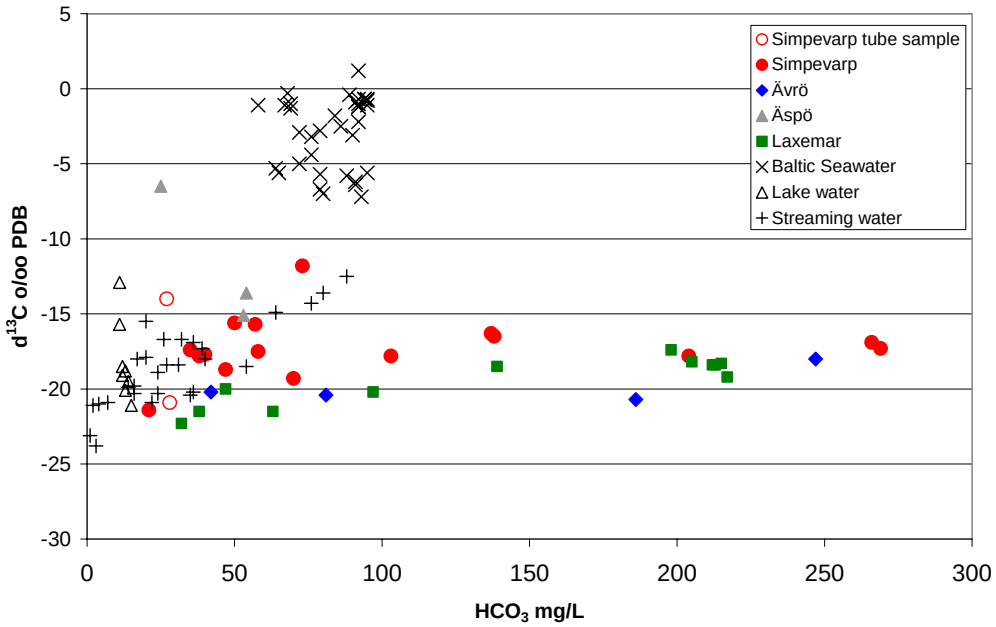

Figure 7.4-6: *$\delta^{13}C$ (HCO_3) versus HCO_3^- in surface waters and groundwaters from Simpevarp, Laxemar Äspö and Ävrö.*

7.4.3 Sulphur

Sulphur isotope ratios, expressed as $\delta^{34}S$ ‰ CDT, have been measured in dissolved sulphate in Baltic Sea waters, surface waters and groundwaters from the Simpevarp area. Over 200 analyses have been performed of which 30 are groundwaters from boreholes KSH01A+B and KSH02 at Simpevarp with two exceptions; one from Laxemar (HLX10) and one from Ävrö (KAV04). The isotope results are plotted versus SO_4^{2-} contents (Fig. 7.4-7) and versus Cl contents (Fig. 7.4-8). Unfortunately, neither SO_4^{2-} nor Cl contents were measured in 10 of the groundwater samples analysed for $\delta^{34}S$. Better coordination of these measurements is considered essential for continued sampling and analyses in the area.

The recorded values vary within a wide range (-1 to +24 ‰ CDT) indicating different sulphur sources for the dissolved SO_4^{2-}. For the surface waters (Lake and running Stream waters) the SO_4^{2-} content is usually below 50 mg/L and the $\delta^{34}S$ relatively low but variable (-1 to +15 ‰ CDT) with most of the samples in the range 2-9 ‰ CDT. These relatively low values indicate that atmospheric deposition and oxidation of sulphides in the overburden is the origin for the SO_4^{2-}. The Baltic Sea waters cluster around the 20 ‰ CDT marine line but show a relatively large spread (16-23 ‰ CDT). The reason for this is not fully understood but suggestions include: a) contribution from land discharge sources (e.g. streams) to various degrees (low values), and b) potential bacterial modification creating high values in the remaining SO_4^{2-}.

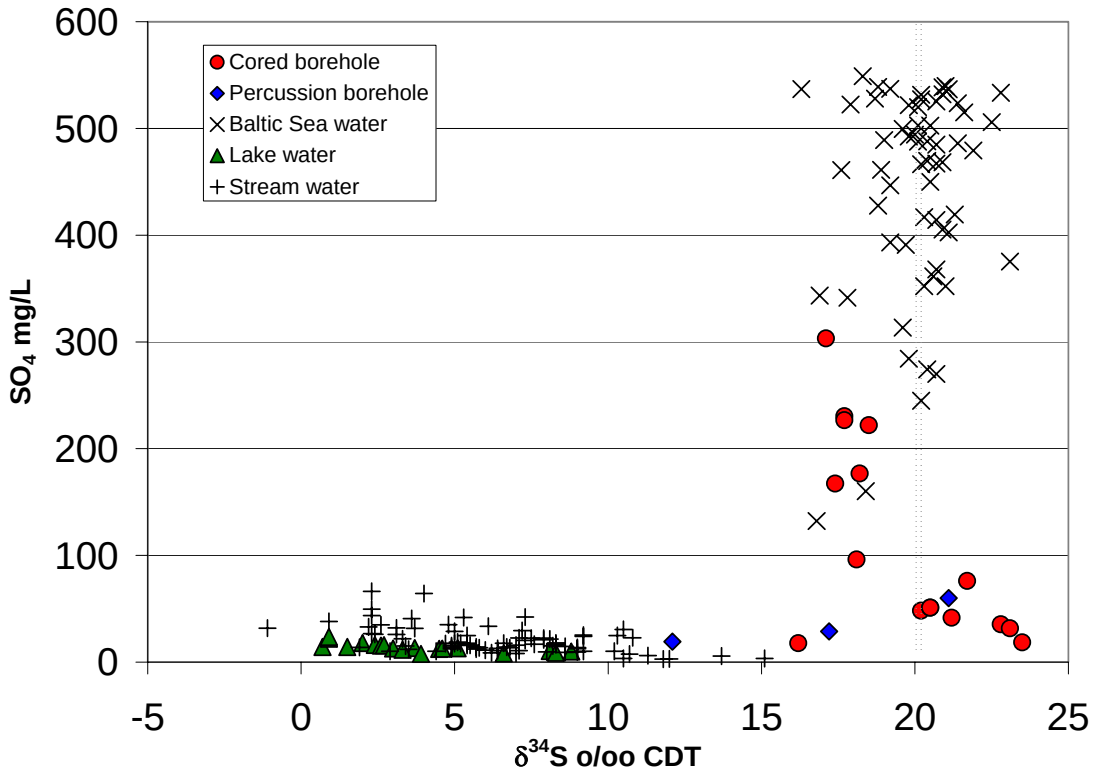

***Figure 7.4-7**: Plot of $\delta^{34}S$ versus SO_4^{2-} in surface waters and groundwaters. The grey line indicates the marine value at around 20 ‰ CDT.*

The borehole groundwaters (Fig. 7.4-8) show $\delta^{34}S$ values in the same range as the Baltic Sea waters but with a clear indication of $\delta^{34}S$ values greater than +21 ‰ CDT in samples with low SO_4^{2-}. These latter values are interpreted as a product of sulphate reduction taking place in groundwaters identified in Figure 7.4-8 with a chloride content between 5000 and 6300 mg/L. The five groundwaters with higher salinities share lower $\delta^{34}S$ but higher SO_4 contents. The $\delta^{34}S$ values of these groundwaters are, however, still within the range for the analysed Baltic Sea waters. The SO_4^{2-} contents are still not high enough to invoke dissolution or leaching as a mechanism, more likely processes are in-mixing of marine waters although in-mixing of SO_4^{2-} from deep brine waters (clearly indicated in deeper groundwaters discussed in section 7.2) cannot be excluded. Deep salin SO_4^{2-} sources may have resulted from the leaching of sediments and/or dissolution of gypsum previously present in fractures. Lowering of the $\delta^{34}S$ signature by oxidation of sulphides seems to be less probable for the groundwater samples and is not supported by fracture mineral investigations (Drake and Tullborg, 2004; P-report in press).

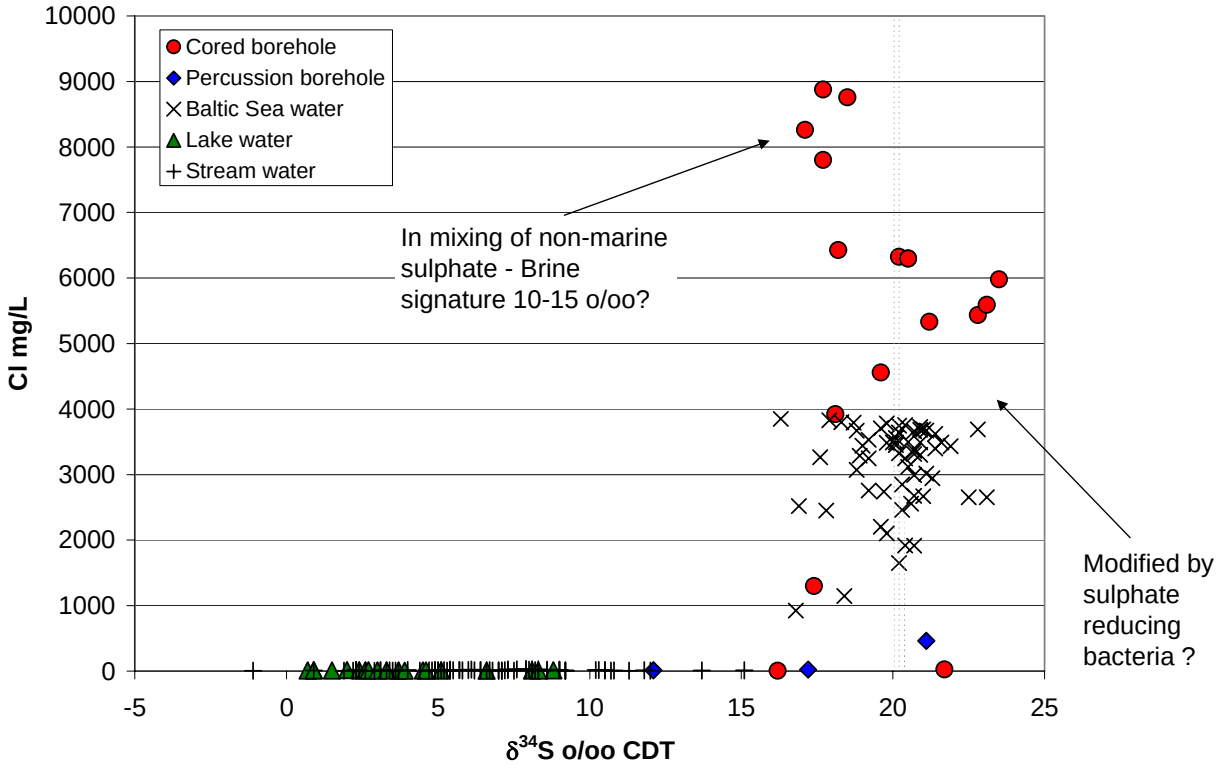

***Figure 7.4-8**: Plot of $\delta^{34}S$ versus Cl in surface waters and groundwaters. The grey line indicates the marine value at around 20 ‰ CDT.*

As discussed in section 7.2, the SO_4 content in deep groundwaters from the Oskarshamn area show different trends versus Cl content (Fig. 7.2-23). The Laxemar samples show relatively high SO_4 content in the saline waters, whereas the KOV01 samples show extremely low values. The most saline water at Simpevarp (16800 mg/L Cl) has a SO_4

content of around 600 mg/L. Geochemical modelling (Gimeno et al., 2004) indicates dissolution of gypsum as a possible source for SO_4 in the groundwaters. A few observations of fracture gypsum in the lower part of borehole KSH03A (the part that is beneath the Baltic Sea east of Simpevarp; Fig. 1-2) have been documented. Unfortunately, no $\delta^{34}S$ measurements are so far available from this gypsum or from the waters at Simpevarp with chloride contents greater than 9000 mg/L.

7.4.4 Strontium

Strontium isotope ratios ($^{87}Sr/^{86}Sr$) have been measured in groundwater samples and Baltic Sea waters from the Simpevarp area and these are plotted versus strontium content in Figure 7.4-9. Also included in this diagram are groundwater analyses from Forsmark and a few analyses from Laxemar and Ävrö.

^{87}Sr is a radiogenic isotope produced by the decay of ^{87}Rb (half-life $5x10^{10}$a). Marine waters show a distinct Sr isotope signature (0.7092) which is very close to the measured values in the Baltic Sea waters, whereas groundwaters from the different sites (Fig. 7.4-9) show values significantly more enriched in radiogenic Sr. Water/rock interaction processes involving Rb-containing minerals are the reason for this. The relatively small variation in Sr isotope ratios within each area, particularly at the Simpevarp, Ävrö and Laxemar sites, is probably an indication that ion exchange reactions with clay minerals along the groundwater flow paths is an important process. For the Simpevarp-Laxemar area there is a tendency towards higher contents of radiogenic Sr in the groundwaters with greatest salinity (and thus the highest Sr contents measured). Because of the limited data it is not possible to explain this observation, but in the absence of any mineralogical reasons, it is likely that greater residence times for these deep saline groundwaters result in more extensive mineral/water interactions. The higher $^{87}Sr/^{86}Sr$ ratios in the Forsmark samples are most probably due to differences in the composition of the bedrock and fracture minerals compared to Simpevarp.

The possibility of tracing marine components by the use of Sr isotopes is often debated. Clay minerals in the fractures may, however, make such interpretations difficult. For example, the strong present-day major ion Littorina Sea signature in the Forsmark groundwaters is not reflected by any marine Sr isotope imprint. Instead, modification of the Sr isotope values is probably attributable to ion exchange processes.

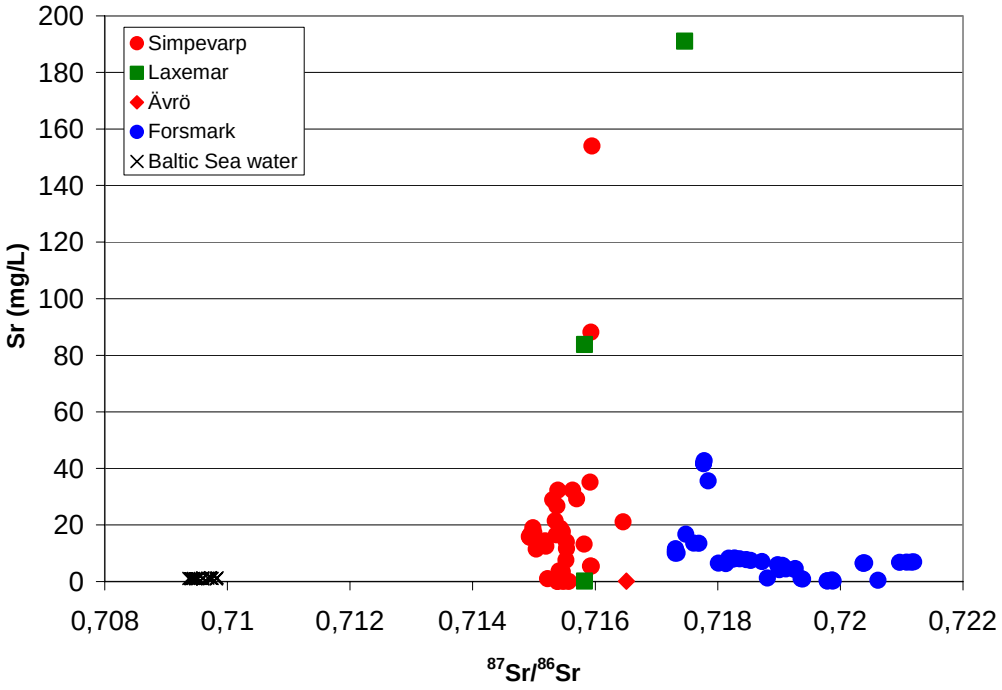

Figure 7.4-9: *Plot of $^{87}Sr/^{86}Sr$ ratios versus Sr in groundwaters from Simpevarp, Laxemar, Ävrö and Forsmark. Also included are Baltic Sea waters from Simpevarp and Forsmark.*

7.4.5 Chlorine

Stable chlorine isotopes have been analysed on waters from the Simpevarp area. Figure 7.4-10 plots $\delta^{37}Cl$ vs Cl for the Simpevarp, Laxemar, Ävrö and Forsmark sites, including Baltic Sea and surface Lake and Stream waters from Simpevarp. According to Frape et al. (1996) modern Baltic and possibly palaeo-Baltic waters may be recognised by negative $\delta^{37}Cl$ signatures related to salt leachates from Palaeozoic salt deposits south of the Baltic Sea; influence by water-rock interaction tends to result in positive $\delta^{37}Cl$ signatures. Clark and Fritz (1997) also show a clear distinction between the Fennoscndian and Canadian Shield crystalline rock groundwaters and groundwaters from sedimentary aquifers.

Taking into consideration the analytical uncertainty of around ±0.2 ‰, Figure 7.4-10 shows that the Simpevarp cored borehole groundwaters are characterised by positive values (+0.14 to +0.75 ‰ SMOC). The Baltic Sea waters fall within the range of -0.28 to +0.27 ‰ SMOC and the surface Stream waters and the percussion borehole groundwaters with very low Cl contents show the largest spread in $\delta^{37}Cl$ values (-0.03 to +0.44 ‰ SMOC). These data suggest that the deeper cored borehole groundwaters are characterised by water/rock interaction processes, whilst the near-surface percussion borehole groundwaters are mainly marine derived. The distribution of Baltic Sea and surface Lake and Stream waters suggest some mixing components of marine-derived and deeper groundwater sources.

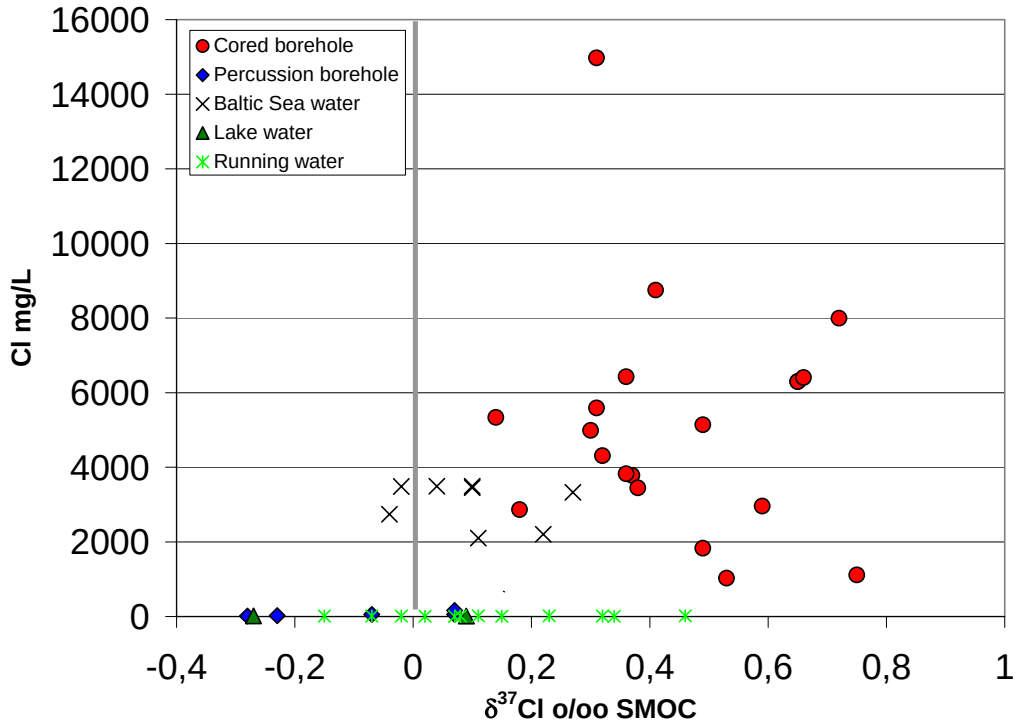

Figure 7.4-10: *Plot of δ^{37}Cl versus Cl in surface and near-surface waters, groundwaters, and Baltic Sea waters from Simpevarp.*

For comparison δ^{37}Cl values for groundwaters from Laxemar and Forsmark have been plotted together with the Simpevarp data (Fig. 7.4-11); additional Baltic Sea samples from the Forsmark area have been included also. For the groundwaters with Cl contents around 5000 mg/L there is a large variation in δ^{37}Cl values; most of the Forsmark samples show slightly negative values whereas the Simpevarp samples show values on the positive side. For groundwaters with higher Cl contents (>6000 mg/L) the Simpevarp and Laxemar samples show values greater than 0.3 ‰ SMOC. The Forsmark sample (only one available so far) shows 0.09 ‰ SMOC. This plot therefore suggests that for groundwaters containing around 5000 mg/L Cl, the Forsmark data indicate a greater marine signature involved (Littorina Sea?).

This is further emphasised by plotting the Br/Cl ratios against δ^{37}Cl (Fig. 7.4-12). This plot shows that groundwaters significantly enriched in Br (i.e. Simpevarp and Laxemar), compared to marine waters (i.e. Baltic Sea) and those groundwaters with a marine signature (i.e. Forsmark), display positive δ^{37}Cl values. The Forsmark groundwaters characterised by more marine-derived Br/Cl ratios cluster closer to 0 ‰ SMOC with a similarily large spread of values as for the Baltic Sea samples. At Forsmark the more positive values reflect deeper groundwaters from the cored boreholes where mixing with marine waters is less marked.

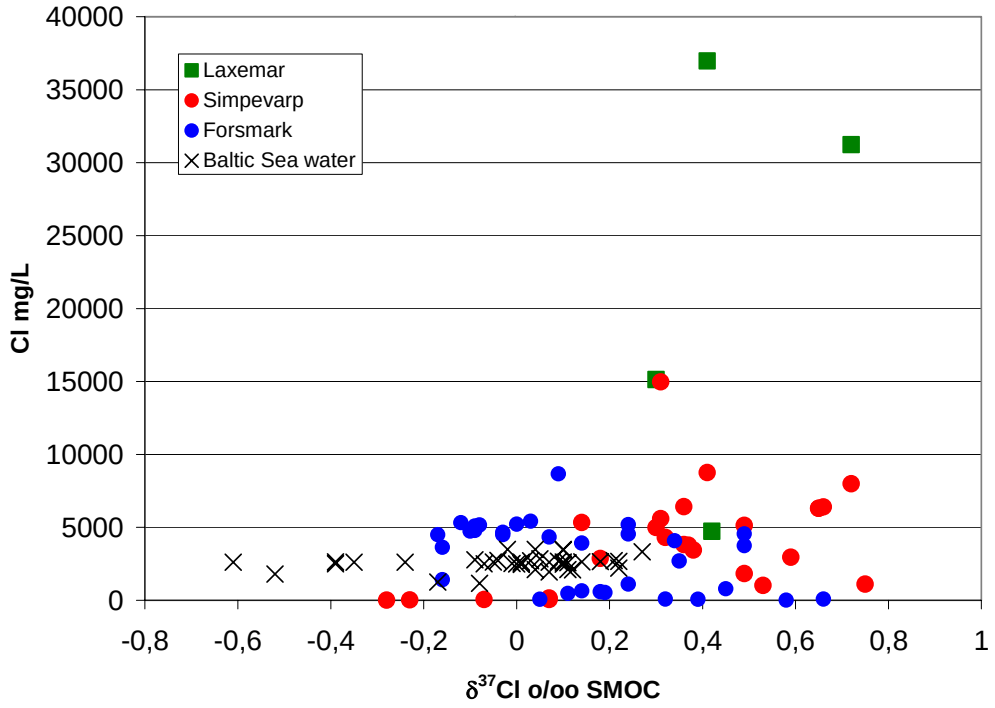

Figure 7.4-11: *Plot of δ^{37}Cl versus Cl in groundwaters from Simpevarp, Laxemar and Forsmark, and Baltic Sea waters from Simpevarp and Forsmark.*

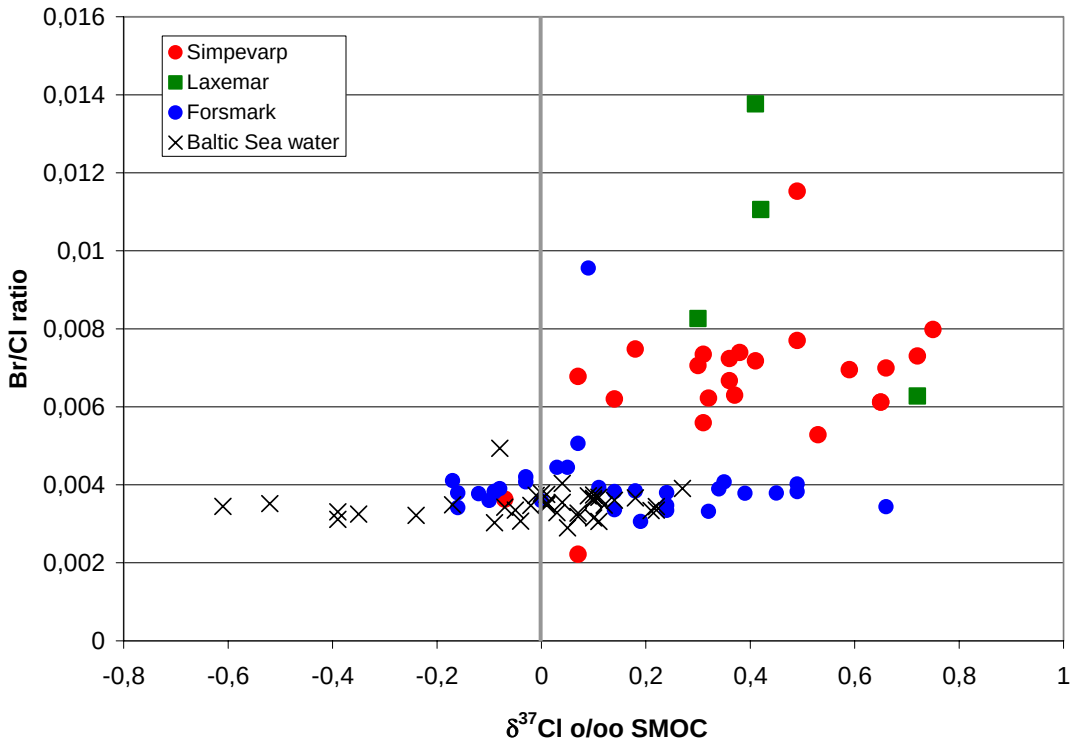

Figure 7.4-12: *Plot of δ^{37}Cl versus Br/Cl ratio in groundwaters from Simpevarp, Laxemar and Forsmark, and Baltic Sea waters from Simpevarp and Forsmark.*

7.4.6 Uranium

A small number of uranium analyses have been carried out including surface waters, Baltic Sea waters and groundwaters from cored boreholes. The uranium contents are below 2 µg/L in all the analysed waters (Fig. 7.4-13). The surface waters show values between 0.16 and 1.9 µg/L whereas the Baltic Sea waters all display values around 0.8 µg/L. Most of the groundwater samples are low in uranium and seven out of nine samples show values ≤ 0,2 µg/L. Higher uranium in surface and near-surface waters is usually observed and is caused by oxidising conditions at the surface. The mobility of the oxidised and dissolved uranium is highly dependent on access to complexing agents, mostly in form of HCO_3^- which is produced in the soil cover and the near-surface environment. Uranium transported into the bedrock aquifer is often found sorbed or incorporated in, especially, Fe(III)oxides along the flow paths. Studies of $^{234}U/^{238}U$ in groundwater and $^{230}Th/^{234}U/^{238}U$ in fracture coatings from water-conducting fractures can be used to determine dissolution/accumulation processes during the last 1 Ma. Unfortunately no such data are available at this stage of the site investigations.

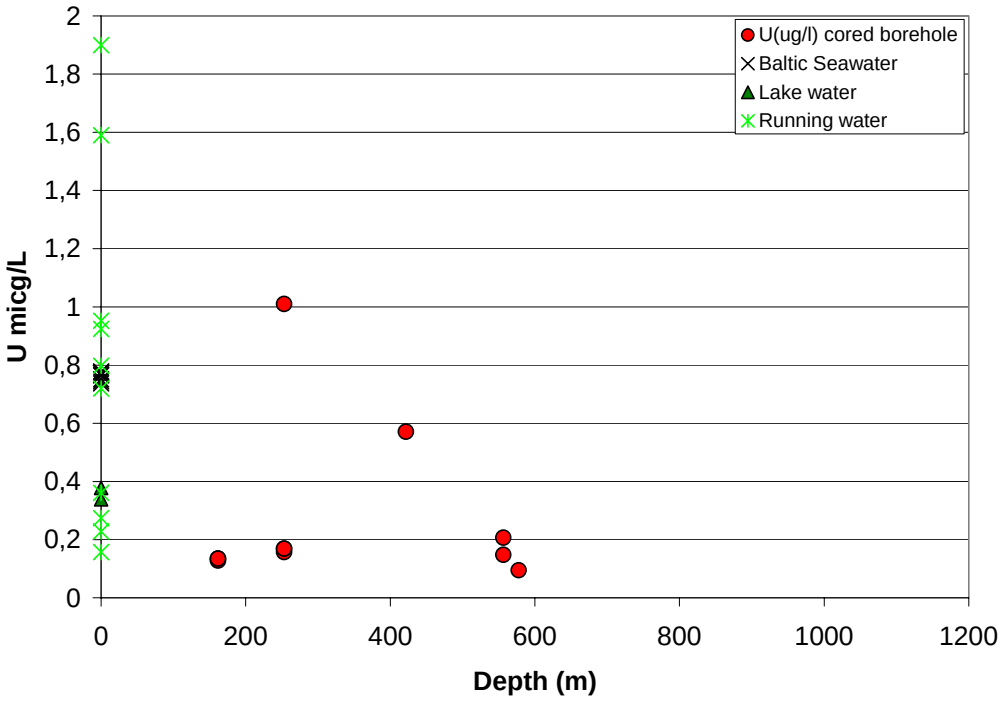

Figure 7.4-13: *Plot of U versus depth in surface waters, Baltic Sea waters and groundwaters from the Simpevarp site.*

There is a tendency towards higher uranium contents in waters with higher HCO_3^- (Fig. 7.4-14). This is also indicated in the plot of the POM groundwater data (7.4-15). It should be noted, howvever, that the uranium contents are generally very low in the analysed waters thus reflecting large uncertainties.

Figure 7.4-15 shows uranium versus depth for the POM samples. The values are generally low and the groundwaters from the greatest depths show values as low as 0.02 µg/L

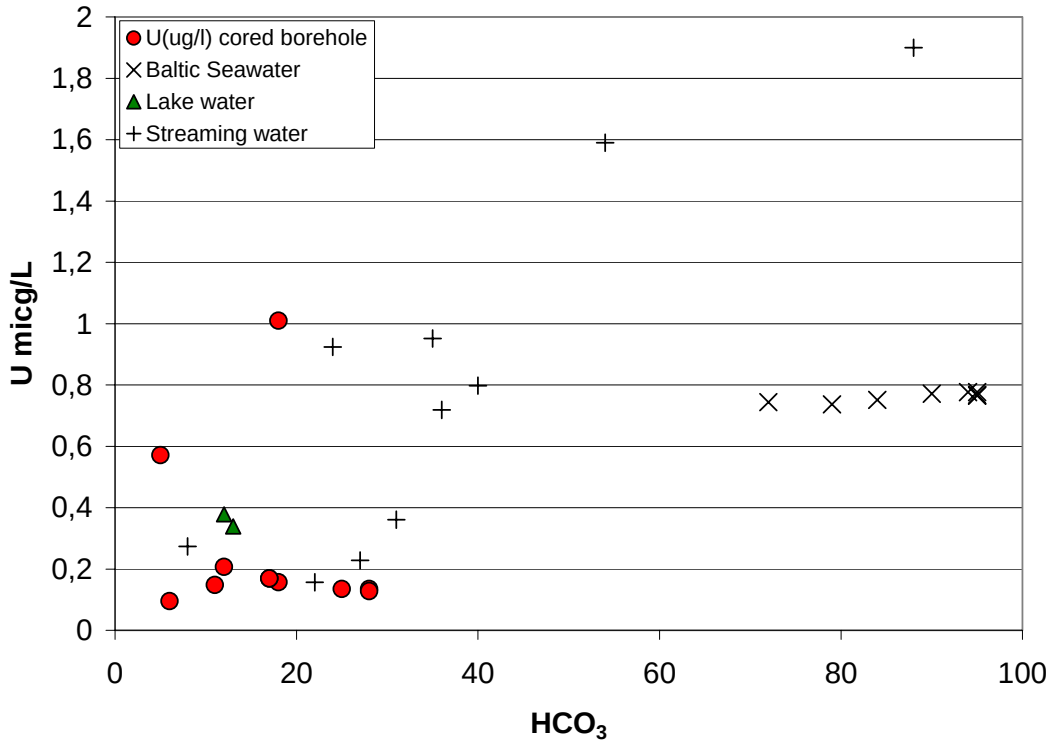

Figure 7.4-14: *Uranium versus bicarbonte content in surface waters, Baltic Sea waters and groundwaters from Simpevarp*

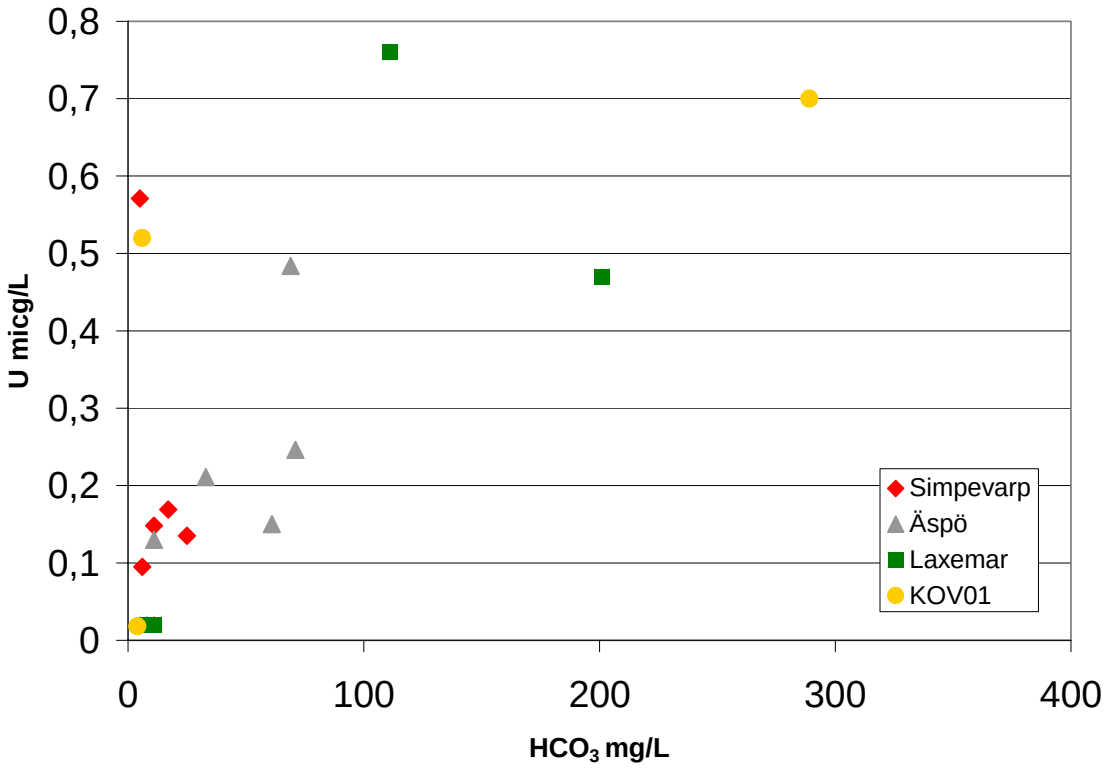

Figure 7.4-15: *Uranium versus bicarbonate in groundwaters from Simpevarp, Äspö, Laxemar and Oskarshamn (KOV01).*

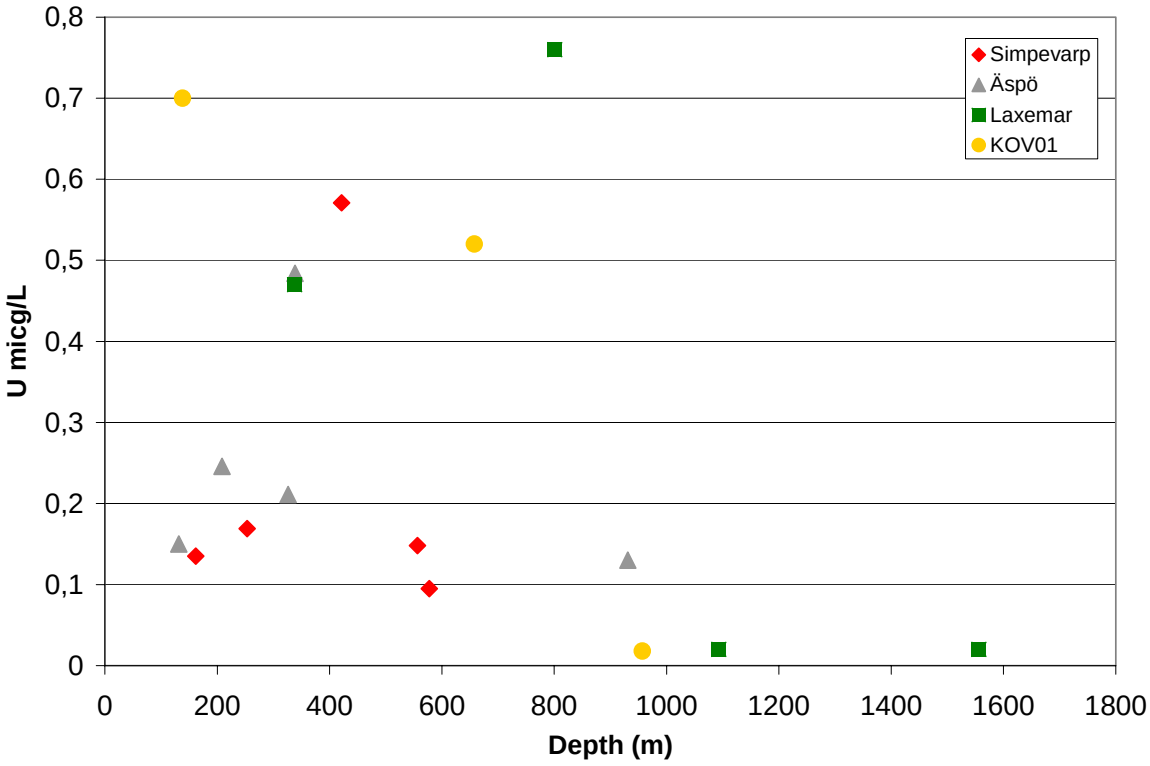

Figure 7.4-16: *Uranium versus depth in groundwaters from Simpevarp, Äspö, Laxemar and Oskarshamn (KOV01).*

7.4.7 Boron

Due to the large relative mass difference between ^{10}B and ^{11}B and the high chemical reactivity of boron, significant isotope fractionation produces large variations in the $^{11}B/^{10}B$ ratios in natural samples from different geological environments. This results in high isotopic contrasts of potential mixing sources and also in process-specific changes in the isotope signature (Barth, 1993). Boron (^{11}B) has also been used as an indicator of permafrost conditions as it appears to become isotopically enriched in the fluid phase during freeze-out conditions. For example, deep saline groundwaters characterised by negative $\delta^{18}O$ values tend to correlate with high ^{11}B values.

The SICADA database reports only ^{10}B which is inadequate to carry out the full evaluation using boron and its isotopes. It is therefore recommended that future groundwater analysis should include boron and the $^{11}B/^{10}B$ ratios.

7.5 Calcite isotope studies

In order to discriminate between the different generations of calcite and provide palaeohydrogeological information of past hydrochemical conditions, 39 samples were analysed for $\delta^{13}C$/ $\delta^{18}O$, of which 15 were selected for $^{87}Sr/^{86}Sr$ and a smaller set (9 samples) analysed chemically. The calcites represent both sealed and open fractures and the results are documented in Drake and Tullborg (2004; in press). In some open fractures it was possible to sample calcites grown in open space voids and showing euhedral crystal forms. Observations have been noted of the crystal morphology when possible since there is a relationship between calcite morphology (long and short C-axis) and groundwater salinity that has been documented from the Sellafield site in the U.K. (Milodowski et al., 1998). Indications from the Simpevarp study show that fresh water carbonates usually have short C-axis (nailhead shaped crystals) whereas calcite precipitated from saline waters preferably show long C-axis (scaleohedral shapes). Equant crystals are common in transition zones of brackish water. Concerning the KSH01A+B samples (from depths between 129-361 m) all but one show equant to scalenohedral forms. This is in good agreement with the occurrence of saline water at relatively shallow depths (150 m) in the bedrock.

The $\delta^{13}C$/ $\delta^{18}O$ values for the KSH01A+B calcites are plotted together with previously analysed calcites from Äspö and Laxemar (Fig. 7.5-1). The calcites show $\delta^{18}O$ values ranging from -6 to -22 ‰ PDB and $\delta^{13}C$ values from -26 to –2 ‰ PDB. The calcites showing the lowest $\delta^{18}O$ values have the highest $\delta^{13}C$, typical for hydrothermal calcites devoid of any biogenic carbon. Calcites with higher $\delta^{18}O$ values indicate possible precipitates from meteoric or brackish Baltic Sea water, based on fractionation features and ambient temperatures in the range of 7-15 ^{o}C (O´Neil et al., 1969). These calcites also show a larger spead in their $\delta^{13}C$ carbon isotope values supporting interaction with biogenic carbon. Extreme $\delta^{13}C$ values (as low as -84 ‰ PDB) have been recorded in Äspö drillcores and indicate biogenic activity in the groundwater aquifers causing *in situ* disequilibria. The lowest values in KSH01A+B (-20 to -26 ‰ PDB) are indications of the same process. It should be noted that the fractionation between HCO_3^- and $CaCO_3$ is only a few per mil; therefore the $\delta^{13}C$ value in the calcite reflects largely the $\delta^{13}C$ value in the bicarbonate at the time of calcite formation.

Most of the calcites with euhdral crystals show $\delta^{18}O$ values between -6 and -10 ‰ PDB, except for a group of three samples with scalenoedral shapes showing values of around -2 to -13 ‰. This population has earlier been identified and interpreted as reflecting ‘warm brine’ precipitates (Bath et al., 2000; Tullborg, 2004).

The highest $\delta^{18}O$ values, close to zero, that have been found in the calcites from the Äspö drillcores have been interpreted as possibly representing precipitates from marine waters of Oceanic-type since they are not found in the groundwaters from drillcore KSH01A+B. This may be due to the relatively small set of samples analysed from the Simpevarp area.

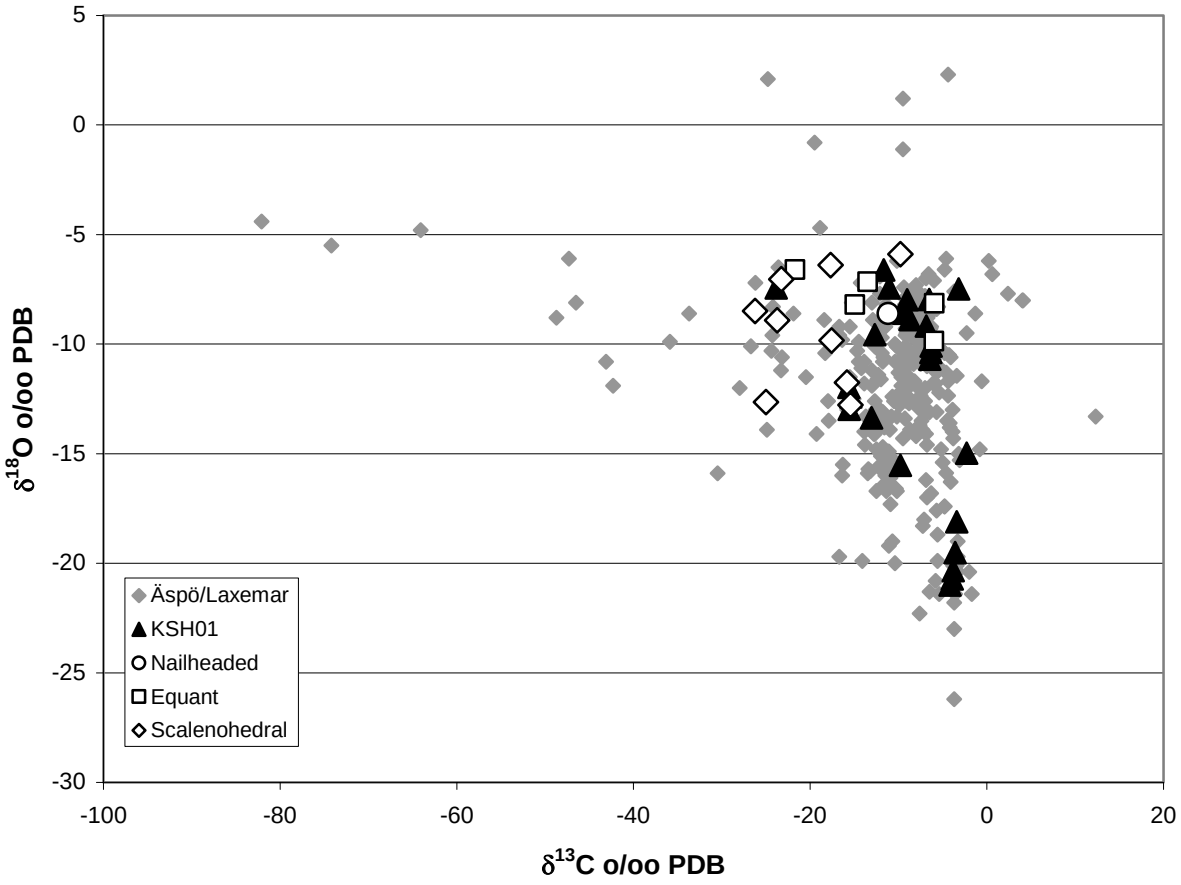

Figure 7.5-1: *Plot of $\delta^{13}C$ versus $\delta^{18}O$ for fracture calcites in KSH01A+B. Also included are earlier analysed samples from Äspö/Laxemar (Bath et al., 2000;Wallin and Peterman, 1999; Tullborg, 1997). Note that crystal shapes have been distinguished when possible.*

Figures 7.5-2 and 7.5-3 show $\delta^{18}O$ and $\delta^{13}C$ plotted against depth respectively for KSH01A+B. These plots indicate that fractures in the upper 400 metres have been more open to low temperature groundwater circulation (i.e. possible interaction with Meteoric/Baltic Sea water) and that calcites with carbon of biogenic origin are common down to 300 m. The distribution of the calcite isotope values versus depth are in agreement with the differential flow logging results, showing low hydraulic conductivity below 300 metres and even lower hydraulic conductivity in the bottom 600 metres of the borehole. The sections sampled for groundwater chemistry are from 156-167 m, 245-261 m and 548-565 m along the core length (which is similar to the vertical depth since the borehole is subvertical). The salinities of the present day groundwaters from these depths range from approx. 4000-8000 mg/L Cl (increasing with depth) and the $\delta^{18}O$ values in the same groundwaters range from -12 to -14 ‰ SMOW.

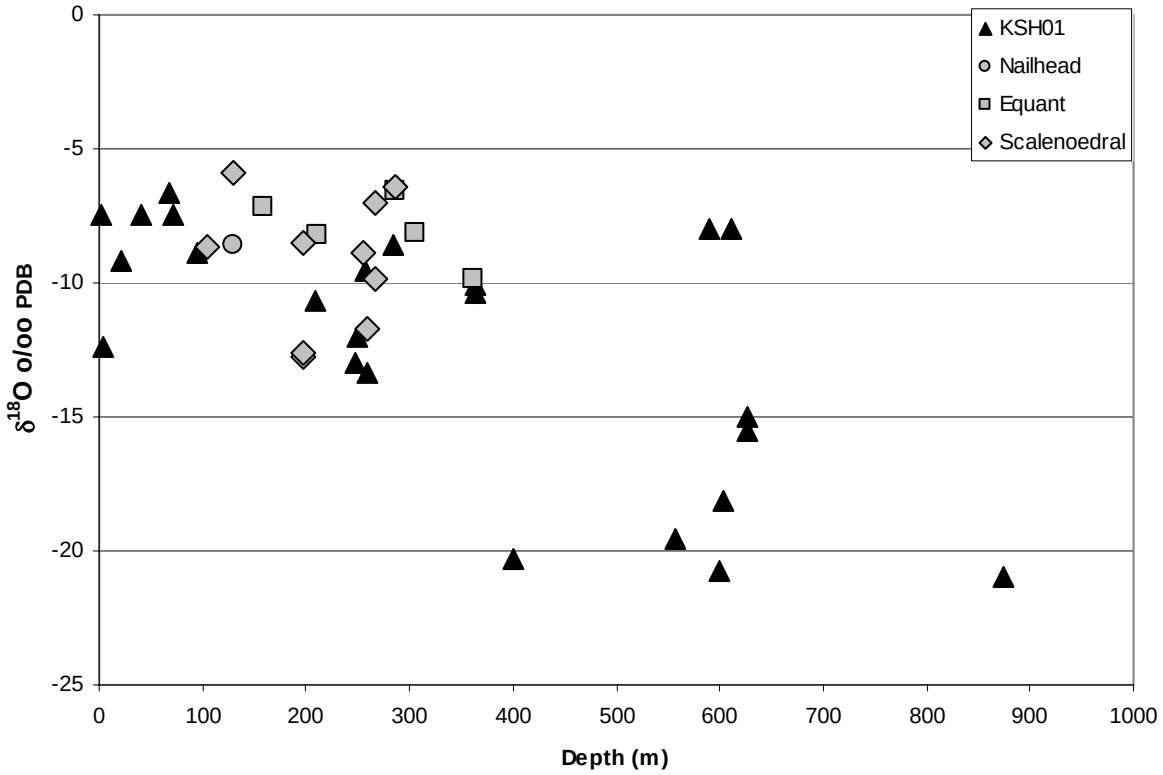

Figure 7.5-2*: Plot of $\delta^{18}O$ versus depth for fracture calcites in borehole KSH01A+B. Crystal shapes are indicated when possible.*

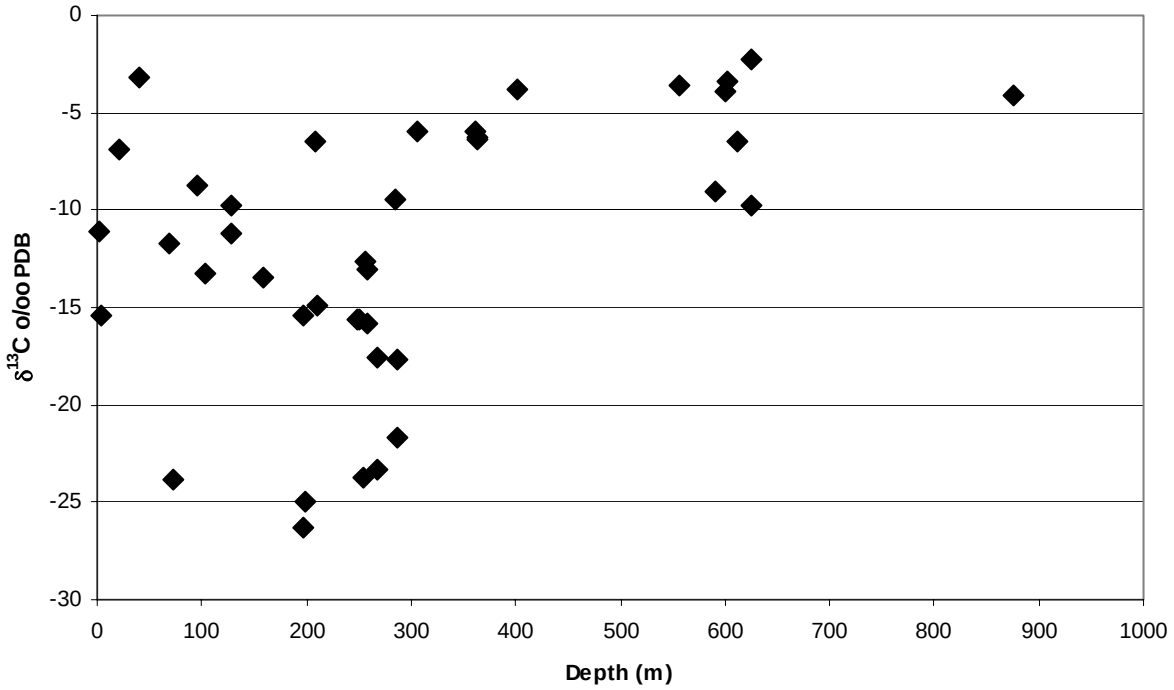

Figure 7.5-3: *Plot of $\delta^{13}C$ versus depth for fracture calcites in borehole KSH01A+B.*

The strontium isotope values in the fracture calcites range between 0.707551 and 0.715985 and show a positive correlation when plotted against $\delta^{18}O$ (Fig. 7.5-4). The calcites showing the lowest Sr and $\delta^{18}O$ values are usually higher in strontium content and often precipitated with hydrothermal minerals. This is in accordance with earlier observations made by Wallin and Petermann (1999) and can be explained by hydrothermal activity that took place relatively early in the geological history of the bedrock. The calcites with Sr isotope values close to present groundwater values in the Simpevarp area (0.715 to 0.716) show $\delta^{18}O$ values around -6.4 and -8.5 ‰ PDP, i.e they are of possible recent origin, which in this case probably means Quaternary.

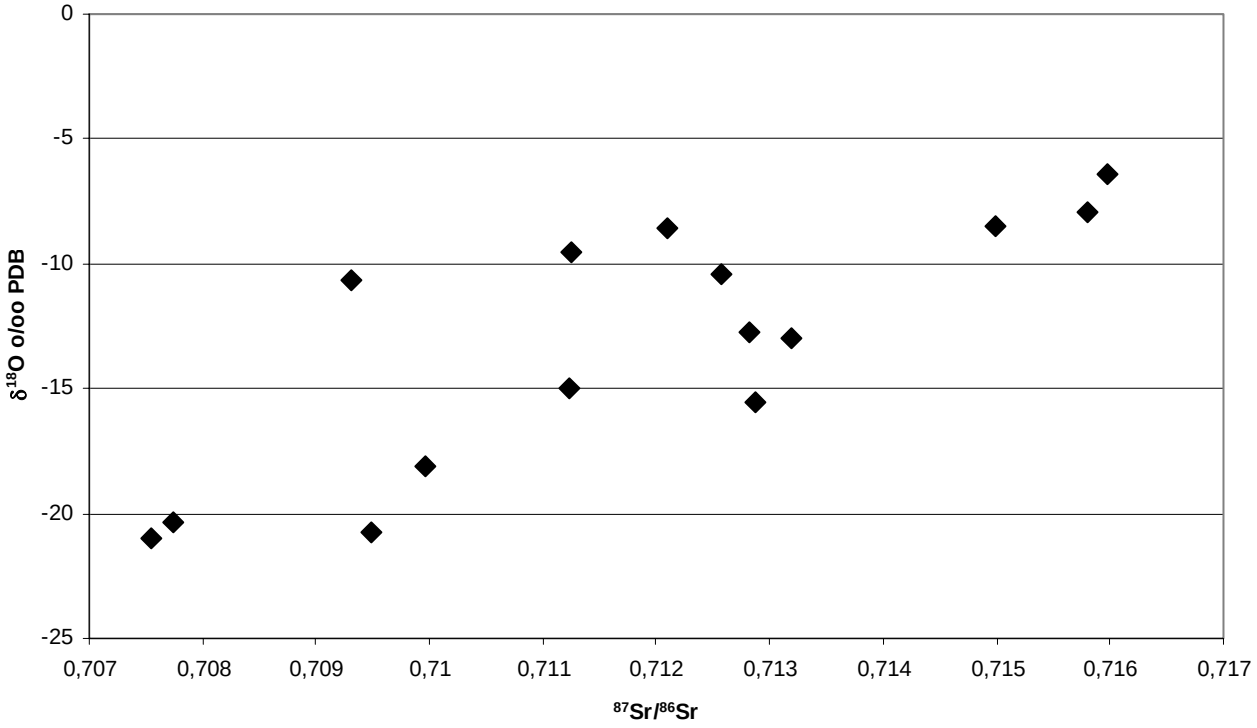

Figure 7.5-4: *Plot of Sr isotope ratios versus $\delta^{18}O$ for fracture calcites in borehole KSH01A+B.*

Trace element analyses made on leachates from calcite samples are reported in Drake and Tullborg (2004, in press). From the results it is obvious that in some samples either some contaminant minerals have also been dissolved, or, that ion exchanged elements are released from clay minerals included in the calcite samples. For example, sample KSH01:611 m shows a very high content of Ba (4852 ppm) which may be explained by the dissolution of Ba-zeolites present in the sample.

Generally the trace elment contents of Sr, Mn and REEs correspond to earlier observations from Äspö/Laxemar (Bath et al., 2000; Tullborg, 2004). Samples of hydrothermal calcites (low $\delta^{18}O$ and high $\delta^{13}C$) show generally Sr values higher than 100 ppm, low REE contents and usually non-fractionated REE patterns, or, in the case of KSH01:401.25 m, enrichment of heavy REEs (Fig. 7.5-5). Samples with the highest La and Mn contents are found in the uppermost 400 metres and are usually associated with calcites with lower $\delta^{13}C$ indicating reducing conditions due to microbial activity.

Small negative Ce anomalies are indicated in two samples: KSH01:257.80 m and KSH01:208 m. The REE contents of the latter are so low that their significance can be questioned but in the 257 m sample it may indicate that groundwaters have passed through a redox zone where Ce has been oxidised and immobilised. The resulting negative Ce-anomaly in the groundwater, therefore, could have been transported to the fracture calcite. It should be noted that the Mn content in this sample is low.

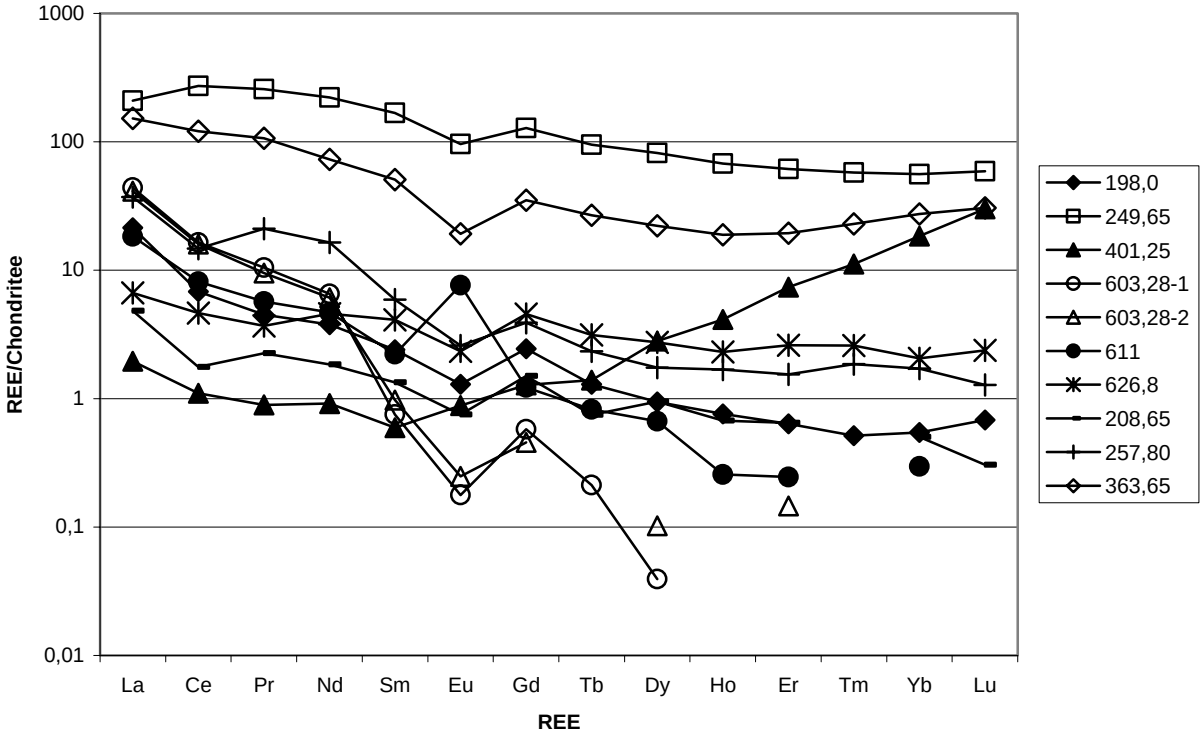

Figure 7.5-5: *Chondrite normalised REE patterns for fracture calcites from KSH01A+B. Note that these analyses are made on leacheates of calcite samples which contain small amounts of contaminant minerals..*

In summary, isotopic evidence from calcites in borehole KSH01A+B supports the results from the hydrogeological and hydrochemical studies which show that the upper part of the bedrock at Simpevarp is much more hydraulically conductive and dynamic than the deeper part (>300 m) and has probably been so for a very long time. The number of open fractures and the amounts of calcite in the deeper fractured bedrock is limited. Furthermore, the stable isotope ratios support the decreased interaction with biogenic carbonate at depths greater than 300 metres. The morphology of the calcites formed in open fractures show crystal shapes typical for brackish or saline groundwater carbonates with one exception. This is in agreement with the present groundwater chemistrry were saline groundwaters (<5000 mg/L Cl) are sampled already at a depth of 150 m.

7.6 Evidence of redox indicators

Manganese (Mn^{2+}) was singled out as a potential redox indicator in the groundwater system and all available data are plotted against depth in Figure 7.6-1. Mn^{2+} is produced by microbes during the oxidising of organic material under anaerobic conditions (Hallbeck, 2004). It should be emphasised that the presence of Mn^{2+} in groundwater is a strong indication of reducing conditions, but its absence (or very low content) in deep groundwaters can not be taken as an indication of oxidising conditions.

Figure 7.6-1 shows no appparent marked trend when all data are viewed, however considering the more reliable cored borehole data there is a sharp decrease from dilute groundwater values (0-100 m interval) followed by a levelling off to around 400 m and then a larger spread of values including lower Mn contents within the 400-600 m interval (i.e. the interval suspected as containing a Littorina Sea component). At depths greater than 600 m, where there is a marked salinity increase (cf. Fig. 7.2-8), low manganese values are indicated by the deepest groundwater sampled. Of the surface waters, the Lake samples show the greatest spread in manganese content, the Stream samples less.

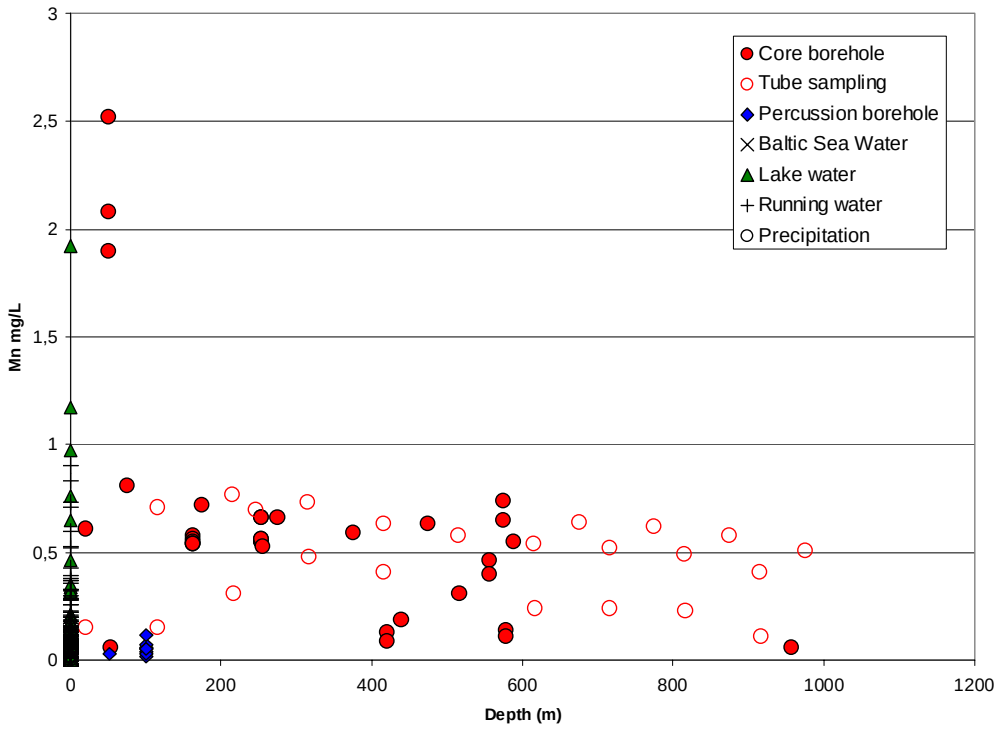

Figure 7.6-1: *Variation of Mn with depth*

The relationshop of manganese with bicarbonate is shown in Figure 7.6-2. The three highest manganese values from the cored boreholes correlate with high bicarbonate in the 0-100 m interval. Even within the 100-600 m interval most of the cored borehole

data show a weak relationship equating higher manganese with higher bicarbonate. The surface-derived waters show no significant trends.

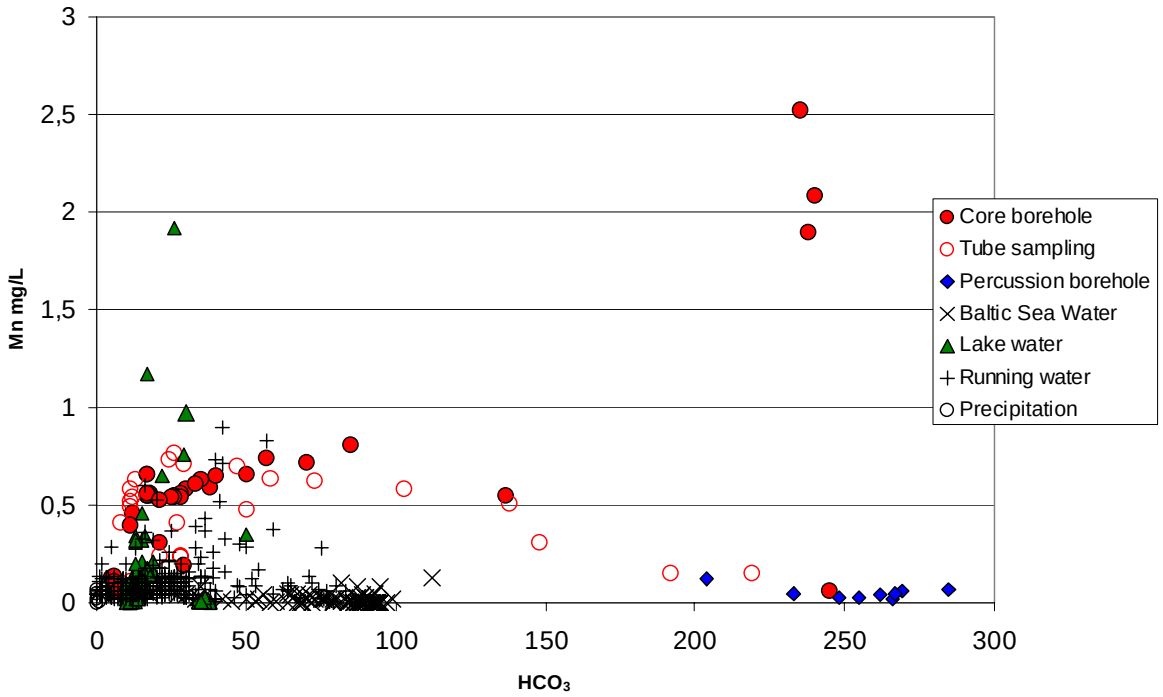

Figure 7.6-2: *Plot of Mn vs HCO_3 for all Simpevarp data*

With the limited data available it is too early to draw any fast conclusions; on-going and future microbe studies (Hallbeck, 2004) should contribute significally to this discussion for the Laxemar Model v. 2.1 Stage.

7.7 Evidence of a Littorina Sea signature

The Littorina stage in the postglacial evolution of the Baltic Sea commenced when the passage to the Atlantic Ocean opened through Öresund in the southern part of the Baltic Sea. The relatively high sea level together with the early stages of isostatic land uplift led to a successively increasing inflow of marine water into the Baltic Sea. Salinities twice as high as modern Baltic Sea have been estimated for a time period of about 2000 years starting some 7000 years ago (cf. description of the post glacial scenario and references therein). From shore displacement curves it is clear that Simpevarp and Laxemar in part were covered by the Littorina Sea. Due to the topography of the area and the on-going isotstatic land uplift, the Laxemar area was probably influenced only to a small degree, whereas the Simpevarp peninsula was covered for several thousands of years until eventual emergence during uplift initiated a recharge meteoric water system some 4000 to 5000 years ago. This recharge system effectively flushed out much of the Littorina Sea water.

The Forsmark area, in contrast, has been covered by the Littorina Sea for a much longer period of time and the low topography implies that it reached several tens of kilometres further inland. Furthermore, the present meteoric recharge stage following uplift and emergence has only prevailed for less than 1000 years such that any flushing out of the Littorina Sea component is less pronounced. Stronger evidence of a Littorina Sea water signature can therefore be expected in groundwaters at Forsmark.

Comparison of Forsmark data with the Simpevarp-Äspö-Laxemar-Oskarshamn (KOV01) data (the POM data) indicates large differences in the character and origin of the groundwaters, especially for brackish groundwaters with chloride contents of around 4000-6000 mg/L Cl. This is exemplified in three plots showing chloride versus magnesium, bromide and $\delta^{18}O$ (Figs. 7.7-1, 7.7-2 and 7.7-3). The magnesium versus chloride plot (Fig, 7.7-1) clearly shows the difference between the Forsmark and Simpevarp groundwaters characterised by chloride contents up to 5500 ppm Cl; characteristically the Forsmark samples closely follow the modern marine (Baltic Sea) trend. Those few groundwaters that plot within the Simpevarp group are from greater depths in the bedrock and, as such, have been influenced by mixing with deeper non-marine saline groundwaters. A few samples from Äspö (KAS06 and HAS02; Fig. 7.7-4) also show relatively high Mg contents, although not as high as in the Forsmark groundwaters with similar chloride contents. Most of the POM groundwaters show low Mg values although small increases are observed for samples in the chloride interval 4000-6300 mg/L.

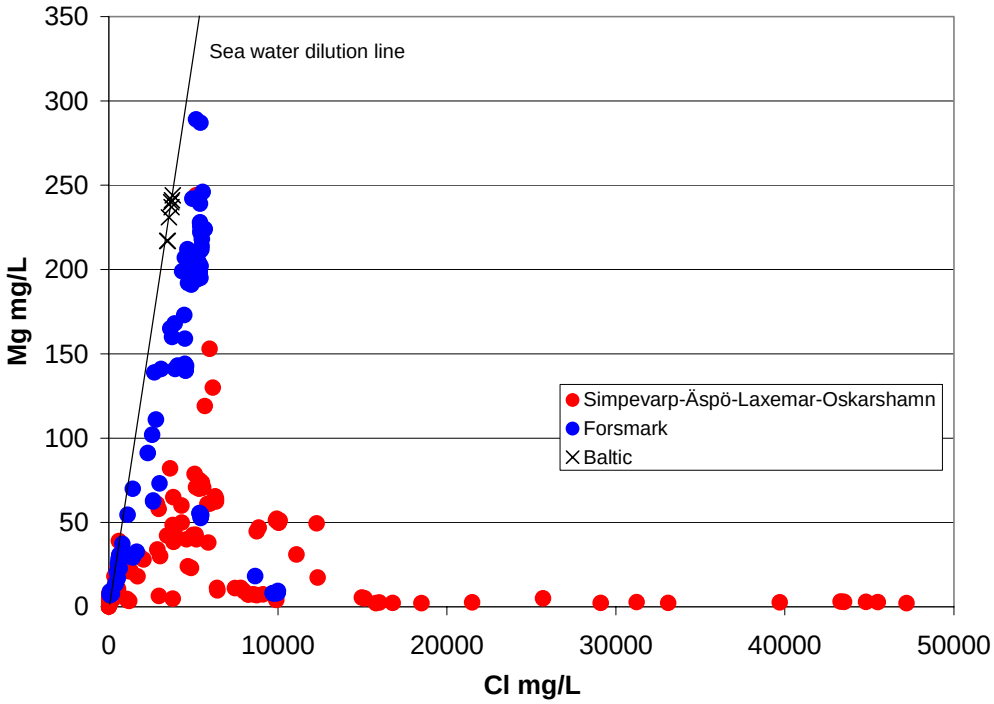

Figure 7.7-1: *Mg versus Cl for groundwaters from Forsmark and the POM sites (Simpevarp-Äspö-Laxemar-Oskarshamn (KOV01)). Baltic Sea waters from Simpevarp and Forsmark are included for reference.*

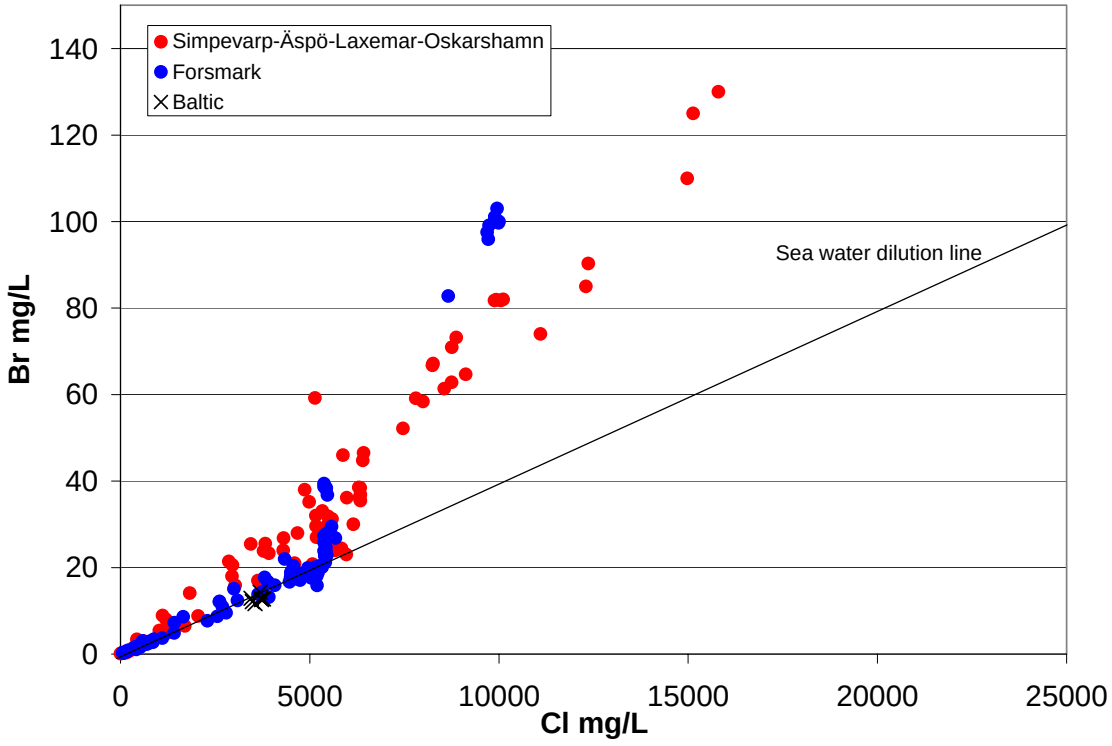

Figure 7.7-2: *Br versus Cl for groundwater samples from Forsmark and the POM sites (Simpevarp-Äspö-Laxemar-Oskarshamn (KOV01)). Baltic Sea waters from Forsmark and Simpevarp are included for reference.*

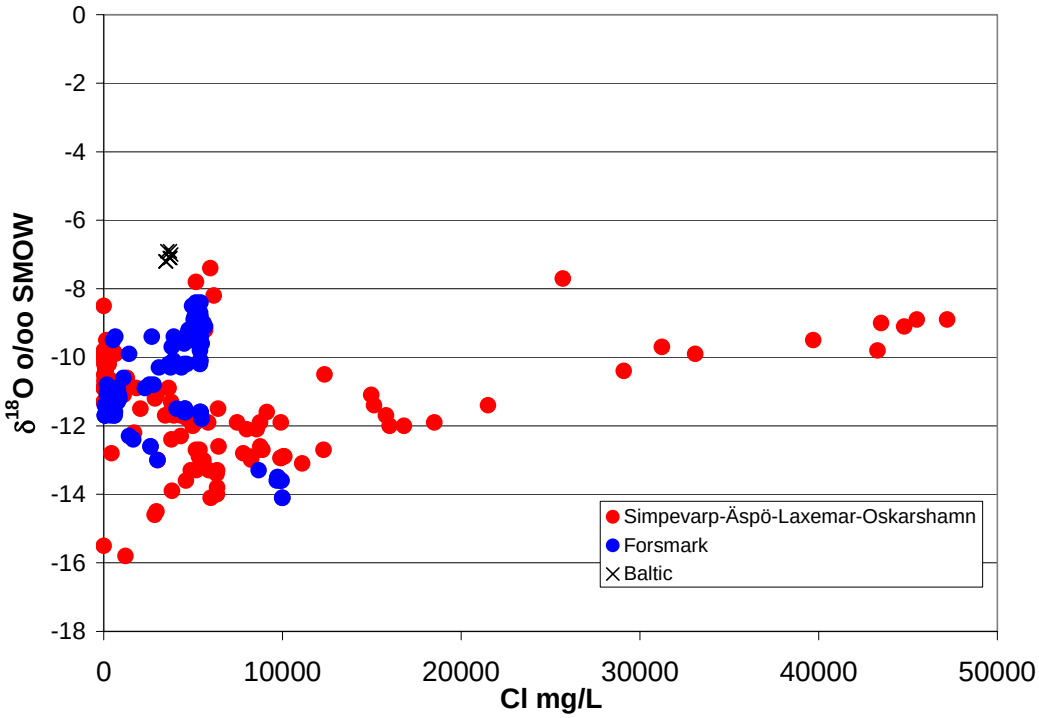

Figure 7.7-3: *$\delta^{18}O$ versus Cl for groundwaters from Forsmark and the POM sites (Simpevarp-Äspö-Laxemar-Oskarshamn (KOV01)). Baltic Sea waters from Simpevarp are included for reference.*

The bromide versus chloride plot (Fig. 7.7-2) underlines the marine signature for most of the Forsmark groundwaters up to contents of 5500 mg/L Cl, whereas marine signatures only are obtained in a few of the POM groundwaters. This observation is strengthened in the $\delta^{18}O$ versus chloride plot (Fig. 7.7-3) which shows deviating groundwater trends for Forsmark and Simpevarp.

Generally, with a few exceptions, the brackish to saline groundwaters up to 5500 mg/L Cl at Forsmark show indications of a marine origin in terms of: a) Br/Cl ratios, b) Mg values ≥100 mg/L, and c) $\delta^{18}O$ values higher than meteoric waters (due to in-mixing of marine waters). In contrast, for the Äspö-Simpevarp-Laxemar samples these criteria are only fulfilled in samples from KAS06 and one sample in KSH03A. In both cases the groundwater samples have been collected from fracture zones outcropping close to the shoreline or under the Baltic Sea.

The chloride content and $\delta^{18}O$ value for the Littorina Sea at maximum salinity is difficult to determine precisely. Interpretations of salinities based on fossil fauna together with $\delta^{18}O$ analyses of the fossils has resulted in suggested salinities around 6500 mg/L Cl and $\delta^{18}O$ values ~ -4.5‰ SMOW (Donner, 1994; Pitkänen et al., 2003). In Figure 7.7-4 (Cl versus $\delta^{18}O$) groundwaters from the POM area show Br/Cl ratio < 0.0045 and magnesium values > 100 mg/L. For comparison are included a small set of samples from Forsmark and the values for selected groundwaters at Olkiluoto considered to contain the largest proportion of Littorina Sea water (Pitlkänen et al., 2003). As can be seen in the figure these values cluster along a mixing line from the suggested Littorina Sea composition to a typical glacial meltwater. Notably, none of the Simpevarp bedrock groundwaters sampled so far show values in total agreement with a Littorina Sea component. At least two explanations can be suggested: 1) the cluster

represents the Littorina Sea at the time when the water intruded, and 2) the Littorina Sea water was mixed with glacial meltwater in the bedrock.

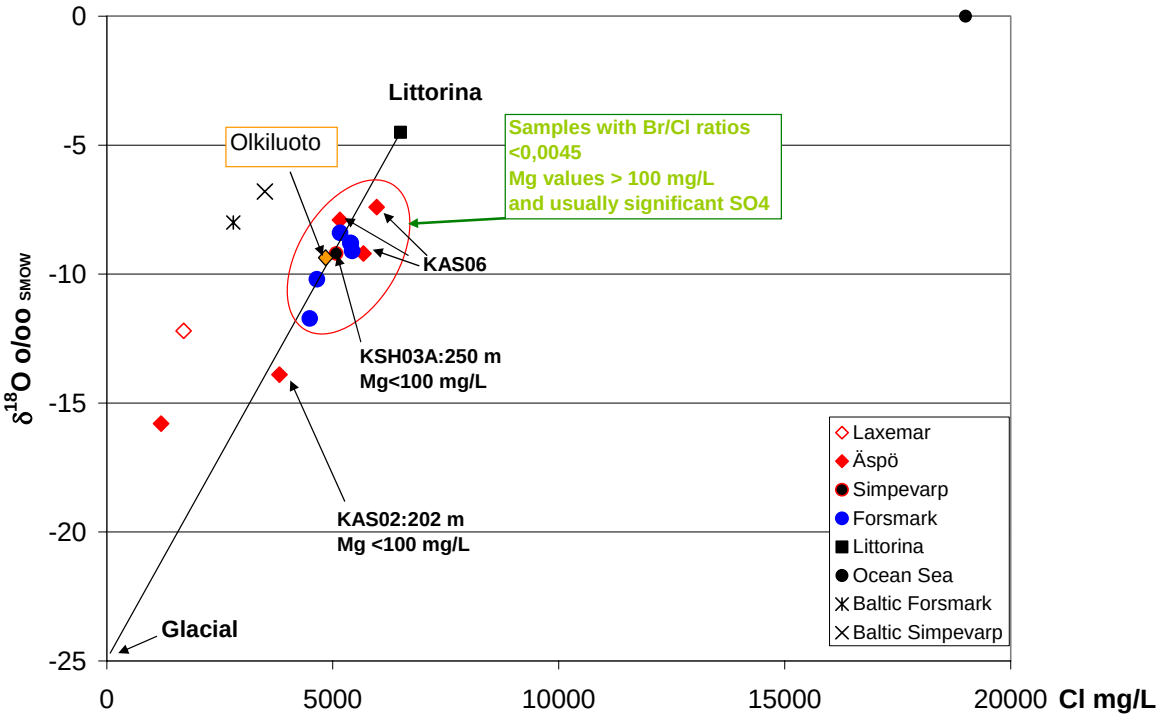

Figure 7.7-4: *$\delta^{18}O$ versus chloride content for potential marine groundwaters from Simpevarp, Äspö, Forsmark and Olkiluoto, the latter from Pitkänen et al. (2003).*

In conclusion, groundwaters from the Äspö, Laxemar and Simpevarp sites at best only show a weak presence of a Littorina Sea water component. However, based on the post glacial scenario for the region, it is reasonable to assume that Littorina Sea water penetrated into the bedrock but has been flushed out subsequently by later recharge meteoric waters during early uplift. This has been facilitated by the fact that the maximum penetration of these Littorina waters appear to have been restricted to shallow depths (approx. 150-300 m). Greater penetration depths may have occurred along some of the sub-vertical structures in the area, but to date there is an absence of data to support this.

Some contributions of ion exchange processes to enhanced magnesium contents in a number of the POM groundwaters must also be considered. The nature of such magnesium sources are presently uncertain, but water/rock interaction through weathering processes and/or removal by ion exchange processes of earlier marine sources from near-surface sediments to subsequent recharging meteoric waters could be invoked.

7.8 Conclusions

7.8.1 Main elements

- Overall depth trends show increasing TDS with increasing depth. In particular the Ca/Na and Br/Cl ratios increase markedly.
- Sulphate and Mg show an overall decrease with depth with greater dispersion from approx. 200-600 m. Bicarbonate decreases sharply with depth.
- Ca/Mg and Br/Cl ratios versus Cl content indicate a deep, non-marine source of the salinity for most of the borehole samples. This is similar to groundwaters from the Äspö, Laxemar and Oskarshamn (KOV01) boreholes.
- Deep groundwaters at Simpevarp and Äspö (1000 m) are Na-Ca-Cl in type; deep groundwaters at Oskarshamn (KOV01; 1000 m) and at Laxemar (1700 m) are Ca-Na-Cl in type. Since Laxemar is inland and Oskarshamn is close to the coast, this could be an indication of discharging very deep groundwaters at Oskarshamn. At greater depths below Simpevarp and Äspö than presently sampled, Ca-Na-Cl groundwaters therefore might be expected..
- A small set of brackish groundwaters (1000-6000 mg/L Cl), located around 150-300 m depth, show marine signatures of possible Littorina Sea origin. These are located in fracture zones close to or under the Baltic Sea.
- $\delta^{18}O$ versus Cl indicates a contribution of glacial waters to the brackish and deeper saline water samples.
- The SO_4 contents show a large variation for the brackish and saline groundwaters. In the brackish groundwaters with 5000-6300 mg/L Cl, microbially mediated sulphate reduction is taking place. The SO_4^{2-} contents in the more highly saline groundwaters are still not high enough to invoke dissolution or leaching as a mechanism. More likely processes are in-mixing of marine waters although in-mixing of SO_4^{2-} from deep brine waters cannot be excluded. Deep saline SO_4^{2-} sources (> 20 000 mg/L Cl) may have resulted from the leaching of sediments and/or dissolution of gypsum previously present in fractures.

7.8.2 Isotopes

- The isotope data from the boreholes are still relatively few and often do not correspond to the most representative samples. To compensate, most of the available data have been plotted with the objective of determining trends rather than far reaching conclusions.
- With respect to tritium, generally the Baltic Sea samples show somewhat higher values (10.3-19.3 TU) compared to the meteoric surface waters (7.8-15 TU). The successive lowering of the tritium contents versus time elapsed since the bomb tests may explain the higher values in the Baltic Sea (due to reservoir effects). Note that the precipitation values are very few, show a large variation in tritium and therefore are not considered very conclusive. Continued systematic sampling of precipitation for tritium analyses is recommended.
- For carbon, plots of ^{14}C versus $\delta^{13}C$ versus HCO_3^- show that there is no real correlation between ^{14}C and $\delta^{13}C$, i.e. there is no indication of a change in $\delta^{13}C$ with age. Breakdown of organic material plays a major role and has occurred either in the near-surface (being transported downwards) or that *in situ* production have taken place. An organic origin is also supported by the $\delta^{13}C$

versus HCO_3^- plot where the groundwater samples showing the highest HCO_3 contents show relatively homogenous $\delta^{13}C$ values.
The plot of tritium versus ^{14}C for surface waters from Simpevarp show a distinct decrease in ^{14}C content in the Lake and Stream waters, whereas the tritium values remain the same or show a small decrease. The explanation is that HCO_3^- added to the waters originates either from calcites devoid of ^{14}C or due to microbial oxidation of organic material with lower (or no) ^{14}C. This is the pattern expected for near-surface waters.

- Marine waters show a distinct Sr isotope signature (0.7092) which is very close to the measured values in the Baltic Sea waters, whereas groundwaters from the different sites show values significantly more enriched in radiogenic Sr. Water/rock interaction processes involving Rb-containing minerals are the reason for this. The relatively small variation in Sr isotope ratios within each area, particularly at the Simpevarp, Ävrö and Laxemar sites, is probably an indication that ion exchange reactions with clay minerals along the groundwater flow paths is an important process. For the Simpevarp-Laxemar area there is a tendency towards higher contents of radiogenic Sr in the waters with highest salinities (and thus the highest Sr contents measured). Because of the limited data it is not possible to explain this observation, but in the absence of any mineralogical reasons, it is likely that greater residence times for these deep saline groundwaters result in more extensive mineral/water interactions.
- The borehole groundwaters generally show $\delta^{34}S$ values in the same range as the Baltic Sea waters but with a clear indication in the brackish groundwaters of $\delta^{34}S$ values greater than +21 ‰ CDT in samples with low SO_4^{2-}. This may be explained by modification of the isotope ratios by sulphur-reducing bacteria. The higher saline groundwaters share lower $\delta^{34}S$ but higher SO_4^{2-} contents. The $\delta^{34}S$ values of these deeper groundwaters are, however, still within the range for the analysed Baltic Sea waters.
- The $\delta^{37}Cl$ data suggest that the deeper cored borehole groundwaters are characterised by water/rock interaction processes, whilst the near-surface percussion borehole groundwaters are mainly marine derived. The distribution of Baltic Sea and surface Lake and Stream waters suggest some mixing components of marine-derived and deeper groundwater sources.

7.8.3 Trace elements

- Only a few data exist for the majority of groundwaters and even some of these are incomplete.
- Sr, Cs and Rb show a positive correlation with depth (and therefore Cl).
- Ba varies considerably but a negative correlation with SO_4^{2-} is indicated, possibly explained by the solubility control of barite.
- Mn contents show large variations in near-surface waters, usually uniform or slightly decreased values in groundwaters down to 600 metres depth, and decreasing values at greater depths.
- The uranium contents are below 2 µg/L in all the analysed waters. The surface waters show values between 0.16 and 1.9 µg/L whereas the Baltic Sea waters all display values around 0.8 µg/L; most of the groundwater samples are low in uranium ($\leq$ 0,2 µg/L). Higher uranium in surface and near-surface waters is usually observed and is caused by oxidising conditions at the surface. The mobility of the oxidised and dissolved uranium is highly dependent on access to

complexing agents, mostly in form of HCO_3^- which is produced in the soil cover and the near-surface environment.

7.8.4 Calcites

Isotopic evidence from calcites sampled from borehole KSH01A+B supports the results from the hydrogeological and hydrochemical studies which show that the upper part of the bedrock at Simpevarp is much more hydraulically conductive and dynamic than the deeper part (>300 m) and have probably been so for a very long time. The number of open fractures and the amounts of calcite in the deeper fractured bedrock is limited. Furthermore, the stable isotope ratios support the decreased interaction with biogenic carbonate at depths greater than 300 metres in KSH01A+B. The morphology of the calcites formed in open fractures show crystal shapes typical for brackish or saline groundwater carbonates with one exception. This is in agreement with the present groundwater chemistrry were saline groundwaters (>5000 mg/L Cl) are sampled already at a depth of 150 m.

8 Visualisation of the Simpevarp data

Visualisation of the hydrogeochemical evaluation documented in this report is in the form of a vertical transect through the Laxemar and Simpevarp sites. The vertical extent of the transect is to approx. 1700 m to accommodate the deepest borehole (KLX02) in the Laxemar site. The approach to locate and construct the transect was carried out as follows.

The position of a WNW-SSE transect was chosen to intersect the Laxemar and Simpevarp sites, approximately along the main regional groundwater direction as approximately shown in Figure 8.1. In this figure the relationship of the groundwater flow direction to the distribution of the major structural features is also indicated.

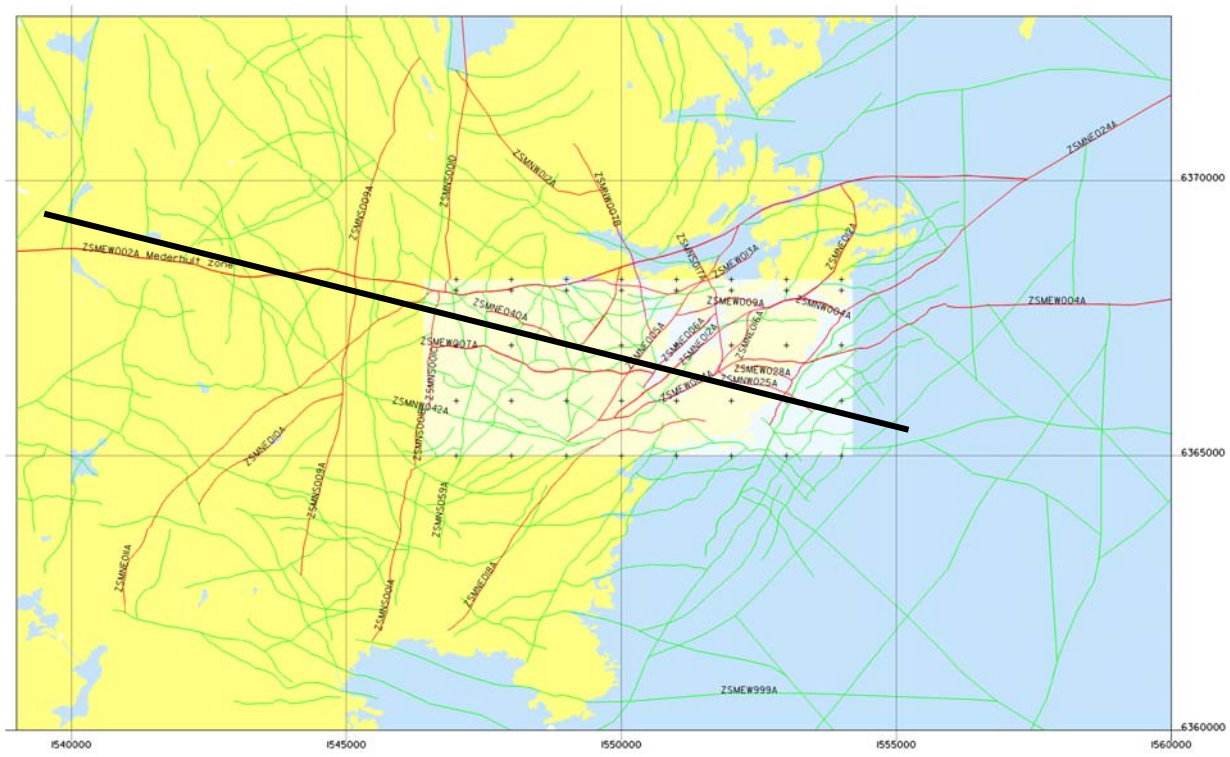

Figure 8.1: *Structural map of the region including and surrounding the Laxemar and Simpevarp sites (lighter boxed area). The black line represents the approximate main groundwater flow direction through the investigated sites. The major structural components intersected are also indicated (I. Rhén, written comm., 2004)*

Within the Simpevarp and Laxemar sites the transect was adjusted to either intersect or pass in the close vicinity of the boreholes of interest, i.e. KLX01, KLX02, HSH02, KSH01A+B, KSH02 and KSH03A (Fig. 8.2). Note that boreholes KLX03 and KLX04 are not included in this present 1.2 model version.

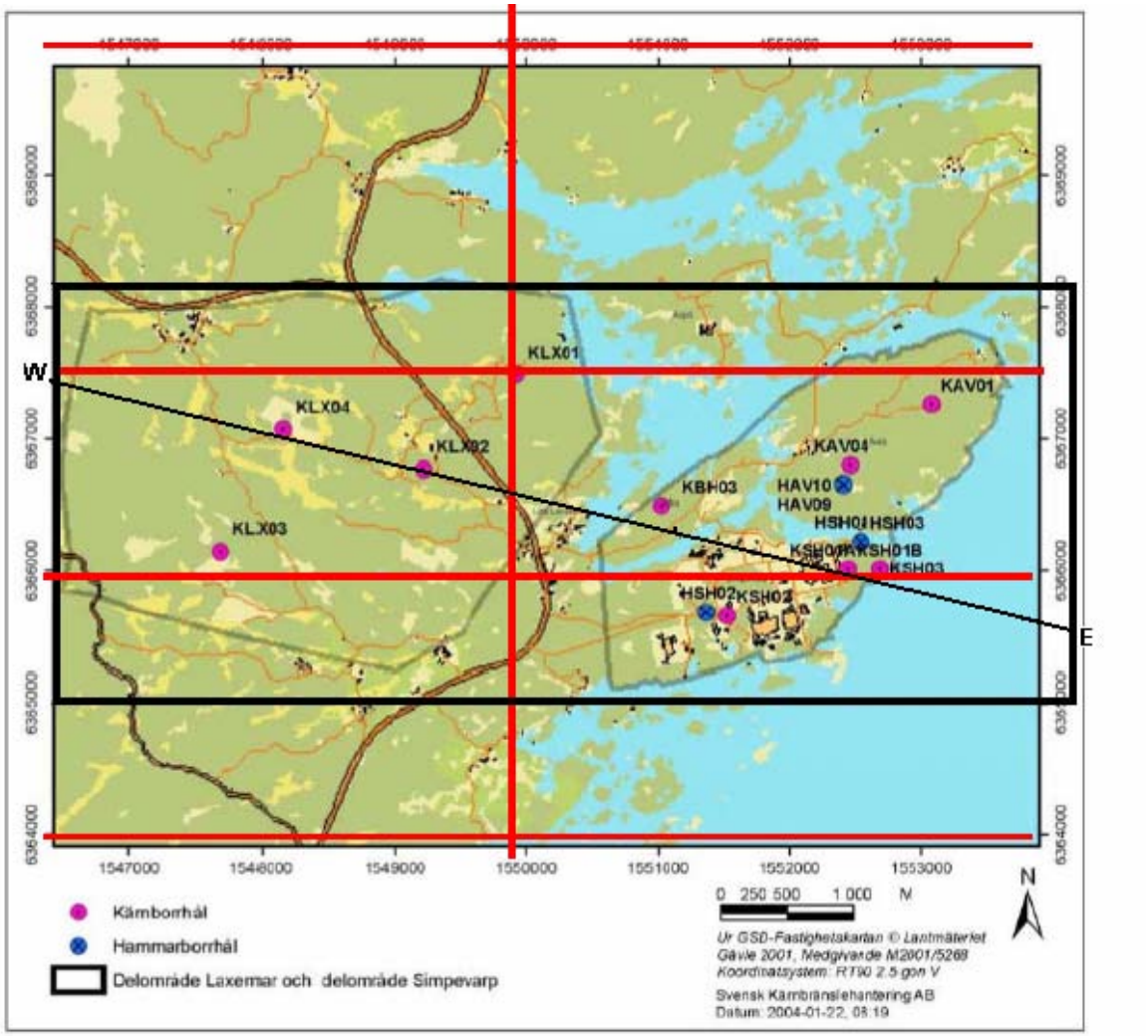

Figure 8.2*: Map showing the location of the sampling points and boreholes in the Simpevarp and Laxemar sites. Boxed in black is the local model area and the vertical NNW-SSE transect profile (black diagonal W-E line) used for the visualisation is also indicated. (I. Rhén written comm., 2004).*

A modelled 2-D version of the vertical transect to 2000 m was produced (Fig. 8.3) showing the position of the main structures, the location (actual or extrapolated) of the boreholes, and the known geology to 1000 m. Using this modelled section as a base, a schematic manual version then was produced to facilitate illustrating the most important structures/fault zones and their potential hydraulic impact on the groundwater flow (Fig. 8.4). This hydraulic information was then integrated with the results of the

hydrogeochemical evaluation results to produce the vertical and lateral changes in the groundwater chemistry (Fig. 8.4).

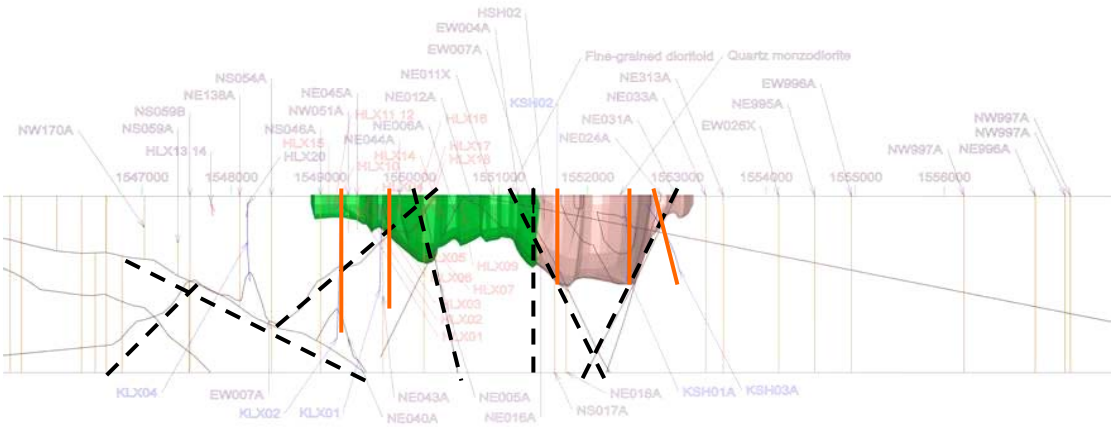

Figure 8.3: *Modelled 2-D version of the vertical transect showing the many intersected structures, the known geology from drilling, and the location (actual or extrapolated) of the boreholes used in the hydrogeochemical characterisation (F. Hartz, written comm., 2004). Accentuated are the more important structures (black hatch lines) and the borehole locations (orange lines). The major geological units present are fine-grained dioritoids (green colour) and quartz monzodiorites (grey/pink colour).*

8.1 Hydrogeology

The WNW-SSE transect in Figure 8.1 shows that in the Simpevarp area the main intersected structures have an approximate NE-SW orientation; in the Laxemar area the transect is mostly parallel to the main WNW-SSE structural trends. The former are considered sub-vertical whilst at Laxemar the structures tend to dip at shallower angles to the SW or NE. Combined, these structures effectively divide both the Simpevarp and Laxemar areas into structural compartments as illustrated in Figures 8.3 and 8.4. It is also believed that each major structural compartment will be characterised by its own local hydraulic groundwater flow regime (Fig. 8.4). Most of the vertical to sub-vertical fracture zones are considered as discharging groundwater pathways; one zone which is also potentially a recharge feature is tentatively indicated by a (?) in blue font close to the Laxemar area.

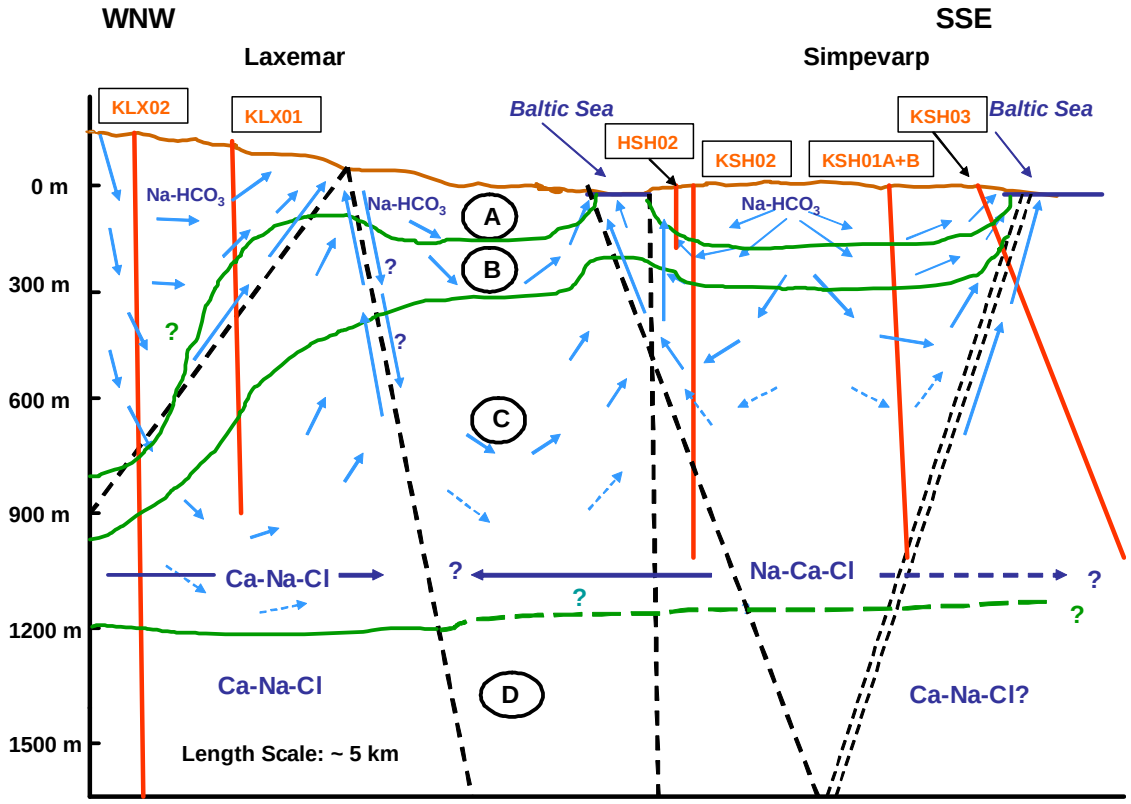

Figure 8.4: *Schematic 2-D model based on Figure 8.3 integrating the major structures, the major groundwater flow directions and the different groundwater chemistries (A-D).*

The groundwater flow regimes at Laxemar/Simpevarp are considered local and extend down to depths of around 600-1000 m depending on local topography. Close to the Baltic Sea coastline where topographical variation is small, groundwater flow penetration to depth will subsequently be less marked. In contrast, Laxemar is charactersied by higher topography resulting in a much more dynamic groundwater circulation which appears to extend to 1000 m depth in the vicinity of borehole KLX02 (Fig. 8.4).

8.2 Hydrochemistry

The marked differences in the groundwater flow regimes between the Laxemar and Simpevarp areas are reflected in the groundwater chemistry. Figure 8.4 shows four major recognised hydrochemical groups of groundwaters denoted by A-D. Question marks are inserted where there is a degree of uncertainty, i.e.:

a) Between groundwater types A and B close to borehole KLX02 at Laxemar. There is some uncertainty whether dilute recharge Na-HCO_3 waters extend to the depth indicated. Some short-circuiting of groundwater flow paths by borehole KLX02 may be occurring.

b) Between types C and D within the Simpevarp site. The extent of Na-Ca-Cl groundwaters below 1000 m is unknown. In addition, it is uncertain whether there is an eventual transition to Ca-Na-Cl groundwater types at even greater depths.

In terms of depth location, chemistry, major reactions and main mixing processes, the main features of these four groundwater types are summarised below.

8.2.1 TYPE A – Shallow (<200 m) at Simpevarp but deeper (0-900 m) at Laxemar

- Dilute groundwater (< 1000 mg/L Cl; 0.5-2.0 g/L TDS)
- Mainly Na-HCO_3 in type
- Redox: Marginally oxidising close to the surface, otherwise reducing
- Main reactions: Weathering; ion exchange (Ca, Mg); dissolution of calcite; redox reactions (e.g. precipitation of Fe-oxyhydroxides); microbially-mediated reactions (SRB)
- Mixing processes: Mainly meteoric recharge water at Laxemar; potential mixing of recharge meteoric water and a modern sea component at Simpevarp; localised mixing of meteoric water with deeper saline groundwaters at Laxemar and Simpevarp

8.2.2 TYPE B – Shallow to intermediate (150-300 m) at Simpevarp but deeper (approx. 900-1100 m) at Laxemar)

- Brackish groundwater (1000-6000 mg/L Cl; 5-10 g/L TDS)
- Mainly Na-Ca-Cl in type but some Na-Ca(Mg)-Cl(Br) types at Simpevarp; transition to more Ca-Na-Cl types at Laxemar
- Redox: Reducing
- Main reactions: Ion exchange (Ca, Mg); precipitation of calcite; redox reactions (e.g. precipitation of pyrite)
- Mixing processes: Potential residual Littorina Sea (old marine) component at Simpevarp, usually in fracture zones close to or under the Baltic Sea; potential glacial component at Simpevarp and Laxemar; potential deep saline (non-marine) component at Simpevarp and at Laxemar

8.2.3 TYPE C - Intermediate to deep (>300 m) at Simpevarp but deeper (approx. 1200 m) at Laxemar

- Saline (6000-20 000 mg/L Cl; 25-30 g/L TDS)
- Mainly Na-Ca-Cl with increasingly enhanced Br and SO_4 with depth at Simpevarp; mainly Ca-Na-Cl with increasing enhancements of Br and SO_4 with depth at Laxemar
- Redox: Reducing
- Main reactions: Ion exchange (Ca)

- Mixing processes: Potential glacial component at Simpevarp and Laxemar; potential deep saline (i.e. non-marine and/or non-marine/old Littorina marine) component at Simpevarp, deep saline (non-marine) component at Laxemar

8.2.4 TYPE D – Deep (> 1200 m) only at Laxemar

- Highly saline (> 20 000 mg/L Cl; to a maximum of ~70 g/L TDS)
- Mainly Ca-Na-Cl with higher Br but lower SO_4 compared to Type C groundwaters
- Redox: Reducing
- Main reactions: Water/rock reactions under long residence times
- Mixing processes: Probably long term mixing of deeper, non-marine saline component by diffusion

Deep groundwaters at Simpevarp and Äspö (1000 m) are Na-Ca-Cl in type; deep groundwaters at Oskarshamn (KOV01; 1000 m) and at Laxemar (1700 m) are Ca-Na-Cl in type. Since Laxemar is inland and Oskarshamn is close to the coast, this could be an indication of very deep discharging groundwaters at Oskarshamn. Therefore, at greater depths below Simpevarp and Äspö than presently sampled, Ca-Na-Cl groundwaters might be expected..

8.3 Support for Littorina

The palaeoevolution of the Simpevarp area implies that a Littorina Sea component should be present in the groundwaters and this possibility has been discussed in section 7.7. Hard evidence (although good indications exist) is still lacking since the Littorina Sea component has been largely flushed out, or it has not been seen yet because of the limited number of boreholes. In the Simpevarp area it would seem that any penetration of Littorina Sea water would be restricted hydrogeologically to the upper 100-150 m, and therefore easily flushed out during land uplift and emergence from the Baltic Sea during isostatic rebound. Limited penetration of Littorina Sea water to greater depths probably has occurred, especially along the sub-vertical fractures and evidence of existing pockets and/or lenses may still be discovered by subsequent investigations.

9 References

Andersson, P., Byegård., J., Dershowitz, B., Doe, T., Hermanson, J., Meier, P., Tullborg, E.L. and Winberg, A., 2002. Final report of the TRUE Block Scale. 1. Characterisation and model development SKB Technical Report TR-02-13. ISSN 1404-0344.

Barth, S., 1993. Boron isotope variations in nature: A synthesis. Geol. Rundsch, 82, 640-641.

Bath, A., Milodowski, A., Ruotsalainen, P., Tullborg, E-L., Cortés Ruiz, A. and Aranyossy, J-F., 2000. Evidences from mineralogy and geochemistry for the evolution of groundwater systems during the quaternary for use in radioactive waste repository safety assessment (EQUIP project). EUR report EN 19613.

Bäckblom, G and Stanfors, R., 1989. Interdisciplinary study of post-glacial faulting in the Lansjärv area, northern Sweden. SKB Tech. Rep. (TR-89-31), SKB, Stockholm, Sweden.

Clark, I., Fritz, P., 1997. Environmental isotopes in hydrogeology. Lewis Publishers, New York.

Drake, H and Tullborg E-L., 2004. Fracture mineralogy – results from XRD, microscopy, SEM/EDS and stable isotopes analyses. SKB- P-report , in press.

Frape, S.K., Byrant, G. Blomqvist, R. and Ruskeeniemi, T., 1966. Evidence from stable chlorine isotopes for multiple sources of chloride in groundwaters from crystalline shield environments. In: Isotopes in Water Resources Management, 1966. IAEA-SM-336/24, Vol. 1, 19-30.

Gascoyne, M., 2004. Hydrogeochemistry, groundwater ages and sources of salts in a granitic batholith on the Canadian Shield, southeastern Manitoba. Appl. Geochem., 19, 4, 519-560.

Gimeno, M.J., Auqué, L.F. and Gómez, J.B., 2004. Simpevarp Hydrogeochemical Site Description Model v. 1.2, October (Submitted).

Gurban, I. and Laaksoharju, M., 2004. Simpevarp Hydrogeochemical Site Description Model v. 1.2, October (Submitted).

Hallbeck, L., 2004. Simpevarp Hydrogeochemical Site Description Model v. 1.2, October (Submitted).

Laaksoharju, M., Smellie, J., Nilsson, A-C. and Skårman, C., 1995. Groundwater sampling and chemical characterisation of the Laxemar deep borehole KLX02. SKB Tech. Rep. (TR-95-05), SKB, Stockholm, Sweden.

Landström, O. and Tullborg, E-L., 1995. Interactions of trace elements with fracture filling minerals from the Äspö Hars Rock laboratory. SKB Tech. Rep. (TR-95-13), SKB, Stockholm, Sweden.

Landström, O., Tullborg, E-L., Eriksson, G. and Sandell, Y. 2001. Effects of glacial/post-glacial weathering compared with hydrothermal alteration - implications for matrix diffusion. SKB Tech. Report (R-01-37), SKB, Stockholm, Sweden.

Pitkänen, P., Luukkonen, A., Ruotsalainen, P., Leino-Forsman, H. and Vuorinen, U., 1999. Geochemical modelling of groundwater evolution and residence time at the Olkiluoto site. Posiva Tech Rep. (98-10), Posiva, Helsinki, Finland.

Pitkänen, P., Partamies, S. and Luukkonen, A., 2004. hydrogeochemical interpretation of baseline groundwater conditions at the Olkiluoto site. Posiva Tech. Rep. (2003-07), Posiva, Helsinki, Sweden.

Munier, R., 1993. Segmentation, fragmentation and jostling of the Baltic shield with time. Thesis, Acta Universitatus Upsaliensis 37.

O´Neil, J.R., Clayton, R.N. and Mayeda, T.K., 1969. Oxygen isotope fractionation in divalent metal carbonates. J. Chem. Phys. 51, 5547-5558.

Smellie, J.A.T., Larsson, N-Å., Wikberg, P. and Carlsson, L., 1985. Hydrochemical investigations in crystalline bedrock in relation to existing hydraulic conditions: Experience from the SKB test-sites in Sweden. SKB Tech. Rep. (TR-85-11), SKB, Stockholm, Sweden.

Smellie, J.A.T., Larsson, N-Å., Wikberg, P., Puigdomenech, I. and Tullborg, E-L., 1987.

Hydrochemical investigations in crystalline bedrock in relation to existing hydraulic conditions: Klipperås test-site, Småland, southern Sweden. SKB Tech. Rep. (TR-87-21), SKB, Stockholm, Sweden.

Smellie, J.A.T. and Wikberg, P., 1989. Hydrochemical investigations at the Finnsjön site, central Sweden. J. Hydrol., 126, 147-169.

Smellie, J. and Laaksoharju, M., 1992. The Äspö Hard Rock Laboratory: Final evaluation of the hydrogeochemical pre-investigations in relation to existing geological and hydraulic conditions. SKB Tech. Rep. (TR-92-31), SKB, Stockholm, Sweden.

Stanfors, R., Rhén, I., Tullborg, E-L. and Wikberg, P., 1999. Overview of geological and hydrogeological conditions of the Äspö Hard Rock laboratory site. App. Geochem., 14, 819-834.

Tullborg, E-L., 1997. Recognition of low temperature processes in the Fennoscandian shield. Ph D Thesis, Earth Science Centre A17, Göteborg University, ISSN 1400-3813. 35 pp.

Tullborg, E-L., 2004. Palaeohydrogeological evidence from fracture filling minerals: Results from the Äspö/Laxemar area. Mat. Res.Soc. Symp. Vol 807, 873-878.

Wallin, B. and Peterman, Z., 1999. Calcite fracture fillings as indicators of palaeohydrogeology at Laxemar at the Äspö Hard Rock Laboratory, southern Sweden. App. Geochem, 14, 953-962.

Appendix 1: Fracture filling studies

Results from XRD analyses

Samples for XRD identification have been sampled mainly from open and usually water conducting fractures containing friable clayish coatings, often of fault gouge type. The fine fraction from each sample was separated and oriented samples on glass were prepared for clay mineral identification. All the fractures sampled belong to the uppermost 600 metres of borehole KSH01A+B; at greater depths the borehole is characterised by very low hydraulic conductivities and a low frequency of originally open fractures.

Most of the samples contain quartz, K-feldspar and albite in addition to calcite, chlorite and clay minerals (Table 1-1). From earlier identifications of open fractures at Äspö (e.g. within the TRUE experiment sites) it is known that altered rock fragments dominate the gouge material (Andersson et al., 2002). It is therefore probable that most of the quartz and feldspar, together with the few observations of amphibole and biotite, belong to these rock fragments even though contamination due to incorporation of material from the wall rock can not be ruled out. The total clay mineral content in the open fractures is very difficult to determine satisfactorily and the XRD analyses should not be regarded as necessarily representative for the entire fracture filling but rather for the specific sample analysed. In fractures filled with fault gouge a reasonable estimate is, however, that the amount of clay minerals (excluding chlorite) usually does not exceed 10-20 weight %. Thin coatings attached to the fracture wall can consist of 90-100% chlorite and clay minerals. The amounts are relatively small as these coatings are usually thin (<100 μm) but their surface can be very large (cf. SEM photo of mixed-layer clay coating (Fig. 1-1).

Minerals constituting less than 5-10% may not be detected. This, however, means that haematite and pyrite, for example, which have been detected in some of the XRD samples, are likely to be present in several of the other samples as well.

Smectite, a clay mineral with significant swelling properties, has been identified in three of the samples (at 3.7 m, 24 m and 289.8 m).

Results from microscopy and SEM studies

The fractures sampled for microscopy comprise open as well as sealed fractures from the entire borehole with the main focus on the uppermost 600 metres. All sample descriptions and results from SEM/EDS analyses of different fracture minerals are compiled in Drake and Tullborg (2004; in press). The aim of the microscopy, in addition to identification of minerals, has been to establish the different mineral parageneses and to study primarily chlorite and calcite.

Figure 1.1: *Drillcore sample KSH01A:603,11 m showing prehnite in a sealed fracture cut by discordant calcite fillings. Note the red staining and chloritisation of the wall rock.*

Blue line shows location of thin section.

Table 1.1: XRD analyses of fracture material from open fractures in borehole KSH01A+B (Analyses carried out by SGU, Uppsala)

Sample **Core length**	**Qtz**	**K-fsp**	**Alb**	**Ca**	**Chl**	**Py**	**Hem**	**Amp**	**Bi**	**Pre**	**Epi**	**Apo**	**Clay**	***Corr***	***M-I*** ***Clay***	***Ill***	***Smec***
3,7-3,87	x			xxx	(x)								xx	yy'			y
24,0	xx	xx	x		x	x		x					x				yy
67,8-67,9	xx	xx	xx	x	xx								x		yy	(y)	
81,35	xx	xx	xx	x	x								x		y	yy	
82,2	xx	xx	xx	x	xx								x		yy	y	
95,0		xx	xx	xxx	x			x			x		x	y	y	(y)	
130,83	xx		x	xxx	x			x					(x)*				
159,20 m (I)	xx	x	x	xxx	xx			x					x	yy			
159,20 m (II)	xx	xx	x	xx	xxx			X					xx*			y	
178,25-178,35			xx	xx	x							xxx	x	yy			
249,0	x	x	x	xx	x								(x)*				
250,4	xx	xx		x	xx		x						(x)			(y)	
255,78-255,93	xx	xx		x	xx		x						X	yy'			
259,3	xx	xx		xx	xx		x										

													X		YY	Y	
267,97-268,02	xx	xx		Xx	xx		x						XX	YY			
289,8-289,95	xx	xx			xxx								X				YY
290,9	xx	x	xxx	xx	xx								X	YY			
306,77	x	x	x	xxx	x								X	YY			
325,93	xx		x		x				xx			xx	X	YY			
447,34	xx	x			xx					xx	x	xx	X	YY			
514.46	xx			xx	xx								X	Y	YY		
558,60-558,65	xx	xx		x	xx		x						X	YY			
590,35-590,52	xx	xx	xx		xx								X		Y	YY	

Qz=quartz, K-flsp=K-feldspar usually adularia, Alb =Na-plagioclase (albite), Chl= chlorite, Py=pyrite, Hem=hematite

Amp=amphibole, Bi =biotite, Pre=prehnite, Ep=epidote, Apo=apophyllite, Clay = presence of clay minerals indicated in the random oriented sample, the clay minerals are identified in fine fraction oriented sample, results are marked with y.

xxx = dominates the sample, xx= significant component, x= minor component, OBS this is only semi-quantitative.

Corrensite = swelling mixed layer clay with chlorite/smectite or chlorite/vermiculite regularly interlayered, M-l clay = mixed layer clay with illite/smectite layers, ill = illite, Smec= smectite *= indicates swelling chlorite, ‘ =indicates corrensite without 1:1 layering.

yy= dominating clay mineral in the fine fraction, y = identified clay mineral in the fine fraction.

( ) = potentially present

* = swelling chlorite

Appendix 2: Accompanying document to recommended (representative) modelling groundwater compositions for Simpevarp and the POM sites

The Simpevarp table of groundwater compositions presented below, together with some of the POM (***P***latsundersökningar i ***O***skarsha***M***n) sites, was evaluated to derive a standard set of groundwater chemical data for modelling purposes. The evaluation was based on several criteria:

- As near a complete set of major ion analytical data
- As near a complete set of isotope data (particularly tritium contents)
- Charge balance
- Drilling water content
- Intimate knowledge of the investigated sites

Below is the tabulated list of chosen borehole sections. Note the following:

- A charge balance of ±5% was considered acceptable. In some cases groundwaters were chosen when exceeding this range to provide a more representative selection of groundwaters. These groundwaters should therefore be treated with some caution when used in the modelling exercises..
- In many cases the drilling water content was either not recorded or not measured (denoted by ‘nd’). Acceptable (i.e. OK) refers to less than 1% drilling water. In some cases groundwaters were chosen when exceeding this range to provide a more representative selection of groundwaters. These groundwaters should therefore be treated with some caution when used in the modelling exercises.
- Some of the tritium data was analysed with a lower detection limit of 8TU; below this limited is indicated by < 8TU. Other references to ‘< detection’ refer to much more accurate analyses where the detection limit lies around 0.02TU. In some places an approximate value is suggested in parenthesis since no recorded value was available.
- Tube samples are indicated with a blue background in the table.
- Samples determined as being less representative (i.e. excessive drilling water component and/or incomplete tritium data), and should be used therefore with some caution, are highlighted in green.

Borehole	Sample No.	Borehole section (m)	Charge balance error (%)	Drilling water content (%)	Tritium content (TU)
Laxemar					
HLX10	3904	0-200	OK	OK	7.2
KLX01	1537	272-277	OK	4.60	< 8
	1528	456-461	OK	13.70	< 8
	1516	680-702	OK	2.60	< 8
	1633	680-702	OK	1.99	< 8
	1761	830-841	OK	OK	nd
	1773	910-921	OK	OK	nd
	1774	910-921	OK	OK	nd
	1785	999-1078	OK	1.84	nd
KLX02	2406	0-50	OK	nd	nd (~8.5)
	-1	81-131	6.86	nd	nd
	-1	131-181	6.25	nd	11.8
	-1	181-231	5.94	nd	15.2
	-1	231-281	6.19	nd	12.7
	-1	281-331	5.95	nd	5.1
	2738	315-321.5	OK	OK	nd (~10.0)
	2705	335-340.8	OK	OK	nd
	2421	400-450	OK	nd	nd (~8.0)
	2424	500-550	OK	nd	10.0
	-1	581-631	7.67	nd	8.4
	2427	700-750	2.37	nd	10.0
	-1	731-781	5.42	nd	19.4

	2712	798-803.2	OK	OK	nd (~15.0)
	-1	831-881	OK	nd	12.7
	-1	931-981	OK	nd	13.5
	-1	981-1031	OK	nd	11.0
	-1	1031-1081	OK	nd	10.1
	2722	1090-1096	OK	nd	nd (~15.0)
	-1	1131-1181	OK	nd	0.23
	2934	1155-1165	OK	nd	2.5
	-1	1181-1231	OK	nd	< detection
	-1	1231-1281	OK	nd	< detection
	-1	1281-1331	OK	nd	< detection
	2931	1345-1355	OK	nd	< detection
	-1	1331-1381	OK	nd	< detection
	-1	1381-1431	OK	nd	< detection
	-1	1431-1481	OK	nd	< detection
	-1	1481-1506	OK	nd	< detection
	-1	1531-1581	OK	nd	< detection
	2731	1420-1705	OK	OK	< detection
Simpevarp					
HSH02	3886	0-200	OK	nd	11.0
HSH03	5858	0-200	OK	OK	7.5
KSH01A	5263	156-167	OK	2.39	0.8
	5268	245-261.5	OK	8.02	0.8
	5288	548-565	OK	10.74	1.1
KSH02	5653	91-141	OK	2.35	10.0

	5655	191-241	OK	5.88	8.6
	5810	419-424	OK	1.48	< 8
	5856	575-580	OK	OK	< 8
KSH03	5801	0-100.6	OK	nd	8.8
Precipitation	6005	-	OK	-	14.8
Äspö					
HAS02	2	44-93	OK	nd	1.0
HAS03	2	48-100	OK	nd	35
HAS05	1	40-100	OK	nd	24
HAS07	2	71-100	OK	nd	1.0
HAS13	1622	0-100	OK	nd	1.2
KAS02	1548	202-214	OK	OK	0.3
	1474	308-344	OK	OK	8.0
	1433	530-535	OK	OK	0.5
	1560	860-924.04	OK	OK	0.9
KAS03	1569	129-134	OK	OK	0.1
	1437	196-222	OK	nd	< 8
	1448	248-251	OK	OK	< 8
	1441	347-373	OK	OK	< 8
	1445	453-480	OK	2.13	< 8
	1452	609-623	OK	2.23	< 8
	1582	860-1002.06	OK	OK	0.82

KAS04	1603	334-343	OK	OK	0.5
	1588	440-480.98	OK	OK	0.03
KAS06	1606	204-277	OK	OK	3.8
	1610	304-377	OK	OK	0.3
	1614	389-406	OK	OK	0.6
	1618	439-602.17	OK	OK	3.5
Ävrö					
HAV04	2	35-100	OK	nd	< detection
HAV05	2	50-100	OK	nd	< detection
HAV06	2	73-100	OK	nd	< detection
HAV10	2	69-100	OK	nd	< detection
KAV01	1374	558-563	OK	nd	8
	1354	635-743.6	OK	nd	< detection
KAV04A	5909	0-100.2	OK	OK	2.8

Appendix 3: Examples of groundwater samples which do not meet the criteria for representativeness in the Nordic Table

Row	Sample	Lack of major ions	Lack of ^{18}O /D	Salinity variation	Lack of time series	Early or 'First Strike' importance	Miscellaneous
4	?			?	X	X	44-93m
6	?			?	X	X	48-100m
8	?	Br		?	X	X	45-100m
10	?	Br		?	X	X	40-100m
12	?			?	X	X	71-100m
14	1620			?	X	X	0-100m
142	1606			X			
162	2279			?	X	X	0-2.5m
204	3814			?	X	X	6-32.5m
208	?	Br		?	X	X	5.8-25m
230	2894			?	X	X	0-15m
241	3453			?	X	X	1-3.6m
244	1800			?	X	X	40-90m
308	2139	Br					
318	2179	Br					
377	6215			?	X	X	?m
381	3740	Br					
389	2614			?	X	X	52-54m
402	2984			?	X	X	111-138m
418	2291			?	X	X	0-37.27m
427	2874			X			187-190m
444	3858			?	X	X	236-241m
454	2517		X	?	X	X	0-8.52m
458	2677		X				8.69-9.34m
466	2297			?	X	X	0-15.8m
484	2300			?	X	X	36.93-37.93m

Row	Sample	Lack of major ions	Lack of ^{18}O /D	Salinity variation	Lack of time-series	Early or 'First Strike' importance	Miscellaneous
497	2302			?	X	X	8.56-15.06m
500	3049			?	X	X	0-10,4m
509	6010		X	?	X	X	7.5-13m
519	2342			?	X	X	6.55-27.05mm
521	2303			?	X	X	28.05-29.55m
526	2304			?	X	X	22.51-25.51m
543	2247			?	X	X	165-180m
544	2248			?	X	X	193.9-208.9m
570	2594			?	X	X	15-18m
576	2588			?	X	X	15-18m
580	2592			?	X	X	21-24m
589	2595			?	X	X	5-6m
599	2579			?	X	X	11-12m
609	2886			?	X	X	12.3-19.8m
623	2928			?	X	X	1.3-5.3m
634	2619			X		X	18-40m
640	2575			?	X	X	1-3m
641	2578			?	X	X	8-9m
645	2889			?	X	X	8.3-16.3m
647	2892			?	X	X	17.3-22.3m
651	2908			?	X	X	1.3-7.3m
654	2514			X		X	4.5-21m
662	2622			X	X	X	22-50m
668	3463			X	X	X	43-50.1m
672	?			X	X	X	202-214.5m
682	?	Br		?	X	X	314-319m
683	?	Br		?	X	X	463-468m
684	?	Br		?	X	X	530-535m
685	?	Br		?	X	X	802-924.04m
697	1990	Br					309-345m
714	1989	Br					800-854m

Row	Sample	Lack of major ions	Lack of ^{18}O /D	Salinity variation	Lack of time-series	Early or 'First Strike' importance	Miscellaneous
716	?	Br		?	X	X	860-924.04m
721	?	Br		?	X	X	129-134m
737	?	Br		?	X	X	196-222m
738	?	Br		?	X	X	248-251m
739	?	Br		?	X	X	347-373m
740	?	Br		?	X	X	453-480m
741	?	Br		?	X	X	609-623m
742	?	Br		?	X	X	690-1002.06m
752	1913	Br					533-626m
770	?	Br		?	X	X	860-1002.06m
777	?	Br		?	X	X	226-235m
782	?	Br		?	X	X	334-343m
791	1999	Br					332-392m
792	?	Br		?	X	X	440-480.98m
800	1659	Br					320-380m
812	1660	Br					440-549.6m
818	1688	Br		?	X	X	191-249m
820	?	Br		?	X	X	204-277m
825	?	Br		?	X	X	304-377m
826	?	Br		?	X	X	389-406m
833	1687	Br					431-500m
835	?	Br		?	X	X	439-602.17m
836	?	Br		?	X	X	191-290m
844	1690	Br					191-290m
913	1906	Br	X				47-64m
917	1894	Br	X				153-183m
930	1878	Br	X				278-329m
933	?	Br	X				151-190m
941	1903	Br					191-220m
947	1923	Br					131-138m
953	1927	Br					147-175m

Row	Sample	Lack of major ions	Lack of ^{18}O /D	Salinity variation	Lack of time-series	Early or 'First Strike' importance	Miscellaneous
977	3678			?	X	X	8.85-9.55m
983-990				?	X	X	10-33m
996-1008				?	X	X	5-54.69m
1112	3835			?	X	X	100.25-134.15m
1123	3845			?	X	X	59.58-65.58m
1124	3846			?	X	X	66.58-74.08m
1128	3848			?	X	X	89.08-92.58m
1134	2832			?	X	X	0-17.26m
1137	3153			?	X	X	12.64-12.84m
1142	3155			?	X	X	43.7-43.9m
1147	3157			?	X	X	15-21.42m
1151	3156			?	X	X	9.23-9.43m
1255	6181	X					7.05-16.94m
1423	2347			X	X	X	11.55-13.55m
1425	2348			X		X	14.55-15.55m
1435	2346			X	X	X	8.92-11.42m
1470	2345			?	X	X	11.92-13.92m
1474	2340			X	X	X	14.92-23.42m
1482	3677			?	X	X	9.61-9.81m
1498	2369	Br	X				3-90.48m
1926	?		X				5.7-19.3m
1939	?		X	?	X	X	5.8-20m
1945	?	Br	X	?	X	X	6-19m
1961	?	Br		X		X	6-19.8m
1969	?	Br	X	X	X	X	5.7-19m
1992	?	Br		?	X	X	1-19.8m
2001	?			X		X	5-19.7m
2007	?	Br		?	X	X	1-10.5m
2028	?	Br		?	X	X	6-20m
2030	?	Br		?	X	X	6-20.3m
2032	?	Br		?	X	X	4.5-20m

Row	Sample	Lack of major ions	Lack of ^{18}O /D	Salinity variation	Lack of time-series	Early or 'First Strike' importance	Miscellaneous
2036	?	Br		?	X	X	6-19m
2038	?	Br		?	X	X	6-19.9
2039	?	Br		?	X	X	6-20m
2129	?	Br		X			6-20.5m
2182	2023			?	X	X	6-20.3m
2184	?	Br		?	X	X	0-20.3m
2188	2052			X			6-50m
2216	2025			X	X	X	6-20m
2219	?			X		X	5.9-19.2m 3.57% Drilling
2254	?			?	X	X	0-20m
2255	?			?	X	X	3.6-20.20m
2256	?	Br	X	?	X	X	3.7-19.8m
2257	?	Br	X	?	X	X	0-40m
2258	3796			?	X	X	1.35-38.7m
2262	2173			X		X	6-38.7m
2278	?	Br		?	X	X	0-19.9m
2279	2202	Br		?	X	X	5.9-20m
2280	?	Br		?	X	X	6-20.4m
2282	2244			?	X	X	5.8-20m
2283	?	Br	X	?	X	X	5.8-20m
2285	2175			?	X	X	5.7-19.8m
2291	2199			?	X	X	5.8-20m
2292	2242			?	X	X	5.8-20m
2313	2245			X	X	X	5-20m
2315	2246			X	X	X	6-19.4m
2320	2227			X	X	X	5.9-20m
2324	2240			X	X	X	5.7-20m
2333	2327			X		X	5.7-20m
2343	2219			?	X	X	6-20.4m
2344	2220			?	X	X	5.8-18.85m
2347	2222			?	X	X	6-20.4m

Row	Sample	Lack of major ions	Lack of ^{18}O /D	Salinity variation	Lack of time-series	Early or 'First Strike' importance	Miscellaneous
2348	2221			?	X	X	5.8-20.4m
2349	2215			?	X	X	5.7-21.8m
2350	2216			?	X	X	5.6-17.3m
2352	2237			?	X	X	5.7-19.6m
2354	2238			?	X	X	5.8-20.3m
2358	2218			?	X	X	5.7-20.3m
2359	2211			?	X	X	6-20.3m
2362	2212			?	X	X	5.9-19.8m
2030	?	Br		?	X	X	6-20.3m
2032	?	Br		?	X	X	4.5-20m
2036	?	Br		?	X	X	6-19m
2038	?	Br		?	X	X	6-19.9
2039	?	Br		?	X	X	6-20m
2129	?	Br		X			6-20.5m
2182	2023			?	X	X	6-20.3m
2184	?	Br		?	X	X	0-20.3m
2188	2052			X			6-50m
2216	2025			X	X	X	6-20m
2219	?			X		X	5.9-19.2m 3.57% Drilling
2254	?			?	X	X	0-20m
2255	?			?	X	X	3.6-20.20m
2256	?	Br	X	?	X	X	3.7-19.8m
2257	?	Br	X	?	X	X	0-40m
2258	3796			?	X	X	1.35-38.7m
2262	2173			X		X	6-38.7m
2278	?	Br		?	X	X	0-19.9m
2279	2202	Br		?	X	X	5.9-20m
2280	?	Br		?	X	X	6-20.4m
2282	2244			?	X	X	5.8-20m
2283	?	Br	X	?	X	X	5.8-20m
2285	2175			?	X	X	5.7-19.8m

Row	Sample	Lack of major ions	Lack of ^{18}O /D	Salinity variation	Lack of time-series	Early or 'First Strike' importance	Miscellaneous
2291	2199			?	X	X	5.8-20m
2292	2242			?	X	X	5.8-20m
2313	2245			X	X	X	5-20m
2315	2246			X	X	X	6-19.4m
2320	2227			X	X	X	5.9-20m
2324	2240			X	X	X	5.7-20m
2333	2327			X		X	5.7-20m
2343	2219			?	X	X	6-20.4m
2344	2220			?	X	X	5.8-18.85m
2347	2222			?	X	X	6-20.4m
2348	2221			?	X	X	5.8-20.4m
2349	2215			?	X	X	5.7-21.8m
2350	2216			?	X	X	5.6-17.3m
2352	2237			?	X	X	5.7-19.6m
2354	2238			?	X	X	5.8-20.3m
2358	2218			?	X	X	5.7-20.3m
2359	2211			?	X	X	6-20.3m

Appendix 2: Explorative analyses of Carbon signatures

Contribution to the model version 1.2

Gunnar Buckau

Institute for Nuclear Waste Disposal

Research Center Karlsruhe

November 2004

Table of contents

1. Introduction

The HAG program makes use of complementary approaches for determination of the past, present and future hydrological situation at Swedish candidate sites. The use of complementary approaches is the basis for providing trust in the overall outcome. The program furthermore deduces information about key geochemical processes. Understanding of such processes will be important if the aquifer system in the disposal far-field will be part of the long-term safety barrier system.

The hydrological modeling is based on combining physical modeling (pressure gradients and permeability distribution) with (isotope-)geochemical identification of end-members and their respective contributions at given (sampling) positions. Different physical modeling approaches are used. Determination of the end-members (groundwater contributors) is based on principle component analysis (PCA) of a large number of groundwater data from different Nordic aquifer systems. These different principle components (groundwater contributors) reflect actual past and present contributors.

The present contribution deals with interpretation of the carbon inventory in such systems. Interpretation of the carbon inventory and how this inventory has evolved contributes to understanding of the nature of the principle groundwater contributors, key geochemical processes and possibly in some cases to the origin and age of the contributors. The work thus aims at contributing to provision of trust in the hydrological interpretation and determination of key geochemical processes.

2. General objectives

The general objectives of the HAG program is to provide trustworthy description of the past, present and future hydrological situation at Swedish candidate sites, and to provide information on key geochemical processes. It should also provide information about the geochemical response to disturbances from repository construction, operation and closure, as well as potential release of both waste and engineered structure material from the repository near-field to the far-field (aquifer system).

3. Objectives of the present contribution

The objectives of the present contribution are (i) to provide a methodology for interpretation of the groundwater carbon inventory, (ii) to provide tools for extending the database by relevant carbon inventory descriptors, and (iii) to outline future activities. For this purpose a limited number of groundwater samples from Äspö and Ävrö are investigated.

4. Approach

Data from eight Äspö and Ävrö groundwater samples are evaluated primarily with respect to their carbon inventories. Isotopic data ($^{18}O/D$ and tritium) of the groundwater matrix are also used as supporting information. The limited number of data allows for evaluation in some detail of individual groundwater points. A broad input for hydrological modeling is not provided, however, the limited number of results support an emerging overall picture of rapid groundwater mixing also at considerable depth.

The carbon inventory is analyzed from the viewpoint of different sources/recharge conditions. Some indicators for important geochemical reactions are used.

The basic approach is to assume that there is one recharge source where the carbon inventory is diluted by carbonate dissolution along a flow/mixing regime. As shown by the data, this is not the case, but rather mixing of different sources should be considered. However, not only compliance with but also deviation from this simple approach/picture, allows drawing some important conclusions.

5. Data used

Data for the eight groundwater samples are extracted from the HAG groundwater database. The data are given in Table 1. In some cases, recalculation of original data and estimation is used (cf. below).

Table 1: Data used for Äspö and Ävrö waters

Samples	Origin	Depth (m)	pH	DIC (mmol/L)	C-13 (permil)	DIC biogenic (mmol/L)	C-14 (pmc)	DOC (mgC/L)	Tritium (TU)
KAS02	Äspö	-466	8.2	0.41	-6.5	0.099	18.59	3	8
KAS03	Äspö	-209	7.7	0.89	-13.6	0.448	7.25	1	8
KAS03	Äspö	-250	8	0.87	-15.1	0.487	8.80	<0.5	8
KAV01	Ävrö	-423	6.8	4.07	-20.7	3.12	68.48	9.6	19
KAV01	Ävrö	-527	7	1.56	-20.4	1.19	65.76		13
KAV01	Ävrö	-561	7.2	0.77	-20.2	0.576	50.95		8
KAV04A	Ävrö	-50	8.4	4.05	-18	2.7	47.61		2.8

Depth is calculated as average from accessible length in borehole.

^{14}C is calculated from the age given in the original table (^{14}C age relative to 100 pmc (percent modern carbon)).

DIC: Dissolved inorganic carbon. The data provided only contain bicarbonate but not other dissolved carbonate species. A rough estimate of contributions from H_2CO_3 is used at pH below 7.7. Between pH 7.7 and 8.4, DIC is set to be equal with the bicarbonate concentration. For a better evaluation, calculation of the different dissolved carbonate species by exact correction of ionic strength etc., would be preferable. This is especially true for calculation of

DIC biogenic for the water samples from the other systems, including evaluation of the ^{14}C concentration of the biogenic DIC inventory. During the HAG meeting 16-17 August it was decided to calculate and add to the database the ionic strength corrected DIC inventory with its contributors.

DIC(biogenic) or $DIC_{biogenic}$: This refers to the calculated amount of DIC with a ^{13}C content of –27 ‰ (rel. PDB) (plant material from the C-3 plant cycle) assuming that (i) the residual amount of DIC originates from dissolution of calcite of marine origin (with a ^{13}C content of zero (rel. PDB)) and without additional isotope fractionation processes. This is an oversimplification and thus $DIC_{biogenic}$ should be understood as an operational term as described.

6. DIC versus pH

In general, the starting point for the DIC inventory is plant material from the C-3 plant cycle. The DIC inventory in recharge from the soil zone is dominated by "soil gas", i.e. dissolved carbon dioxide and associated species at pH in the order of around 5. Along with residence in the aquifer system, carbonate minerals are dissolved and pH is increasing. The carbonate minerals of marine origin have a ^{13}C value of around zero (reference value). If the dominating acid-base process is dissolution of carbonate minerals by carbonic acid from soil-CO_2, the ^{13}C value will decrease from –27 ‰ to a 50/50 mixture with a ^{13}C value of around –13.5 ‰. The dissolution of marine carbonate takes place already at low depth and thus direct measurement of dissolved soil CO_2 is seldom possible even in shallow groundwater.

Based on this simple picture, and if other processes are of subordinate magnitude, the recharge groundwater with somewhere around pH 5 experiences an increase in the DIC inventory in association with progressive increase in pH. The process stops as ^{13}C has reached a value of around –13.5 ‰. This simple evolution of the carbonate inventory of groundwater is not found in the Äspö and Ävrö waters.

The evolution of ^{13}C and pH for Äspö and Ävrö waters is shown in Fig. 1. One could imagine a simple evolution of the sequence KAV01 (423 m), KAV01 (527 m), KAV01 (561 m) to KAS03 (209 and 250 m). KAV04 must have a very different origin or be severely affected by geochemical reactions. As it turns out, this water at around 50 m depth is probable strongly influenced by discharge of old groundwater. KAS02 (426 m) has a ^{13}C value significantly below –13.5 ‰ and thus must be subject to considerable influence of geochemical reactions, especially carbonate sediment dissolution from acid generating reactions (for example microbial sulfate reduction).

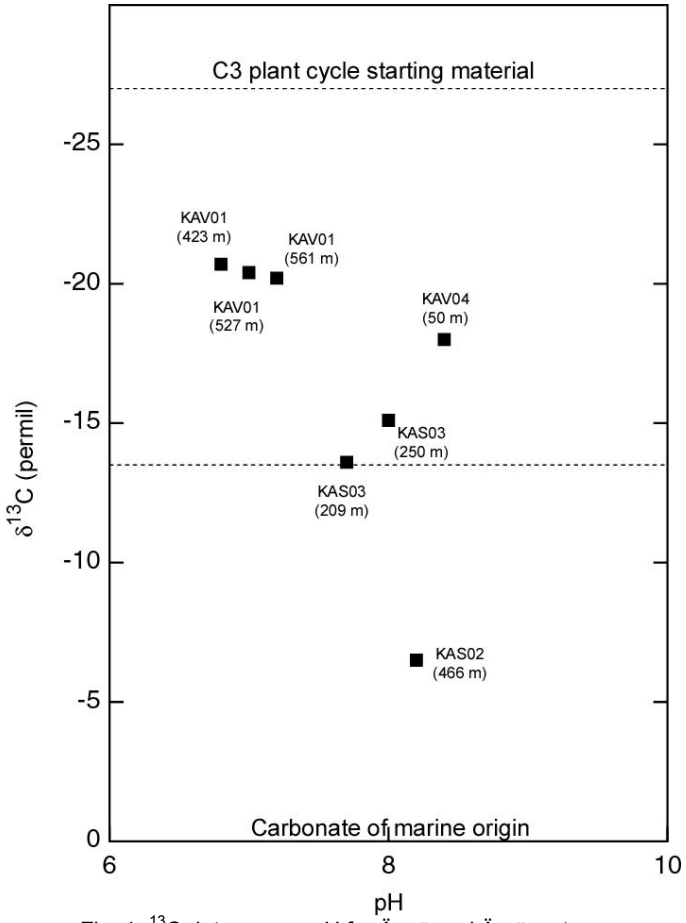

Fig. 1: ^{13}C data versus pH for Äspö and Ävrö waters

7. DIC inventory and ^{13}C

Groundwater can be grouped by differences in the concentration of biogenic DIC, especially from recharge where plant originating organic matter is not present in the sediments (such as brown coal in some sandy sediments). For this purpose, the DIC concentration is plotted against the ^{13}C values. As DIC is dissolved in the groundwater regime, assuming exclusive origin in marine sediments, the mixing of recharge DIC (DIC biogenic, soil gas from plant material) and DIC with zero ^{13}C value (marine carbonate sediments) results in the ^{13}C value approaching that of marine sediments with increasing dissolution. The principle evolution is shown in Fig. 2.

The figure shows, that KAS02 (466 m) has a very low DIC biogenic source term or has lost DIC by, for example precipitation or methane generation. In the case of methane generation, the DIC concentration decreases along with a lowering in the negative ^{13}C value (i.e. the depletion in ^{13}C to ^{12}C relative to a reference is decreasing, or in other words, the ^{13}C content in the residual DIC inventory is increasing). The reason for the latter is microbial preference for ^{12}C. It furthermore shows that despite geochemical resemblance in the sequence KAV01 (423, 527 and 561 m) and KAS03 (208 and 250 m), only KAV01 (561 m) and the two KAS03 waters can have a comparable DIC biogenic source term. As already noticed in Fig. 1,

KAV04 probably deviates from the other ones (or has a similar origin as KAV01 (423 m) and remains at a high ^{13}C value due to lack in marine carbonate minerals or very slow dissolution kinetics.

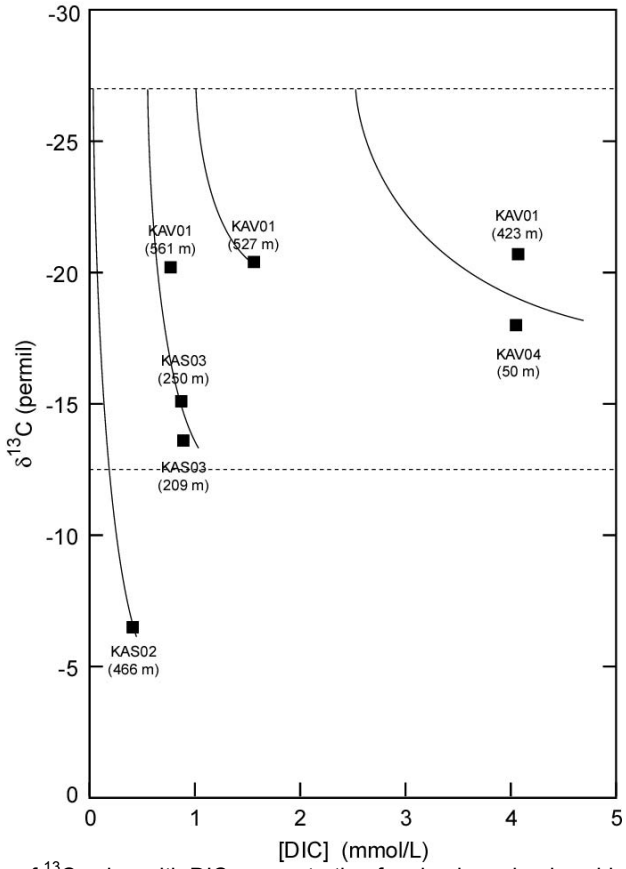

Fig. 2: Principle evolution of ^{13}C value with DIC concentration for simple carbonic acid neutralization by marine sediment dissolution.

In order to quantify the DIC biogenic source term, dilution of the biogenic inventory with DIC from marine sediments is either calculated by the mixing of the two DIC sources or by plotting the inverse of the DIC (total) inventory against the ^{13}C value. This does not mean that the basic approach of only two sources is held correct, but it is a tool for classification of the water. The calculated numbers are given in Table 1 and the graphical illustration is given in Fig. 3 (by extrapolation to –27 ‰) The waters do not group well together and thus either have very different origin/recharge conditions, have additional contributors and/or are subject to significant geochemical reactions.

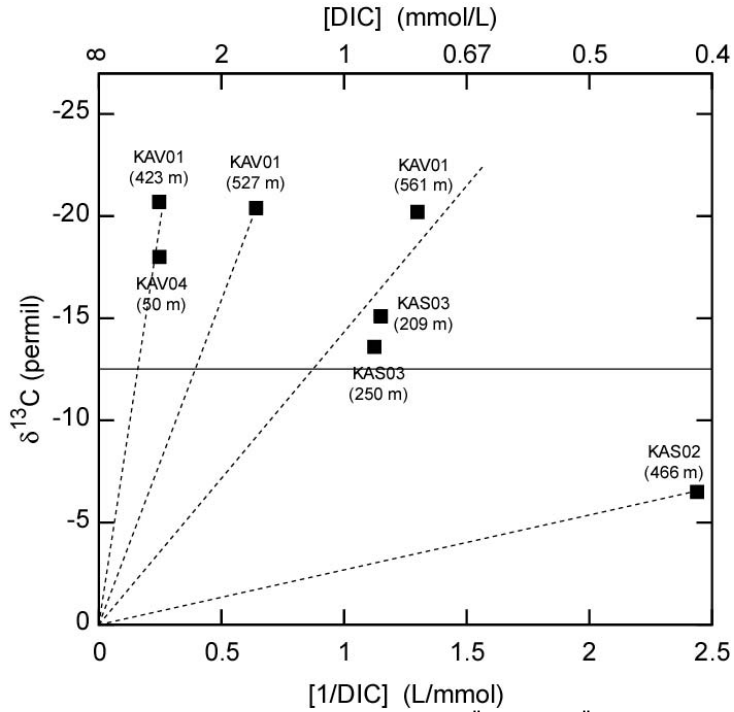

Fig. 3: Quantification of DIC biogenic (recharge source term) in Äspö and Ävrö waters using simplest mixing approach. The dotted lines represent one source term/origin with a ^{13}C value of zero for infinite dilution with marine carbonate dissolution and the DIC biogenic extrapolated to upper scale (^{13}C contributor of –27 ‰).

8. ^{14}C groundwater dating with ^{18}O/Deuterium content

Groundwater age is a discussion in itself. An age in a strict sense can only be given for an isolated flow path with no considerable mixing of groundwater of different origin. That hardly exists. Nevertheless, the ^{14}C inventory can be quantified and some conclusions can be drawn. The approach for quantification of the ^{14}C inventory goes in two steps. Step number one is to assume that ^{14}C is only found in DIC biogenic, i.e. from soil gas with recharge. For this purpose, the ^{14}C inventory is calculated as if ^{14}C originates exclusively from biogenic DIC (-27 ‰). The calculation is simply multiplication of the measured ^{14}C value by the fraction of DIC that is of biogenic origin.

The second step is to take regard for the elevation in ^{14}C as a consequence of nuclear atmospheric testing. This is shown in Fig. 4. With exception for KAS04 (209 and 250 m), all waters fall on a correlation indicating a common ^{14}C concentration of pre-nuclear atmospheric testing of 65±5 pmc. This number is very reasonable as can be seen from comparison with recharge groundwater from the Gorleben aquifer system (about 55 pmc). The ages given in the original Excel table are conventional ages based on a starting ^{14}C concentration of 100 pmc, with no relevance for actual groundwater age or age of a DIC inventory. The relatively shallow KAV04 shows a relatively small contributor of groundwater carrying tritium for nuclear atmospheric testing. This leads to the conclusion, that a main contribution originates from deeper regions discharging in this area. This is also in agreement with above finding that the DIC inventory shows deviation from a simple carbonic acid carbonate dissolution route.

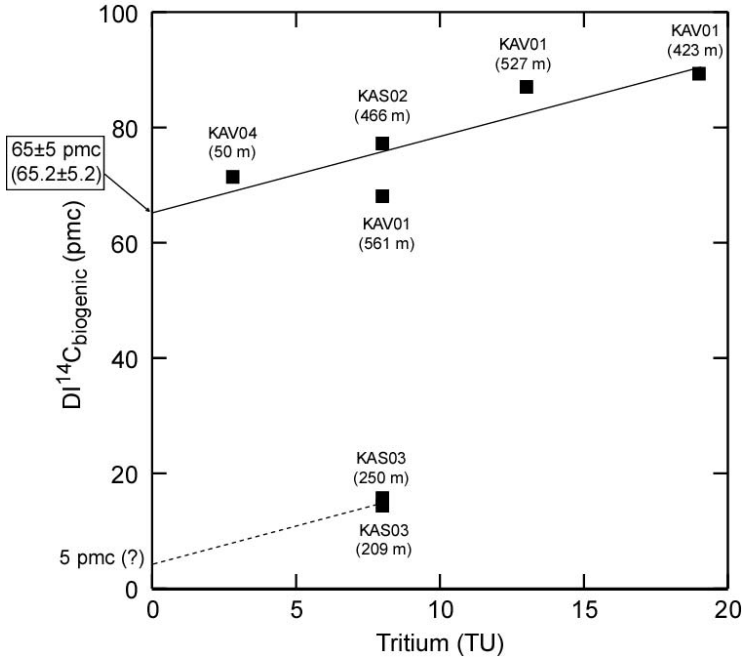

Fig. 4: Evaluation of ^{14}C source term prior to nuclear atmospheric testing. The pre-nuclear atmospheric testing source term for DIC biogenic is found to be 65±5 pmc, with exception for KAS03 (209 and 250 m) waters.

With respect to all waters except for the two KAS03, the conclusion is clear. The waters contain different fractions of very young groundwater (nuclear atmospheric testing tritium and associated elevation of ^{14}C). The residual Holocene contributors show different origin with respect to the concentrations of biogenic DIC and the dissolution of carbonate sediments (dilution of biogenic DIC inventory). Their DIC biogenic, however, show no significant ^{14}C decay and thus no significant age relative to the half-life of ^{14}C (5730 a). It is especially noteworthy, that KAS02 with its very small DIC biogenic origin shows the same ^{14}C concentration of this small biogenic DIC inventory as the other waters. In this context it must be underlined that the ^{14}C dating of DIC biogenic refers to the Holocene contributors. If other contributors have low overall DIC contributions, they will be overwhelmed by the DIC of Holocene recharge origin with its high DIC content from soil CO_2.

The question remaining is the ^{14}C inventory of the two KAS03 waters. These DIC inventories do not show a deviating behavior with respect to DIC concentration, ^{13}C value and the inventory of DIC biogenic (very comparable to KAV01 (561 m)). The approach of mixing of very recent tritium influenced DIC biogenic from recharge and another DIC biogenic contributor is visualized in Fig. 4. In this case the other DIC biogenic source should have a ^{14}C concentration of around 5 pmc. The problem with this number is that corresponds to an age of about 21.000 years. 21.00 years ago there was no soil and vegetation layer over the Äspö and Ävrö region. Consequently all assumptions used for calculating this number are invalid. The solution can be found in Fig. 5. The KAS03 waters are dominated by glacial water. The origin and isotopic composition of the glacial DIC inventory is not known. Therefore, ^{14}C values cannot be used for dating of the DIC inventory, and consequently also not for the groundwater. The reason that the DIC inventory can be dated for the other groundwater samples is that the glacial water DIC inventory is sufficiently low and thus mixing with glacial water does not

completely change the dominance of Holocene/soil CO_2 DIC inventory. This means that the groundwater KAS02 (466 m) and KAV01 (561 m) have at least three contributors, namely very young recharge (the fraction given by the respective tritium concentrations), Holocene contributors showing no significant ^{14}C decay (with large uncertainty) and Pleistocene contributors (given by the stable isotopes ^{18}O and deuterium).

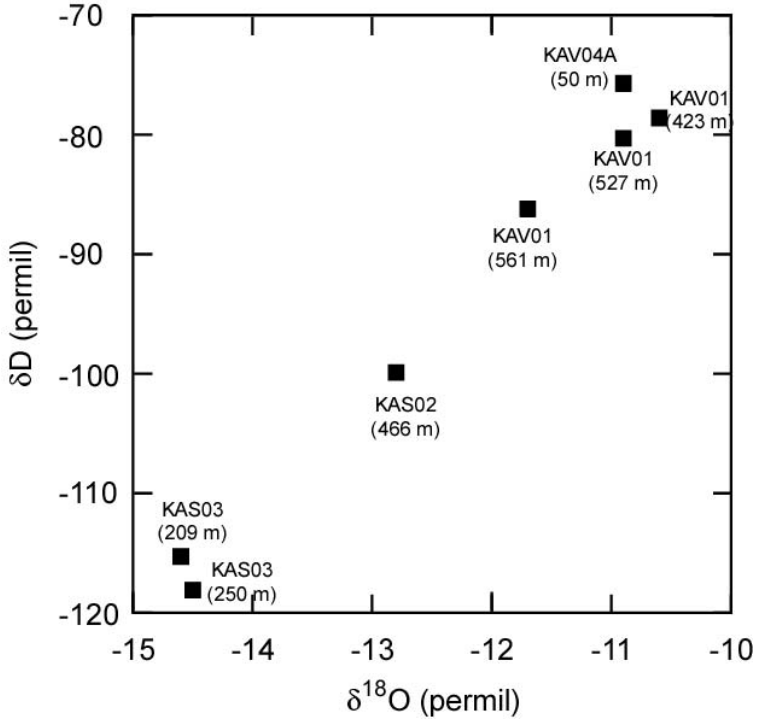

Fig. 5: Deuterium versus ^{18}O for Äspö and Ävrö waters.

9. Cogeneration of DOC and DIC biogenic.

DIC biogenic and DOC (especially the sum of humic and fulvic acid) correlate with each other. The reason is the common origin in microbial turnover of organic material. In Fig. 6, data for the present waters are shown. Unfortunately only few DOC data are available. Comparison with the Gorleben aquifer system shows the same order of magnitude in the dependency. Given that the relation for the Gorleben data are extracted by reading from a graphical representation, the agreement with the present waters is acceptable.

In principle, the data should go through the origin (with no microbial activity there is neither DIC biogenic nor DOC (humic and fulvic acid). The Gorleben data, however, show the potential for a rest term of DIC biogenic at zero DOC. Given the uncertainty in both the present and the Gorleben data, one may either lay a straight line through the origin or accept a rest term of DIC biogenic at zero DOC. The dependency of DIC biogenic co-generated with DOC is very similar between the two systems and thus relies on the same mechanism (microbial decomposition of organic source material). KAS02 (466 m) shows a ^{13}C value below –13.5 ‰ and thus is subject to acid generating processes. It also shows an exceptionally small

concentration of DIC biogenic. The other two values from glacial dominated waters and KAV01 (423 m), despite being very few data, resemble the relation found in Gorleben.

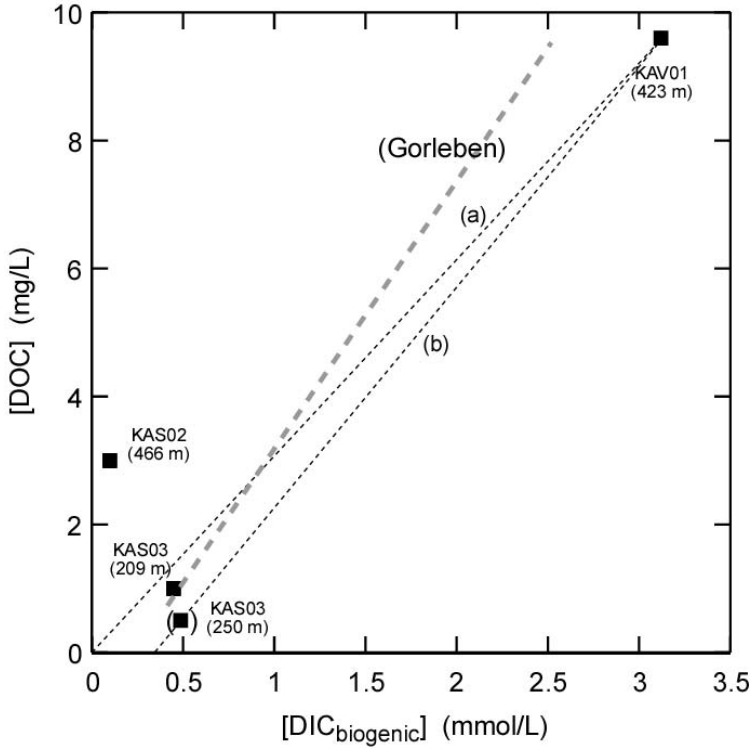

Fig. 6: Relation between DOC and DIC biogenic in Gorleben aquifer system and the Äspö and Ävrö waters. Two different lines are plotted for the Äspö/Ävrö data, namely (a) for strict relation between the two variables including going through the origin and (b) allowing for a rest term of DIC biogenic for zero DOC concentration. The value for KAS02 is not regarded for these correlation lines

10. Summary of results

Results may be summarized as shown in Table 2. As a reminder (cf. above) there is a clear difference between the age of the groundwater or rather mixing of different groundwater contributors of different age/origin on one hand and the age or mixing ratios of constituents in the groundwater. In simple terms, a groundwater may consist of 50/50 Holocene and Pleistocene water. Nevertheless, the DIC may be dominated by the Holocene contributor and thus show a more or less exclusively Holocene carbon signature, not representative for the entire groundwater body.

With exception for KAS02 (466 m), all waters show an expected basic behavior in the carbon inventory evolution. With exception for the glacial waters, the DIC inventory shows no significant ^{14}C decay. This is also in agreement with the considerable contributions of tritium. The in principal glacial waters KAS03 (209 and 250 m) show considerable intermixing with young tritium water. Dating of DIC inventory of glacial origin not possible because source term data are unknown. The lowest tritium content is found in the relatively surface near

KAV04 (around 50 m). The DIC inventory shows no significant ^{14}C decay. This is in agreement with a mixture of different contributors discharging in this area.

Table 2: Overview of results for Äspö and Ävrö waters

Samples	Origin	DIC and pH	DIC and C-13*	C-14 and O-18/D dating	DOC and DIC microbial co-generation
General comment		General trend as expected	Large differences in DIC biogenic	Consistent results (Precondition: Correction for Nuclear atmospheric testing)	General trend as in Gorleben aquifer system
KAS02 (466 m)	Äspö	Acid generating processes or vastly different origin	Exceptionally low DIC biogenic	More than half is of glacial origin; ^{14}C of DIC inventory is "typical Holocene"	Exceptionally high DOC or exceptionally low DIC ? (Methane generation (?))
KAS03 (209 m)	Äspö	O.K.	1	Glacial Very low C-14 of non-tritium dependent contributor	O.K.
KAS03 (250 m)	Äspö	O.K.	1	Glacial Very low C-14 of non-tritium dependent contributor	(O.K.)
KAV01 (423 m)	Ävrö	O.K.	2	"Typical Holocene"	O.K.
KAV01 (527 m)	Ävrö	O.K.	3	"Typical Holocene"	-
KAV01 (561 m)	Ävrö	O.K.	1	Affected by glacial water DIC inventory slightly lower than "Typical Holocene"	-
KAV04A (50 m)	Ävrö	O.K.	2	DIC: "Typical Holocene" Surface near but low in tritium -> up-lift ?	-

*: "1", "2" and "3" represent grouping of groundwater with similar DIC biogenic concentrations

11. Caution

The approach used is a very simple and straightforward one. It makes use of simple assumptions such as the DIC biogenic inventory having a ^{13}C value of –27 ‰, the same as in the source material for recharge under C-3 plant material soil and vegetation. If there are recharge contributors from lakes or wetland with standing water with DIC exchange/isotopic fractionation with the atmosphere, such simple approaches are not valid. The same is true if there is microbial methane generation, considerable precipitation of DIC or other non-identified processes. The idea of the approach, however, is that by this simple approach, systems/samples can be identified that basically follow this simple route in the development of the DIC inventory and deviations can be identified for further clarification.

12. Next steps

During the HAG meeting, 16-17 August 2004 it was shown that the basic conclusions are in agreement with progress in hydrological understanding. For this reason the basic approach should be followed up.

The next steps proposed are:

- Introduce calculated concentrations of carbonic acid, carbonate and DIC (decided during the meeting)

- Introduce original ^{14}C data (conventional ^{14}C ages are not ages but a measure for relative ^{14}C activity)

- Normalize tritium data to a given year in order to avoid misinterpretation of very young (< 40 a) contribution based on decay between different sampling and analysis dates (normalization to18 August 2004 was decided at the meeting)

- Introduce the concentration of DIC biogenic (based on operational definition as the DIC total multiplied by the ^{13}C value (in ‰) and divided by –27 (‰) as the value for the C-3 plant source material

- Introduce the ^{14}C concentration of DIC biogenic, i.e. the ^{14}C value of the total DIC inventory (measured value) multiplied by the fraction of DIC being DIC biogenic ($DI^{14}C_{biogenic} = {}^{14}C_{measured} \times DIC_{biogenic}/DIC_{total}$)

- Combine principle component analysis with these calculated numbers for the carbon inventory in order to identify their values/ranges for different groundwater contributors (end-members)

For this purpose, complementing the presently partly scarce data by analysis of ^{14}C in further samples is a key issue.

13. Outcome aimed for in the continuation

Thorough analysis of the ^{14}C concentration of Holocene contributors (corrected for very young tritium containing contributor with the associated ^{14}C elevation from nuclear atmospheric testing) should allow for identification of the age by ^{14}C decay relative to the source term of recent (pre-nuclear atmospheric testing) contributor, however, younger than the elevation over sea level (vegetation/soil layer source term).

Identification of carbon inventory in different contributors (end-members) may contribute to the understanding/verification of their origin/composition.

Further analysis of data from different aquifer systems should allow for identification of key geochemical carbon inventory processes.

14. Open issues

The inclusion of organic carbon should be considered in order to identify the nature of different groundwater contributors. The isolation and characterization of organic carbon fractions (especially humic and fulvic acids) has in principle been decided upon in the program planning. Given the considerable effort involved, a plan for selection of samples and their analysis should be considered.

Appendix 3: Explorative analyses of microbes, colloids and gases

Contribution to the model version 1.2

Lotta Hallbeck

Vita vegrandis

November 2004

1 Microbiology and microbial model

1.1 Introduction

To understand the present undisturbed conditions the following parameters are of interest for hydrogeochemical site description modelling: pH, Eh, S^{2-}, S^0, SO_4, HCO_3^-, HPO_4^{2-}, nitrogen species and TDS together with colloids, fulvic and humic acids, dissolved organic compounds and microorganisms. Further, for a full understanding it is necessary to be able to predict how the conditions will change during the construction of a repository and during the following phases of the storage of spent nuclear waste. This part of the report will deal with the microbial data available so far from the site investigation in the Simpevarp area.

Microbial parameters of interest are the total number and the presence of different metabolic groups of microorganisms (Pedersen, 2001). These data will indicate activity of specific microbial populations at a certain site and how they may affect the geochemistry. The groups cultured for the microbial part of the site investigation were iron-reducing bacteria (IRB), manganese-reducing bacteria (MRB), sulphate-reducing bacteria (SRB), auto- and heterotrophic methanogens and auto- and heterotrophic acetogens.

MPN, "most probable number of microorganisms", is a statistical cultivation method for numbering the most probable number of cultivable metabolic groups of microorganisms (Am. Publ. Health Ass1992).

1.2 Available data

At the data freeze for model version 1.2, 30 April 2004, microbial data from 3 depths in borehole KSH01A were available. In this report these data are analysed in comparison to chemistry and gas data of importance for the different microbial processes.

Table 1 The MPN of different metabolic groups tested with groundwater from three depths in borehole KSH01A in Simpevarp.

Metabolic group	KSH01A (156,5–167 m)	KSH01A (245–261,6 m)	KSH01A (548–565 m)
Iron-reducing bacteria	analysed	analysed	analysed
Manganese-reducing bacteria	analysed	analysed	analysed
Sulphate-reducing bacteria	analysed	analysed	analysed
Autotrophic methanogens	not analysed	analysed	analysed
Heterotrophic methanogens	not analysed	analysed	analysed
Autotrophic acetogens	not analysed	not analysed	analysed
Heterotrophic acetogens	not analysed	analysed	analysed

1.3 Evaluation of the microbial data

1.3.1 Total number of cells and total organic carbon, TOC

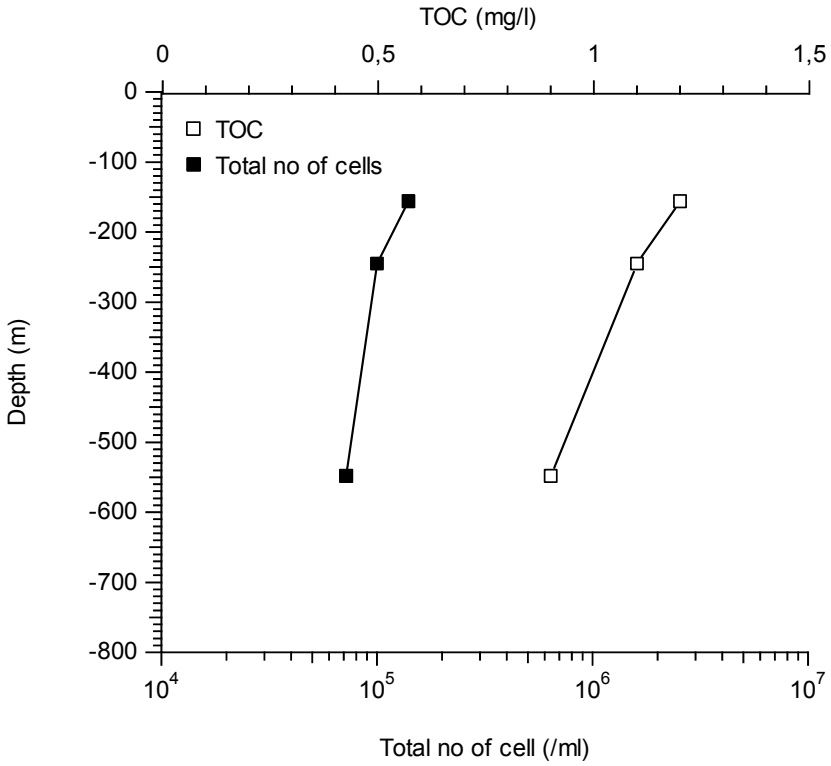

Figure 1 Total number of cells and total organic carbon (TOC) at three depths in borehole KSH01A in Simpevarp.

In Fig. 1 it can be seen that the total numbers of cells at the three depths in KSH01A were from 10^5 per millilitre for level 156,5–167 m down to 7 x 10^4 per millilitre at level 548–565 m. These data are similar to the numbers found in other boreholes in the Äspö area (Pedersen, 2001). The TOC values follow the decreasing trend with depth also in agreement with earlier studies (Pedersen, 2001).

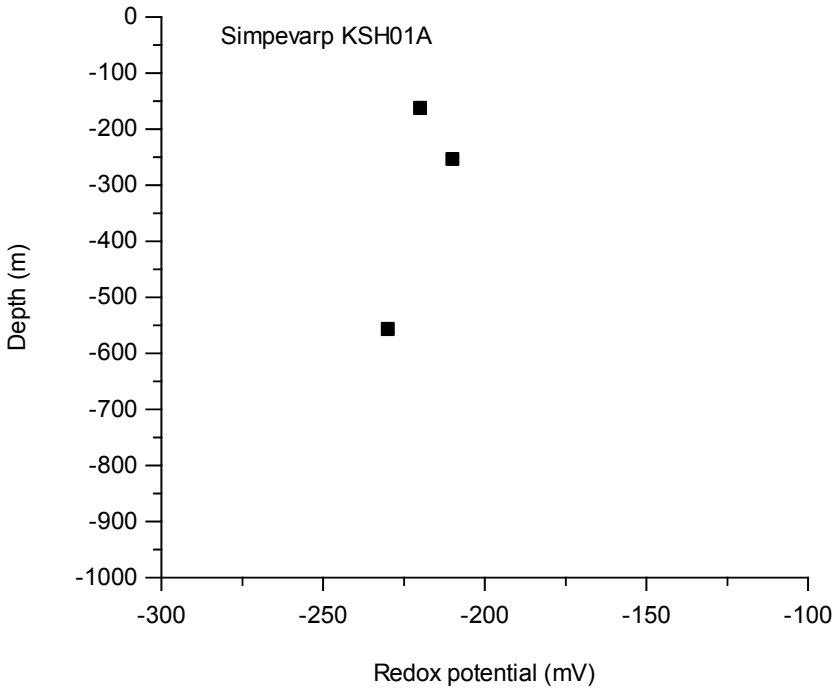

Figure 2. Measured redox potentials at three depths in borehole KSH01A in the Simpevarp area.

1.4 Redox potential in groundwater

Fig. 2 shows the measured redox potentials in groundwater from the different depths in KSH01A. The values were more negative compared to some other boreholes in the Fennoscandian Shield, especially at the shallowest depth observed here. The redox values in combination with the microbial data will be discussed in section 1.12.

1.5 Iron-reducing bacteria, Fe^2 and Fe_{tot}

In KSH01A the numbers of iron-reducing bacteria (IRB) were very low, below 10 per millilitre at all three levels (Fig. 3). The reason for this may be lack of suitable oxidized iron phases such as $Fe(OH)_3$. This is also reflected in the relatively negative redox potential even at the shallowest depth investigated (see Fig. 2). The iron in the groundwater was in the form of ferrous iron as can be seen in Fig. 3.

The iron reducers probably do not affect the geochemistry significantly in this borehole environment. On the other hand, their presence makes it possible for them to thrive if the circumstances change to more favourable conditions for them. Such conditions could arise when reduced iron has oxidised during the construction of a repository.

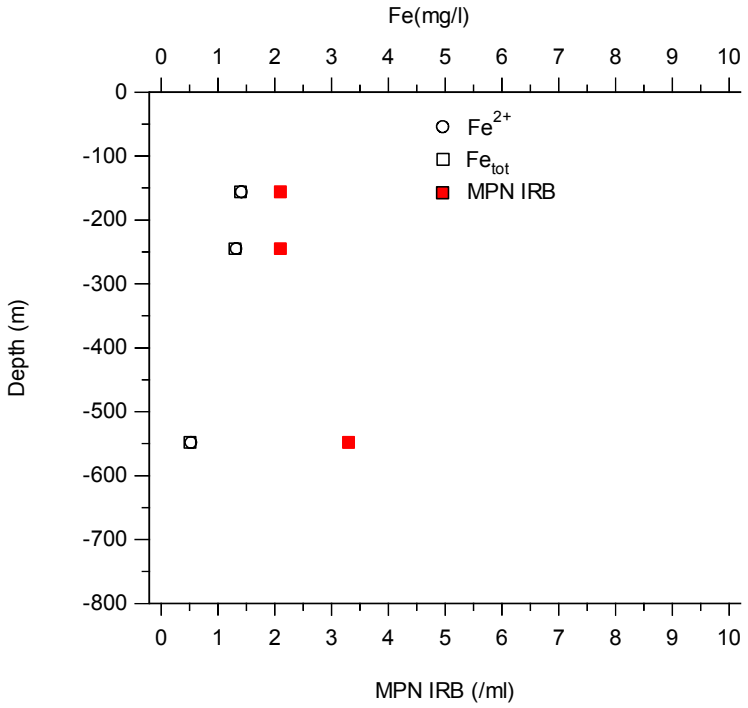

Figure 3. Most probable number of cells (MPN) for iron-reducing bacteria (IRB) and Fe^{2+} and Fe_{tot} versus depths at three levels in borehole KSH01A in the Simpevarp area.

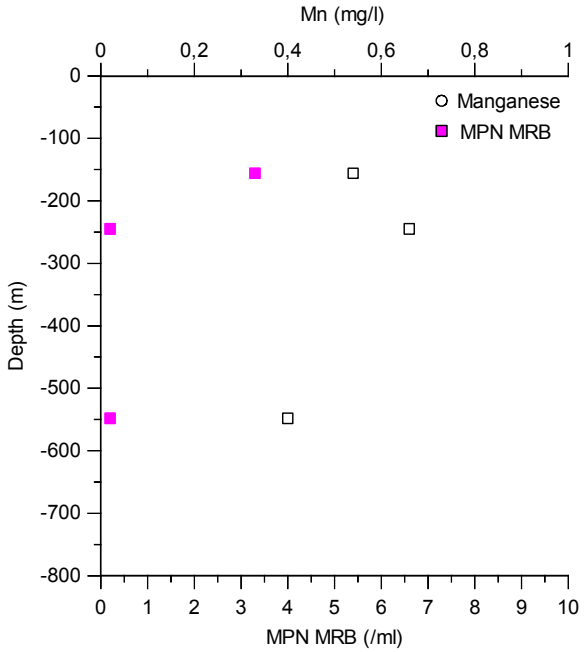

Figure 4. Most probable number of cells (MPN) for manganese-reducing bacteria (MRB) and manganese versus depths at three levels in borehole KSH01A in the Simpevarp area.

1.6 Manganese-reducing bacteria and manganese

Fig. 4 shows that the number of manganese-reducing bacteria (MRB) was also low at all three depths. This can be expected for the same reason as given for iron reducers. Absence of oxidised manganese compound and thus a low redox potential makes the environment unsuitable for manganese reducers. There is no speciation of the manganese values but the manganese in solution is in the Mn^{2+} state due to the insolubility of MnO_2, the form that Mn(IV) will have in natural water within pH range 5–8.The MPN results for MRB indicate that they do not participate to any larger extent in the microbe-geochemistry interactions in the investigated borehole environment.

1.7 Sulphate-reducing bacteria, sulphate and sulphide

The numbers of sulphate-reducing bacteria (SRB) were relatively high compared to iron- and manganese-reducers. The highest value was found at the shallowest depth, 156,5–167 m, with 160 cells per millilitre. The sulphate concentration was low at this depth possibly because of reduction by the SRBs. The hydrogen sulphide values were low at all depths, which may seem contradictory to the large number of SRB. One explanation for this could be formation and precipitation of pyrite in the fractures. Pyrite has been found in the fracture minerals during analysis made on drill cores from KSH01A (Laaksoharju et al., 2004).

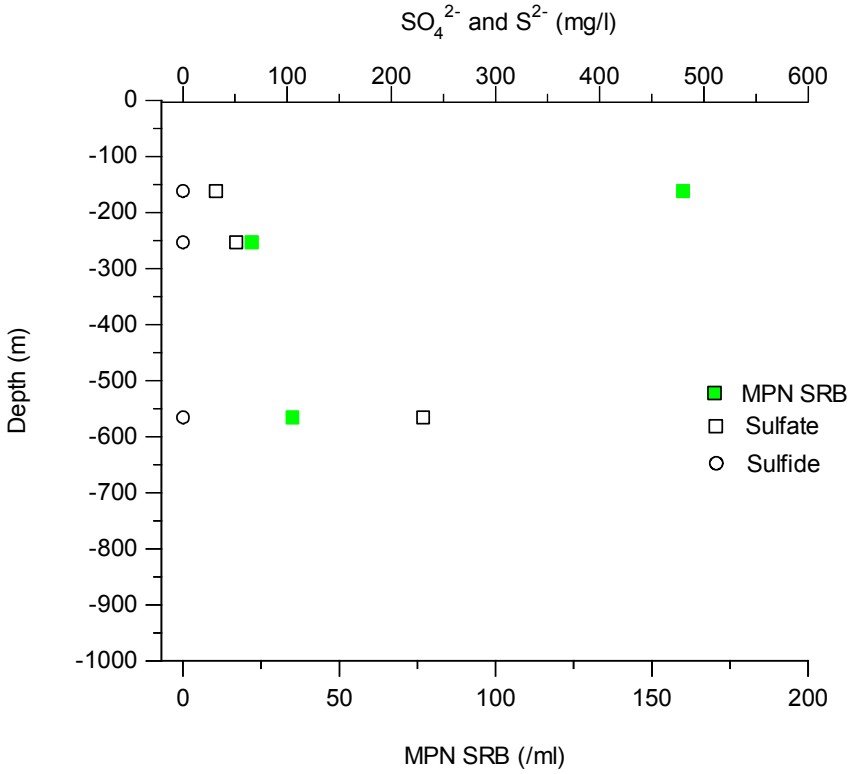

Figure 5. Most probable number of cells (MPN) for sulphate-reducing bacteria (SRB), sulphate and sulphide versus depths at three levels in borehole KSH01A in the Simpevarp area.

1.8 Methanogens

In Fig.5 the MPN numbers for the two different types of methanogens, autotrophic and heterotrophic, together with methane and hydrogen concentrations are plotted versus depth. At level 245–261,5 m it can be seen that the MPN for heterotrophic methanogens was 700 per millilitre. This corresponds to an increased concentration of methane at this depth but also with an increased concentration of hydrogen. The heterotrophic methanogens do not use hydrogen as energy source therefore a correlation between heterotrophic methanogens and hydrogen is not expected. At the deepest level the number of methanogens decreased followed by a decrease in methane. The hydrogen concentration is at almost the same value as at the 245–261.5 m level.

There are no isotopic data available for the detected methane and, therefore, it is not possible to conclude the origin of the methane (see also the part about hydrocarbons in 3.2.3). The

hydrogen probably originates from deep crustal degassing as discussed in the chapter on Gases in this report (Chapter 3).

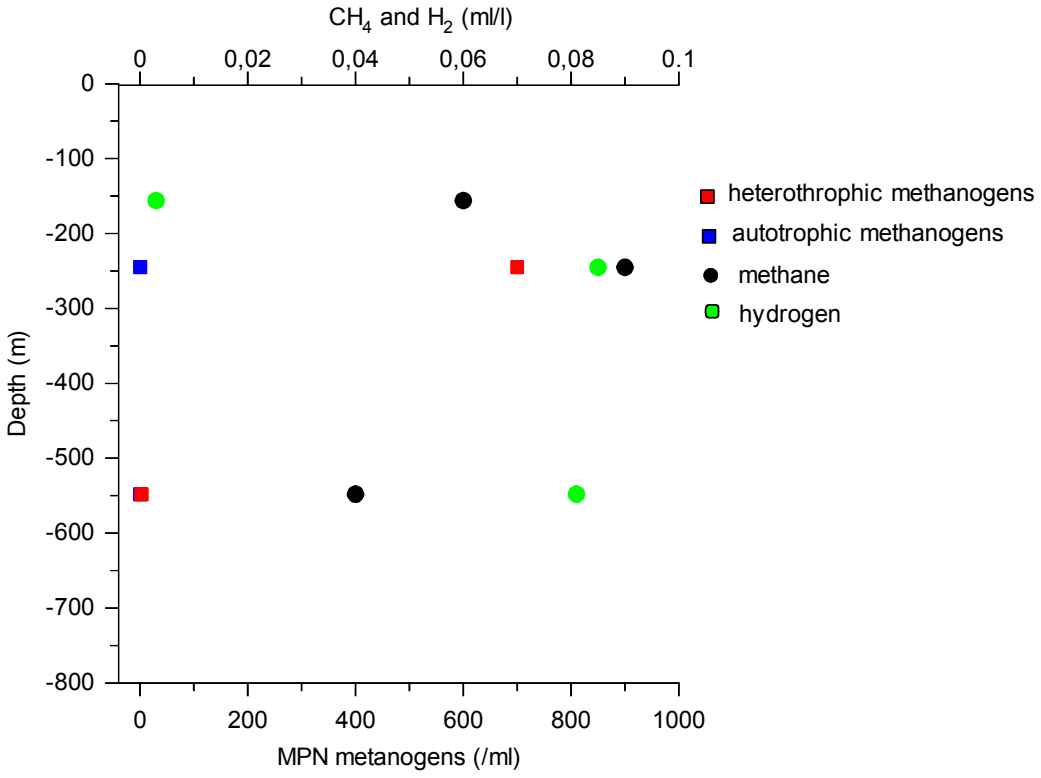

Figure 6 Most probable number of cells (MPN) for auto- and heterotrophic methanogens, methane and hydrogen versus depths at three levels in borehole KSH01A in the Simpevarp area.

1.9 Acetogens

MPN measurements for both auto- and heterotrophic acetogens were reported from the lowest level only, 548–565,5 m, in KSH01A at the time for the data freeze. As can be seen in Figure 7, there was a high amount of heterotrophic acetogens at level 245–261.5 m but both autotrophic and heterotrophic acetogens were below 0.2 per ml at the deepest level studied. These data together with the methanogen data suggest that the microbial activity is highest at

the 245–261.5 m level. The result from acetogenic activity is production of acetate. So far, there are no acetate data available; however, acetate could be an important parameter to measure in the future.

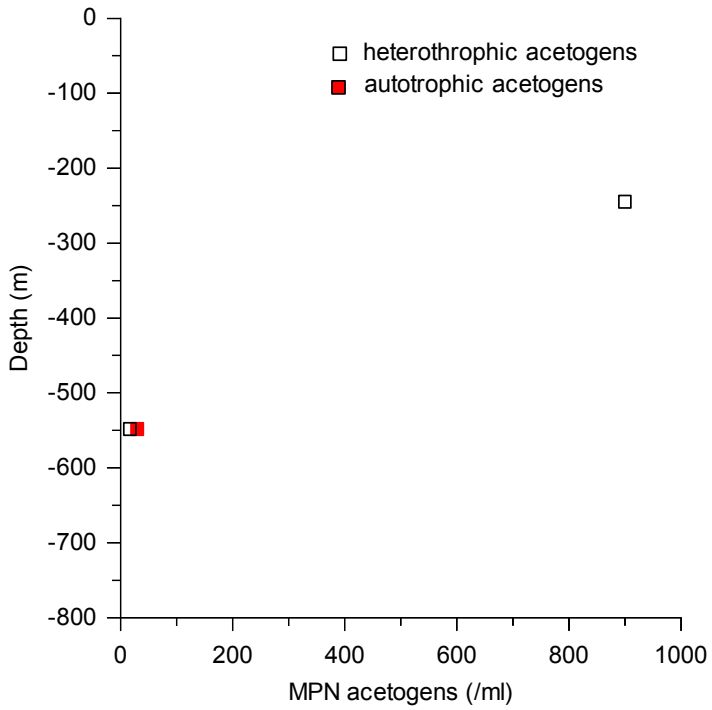

Figure 7 Most probable numbers of cells (MPN) for auto- and heterotrophic acetogens versus depths at 1 respectively 2sections in borehole KSH01A in the Simpevarp area.

1.10 Total number of cells versus MPN

From a comparison to the total number of cells found in groundwater from the three levels versus the MPN numbers obtained from culturing it can be seen that it is a small percentage of the total numbers that was cultured. Table 2 shows that the percentages were 0.12, 1.6 and 0.085. Even though the sampling from the first level did not include methanogens and acetogens, the percentage of cultivable cells is higher than at the deepest level. One explanation for this might be that, the more reduced the environment, the more difficult it is to obtain the correct culture conditions or that organisms at this level possess metabolisms that are not yet explored.

In general, it can be concluded that even if the MPN numbers are too low, the proportion of the different metabolic groups registered is correct. This is supported by the agreement between cultured microorganisms and measured redox values (see section 1.12).

Table 2. The percentage of the total number of cells cultured with MPN in the analysed sections in KSH01A.

Borehole (section, m)	Cells cultured (%)	
	MPN	Lower – upper 95% confidence limits
KSH01A (156,5–167)	0.12	0.043 – 0.38
KSH01A (245–261,6)	1.6	0.61 – 5.1
KSH01A (548–565)	0.085	0.051 – 0.37

1.11 Correlations

In the evaluation of data for different microorganisms, correlations between the presence of the microorganisms and one or more parameters involved in the metabolism of the respective microorganism should be tested for. In Fig. 8 the MPN values for iron-, manganese- and sulphate-reducing bacteria are plotted versus ferrous iron, manganese and sulphate, respectively. Since there are few data available for this model version, good correlations should not be expected for these types of microorganisms that possess a significant variability in appearance. Figure 8c, section 548 m and 156 m, shows a trend that is common for sulphate-reducing bacteria: low sulphate values correlate with high occurrence of SRB. The low sulphate values are possibly due to reduction by SRB to sulphide. If MPN for SRB were plotted versus produced sulphide it would show an opposite trend. However, in the groundwater of KSH01A the sulphide seems to be precipitated as iron sulphide (pyrite), and the values are therefore very low (Laaksoharju, 2004).

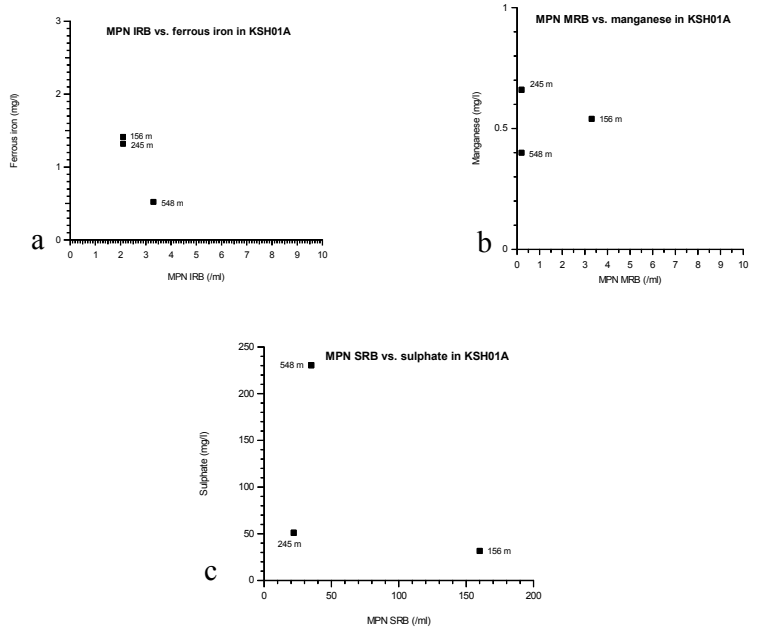

Figure 8. MPN values for (a) IRB versus ferrous iron, (b) MRB versus manganese, and (c) SRB versus sulphate in borehole KSH01A in the Simpevarp area. Numbers in the figure indicate the borehole section centre.

1.12 The microbial model

Fig. 9 shows the distribution of the different microbial groups found at the three sampled levels in KSH01A and the measured redox potentials from Fig. 2. The redox potential is rather negative and relatively similar at the three depths, –220, –210 and –230 mV.

To the right in Fig.9 is a so-called redox ladder with different microbial respiration redox couples placed at their respective E_0'. The vertical red line in this figure marks the redox interval measured in KSH01A. These redox values coincide with where sulphate reducers and methanogens can be found and correlate very well with the MPN results for this borehole. If iron- and manganese-reducers were to be found, the measured redox values had to be at least 50 mV higher. In the table in Appendix 1 the calculated redox values for the three levels are provided. The table shows that the redox pairs $SO4^{2-}/S^{2-}$ and CH_4/CO_2 give values that agree with the measured redox potentials and by that also with the microorganisms found.

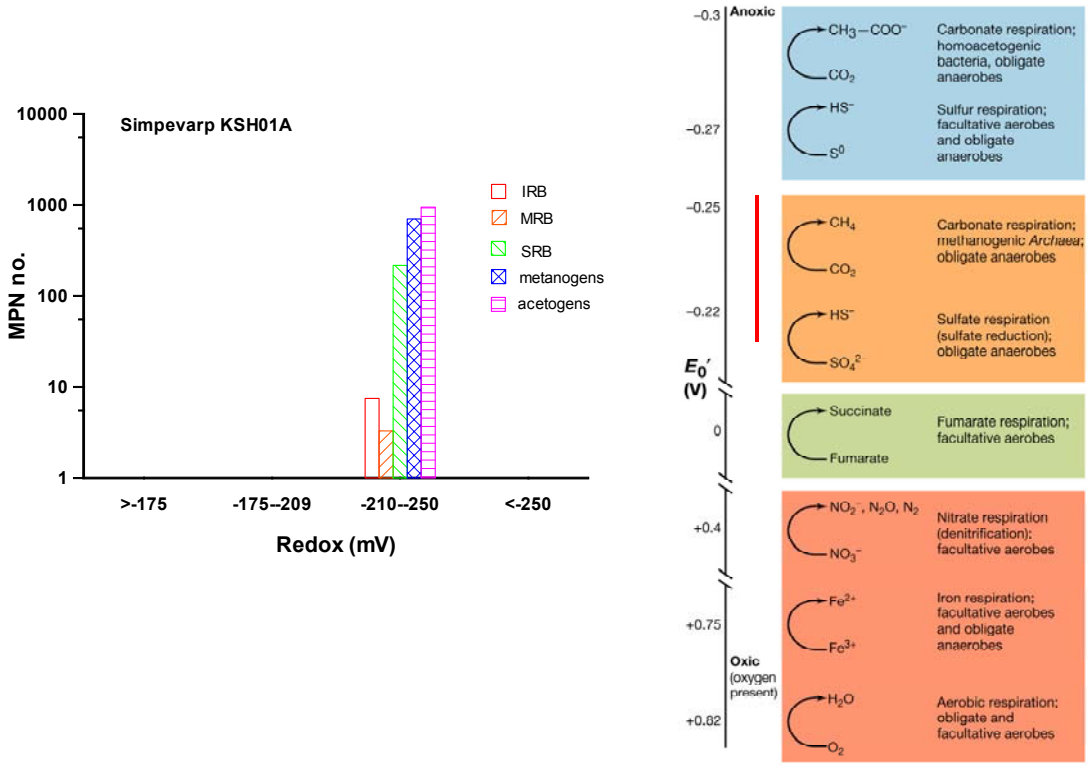

Figure 9. The sum of the most probable number of microorganisms plotted versus intervals of redox values. The data are from sampling of groundwater in borehole KSH01A in the Simpevarp area.

In Fig. 10 the MPN data are plotted versus depth. Here it can be seen that a higher number of microorganisms were found in the depth interval 101–300 m, that is, the two shallowest sampling points than at the deepest, 548–565,5 m. Since there are two sampled depths at the 101–300 m interval, the sum of MPN values was divided by 2. This finding indicates that the number of microorganisms is higher in the groundwater from the shallower sites.

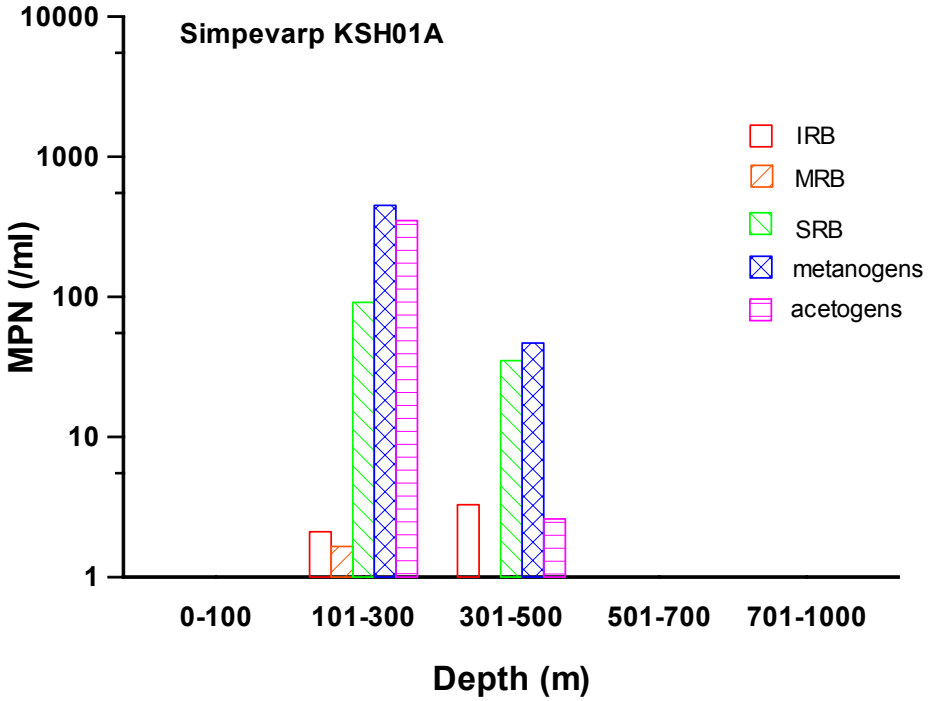

Figure 10 The sums of most probable number (MPN) of microorganisms plotted versus depth intervals. The data are from sampling of groundwater in borehole KSH01A in the Simpevarp area.

Fig. 11 shows a one-dimensional redox model of borehole KSH01A including the 3 sampling sites and intercepting structures. These structures were found by groundwater sampling, together with BIPS and Flowlog measurements. Flow measurements showed that the fracture zone at 245–261.6 m covers a large area but that each fracture had a low flow. The low flow velocity was probably due to clay formation in the fractures (Laaksoharju et al., 2004).

Fig. 11 also shows that in the shallowest part of the borehole, 156.5–167 m, the sulphate-reducing bacteria were predominant. The measured and the calculated redox value with the redox pair SO_4^{2-}/S^{2-} support this finding. In version 1.1, pyrite was reported as one of the minerals found in fracture fillings; this too supports the microbiological data and gives an explanation to why the measured sulphide data at this depth were very low.

At the next sampling depth, 245–261.6 m, heterotrophic methanogens and acetogens dominated. The measured and calculated redox values this time with CO_2/CH_4 as redox pair correspond with the redox interval where these types of microorganisms can be found.

Finally, the deepest site has in general very low numbers of cultivable microorganisms. The flow at this site was lower than at the depth above, and the redox value was low. The lowest measured redox value at this depth was –230 mV (Appendix 1). The E_0' where autotrophic acetogenesis takes place is around –300 mV (Fig.9) and the measured low redox strengthens the suggestion that acetogens would be the most active at this depth even though MPN numbers were very low. A reason for this might be that the MPN method is difficult to apply to autotrophic organisms and that the MPN method therefore gives lower values than in reality.

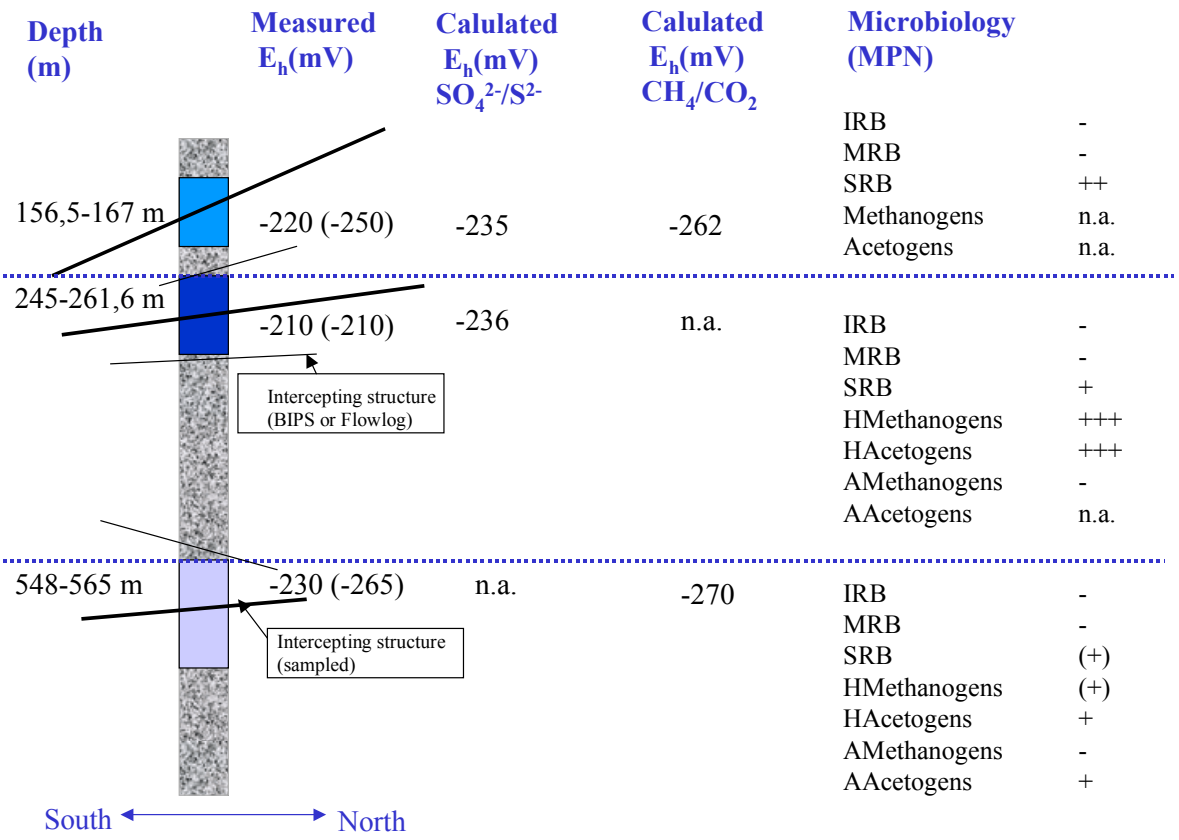

Figure 11 One-dimensional biogeochemical model of borehole KSH01A in Simpevarp. This model is made with data available in SICADA 30 April 2004, the time for data freeze 1.2.

n.a.= not analysed.

1.13 Conclusions

- As there were only three sets of microbiological data available, and from only one borehole, this model version is one-dimensional.
- Redox potentials in borehole KSH01A were in general low, below –200 mV at all sampled depths.
- Sulphate-reducing bacteria dominated at the shallowest level, 156.5–167 m.
- At the mid level, 245–261.6 m, heterotrophic methanogens and acetogens were in the majority.
- At the deepest level, autotrophic and heterotrophic acetogens were found but only in low numbers.
- The high numbers of microorganisms at the level 245–261.6 m were probably due to the large fracture area with high amounts of fracture surfaces inducing significant perturbations and profitable gradients for life.
- The microbial species abundance and activity in borehole KSH01A seem to be in close correlation with the redox potential.

2 Colloids

2.1 Introduction

Particles in the size range 10^{-3} to 10^{-6} mm are regarded as colloids. Their small size prohibits them to settle which render them a potential to transport radionuclides in groundwater. The aim of the study of colloids in the site investigation of Simpevarp 1.2, was to quantify and determine the composition of colloids in groundwater from boreholes. The results will be included in the modelling of the hydrochemistry at the site.

This set of data, from the data freeze of 30th of June, included colloid data from 2 boreholes, sampled during 1987, 1988 and 1989. Data from colloid analyses made for the site investigation have not been reported to SICADA in time for the data freeze.

2.2 Methods

The method used was on-line filtering with the same volume of water passing through filters with 0.4, 0.2 and 0.05 μm pore size, respectively. The mineral composition of the colloids on the filters was determined with energy dispersive X-Ray Fluorescence (XRF) and the quantities of the analysed elements were recalculated in μg l^{-1} (ppb) considering the water flow (ml h^{-1}) registered through the filters (Laaksoharju et al., 1995). The elements analysed were calcium (Ca), iron (Fe), sulphur (S), manganese (Mn), Aluminium (Al) and silica (Si).

2.2.1 Databases

The data used were extracted from the file *All_data_POM_Area.xls* provided by Maria Gimeno at the Projectplace. The data used here are compiled in table 2.1. The total data set can be found in Appendix 1.

2.2.2 Evaluation of the colloid data

During the evaluation of the primary data, a decision was taken to exclude data from Laxemar, KLX01, 691 m sampled 1988-11-03 because of extremely high iron values that probably were due to a sampling artefact (Table 2). All other data available were used in the evaluation.

In a report by Laaksoharju, 1995, calcium values calculated as calcite and sulphur values calculated as pyrite were both withdrawn from the total amount of colloids. In this presentation the same approach was used with the exception that the sulphur values are not recalculated as pyrite but are shown as sulphur.

2.3 Colloids versus depth

In a valuation of the background values for colloids in groundwater, the amount of colloids versus depth is studied. It can be seen in Figure 1 that the amount of colloids decreases with depth in KLX01 but not in KAV01. Further, the amount does not vary much at the different

depth. The sampled depths were 422.5 m, 525.5 m and 560.5 m respectively and they differ only 140 m in depth, which is not much in relation the total depth explored.

The average amount of colloids in this study is 63±49 μg l^{-1} and is in agreement with colloid studies from Switzerland (30±10 and 10±5 μg 1^{-1}) and Canada (300±300 μg $1^{-}1$) where they used the same approach as here (Laaksoharju, 1995).

Table 1 Element analyses of colloid fractions from borehole KAV01, Ävrö.

Borehole	KAV01 422.5 m			KAV01 525.5 m			KAV01 560.5 m		
Filter pore size (μm)	0.05	0.2	0.4	0.05	0.2	0.4	0.05	0.2	0.4
Chloride (mg l^{-1})	500	500	500	1600	1600	1600	4200	4200	4200
Colloid phase (μg l^{-1})									
Ca as Calcite $CaCO_3$	161	124	177	414	402	182	648	434	254
Fe as $Fe(OH)_3$	7.5	12.6	14.2	12.5	8.61	10.1	15.2	6.32	15.0
S as sulphur	9.25	14	11	19.5	18	13	23.5	12	11
Mn as $Mn(OH)_2$	2.22	1.78	2.67	1.94	2.67	0.81	0	0	0
Al as K-Mg-Illite clay: $K_{0.6}Mg_{0.25}Al_{2.3}Si_{3.5}O_{10}(OH)_2$	0	0	0	0	0	0	1.44	4.33	5.05
Si as SiO_2	0	2.78	2.14	0	0	0	0	0	6.10
Sum, ppb, (μg l^{-1})	179.97	155.16	207.01	447.94	431.28	205.91	688.14	456.65	291.15
Sum omitting calcite	18.97	31.16	31.01	33.94	29.28	23.91	40.14	22.65	37.15
Sum omitting calcite and sulphur	9.72	17.16	20.01	14.44	11.28	10.91	16.64	10.65	26.15

Table 2 Element analyses of colloid fractions from borehole KLX01, Laxemar.

Borehole	KLX01, 458,5 m			KLX01, 691 m (1)			KLX01, 691 m (2)		
Filter pore size (μm)	0.05	0.2	0.4	0.05	0.2	0.4	0.05	0.2	0.4
Chloride (mg l^{-1})	1700	1700	1700	4800	4800	4800	4500	4500	4500
Colloid phase (μg l^{-1})									
Ca as Calcite $CaCO_3$	174.74	403.39	167.25	1432.85	1869.70	843.74	685.22	1160.76	871.19
Fe as $Fe(OH)_3$	6.32	5.55	11.48	6.89	19.14	754.1	14.16	7.6	21.05
S as sulphur	32	34	21	47	78	34	26.5	20	29
Mn as $Mn(OH)_2$	0	0	0	0	0	10.04	0	0	0
Al as K-Mg-Illite clay: $K_{0.6}Mg_{0.25}Al_{2.3}Si_{3.5}O_{10}(OH)_2$	8.12	46.9	24.9	16.96	227.31	83.0	0	0	16.24
Si as SiO_2	6.10	19.04	9.84	3.63	29.95	98.40	2.78	6.42	5.35
Sum ppb, (μg l^{-1})	227.28	508.88	234.47	1507.33	2224.1	1823.28	728.66	1194.78	942.83
Sum omitting Calcite	52.54	105.49	67.22	74.48	354.4	979.54	43.44	34.02	71.64
Sum omitting calcite and sulphur	20.54	71.49	46.22	-	-	-	16.94	14.02	42.64

Italic numbers were omitted from the modelling

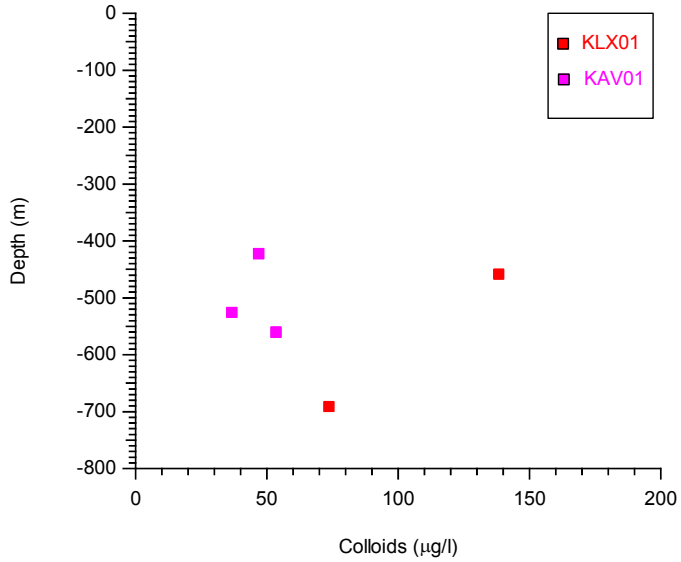

Figure 1 Colloids (µg l^{-1}) plotted versus depth in samples from borehole KLX01 in Laxemar and KAV01 in Ävrö.

2.4 Colloids versus chloride

In groundwater with a high chloride concentration the amount of colloids usually decreases because higher ion strength increases the precipitation of different solid particles. This can be seen in Fig. 2 for the data from KLX01 but not for KAV01.

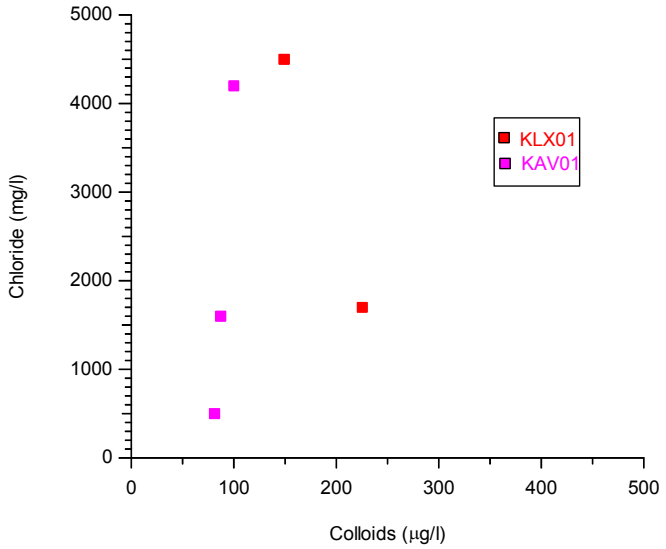

Figure 2 Colloids (μg l^{-1}) plotted versus amount of chloride in the groundwater in samples from boreholes KLX01 in Laxemar and KAV01 in Ävrö.

2.5 Colloids versus iron

High iron concentrations in groundwater force the precipitation of other compounds by its ability for co-precipitation, which produces larger particles. Thus the amount of colloids will decrease with increasing iron concentration. Fig.3 shows the colloids versus the iron content in groundwater from KLX01 and KAV01. Here it can be seen that in KLX01 with low iron values, the amount of colloid is relatively higher compared to the colloid amount in KAV01. The iron values in KAV01 are 10–25 times higher than the corresponding values in KLX01.

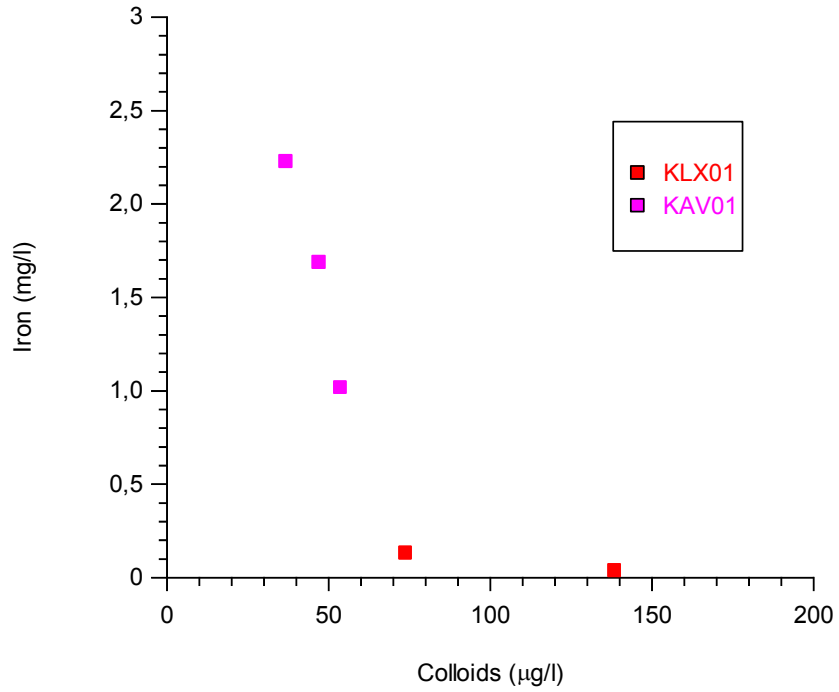

Figure 3 Colloids (μg l^{-1}) plotted versus iron in groundwater in samples from borehole KLX01 in Laxemar and KAV01 in Ävrö.

2.6 Composition of the colloids

The composition of the colloids has also been studied. Table 1 and 2 show the values for the elements analysed, calcium (Ca), iron (Fe), sulphur (S), manganese (Mn), Aluminium (Al) and silica (Si), and the recalculated colloid phases calcite, iron hydroxide, manganese dioxide, K-Mg-Illite clay and silica oxide. Sulphur was not recalculated to any other colloid phase.

Fig. 4 shows the composition of the colloids sampled from different depths in the two boreholes. In this figure sulphur is shown. In Fig. 5 on the other hand these values are omitted. In both figures the calcite is omitted since it is considered as an artefact due to pressure changes during sampling

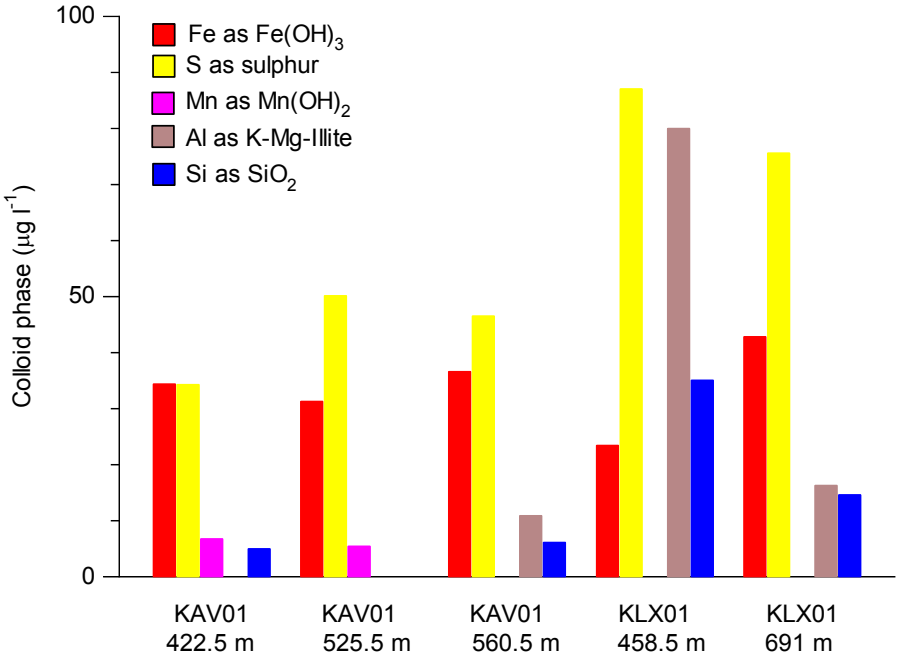

Figure 4. The composition of colloids sampled from two boreholes, KAV01 and KLX01 in the Simpevarp area. Calcite values are omitted in this figure.

In Figures 4 and 5 it can be seen that manganese oxides are only present in KAV01 groundwater. On the other hand K-Mg-Illite can only be found at the lowest depth in KAV01 but at both 458.5 m and 691 m in KLX01hetero. The K-Mg-Illite value at 458.5 m is very much higher than the others and it can be discussed if this also might be an artefact from the sampling method.

2.7 Conclusion

The data available seems to agree with the amount of colloids reported earlier from Äspö and Bangombe (Laaksoharju et al.1995, Pedersen, 1996). Still, because of the few data available it is difficult to draw conclusion from this analysis. Especially the lack of data for numbers of particles makes it difficult to make calculations of possible binding sites for radionuclides in the different colloid fractions. It will, however, be a very different situation when the data from sampling in connection with the ongoing site investigation are reported into the SICADA.

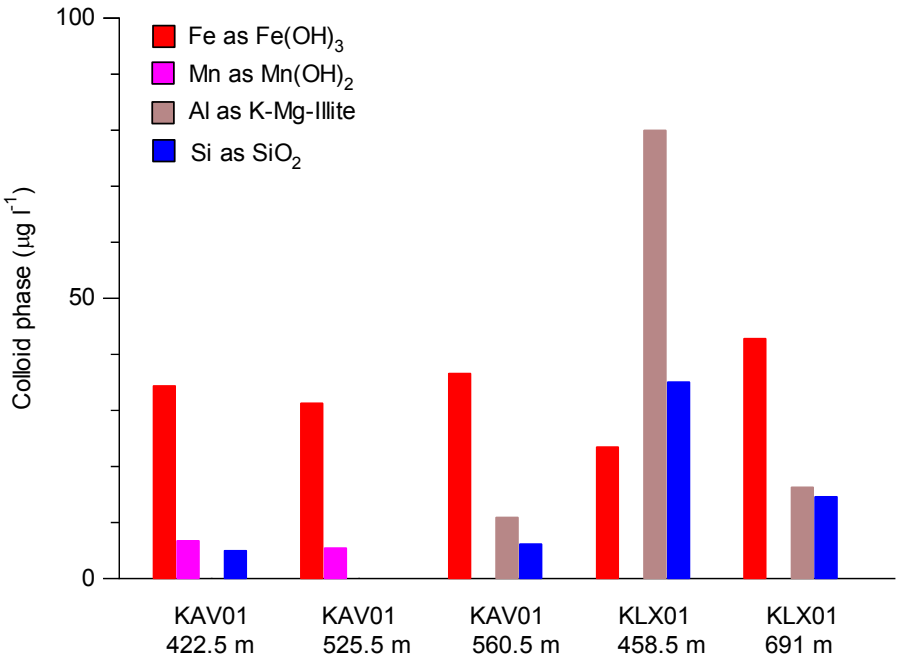

Figure 5. The composition of colloids sampled from 2 boreholes, KAV01 and KLX01 in the Simpevarp area. Calcite and sulphur values are omitted in this figure.

3 Gases

3.1 Introduction

Earlier studies of groundwater in the Fennoscandian shield have shown high amounts of dissolved gasses. If the sum of gas reaches above saturation gas bubbles may form. The surface of such bubbles can adsorb different compounds in the groundwater such as radionuclides. The bubbles will move rapidly in groundwater and can cause dispersion of radionuclides to large areas and especially to the ground surface. In a site investigation it is therefore of great importance to evaluate and include gas data in hydrogeochemical models. Some gases are involved in microbiological reactions. These gases are methane, carbon dioxide and hydrogen. Methane is produced by methanogens in reduced environments and can be used as substrate by methanotrophic bacteria. Carbon dioxide is used as carbon source for autotrophic organisms and is the end product in microbial degradation. Hydrogen is energy and electron source for methanogens, acetogens and some other autotrophic microorganisms, i.e. sulphate reducers. It is also one of the end products in microbiological fermentation.

In this study up to 12 gases were analyzed: helium, argon, nitrogen, carbon dioxide, methane, carbon monoxide, oxygen, hydrogen, ethyne, ethene, ethane and propane. They are listed in the row for borehole KSH01A in Table 1. This borehole is the only one that was complete regarding analysed gas components. Numbers for the total volume of gas were available only for 5 depths in 2 of the boreholes. They contain between 44 and 80 ml l^{-1} and this is in accordance with volumes found at other places in the Fennoscandian shield. The highest amounts of gas have been found in deep groundwater in Olkiluoto in Finland with volumes up to above 1000 ml l^{-1} (Pitkänen, 2004). The gas volume data from KLX01 does not include propane (C_3H_8), oxygen, argon or hydrogen and volume from this borehole should, therefore, not be compared to the volumes from KSH01A.

Table 1 shows the boreholes and depths from which data have been available for this report.

3.2 The dissolved gasses

In this report gas data from the boreholes KLX01 and KSH01A will be discussed. They are represented by red and black symbols, respectively, in the Figures 1-3.

3.2.1 Nitrogen and helium

Fig. 1 shows that the amount of nitrogen decreases with depth in KLX01 but in KSH01A it is the opposite trend. It has to be noticed that the data from KSH01A are from shallower water and from KLX01 from below 600 m. The nitrogen concentration in groundwater from Olkiluoto, Finland, showed an increasing trend with depth down to 1100 m (Pitkänen, 2004).

Helium concentration in both boreholes in the Simpevarp area showed a slight decrease with depth but there is little variation among the data. Helium concentrations in Olkiluoto increased with depth following the nitrogen concentration.

The origin of nitrogen and helium in groundwater is considered to be crustal degassing of the bedrock. Another source for helium can be radioactive decay, also this in the bedrock.

Table 1 Boreholes, depths, gasses analyzed and gas volumes available in SICADA for analysis in Simpevarp model version 1.2.

Borehole	Depth centre (m)	Sampling date	Gases analyzed	Gas volume (ml l^{-1})
KAS02	208.25	1989-01-11	He, N_2, CH_4, CO	
	892.02	1089-01-31	N_2, CO_2, CH_4, CO	
KAS03	131.5	1989-02-21	N_2, CO_2, CH_4, CO	
	931.03	1989-03-15		
KAS04	338.5	1989-04-27	He, N_2, CO_2, CH_4	
	460.49	1989-04-03	He, N_2, CO_2, CH_4, CO	
KLX01	682.5*	1988-11-03/01	He, N_2, CO_2, CH_4, CO, C_2H_2, C_2H_4, C_2H_6	69
	835.5	1990-10-09		44
	915.5	1990-10-31		44
KSH01A	161.75	2003-03-28	He, Ar, N_2, CO_2, O_2, CH_4, H_2, CO, C_2H_2, C_2H_4, C_2H_6, C_3H_8	79.8
	556.5	2003-06-23		76,4

*duplicate sampling

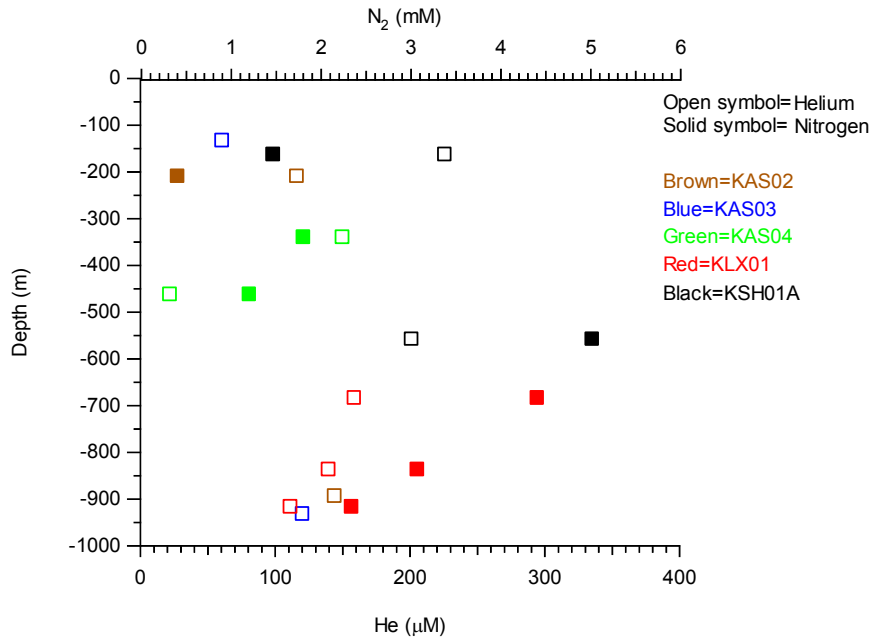

Figure 1. The concentrations of nitrogen and helium plotted versus depth in samples from boreholes in the Äspö, Laxemar and Simpevarp areas.

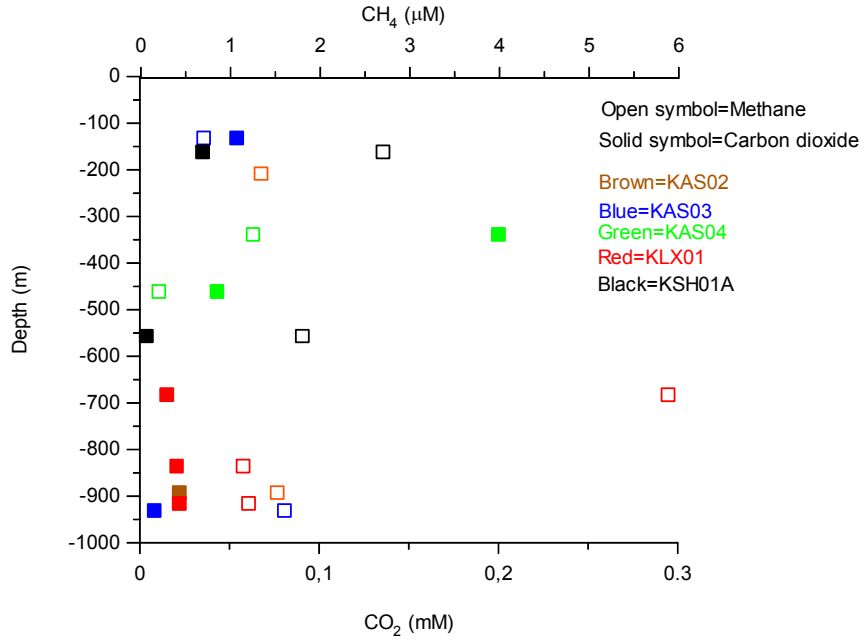

Figure 2. Carbon dioxide and methane plotted versus depth in samples from boreholes in the Äspö, Laxemar and Simpevarp areas.

3.2.2 Carbon dioxide and methane

Carbon dioxide in groundwater is a dissociation product of dissolved carbonates from fractures in the bedrock. The carbon dioxide concentrations in samples from the Simpevarp area are fairly constant in the different boreholes with values below 0.1 mM. There is a slight tendency that the concentration decreases with depth down to 500–600 m and below that the values are more or less constant. This pattern has also been observed for carbon dioxide concentrations in groundwater from the Olkiloto Site in Finland. (Pitkänen, 2004*)*

Methane is found in low concentrations, 0.5 – 3 μM, in all boreholes at all depths but no trend in concentrations appears due to the very restricted amount of available data. In KSH01A, the value for the deepest depth 556.5 m, is lower than for 161.75 m, 1.8 μM compared to 2.7 μM, respectively.

The origin of methane in groundwater can be either biotic or abiotic. The biotic methane is produced by methanogenic *Achaea*, a group of prokaryotic organisms. They can utilize either C1-compounds or acetate. This is exemplified with acetate in Equation 1. They can also fixate carbon dioxide with hydrogen gas as energy and electron source (Eq. 2). The origin of their substrate can be biodegraded organic matter as in sea and lake sediments or composts. It can also be carbon dioxide and hydrogen with origin in the mantle (Apps & Van de Kamp, 1993).

$$CH_3COOH \rightarrow CH_4 + CO_2 \qquad \text{(Eq.1)}$$

$$CO_2 + 4H_2 \rightarrow CH_4 + 2H_2O \qquad \text{(Eq.2)}$$

The abiogenic methane is produced in, for example, hydrothermal systems during water–rock interactions involving the Fischer-Tropsch synthesis reaction, which is the same as Eq.2 above. This methane can act as precursor for polymerisation to higher hydrocarbons such as short chain alkanes (see below).

The isotopic carbon signature of methane can reveal the source of the methane but there are no such data available in the SICADA.

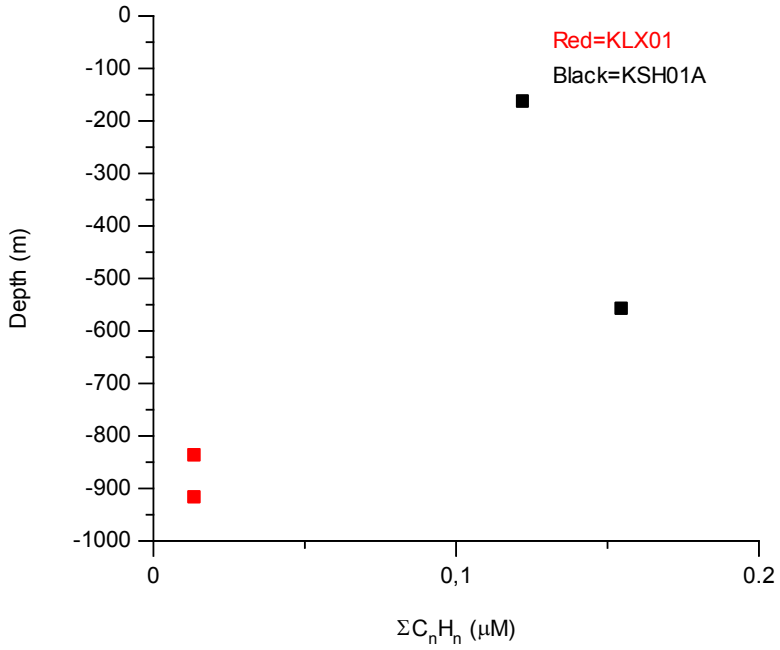

Figure 3 *Total concentrations of hydrocarbons, except methane, versus depth in two boreholes in Laxemar and Simpevarp.*

3.2.3 Hydrocarbons

Data for hydrocarbons (HC) are available for two boreholes, KLX01 and KSH01A. Unfortunately, all compounds were not measured for both boreholes and this is why these values differ (Fig.3).

The data from KSH01A contain the C1, C2 and C3 hydrocarbons that usually are measured and the discussion will only deal with these. As can be seen in Fig. 3, the concentration of hydrocarbons increases with depth. The hydrocarbons come from a deep abiogenic source and move slowly by diffusion towards the surface. Calculating the C1/(C2+C3) ratio can elucidate the source of the methane found. If this ratio is high, over 103, it is considered as microbiological methanogenesis, thermogenic and abiogenic methanogenesis will give a ratio around 101 (Sherwood-Lollar et al., 1993, 2002; Clark and Fritz, 1997; Whiticar, 1999). The calculation for data from KSH01A gives the ratios 33 and 12, respectively. This indicates, referring to the theory above, that most of the methane originates from an abiogenic source, but it cannot be excluded that some of the methane has biogenic origin. To be conclusive in this statement, more HC data need to be generated together with stable isotope values for methane and hydrocarbons.

3.2.4 Hydrogen

Hydrogen is an important gas in several anaerobic microbial metabolisms such as methanogenesis and acetate production by acetogens. There are also autothrophic iron- and sulphate-reducing bacteria that can use hydrogen as energy and electron source concomitant with iron or sulphate reduction.

There are at least six possible processes in which crustal hydrogen is generated: (1) reaction between dissolved gases in the C-H-O-S system in magmas, especially in those with basaltic affinities; (2) decomposition of methane to carbon (graphite) and hydrogen at temperatures above 600°C; (3) reaction between CO_2, H_2O, and CH_4 at elevated temperatures in vapours; (4) radiolysis of water by radioactive isotopes of uranium, thorium and their decay daughters, and potassium; (5) cataclasis of silicates under stress in the presence of water; and (6) hydrolysis by ferrous minerals in mafic and ultramafic rocks (Apps and Van de Kamp 1993). It is important to explore the scale of these processes and the rates at which the produced hydrogen is becoming available for deep microbial ecosystems.

Measurement of hydrogen is a complicated issue because of its tendency to diffuse through most materials. In the compilation of data from the Simpevarp area there is only one certain hydrogen value and that is 3.62 μM in KSH01A at 556.5 m depth. This is a relatively high value compared to data from other Nordic sites (Pedersen 2000). Discussion of trends for the concentration of hydrogen has to remain until more data are available.

3.3 Conclusion

- So far, the amount of gas data are very limited and exclude any considerable analysis of the impact of gases on geochemistry and microbiology.
- The available gas data for the Simpevarp area show that the gas content is in the same order of magnitude as in most of the Nordic sites studied.
- The gases are probably mostly mantle-generated.
- Gases are probably oversaturated in relation to atmospheric pressure but not at depth.

4 References

American Public Health Association.1992.Estimation of bacterial density, 977–980. In: Standard methods for the examination of water and wastewater, 18th ed. American Public Health Association, Washington, D.C.

Apps J A. and Van de Kamp PC .1993. Energy gases of abiogenic origin in the Earth's crust. The future of energy gases. US Geological Survey Prof. Pap. 1570, 81–132.

Clark I. Fritz P. 1997. Environmental isotopes in hydrogeology. Lewis Publishers, Boca Raton, 328 p.

Laaksoharju M. Degueldre C. Skårman C. 1995. Studies of colloids and their importance for repository performance assessment. SKB Technical Report TR-95-24, Stockholm, Sweden.

Pedersen, K. (ed). 1996. Bacteria, colloids and organic carbon in groundwater at the Bangombé site in the Oklo area. SKB Technical Report TR-96-01, Stockholm, Sweden.

Pedersen, K. (2001) Diversity and activity of microorganisms in deep igneous rock aquifers of the Fennoscandian Shield. In Subsurface microbiology and biogeochemistry. Fredrickson, J. K. & Fletcher, M., Eds. New York: Wiley-Liss Inc., 97–139.

Pitkänen P. Partamies S. Luukonen A. 2004. Hydrochemical interpretation of baseline groundwater conditions at the Olkiluoto site. POSIVA 2003-07, Posiva, Olkiluoto, Finland.

Sherwood-Lollar B. Frape S K. Weise S M. Fritz P. Macko S A. Welham J A. 1993. Abiogenic methaogenesis in crystalline rocks. Geochimica et cosmochemica Acta 57, 5087–5097.

Whiticar M J. 1990. A geochemical perspective of natural gas and atmospheric methane. Organic Geochemistry 16, 531-547.

5 Appendix 1

Area	Bore hole	Depth centre (m)	FILTER POR	Number of samples	Volume filtered (ml)	Al P (ug/l)	Ca P (ug/l)	Fe P (ug/l)	Mn P (ug/l)	Si P (ug/l)	S P (ug/l)	Fe (mg/l)	Fe2+ (mg/l)	
Ävrö 1987	KAV01	422,5	0.05	2	800	b.d.*	64.5 ±28.5**	4.1±0.85	1.4±0.85	b.d.	9.25±3.8	1.67±0	1.67±0	
		422.5	0.2	1	800	b.d.	50	6.6	1.1	1.3	14	1.67	1.67	
		422.5	0.4	1	800	b.d.	71	7.4	1.5	1	11	1.67	1.67	
Ävrö	KAV01	525.5	0.05	2	550	b.d.	166 ±20	6.55±1.85	1.2±0.1	b.d.	19.5±0.5	2.3±0	2.3±0	
		525.5	0.2	1	550	b.d.	161	4.5	1.5	b.d.	18	2.3	2.3	
		525.5	0.4	1	550	b.d.	73	5.3	0.5	b.d.	13	2.3	2.3	
Ävrö	KAV01	560.5	0.05	2	485	0.4±0	259.5 ±116.5	7.95±6.05	b.d.	b.d.	23.5±6.5	1.04±0	1.03±0	
		560.5	0.2	1	485	1.2	174	3.3	b.d.	b.d.	12	1.04	1.03	
		560.5	0.4	1	485	1.4	102	7.8	b.d.	1.2	11	1.04	1.03	
Laxemar 1988	KLX01	458.5	0.05	2	350	2.25± 0.85	70 ±29	3.3±2.3	b.d.	2.85±0.85	32±13	0.028	0.027	

		458.5	0.2	1	350	13	162	2.9	b.d.	8.9	34	0.028	0.027	
		458.5	0.4	1	350	6.9	67	6	b.d.	4.6	21	0.028	0.027	
Laxemar	KLX01	691	0.05	2	385	4.7±1.8	574 ±66	3.6±0.75	b.d.	1.7±1.7	47±0	0.048±0	0.037±0	
		691	0.2	1	385	63	749	10	b.d.	14	78	0.048	0.037	
		691	0.4	1	385	23	338	394	6.2	46	34	0.048	0.037	
Laxemar	KLX01	691	0.05	2	400	b.d.	274.5± 23.5	7.4±0.4	b.d.	1.3±0	26.5±2.5	0.154	0.140	
		691	0.2	1	400	b.d.	465	4.3	b.d.	3	20	0.154	0.140	
		691	0.4	1	400	4.5	349	11	b.d.	2.5	29	0.154	0.140	

*below detection limit

**mean value and standard deviation

Appendix 4: Mass balance modelling

Contribution to the model version 1.2

María J. Gimeno, Luis F. Auqué and Javier B. Gómez

Department of Earth Sciences, University of Zaragoza

November 2004

Introduction

For this new Site Descriptive Modelling phase in Simpevarp (Simpevarp 1.2), the chosen formalism has been to include all relevant data in the Simpevarp and Laxemar subareas together with the available information from Äspö (before the tunnel construction) and Ävrö.

Most of the data from the Äspö, Ävrö and Laxemar subareas included in this 1.2 data freeze have been previously used for the geochemical evaluations performed in the framework of the SKB program (e.g. Smellie and Laaksoharju, 1992; Laaksoharju *et al.*, 1995; Laaksoharju, 1997; Laaksoharju *et al.*, 1999). Many samples have also participated in intercomparison projects related to geochemical and hydrogeochemical modelling methodologies (e.g. Luukkonen and Kattialoski, 2001) and to site intercomparison at the scale of the Scandinavian shield (Puigdomenech, 2001). Finally, some of them have been used as basic input data in safety assessment exercises such as SR-97 (Laaksoharju *et al.*, 1998) or SITE-94 (Glynn and Voss, 1999).

There are some additional specific studies where part of these dataset has previously been analysed. The classical work by Grenthe *et al.* (1992) on the redox conditions in the Swedish groundwaters uses several of these samples. Moreover, there are abundant works related to the fracture filling mineralogy in Äspö and Laxemar (Tullborg *et al.*, 1999; Wallin and Peterman, 1999), to the microbiology of some of the boreholes included in this data freeze (Pedersen *et al.*, 1997; Haveman and Pedersen, 2002), and to the associated colloids (e.g. Ducker and Ledin, 1998).

As this short bibliographic review shows, there is an important amount of information available from previous works on the dataset provided for Simpevarp 1.2. This information covers a very broad range of topics, from results on the effective processes operating in the system, to different methodological issues, alternative interpretative hypothesis, geochemical modelling strategies, and multidisciplinary approaches.

This fact frames phase Simpevarp 1.2 in a completely different context from the previous work done for Simpevarp 1.1. The contribution of the authors is now focussed on three main points:

(1) Evaluation of primary data. Here the main hydrogeochemical characters of the studied subareas are analysed as a whole. The analysis is performed following the same methodology (ion-ion plots) used in the previous Simpevarp 1.1 report, but, the internal structure of the chapter is different and is based on the different compositional systems, that is, carbonate, sulphate and silica systems, integrating chemical contents with some geochemical modelling results (SI calculations). This integrated presentation makes much easier the analysis of some specific aspects, which have allowed the proposal of new hypothesis and suggestions, as the meaning of the high sulphate contents in Laxemar (considered problematic in previous works, Laaksoharju *et al.*, 1997), or the evolution of Sr in the more saline groundwaters (not previously analysed, as far as the authors know).

(2) Geochemical modelling. Taking into account the amount of previous works on this topic, efforts have been driven towards two main aspects which, from the authors' point of view, have been less studied:

a. Speciation-solubility calculation in the more saline waters. In Simpevarp 1.2, some water samples in Laxemar subarea have very high ionic strengths (salinities). Under these conditions, the activity coefficient approach for charged species must be verified before modelling.

b. Proposal of a preliminary conceptual model about reaction and mixing-reaction processes involving the aluminosilicate phases. Its study is particularly problematical but unavoidable because they are present as fracture fillings in this system.

(3) Redox processes. Traditionally, the redox state control in the studied groundwaters has been assigned either to iron oxides / oxihydroxides or to sulphides, in most cases excluding each other. The analysis performed by the authors in Simpevarp 1.1 (and Forsmark 1.1), suggests that the control is mainly exerted by the sulphidic system in detriment of the iron system. The increase in the number of samples from different subareas and depths has allowed an in-depth reevaluation of the problem.

1 State of knowledge at previous model version

The main findings from the 1.1 phase can be summarised as follows.

The chemistry of fresh, non-saline groundwaters is mainly controlled by water-rock interaction processes. The identified heterogeneous reactions are: a) organic matter decomposition, b) dissolution of calcite, plagioclase, biotite and gypsum (or sulphides), and c) Na-Ca exchange and precipitation of some phyllosilicates, all of them with very low mass transfers. The Cl (132 mg/L) end members in this group show a small contribution from mixing with a marine end member.

As for the saline groundwaters, their chemistry is mainly controlled by the mixing of multiple end members. The mixing process seems to be a combination of a saline end-member (Brine) with several "dilute" end-members. Among these dilute end-members, Glacial Meltwater is always present, with a contribution of 30-50%, together with a meteoric end-member with a similar contribution. The presence of a marine end-member (Litorina or Sea Sediment) is not clear because it always appears in low proportion (< 17%). The heterogeneous reactions identified during mixing include organic matter decomposition, dissolution of plagioclase, biotite and Fe-chlorite (or Fe $(OH)_3$), precipitation of calcite, illite and SiO_2 phases (or phyllosilicates), the possible actuation of bacterial sulphate reduction processes with the simultaneous precipitation of iron sulphides, and, finally, ionic exchange between Na and Ca.

2 Evaluation of primary data

For this new Site Descriptive Modelling phase in Simpevarp (Simpevarp 1.2), the chosen formalism has been to include all relevant data in the Simpevarp and Laxemar subareas together with the available information from Äspö (before the tunnel construction) and Ävrö. This dataset was supplied by SICADA as Data Freeze 1.2, and includes old (Data Freeze 1.1 and pre-Data Freeze 1.1) and new (post-Data Freeze 1.1) samples. The number of samples included in this data freeze is shown in Appendix A[1], separated by subareas, indicating the number of samples with complete chemical data and the number of representative samples.

The dataset consists of 1518 water samples (Table 1): 964 from Simpevarp, 302 from Laxemar, 152 from Äspö, and 100 from Ävrö. Samples reflecting surface conditions (precipitation, streams, lakes and sea water) comprise a total of 822 samples (766 from Simpevarp and 56 from Laxemar). Of the remaining 696 samples from the four subareas, 63 samples are from percussion-drilled boreholes and 633 from core-drilled boreholes; some of these borehole samples represent repeated sampling from the same isolated location or samples in a non-packered, open borehole (tube sampler; 168 samples) and shallow soil pipe waters (23 samples).

From the total dataset only 174 surface samples and 144 groundwater samples were analysed for all the major elements, stable isotopes and tritium at the time of Data Freeze 1.2. There are some samples with additional information, mainly on colloids, dissolved gasses and microbes, which are also shown in table 1. This means that 21% of the samples could be used for a detailed evaluation concerning the origin of the waters. However, not all these samples have actually been used for the evaluation. According to the work done by Smellie and Tullborg (this issue) regarding the representativity of the groundwater samples, only 81 out of 144 samples with complete chemical data have been considered representative. How this dataset has been used in the different models is listed in Appendix B.

Analysed data include the same set of parameters as in the previous stage (see table of chemical analysis). The pH and conductivity values used in the following were the ones determined in the laboratory. There are no data for Eh and temperature for the surface waters but there are some continuous logging Eh, pH and temperature data from several boreholes at different depths. The selected Eh, pH and temperature values are included in the table of the chemical analysis.

2.1 Representativity of the data

This analysis is presented in Smellie and Tullborg (this issue).

2.2 Explorative analysis

Following the same approach in groundwater modelling as used in the previous stage (Simpevarp 1.1), the evaluation of this new set of data started with the explorative analysis of different groundwater variables. The evaluation already reported in version

[1] Tables A-1 to A-4 show the number of samples included in the 1.2 data freeze. Tables A-5 to A-7 include the samples taken after 1.1 data freeze.

1.1 (mainly for Simpevarp subarea) will not be repeated here[2]. However, all the new observations and conclusions derived from the analysis of the four subareas will be clearly shown. Moreover, in this second stage the improved knowledge of the local and regional geology and mineralogy will serve as a background to interpret the evolution of the groundwater.

2.2.1 Evaluation of scatter plots for conservative and some non conservative elements

The hydrochemical data have been graphically displayed using X-Y plots to derive trends that may facilitate interpretation. Since chloride is generally conservative in normal groundwaters, its use is appropriate to study hydrochemical evolution trends when coupled to ions, ranging from conservative and non-conservative, to provide information on mixing, dilution, sources and sinks. Moreover, here, chloride acts as a tracer of the main irreversible process operating in the system --mixing--, which will be demonstrated below. Many of the X-Y plots therefore involve chloride as one of the variables. What follows is a preliminary evaluation of the various geochemical trends apparent in the POM area groundwaters.

The evaluation of the hydrogeochemical data uses all representative samples jointly in order to understand the overall large-scale dynamics and evolution of the system. However, in some cases, the evaluation will be focused on particular groundwater samples.

As a general rule chloride increases with depth but it shows a different trend in Laxemar than in the other three subareas (Simpevarp, Äspö and Ävrö; Figure 2-1). Considering only representative samples from the Simpevarp subarea (there are no representative samples deeper than 580 m), chloride gradually increases with depth up to 10 g/L. Äspö and Ävrö samples (up to 1000 and 750 m depth, respectively) show the same progressive increase, but reach chloride contents up to 12 g/L. Laxemar, although close by, is representative of a more mainland environment and involves greater depths. As we already pointed out in the previous report[3] (Laaksoharju *et al.*, 2004a), the Laxemar data show dilute groundwaters extending to approx. 600 m and for KLX02 to around 1000 m before a rapid increase in salinity to maximum values of around 47 g/L Cl at 1700 m. There are still not enough data from Simpevarp (nor from Äspö or Ävrö) to check whether groundwaters there will follow the same rapid increase in salinity with depth as in Laxemar.

[2] In fact, as it can be seen in Table A-7, there are only 7 new representative groundwater samples from the Simpevarp subarea. Fortunately, they correspond to groundwaters deeper than those available for Data Freeze 1.1.

[3] There is only one new representative groundwater sample from Laxemar and it corresponds to a shallow depth (0-200 m).

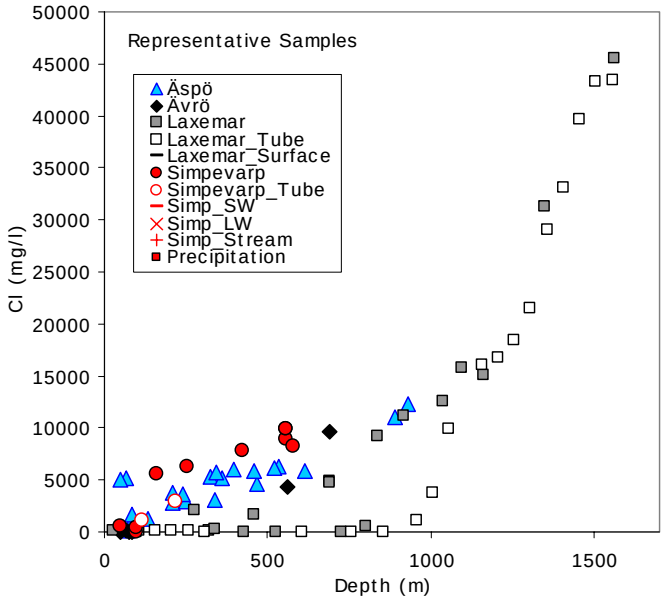

Figure 2-1: *Evolution of chloride with depth in the four subareas of POM (Simpevarp Laxemar, Äspö and Ävrö).*

Bromide shows a linear increase with chloride, indicative of a common geochemical origin for both (Figure 2-2a). Saline groundwaters have a higher bromide content than present Baltic or estimated Litorina Sea waters. They have rather homogenous Br/Cl ratios (higher than sea water, Figure 2-2b) supporting a non-marine origin for the saline groundwaters.

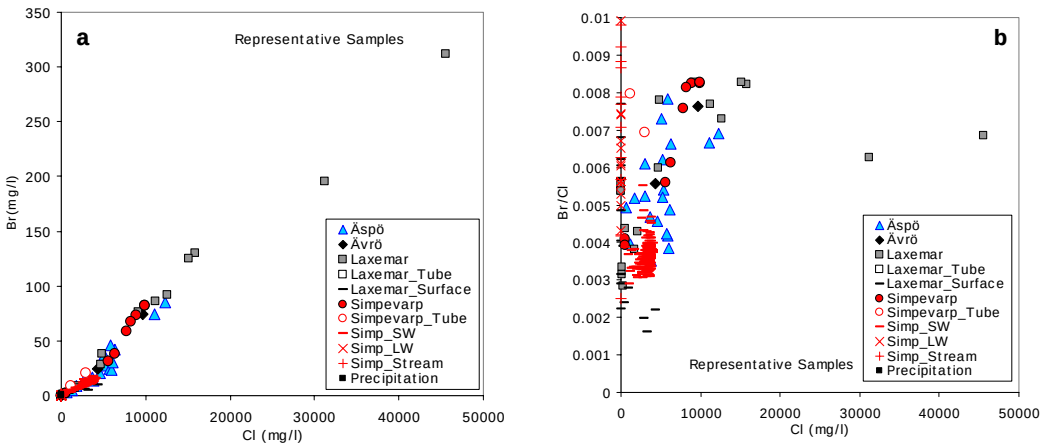

Figure 2-2: *Bromide vs. chloride (a) and Br/Cl ratios (b) in waters from POM area.*

Sodium shows a positive and very good linear correlation with chloride concentration (Figure 2-3), which reflects that mixing is the main process controlling Na content. The deviation of representative groundwater samples from the sea water dilution line can be interpreted as mixing with a saline end member (green triangle labelled “Brine” in Fig. 2.3). This is clearly seen in Laxemar samples (Cl>10000mg/L), which show a conservative behaviour for this element. Simpevarp samples show sodium contents following a line with a slope between SWDL and the line followed by Laxemar samples.

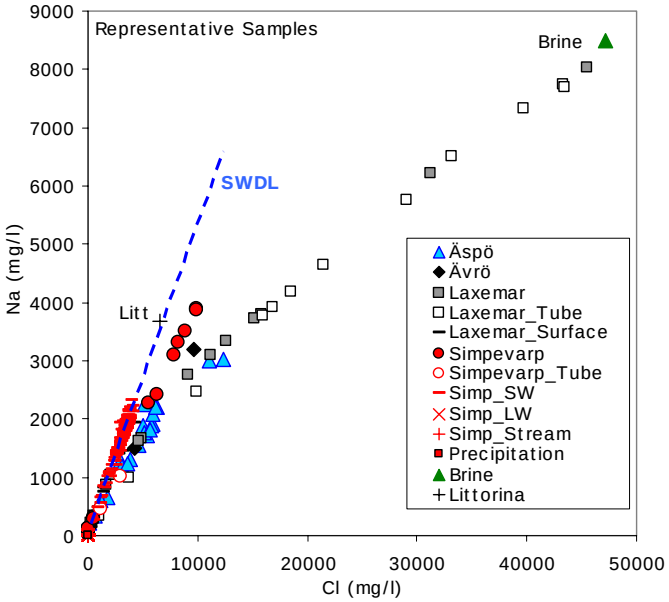

Figure 2-3: *Plot of Na vs Cl for POM area.*

Lithium also shows a linear increase with chloride suggesting a control by mixing. However, its more scattered trend (Figure 2-4) seems to indicate a locally important additional reaction processes such as dissolution of micas (e.g. biotite) and/or ion-exchange in smectite[4].

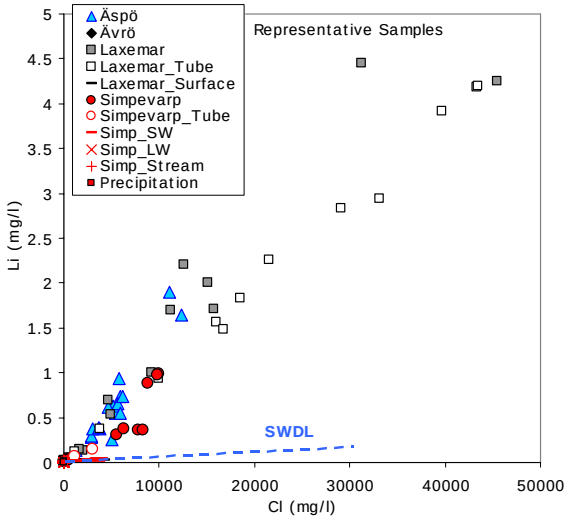

Figure 2-4: *Lithium vs. chloride in waters from POM area.*

Strontium shows a good positive correlation with increasing chloride concentration and even better with increasing calcium (Figures 2-5 a and b). The Cl-Sr linear behaviour points to mixing as one of the main processes controlling Sr and Ca contents, with a common geochemical source (brine). This quasi-conservative behaviour is further discussed below.

[4] Fracture filling/coating mineral identified in Simpevarp in low proportions but with an important specific area.

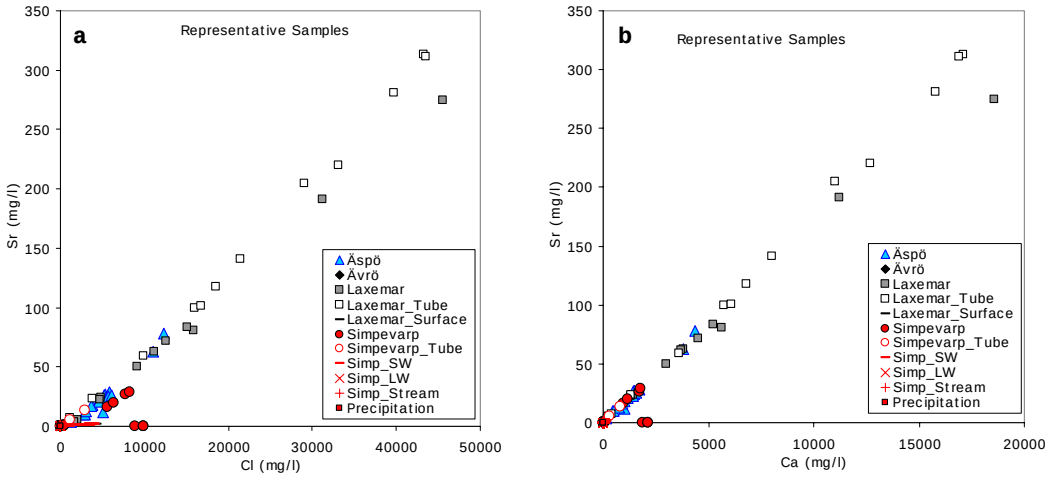

Figure 2-5: *Strontium vs. chloride (a) and calcium (b) in waters from POM area.*

The potassium content in groundwaters (Figure 2-6 *panel a*) increases very slowly with depth (and with chloride), keeping always below the sea water dilution line. This behaviour is common to the four subareas (except two samples from Äspö and two from Simpevarp[5]) showing a global dilution trend towards the saline end member (Brine) although slightly below it. This may reflect the influence of mixing with a saline component in saline groundwaters from Laxemar. Additional water-rock interactions seem to be controlling this element (reaction with clay minerals, or cation-exchange) as suggested by the scattered brackish waters with less than 10000 mg/L Cl.

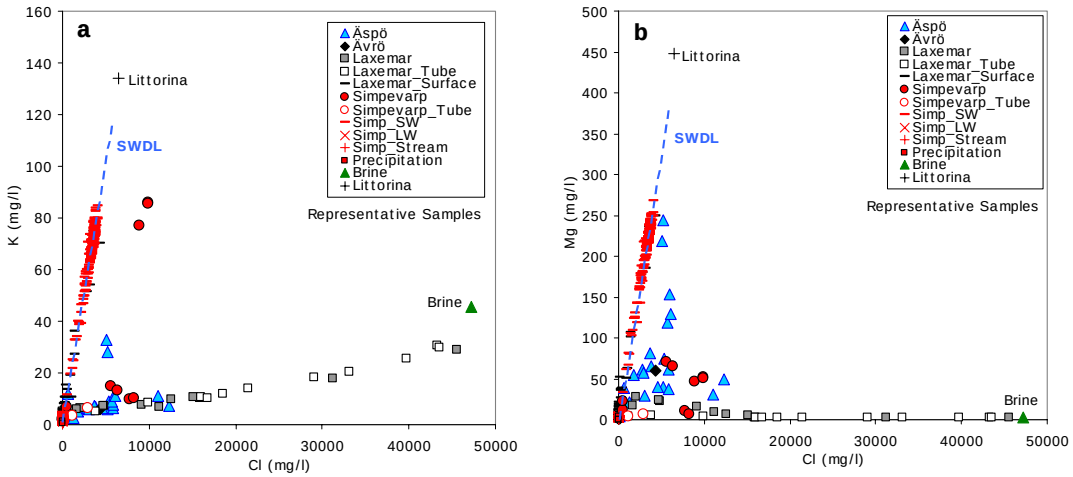

Figure 2-6: *Potassium and magnesium vs. chloride in water samples from POM area.*

Magnesium (also below the SWDL, Figure 2-6 *panel b*) shows a steeper increase with depth in the shallower groundwaters, mainly in Äspö samples, probably related with a Littorina component (Laaksoharju and Wallin, 1997). Deeper groundwaters, however, show a decrease in magnesium, following a trend towards the saline end member. This trend suggests the influence of a magnesium-depleted saline component. The broad scatter, in the 1000-10000 mg/L Cl range, suggests that reactions involving chlorite and montmorillonite could have been operative. Initial K and Mg enrichment in fresh waters

[5] The two samples from Äspö can be the result of mixing with a marine component. The two anomalous samples from Simpevarp are the same with anomalously low Sr content (Figure 2-5) and it seems to be the result of analytical problems for these two elements.

(obscured by the graph scale) is probably caused by mineral weathering (micas, K-feldspars, etc.) in surface conditions.

2.2.2 Evaluation of scatter plots for the calcium carbonate system

Under this heading the evaluation of the main parameters controlling the carbonate system (pH, alkalinity, CO_2 and calcium) is included. Some PHREEQC modelling results (saturation indexes and pCO_2 values) are also included here in order to simplify the description and make the interpretations clearer.

Superficial fresh waters show a wide range of pH values as a consequence of their multiple origin (Figure 2-7). The lowest values are associated with waters with a marked influence of atmospheric and biogenic CO_2; the highest values (up to 8.5 pH units) are associated with the most diluted groundwater. Overall this gives a decreasing trend with chloride when the rest of the groundwater samples are taken into account. Nevertheless, this trend is affected by uncertainties in pH measurements in the laboratory and there are not enough data from continuous logging pH measurements (apart from the analysis reported in phase 1.1) to check them.

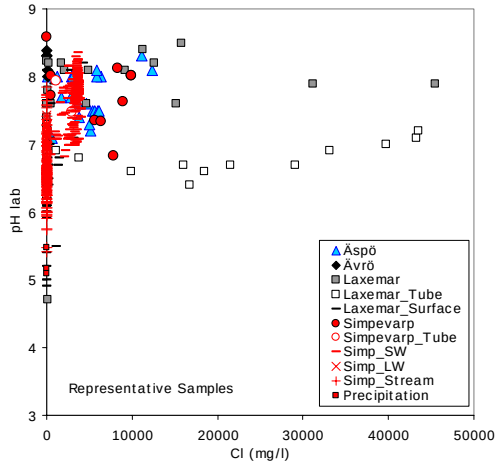

Figure 2-7: *pH vs. chloride content in mg/l (increasing with depth) in POM waters.*

Alkalinity (HCO_3^-) is, together with chloride and sulphate, the third major anion in the system, and is the most abundant in the non-saline waters. Its concentration increases in the shallower groundwaters (Figure 2-8a) as a result of atmospheric and biogenic CO_2 influence and/or calcite dissolution. The alkalinity content reaches equilibrium (or oversaturation) with calcite in the fresh groundwaters (Figures 2-8a and 2-9a) and then decreases dramatically with depth as it is consumed by calcite precipitation, whereas calcium keeps increasing as a result of mixing (Figure 2-8b).

As can be seen in Figure 2-8b, calcium shows a good positive correlation with increasing chloride concentration in saline groundwaters, suggesting that mixing is the main process controlling this element. In spite of the extent of reequilibrium with calcite affecting Ca, the high Ca content of the mixed waters (coming from the brine end member) obliterates the effects of mass transfer with respect to this mineral. This fact justifies the quasi-conservative behaviour of calcium, at least in waters with chloride contents higher than 10000 mg/L. Simple theoretical simulations of mixing between a brine end member and a dilute water, with and without calcite equilibrium, have shown the negligible influence of reequilibrium on the final dissolved calcium contents.

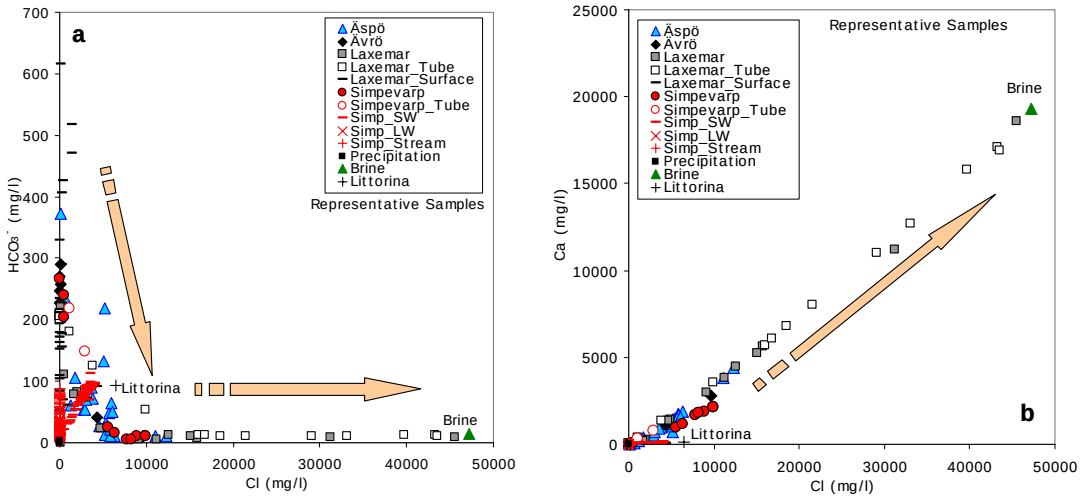

Figure 2-8: *Alkalinity(a) and calcium (b) vs. Cl in waters from POM area*

Figure 2-9 shows the calcite saturation index in the groundwaters. The alkalinity trend described above can be readily explained by looking at this plot. The uncertainty associated with the saturation index calculation (±0.5) is higher than that usually considered (±0.3). This is due to problems during the laboratory measurements of pH (CO_2 outgassing and ingassing), as was described in the report for the previous phase (Laaksoharju *et al.*, 2004a).

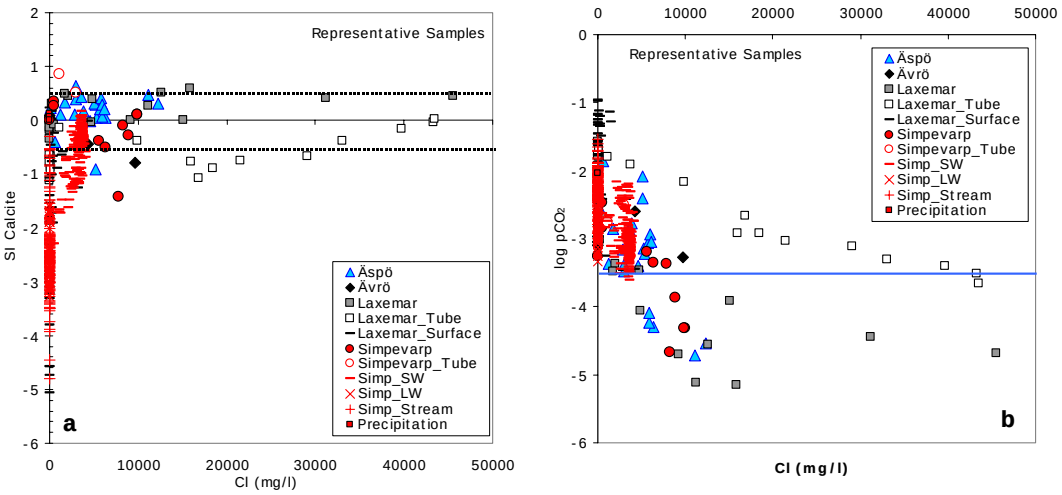

Figure 2-9: *Calculated calcite saturation indexes and partial pressure of CO_2 against chloride for waters from POM area. The dashed lines in panel a represent the uncertainty associated with SI calculations. The blue line in panel b represents the atmospheric value.*

2.2.3 Evaluation of scatter plots for the silica system

The content of dissolved SiO_2 in surface waters indicates a typical trend of weathering, while in groundwaters it has a narrow range of variation indicative of partial reequilibrium (Figure 2-10a). The general process evolves from an increase in dissolved SiO_2 by dissolution of silicates in surface waters and shallow groundwaters to a progressive decrease related to the participation of silica polymorphs and aluminosilicates which control dissolved silica as the residence time of the waters increases. This can be clearly seen in Figure 2-10b.

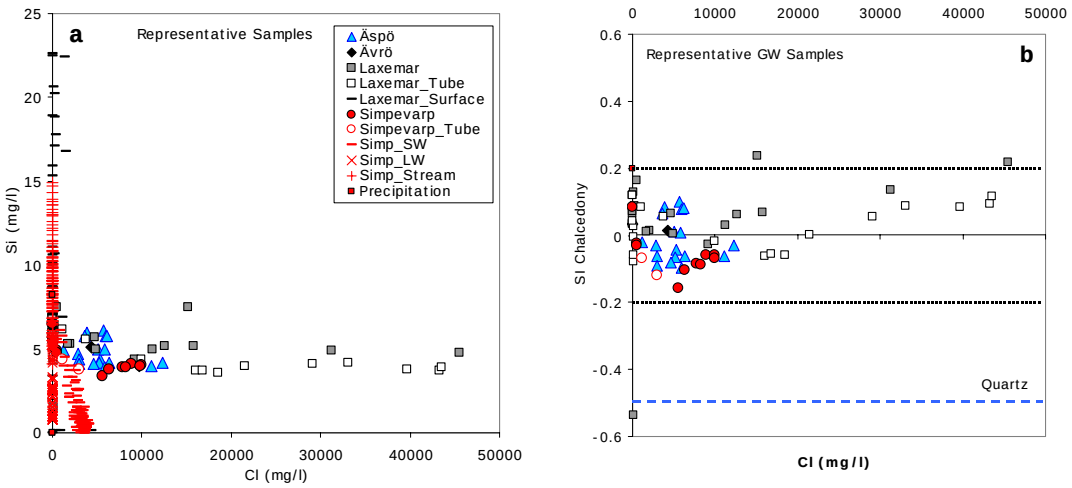

Figure 2-10: *(a) Plot of SiO_2 vs.Cl for all POM waters. (b) Saturation indexes of chalcedony and quartz as a function of Cl in POM waters. The dashed lines represent the uncertainty associated with SI calculations (Deutsch et al., 1982).*

The weathering of rock-forming minerals is the main source of dissolved silica. Superficial waters have a variable degree of saturation with respect to silica phases (quartz and chalcedony), compatible with the weathering hypothesis, and a rather unclear control by secondary phases. This is a rough generalization, useful for this general description but it should be noted that surface waters come from diverse systems (streams, lakes and soil zones) involving contrasting processes (evaporation, biological uptake, etc.; Laaksoharju *et al.*, 2004b) that affect silica concentrations.

Saline groundwaters are oversaturated in quartz and close to equilibrium with chalcedony (Figure 2-10b). Saturation indices are relatively constant and independent of chloride content; this suggests that the groundwater has already reached, at least, an apparent equilibrium state associated with the formation of aluminosilicates or secondary siliceous phases like chalcedony, which seems to be controlling dissolved silica.

The lack of QA aluminium data for Simpevarp groundwaters precludes a speciation-solubility analysis of aluminosilicates. Therefore, activity diagrams were used to study the relationship between silicate minerals and their stability. This analysis will be discussed later (Modelling part, 3.2).

2.2.4 Evaluation of scatter plots for the sulphate system

Figure 2-11a, showing SO_4 vs Cl, indicates an obvious modern Baltic Sea water dilution trend affecting the groundwater samples (from the four subareas) representing a separate saline dilution trend already pointed out in the previous phase. In general, these groundwater data lend support to the absence of a significant postglacial marine component, suggesting instead the mixing with deeper, more saline waters of a non-marine origin. Perhaps the most interesting aspect is the different evolution shown by sulphate in all POM waters (which increases with salinity), with respect to sulphate behaviour in other sites. Figure 2-11b shows the sulphate contents in Olkiluoto and Forsmark[6] sites. In both cases, after an initial increase in sulphate (reaching the

[6] Forsmark data are more limited in salinity than Olkiluoto data, but the trend shown by the more saline waters in Forsmark follows the same evolution.

maximum values when salinity is around 5000-6000 mg/L of Cl) there is a clear decrease towards zero. For the same chloride content, sulphate concentration in the POM area is clearly higher.

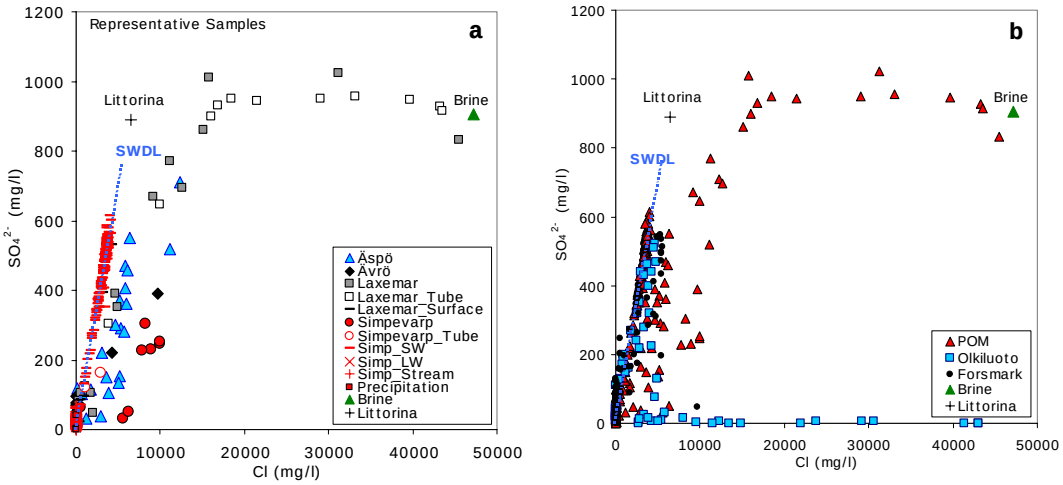

Figure 2-11: *(a)Plot of SO_4 vs Cl for all POM data. (b) Plot comparing POM data with Forsmark and Olkiluoto samples.*

This contrasting behaviour must be related to the process controlling the sulphate content in these waters. Analysing the saturation state of waters with respect to gypsum some conclusions can be drawn. This analysis was also done for the previous phases (Simpevarp 1.1 and Formark 1.1) but the results there indicated that the waters were clearly undersaturated with respect to gypsum, so the plot was not included in the report (Figure 2-12b). In this phase, as the range of salinity in the samples has increased, an interesting behaviour can be observed. For the whole set of POM groundwaters, the gypsum SI trend indicates a clear evolution towards equilibrium (Figure 2-12a) which is reached at chloride values of 10000 mg/L and maintained even in the most saline waters. This equilibrium, defined mainly in the most saline and deepest groundwaters from Laxemar, introduces a new controlling phase in the groundwater system. Moreover, it can help to solve the uncertainties reported in previous works (Laaksoharju and Wallin, 1997) on the odd sulphate behaviour in Laxemar waters. In fact, Laaksoharju *et al.* (1995) reported the presence of gypsum as a fracture filling mineral in this subarea, though in small amounts. In addition, the influence of gypsum as sulphate limiting phase has been already reported in the Canadian Shield (Gascoyne, 2004).

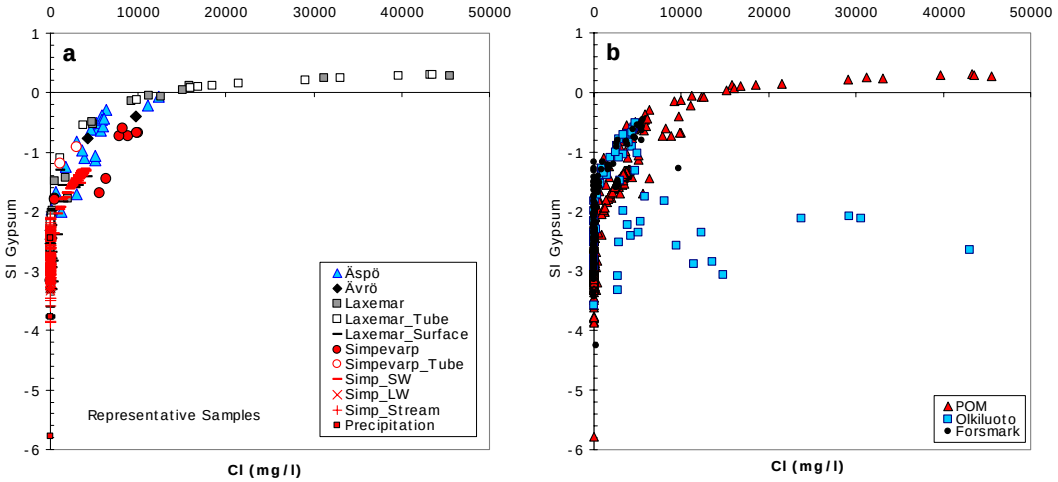

igure 2-12: *(a)Plot of Gypsum saturation index vs Cl for all POM data. (b) Plot comparing POM data with Forsmark and Olkiluoto samples.*

The behaviour of other sulphate minerals, like celestite ($SrSO_4$), was also checked. Figure 2-13a shows the saturation index calculated for these waters with respect to celestite. The SI trend is similar to the one shown by gypsum and, therefore, celestite should be considered as another possible new controlling phase in this groundwater system. As far as the authors know, celestite has not been identified in the system.

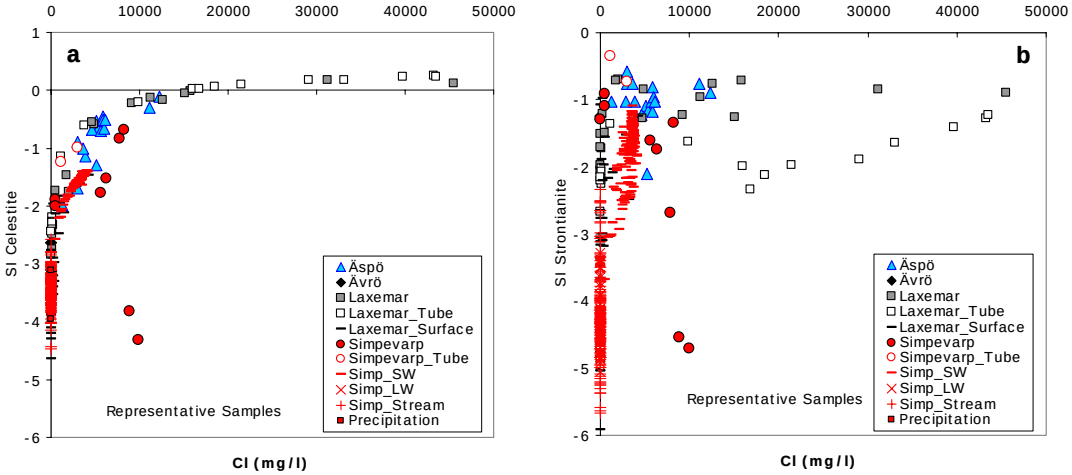

Figure 2-13: *Celestite(a) and Strontianite (b) saturation indexes vs Cl for all POM data.*

SI calculations indicate that celestite and gypsum saturation is approached when Cl > 10000 mg/l. As these high-chloride waters are in equilibrium with calcite, the application of the Gibbs phase rule to the $CaCO_3$-$SrCO_3$-$CaSO_4$-$SrSO_4$ system (at constant T and P) indicates that these waters cannot be in equilibrium with strontianite ($SrCO_3$). At calcite, gypsum and celestite equilibrium, the strontianite saturation index is defined for a particular T and P by:

$$SI_{strontianite} = \log \frac{k_{calcite} k_{celestite}}{k_{gypsum} k_{strontianite}}$$

Using thermodynamic data from WATEQ4F database, the SI for strontianite is expected to be near –1.2 (15ºC), which fits the observed values very well (Figure 2-13b).

As a result of these new observations, it is worth considering that Ca and Sr (clearly related by mixing and reaction processes, as their good linear correlation suggested, Figure 2-5) could be controlled by gypsum and celestite. Figure 2-14 shows the same good relation between Ca and Sr in Forsmark and Olkiluoto. The only difference is the slope of the line.

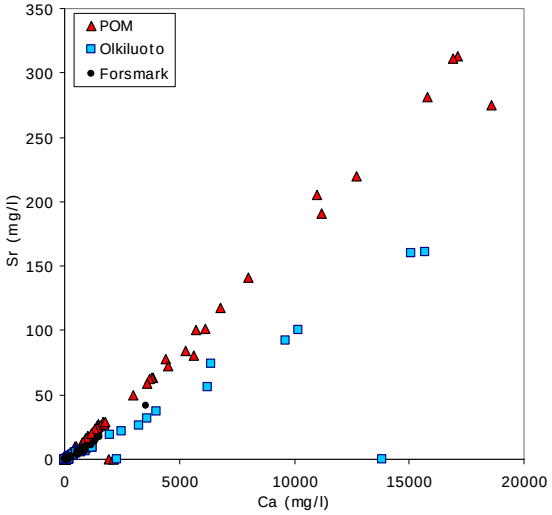

Figure 2-14: *Strontium vs. calcium in waters from POM area, Forsmark and Olkiluoto.*

This difference is even more evident in Figure 2-15 where Ca/Sr molar ratio has been plotted against salinity for the POM waters in panel (a) and for POM, Forsmark and Olkiluoto in panel (b). Ca/Sr ratios in surface and shallow groundwaters show a very wide range of variation for the three sites. This is easily explained as a result of the weathering of different rocks, minerals and, therefore, Ca/Sr ratios.

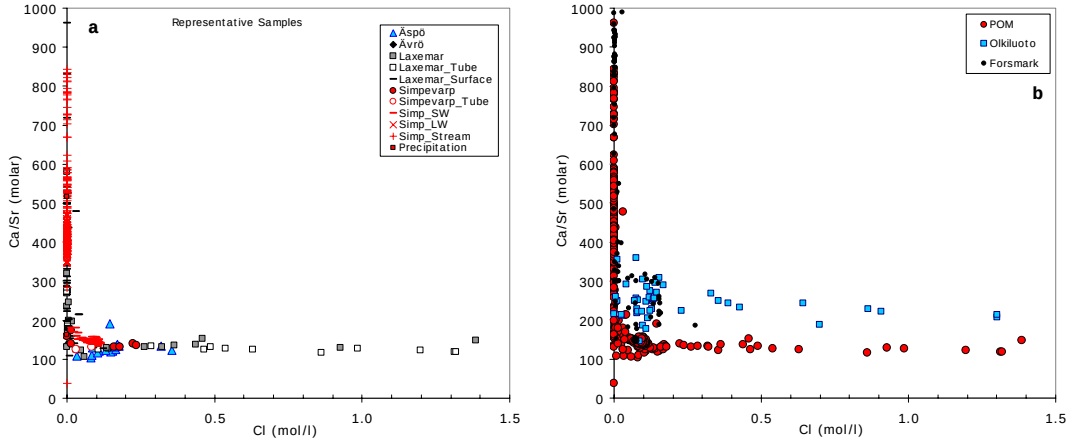

Figure 2-15: *Ca/Sr molar ratios in waters from POM area (a) and together with Forsmark and Olkiluoto.*

As for the groundwaters, Ca/Sr ratios show a constant value of around 120 for salinities higher that 0.1 mol/l Cl in the POM area. Though also showing a constant value for the same ranges of salinities, Olkiluoto waters (with a broader range of salinity than Forsmark) have a Ca/Sr ratio of around 230. The most interesting observation here is that these ratios agree with those in their respective brine end-members.

This suggests that in the more saline groundwaters, elements (in this case Ca and Sr) are inherited from the saline end-member and controlled by mixing, in spite of the specific

equilibrium situations (as has been found in the POM area). Another conclusion can be drawn: this situation of equilibrium must produce only small mass transfers compared with the contents of the mixed waters.

3 Geochemical Modelling

Speciation-solubility calculations (some already described in the explorative analysis) and reaction-path modelling have been carried out with PHREEQC (Parkhurst and Appelo, 1999) using the WATEQ4F thermodynamic database[7]. The principles of speciation-solubility calculations were described in the previous report (Laaksoharju *et al.*, 2004). The specific reaction-path calculations performed here will be presented later.

Geochemical modelling calculations are used to investigate the processes that control water composition at the POM area.

This chapter is divided into three main sections dealing with: (a) the validity check of the thermodynamic code PHREEQC when working with the most saline waters included in the dataset; (b) the consequences of mixing and reaction for some problematic minerals in the aluminosilicates-system; and (c) the redox state of the system.

3.1 High Ionic Strength waters

When modelling high saline waters the validity of the approach used to calculate the activity coefficients must be checked. In PHREEQC this approach depends on the database selected for the calculations. With WATEQ4F database the model used is the same implemented in all the USGS geochemical codes from the old WATEQ onwards (hereinafter USGS approach), that is: (a) for Ca, Mg, Na, K, Cl, SO4, HCO3, CO3, H2CO3 and Sr, Truesdell & Jones' activity coefficient equation (or WATEQ-type Debye-Hückel); and (b) for the other species (for which the required data to implement the previous activity model are lacking) the extended Debye-Hückel or the Davies equation. Regarding the validity of the USGS approach, most geochemical text books report that Truesdell & Jones' approach is valid up to 4-6 molal ionic strength. This is only true for simple solutions (Na-Cl dominated solutions). For complex solutions, when ion pairing increases, the USGS approach "mixes" the T-J equation for the main species with the Davies equation for the other species, decreasing the validity of the approach as a whole. For these complex solutions, the suggested limit of application of the USGS approach is 2 molal. But our own experience in geochemical modelling of natural brines (comparing approaches and using many different codes) suggests that the validity of the USGS approach must be also verified in the range 1-2 molal.

In the previous phase this analysis was not necessary as all Data Freeze 1.1 Simpevarp groundwaters were below 0.3 molal, clearly in the range of the USGS approach validity. However, the inclusion of Laxemar groundwaters in this new dataset makes this analysis necessary as they reach ionic strengths of 1.8-1.9 (similar to the Brine end member). For these values, the use of other approach is justified and is presented here. The most suitable approach for this kind of solutions is Pitzer's formalism for the activity coefficient calculations. The geochemical code PHRQPITZ (Plummer *et al.*, 1998) implements Pitzer's formalism, and its results have been compared with those obtained by PHREEQC with WATEQ4F database.

[7] The selection of this thermodynamic database is justified in Appendix B.

To properly perform the comparison, the solution density must be taken into account. This parameter is not directly measured in groundwaters and therefore, a computer code was used (SOLDEN, Sánchez Moral, 1994) to calculate it using the Redlich-Meyer equation.

First of all, the density calculation was tested with some saline groundwaters from Olkiluoto (only slightly less concentrated than the more saline Laxemar groundwaters) for which the density has been measured. The results of this test are shown in table 3-1. Table 3-2 shows the calculated density for the three most saline Laxemar samples (at the temperature measured in the borehole) and for the Brine end member (at 25ºC).

The three saline samples were fed into PHREEQC and PHRQPITZ together with the calculated densities, and the main results are compared in table 3-3.

Table 3-1*: Calculated density values for some Olkiluoto saline groundwaters. Comparison with the measured values.*

	Measured	Calculated density
KR12/737/1	1.033	1.031±0.001g/cm3
KR12/747/1	1.035	1.033 ±0.001g/cm3

Table 3-2*: Calculated density values for some Laxemar saline groundwaters and for Brine end member.*

sample	Calculated density
2731	1.05±0.002g/cm3
2931	1.033 ±0.002g/cm3
2722	1.021 ±0.002g/cm3
“Brine”	1.051 ±0.002g/cm3

Table 3-3*: Calculated ionic strength and saturation indexes for three saline samples from Laxemar using the approach included in PHREEQC AND PHRQPITZ.*

	2731		**2931**		**2722**	
	PHREEQC	PHRQPITZ	PHREEQC	PHRQPITZ	PHREEQC	PHRQPITZ
Ionic Strength	1.79	1.81	1.15	1.18	0.59	0.61
SIcalcite	0.74	0.71	0.44	0.49	0.64	0.61
SI gypsum	0.18	0.033	0.20	0.074	0.09	0.03
SI celestite	0.04	-0.093	0.13	0.05	-0.5	-0.11

The first row shows that the calculated ionic strength is almost the same with the two codes. The same is valid for the calcite saturation index. However, there are some differences, as expected, in the SI of the sulphate mineral phases gypsum and celestite. For both minerals (in the three samples) the saturation index calculated by PHRQPITZ (the most suitable approach for these solutions) indicates a numerical saturation closer to equilibrium than the results from PHREEQC. However, even these differences are inside the precision range accepted for this kind of phases(± 0.2 SI units). These results strengthen the hypothesis of sulphate minerals as controlling phases in deep saline waters.

Moreover, they confirm the validity of PHREEQC to calculate the activity coefficients of the saline waters studied here. They are sodium-chloride waters in which the concentration of the other main components is not high enough to produce important deviations in the Truesdell and Jones’ equation.

3.2 The aluminosilicate system

The mineralogical results from KSH01A + B have demonstrated the presence of a complex sequence of fracture fillings. Apart from chlorite and calcite, epidote, prenhite, laumontite, Ba-zeolite, adularia, albite, hematites and pyrite have also been reported. Small amounts of outermost coatings with smectite, interstratified clay minerals and illite, with high surface area, have also been identified. This set of minerals is common to the other subareas (e.g., Äspö).

Besides the granite rock forming minerals, some of these fracture filling phases are aluminosilicate minerals with which waters have been in contact during their geochemical evolution. Therefore they are important water-rock interaction phases. However, as already pointed out, the lack of aluminium data for POM groundwaters precludes a speciation-solubility analysis, limiting their analysis to stability diagrams.

The accuracy of these diagrams depends on pH and is therefore affected by uncertainties in its value. Uncertainties in the equilibrium constants of the aluminosilicates (especially the phyllosilicates) also affect the conclusions drawn from these diagrams and the results of any theoretical model performed with them (e.g. Laaksoharju and Wallin, 1997; Trotignon *et al.*, 1997, 1999). In this context the study of aluminosilicate phases have been limited to those with lower uncertainties and using thermodynamic data that have already given reasonable results in systems similar to the one studied here. That means that the aluminosilicate system here is reduced to adularia, albite, kaolinite, laumontite, prenhite and chlorite, and the selected thermodynamic data are the ones calculated at 15ºC by Grimaud *et al.* (1990) for the Stripa groundwaters.

The following description includes a general evaluation of the POM groundwaters from their position in the stability diagrams and a discussion on the effects of mixing and reaction in the more saline and older groundwaters[8]. This discussion is illustrated with a theoretical equilibrium modelling. The question of the origin of the saline groundwaters (brine end member) is not discussed here, and the model just assumes that they are already in the system, participating in mixing processes. Nevertheless, the last part of this chapter deals with the potential use of this modelling approach to predict the chemical characteristic of these very old saline groundwaters.

3.2.1 The Stripa diagrams

The set of thermodynamic data used to construct the stability diagrams was calibrated for Stripa groundwaters (Grimaud *et al.*, 1990). Figure 3-1 shows the diagrams with Stripa waters plotted. The trends followed by the waters were interpreted as a result of water-rock interaction processes. The authors used chloride as marker of the irreversible process assuming that it was mainly conditioned by reaction with the rock[9]. This control of chloride is the main difference with respect to what is found in the POM waters, where chloride is controlled by mixing.

[8] In this section different diagrams and computer simulations for POM groundwaters are presented, in some of the cases together with other sites (Olkiluoto and Stripa).

[9] Only for the most saline waters (700 mg/l Cl) a mixing component with brines was suggested (Grimaud *et al.*, 1990)

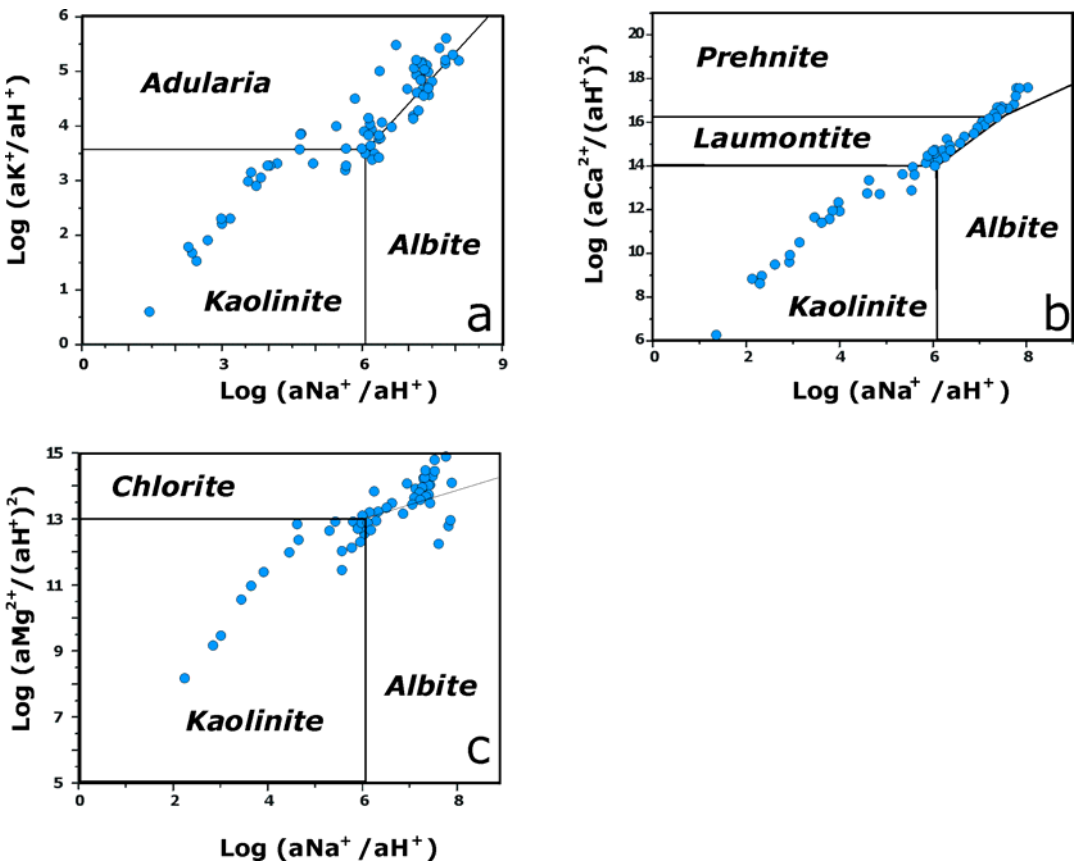

Figure 3-1: *Aqueous activity diagrams for some aluminosilicate minerals at 15ºC, 1 bar. The field boundaries correspond to the data of Grimaud et al. (1990). The displacement from the model line for some of the trends in data could be due to incorrect pH values.*

Figure 3-2 shows the diagram kaolinite-albite-adularia (the same as the one shown in figure 3-1a) for the POM waters. Green and blue arrows show the main trends that can be distinguished. The first trend (green arrows) crosses the kaolinite stability field and goes towards the limit with adularia. This trend is defined by surface and shallow groundwaters. They are modern waters with low chloride contents and whose geochemical evolution is the result of water-rock interaction.

The evolution path of these waters in the kaolinite field shows a slope around 2, typical of weathering-alteration processes in granitic materials. This trend represents the effects of a progressive dissolution of the rock forming minerals (calcite, chlorite, plagioclase, K-feldspars, etc; see the steady increase of the ratios for Ca and Mg in Figures 3-3 and 3-4). Along this process, partial reequilibria with phyllosilicates (e.g. kaolinite) can be reached. Ionic exchange and, finally, calcite precipitation can also take place.

Waters close to or on the kaolinite-adularia boundary would correspond to the more evolved samples in this water-rock interaction process. A special case is certain Laxemar groundwaters, which are very diluted (30-150 mg/L Cl) but at great depths (up to 700 m in KLX02 borehole). The position of these samples in the diagram would support a meteoric origin without a mixing component with more saline waters, but with a residence (reaction) time longer than the shallower groundwaters.

Laxemar waters taken by tube sampling are placed in the kaolinite field but this is uncertain due to the possible "artificial mixing" during sampling, and, probably, to the pH measurements.

The second trend (blue arrow) evolves parallel to the adularia-albite limit indicating an equilibrium situation. Brackish and saline groundwaters from the POM area follow this second trend. This result is very similar to Stripa waters (compare the figures and scale) but there is an important difference: maximum chloride contents in Stripa only reach 700 mg/L, whereas POM groundwaters, plotted in the same position, reach chloride values up to 45000 mg/L. Stripa groundwaters' residence time has been estimated as being approximately 100000 years (Fontes *et al.*, 1989). That means that even in that time, water-rock interaction provides only 700 mg/L of chloride. It is clear, therefore, that an additional source of salinity is needed in the POM waters to justify much higher chloride values in much younger waters. This source is the mixing with a saline component (marine and/or non marine).

Another interesting finding is that in the trend parallel to the adularia-albite limit the range of salinity in the POM groundwaters is very broad, including not only the most saline waters (close to brine end member composition), but also waters with around 5000 mg/L Cl. This points again to the important effects of mixing in these waters, as it has been repeatedly reported in previous works (Laaksoharju and Wallin, 1997; Laaksoharju *et al.*, 1999).

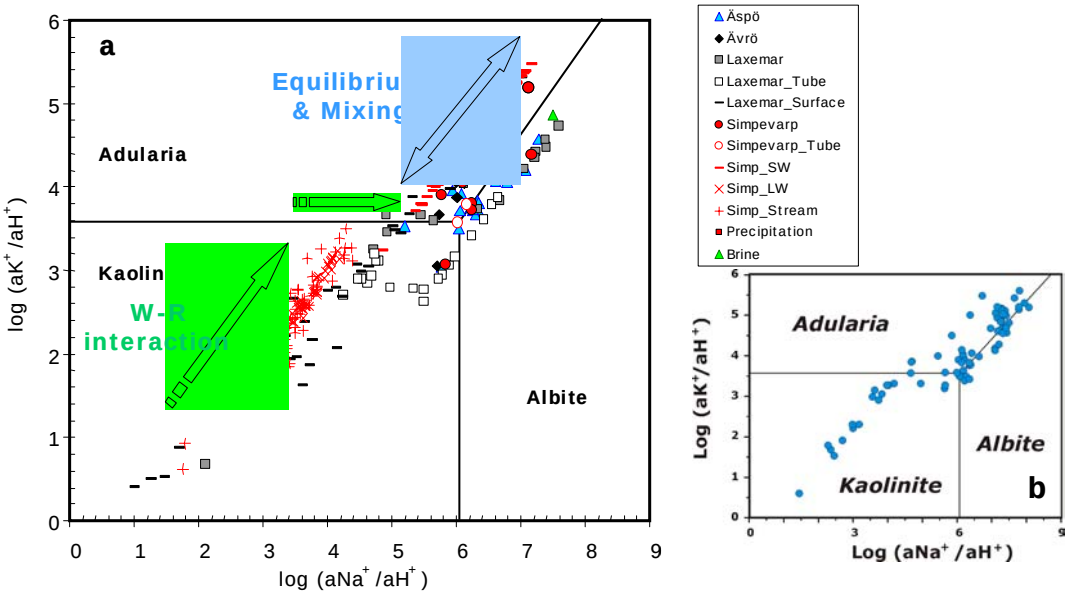

Figure 3-2: *Stability diagrams for kaolinite, adularia and albite in the POM waters (a) and in Stripa groundwaters (b). Saline end member is also plotted in the POM diagram (red triangles).*

The next stability diagram depicts the kaolinite, laumontite, prehnite and albite stability fields (Figure 3-3). Comparing the Stripa and POM trends, it seems that the more evolved POM groundwaters could be in equilibrium with a different laumontite phase (different equilibrium constant) than the Stripa groundwaters. This hypothesis must be tested in future works.

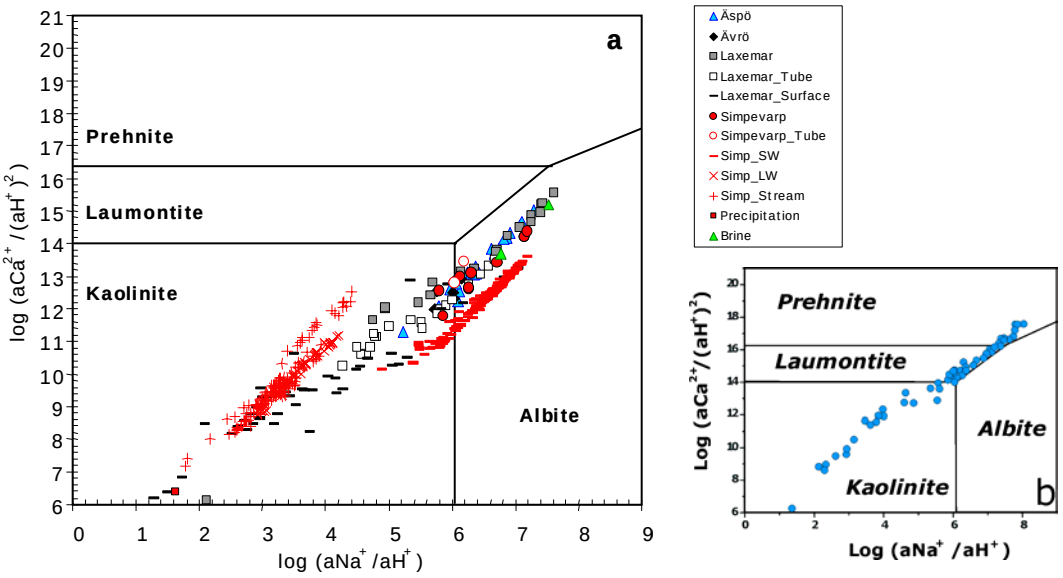

Figure 3-3: *Stability diagrams for kaolinite, Laumontite, Prehnite and albite in the POM waters.*

The third diagram calibrated with Stripa groundwaters shows the kaolinite, chlorite and albite stability fields (Figure 3-4). In this case, saline groundwaters from POM are in the stability field of albite, but some are close to the chlorite border, indicating that this mineral could be a limiting phase at some depth. In any case, it must be taken into account that the chlorite phase used in the diagram is a pure Mg-phase, whereas in Äspö and Simpevarp chlorite shows a greater compositional complexity, with a significant fraction of Fe in reduced form.

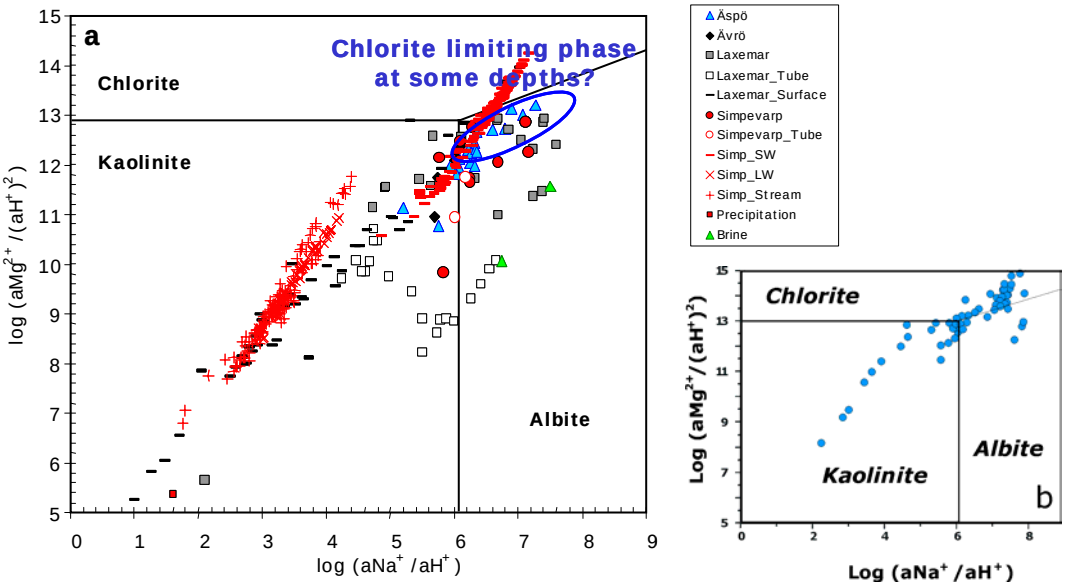

Figure 3-4: *Stability diagrams for kaolinite, chlorite and albite in the POM waters (a) and in Stripa waters (b).*

Some additional stability diagrams were analysed and are presented in Appendix C.

In Figure 3-5 the POM samples have been plotted together with those of Olkiluoto (Pitkänen *et al.*, 2004). Olkiluoto waters occupy the same location as POM waters. Although not presented here, the same match is observed in diagrams 3-3 and 3-4. Olkiluoto samples in the kaolinite stability field and in the kaolinite-adularia boundary

correspond to subsurface or shallow groundwaters whose chemistry is controlled by water-rock interaction. Samples located on the adularia-albite boundary correspond to brackish and saline groundwaters characterised by having undergone complex mixing processes (between Meteoric, Littorina, Glacial and Saline end members, Pitkänen *et al.*, 2004).

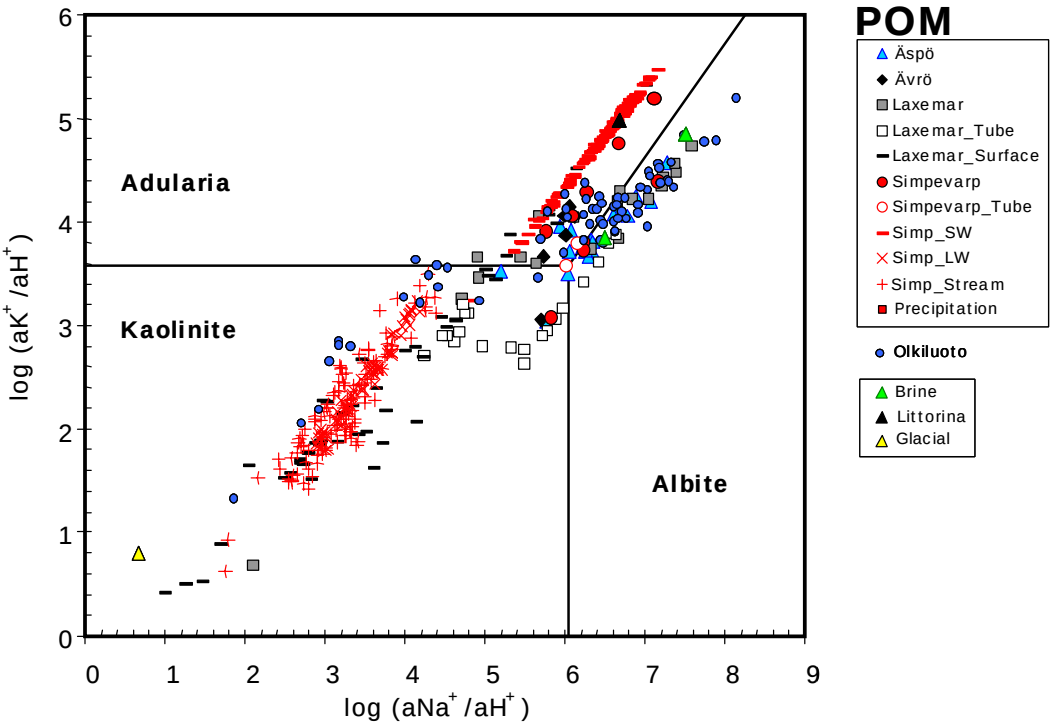

Figure 3-5: *Stability diagram for kaolinite, adularia and albite. Together with the POM waters, the Olkiluoto waters (Pitkänen et al., 2004) and the theoretical end members (Brine, Littorina and Glacial) have been plotted in this diagram.*

The position of the theoretical end members is also shown in Figure 3-5 (Brine, Littorina and Glacial; Meteoric is close to Glacial). It is fairly clear that the evolution path of these waters is the result of (a) reaction between diluted waters (surface and shallow groundwaters) and rock, (b) mixing in depth with more saline groundwaters in different proportions as a function of location and residence time, and (c) the simultaneous interaction of these deep waters with the rock.

3.2.2 Theoretical simulations based on the stability diagrams.

As shown above, POM groundwaters on the adularia-albite boundary include samples with broadly different salinities, chemical contents and depths, but with an apparent similar equilibrium situation. In the first instance, they could be interpreted as the result of different mixing episodes among different end members at different times during the site evolution. Alongside this main process, there would be re-equilibration periods (reaction with rock) following the disequilibrium created by the successive mixing episodes.

The chemistry of the groundwaters is then the result of a complex sequence of mixing and reaction. The relative contribution of the two processes has usually been evaluated by means of inverse mass balance calculations (Laaksoharju *et al.*, 2004a, b; Pitkänen *et al.*, 2004). In this report a direct mixing and reaction calculation has been chosen.

The modelling starts with the assessment of the oldest mixing episode between the saline and the glacial end members (8000-10000 BC). This simulation has a real counterpart in some groundwater samples in the POM area barely modified by subsequent mixing episodes (Laaksoharju and Wallin, 1997). Moreover, these samples represent the best examples of a reequilibrium with the studied mineral phases after mixing.

There is no pH value for the Brine end member and therefore the influence of this parameter in the apparent equilibrium situation has also been modelled. Three different pH values were selected, 7, 8 and 8.5. Figure 3-6 shows the location of the Brine end member with the three different pH values (green triangles). The points lie on a line parallel to and very close to the adularia-albite boundary.

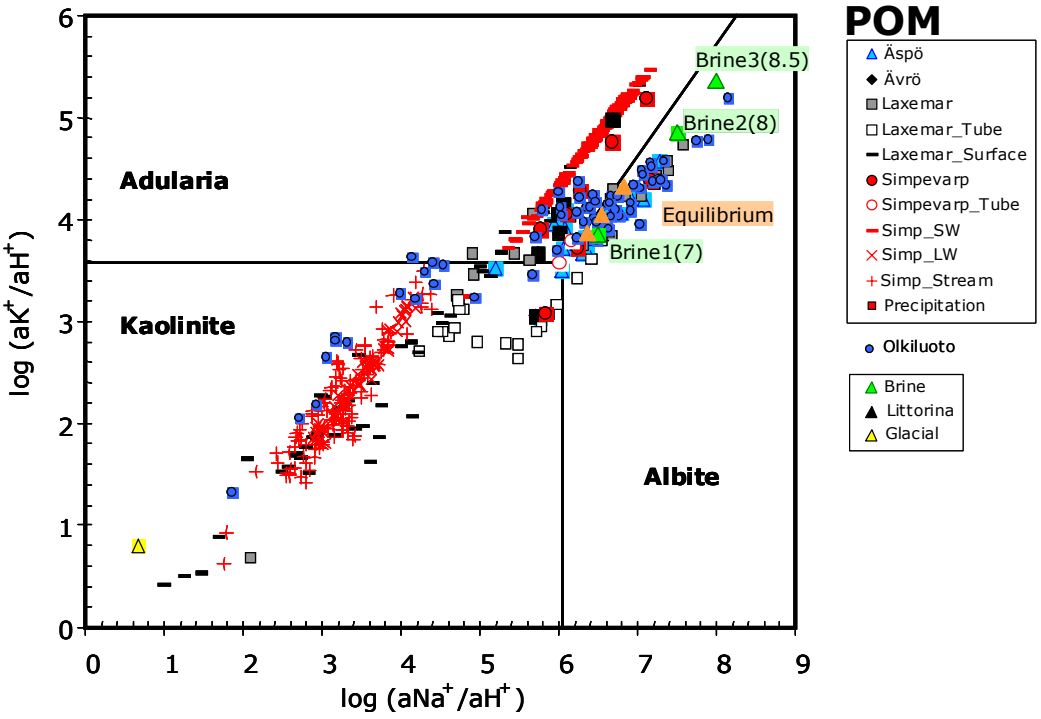

Figure 3-6: *Stability diagram for kaolinite, adularia and albite. In this plot, the result of the equilibrium simulation of the Brine end member (with different pH values) is shown.*

Assuming that this end member had enough contact time with the bedrock to attain equilibrium, the second step in the modelling is the simulation of an equilibrium of the Brine end member (at the three pH values) with a mineral set formed by albite, adularia, calcite and chalcedony[10]. The location of the three different brines *in equilibrium with the selected mineral set* is also shown in Figure 3-6 (orange triangles). They plot on the adularia-albite boundary very close by together. The calculated equilibrium pH values are between 7 and 7.6, a narrower range than the initially considered (7-8.5). This fact indicates that pH uncertainties in the Brine end member represent only a slight displacement parallel to the adularia-albite equilibrium line, making reasonable the assumption of equilibrium with these phases. Moreover, the mass transfer produced during Brine equilibration is negligible, of the order of 0.1-0.001 mmol/L. This

[10] Additional simulations, using different sets of minerals, though not given here, were also performed.

circumstance supports the initial assumption of equilibrium with these minerals in the old brines.

Following the pH sensitivity analysis, a sample was selected as representative of the saline end member (Laxemar #2731 from KLX02 borehole; BL in Figure 3-7), with a measured pH value and a chemical composition similar to the Brine end member.

The next modelling step is a mixing calculation. The saline sample (Saline) was mixed with the Glacial end member (dilute water) in three different proportions: 63% Saline - 37% glacial (Mix 1), 24% Saline-76% glacial (Mix 2) and 5% Saline-95% glacial (Mix 3). The first two mixing proportions coincide with those calculated for samples 2931 and 1773, respectively (Laaksoharju *et al.*, 1995; Laaksoharju and Wallin, 1997). The third proportion has been chosen as an extreme value with a dominant diluted component. The position of these mixed waters is plotted in the stability diagram (Figure 3-7).

After mixing, the equilibrium of the mixed waters with different combinations of calcite, chalcedony, albite, adularia and kaolinite was simulated in order to measure its effects in the final composition of these waters. The results are shown in figures 3-7b, c and d.

Groundwaters that result from simple mixing (in the range of mixing proportions considered here) plot on a line parallel to the adularia-albite equilibrium boundary: Mix 1 plots in the albite field close to the boundary, and Mix 2 and 3 inside the kaolinite stability field. However, sample 1773, which has the same mixing proportions as Mix 2, plots on the adularia-albite boundary and not inside the kaolinite field as predicted by only-mixing[11]. This fact suggests that after mixing some mineral reequilibrium processes have taken place, modifying the position of the mixed samples in the diagram.

Any of the simulated reequilibrium situations lead the waters towards a point in the vicinity of the adularia-albite boundary, even when equilibrium with respect to these phases is not imposed (see, for instance, the position of samples in equilibrium with calcite and chalcedony; Figure 3-7b,c,d). Moreover, all the simulations produced mass transfers not higher than 0.1 mmol/L (Table 3-4). The effects of this mass transfer on the chemical contents of waters is insignificant compared with the effect of mixing for elements such as Na or Ca (and obviously Cl or Br), with variations due to the mixing of hundreds (even thousands) of milimols. The magnitude of the mineral mass transfers obtained from this analysis agrees very well with results obtained from mass balance calculations for this type of mixing processes.

These results indicate that reequilibrium-reaction processes are important in the control of some parameters such as pH, Eh, and some minor-trace elements, and lead the waters towards the adularia-albite boundary. However, the main compositional changes are controlled by the magnitude of the mixing process. Besides, the extent of the reaction processes can be influenced by chloride concentration, also controlled by mixing.

[11] There are no real samples with the same mixing proportions as Mix 3.

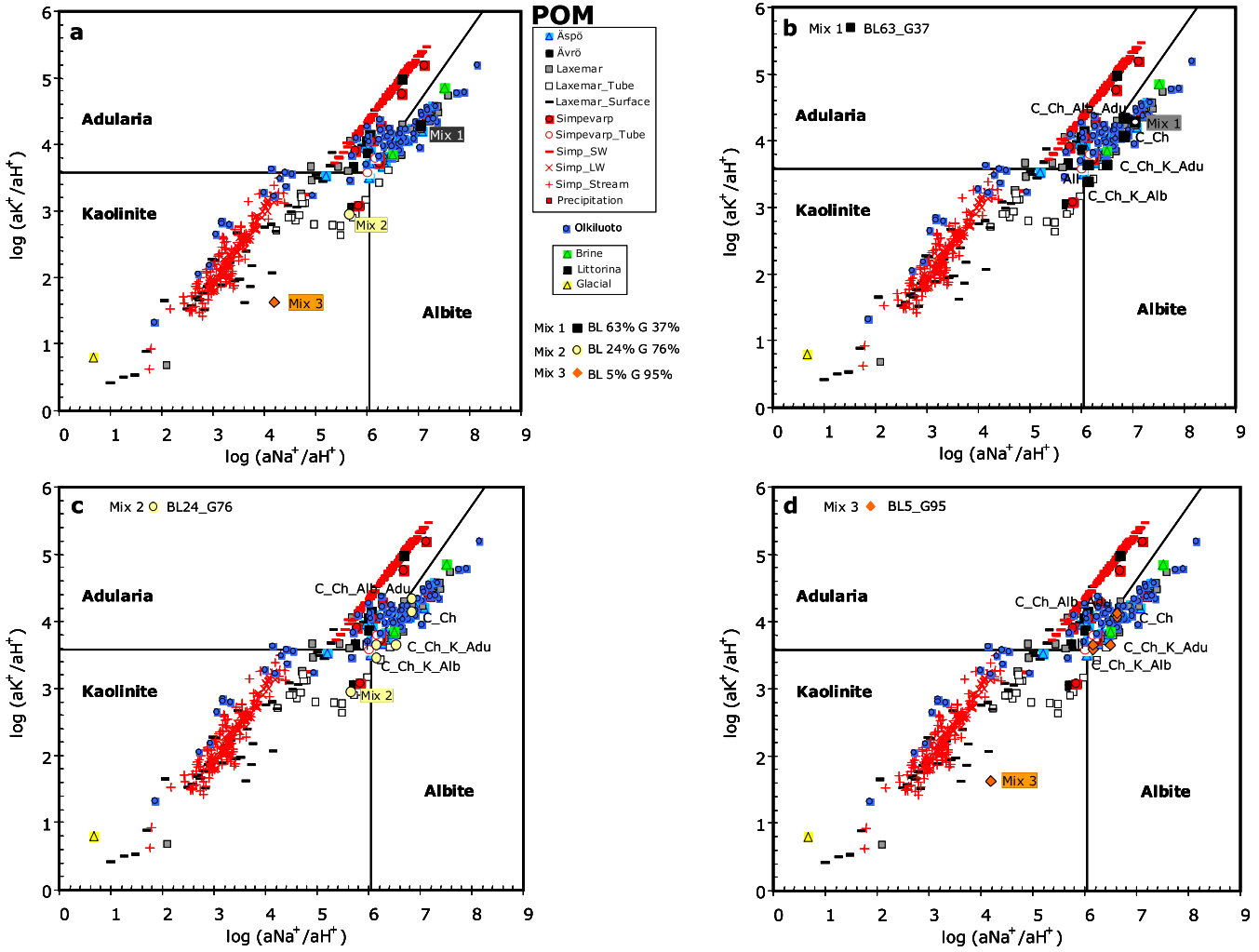

Figure 3-7: *Graphical representation of simulations in the stability diagram for kaolinite, adularia and albite. Location of the samples as a result of (a) a simple mixing processes, (b) Mix 1 and different reequilibrium reactions (C: calcite; Ch: chalcedony; Alb: albite; Adu: adularia; K: kaolinite; All: all these minerals); (c) Mix 2 and different reequilibrium reactions; and (d) Mix 3 and different reequilibrium reactions.*

Table 2-4: *Calculated mass transfers (mol/L) in the three mixing proportions analysed above. Only two examples are shown here: the equilibrium with the whole set of minerals, and the equilibrium with calcite, chalcedony, albite and adularia.*

Mass Transfers	63% Brine - 37% Glacial		24% Brine - 76% Glacial		5% Brine - 95% Glacial	
	The whole assemblage	C-Alb-Adu-Ch	The whole assemblage	C-Alb-Adu-Ch	The whole assemblage	C-Alb-Adu-Ch
Calcite (C)	3.57E-04	4.05E-06	2.46E-04	1.49E-05	1.20E-04	2.40E-05
Albite (Alb)	8.10E-04	4.13E-04	3.61E-04	1.12E-04	1.05E-04	6.62E-06
Adularia (Adu)	4.11E-04	4.13E-04	1.11E-04	1.12E-04	6.46E-06	6.70E-06
Kaolinite (K)	1.99E-04		1.25E-04		4.93E-05	
Chalcedony (Ch)	8.53E-04	3.72E-05	5.90E-04	9.21E-05	3.18E-04	1.25E-04
pH eq.	6.91	7.60	7.34	8.03	8.07	8.54

This thermodynamic analysis is still in progress and will be complemented with the simulation of the following evolution steps: mixing with Littorina end member (plus reaction) and with a meteoric end member (plus reaction). The first attempts with Littorina have shown that the final waters plot in similar locations in the stability diagram and that small mass transfers are obtained for the key minerals.

3.2.3 Uncertainties associated with the theoretical simulations

There are several kinds of uncertainties associated with the previous analysis. The first, already introduced above, is related to the equilibrium constants selected to construct the stability diagrams and used in the modelling calculations. Only phases with small thermodynamic uncertainties (e.g. adularia and albite) have been included in the calculations. Laumontite and chlorite require a more detailed evaluation as they are more problematic with respect to their thermodynamic uncertainties (laumontite) and their compositional heterogeneity in the system (chlorite). Mineral phases such as zeolites, smectite, illite or epidote, are common as fracture fillings in this system and could contribute to the control of the chemical contents. However, they have not been considered in the calculations due to their thermodynamic uncertainties (equilibrium solubility constants not well defined). The uncertainties related to this simple equilibrium model would be minimised if aluminium data in the studied waters were available (Trotignon *et al.*, 1997).

The second type of uncertainty is associated with the ambiguity between the possible control by aluminosilicate dissolution-precipitation or by ionic exchange in clay minerals. This last process involving illite, smectites or zeolites could be an alternative way to express constraints on cations like K^+, Na^+ or Ca^{2+} in low temperature systems. The ionic exchange control on the groundwater composition can be especially effective in the most recent mixing event, with short interaction (reequilibrium) time with minerals.

Therefore, this uncertainty means that aluminosilicate dissolution-precipitation and ionic exchange in clay minerals can result in the same water chemistry. This typical ambiguity is present in the studied sites. POM and Olkiluoto data plot together in the

stability diagram used in this work, as shown above (Figures 3-5, 3-6 and 3-7), but they also plot in the same position in other stability diagrams involving different clay minerals (used by Pitkänen *et al.*, 1999 for Olkiluoto samples). Figure 3-8 shows just one of these diagrams, but the trend is the same in all of them. From this diagram, some kind of process involving Na and Ca exchange in montmorillonite could be called upon to explain some of the more evolved POM and Olkiluoto groundwaters.

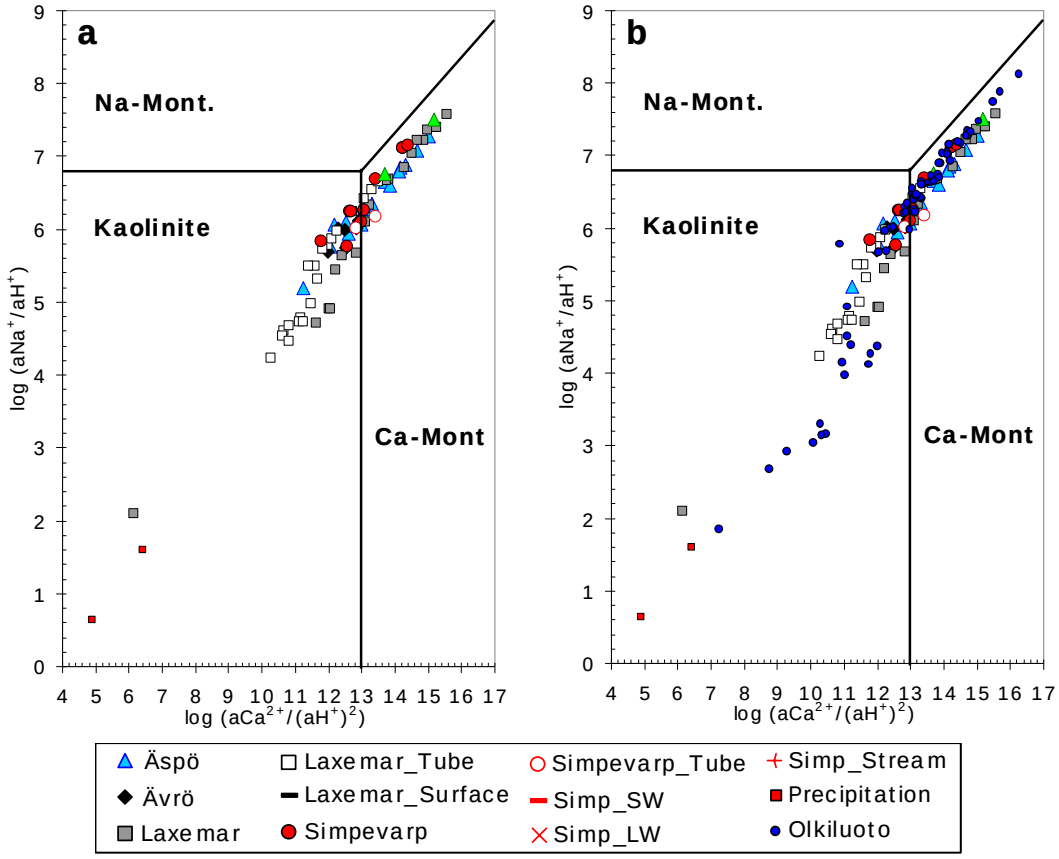

Figure 3-8: *Aqueous activity diagram for some aluminosilicate minerals at 7ºC, 1 bar. The field boundaries were calculated with data from Helgeson (1969) and a logarithmic silica activity of –4. (a) POM waters; (b) POM and Olkiluoto waters.*

In the POM area the presence of laumontite, adularia, etc. in the open fractures has been reported, together with calcite, clay minerals and sulphides. In Olkiluoto, only calcite, sulphides and clay minerals have been reported. So, in spite of the mineralogical differences between the two sites, their groundwaters could be interpreted in the same way.

This duality in the interpretation or in the conceptual approach is not new. For instance, in the ARCHIMEDE project (Griffault *et al.*, 1996) both conceptual models (dissolution-precipitation vs. ion exchange) were successfully applied to predict the groundwater geochemical evolution in the Boom Clay Formation (Mol, Belgium). A thorough discussion on this topic can be found in Beaucaire *et al.* (2000).

3.2.4 Additional application of "equilibrium assemblages"

The thermodynamic approach applied in the previous section to assess mixing and reaction processes provides an ideal tool for predicting the composition of groundwaters with long residence times. This is the case of the "old brine end members" used in the

Scandinavian Shield. These groundwaters can be considered as having reached a "global" equilibrium with calcite, chalcedony and different aluminosilicaltes. This kind of approach was used by Michard and co-workers (e.g. Michard, 1980; Michard *et al.*, 1986) to predict the composition of some granitic thermal groundwaters assuming thermodynamic equilibrium between the water and a selected mineral assemblage, as a function of chemical contents not controlled by mineral equilibria (e.g. Cl). This model was also applied by Grimaud *et al.* (1990) to the low temperature granitic groundwaters at Stripa.

More recently, Trotignon *et al.* (1997, 1999) applied the same concept to Äspö groundwaters (from KAS02 and KAS03 boreholes) and reported a high sensitivity of the predictions to the mineral equilibrium constants, mainly from laumontite. They found a reasonable fit between the predicted values and the measured concentrations for the assemblage calcedony + kaolinite + albite + adularia + laumontite with the selected equilibrium constants.

Here, Trotignon's approach was extrapolated[12] to calculate "brine compositions" using the same assemblage (calcedony, kaolinite, albite, adularia and laumontite) plus calcite and gypsum (saline waters in POM area are in equilibrium with this mineral as explained before), and the thermodynamic data from Grimaud *et al.* (1990) except for kaolinite and laumontite. The equilibrium constants for these minerals were taken from Trotignon's best fit.

The procedure consists of the following steps: pure water (Glacial end member) was equilibrated with the selected mineral assemblage imposing, simultaneously, different chloride concentrations up to "brine" values. PHREEQC was used to simulate this process. The results obtained for the Brine end member and for the more saline water in Olkiluoto (KR12/741/1; Pitkänen *et al.*, 2004) are shown in table 3-5.

Comparing the predicted values with the real ones, it is clear that in most cases the fit is quite good (pH, Na, Ca, SiO_2). But, more interesting, the predictions are able to reproduce the main groundwater features: pH values close to 8 and very low alkalinity. Considering the thermodynamic uncertainties associated to these calculations, one can say that in general the results are fairly good.

A plot of the concentration data on table 3-4 as a function of chloride concentration (Figure 3-9) shows some other interesting facts. It makes clear that the concentration of elements controlled by equilibrium with the mineral assemblage depends on chloride content. This conclusion is not new (Michard, 1987) but it has important implications in the context of the mixing and reaction processes that affect this kind of systems. For the oldest mixing event, it clearly shows that chloride is more than a useful conservative element to compute mixing proportions. Therefore, it could be concluded that in the POM area mixing is the main irreversible process. It controls chloride concentration and then, this concentration determines the re-equilibrium path (water-rock interaction) triggered by mixing.

This result emphasizes the important effort made in the Swedish (and Finish) framework to characterize the mixing process. Moreover, it justifies the selection of

[12] The groundwaters analysed in their work were saline, but only up to 10000mg/L chloride. In order to be confident with the simulations performed in this report, the authors first reproduced Trotignon's results (analysis not presented here) and then extrapolated the approach to the more saline waters found in the POM area.

chloride as the main descriptive variable when studying the geochemical evolution of these systems.

Table 3-5: *Predicted and observed concentrations for the brines in POM area (Brine end member) and in Olkiluoto (the more saline sample with complete analytical data, in the site).*

Increasing chloride concentration

	Initial water			Prediction			Prediction
	Glacial	Equilibrium with the selected mineral assemblage	Olkiluoto Brine	Olkiluoto Br (Theor)	Equilibrium with the selected mineral assemblage	Brine end member	Brine (Theor)
mCl	1.41E-05		0.8754	0.8833		1.442	1.443
pH	5.8		8.3	7.95		7-8	7.8
mNa	7.39E-06		0.366	0.375		0.400	0.490
mK	1.02E-05		0.0005	0.00145		0.00126	0.00213
mCa	4.49E-06		0.258	0.261		0.521	0.490
mH_4SiO_4	1.42E-04		9.79E-05	9.30E-05		6.67E-05	7.40E-05
mAlkalinity	1.97E-06		1.32E-04	5.39E-05		2.50E-04	4.56E-05
mSO_4	5.20E-06		5.38E-05	7.27E-03*		5.14E-03	5.36E-03

* The equilibrium with gypsum assumption is not valid in these waters as they are clearly undersaturated (Figure 2-12).

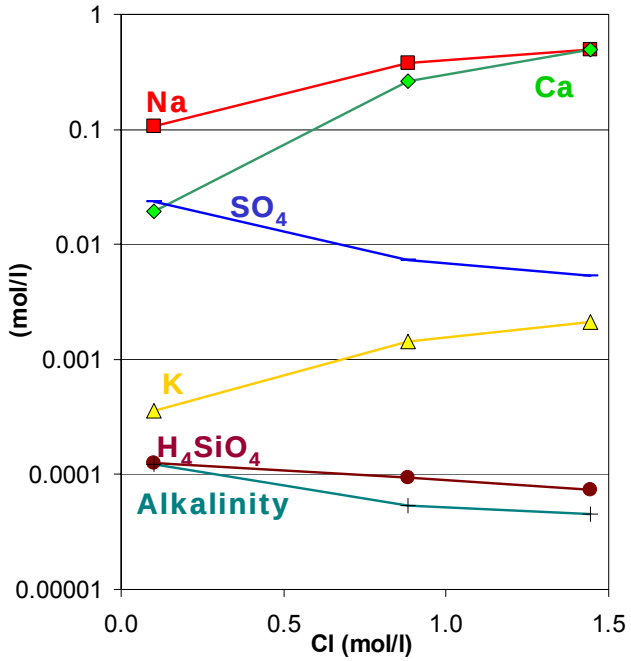

Figure 3-9: *Evolution of chemical contents as a function of chloride, keeping the equilibrium with the mineral assemblage (see text).*

3.3 The redox system modelling

In this section the results from the modelling of the redox state in the POM area are presented. For Simpevarp 1.2, the amount of suitable data for a redox study is greater than for Simpevarp 1.1 and, therefore, this study is more complete. The two possibilities suggested in previous studies about the redox state of the groundwaters have been revisited, namely: (a) the iron system controls the redox state (Grenthe *et al.*, 1992); and (b) the sulphur system controls the redox state (e.g. Nordstrom and Puigdomenech, 1986). Some of the samples supplied with Data Freeze 1.2 have been previously used to back up both interpretations (Grenthe *et al.*, 1992; Glynn and Voss, 1999).

For this modelling exercise samples with enough redox data were selected. This includes Eh and pH[13] data from continuous logging (from this data freeze and from previous reports, Smellie and Laaksoharju, 1992; Laaksoharju *et al.*, 1995), analytical data[14] for Fe^{2+}, S^{2-} and CH_4, and microbiological information.

Apart from the samples delivered with Data Freeze 1.2, some additional samples from Finnsjon, Fjallweden, Klipperas and KOV01 were also analysed in order to verify some results. As they add no new insight, they have not been referred to in the text.

The microbiological information available from Data Freeze 1.2 refers only to the Simpevarp subarea. Nevertheless, additional data taken from previous works on the POM subareas have been also incorporated (especially from boreholes and depths equivalent to those included in Data Freeze 1.2).

These selection criteria have drastically reduced the number of suitable samples for the redox characterization of the system. In spite of this, the selected samples cover the four subareas (Äspö, Ävrö, Laxemar and Simpevarp) and a wide range of depths (130 to 930 m; Table 3-6). Moreover, they have continuous Eh logging, redox pair concentrations and even microbiological information and thus, a combination of these three data sets can be made.

3.3.1 The redox pair calculations

3.3.1.1. Methodology

The redox pair calculations include the following pairs: the dissolved SO_4^{2-}/S^{2-} and CH_4/CO_2 redox pairs and the heterogeneous $Fe(OH)_3/Fe^{2+}$, pyrrhotite (or FeS)/SO_4^{2-} and pyrite/ SO_4^{2-} couples. As in previous reports (Laaksoharju *et al.*, 2004 a, b) dissolved Fe^{3+}/Fe^{2+} and Fe^{3+}-clay/Fe^{2+}-clay (Banwart, 1999) were also tried but the results are not presented here[15].

Iron oxides (including hematite) and oxihydroxides are common fracture filling minerals in the POM area (Wallin and Peterman, 1999; Tullborg *et al.*, 1999).

---

[13] In order to minimize the pH uncertainties effects on the redox calculations (Laaksoharju *et al.*, 2004a, b).

[14] A more detailed discussion about this can be seen in Appendix D.

[15] Differences between total iron and Fe^{2+} concentrations are too small to obtain reliable figures with the Fe^{3+}/Fe^{2+} homogeneous redox couple, and calculated Eh values are always oxidizing. Fe^{3+}-clay/Fe^{2+}-clay provide, in general, much more oxidizing values than any other redox couple or Eh measurements (Figure 3-10).

Therefore, several calibrations were employed to model the redox potential with the $Fe(OH)_3/Fe^{2+}$ heterogeneous pair.

(1) The calibration proposed by Grenthe *et al.* (1992). According to these authors, Eh values in Swedish groundwaters can be estimated with the $Fe(OH)_{3(s)}/ Fe^{2+}$ heterogeneous redox couple,

$$Fe(OH)_{3(s)} + 3H^+ + e^- \rightarrow Fe^{2+} + 3H_2O, \qquad (1)$$

by means of the equation

$$Eh = E^{0*} - 2.303\frac{RT}{F}\left(3pH + \log\left[Fe^{2+}\right]\right) \qquad (2)$$

where $E^0* = 707 \pm 59$ mV at 10 ºC (the average Swedish groundwater temperature), F is Faraday constant (23.061 cal V^{-1} equivalent^{-1}), R is the gas constant (1.98717 cal deg^{-1} mol^{-1}) and T is the temperature (K). The E^0* value determined by Grenthe *et al.* (1992) is based on a fit of equation (1) to Eh, pH and Fe^{2+} data from SKB groundwaters from different sites. $Fe(OH)_3$ solubility product obtained from this fit is intermediate between freshly precipitated amorphous hydroxide and crystalline goethite. In fact, the solubility product is the one proposed by Langmuir (1997) for lepidocrocite. Equation (2) is usually employed to estimate Eh values from pH and Fe^{2+} concentration data (e.g. Smellie and Laaksoharju, 1992). For the fit, Grenthe *et al.* (1992) used Fe^{2+} concentration data corrected only for the $FeCO_3^0$ ion pair. But Fe^{2+} speciation is usually more complex than the simple correction made by these authors. Following Glynn and Voss (1999), in this study two sets of Eh values were calculated with equation (1), one considering Fe^{2+} analytical data and the other considering the Fe^{2+} species' activities obtained from the speciation-solubility calculations with WATEQ4F database.

(2) The calibration suggested by Bruno *et al.* (1999) using the thermodynamic data for amorphous and microcrystalline $Fe(OH)_3$ in reaction (1).

The redox potential for the SO_4^{2-}/S^{2-} and CH_4/CO_2 homogeneous redox pairs was calculated by PHREEQC with WATEQ4F database. A sensitivity analysis was performed with the thermodynamic values included in LLNL database and in NAGRA database (release 26-Aug-2002; Hummel *et al.*, 2002). The results indicate differences not greater than 30 mV for the calculated Eh.

The presence of pyrite as fracture filling mineral is also common in the POM area. It has been reported as minor grains in the outermost coating along hydraulically conductive fractures in Simpevarp, suggesting that pyrite formation is an ongoing process in the system. Pyrrothite or amorphous FeS have not been identified in the system, but these minerals are usually the precursors of pyrite formation. Pyrrothite can precipitate at hematite surface in the presence of sulphate-reducing bacteria (Neal *et al.*, 2001). Moreover, the saturation state of water with respect to these phases suggests an equilibrium state, as given in a previous report (Laaksoharju *et al.*, 2004 a, b). Therefore, pyrite/SO_4^{2-} (using thermodynamic data from WATEQ4F and Bruno *et al.*, 1999), pyrrothite/SO_4^{2-} (data from Bruno *et al.*, 1999) and FeS_{ppt} (data from WATEQ4f) buffers were used to perform the redox calculations.

Table 3-6. *Eh values for the selected samples in the POM area. The potentiometrically measured values are shown for comparion with the values calculated with the different redox pairs.*

Site	Sample	Depth (m)	T (ºC)	pH	Eh (mV)					
					Chemmac	SO_4^{2-}/S^{2-}	CH_4/CO_2	$Fe(OH)_3/Fe^{2+}$ Grenthe(1)	$Fe(OH)_3/Fe^{2+}$ microcrystalline	$Pyrite/SO_4^{2-}$ (2) $Pyrrotite/SO_4^{2-}$
Äspö	1433	532.5	15.3	8	-310	-245.2		-324	-154.5	-270
Äspö	1548	208		7.5	-260	-210.9	-224.3	-258	-83.7	-240
Äspö	1569	131.5	10.2	8	-270	-243.9	-251.9	-313	-137.1	-270
Äspö	1582	931	20.5	8	-270	-263.6	-286.7	-295	-125.6	-270
Äspö	1588	460.5		8.1	-290	-254.0	-268.5	-343	-173.8	-280
Äspö	1603	338.5	12.2	7.9	-280	-251.9	-287.4	-315	-144.3	-270
Ävrö	1374	560.5	15	7.2	-212	-200.5		-226	-49.8	-205
Laxemar	1528	458.5		8.7	-270	-292.3		-401	-232.2	-310
Laxemar	1537	274.5		8.5	-262	-282.3		-396	-200	-300
Laxemar	1633	691		7.9	-265	-248.1		-294	-122	-265
Laxemar	1773	915.5		8.3	-140	-276.8	-306.8	-336	-168.6	-290
Laxemar	2738	318	12.5	8.1	-135	-246.1		-382	-209.5	-280
Simpevarp	5263	161.75	6.3	8.1	-250	-234.9	-261.7	-385	-237.3	-280
Simpevarp	5268	253.25	10.8	8.05	-210	-236.5		-375	-206.5	-270
Simpevarp	5288	556.5	3	8.05	-265		-270	-350	-181.9	-270

(1)Average values with and without the activity correction (±15 mV).

(2)Average values from the two redox pairs considering data of Bruno *et al.* (1999) (±15 mV)

3.3.1.2. Results

The results are summarised in Table 3-6 and Figures 3-10 and 3-11. The Eh calculated with the $Fe(OH)_3/Fe^{2+}$ redox pair and Grenthe's calibration agrees reasonably well with most of the Eh values measured in Ävrö and Äspö. This good fit was expected as these samples were used by Grenthe and co-workers to perform the calibration. The Eh calculated with the same redox pair but for microcrystalline $Fe(OH)_3$ is much more oxidant. On the contrary, the microcrystalline phase gives the best results in the case of Simpevarp and some Laxemar samples, whereas Grenthe's calibration gives much more reducing Eh values (Figure 3-10). This observation was already made in the previous phase (Simpevarp 1.1, Laaksoharju *et al.*, 2004a; and Forsmark, Laarksoharju *et al.*, 2004b). This fact suggests that the groundwater redox state can be controlled by iron oxides and oxihydroxides with different degrees of crystallinity.

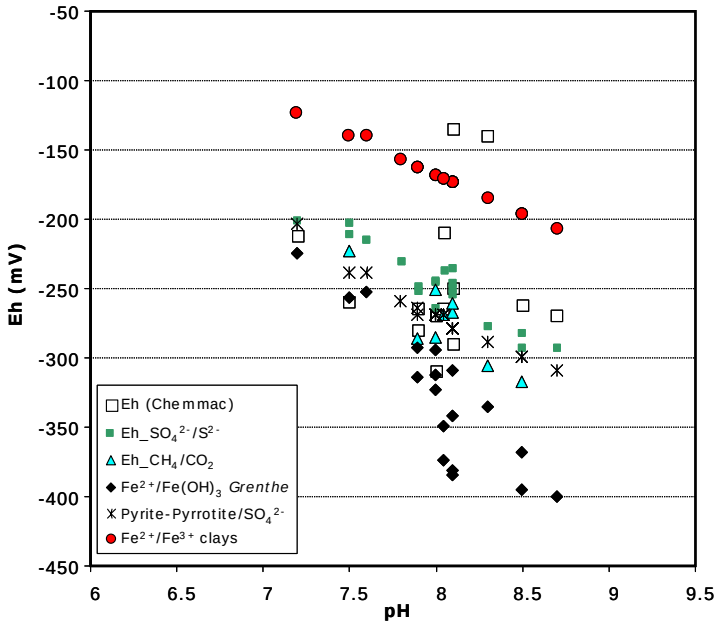

Figure 3-10: *Comparison of redox results for different redox pairs.*

Except for some few samples, the different "sulphur system" redox pairs provide Eh values coincident with the potentiometrically measured Eh. The SO_4^{2-}/S^{2-} homogeneous redox pair gives Eh values similar to the ones obtained from the heterogeneous pairs ($Pyrite/SO_4^{2-}$ and FeS/SO_4^{2-}; Figure 3-11) as calculated with WATEQ4F thermodynamic data. A sensitivity analysis carried out comparing these data to Bruno *et al.*'s (1999) shows only minor differences.

As expected, Eh values obtained with the CH_4/CO_2 pair are close to the ones obtained with SO_4^{2-}/S^{2-} (and also to the remaining sulfur redox pairs). Therefore, they also agree well with the potentiometrically measured Eh.

Table 3-6 shows the global results for the samples from the different POM subareas. In Äspö and Ävrö there is a good agreement between the potentiometrically measured Eh and the value calculated from the following redox pairs: heterogeneous and homogenours sulfur pairs, CH_4/CO_2 and Grenthe's calibration for $Fe(OH)_3/Fe^{2+}$. In Simpevarp, the redox pair results also agree very well with the measured Eh values; however, the iron system seems to be controlled by a microcrystalline hydroxide instead of by an intermediate phase (Grenthe's calibration). Finally, in Laxemar the sulfur redox

pairs show a good agreement with potentiometric Eh; as for the iron hydroxide pair, the best agreement with the measured value is not always obtained with the same pair: in some cases is Grenthe's calibration the one which agrees better with the measured Eh (sample 1633; table 3-6) and in other cases is the microcrystalline phase which agrees better (samples 1528 and 1573). Samples 1773 and 2738 have a potentiometric Eh considerably lower than any other calculated with the redox pairs.

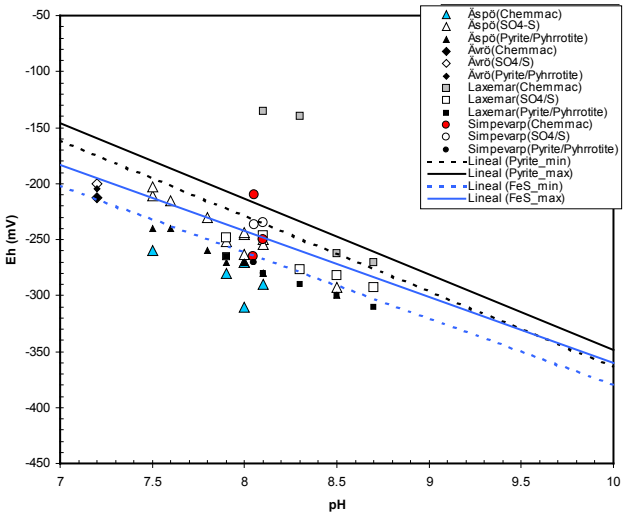

Figure 3-11: *Eh-pH diagram showing the calculated Eh values for the POM samples. The Eh values obtained from potentiometric measurements are plotted using the same symbols as before for each subarea. The Eh values from the SO_4^{2-}/S^{2-} redox pair are represented with open symbols and the values obtained with the pyrite-pyhrrotite/SO_4^{2-} pair, with a filled black symbol. "Pyrite_min" and "Pyrite max" lines represent the equilibrium situation for the range of SO_4^{2-} and Fe^{2+} concentration found in POM groundwaters. The same is valid for the FeS/SO_4^{2-} equilibrium.*

The results given by the sulphur system are more homogenous and in better agreement with each other than those obtained from the $Fe(OH)_3/Fe^{2+}$ redox pair. This suggests that the sulphur system is the main controller of the groundwater redox state, as reported previously (Nordstrom and Puigdomenech, 1986; Glynn and Voss, 1997; Laaksoharju *et al.*, 2004 a, b). The CH_4/CO_2 redox pair gives results in good agreement with the sulphur pairs. In summary, all these redox pairs should be used when characterizing the redox state of these groundwaters. The variable results obtained with the $Fe(OH)_3/Fe^{2+}$ pair do not mean that the iron system does not participate in the redox control of these waters. This is further discussed below.

3.3.1.3. Limitations of SO_4^{2-}/S^{2-} and CO_2/CH_4 pairs

The redox potential for the SO_4^{2-} redox pair can be calculated for waters with pH>7 from the equation:

$$p\varepsilon = \log K - \frac{9}{8} pH + \frac{1}{8} \log \frac{[SO_4^{2-}]}{[HS^-]}$$

As the reaction involve the transfer of 8 electrons, the change in the calculated redox potential amounts only to 1/8 pe unit (or 7 mV) for a tenfold change in the sulphate/sulphide ratio. Therefore, this pair is not very sensitive to changes in the

concentration of S^{2-} and SO_4^{2-} in the studied waters and provides similar values for all of them (Table 3-6).

The same argument is valid for the CO_2/CH_4 pair, whose redox potential can be obtained from:

$$p\varepsilon = \log K - pH + \frac{1}{8}\log\frac{[CO_2]}{[CH_4]}$$

Besides, the log *K* values for both reactions are close enough to produce very similar Eh results. Therefore, the calculated Eh from these redox pairs is only meaningful when concentration values are reliable. This important condition seems to be fulfilled in all the studied waters except in Simpevarp, where S^{2-} data are different in Data Freeze 1.1 and Data Freeze 1.2 and the detection limit is not stated. A value of 0.01 mg/L (Wacker *et al.*, 2003) has been selected for calculations.

In any case, it is always convenient to check the validity of the redox pair results comparing them with the information from the microbial studies and the potentiometric measured Eh values. In spite of the technical difficulties in obtaining reliable Eh values in the boreholes, SKB methodology is a valuable (and indispensable) element in the study of redox conditions.

3.3.2 The iron system

Iron oxihydroxide minerals in natural settings are represented by a series of minerals that range from poorly (ferrihydrite) to well crystalline phases (hematite or goethite), in which poorly crystalline oxides act as precursors to the well-crystallised ones (Appelo and Postma, 1993; Langmuir, 1997). As already stated, different iron oxides-oxihydroxides occur as common fracture fillings in the POM area, from hematite to less crystalline phases generally termed "iron oxides" or "iron oxihydroxides". The redox state of groundwaters can be controlled by any of these phases as demonstrated in previous studies by Grenthe *et al.* (1992) and Bruno *et al.* (1999) in groundwaters from the Scandinavian Shield.

In this report, Grenthe's calibration and the "amorphous-microcrystalline" approach of Bruno *et al.* (1999) have been used to evaluate the uncertainties associated to the crystallinity variations in these iron phases.

The dissolution of ferric oxihydroxide minerals can be represented by the reaction:

$$Fe(OH)_3 + 3H^+ \rightarrow Fe^{3+} + H_2O \qquad (2)$$

The stability constants for amorphous (log *K*=5) and mycrocrystalline (log *K*=3) phases considered by Bruno *et al.* (1999) come from data by Nordstrom *et al.* (1990) for ferrihydrite (mineral term that enclose the less crystalline iron oxihydroxide found in natural systems and usually referred to as hydrous ferric oxide, HFO). Stability constants for the crystalline phases (hematite and goethite) correspond to log *K* values around -2.0 (Langmuir, 1997).

The $Fe(OH)_3$ solubility product proposed by Grenthe *et al.* (1992) and written in terms of reaction (2) correspond to log *K*=1.1 (±1.1). As Grenthe *et al.* (1992) indicate, this value is intermediate between the less crystalline ferric hydroxide (ferrihydrite) and

crystalline goethite. This value is close to that of lepidocrocite, a common intermediate phase between amorphous and crystalline oxides (Langmuir, 1997).

The reaction for the $Fe(OH)_3/Fe^{2+}$ redox pair can be expressed as a reductive dissolution as is shown in reaction (1). From this, the Eh-pH variations (for a fixed Fe^{2+} concentration) can be calculated for the different solubility constants of amorphous, microcrystalline and "lepidocrocite" phases. Figure 3-12 shows these results and serves to explain the reason why, *for the same pH conditions*, Grenthe's calibration always provides more reducing Eh values than those obtained from the microcrystalline phase.

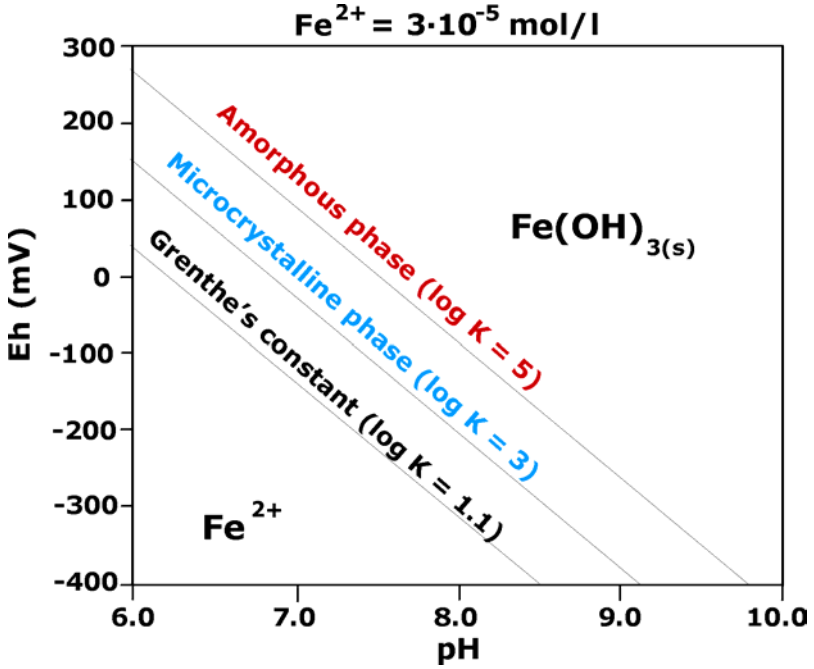

***Figure 3-12**: Eh-pH diagram for the Fe(OH)3/Fe2+ redox pair (reaction 1) at fixed Fe2+ concentration (3·10-5 mol/L). Phase boundaries are calculated for different $Fe(OH)_3$ crystallinities (different log K).*

Figure 3-13 depicts two separated diagrams with the lines for the microcrystalline redox pair (panel a) and the Grenthe's one (panel b) superimposed. In both cases, the range of ferrous iron concentration in the studied waters has been taken into account and therefore, the simple line in Figure 3-12 has became a double line.

It is clear from the figure that some samples agree well with Grenthe's calibration (panel b) whereas others agree better with the microcrystalline phase. From theses diagrams, a continuum in the redox control by iron hydroxides with different crystallinity degrees could be concluded.

The solubility product proposed by Grenthe *et al.* (1992), considering an intermediate phase between ferrihydrite and goethite, is justified if the assumption is made that such a phase is produced during drilling and/or field measurements. It is very difficult to avoid oxygen intrusion and this element is quickly reduced by Fe^{2+} phases or species in solution forming hydrous ferric oxihydroxides which can then play an active role in the electrochemical measurement.

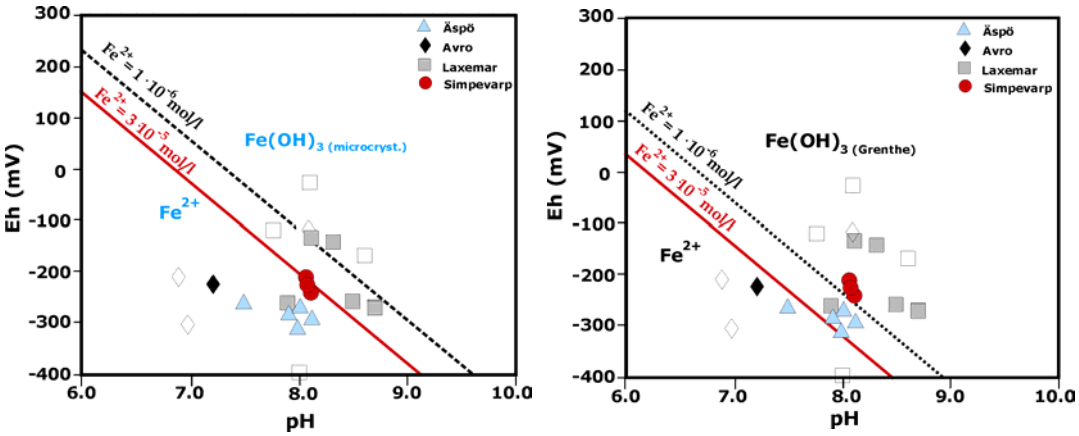

***Figure 3-13**: Eh-pH diagram showing the measured Eh and pH of the selected samples (Table 3-6). (a) $Fe(OH)_3/Fe^{2+}$ phase boundaries for a microcrystalline phase. (b) (a) $Fe(OH)_3/Fe^{2+}$ phase boundaries for a medium crystalline phase from Grenthe et al. (1992). In both cases, the phase boundaries are shown for the range of Fe^{2+} concentration in the POM groundwaters.*

However, the initial $Fe(OH)_3$ formed under such circumstances is expected to have a lower crystallinity (and higher solubility) than the value deduced by Grenthe *et al.* (1992), as has been observed in different natural systems (Appelo and Postma, 1993; Langmuir, 1997). When this amorphous phase precipitates, a process of partial recrystallization will increase its crystallinity, eventually reaching Grenthe's solubility product.

This conclusion is in agreement with the observed transformations of the Fe-oxyhydroxides in nature through recrystallization from an initial precipitate of freshly amorphous phases to goethite. This recrystallization (Ostwald ripening) involves a decrease in surface area, solubility and reactivity, together with an increase in thermodynamic stability and crystallite size (Figure 3-14).

Therefore, the apparent control of Eh by ferrihydrite or any other more crystalline $Fe(OH)_3$ in different groundwaters could be explained in terms of this recrystallization processes. The time scale of the aging process is difficult to quantify due to the multiple steps involved. But the available information for the net recrystallisation process suggests that it is a very quick process.

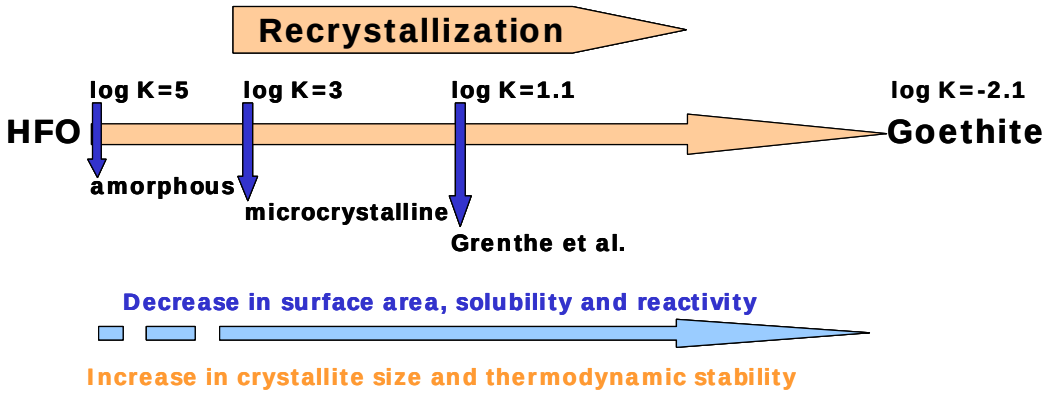

***Figure 3-14**: Schematic representation of recrystallisation processes affecting iron oxides-oxihydroxides in natural systems. Effects on crystallinity and other properties are also shown.*

The recrystallization reaction rate has been studied in the laboratory and in natural systems. In the latter, a rate of several years has been reported (Langmuir, 1997). Laboratory experiments performed by Schwertmann and Murad (1983) indicate that at neutral pH values (6-7) the reaction has a half life of 110-160 days. This rate increases strongly with pH. Therefore, HFO are expected to be absent in old groundwater systems without dissolved O_2 because they would have recrystallized to goethite a long time ago.

This observation would also explain the observations of Trotignon *et al.* (2002) in the replica experiment of the REX project. The Eh potential measured during different O_2 "pulses" of the experiment (spanning 6-12 days) are in agreement with a calculated $Fe(OH)_3$ log *K* of 4. However, during the long anoxic periods between pulses (up to three months) the system reaches equilibrium with goethite.

The consequences of the recrystallization process can be summarised as follows: HFO phases do not appear to be "old phases" in the system, in agreement with Grenthe *et al.* (1992). They can be promoted by drilling and measurement operations. So, one would be measuring the "reductive capacity of the system" rather than its pristine conditions. As a conclusion, when applying the $Fe(OH)_3/Fe^{2+}$ redox pair one can obtain a different Eh value depending on the "instantaneous" degrees of crystallinity (different log *K*) of the oxihydroxides, due to the their fast recrystallization rate.

3.3.3 The sulphur system

Sulphide and iron concentrations shows no clear trend with depth in the POM area (Figure 3-15). High S^{2-} and Fe^{2+} contents appear at 600 and 800 m depth. However, high sulphide waters have generally low ferrous iron concentrations and *vice versa* (Figure 3-16).

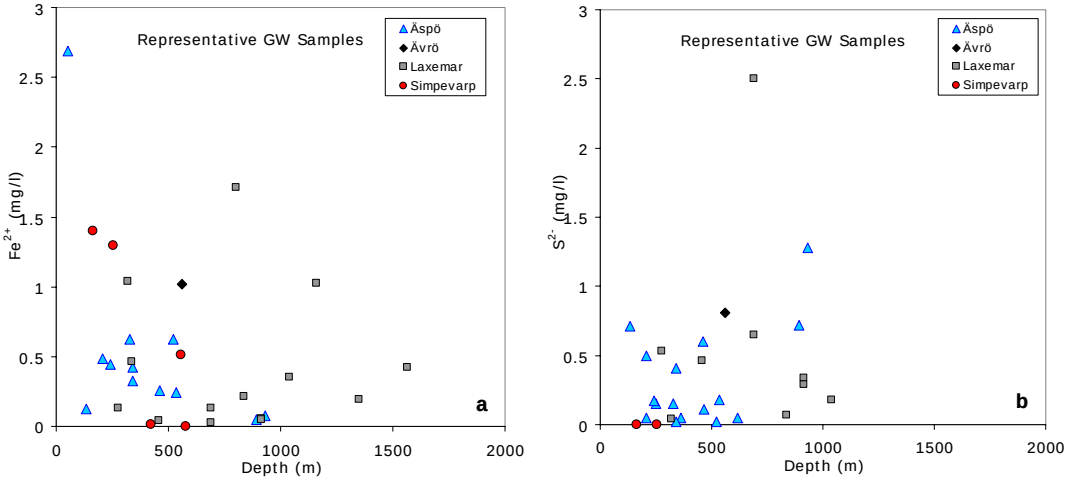

Figure 3-15: *Depth evolution of ferrous iron (a) and sulphide (b) in the four subareas of POM (Simpevarp Laxemar, Äspö and Ävrö).*

Speciation-solubility calculations show that all the waters considered in this redox analysis are slightly oversaturated or near equilibrium with respect to the amorphous iron sulphide (FeS_{ppt} from WATEQ4F database), in agreement with previous results by Glynn and Voss (1999). This could suggest that precipitation of iron sulphides is an active process in the system, controlling the concentrations of both elements in solution.

The combination of very low iron and high sulphide contents is common in sulphidic environments as a result of sulphur phases precipitation. This is true if the intensity of the sulphate reduction processes and the release of dissolved sulphide dominate over Fe^{2+} release to solution. However, if a source of Fe^{2+} dominates (e.g. ferric oxides or oxihydroxides as fracture filling minerals), relatively high Fe^{2+} concentrations can keep dissolved sulphide at the low levels detected in other groundwaters, even though sulphate reduction might produce substantial amounts of sulphide. Therefore, sulphate reducing bacteria (SRB) can play a fundamental role in this balance and in the precipitation process.

SRB and sulphate reducing activity have been detected in the Äspö subarea (Laaksoharju and Wallin, 1997; Motamedi and Pedersen, 1998; Haveman and Pedersen, 2002) reaching 450-600 m depth. SRB have been also detected in the Simpevarp subarea (in the three sections examined in KSH01A borehole: 161.75m, 253.25m and 556.5m depth; Hallbeck, this report). However, the presence of SRB bacteria is not correlated with a clear decrease in SO_4^{2-} or an increase in S^{2-} (Pedersen, 2000; Pitkänen *et al.*, 2004; Hallbeck, this report). This last observation on the dissolved S^{2-} can be explained by active precipitation of sulphide minerals. The presence of pyrite in the outermost part of the fracture fillings support the idea that this process is not too old (Tullborg, this issue).

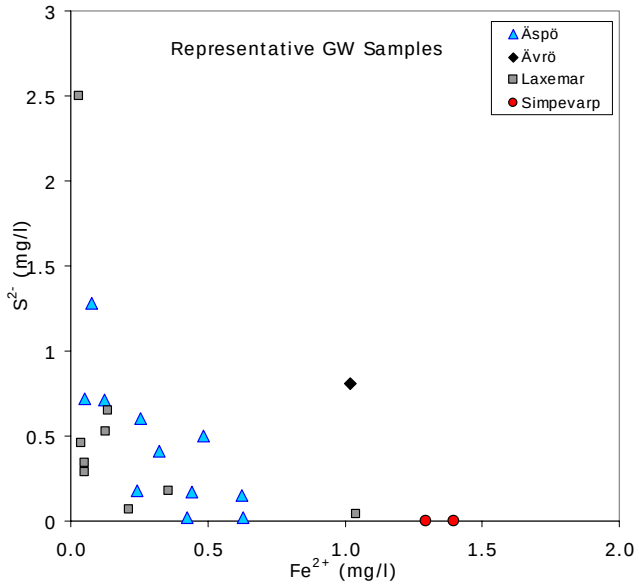

Figure 3-16: *Depth evolution of ferrous iron (a) and sulphide (b) in the four subareas of POM (Simpevarp Laxemar, Äspö and Ävrö).*

All these lines of evidence appear to converge, especially in the Simpevarp subarea. Waters from KSH01A borehole show very high Fe^{2+} and very low S^{2-} concentrations compared with the rest of the representative samples in the POM area (Figure 3-16), in spite of the presence of SRB. FeS_{ppt} saturation indexes in these groundwaters are between +0.03 and +0.13, suggesting an equilibrium situation mediated by monosulphide precipitation. In fact, this situation can be related to the control of the iron system by less crystalline oxihydroxides, as suggested by the above redox pair analysis.

The reductive dissolution of oxihydroxides by hydrogen sulphide (with simultaneous FeS minerals precipitation) is a well known process in natural systems. The

effectiveness of the process depends on the reactivity of the oxides towards dissolved sulphide: amorphous, less crystalline oxihydroxides are much more reactive (both in abiotic and in bacterially-mediated reactions) than crystalline ones (Canfield *et al.*, 1992), quickly depleting dissolved sulphide towards the very low concentrations observed (Poulton *et al.*, 1992).

Clearly, more data are needed to verify this suggestion, but, if true, the implications are very important. The borehole disturbance that promotes amorphous iron oxihydroxide precipitation also affects the sulphur system. As before, it can be concluded that what is measured is the reductive capacity of the groundwater system.

Redox modelling demonstrates the good buffer capacity of the system and suggests the possibility that the original (not disturbed) redox conditions would have been more reducing than those found in this analysis. This result might well deserve more detailed studies.

3.3.4 Conceptual model for the redox system

The redox state of groundwaters in the POM area appears to be well described by sulphur redox pairs in agreement with some previous studies in this area (Glynn and Voss, 1999; Laaksoharju *et al.*, 2004a) and in other sites from the Fennoscandian Shield (Nordstrom and Puigdomenech, 1986; Laaksoharju *et al.*, 2004b; Pitkänen *et al.*, 2004). Besides, from the analysis performed here it can be concluded that CH_4/CO_2 is another important redox pair in determining the redox state.

The presence of sulphate reducing bacteria and methanogens widely distributed in the Äspö and Simpevarp subareas can be related to this successful description and supports that the sulphur and methane redox pairs could be the prevailing ones in controlling a microbiologically mediated redox state. High quality measurements of S^{2-} and CH_4 are needed to pursue this approach.

However, in agreement with Grenthe *et al.* (1992), the work presented here also supports the fact that the iron system contributes to the control of the redox state through different oxide-oxihydroxides. The issue is to clearly identify its real contribution, due to the variable crystallinity of the phases involved and their evolution by, probably fast, recrystallisation. This fact indicates that more than one iron phase could be controlling the Eh in different groundwaters, although theoretically, with enough time, they could all eventually tend to an equilibrium with goethite and therefore to lower Eh values than the measured ones.

The interaction between the iron and sulphur systems is evident through sulphate reducing bacteria and sulphide mineral precipitation. Several lines of reasoning indicate that this process is effective at different levels in the POM area. For instance, recent pyrite coatings have been identified in the fracture fillings of Simpevarp, which is an additional support to the good results of sulphur redox pairs. However, the influence of iron oxihydroxide crystallinity on sulphides precipitation has also been rated in the Simpevarp subarea as an important factor.

Therefore, although the sulphur system can be considered the best suited to characterise the redox state of the groundwaters, a better understanding of the iron system is needed to assess its particular contribution to the redox state or to the reductive capacity of these groundwater systems.

4 Hydrogeochemical conceptual model

Groundwater in the POM area can be divided into three groups based on their salinity:

(1) Saline groundwaters. Mixing with a brine end member is responsible, directly or indirectly, for most of their chemical content, specially from Cl concentrations haigher than 10000 mg/L upwards. Their alkalinity is low, and controlled by equilibrium with calcite. pH is controlled by calcite equilibrium and, possibly, aluminosilicate reactions. In contrast to other Fennoscandian sites, sulphate is controlled by gypsum (and gypsum has been identified in fracture fillings) in high saline groundwaters. The old mixed waters tend, with time, to re-equilibrate with a relatively constant mineral assemblage, irrespective of their initial elemental contents. These reactions are slow and can be approached by equilibrium modelling (with aluminosilicates), although other alternatives can be explored (clay minerals).

(2) Brackish groundwaters. They have been submitted to more complex mixing processes, with participation of all possible end-members. A combination of slow and fast chemical reactions (eg. Na-K-Ca ion exchange, calcite precipitation, etc) have operated on the mixed waters

(3) Non saline groundwaters. These waters are the result of "pure" water-rock interaction or mixing of the previous types with recent waters. They lack a clear thermodynamic control; if there is any, it is by fast chemical reactions (ionic exchange, surface complexation reactions, calcite dissolution-precipitation, etc.) coupled with the more important irreversible processes (RFM dissolution, decomposition of organic matter, etc.).

The redox state of groundwaters in the POM area appears to be well described by sulphur redox pairs in agreement with some previous studies in this area and in other sites from the Fennoscandian Shield. Besides, from the analysis performed here it can be concluded that CH_4/CO_2 is another important redox pair in determining the redox state. Therefore, although the sulphur system can be considered the best suited to characterise the redox state of the groundwaters, a better understanding of the iron system is needed to assess its particular contribution to the redox state or to the reductive capacity of these groundwater systems.

5 References

Appelo, C.A.J. and Postma, D. (1993). *Geochemistry, Groundwater & Pollution.* Balkema, Rotterdam, The Netherlands, 536 p.

Ball, J.W. and Nordstrom, D.K. (2001). *User's manual for WATEQ4F, with revised thermodynamic data base and test cases for calculating speciation of major, trace, and redox elements in natural waters.* (Open File Report 91-183), USGS, USA.

Banwart, S.A. (1999). Reduction of iron (III) minerals by natural organic matter in groundwater. *Geochim. Cosmochim. Acta,* **63**(19/20), 2919-2928.

Beaucaire, C., Pitsch, H., Toulhoat, P., Montellier, S. and Louvat, D. (2000). Regional fluid characterisation and modelling of water-rock equilibria in the Bloom clay Formation and in the Rypelian aquifer at Mol, Belgium. *Appl. Geochem.,* **15**, 667-686.

Berner, U. (1995). *Kristallin-I: estimates of solubility limits for safety relevant radionuclides.* (Technical Report NTB 94-08), NAGRA, Wettingen, Switzerland, 60 p.

Bethke, C. (1994). *The Geochemist's Workbench. A users guide to Rxn, Act2, React, Tact and Gtplot.* 213 p.

Bottomley, D.J., Gascoyne, M. and Kamineni, D.C. (1990). The geochemistry, age and origin of groundwater in a mafic pluton, East Bull Lake, Ontario, Canada. *Geochim. Cosmochim. Acta,* **54**, 993-1008.

Bruno, J., Cera, E., de Pablo, J., Duro, L., Jordana, S., and Savage, D. (1997). *Determination of radionuclide solubility limits to be used in SR 97. Uncertainties associated to calculated solubilities.* (Technical Report SKB TR 97-33), SKB, Stockholm, Sweden, 184 p.

Bruno, J., Cera, E., Grivé, M., Rollin, C., Ahonen, L., Kaija, J., Blomqvist, R., El Aamrani, F.Z., Casas, I., de Pablo, J. (1999). *Redox Processes in the Palmottu Uranium Deposit. Redox measurements and redox controls in the Palmottu System.* (Technical Report), Quantisci, Barcelona, Spain, 76 p.

Bruno, J., Duro, L. and Grivé, M. (2002). The applicability and limitations of thermodynamic geohemical models to simulate trace element behaviour in natural waters. Lessons learned from natural analogue studies. *Chem. Geol.,* **190**(1-4), 371-393.

Bruno, J., Duro, L. and Grivé, M. (2001). *The applicability and limitations of the geochemical models and tools in simulating radionuclide behaviour in natural waters. Lessons learned from the Blind Predictive Modelling exercises performed in conjunction with Natural Analogue studies.* (Technical Report SKB TR-01-20), SKB, Stockholm, Sweden, 63 p.

Canfield, D.E., Raiswell, R. and Bottrell, S. (1992). The reactivity of sedimentary iron minerals toward sulfide. *Am. J. Sci.,* **292**, 659-683.

Cramer, J.J. and Nesbitt, W. (1994). Groundwater evolution and redox geochemistry. In: Cramer, J.J. and Smellie, J.A.T. (Eds.) *Final Report of the AECL/SKB Cigar Lake Analog Study.* (Tech. Rep SKB TR 94-04), AECL, Pinawa, Manitoba, Canada, pp. 191-207.

Deutsch, W.J., Jenne, E.A. and Krupka, K.M. (1982). Solubility equilibria in basalt aquifers: The Columbia Plateau, Eastern Washington, USA. *Chem. Geol.,* **36**, 15-34.

Düker, A. and Ledin, A. (1998). Properties of the particulate phase in deep saline groundwater in Laxemar, Sweden. *Wat. Res,* **32**(1), 186-192.

Fontes, J.-Ch., Louvat, D. and Michelot, J.-L. (1989). Some constraints on geochemistry and environmental isotopes for the study of low fracture flows in crystalline rocks - The Stripa case. In: International Atomic Energy Agency (Eds.) *Isotopes techniques in the study of the Hydrology of Fractured and Fissured Rocks.* IAEA, Vienna, Austria.

Gascoyne, M. (2004). Hydrogeochemistry, groundwater ages and sources of salts in a granitic batholith on the Canadian Shield southeastern Manitoba. *Appl. Geochem.,* **19**, 519-560.

Gimeno, M.J., Peña, J. and Pérez del Villar, L. (2001). Geochemical modelling of groundwater evolution in the Palmottu natural system. In von Maravic, H. (Eds.) Book of Abstracts. 8th EC-Natural Analogue Working Group Meeting, Strasbourg, France, March 23-25, 1999. EC NST, Luxembourg, Luxembourg.

Glynn, P.D. and Voss, C.I. (1999). *SITE-94. Geochemical characterization of Simpevarp ground waters near the Äspö Hard Rock laboratory.* (Technical Report SKI R 96-29), SKI, Stockholm, Sweden, 210 p.

Gómez, P., Turrero, M.J., Garralón, A., Ortuño, F. and Valladares, J. (1998). Hydrogeochemical characterization of Bangombé groundwater. In: Louvat, D. and Davies, C. (Eds.) OKLO Working Group. Proceedings of the first joint EC-CEA workshop on the OKLO-natural analogue Phase II project. Sitges, Spain, June 18-20, 1997. CEE, Luxembourg, Luxembourg, pp. 215-225.

Gómez, P., Turrero, M.J.; Martínez, B.; Melón, A., Mingarro, M., Rodríguez, V., Gordienko, F., Hernández, A., Crespo, M.T., Ivanovich, M., Reyes, E., Caballero, E., Plata, A., and Fernández, J.M. (1996). Hidrogeochemical and isotopic characterisation of the groundwater from El Berrocal site, Spain. Topical Report 4. In: ENRESA (Eds.) *Characterisation and validation of natural radionuclide migration processes under real conditions of the fissured granitic environment. Topical Reports, Vol. II, Hydrogeochemistry.* (Publicación Técnica No Periódica PTNP 02/96), ENRESA, Madrid, Spain, pp. 7-358.

Grenthe, I., Stumm, W., Laaksoharju, M., Nilsson, A.C. and Wikberg, P. (1992). Redox potentials and redox reactions in deep groundwater systems. *Chem. Geol.,* **98**, 131-150.

Griffault, L., Merceron, T., Mossmann, J.R., Neerdael, B., De Canniére, Beaucaire, C., Daumas, S., Bianchi, A. and Christien, R. (1996). *Acquisition et regulation de la chimie des eaux en milieux argileux pour le project de stockage de déchets radioactifs en formation géologique. Project Archimede argile.* (Report EUR 17454), 176 p.

Haveman, S.A. and Pedersen, K. (2002). Distribution of culturable microorganisms in Fennoscandian Shield groundwater. *FEMS Microbiology Ecology,* **39**, 129-137.

Helgeson, H.C. (1969). Thermodynamics of hydrothermal systems at elevated temperatures and pressures. *Am. J. Sci.,* **267**, 729-804.

Helgeson, H.C., Delaney, J.M., Nesbitt, H.W. and Bird, D.K. (1970). Summary and critique of the thermodynamic properties of rock forming minerals. *Am. J. Sci.,* **278**, 229.

Hummel W., Berner U., Curti E., Pearson F.J. and Thoenen T. (2002). *Nagra/PSI Chemical Thermodynamic Data Base 01/01.* (Technical Report NTB 02-16), Nagra, Wettingen, Switzerland.

Iwatsuki, T. and Yoshida, H. (1999). Characterizing the chemical containment properties of the deep geosphere: water-rock interactions in relation to fracture systems within deep crystalline rock in the Tono area, Japan. In: Metcalfe, R. and Rochelle, C.S. (Eds.) *Chemical containement of waste in the geosphere.* Geological Society of London, London, UK, pp. 71-84.

JNC (1999). *H-12. Project to stablish the scientific and technical basis for HLW in Japan.* (Supporting Report JNC SR-3), JNC, Japan.

Laaksoharju, M. and Wallin, B. (Ed.) (1997). Evolution of the groundwater chemistry at the Äspö Hard Rock Laboratory. Proceedings of the second Äspö International Geochemistry Workshop, Äspö, Sweden, June 6-7, 1995. SKB, Stockholm, Sweden.

Laaksoharju, M., Gimeno, M., Auqué, L., Gómez, J., Smellie, J., Tullborg, E-L. and Gurban, I. (2004). *Hydrogeochemical evaluation of the Forsmark site, model version 1.1.* (Report SKB R 04-05), SKB, Stockholm, Sweden, 342 p.

Laaksoharju, M., Gurban, I. and Skarman, C. (1998). *Summary of hydrochemical conditions at Aberg, Beberg and Ceberg.* (Technical Report SKB 98-03), SKB, Stockholm, Sweden.

Laaksoharju, M., Smellie, J. A.T., Nilsson, A-C and Skarman, C. (1995). *Groundwater sampling and chemical characterisation of the Laxemar deep borehole KLX02.* (Technical Report SKB 95-05), SKB, Stockholm, Sweden.

Laaksoharju, M., Smellie, J., Gimeno, M., Auqué, L., Gómez, J., Tullborg, E-L. and Gurban, I. (2004). *Hydrogeochemical evaluation of the Simpevarp area, model version 1.1.* (Report SKB R 04-16), SKB, Stockholm, Sweden, 398 p.

Laaksoharju, M.; Tullborg, E.L.; Wikberg, P.; Wallin, B. and Smellie, J. (1999). Hydrogeochemical conditions and evolution at the Äspö HRL, Sweden. *Appl. Geochem.,* **14**, 835-860.

Langmuir, D. (1997). *Aqueous Environmental Geochemistry.* Prentice Hall, Upper Saddle River, NJ, USA, 600 p.

Luukkonen, A. and Kattilakoski, E. (2001). *Äspö Hard Rock Laboratory. Groundwater flow, mixing and geochemical reactions at Äspö HRL. Task 5. Äspö Task Force on groundwater flow and transport of solutes.*. (Progress Report SKB IPR-02-41), SKB, Stockholm, Sweden.

Michar, G. (1980). Contrôle des concentrations d'éléments dissous dans les eaux thermales et géothermales. *J. fr. Hydrol.,* **11**, 7-16.

Michard, G. (1987). Controls of the chemical composition of geothermal waters. *Chemical Transport in Metasomatic Processes,* , 323-353.

Michard, G., Sanjuan, B., Criaud, A., Fouillac, C., Pentcheva, E., Petrov, P.S., Alexieva, R. (1986). Equilibria and geothermometry in hot alkaline waters from granites of SW Bulgaria. *Geochem. J.,* **20**, 159-171.

Motamedi, M. and Pedersen, K. (1998). Desulfovibrio aespoeensis sp. nov., a mesophilic sulfate-reducing bacterium from deep groundwaters at Äsö hard rock laboratory, Swden. *Int. J. Syst. Bacteriol.,* **48**, 1:311-5.

NAGRA (1994). *Kristallin-I. Safety Assessment Report.* (Technical Report NTB TR 93-22), NAGRA, Wettingen, Switzerland, 396 p.

Neal, A.L., Techkarnjanaruk, S., Dohnalkova, A., McCready, D., Peyton, B.M. and Geesey, G.G. (2001). Iron sulfides and sulfur species produced at hematite

surfaces in the presence of sulfate-reducing bacteria. *Geochim. Cosmochim. Acta,* **65**(2), 223-235.

Nordstrom, D.K. and Archer, D.G. (2002). Arsenic Thermodynamic Data and Environmental Geochemistry. In: Welch, A.H. and Stollenwerk, K.G. (Eds.) *Arsenic in Ground Water: Geochemistry and Ocurrence.* Kluwer Academic Publishers, Boston, USA, pp. 1-26.

Nordstrom, D.K. and Puigdomenech, I. (1986). *Redox chemistry of deep ground-waters in Sweden.* (Technical Report SKB TR 86-03), SKB, Stockholm, Sweden, 30 p.

Nordstrom, D.K., Ball, J.W., Donahoe, R.J. and Whittemore, D. (1989). Groundwater chemistry and water-rock interactions at Stripa. *Geochim. Cosmochim. Acta,* **53**, 1727-1740.

Nordstrom, D.K., McNutt, R.H., Puigdoènech, I., Smellie, J.A.T. and Wolf, M. (1992). Groundwater chemistry and geochemical modelling of water-rock interactions at the Osamu Utsumi mine and the Morro do Ferro analogue study sites, Poços de Caldas, Minas Gerais, Brazil. *J. Geochem. Explor.,* **45**, 249-287.

Nordstrom, D.K., Plummer, L.N., Langmuir, D., Busenberg, E., May, H.M., Jones, B.F. and Parkhurst, D. (1990). Revised chemical equilibrium data for major water-mineral reactions and their limitations. In: Melchior, D.C. and Basset, R.L. (Eds.) *Chemical Modeling of Aqueous Systems II.* pp. 398-413.

Parkhurst, D.L. and Appelo, C.A.J. (1999). *User´s guide to PHREEQC (Version 2) , a computer program for speciation, batch reaction, one dimensional transport, and inverse geochemical calculations.* (Science Report WRRIR 99-4259), USGS, 312 p.

Parkhurst, D.L., Thorstenson, D.C. and Plumer, L.N. (1990). *PHREEQE, a computer program for geochemical calculations. Revised by J.V. Tisaranni & P.D. Glynn.* (Technical Report USGS R-80--96), USGS, USA, 193 p.

Parkhurst, D.L., Thorstenson, D.C. and Plumer, L.N. (1980). *PHREEQE, a computer program for geochemical calculations.* (Technical Report USGS R-80--96), USGS, USA, 193 p.

Pearson, F.J. Jr. and Berner, U. (1991). *Nagra thermochemical data base - I. Core data.* (Technical Report NTB 91-17), NAGRA, Wettingen, Switzerland, 70 p.

Pearson, F.J. Jr., Berner, U. and Hummel, W. (1992). *Nagra thermochemical data base - II. Supplemental Data 05/92.* (Technical Report NTB 91-18), NAGRA, Wettingen, Switzerland, 250 p.

Pedersen, K, Ekendahl, S. Tullborg, E-L, Furnes, H. Thorseth, I, and Tumyr, O. (1997). Evidence of ancient life at 207 m depth in a granite aquifer. *Geology,* **25**, 827-830.

Pitkänen, P., Luukkonen, A., Ruotsalainen, P., Leino-Forsman, H. and Vuorinen, U. (1999). *Geochemical modelling of groundwater evolution and residence time at the Olkilouto Site.* (Technical Report POSIVA 98-10), POSIVA, Helsinki, Finland, 184 p.

Pitkänen, P., Partamies, S. and Luukkonen, A. (2004). *Hydrogeochemical interpretation of baseline groundwater conditions at the Olkiluoto Site.* (Technical Report POSIVA 2003-07), POSIVA, Helsinki, Finland, 159 p.

Plummer, L.N., Jones, B.F. and Truesdell, A.H. (1976). *WATEQF. A FORTRAN IV version of WATEQ, a computer program for calculating chemical equilibrium of natural waters.* (Report USGS 76-13), USGS, USA, 61 p.

Plummer, L.N., Parkhurst, D.L., Fleming, G.W. and Dunkle, S.A. (1988). *A computer program incorporating Pitzer's equations for calculation of geochemical reactions in brines.* (Technical Report USGS R-88-4153), USGS, USA.

Plummer, L.N., Prestemon, E.C. and Parkhurst, D.L. (1994). *An interactive code (NETPATH) for modelling NET geochemical reactions along a flow PATH-version 2.0.* (Report USGS 95-4169), USGS, USA.

PNC (1992). *Research and development on geological waste disposal of high-level radioactive waste. First Progress Report.* (Progress Report PNC TN1410 93-059.), pnc.

Poulton, S.W., Krom, M.D., Van Rijn, J. and Raiswell, R. (2002). The use of hydrous iron (III) oxides for the removal of hydrogen sulphide in aqueous systems. *Water Research,* **36**, 825-834.

Puigdomenech, I. (Ed.) (2001). *Hydrochemical stability of groundwaters sourrunding a spent nuclear fuel repository in a 100000 year perspective.* (Technical Report SKB TR 01-28), SKB, Stockholm, Sweden, 83 p.

SKB (1999). *SR 97. Processes in the repository evolution. Background report to SR 97.* (Technical Report SKB TR 99-07), SKB, Stockholm, Sweden.

SKI (1996). *SKI SITE-94. Deep repository performance assessment project. 2 vols.* (Technical Report SKI R 96/36), SKI, Stockholm, Sweden, 305-660 p.

Smellie, J.A.T. and Laaksoharju, M. (1992). *The Äspö Hard Rock Laboratory: Final evaluation of the hydrogeochemical pre-investigations in relation to existing geologic and hydraulic conditions.* (Technical Report SKB TR 92-31), SKB, Stockholm, Sweden, 239 p.

Trotignon, L., Beaucaire, C., Louvat, D. and Aranyossy, J.F. (1999). Equilibrium geochemical modelling of Äspö groundwaters: a sensitivity study of thermodynamic equilibrium constants. *Appl. Geochem.,* **14**, 907-916.

Trotignon, L., Beaucaire, C., Louvat, D. and Aranyossy, J.F. (1997). Equilibrium geochemical modelling of Äspö groundwaters: a sensitivity study to model parameters. In: Laaksoharju, M. and Wallin, B. (Eds.) *Evolution of the groundwater chemistry at the Äspö Hard Rock Laboratory.* (Report SKB 97-04), SKB, Stockholm, Sweden.

Trotignon, L., Michaud, V., Lartigue, J.E., Ambrosi, J.P., Eisenlohr, L., Griffault, L., De Combarieu, M. and Daumas, S. (2002). Laboratory simulation of an oxidizing perturbation in a deep granite environment. *Geochim. Cosmochim. Acta,* **66**(14), 2583-2601.

Tullborg, E.L., Landström, O. and Wallin, B. (1999). Low temperature trace element mobility influenced by microbial activity - indications from fracture calcite and pyrite in crystalline basement. *Chem. Geol.,* **157**(3-4), 199-218.

Van der Lee, J. and De Windt, L. (1999). *CHESS tutorial and Cookbook. Updated for version 2.4..* (Technical Report TR CIG/LHM/RD/99/05), EMP, Paris, France.

Vieno, T. and Nordman, H. (1999). *Safety assessment of spent fuel disposal in Hästholmen, Kivetty, Olkiluoto and Romuvaara. TILA-99.* (Technical Report POSIVA 99/07), POSIVA, Helsinki, Finland, 253 p.

Vuorinen, U., Kulmala, S., Hakanen, M., Ahonen, L. and Carlsson, T. (1998). *Solubility database for Tila-99.* (Technical Report POSIVA 98-14), POSIVA, Helsinki, Finland, 117 p.

Wallin, B. and Peterman, Z. (1999). Calcite fracture fillings as indicators of paleohydrology at Laxemar at the Äspö Hard Rock Laboratory, southern Sweden. *Appl. Geochem.,* **14**, 953-962.

Wescot, R.G., Lee, M.P., Eisenberg, N.A., McCartin, T.J. and Baca, R.G. (1995). *NRC Iterative Performace Assessment Phase 2.* (Technical Report NRC IPA-2), NUREG, USA, 544 p.

Appendix A: Samples supplied in the 1.2 datafreeze

Table A.1: *Number of samples supplied in the data freeze 1.2 for the Äspö subarea.*

Subarea	Type of Water	Type of sampling	ID code	Sampling Dates	Depths	Number of Samples			
						Total (Data Freeze 1.2)	With Major Elements (ME)	With ME, Stable isotopes & Tritium	Representative
Äspö (before tunnel)	Ground Water	Packered section	HAS02	1987	40-100	2	2		1
			HAS03	1987	40-100	2	2		1
			HAS05	1987	40-100	2	2		1
			HAS06	1987	40-100	2	2		1
			HAS07	1987	70-100	2	2		1
			HAS13	1989	0-100	4	4	1	1 (G)*
			KAS02	1988, 1989	202-214	10	9	1	1
				1988	314-319	8	8	1	0
				1988	308-344	4	4	1	1
				1988	463-468	9	2	1	0
				1988	530-535	5	1	1	1
				1988, 1989	802-924	16	10	2	1 (G)
			KAS03	1989	129-134	9	9	1	1 (G)
				1988	196-222	4	1	1	1
				1988	248-251	3	3	1	1
				1988	347-373	4	2	1	1
				1988	453-480	4	3	1	1
				1988	609-623	4	1	1	1
				1988	690-1002	3	1	1	0
				1989	860-1002	13	13	1	1 (G)
			KAS04	1988	102-202	3	2	0	0
				1988	202-325	2	2	0	0
				1989	226-235	8	8	1	0
				1989	334-343	7	7	1	1 (G)
				1989	440-480	6	6	1	1 (G)
			KAS06	1989	204-277	4	4	1	1
				1989	304-377	4	4	1	1
				1989	389-406	4	4	1	1
				1989	439-602	4	4	1	1
Total Äspö (GW)						**152**	**122**	**23**	**23**

* (G) sample with dissolved gasses.

Table A.2: *Number of samples supplied in the data freeze 1.2 for the Ävrö subarea.*

Subarea	Type of Water	Type of sampling	ID code	Sampling Dates	Depths	Number of Samples			
						Total (Data Freeze 1.2)	With Major Elements (ME)	With ME, Stable isotopes & Tritium	Representative
Ävrö	Ground Water	Packered section	HAV04	1987	35-100	2	2	2	1
			HAV05	1987	50-100	2	2	2	1
			HAV06	1987	73-100	2	2	2	1
			HAV07	1987	69-100	2	2	2	1
			HAV09	2003	15-131	1	0	0	0
			HAV10	2003	12-100	2	0	0	0
		Tube (50 m)	KAV01	2003	33-733	14	0	0	0
		Packered section		1987	420-425	8	6	1 (C)	0
				1987	522-532	9	9	1 (C)	0
				1987	558-563	18	15	1 (C)	1
				1987	635-743	17	4	1	1
			KAV04	2003, 2004	47-50	1	1	0	0
				2003, 2004	0-100	1	1	1	1
				2003, 2004	¿?	21	0	0	0
Total Ävrö (GW)						**100**	**44**	**13**	**7**

(C) sample with colloids.

Table A.3: *Number of samples supplied in the data freeze 1.2 for the Laxemar subarea.*

Subarea	Type of Water	Type of sampling	ID code	Sampling Dates	Depths	Number of Samples				
						Total (Data Freeze 1.2)	With Major Elements (ME)	With ME & Stable isotopes	With ME, SI & Tritium	Representative
Laxemar	Ground Water	Packered Section	HLX01	1987, 1998	19-100	4	3	3	3	0
			HLX02	1998	19-20	1	1	1	0	0
			HLX03	1987, 1998	19-100	3	2	2	2	0
			HLX04	1998	19-20	1	1	1	0	0
			HLX05	1998	19-20	1	1	1	0	0
			HLX06	1987, 1998	19-100	3	3	3	2	0
			HLX07	1987, 1998	19-100	3	3	3	2	0
			HLX08	1998	6-7	1	1	1	0	0
			HLX10	2003	0-200	4	1	1	1	1
			KLX01	1988	272-277	10	9	1	1	1 (G)
				1988	456-461	12	10	1	1	1 (C)
				1988, 1989	680-702	23	17	2	2	2 (G,C)
				1990	830-841	11	6	1	0	1 (G)
				1990	910-921	12	11	1	0	1
				1990	999-1078	11	11	1	0	1
		Tube (50m)	KLX02	1992-1997	0-1681	81	53	53	40	26
		Packered Section		1994	315-321	5	4	1	0	1
				1993	335-340	6	3	1	0	1
				1993, 2002	798-803	8	4	1	0	1
				1993, 1999	1090-1096	12	8	4	0	1
				1999	1155-1165	4	4	4	4	1
				1999	1385-1392	1	1	1	1	0
				1992, 1993	¿?	28	0	0	0	0
			KLX04	2004	¿?	1	0	0	0	0
	Sea Water		PLX	1998-1999		56	56	56	25	49
TOTAL	**Groundwaters**					**246**	**157**	**88**	**59**	**39**
	Surface Waters					**56**	**56**	**56**	**25**	**49**
	Total					**302**	**213**	**144**	**84**	**88**

Table A.4: *Number of samples supplied in the data freeze 1.2 for the Simpevarp subarea.*

Subarea	Type of Water	Type of sampling	ID code	Sampling Dates	Depths	Number of Samples				
						Total (Data Freeze 1.2)	With Major Elements (ME)	With ME & Stable isotopes	With ME, SI & Tritium	Representative
Simpevarp	Ground Water	Packered	HSH02	2003	0-200	7	5	5	5	1
			HSH03	2002,03,04	0-200	10	4	4	4	1
		Tube	KSH01A	2003	1-1000	19	12	11	11	0
		Packered section		2003	156-167	25	6	6	6	1 (M)
				2003	245-261	17	7	7	6	1 (G,M)
				2002	197-313	1	1	1	1	1 (G,M)
				2003	548-565	19	2	2	2	1
		Tube	KSH02	2003	0-991	23	11	8	4	2
		Packered section		2003	419-424	2	2	1	1	1
				2003	411-467	1	1	1	1	0
		Tube		2003	575-580	2	2	2	1	1
		Packered section		2004	957-958	3	1	0	0	0
				2004	958-975	1	0	0	0	0
			KSH03	2003/04	0-100	4	3	3	3	1
		Tube		2003/04	40-990	29	10	1	1	0
		?	KSH03A B			12	0	0	0	0
	Shallow GW		PSM	2004		8	0	0	0	0
			SSM	2003/04		15	3	3	3	1
	Sea W		PSM	2003/04		214	205	64	54	192
	Lake W		PSM	2003/04		151	121	20	18	64
	Running W		PSM	2003/04		394	354	81	71	126
	Precipit		PSM	2002/03		7	7	7	6	2
TOTAL	**Groundwaters (including shallow)**					**198**	**70**	**55**	**49**	**12**
	Surface waters					**766**	**687**	**172**	**149**	**384**
	Total					**964**	**757**	**227**	**198**	**396**

(M) sample with microbial analysis.

POM (TOTAL)	**Ground Waters (including shallow GW)**	**696**	**393**	**179**	**144**	**81**
	Surface Waters (Sea, Lake, Running, Precipitation)	**822**	**743**	**228**	**174**	**433**
	Total	**1518**	**1136**	**407**	**318**	**514**

Table A.5: *Number of samples taken after data freeze 1.1 for the Ävrö subarea.*

Subarea	Type of Water	Type of sampling	ID code	Sampling Dates	Depths	Number of Samples			
						New samples after Data Freeze 1.1	With Major Elements (ME)	With ME, Stable isotopes & Tritium	Representative
Ävrö	Ground Water	Packered sec.	HAV04	1987	35-100				
			HAV05	1987	50-100				
			HAV06	1987	73-100				
			HAV07	1987	69-100				
			HAV09	2003	15-131	1	0	0	0
			HAV10	2003	12-100	2	0	0	0
		Tube (50 m)	KAV01	2003	33-733	14	0	0	0
		Packered sec.		1987	420-425				
				1987	522-532				
				1987	558-563				
				1987	635-743				
			KAV04	2003, 2004	47-50	1	1	0	0
				2003, 2004	0-100	1	1	1	1
				2003, 2004	¿?	21	0	0	0
Total New Ävrö samples						**40**	**2**	**1**	**1**

Table A.6: *Number of samples taken after data freeze 1.1 for the Laxemar subarea.*

Subarea	Type of Water	Type of sampling	ID code	Sampling Dates	Depths	Number of Samples				
						New samples after Data Freeze 1.1	With Major Elements (ME)	With ME & Stable isotopes	With ME, SI & Tritium	Representative
Laxemar	Ground Water	Packered section	HLX01	1987, 1998	19-100					
			HLX02	1998	19-20					
			HLX03	1987, 1998	19-100					
			HLX04	1998	19-20					
			HLX05	1998	19-20					
			HLX06	1987, 1998	19-100					
			HLX07	1987, 1998	19-100					
			HLX08	1998	6-7					
			HLX10	2003	0-200	4	1	1	1	1
			KLX01	1988	272-277					
				1988	456-461					
				1988, 1989	680-702					
				1990	830-841					
				1990	910-921					
				1990	999-1078					
		Tube (50m)	KLX02	1992-1997	0-1681					
		Packered section		1994	315-321					
				1993	335-340					
				1993, 2002	798-803					
				1993, 1999	1090-1096					
				1999	1155-1165					
				1999	1385-1392					
				1992, 1993	¿?					
			KLX04	2004	¿?	1	0	0	0	0
	Sea Water		PLX	1998-1999						
Total New Laxemar samples						**5**	**1**	**1**	**1**	**1**

Table A.7: *Number of samples taken after data freeze 1.1 for the Simpevarp subarea.*

Subarea	Type of Water	Type of sampling	ID code	Sampling Dates	Depths	Number of Samples				
						New samples after Data Freeze 1.1	With Major Elements (ME)	With ME & Stable isotopes	With ME, SI & Tritium	Representative
Simpevarp	Ground Water	Packered	HSH02	2003	0-200	3	3	3	3	0
			HSH03	2002,03,04	0-200	2	1	1	1	1
		Tube	KSH01A	2003	1-1000					
		Packered section		2003	156-167					
				2003	245-261					
				2002	197-313					
				2003	548-565	19	2	2	2	1
		Tube	KSH02	2003	0-991					
		Packered section		2003	419-424	2	2	1	1	1
				2003	411-467					
		Tube		2003	575-580	2	2	2	1	1
		Packered section		2004	957-958	3	1	0	0	0
				2004	958-975	1	0	0	0	0
			KSH03	2003/04	0-100	4	3	3	3	1
		Tube		2003/04	40-990	29	10	1	1	0
			KSH03A B							
	Shallow GW		PSM	2004		8	0	0	0	0
			SSMxxx	2003/04		12	0	0	0	0
	Sea W		PSMxxx	2003/04		94	72	22	16	75
	Lake W		PSMxxx	2003/04		74	56	6	6	30
	Running W		PSMxxx	2003/04		160	118	21	17	63
	Precipit		PSMxxx	2002/03		1	7	7	6	2
TOTAL new samples	**Ground Waters (including shallow GW)**					**85**	**24**	**13**	**12**	**5**
	Surface Waters (Sea, Lake, Running, Precipitation)					**329**	**247**	**50**	**39**	**169**
	Total					**414**	**271**	**63**	**51**	**174**

POM (TOTAL new samples)	**Ground Waters (including shallow GW)**	**130**	**27**	**15**	**14**	**7**
	Surface Waters (Sea, Lake, Running, Precipitation)	**329**	**247**	**50**	**39**	**169**
	Total	**459**	**274**	**65**	**53**	**176**

Appendix B: Why WATEQ4F database?

B.1. The reason for this Appendix

The use of WATEQ4F thermodynamic database has been questioned by INSITE and therefore an explanation about the authors reasons to use it is presented in this Appendix. The two textually written comments concerning this matter are:

Why is the WATEQ4F database used rather than more widely used NEA/HATCHES or NAGRA-PSI databases?.... ..... However the differences for the modelling involved here (i.e. major minerals and aqueous species) are probably negligible. Comments to Forsmark 1.1

Although this is perfectly reasonable (referred to the use of WATEQ4F) *at the present stage of the investigations, one has to bear in mind that in a later stage the calculations will have to be compatible with the ones performed for PA purposes. PA related modelling uses NEA-TDB database, even for the auxiliary data (major components). It would be advisable to look for full compatibility among the various thermodynamic databases as the investigations progress.* Comments to Simpevarp 1.1.

From these comments it seems that the reviewers consider that WATEQ4F database is less used than others, and its use will cause some kind of incompatibility with future PA-related calculations. The following explanation sets to demonstrate that this is not true.

B.2. Why WATEQ4F database?

The WATEQ4F database is one of the most widely used in scientific literature and also in the Performance Assessment context (the same is valid for the WATEQ4F geochemical code). WATEQ4F is the latest version of the WATEQ series developed by the US Geologycal Survey at the end of the sixties. Since then it has been enlarged and improved in successive updates by researchers from this institution. The main latest upgrades in WATEQ4F database are those of Nordstrom *et al.* (1990) and Nordstrom and Archer[16] (2002).

This set of thermodynamic data has been included, in a reduced form, in other geochemical codes from USGS such as: NETPATH (WATEQFP; Plummer *et al.*, 1994) and PHREEQE (Parkhurst *et al.*, 1980, 1990). This latest code is another of the most widely used in geochemical modelling activities and encloses a thermodynamic database that, basically is a reduced subset of WATEQ4F (less elements and minerals).

[16] Authors with a widely recognised prestige in geochemical modelling and thermodynamic data compilation activities.

WATEQ4F in one of the databases distributed with the USGS code PHREEQC (Parkhurst and Appelo, 1999). It is also distributed with other codes developed out of this institution. CHESS (Van der Lee and De Windt, 1999) or Geochemist's Workbench (GWB; Bethke, 1992, 1990) enclose WATEQ4F database among others because of its wide use. Finally, WATEQ4F is frequently used as a source of thermodynamic data both for geochemical studies and for elaboration of other thermodynamic compilations. This is valid in the scientific field and also in PA related geochemical activities.

B.3. WATEQ4F database in the PA context

Here is a brief review of the use of WATEQ4F database (or PHREEQE database) in the main geochemical modelling studies related to PA. These studies refer to natural analogues, underground research laboratories (and Test Sites) and the PA exercises themselves.

B.3.1. Natural Analogue Studies

WATEQ4F database has been widely used in the natural analogue studies at different levels. It has been used in the hydrogeochemical modelling, in the BPM exercises and also as a simple source of data. Some examples include: Cigar Lake (Cramer and Nesbitt, 1994); Poços de Caldas (Nordstrom *et al.*, 1992); El Berrocal (Gómez *et al.*, 1996); Oklo (Gómez *et al.*, 1998); Palmottu (Bruno *et al.*, 1999; Gimeno *et al.*, 2001); Tono Mine (Iwatsuki and Yoshida, 1999); etc. The use of this database is also indicated in the BPM exercises review performed by Bruno *et al.* (2001, 2002).

B.3.2. Underground Research Laboratories and Test Sites

The use of WATEQ4F (or PHREEQE) codes and databases in the geochemical calculations related to these activities is exemplified by the following: Bottomley *et al.* (1990) use WATEQF (Plummer *et al.*, 1976) to study groundwater geochemical evolution at East Bull Lake (WRA, Canada); Beaucaire *et al.* (2000) use PHREEQE to establish the geochemical groundwater evolution model at MOL (Belgium) in the context of ARCHIMEDE project (Griffault *et al.*, 1996).

However, this use is specially significant in the framework of the Swedish program: (a) Nordstrom and Puigdomenech (1986) used WATEQ3 for the analysis of redox states in deep groundwaters; (b) Nordstrom *et al.* (1989) in the context of STRIPA project, used WATEQ4F, the code and the database; (c) Smellie and Laaksoharju (1992) used PHREEQE code and database in the Pre-investigation stage in Äspö; (d) Laaksoharju *et al.* (1995) used PHREEQE code and database for Saturation Index calculations to check the colloids stability; (e). Düker and Ledin (1998) used PHREEQE code and database, to check the stability of colloids at LAXEMAR; (f) Banwart (1999) used PHREEQE (with its own database enlarged with Nordstrom *et al.*, 1990) for geochemical calculations associated with the REDOX experiment at Äspö.

B.3.3. Performance Assessment exercises

Direct use of WATEQ4F or PHREEQE database in PA exercises can be considered at least as wide as any other database. These codes and databases have been used in NRC-

IPA phase II (Wescot *et al.*, 1995), H3 (PNC, 1992), H12 (JNC, 1999), and the two last PA exercises in the Swedish Program: SITE-94 (SKI, 1996) and SR-97 (SKB, 1999).In SITE-94 Glynn and Voss (1999) used WATEQ4F for geochemical evolution of groundwaters and redox conditions. In SR-97 the authors used the results from WATEQFP (NETPATH) to characterize the geochemical evolution of the three considered sites. This use is specified in the main report.

Moreover, WATEQ4F database has also been used, indirectly in other exercises such as KRISTALLIN-I (NAGRA, 1994), TILA-99 (Vieno and Nordman, 1999) and SR-97 through the NAGRA-PSI database (see below).

B.4. WATEQ4F and other databases

It is clear that this thermodynamic database has been widely used in the kind of systems and studies that we are dealing with here. However, the use of other thermodynamic databases have been suggested instead of WATEQ4F. These are: HATCHES NEA, NAGRA-PSI database, and NEA-TDB. Their main features include:

B.4.1. HATCHES NEA

One of the latest versions of this database (HATCHES NEA 13, Oct. 2000) includes most of the data from PHREEQE database. This is explicitly indicated in the log K and ΔH values. The source of data is expressed as "USGS data" or "PHREEQC database", that is, the data from Nordstrom *et al.* (1990).

B.4.2. NAGRA-PSI

The main references about the origin of thermodynamic data enclosed in this database are Pearson and Berner (1991), Pearson *et al.* (1992) and Hummel *et al.* (2002). These authors reported the source of data indicating that they take almost all data from Nordstrom *et al.* (1990) for carbonate, sulphate, silica, aluminium, Fe and Mn inorganic systems (species and minerals). They even justify the use of these data saying that their quality is guaranteed because these are the data included in WATEQ4F and PHREEQE.

This database has been used in PA exercises such as: (a) KRISTALLIN-I for the reference waters and solubility limits calculations (Berner, 1995); (b) in SR-97 the authors created a specific thermodynamic database (SR-97 TDB, Bruno *et al.*, 1997), based on this NAGRA-PSI (that is, Nordstrom *et al.*, 1990) but modified for Np, Am, REE and Th; (c) TILA-99 also used the SR-97 TDB and it was compared with data0.com 02 from EQ3/6 (Vuorinen *et al.*, 1998).

B.4.3. NEA-TDB

NEA-TDB has been frequently used as a source of data for some elements, but up to now no PA has used a complete thermodynamic database called "NEA-TDB". The reason for this is simple: databases supplied as NEA-TDB (up to 2001) with different codes (EQ3/6, CHESS, etc.) contain data for elements of interest for PA (U, Am, Tc, Pu and Np) and a very small set of "auxiliary" data (major components) to be used with the selected data (for instance, the only mineral phase included, common in natural systems, is QUARTZ).

Therefore, to the best of our knowledge, this database is very useful as a source of data for some elements of critical importance in PA, but useless for the hydrogeochemical study of natural systems. In fact, the data for U, Am, Tc, Pu and Np from NEA-TDB are always added to other thermodynamic data bases in all PA exercises.

Conclusions.

The main conclusion from all this description is that not only WATEQ4F database (and also the code) has been widely used in PA exercises, but also its thermodynamic data have been frequently used in safety assessment as the "core" ("auxiliary data") of databases specifically developed for PA calculations (including the Swedish program).

The use of these data favour the comparison of results in our modelling tasks because most of the previous studies in the Swedish sites and/or site characterisation tasks have also used the same thermodynamic data set. But if the use a "normalized" thermodynamic database in PA studies is planned or demanded in relation to Forsmark and Simpevarp now is the time to know it.

Appendix C: Stability Diagrams

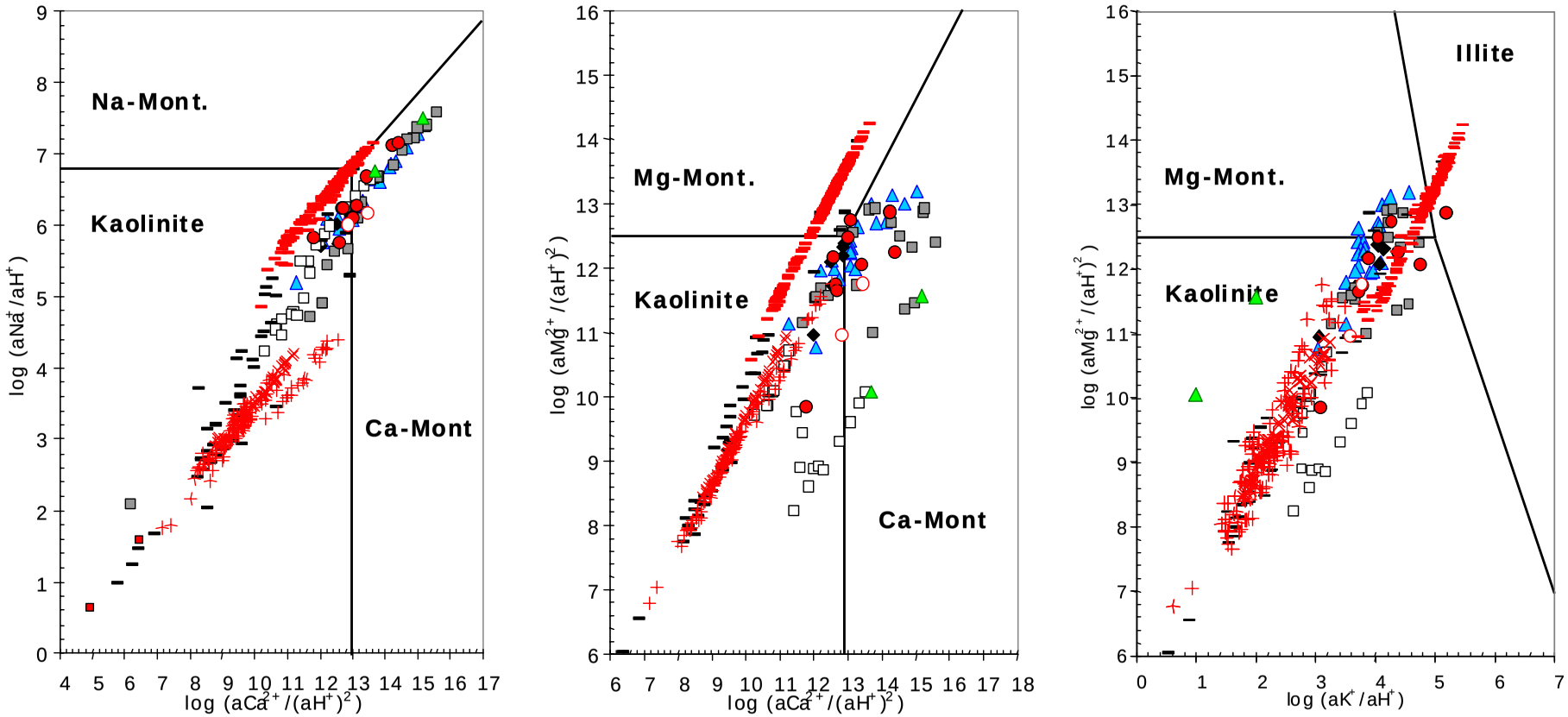

Figure C-1: *Plot of the POM waters in the aqueous activity diagrams for some aluminosilicate minerals at 7ºC, 1 bar. The field boundaries were calculated with data from Helgeson (1969) and a logarithmic silica activity of –4. The legend in shown in next figure.*

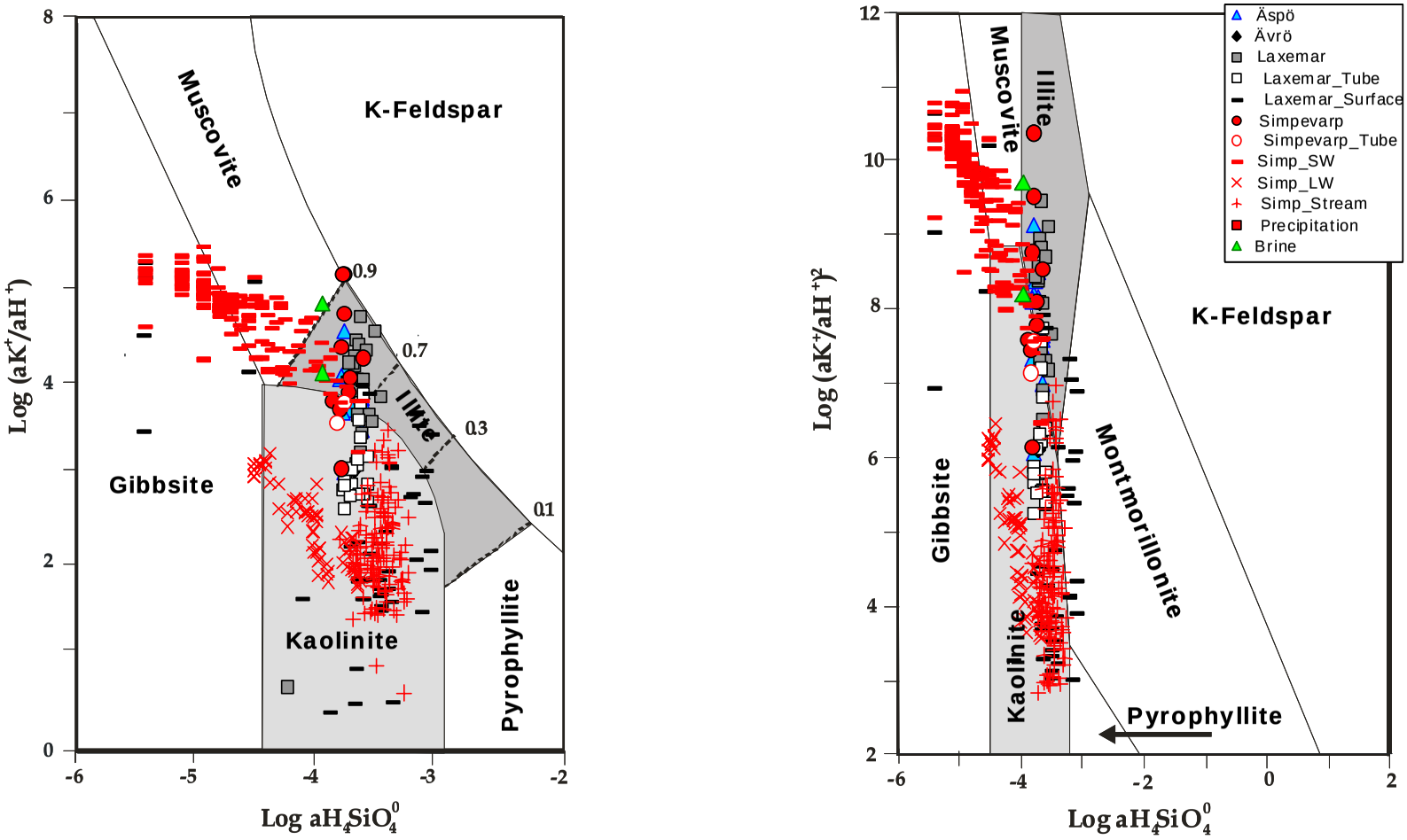

***Figure C-2**: Plot of the POM waters in aqueous activity diagrams for some aluminosilicate minerals at 25°C, 1 bar, including illite. The field boundaries have been calculated with data from Helgeson (1969) and Helgeson et al. (1978) in graph (a) and from Garrels (1984) in graph (b). In graph (a) illite field is contoured to show the stability of different illite fractios in I/S.*

Appendix D: Analytical data for redox pairs calculations

When selecting the samples for the redox characterization of the system, one of the selection criteria was the availability of analytical data for the redox elements: Fe^{2+}, S^{2-} and CH_4. Special attention was paid to the samples with CH_4 data as the redox pair CH_4/CO_2 had not been analysed before.

The availability of analytical data was checked evaluating the representativity of the concentrations with respect to their detection limits. The information about detection limits was not supplied with the 1.2 data freeze, thus, previous reports that include the same samples (Smellie and Laaksoharju, 1992; Laaksoharju *et al.*, 1995) were consulted.

The more recent data (from Simpevarp subarea) present some problems in this sense. Aqueous redox-active species in those samples (see table with the complete chemical analysis in this issued) are in sufficient concentrations for a successful Eh calculation. Total sulphide concentrations are low but above detection limit, with values between $3 \cdot 10^{-7}$ to $7.8 \cdot 10^{-5}$ mol/l; total iron concentration is between 10^{-7} and $1.2 \cdot 10^{-4}$ mol/l, above the theoretical lower limit of iron concentration for a successful Eh measurement if iron pairs control the redox potential (10^{-6} mol /l, Grenthe *et al.*, 1992). Samples 5263 and 5268 from Simpevarp have no data for S^{2-} in the 1.2 data freeze, however the same samples in 1.1 data freeze showed very low, but apparently significative, S^{2-} values (0.0014 to 0.011 mg/L). Wacker *et al.* (2003) reported a sulphide value of 0.01 mg/L for both samples. There is no indication of the detection limit for this element, but in other works, the value considered is, exactly, 0.01 mg/L. All these differences give the idea of the considerable uncertainty related to the analytical values for this fundamental element in the redox study. The authors, here, have assumed a value of 0.01 mg/L as the detection limit for sulphide.

Appendix 5: Water classification, M3 calculations and DIS modelling

Contribution to the model version 1.2

Ioana Gurban [1)] Marcus Laaksoharju[2)]

3D-Terra, Montreal [1)]

Geopoint AB, Stockholm [2)]

November 2004

Contents

1. Introduction

This paper presents the results of the water classification, mixing modelling, 3D visualisation and drilling impact study (DIS)

2. Water type classification

A classical geochemical evaluation and modelling tool AquaChem was used for water type classification of the Simpevarp 1.2 samples. The aim of water classification is to simplify the groundwater information. First the data set was divided into different salinity classes. Except for sea waters, most surface waters and some groundwaters from percussion boreholes are fresh waters according to the classification used for Äspö groundwaters. The rest of the groundwaters are brackish (Cl <5 000mg/L), except for the deeper samples from the KSH01A and KSH02 which are saline (>5 000 mg/L). Most surface waters are of Ca-HCO_3 or Na-Ca-HCO_3 type and naturally the sea water is of Na-Cl type. The deeper groundwaters are mainly of Na-Ca-Cl type. These water classes are illustrated by using different standard plots in Figure 1 and the results are listed for all samples in Appendix 1.

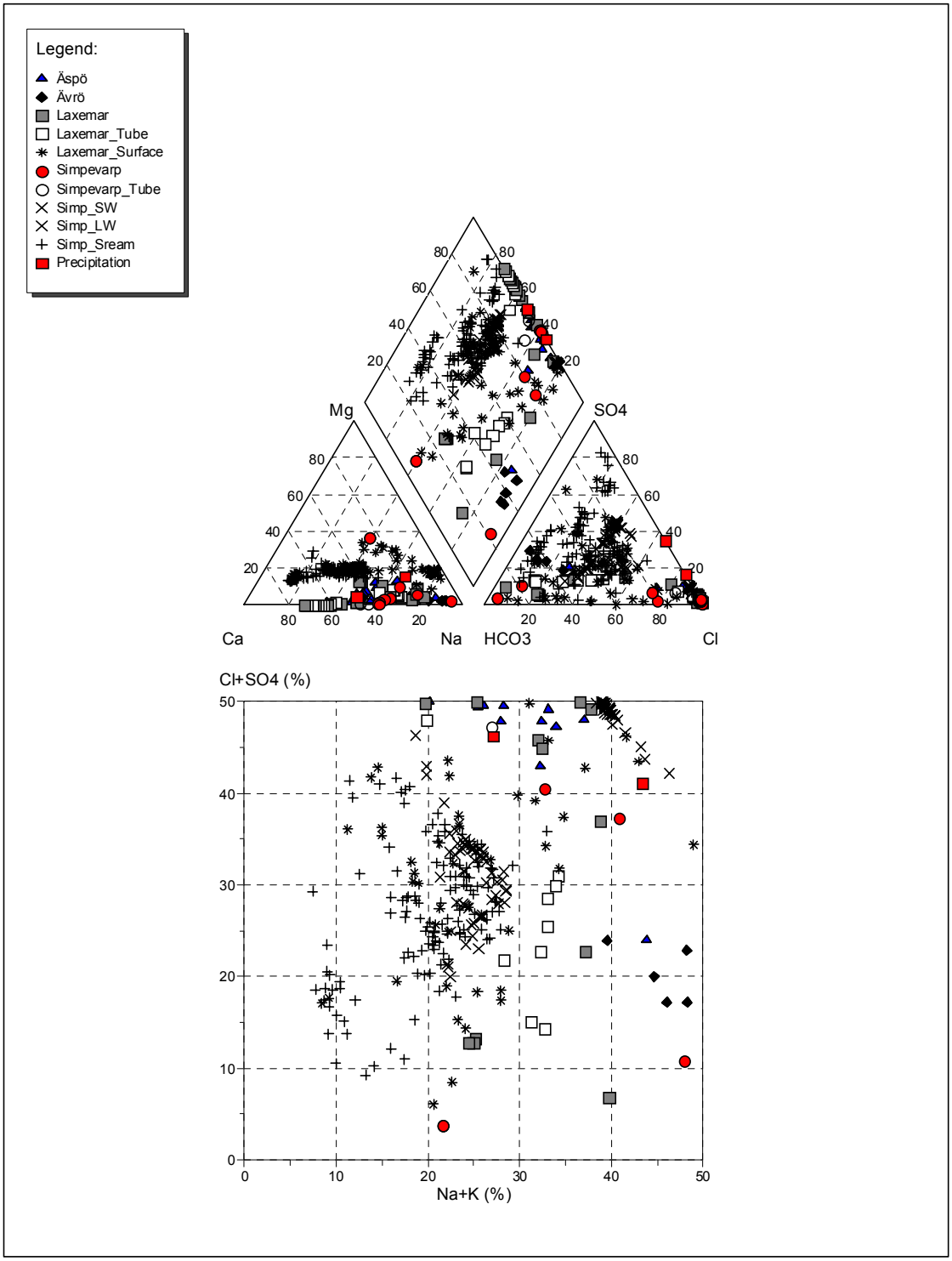

Figure 1*: Multicomponent plots used for classification of the data. From top to bottom: Piper plot and Ludwig-Langelier plot applied on all Simpevarp data using AquaChem.*

3. Descriptive and quantitative modelling by using M3 code

3.1 M3 modelling

A challenge in groundwater modelling is to reveal the origin, mixing and reactions altering the groundwater samples. The groundwater modelling concept M3 (Multivariate Mixing and Mass-balance calculations) Laaksoharju and Skårman, (1995c); Laaksoharju et al., (1999b,) can be used for making judgment on this.

In M3 modelling the assumption is that the groundwater is always a result of mixing and reactions. M3 modelling uses a statistical method to analyse variations in groundwater compositions so that the mixing components, their proportions, and chemical reactions are revealed. The method quantifies the contribution to hydrochemical variations by mixing of groundwater masses in a flow system by comparing groundwater compositions to identified reference waters. Subsequently, contributions to variations in non-conservative solutes from reactions are calculated.

The M3 method has been tested, evaluated, compared with standard methods and modified over several years within domestic and international research programmes supported by the SKB. The main test and application site for the model has been the Äspö HRL (Laaksoharju and Wallin (eds.) 1997; Laaksoharju et al., 1999c). Mixing seems to play an important role at many crystalline and sedimentary rock sites where M3 calculations have been applied such as in different Swedish sites (Laaksoharju et al., 1998), Canada (Smellie and Karlsson, 1996), Oklo in Gabon (Gurban et al., 1998) and Palmottu in Finland (Laaksoharju et al, 1999a).
The features of the M3 method are:

- It is a mathematical tool which can be used to evaluate groundwater field data, to help construct a conceptual model for the site and to support expert judgement for site characterisation.
- It uses the entire hydrochemical data set to construct a model of geochemical evolution, in contrast to a thermodynamic model that simulates reactions or predicts the reaction potential for a single water composition.
- The results of mixing calculations can be integrated with hydrodynamic models, either as a calibration tool or to define boundary conditions.
- Experience has shown that to construct a mixing model based on physical understanding can be complicated especially at site scale. M3 results can provide additional information of the major flow paths, flow directions and residence times of the different groundwater types which can be valuable in transport modelling.
- The numerical results of the modelling can be visualised and presented for non-expert use.

The M3 method consists of 4 steps where the first step is a standard principal component analysis (PCA), selection of reference waters, followed by calculations of mixing proportions, and finally mass balance calculations (for more details see Laaksoharju et al., 1999b; Laaksoharju, 1999d).

For the Simpevarp 1.1 phase (Laaksoharju et al, 2004), 2 models were built: at regional scale and at local scale. 113 samples from Simpevarp met the M3 criteria (data for major elements and isotopes) and were used in the M3 modelling. These samples were from boreholes (core and percussion), soil pipes, lake water, stream water and precipitation. In the present Simpevarp 1.2 phase (applied on data from the called POM area) the version 1.1 is up-dated with the new available data. For Simpevarp 1.2 phase, 2 models are built: at regional scale and at local scale. 326 samples from Simpevarp met the M3 criteria (data for major elements and isotopes) and were used in the M3 modelling. These samples were from boreholes (core and percussion), soil pipes, lake water, stream water and precipitation. From the 326 samples available, 180 are considered representative from hydrochemical point of view and 146 non representative.

3.2 Regional model

The PCA applied on POM (Simpevarp 1.2) data and all Nordic Sites data is illustrated in Figure 2. A total of 326 samples from Simpevarp 1.2 site were used for this plot. Numerical values are listed in Appendix 2 (in the Appendix 2, the olive green samples indicate the representative samples). The PCA in Figure 2 shows a surface water affected by seasonal variation (winter – summer precipitation), a marine trend showing a Baltic Sea water influence and for some Äspö samples a possible Littorina sea water influence. A glacial and finally a deep groundwater trend is shown.

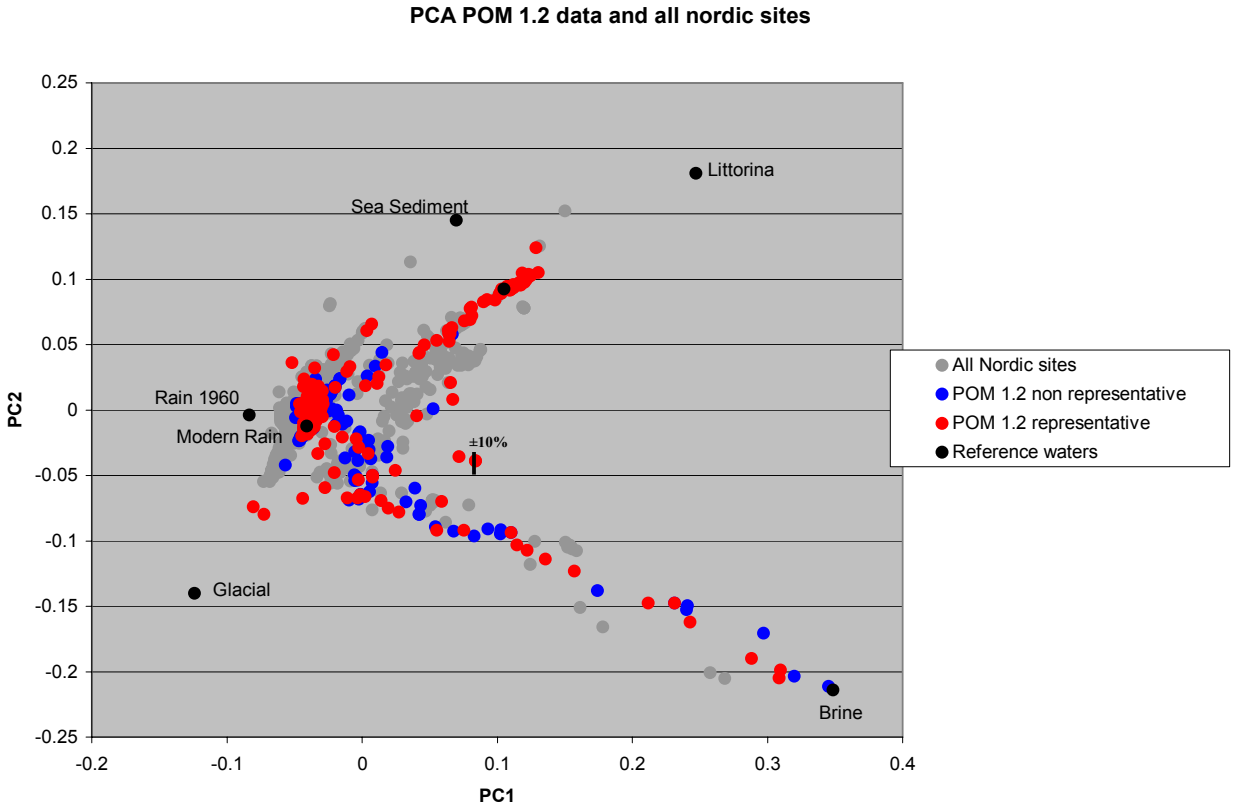

Figure 2. *The picture shows the principal components analysis and the identification of the reference waters. (Variance: First principal component: 0.40824, First and second principal components: 0.63596, First, second and third principal components: 0.74703). The figure*

shows the Nordic samples in grey points, the POM (Simpevarp1.2) representative data in red and the POM (Simpevarp 1.2) non-representative data in blue. The Sea sediment, Littorina, Brine, Glacial and Rain 1960 reference waters are used as end members for the modelling. The model uncertainty ±10% is shown as an error bar; the analytical uncertainty is ±5% and represents therefore half of the error bar.

3.2.1 The reference waters used

The following reference waters were used in the M3 modelling (for analytical data see Table 3-1):

- **Brine type of reference water:** Represents the sampled deep brine type (Cl = 47000 mg/L) of water found in KLX02: 1631-1681m (Laaksoharju et al., 1995a). An old age for the Brine is suggested by the measured ^{36}Cl values indicating a minimum residence time of 1.5Ma for the Cl component (Laaksoharju and Wallin (eds.), 1997).

- **Glacial reference water:** Represents a possible melt-water composition from the last glaciation >13000BP. Modern sampled glacial melt water from Norway was used for the major elements and the $\delta^{18}O$ isotope value (−21 ‰ SMOW) was based on measured values of $\delta^{18}O$ in calcite surface deposits (Tullborg, 1984). The $\delta^{2}H$ value (−158 ‰ SMOW) is a modelled value based on the equation ($\delta H = 8 \times \delta^{18}O + 10$) for the meteoric water line.

- **Littorina Water:** Represents modelled Littorina water (see table 3-1).

- **Modified Sea water (Sea sediment):** Represents Baltic Sea affected by microbial sulphate reduction.

- **Baltic:** Corresponds to modern Baltic sea water.

- **Rain 1960:** Corresponds to infiltration of meteoric water (the origin can be rain or snow) from 1960. Sampled modern meteoric water with a modelled high tritium content was used to represent precipitation from that period.

- **Modern Rain:** Corresponds to modern precipitation.

Table 3-1: Groundwater analytical or modelled data* used as reference waters in the M3 regional modelling for Simpevarp.

	Cl (mg/L)	Na (mg/L)	K (mg/L)	Ca (mg/L)	Mg (mg/L)	HCO_3 (mg/L)	SO_4 (mg/L)	^3H (TU)	δ^2H ‰	$\delta^{18}O$ ‰
Brine	47200	8500	45.5	19300	2.12	14.1	906	0	-44.9	-8.9
Glacial	0.5	0.17	0.4	0.18	0.1	0.12	0.5	0	-158*	-21*
Littorina sea*	6500	3674	134	151	448	93	890	0	-38	-4.7
Sea Sediment	3383	2144	91.8	103	258	793	53.1	0	-61	-7
Baltic	3760	1960	95	234	93.7	90	325	20	-53.3	-5.9
Rain 1960	0.23	0.4	0.29	0.24	0.1	12.2	1.4	2000	-80	-10.5
Modern Rain	0.23	0.4	0.29	0.24	0.1	12.2	1.4	20	-80	-10.5

The selected reference waters with the identification row numbers used in Appendix 2:

- Brine (identification row 327)
- Glacial (row 328)
- Littorina (identification row 329)
- Sea sediment (identification row 330)
- Baltic (identification row 331)
- Rain 1960 (identification row 332)
- Modern rain (identification row 333)

The following six reactions have been considered, with comments on the qualitative outcomes of mixing and mass balance modelling with M3:

1. *Organic decomposition:* This reaction is detected in the unsaturated zone associated with Meteoric water. This process consumes oxygen and adds reducing capacity to the groundwater according to the reaction: $O_2 + CH_2O \rightarrow CO_2 + H_2O$. M3 reports a gain of HCO_3 as a result of this reaction.
2. *Organic redox reactions:* An important redox reaction is reduction of iron III minerals through oxidation of organic matter: $4Fe(III) + CH_2O + H_2O \rightarrow 4Fe^{2+} + 4H^+ + CO_2$. M3 reports a gain of Fe and HCO_3 as a result of this reaction. This reaction takes place in the shallow part of the bedrock associated with influx of Meteoric water.
3. *Inorganic redox reaction:* An example of an important inorganic redox reaction is sulphide oxidation in the soil and the fracture minerals containing pyrite according to the reaction: $HS^- + 2O_2 \rightarrow SO_4^{2-} + H^+$. M3 reports a gain of SO_4 as a result of this reaction. This reaction takes place in the shallow part of the bedrock associated with influx of Meteoric water.
4. *Dissolution and precipitation of calcite:* There is generally a dissolution of calcite in the upper part and precipitation in the lower part of the bedrock according to the reaction: $CO_2 + CaCO_3 \rightarrow Ca^{2+} + 2HCO_3^-$. M3 reports a gain or a loss of Ca and HCO_3 as a result of this reaction. This reaction can take place in any groundwater type.

5. *Ion exchange:* Cation exchange with Na/Ca is a common reaction in groundwater according to the reaction: $Na_2X_{(s)} + Ca^{2+} \rightarrow CaX_{(s)} + 2Na^{+}$, where X is a solid substrate such as a clay mineral. M3 reports a change in the Na/Ca ratios as a result of this reaction. This reaction can take place in any groundwater type.
6. *Sulphate reduction:* Microbes can reduce sulphate to sulphide using organic substances in natural groundwater as reducing agents according to the reaction: $SO_4^{2-} + 2(CH_2O) + OH^- \rightarrow HS^- + 2HCO_3^- + H_2O$. This reaction is of importance since it may cause corrosion of the copper capsules. Vigorous sulphate reduction is generally detected in association with marine sediments that provide the organic material and the favorable salinity interval for the microbes. M3 reports a loss of SO_4 and a gain of HCO_3 as a result of this reaction. This reaction modifies the seawater composition by increasing the HCO_3 content and decreasing the SO_4 content.

3.3 Local model

The local model was based on data from the POM (Simpevarp 1.2) modelling area (Simpevarp, Äspö, Ävrö and Laxemar). The PCA applied on Simpevarp data is illustrated in Figure 3. Figure 3 shows similar trends as Figure 2 but with a higher resolution.

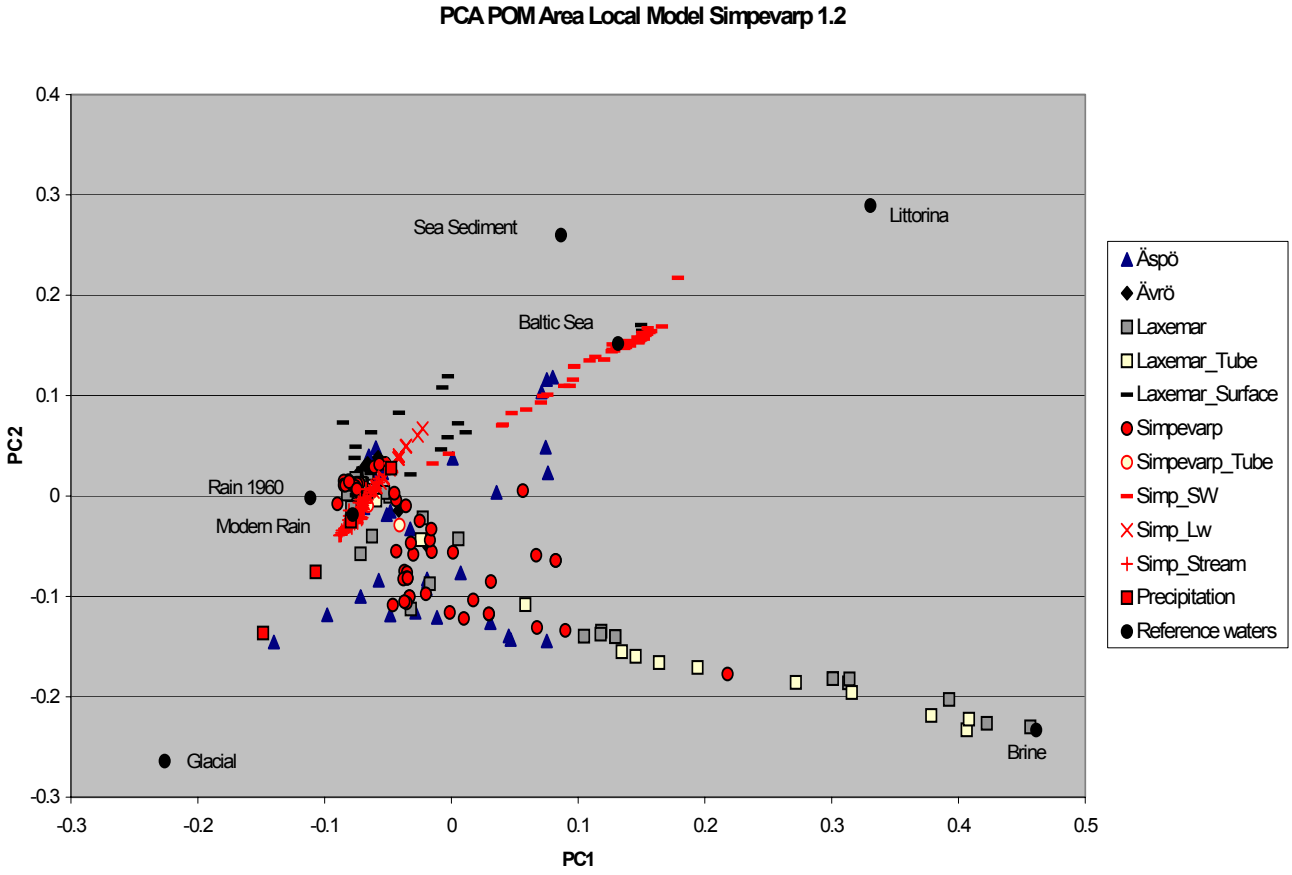

Figure 3. *The picture shows the PCA for the local model for POM (Simpevarp 1.2). The picture shows the principal components analysis and the identification of the reference waters. (Variance: First principal component: 0.41147, First and second principal components: 0.69034, First, second and third principal components: 0.79185). The Sea*

sediment, Littorina, Brine, Glacial and Rain 1960 are used as reference waters for the modelling.

The selected reference waters with the identification row numbers used in Appendix 2 (for groundwater analytical data see Table 3-2:

- Brine (identification row 327)
- Glacial (row 328)
- Littorina (identification row 329)
- Sea sediment (identification row 330)
- Baltic (identification row 331)
- Rain 1960 (identification row 332)
- Modern rain (identification row 333)

Table 3-2: Groundwater analytical or modelled data* used as reference waters in the M3 local modelling for Simpevarp.

	Cl (mg/L)	Na (mg/L)	K (mg/L)	Ca (mg/L)	Mg (mg/L)	HCO_3 (mg/L)	SO_4 (mg/L)	^3H (TU)	δ^2H ‰	$\delta^{18}O$ ‰
Brine	47200	8500	45.5	19300	2.12	14.1	906	0	-44.9	-8.9
Glacial	0.5	0.17	0.4	0.18	0.1	0.12	0.5	0	-158*	-21*
Littorina sea*	6500	3674	134	151	448	93	890	0	-38	-4.7
Sea Sediment	3383	2144	91.8	103	258	793	53.1	0	-61	-7
Baltic	3760	1960	95	234	93.7	90	325	20	-53.3	-5.9
Rain 1960	0.23	0.4	0.29	0.24	0.1	12.2	1.4	2000	-80	-10.5
Modern Rain	0.23	0.4	0.29	0.24	0.1	12.2	1.4	20	-80	-10.5

3.4 Alternative models

In order to try to test alternative models, the Tritium values were normalised to present date. Since the normalised tritium is described by a mathematical formula the normalised tritium data do not give any new information and did not change the appearance of the PCA. In M3 calculations only independent elements could bring new information.

3.5 Scatter plots of M3 modelling results

The measured Cl content, the TDS (SumIons) and the calculated M3 mixing proportions are shown for various core boreholes within the modelling domain (see Figures 4 to 14 and Appendix 3). The figures 4a, 5a, 6a, 7a, 8a, 9a, 10a, 11a, 12a, 13a and 14a represent the all available samples, representative and non representative. The figures 4b, 5b, 6b, 7b, 8b, 9b, 10b, 11b, 12b, 13b and 14b represent only the representative samples. A mixing proportion of less than 10% is regarded as being under the detection limit of the M3 method and is therefore shaded. The mixing proportions have an uncertainty range of ±0.1 mixing units. The purpose

of the plots is to facilitate comparison of the hydrochemical results (Cl, TDS, mixing proportions) with the hydrogeological results. Due to the fact that the hydrogeologists use only 4 reference waters (meteoric, glacial, brine and Littorina), the marine components (Littorina and Sea Sediment reference waters) were added together and called Marine water. In the following pictures, the mixing proportions plotted are: Brine, Glacial, Rain1960 (meteoric) and Marine (the sum of Littorina and Sea Sediment). In Appendix 4 the Cl content, the TDS (SumIons) and M3 mixing proportions for the percussion and core boreholes are listed. Olive green colour indicate representative samples.

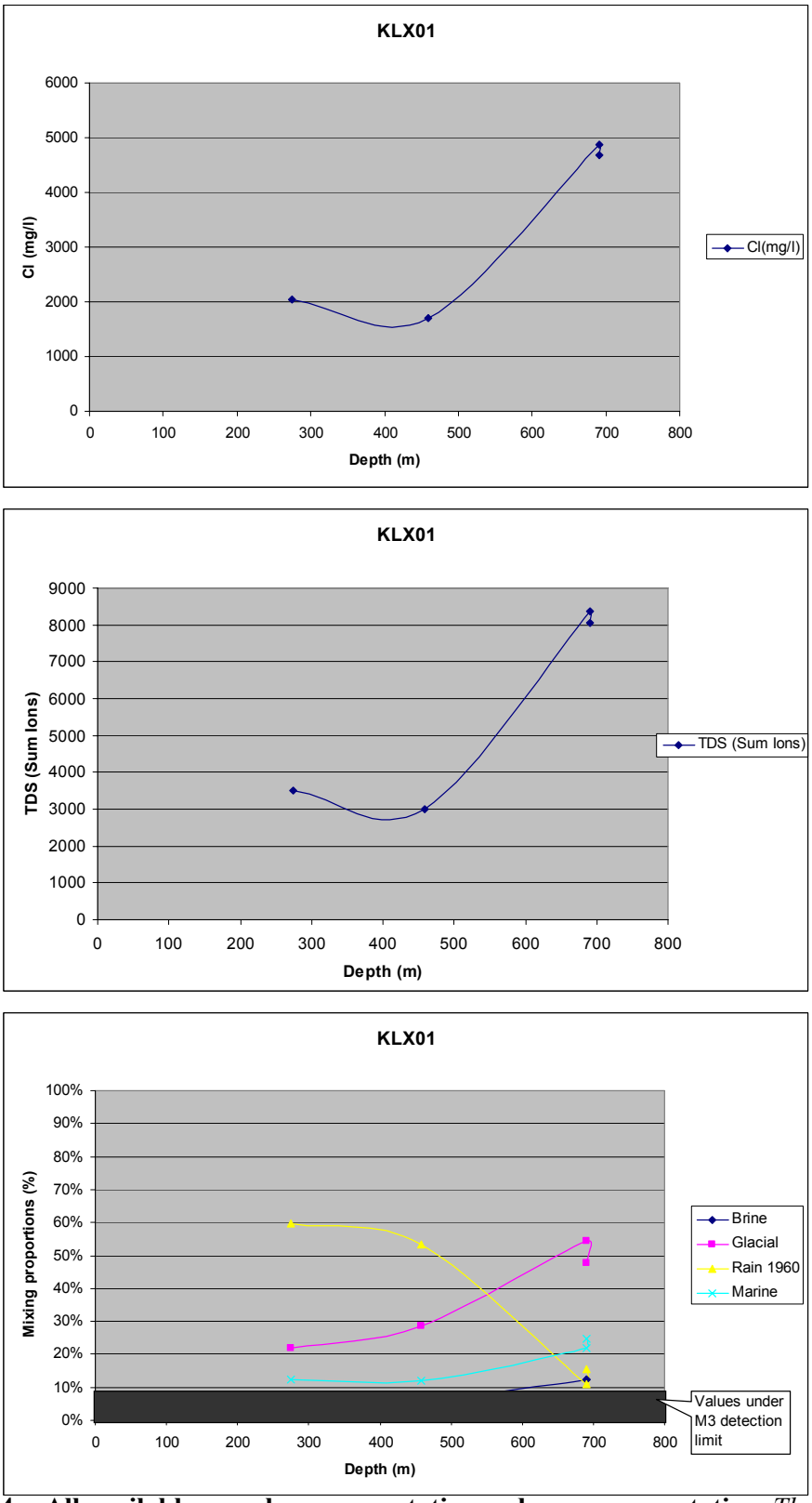

Figure 4a: All available samples representative and non representative: *The measured Cl content is shown in the uppermost figure, the TDS (Sum Ions) in the middle picture and the calculated M3 mixing proportions in the lowermost figure along borehole KLX01.*

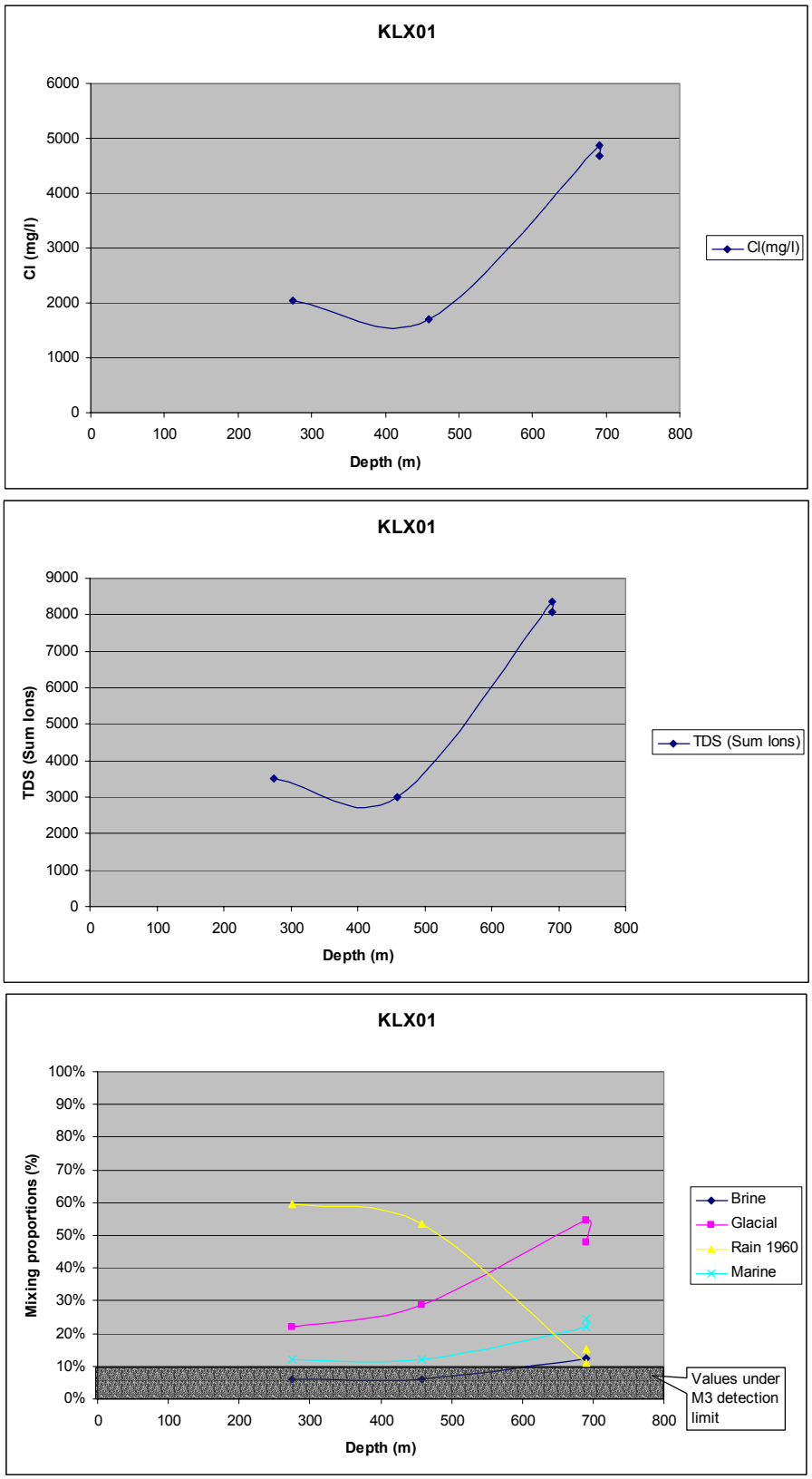

Figure 4b: Representative samples: *The measured Cl content is shown in the uppermost figure, the TDS (Sum Ions) in the middle picture and the calculated M3 mixing proportions in the lowermost figure along borehole KLX01.*

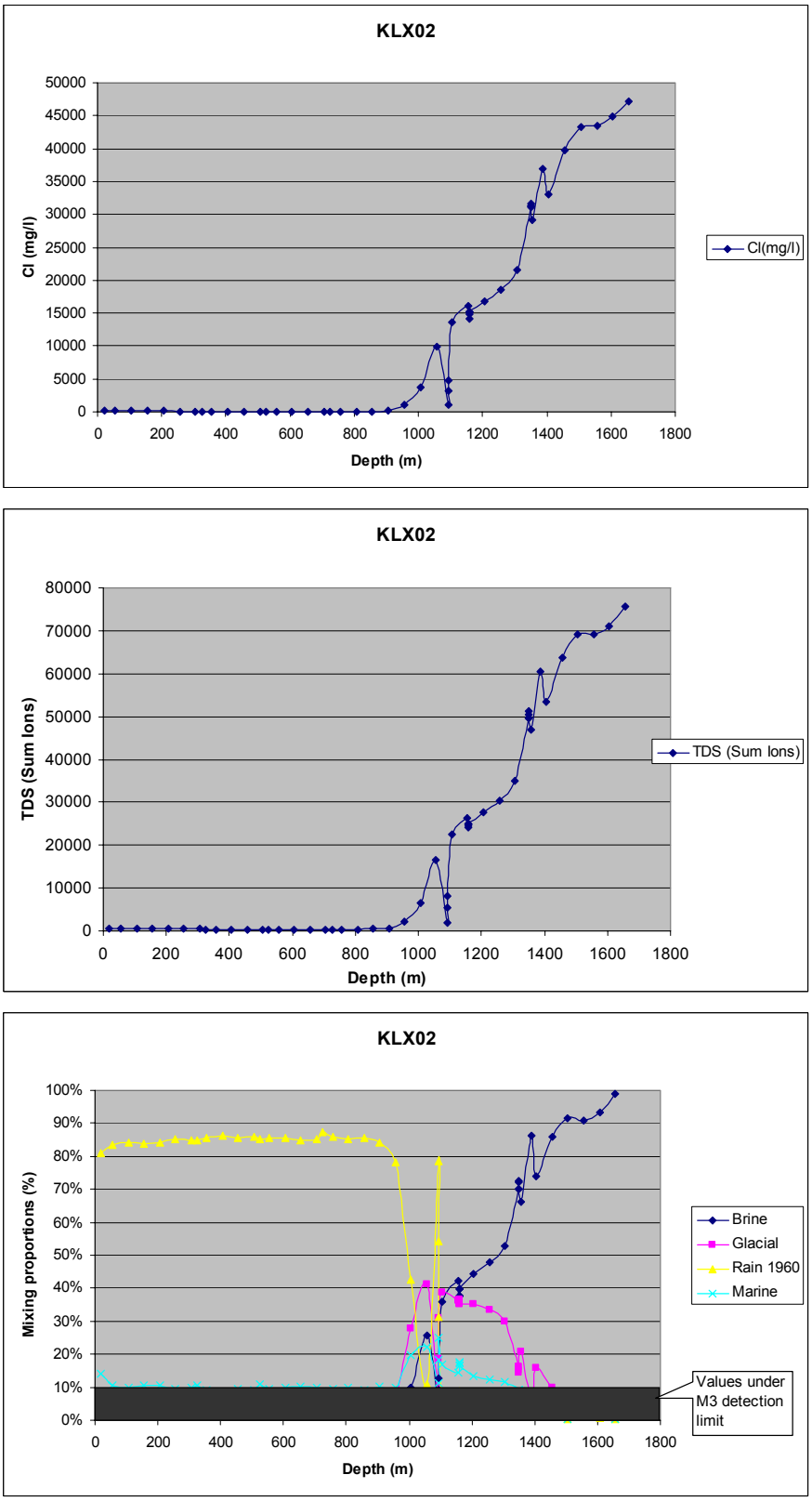

Figure 5a: All available samples representative and non representative: *The measured Cl content is shown in the uppermost figure, the TDS (Sum Ions) in the middle picture and the calculated M3 mixing proportions in the lowermost figure along borehole KLX02.*

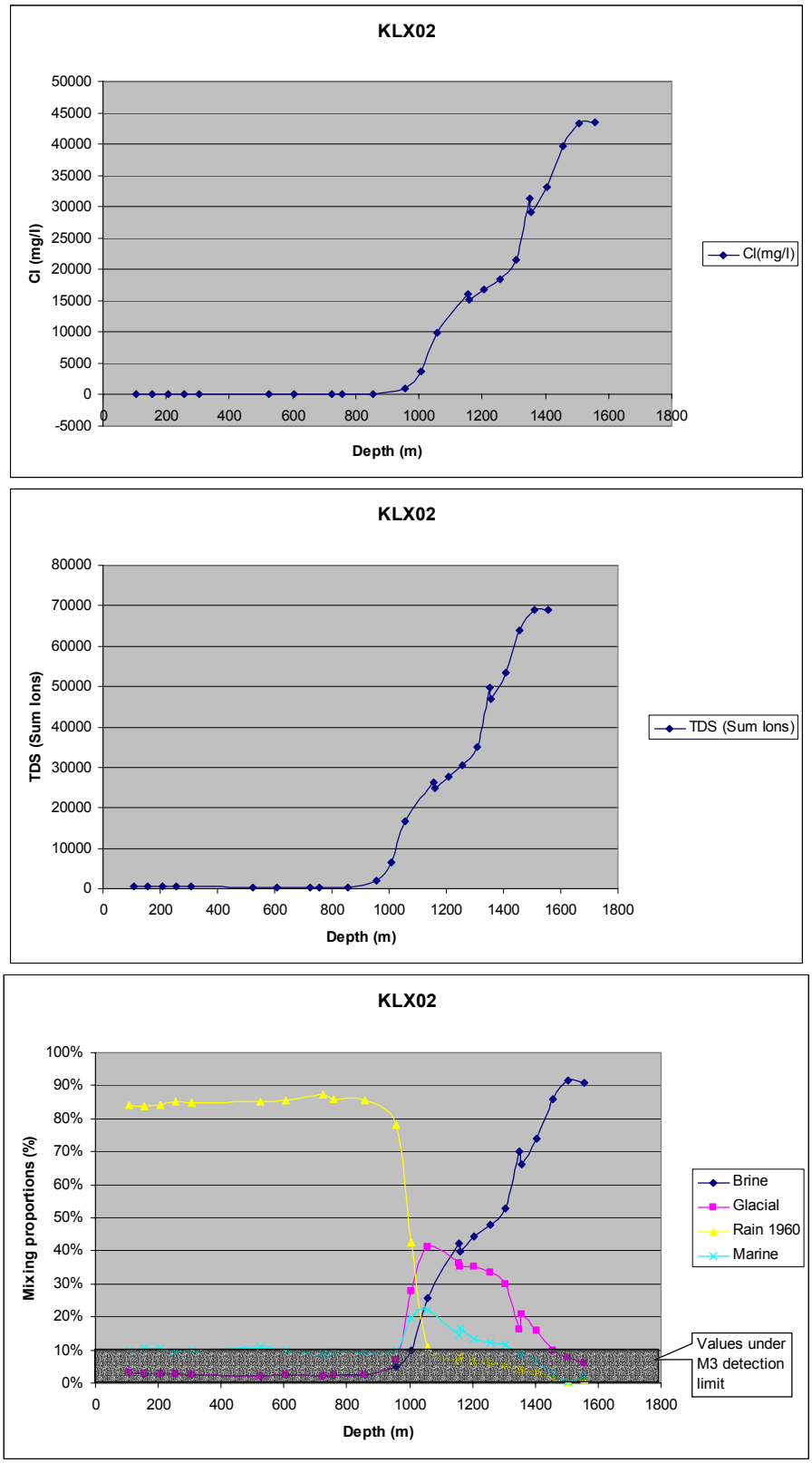

Figure 5b: Representative samples: *The measured Cl content is shown in the uppermost figure, the TDS (Sum Ions) in the middle picture and the calculated M3 mixing proportions in the lowermost figure along borehole KLX02.*

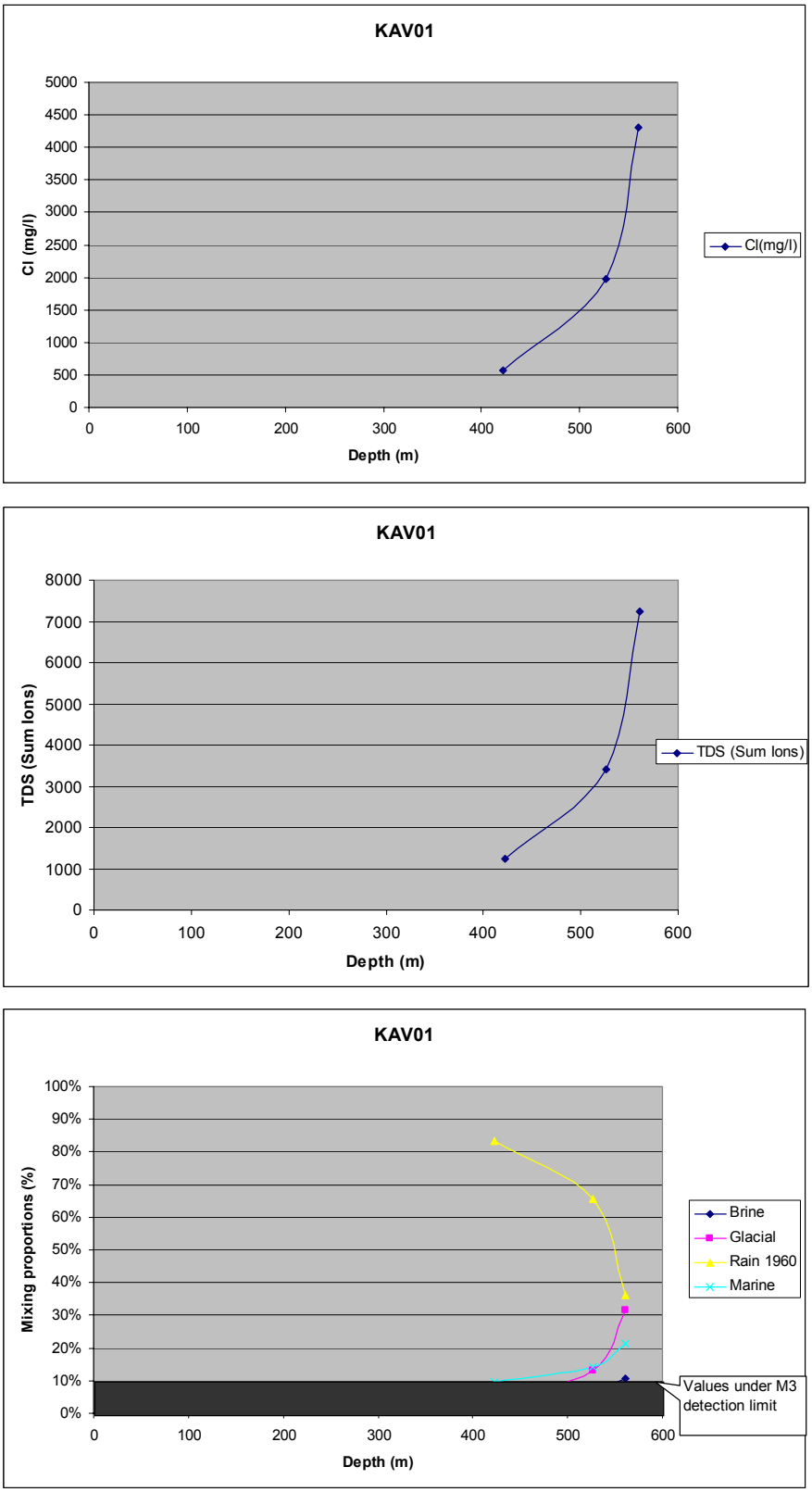

Figure 6a: All available samples representative and non representative: *The measured Cl content is shown in the uppermost figure, the TDS (Sum Ions) in the middle picture and the calculated M3 mixing proportions in the lowermost figure along borehole KAV01.*

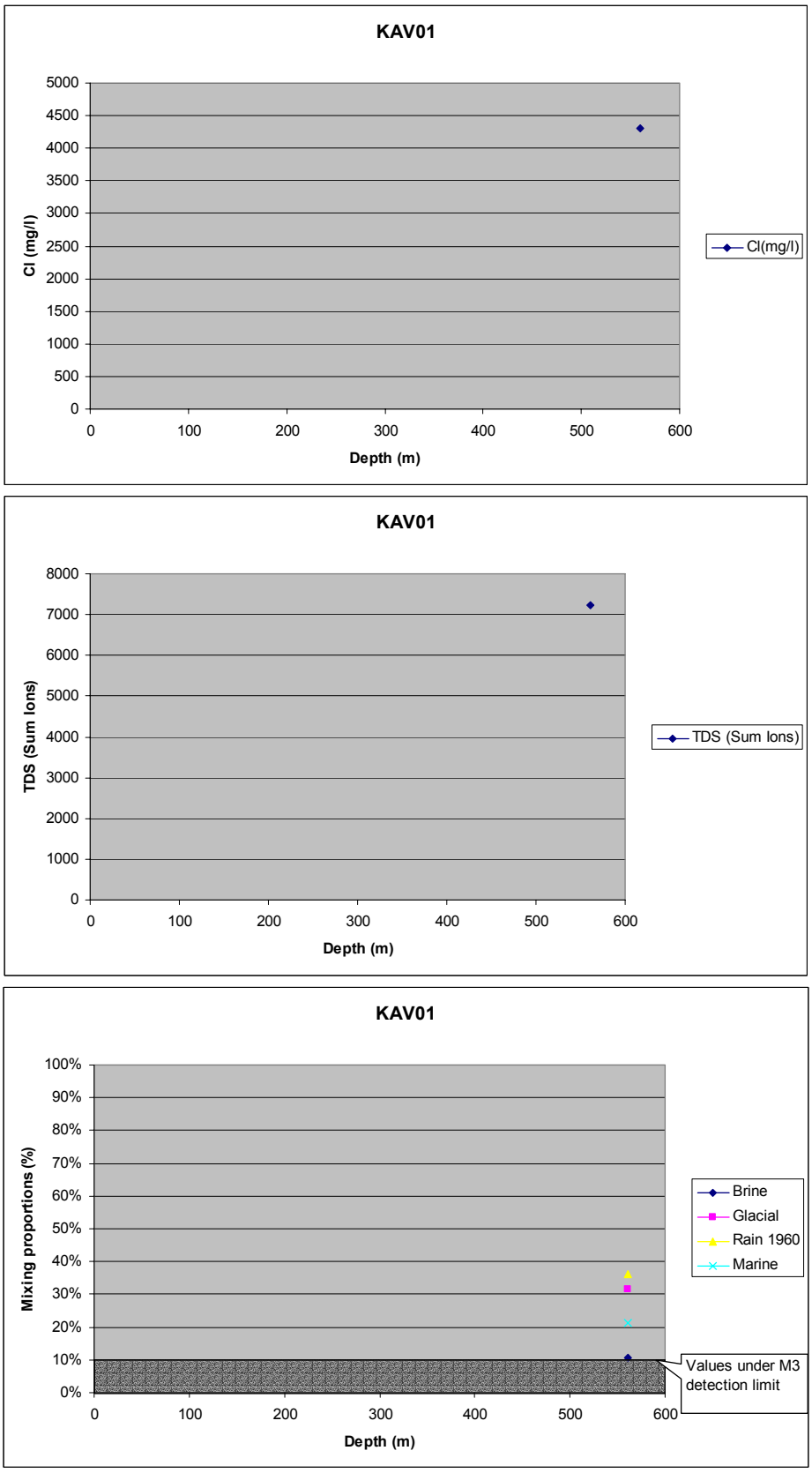

Figure 6b: Representative samples: *The measured Cl content is shown in the uppermost figure, the TDS (Sum Ions) in the middle picture and the calculated M3 mixing proportions in the lowermost figure along borehole KAV01.*

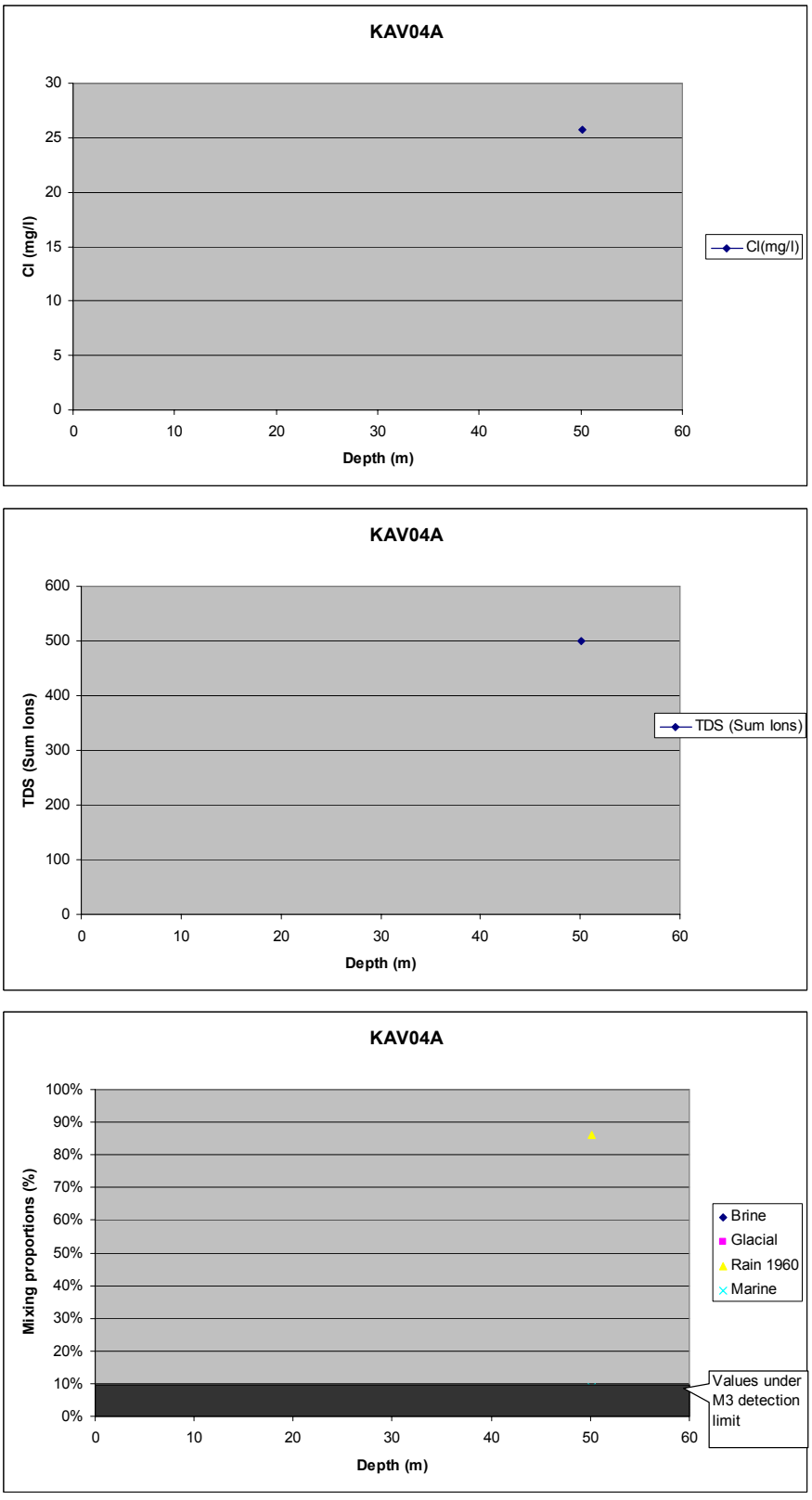

Figure 7a: All available samples representative and non representative: *The measured Cl content is shown in the uppermost figure, the TDS (Sum Ions) in the middle picture and the calculated M3 mixing proportions in the lowermost figure along borehole KAV04A.*

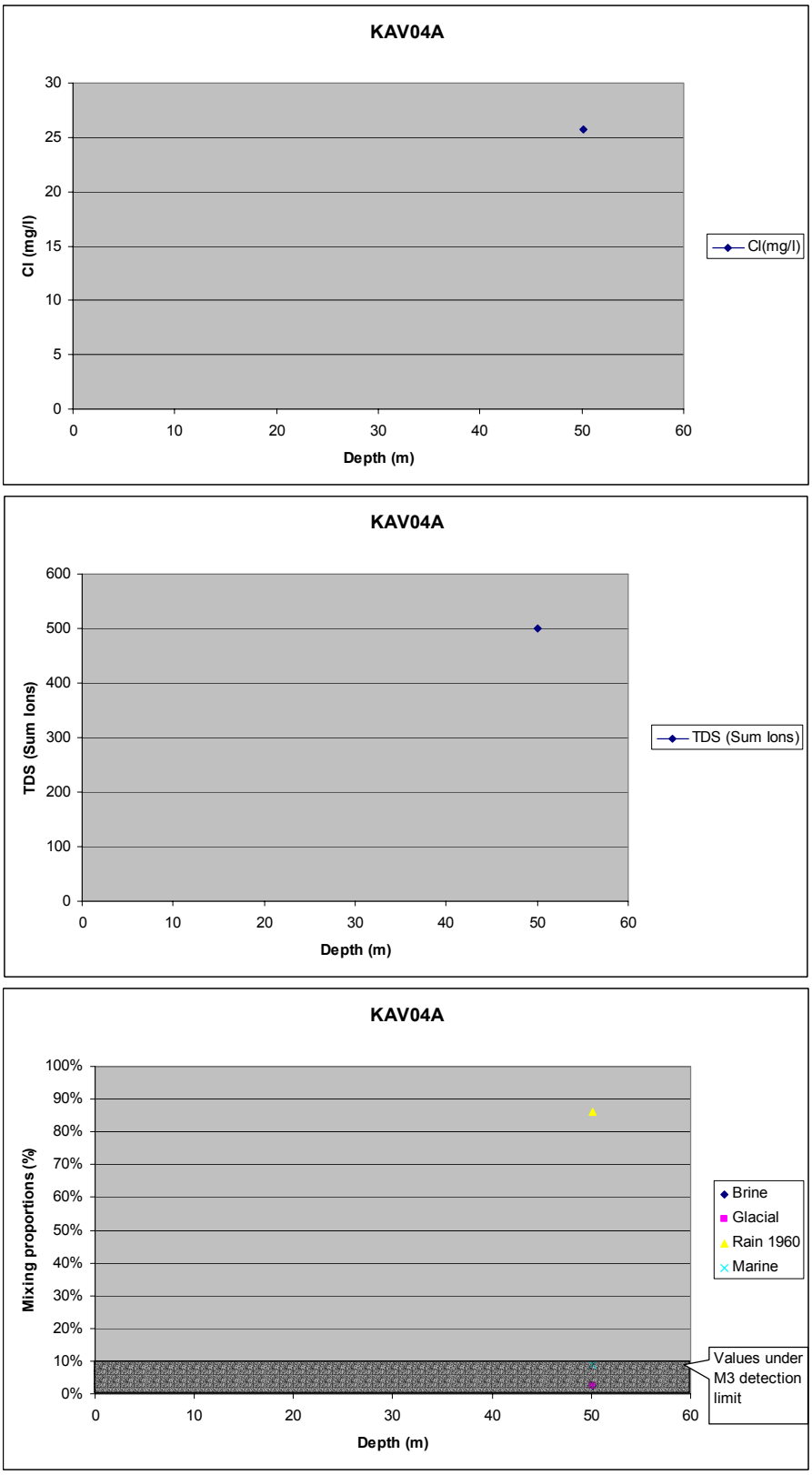

Figure 7b: Representative samples: *The measured Cl content is shown in the uppermost figure, the TDS (Sum Ions) in the middle picture and the calculated M3 mixing proportions in the lowermost figure along borehole KAV04A.*

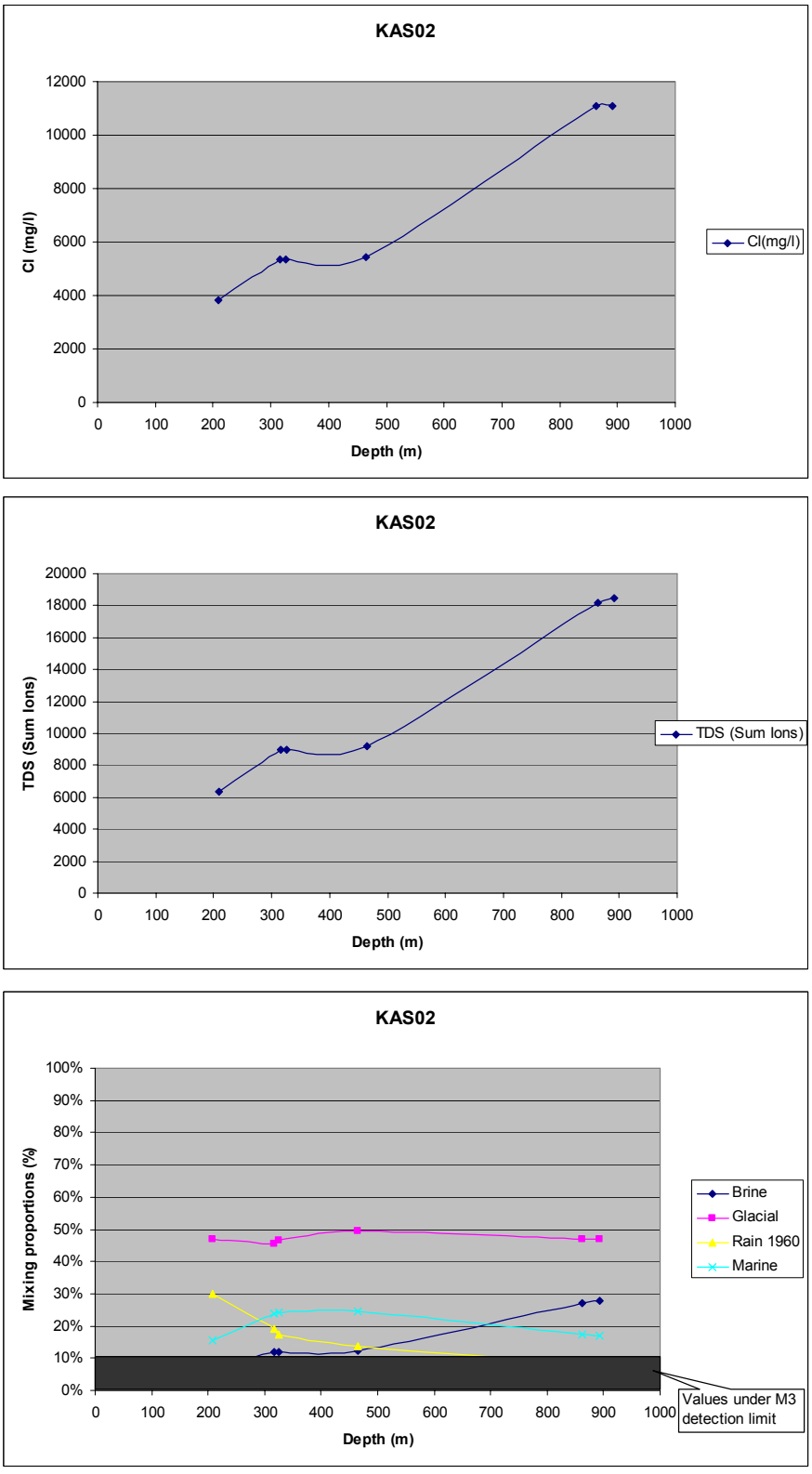

Figure 8a: All available samples representative and non representative: *The measured Cl content is shown in the uppermost figure, the TDS (Sum Ions) in the middle picture and the calculated M3 mixing proportions in the lowermost figure along borehole KAS02.*

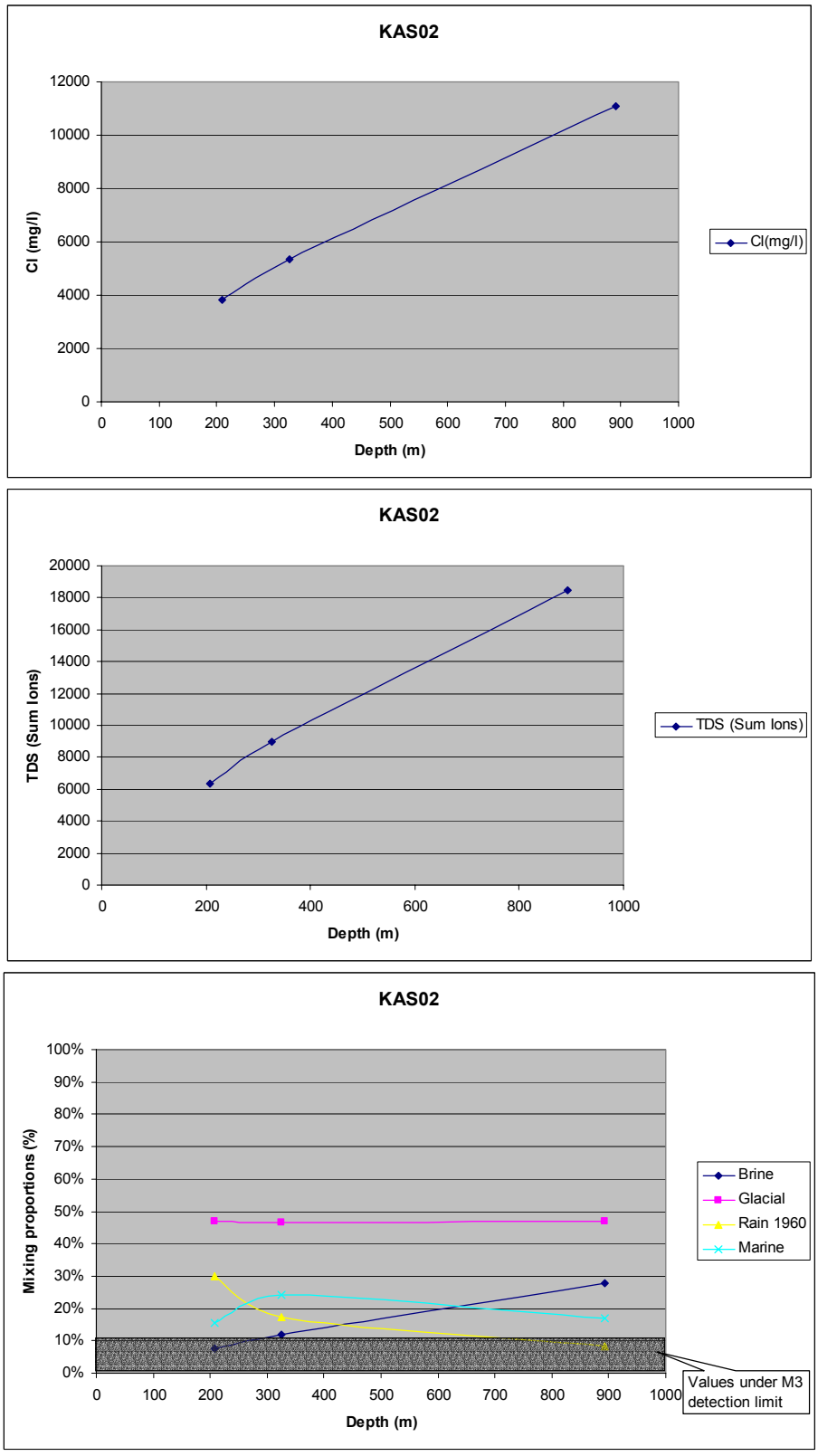

Figure 8b: Representative data: *The measured Cl content is shown in the uppermost figure, the TDS (Sum Ions) in the middle picture and the calculated M3 mixing proportions in the lowermost figure along borehole KAS02.*

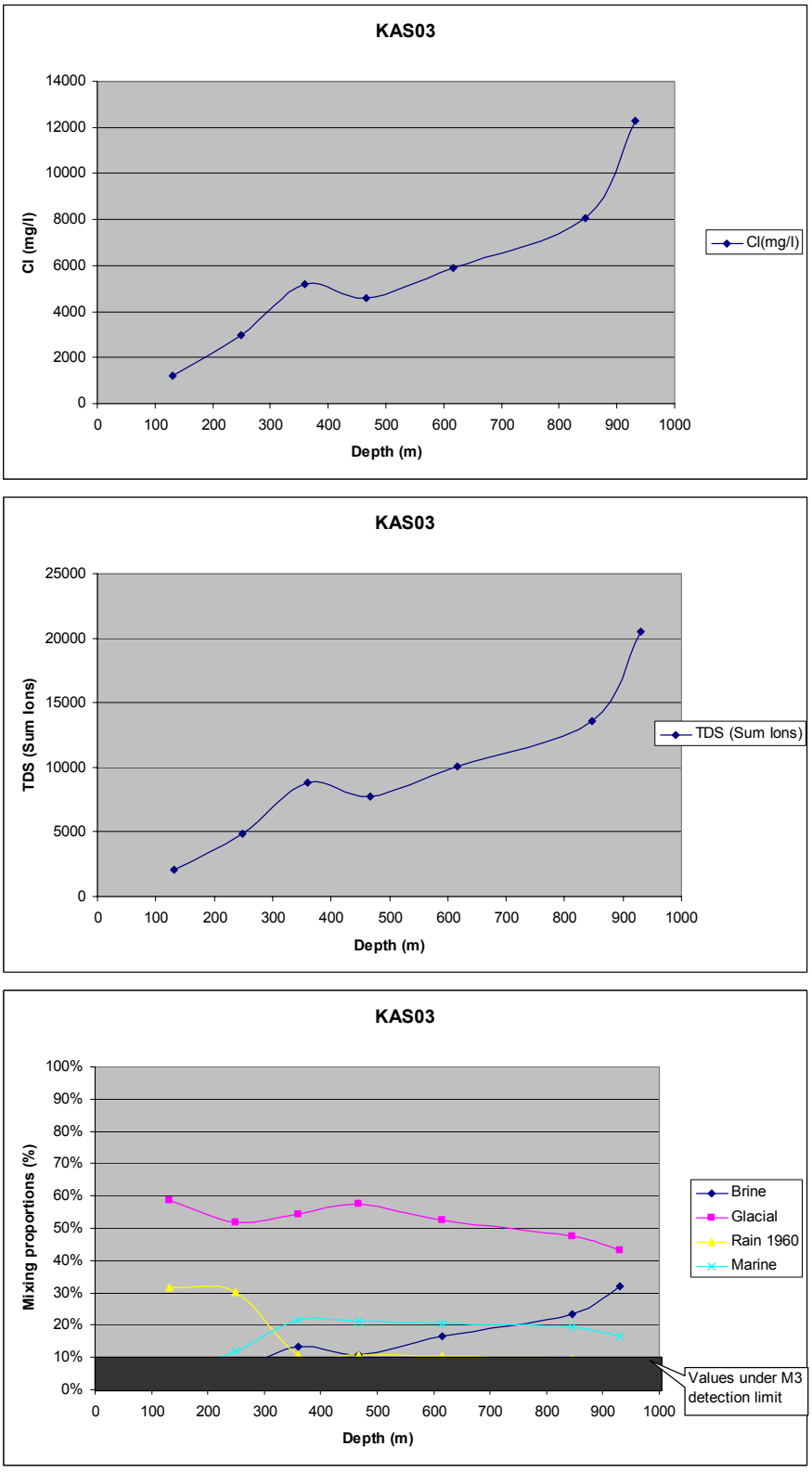

Figure 9a: All available samples representative and non representative: *The measured Cl content is shown in the uppermost figure, the TDS (Sum Ions) in the middle picture and the calculated M3 mixing proportions in the lowermost figure along borehole KAS03.*

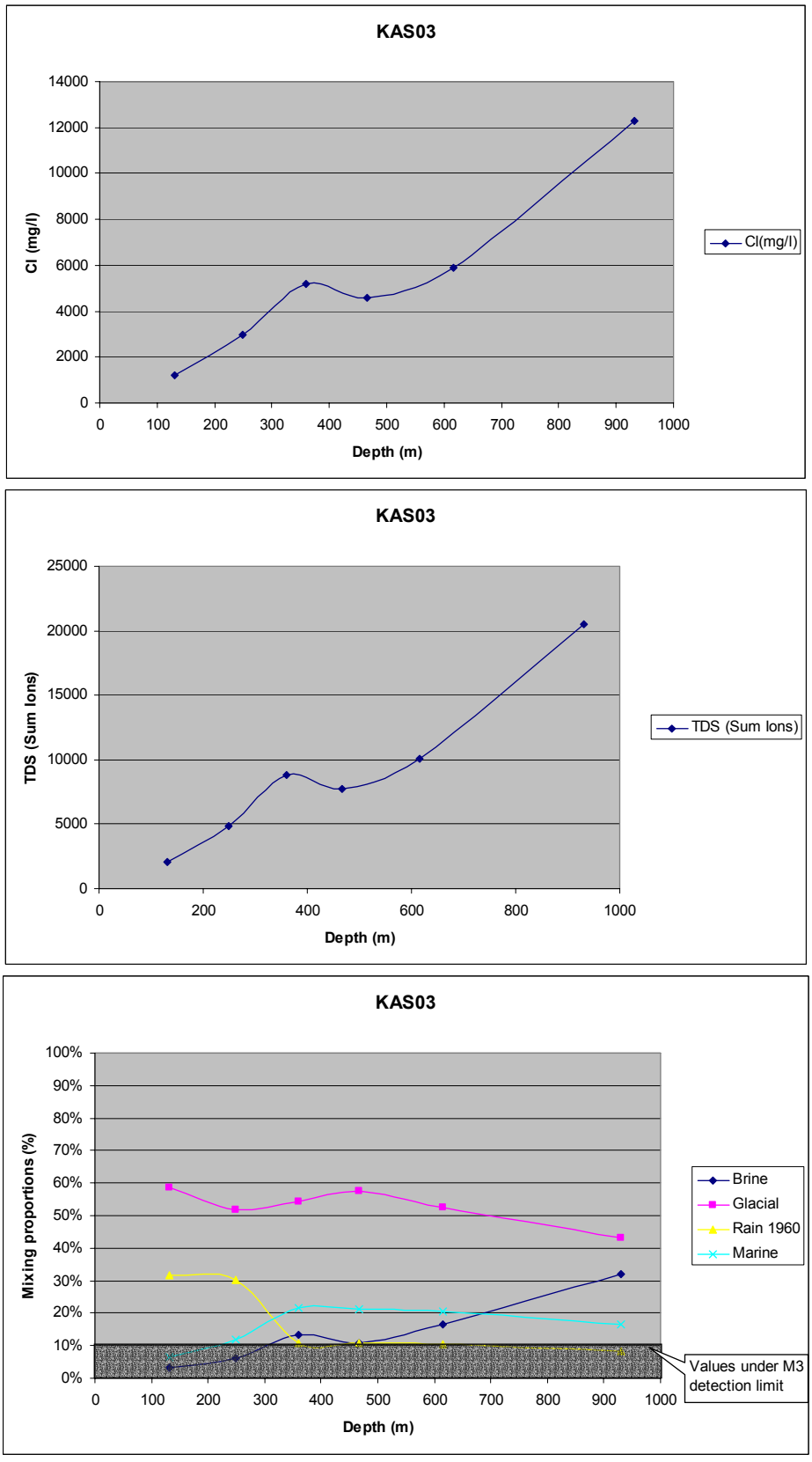

Figure 9b: Representative samples: *The measured Cl content is shown in the uppermost figure, the TDS (Sum Ions) in the middle picture and the calculated M3 mixing proportions in the lowermost figure along borehole KAS03.*

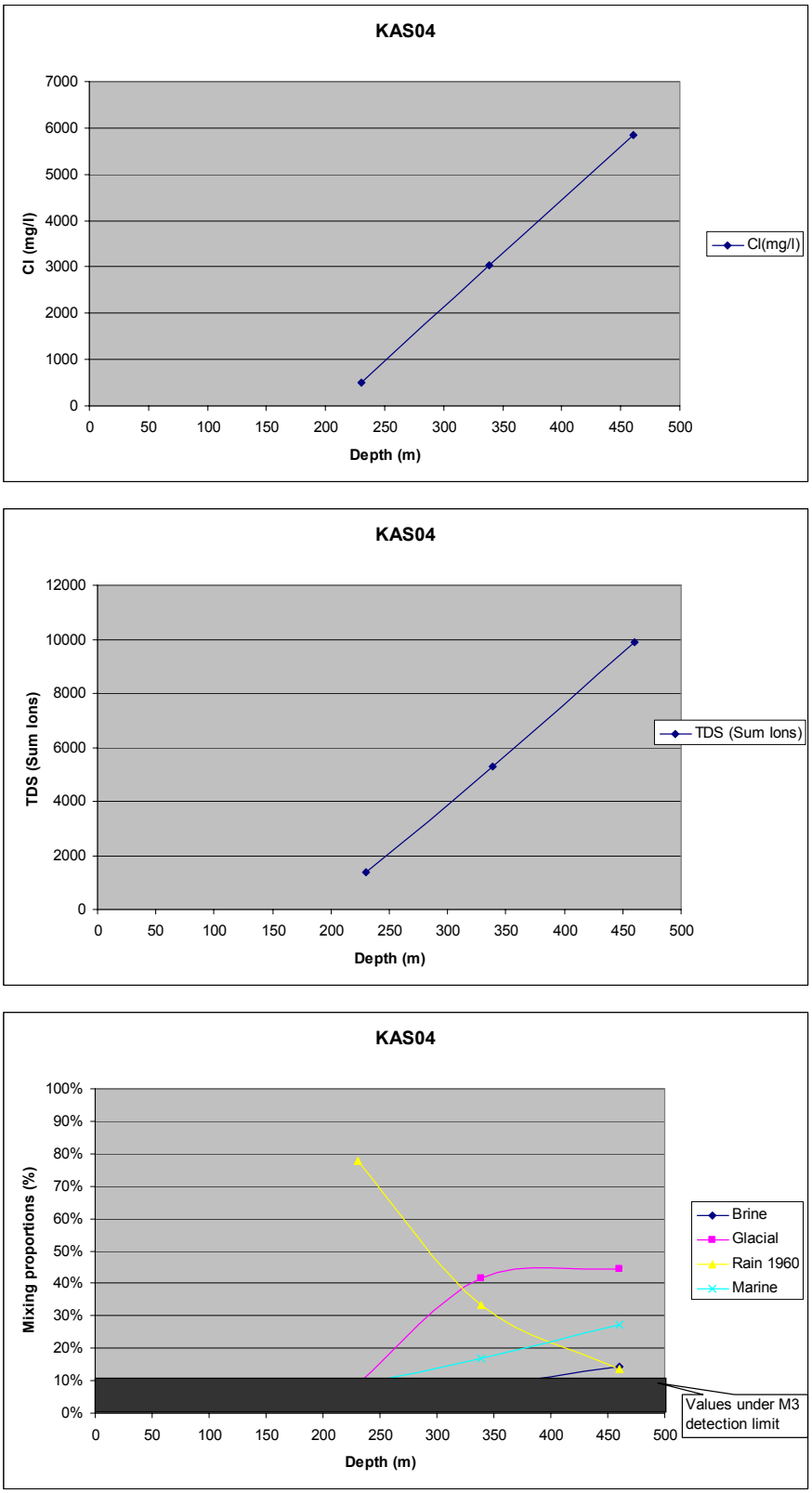

Figure 10a: All available samples representative and non representative: *The measured Cl content is shown in the uppermost figure, the TDS (Sum Ions) in the middle picture and the calculated M3 mixing proportions in the lowermost figure along borehole KAS04.*

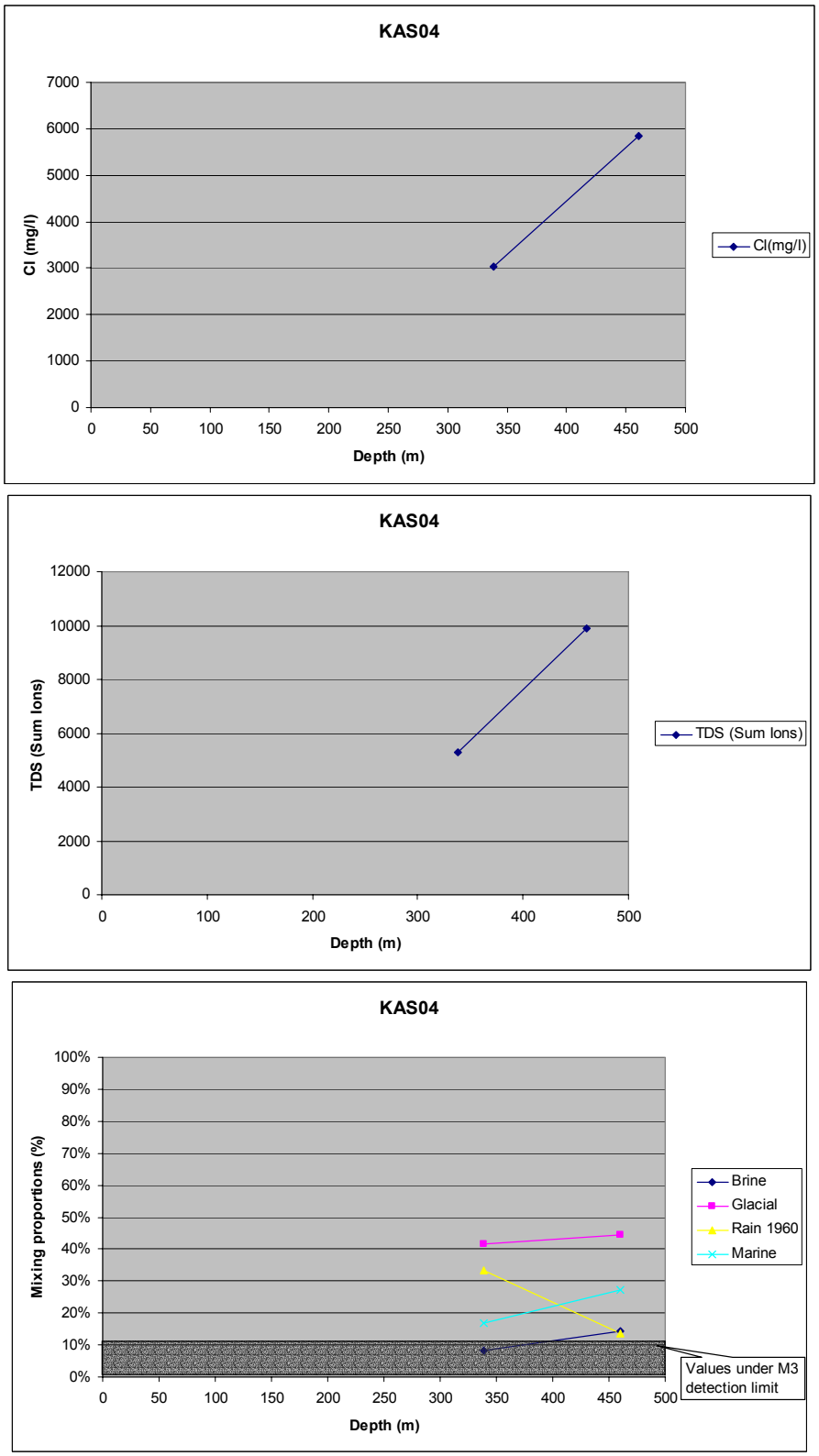

Figure 10b: Representative samples: *The measured Cl content is shown in the uppermost figure, the TDS (Sum Ions) in the middle picture and the calculated M3 mixing proportions in the lowermost figure along borehole KAS04.*

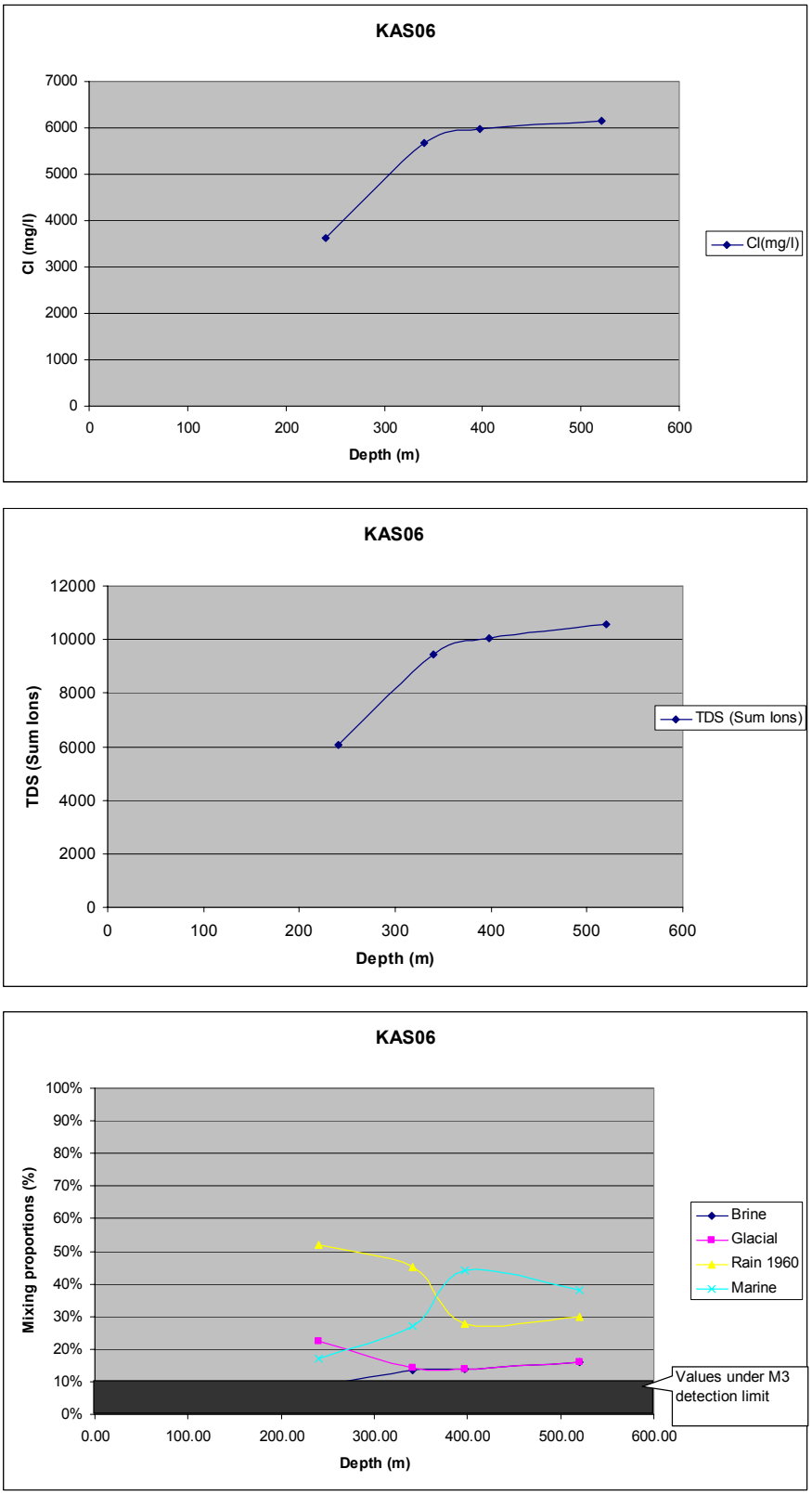

Figure 11a: All available samples representative and non representative: *The measured Cl content is shown in the uppermost figure, the TDS (Sum Ions) in the middle picture and the calculated M3 mixing proportions in the lowermost figure along borehole KAS06.*

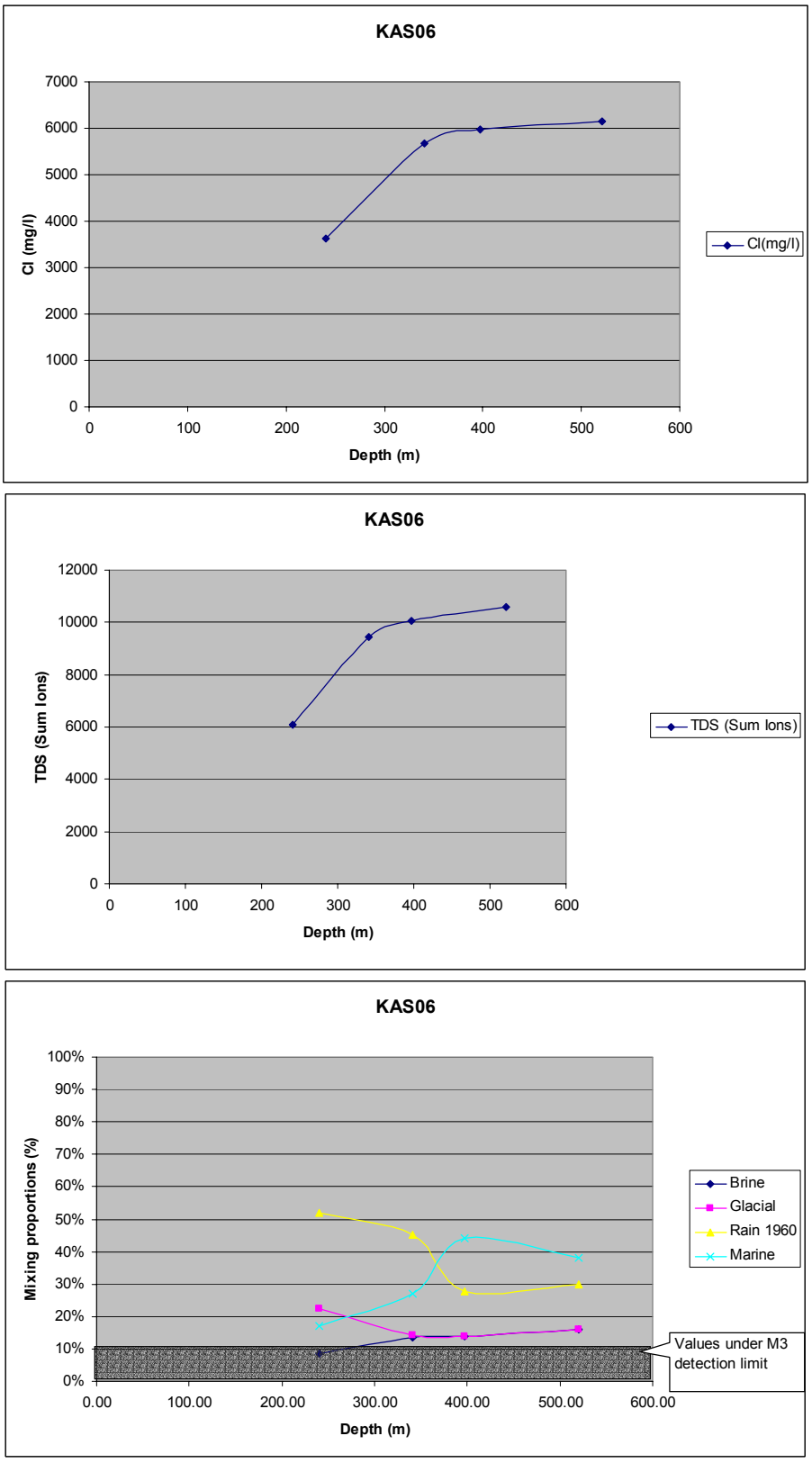

Figure 11b: Representative samples: *The measured Cl content is shown in the uppermost figure, the TDS (Sum Ions) in the middle picture and the calculated M3 mixing proportions in the lowermost figure along borehole KAS06.*

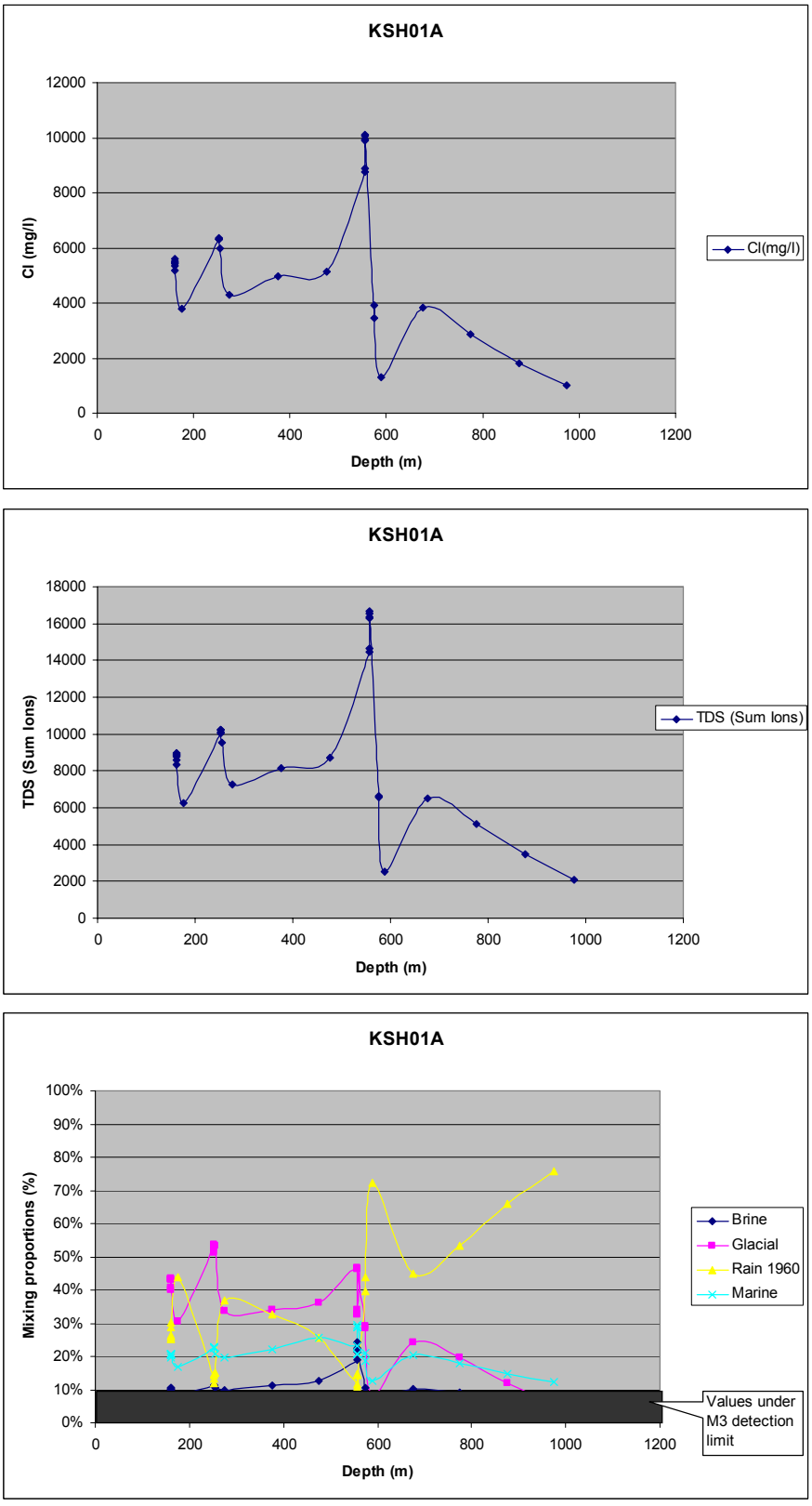

Figure 12a: All available samples representative and non representative: *The measured Cl content is shown in the uppermost figure, the TDS (Sum Ions) in the middle picture and the calculated M3 mixing proportions in the lowermost figure along borehole KSH01A.*

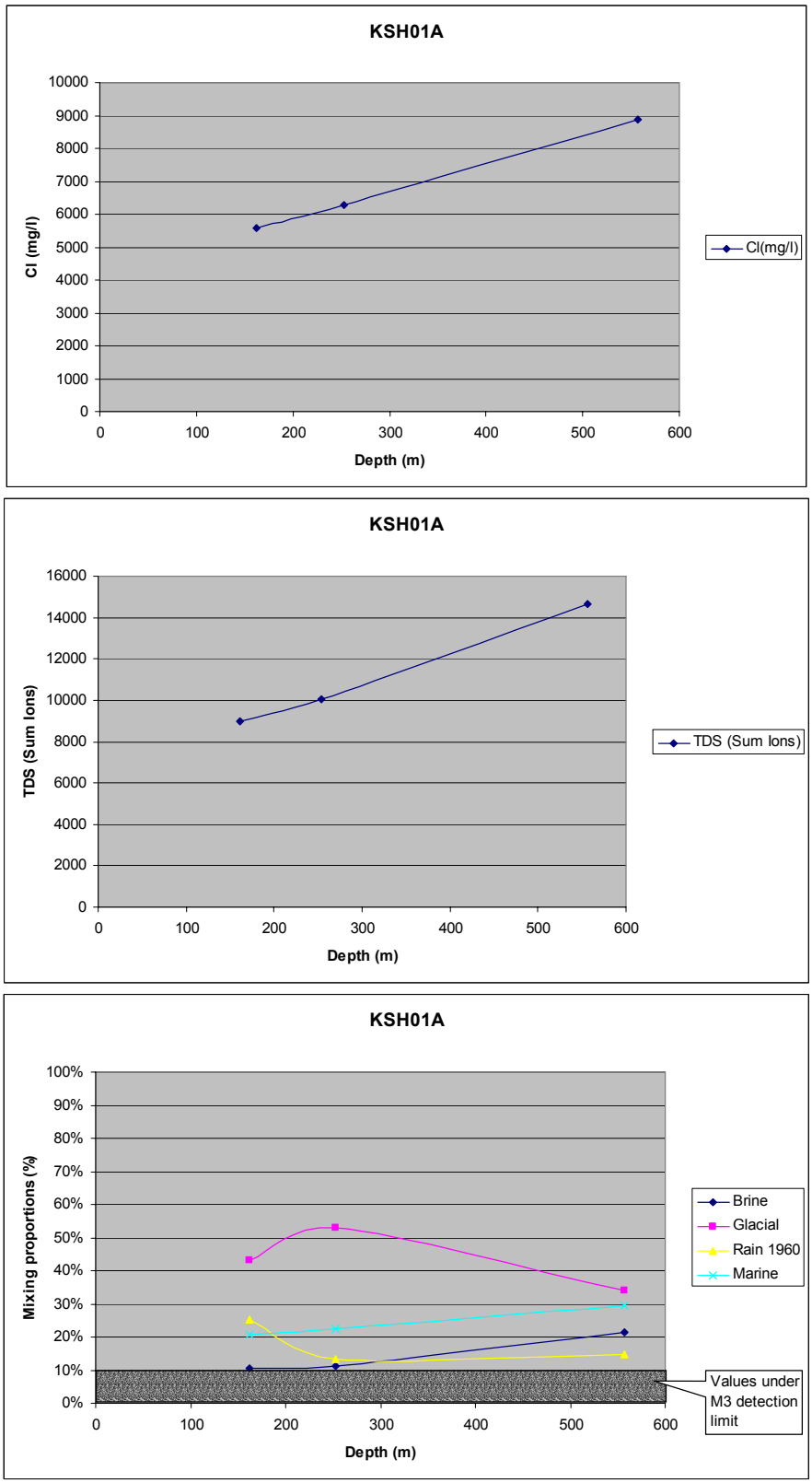

Figure 12b: Representative samples: *The measured Cl content is shown in the uppermost figure, the TDS (Sum Ions) in the middle picture and the calculated M3 mixing proportions in the lowermost figure along borehole KSH01A.*

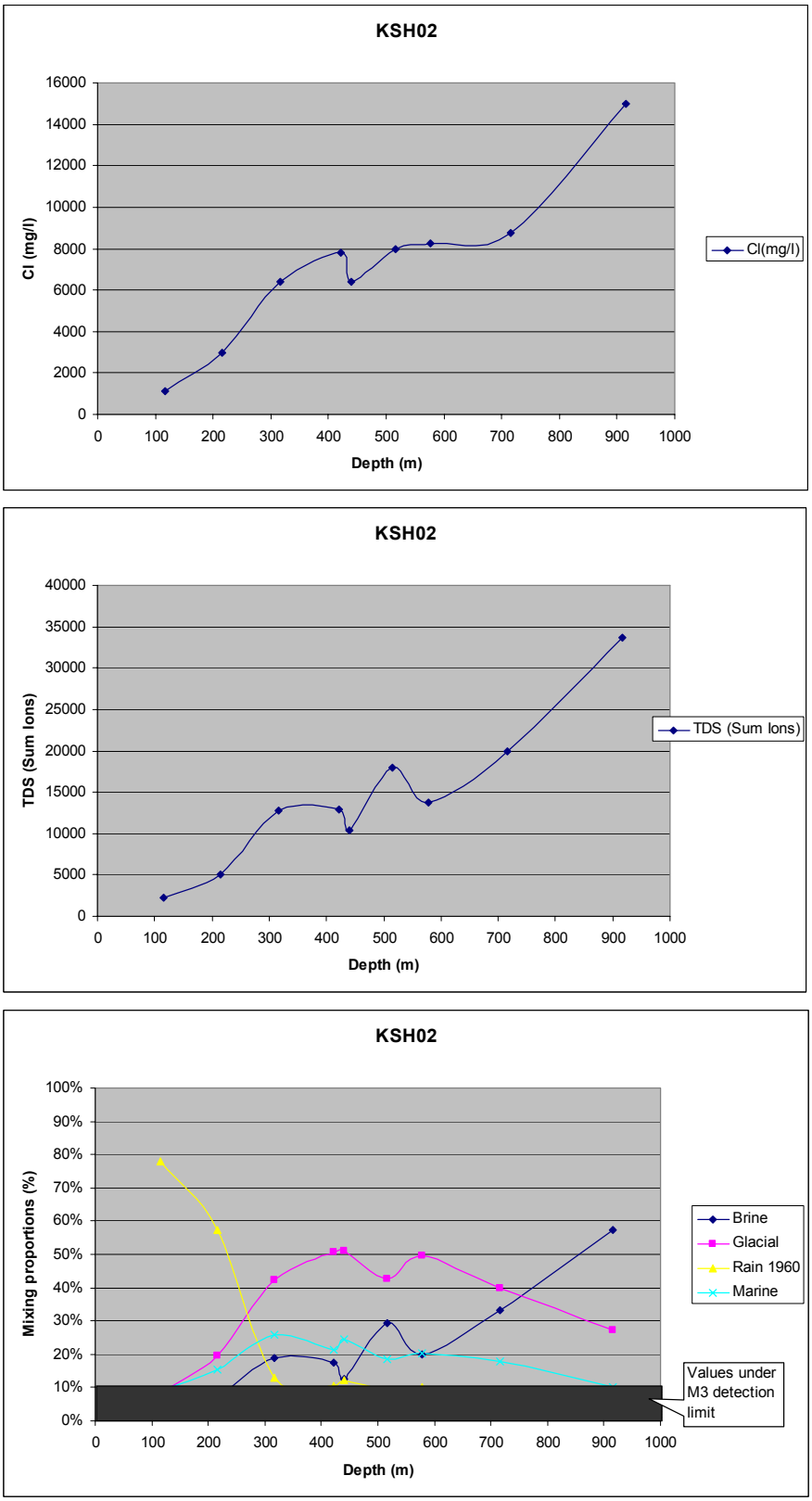

Figure 13a: All available samples representative and non representative: *The measured Cl content is shown in the uppermost figure, the TDS (Sum Ions) in the middle picture and the calculated M3 mixing proportions in the lowermost figure along borehole KSH02.*

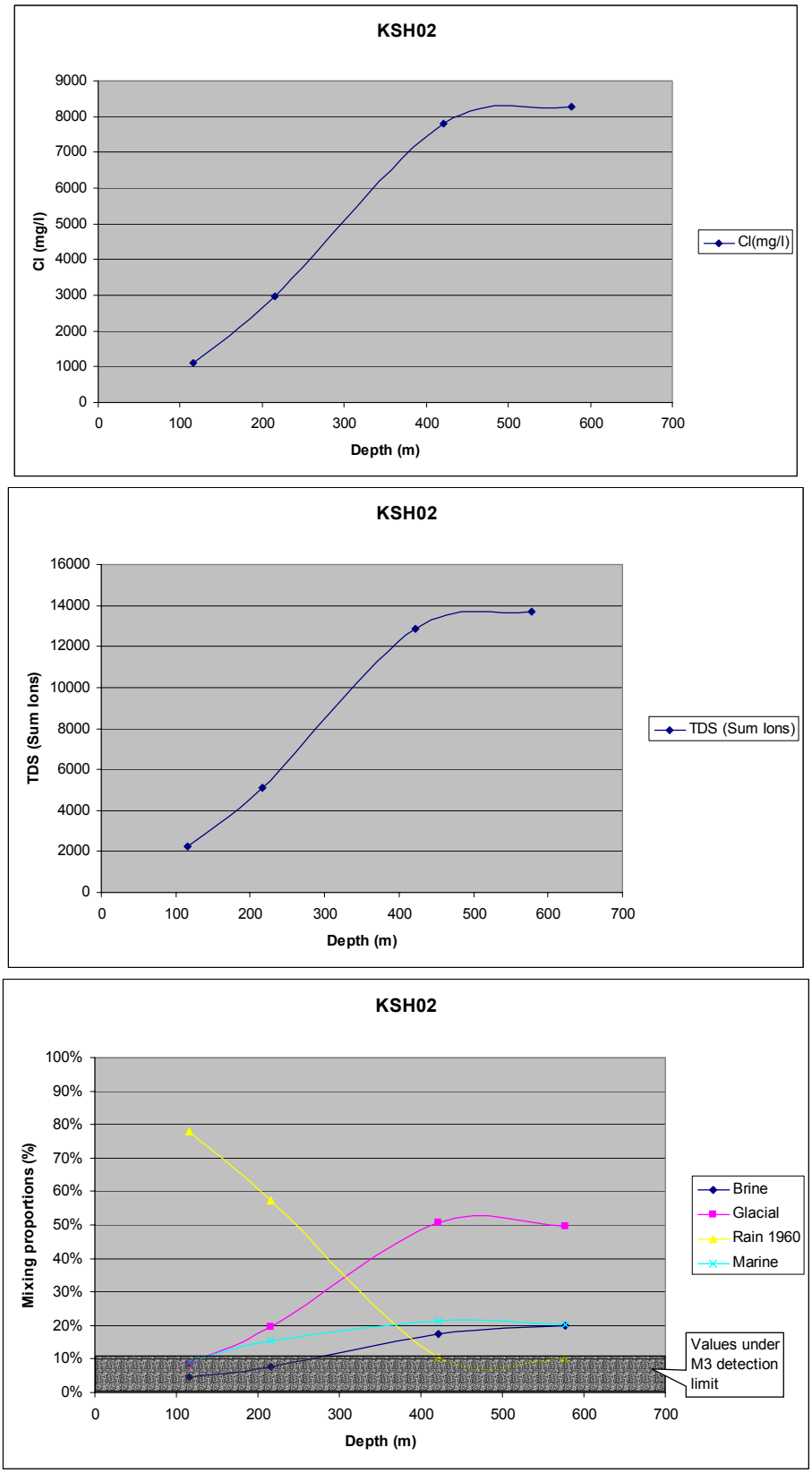

Figure 13b: Representative samples: *The measured Cl content is shown in the uppermost figure, the TDS (Sum Ions) in the middle picture and the calculated M3 mixing proportions in the lowermost figure along borehole KSH02.*

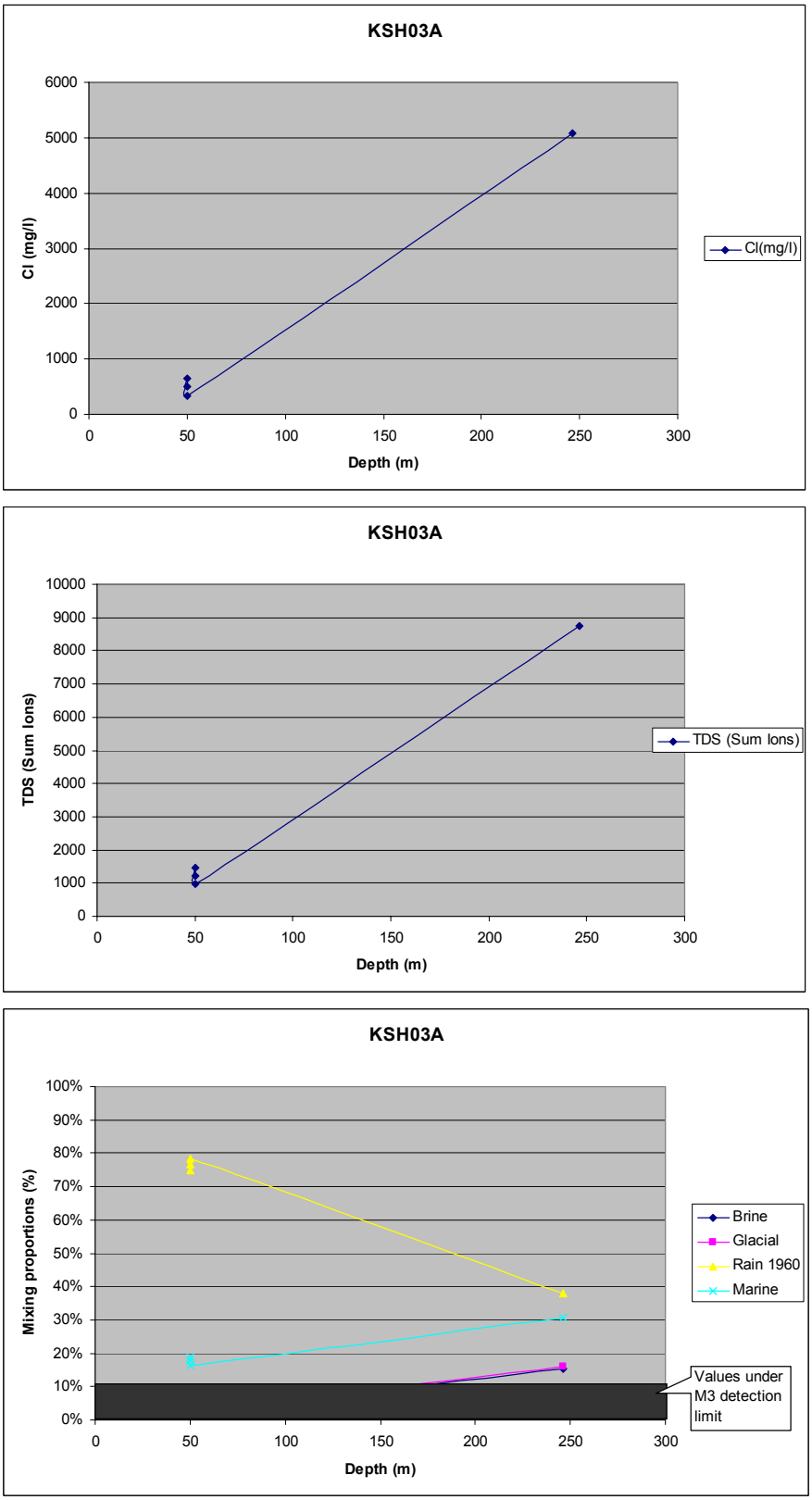

Figure 14a: All available samples representative and non representative: *The measured Cl content is shown in the uppermost figure, the TDS (Sum Ions) in the middle picture and the calculated M3 mixing proportions in the lowermost figure along borehole KSH03A.*

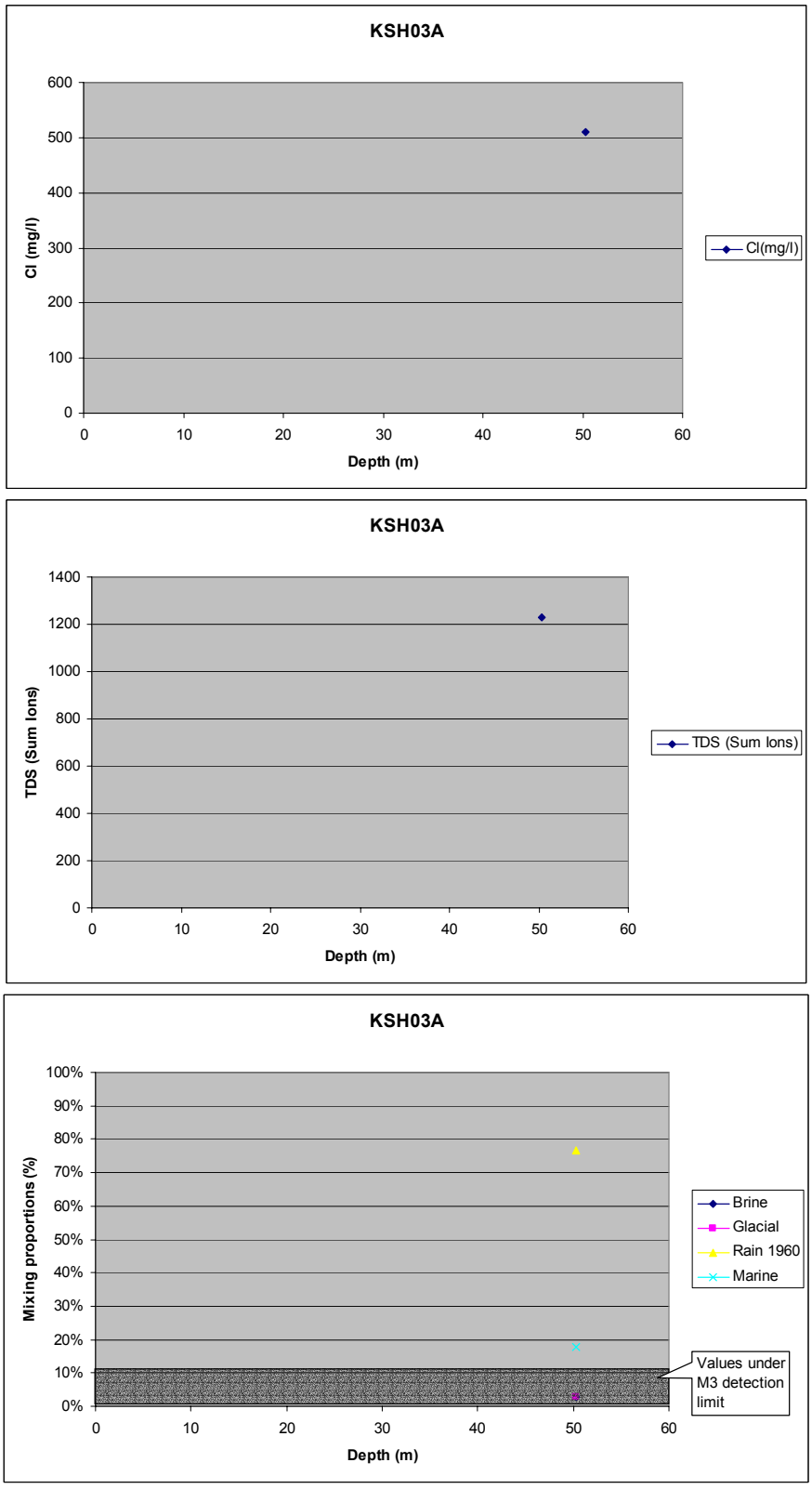

Figure 14b: Representative samples: *The measured Cl content is shown in the uppermost figure, the TDS (Sum Ions) in the middle picture and the calculated M3 mixing proportions in the lowermost figure along borehole KSH03A.*

4. Site specific hydrogeochemical uncertainties

At every phase of the hydrogeochemical investigation programme – drilling, sampling, analysis, evaluation, modelling – uncertainties are introduced which have to be accounted for, addressed fully and clearly documented to provide confidence in the end result, whether it will be the site descriptive model or repository safety analysis and design (Smellie et al, 2002). Handling the uncertainties involved in constructing a site descriptive model has been documented in detail by Andersson et al. (2001). The uncertainties can be conceptual uncertainties, data uncertainty, spatial variability of data, chosen scale, degree of confidence in the selected model, and error, precision, accuracy and bias in the predictions. Some of the identified uncertainties recognized during the Simpevarp modelling exercise and during the DIS exercise are discussed below.

The following data uncertainties have been estimated, calculated or modelled:

- Drilling; may be ± 10-70%
- Effects from drilling during sampling; is <5%
- Sampling; may be ± 10%
- Influence associated with the uplifting of water; may be ± 10%
- Sample handling and preparation; may be ± 5%
- Analytical error associated with laboratory measurements; is ± 5%
- Mean groundwater variability at Simpevarp during groundwater sampling (first/last sample); is about 25%.
- The M3 model uncertainty; is ±0.1units within 90% confidence interval

Conceptual errors can occur from e.g. the paleohydrogeological conceptual model. The influences and occurrences of old water end-members in the bedrock can only be indicated by using certain element or isotopic signatures. The uncertainty is therefore generally increasing with the age of the end-member. The relevance of an end-member participating in the groundwater formation can be tested by introducing alternative end-member compositions or by using hydrodynamic modelling to test if old water types can resign in the bedrock during prevailing hydrogeological conditions.

4.1 Model uncertainties

The following factors can cause uncertainties in M3 calculations:

Input hydrochemical data errors originating from sampling errors caused by the effects from drilling, borehole activities, extensive pumping, hydraulic short-circuiting of the borehole and uplifting of water which changes the in-situ pH and Eh conditions of the sample, or as analytical errors.

Conceptual errors such as wrong general assumptions, selecting wrong type/number of end-members and mixing samples that are not mixed. Methodological errors such as oversimplification, bias or non-linearity in the model, and the systematic uncertainty, which is attributable to use of the centre point to create a solution for the mixing model. An example of a conceptual error is assuming that the groundwater composition is a good tracer for the flow

system. The water composition is not necessarily a tracer of mixing directly related to flow since there is not a point source as there is when labelled water is used in a tracer test.

Another source of uncertainty in the mixing model is the loss of information in using only the first two principal components. The third principal component gathers generally around 10% of the groundwater information compared with the first and second principal components, which contain around 70% of the information. A sample could appear to be closer to a reference water in the 2D surface than in a 3D volume involving the third principal component. In the latest version of M3 the calculations can also be performed in 3D.

Uncertainty in mixing calculations is smaller near the boundary of the PCA polygon and larger near the center. The uncertainties have been handled in M3 by calculating an uncertainty of 0.1 mixing units (with a confidence interval of 90%) and stating that a mixing portion <10% is under the detection limit of the method (Laaksoharju et al., 1999b).

5. Visualisation of the sampling location, Cl, TDS and mixing proportions in 3D with Tecplot

The 3D visualization of the Cl distribution, TDS (SumIons) and mixing proportions in Simpevarp was performed with Tecplot. The purpose of the visualization is to show the hydrochemical results (Cl, TDS, mixing proportions) with the hydrogeological results. Due to the fact that the hydrogeologists use only 4 reference waters (meteoric, glacial, brine and Littorina), the marine components (Littorina and Sea Sediment reference waters) were added together and named Marine water.

The x, y, z coordinates in the model box represent the Easting, Northing and elevation of the midpoint of the sampling section in meters. The modelling domain was set according to the local model used by the hydrogeologists (Figure 15):

Xmin= 1546400
Xmax= 1554200
Ymin= 6365000
Ymax= 6368200
Zmax= 6.125
Zmin= -1625.77

The exception is the Z coordinate, which in the local hydrogeological model is –1100. Since hydrogeochemical data was available from larger depth in borehole KLX02 it was decided to extend the depth of the modelling box to -1626m. The boundary conditions were set according to the box domain as following:

x	y	z	Cl(mg/l)	TDS (SumIons)	Brine	Glacial	Rain 1960	Marine
1546400	6365000	-1625.77	47200	75967.72	1	0	0	0
1546400	6368200	-1625.77	47200	75967.72	1	0	0	0
1554200	6365000	-1625.77	47200	75967.72	1	0	0	0
1554200	6368200	-1625.77	47200	75967.72	1	0	0	0
1546400	6366600	0	0.23	14.86	0	0	1	0
1554200	6366600	0	3760	6557.7	0.09	0.09	0.09	0.73
1546400	6366600	-1625.77	47200	75967.72	1	0	0	0
1554200	6366600	-1625.77	47200	75967.72	1	0	0	0
1550300	6365000	0	3760	6557.7	0.09	0.09	0.09	0.73
1550300	6368200	0	0.23	14.86	0	0	1	0
1550300	6365000	-1625.77	47200	75967.72	1	0	0	0
1550300	6368200	-1625.77	47200	75967.72	1	0	0	0

Due to the data distribution, it was not possible to use the Kriging method for interpolation. The inverse distance algorithm was used instead. From the model domain, a inclined vertical profile which pass through a maximum of sampling point was extracted. The coordinates of the profile are:

X=1546400; Y=6367520
X= 1554200; Y=6365650

The locations of the sampling points used for M3 modelling and the inclined vertical profile are shown in all the figures 16 to 26. The z coordinate was not always available for the surface

samples (sea, lake, streams, soil tubes). Therefore, when necessary, the z coordinate was estimated to be 0. At the scale of the model, this represents an error smaller than 5%.

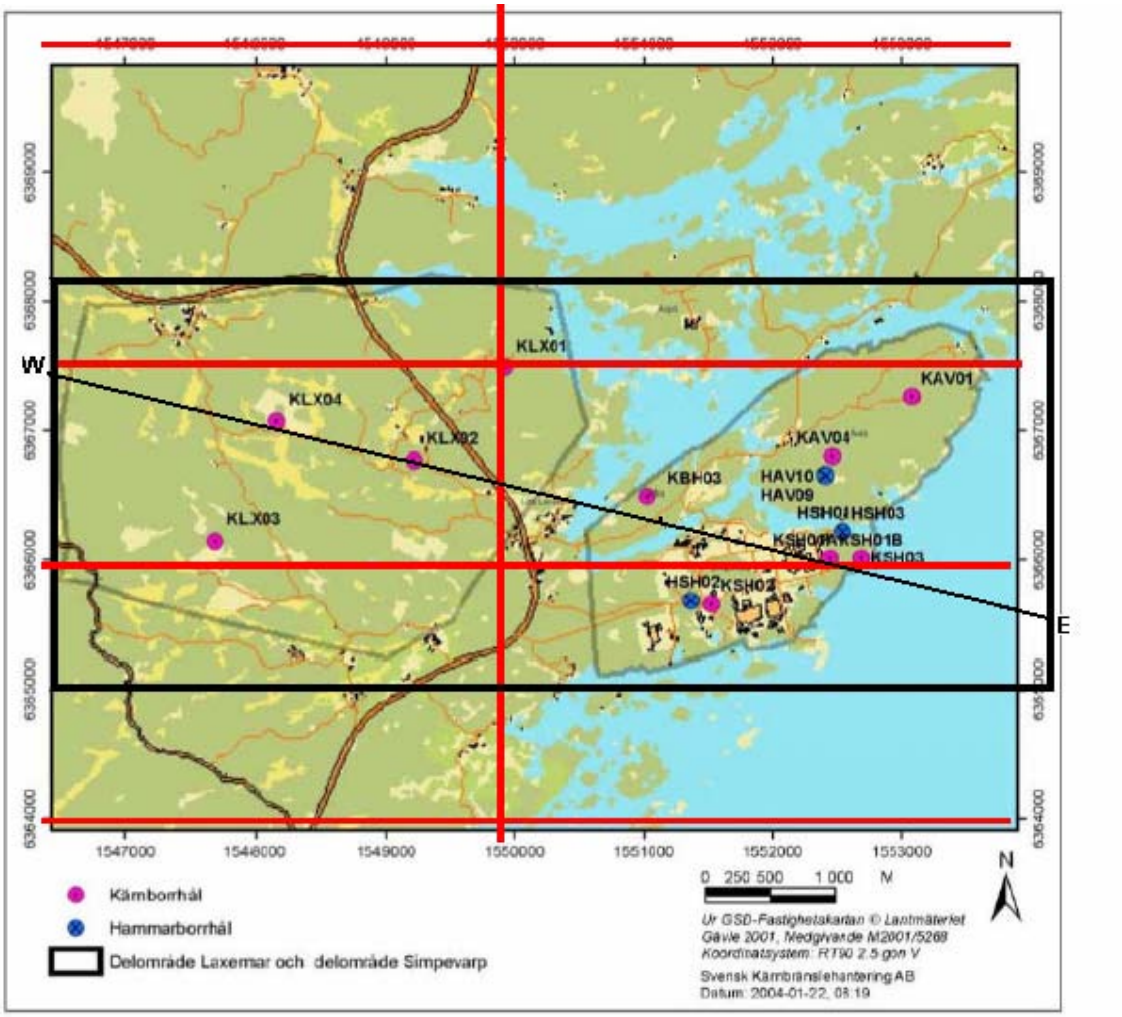

Figure15*: The map showing the location of the sampling points and boreholes in Simpevarp. The thick black line indicate the location of the local model and the inclined thin black line the vertical profile used for the Tecplot visualisation. The red lines indicate cutting planes used by the hydrogeologists (from I. Rhén personal communication, 2004).*

In the following pictures, the mixing proportions presented are: Brine, Glacial, Rain1960 (meteoric) and Marine (the sum of Littorina and Sea Sediment). Figures 16 to 20 show the 3D and the 2D visualisation of the 193 available values in Simpevarp 1.2 data set. These values represent groundwater and surface data. All the available samples, representative and non-representative data, are used for the visualisation. The non-representative samples, like the ones in the deep part of KHS01A can create biad in the results. Indeed, the open hole measurements show very dilute water down to 1000m in the borehole KSH01A. In the figures 18 to 20 this part of the borehole is indicated by a red box.

The figures 21 to 25 show the 3D and the 2D visualisation of the 90 representative samples in Simpevarp. These values represent groundwater and surface data. Only the representative

samples are used in the visualisation. The figure 26 shows the TDS distribution with Tecplot for all the available samples (representative and non-representative) and the distribution of only the representative samples.

5.1 3D Visualisation of the samples location, Cl, TDS and mixing proportions distribution of the representative and non-representative samples in Simpevarp

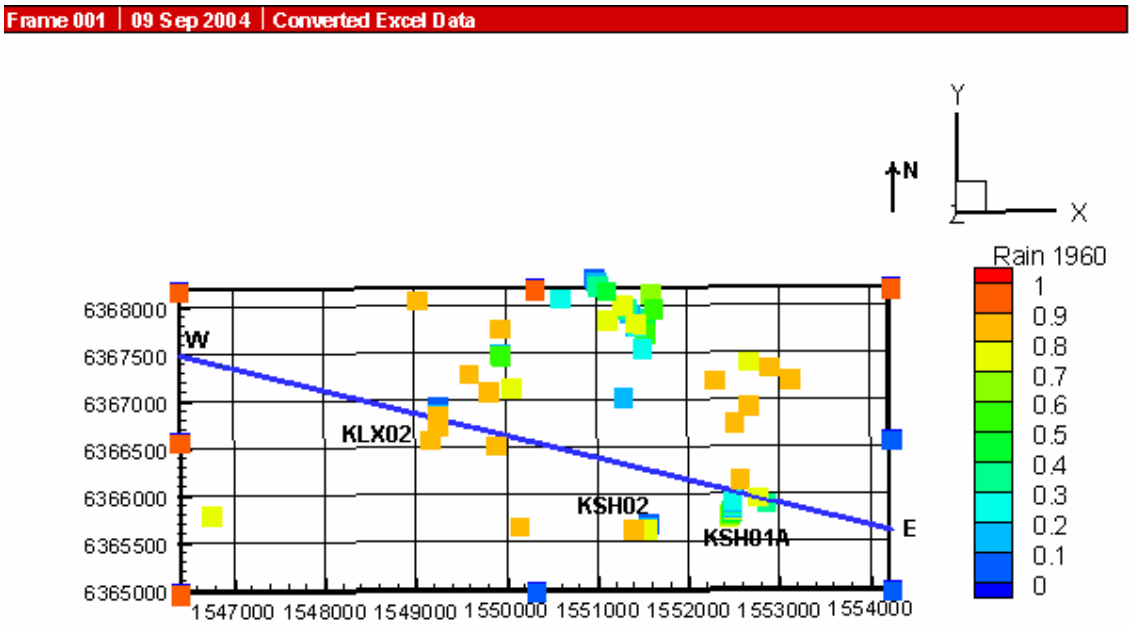

Figure 16: *2D visualisation (top view of the modelling box) of the Rain 1960 distribution in Simpevarp. The figure shows the location of the sampling points used for the M3 modelling and the location of the inclined vertical profile.*

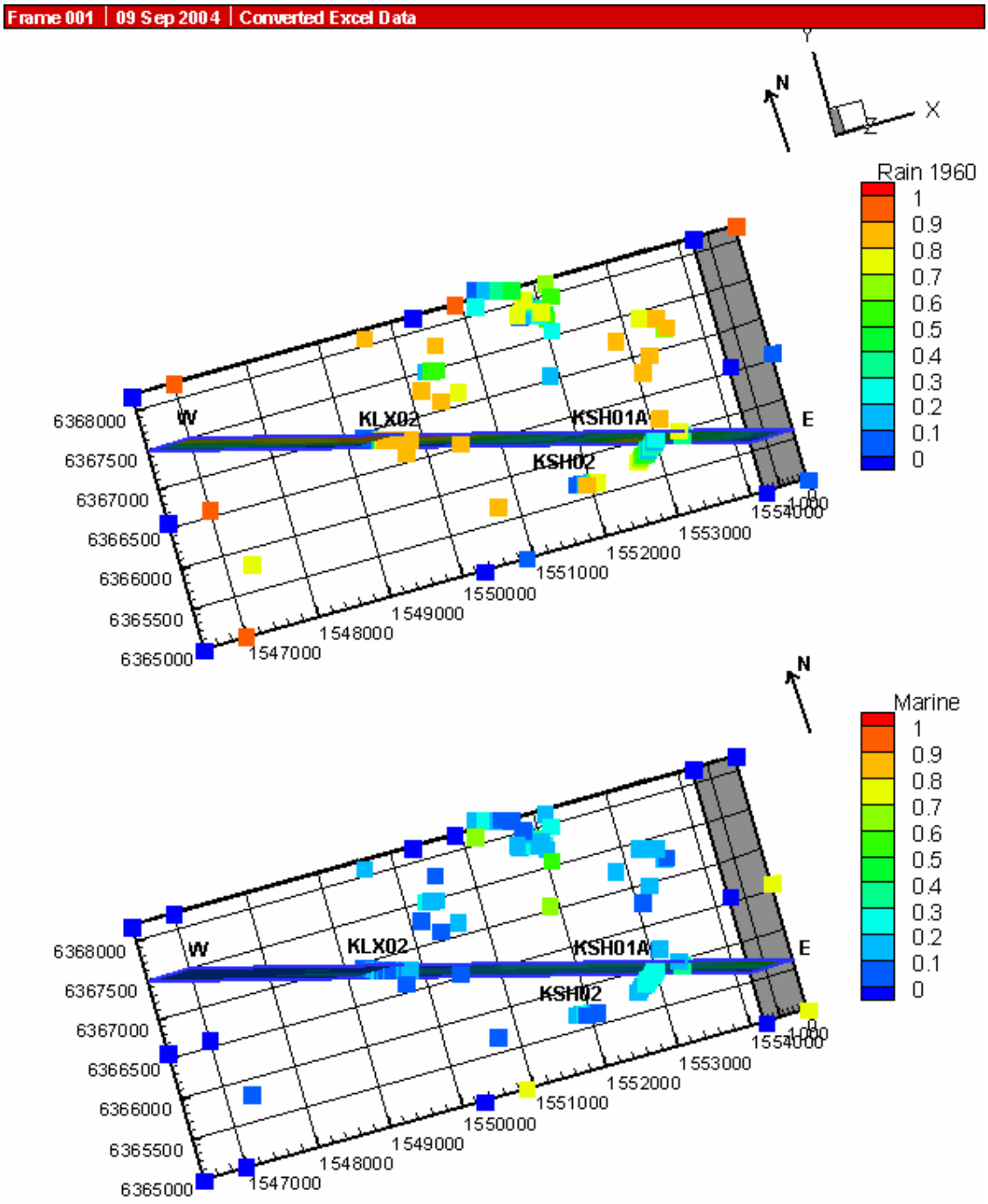

Figure17*: 2D-3D visualisation of the Rain 1960 and Marine distribution in Simpevarp. The figure shows the location of the sampling points used for the M3 modelling and the location of the inclined vertical profile.*

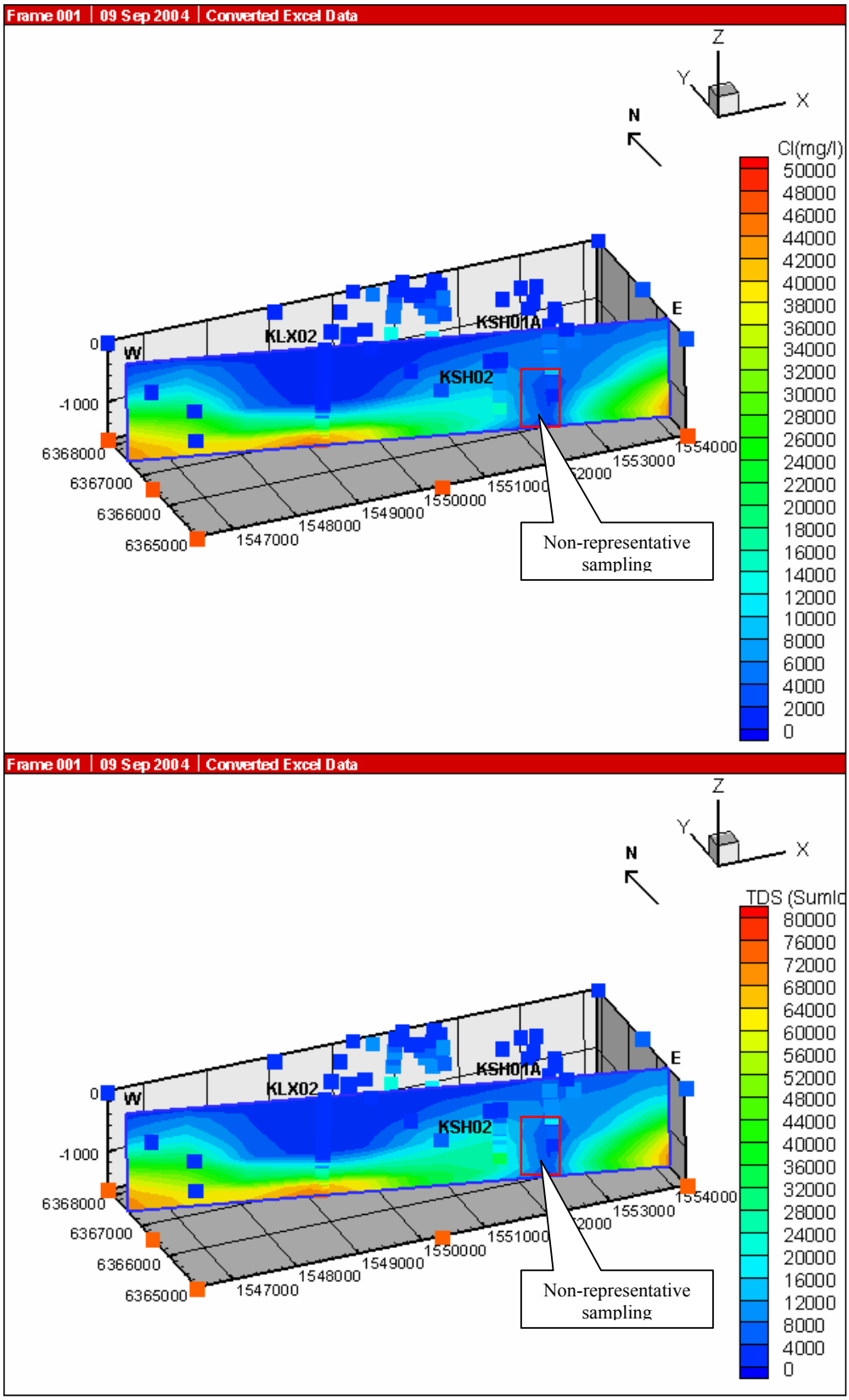

Figure18: *3D visualisation of the Cl and TDS (SumIons) distribution in Simpevarp. The figures show the location of the sampling points used for the M3 modelling and the location of the inclined vertical profile. The depth scale is in meters.*

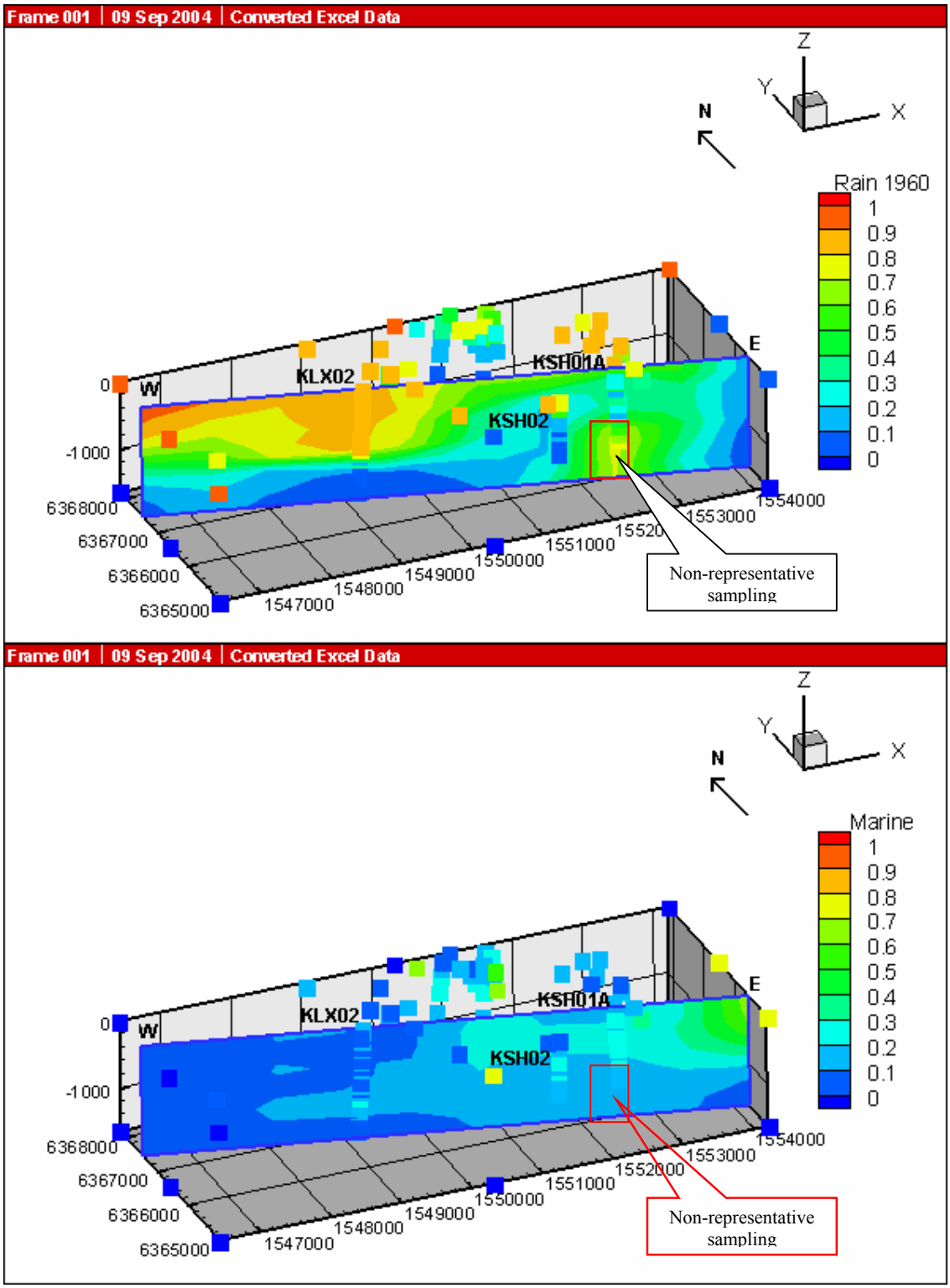

Figure 19*: 3D visualisation of the Rain 1960 and Marine mixing proportions distributions in Simpevarp. The figures show the location of the sampling points used for the M3 modelling and the location of the inclined vertical profile. The depth scale is in meters.*

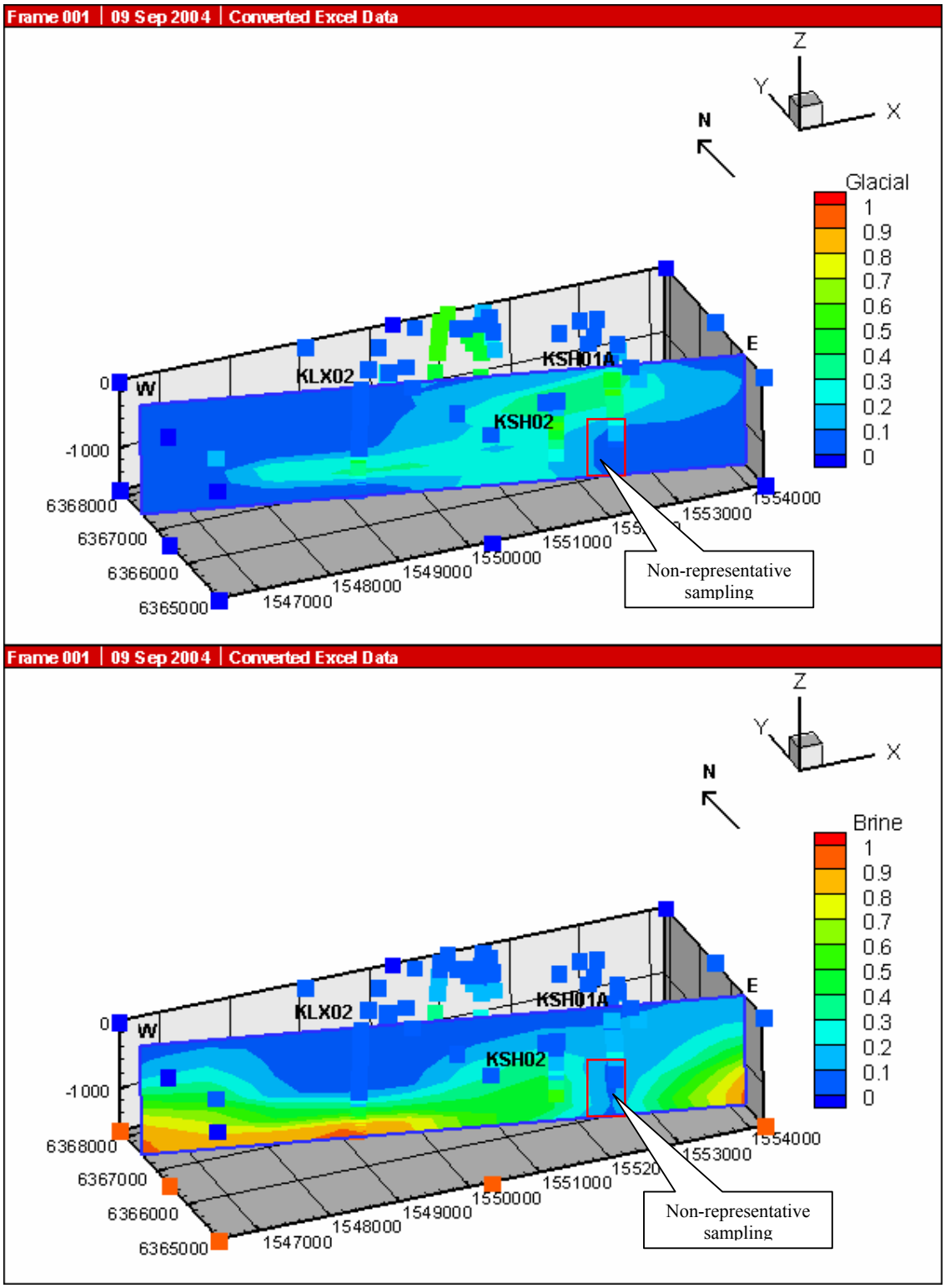

Figure 20: *3D visualisation of the Glacial and Brine mixing proportions distributions in Simpevarp. The figures show the location of the sampling points used for the M3 modelling and the location of the inclined vertical profile. The depth scale is in meters.*

5.2 3D Visualisation of the samples location, Cl, TDS and mixing proportions distribution of the representative samples in Simpevarp

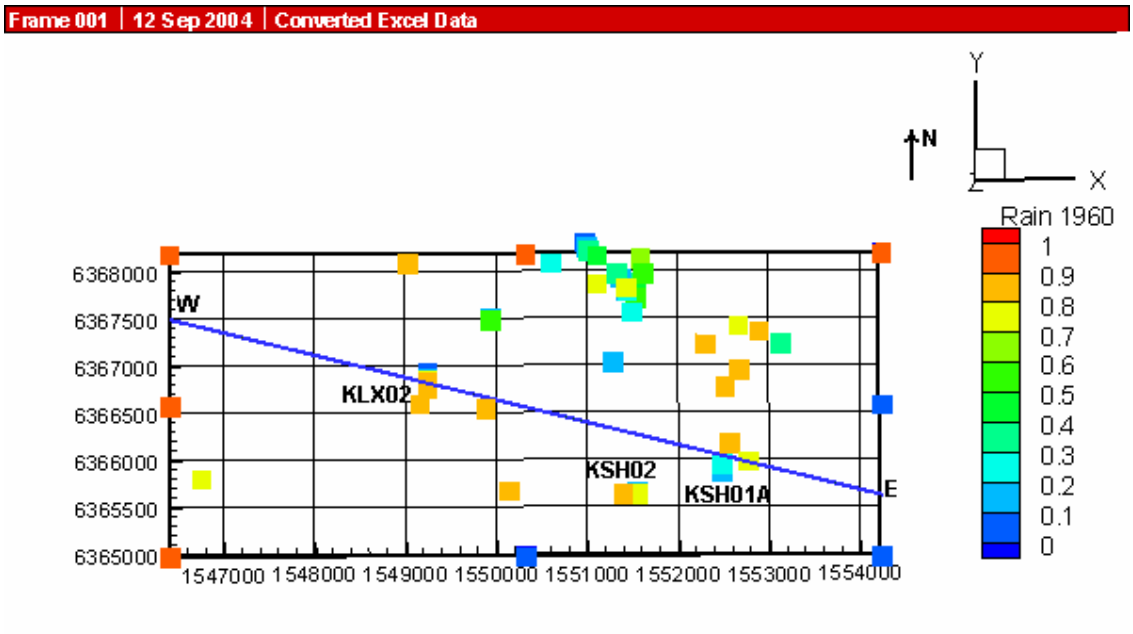

Figure 21*: 2D visualisation (top view of the modelling box) of the Rain 1960 distribution in Simpevarp. The figure shows the location of the representative sampling and the location of the inclined vertical profile.*

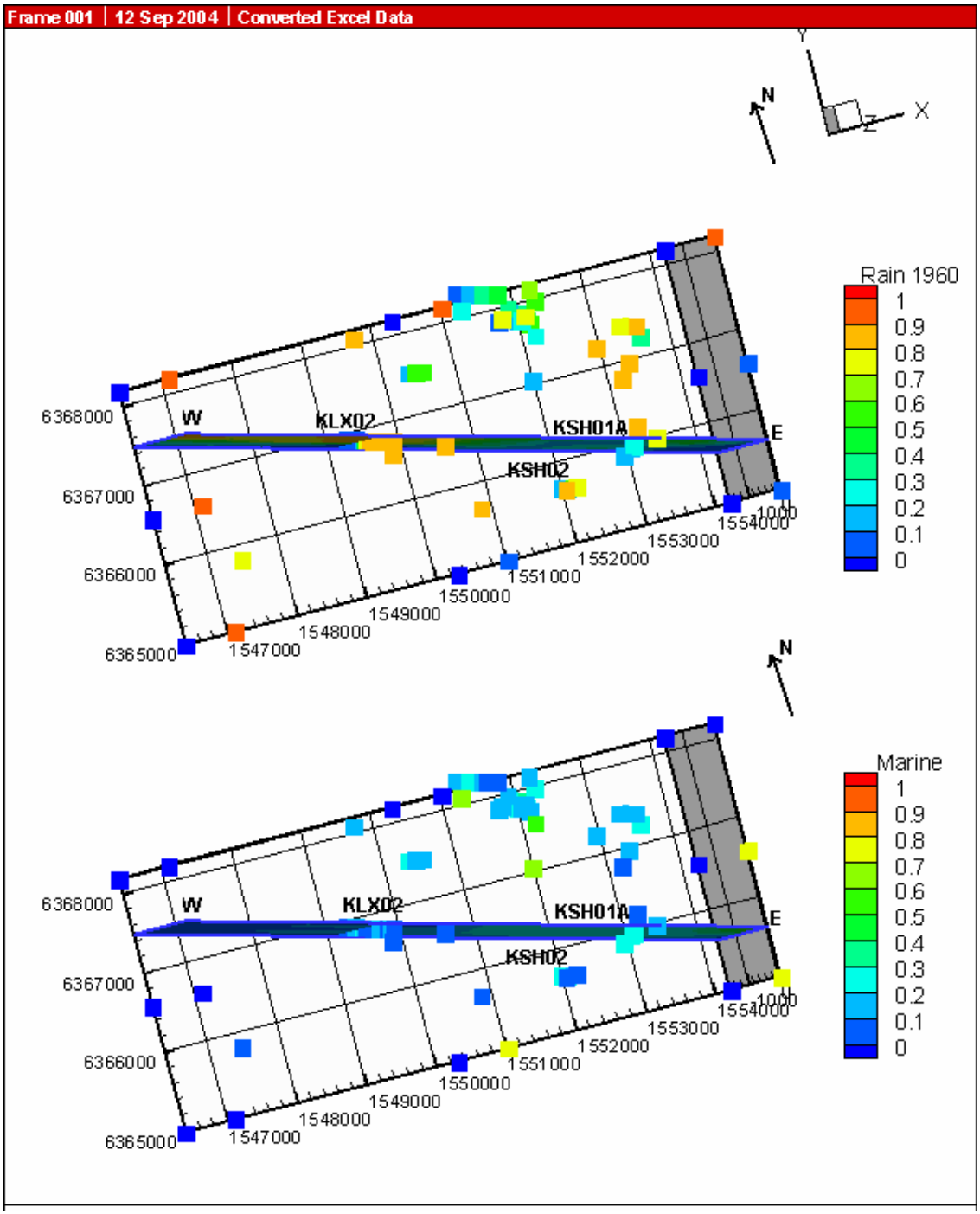

Figure 22: *2D-3D visualisation of the Rain 1960 and Marine distribution in Simpevarp. The figure shows the location of the representative sampling and the location of the inclined vertical profile.*

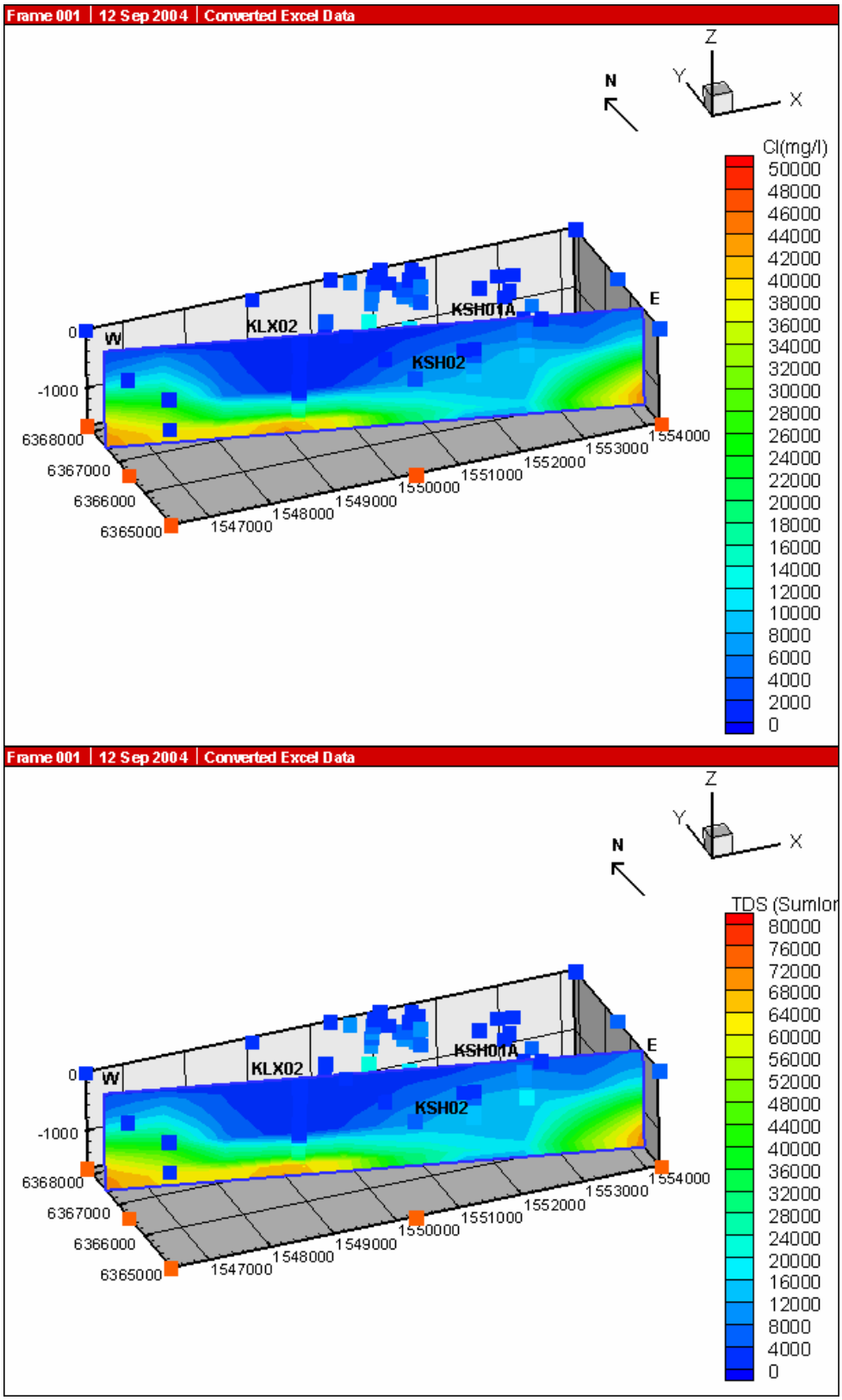

Figure23: *3D visualisation of the Cl and TDS (SumIons) distribution in Simpevarp. The figures show the location of the representative sampling and the location of the inclined vertical profile. The depth scale is in meters.*

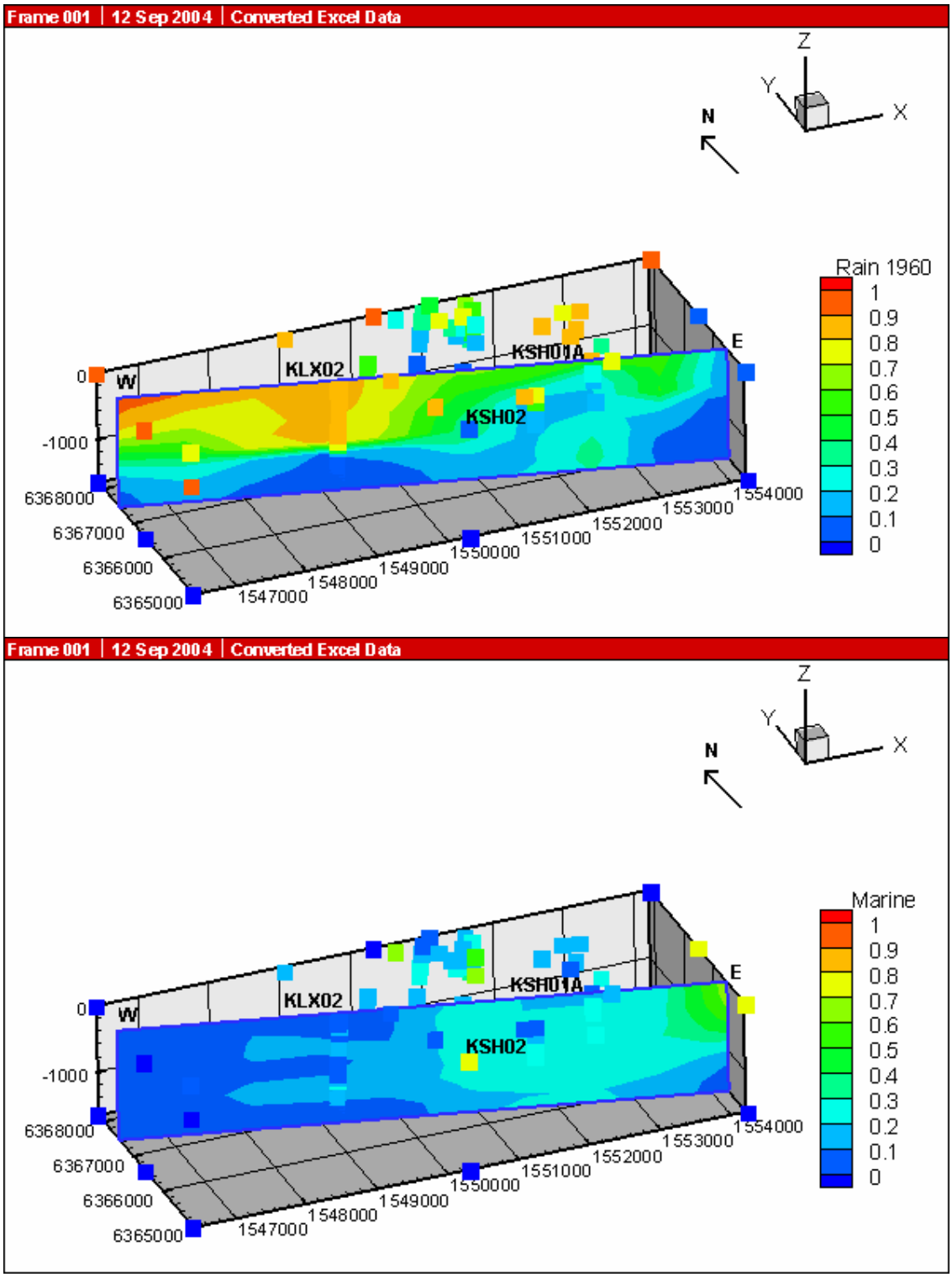

Figure 24: *3D visualisation of the Rain 1960 and Marine mixing proportions distributions in Simpevarp. The figures show the location of the representative sampling and the location of the inclined vertical profile. The depth scale is in meters.*

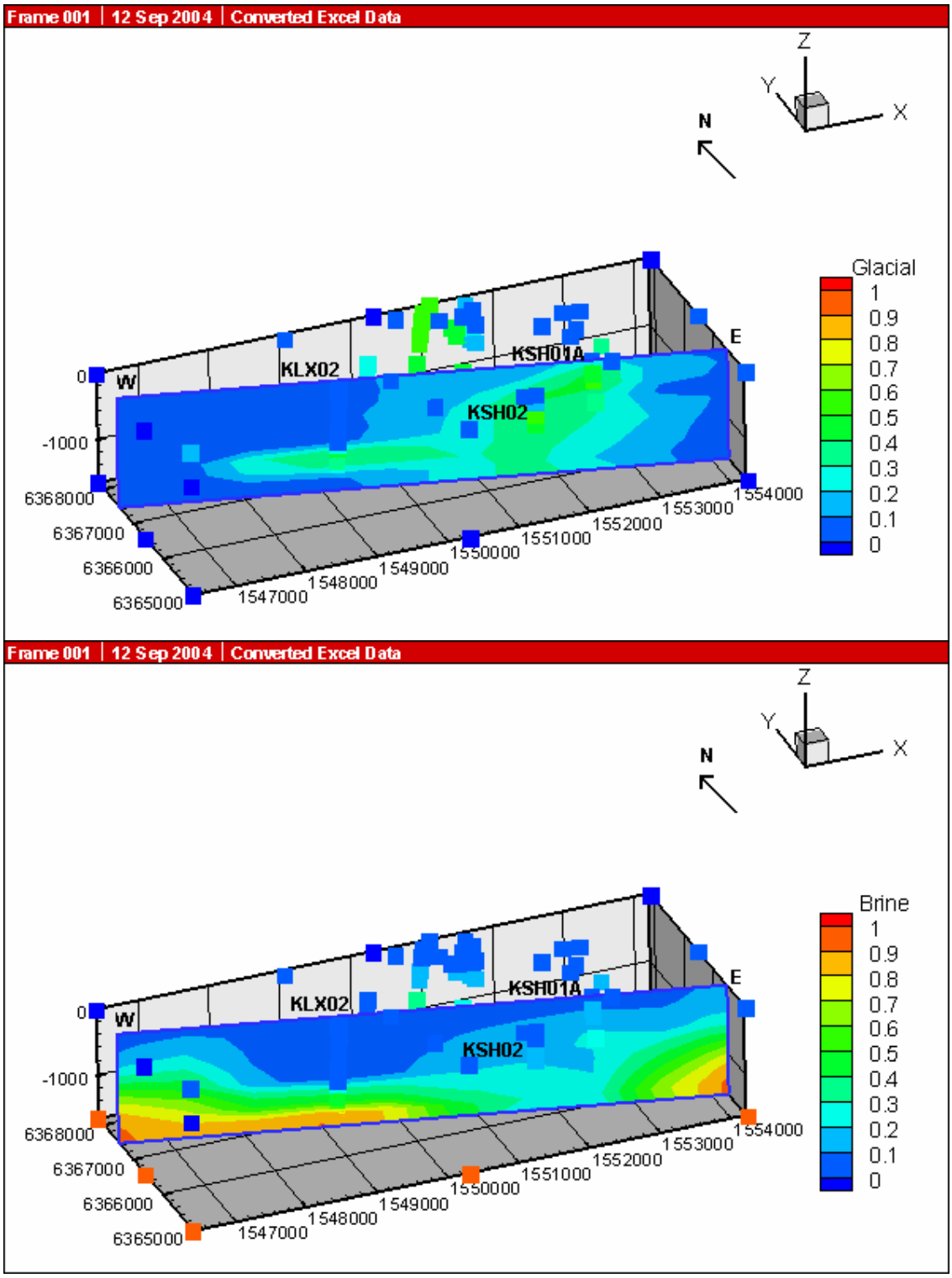

Figure 25*: 3D visualisation of the Glacial and Brine mixing proportions distributions in Simpevarp. The figures show the location of the representative sampling and the location of the inclined vertical profile. The depth scale is in meters.*

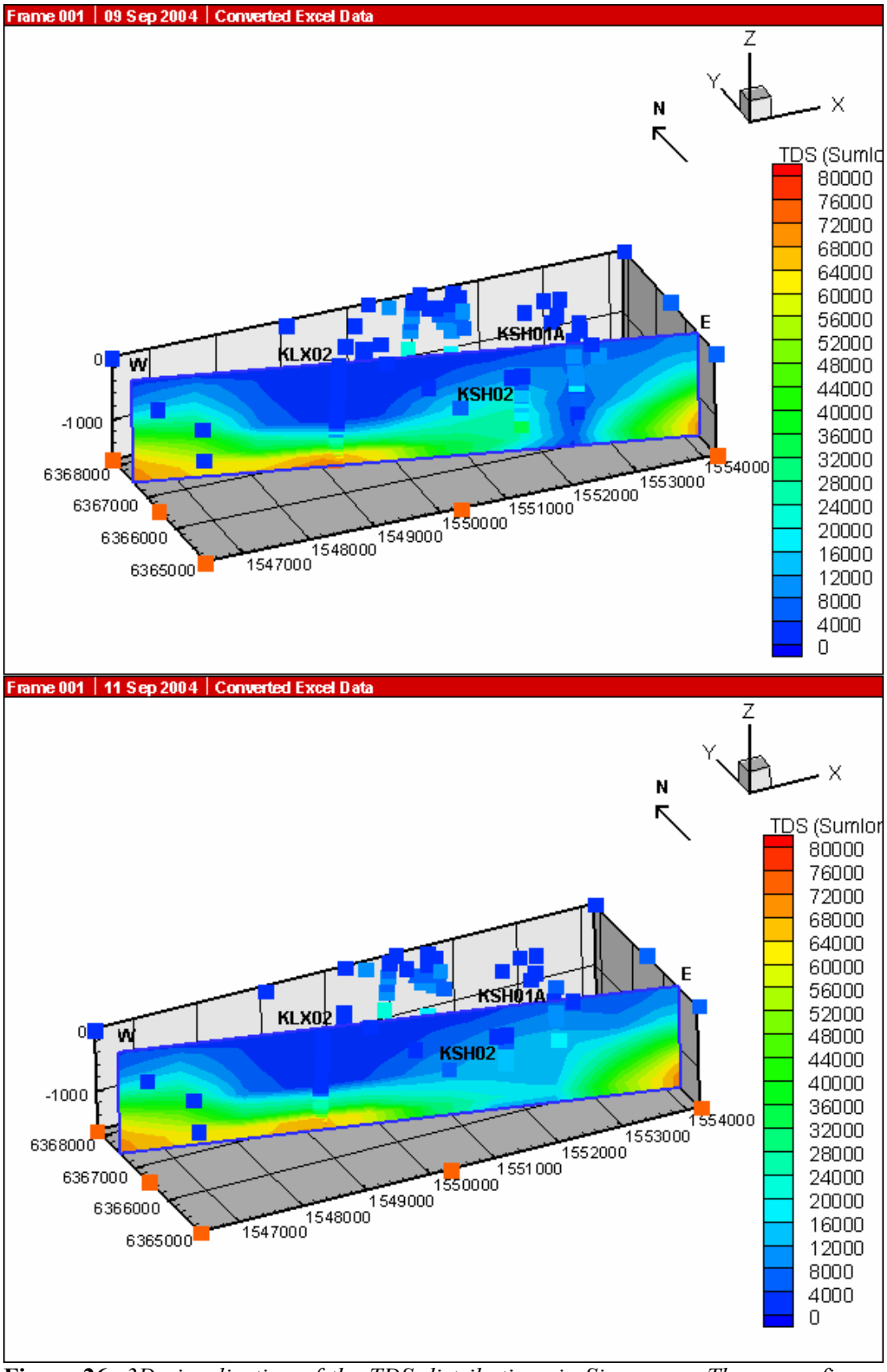

Figure 26*: 3D visualisation of the TDS distributions in Simpevarp. The upper figure shows the TDS distribution of all the sampling points (representative and non-representative). The lower figure shows the distribution of the representative samples and their location. The depth scale is in meters.*

6. DIS (Drilling Impact Study) calculations for Simpevarp

The Drilling Impact Study (DIS, Gurban I and Laaksoharju M, 2003) was used for evaluation of the contamination potential of the groundwater data used for Simpevarp 1.2. The DIS evaluates the impact of the drilling events on the hydrochemistry. DIS was applied on the data from KSH01 for the two uppermost sections (156.5-167 m and 245-261.6 m) during the Simpevarp 1.1 exercise (Laaksoharju et al, 2004). In Simpevarp 1.2 modelling the DIS calculations were applied on section 548-565 m of the KSH01 borehole.

The successful implementation of DIS evaluation required the availability of drilling data stored in SICADA and the results from DIFF (Differential Flow measurements). The DIS evaluation involves the compilation, calculation and interpretation of drilling data and DIFF measurements. The following data are used:

- Drilling water pumped in and out from the borehole during drilling operation;
- The drilled length versus time;
- Water pressure along the borehole during drilling;
- Drawdown during drilling;
- Uranine concentration in the drilling water pumped in and out from the borehole during drilling;
- The DIFF measurements performed in the borehole records the hydraulic conductivity along the borehole.

The evaluation work started by collecting data from the drilling and drilling related activities. The representativity of the drilling data and drilling activities were judged and the data used for the DIS calculations were selected. The Figures 27 to 30 show examples of evaluations and calculations used in the DIS modelling. The accumulated drilling water pumped in and out from the whole borehole (Figure 27), the accumulated drilling water in the section KSH01: 548-565m (Figure 28). The readings for uranine concentration in the drilling water pumped in and out from the borehole and the difference are presented in the Figure 29. The intention was to use 0.160mg/l uranine in the flushing water and this was used in the calculations, but in reality this value may vary. The DIFF measurements (Figure 30) show a hydraulic conductivity K (m/s) around $7*10^{-8}$ m/s for the section 548-565 m in KSH01. This value was used in the modeling.

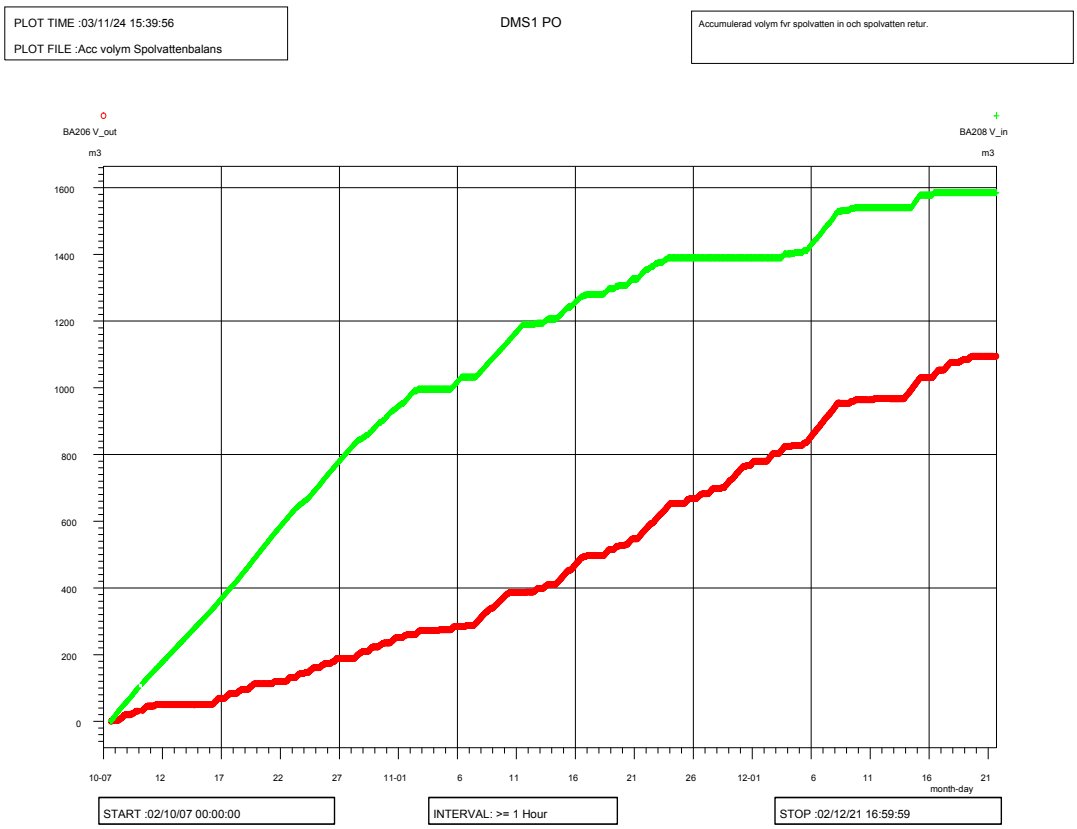

Figure 27*: Accumulated drilling water volume pumped in (in green) and drilling water volume pumped out (in red) in KSH01 with time. The monitoring of the amount of drilling water pumped into the borehole is of varying quality indicated by 2 or 3 platoes with no inflow. During the "platoe period" drilling was conducted and water is still pumped in. The error is explained by a sensor problem.*

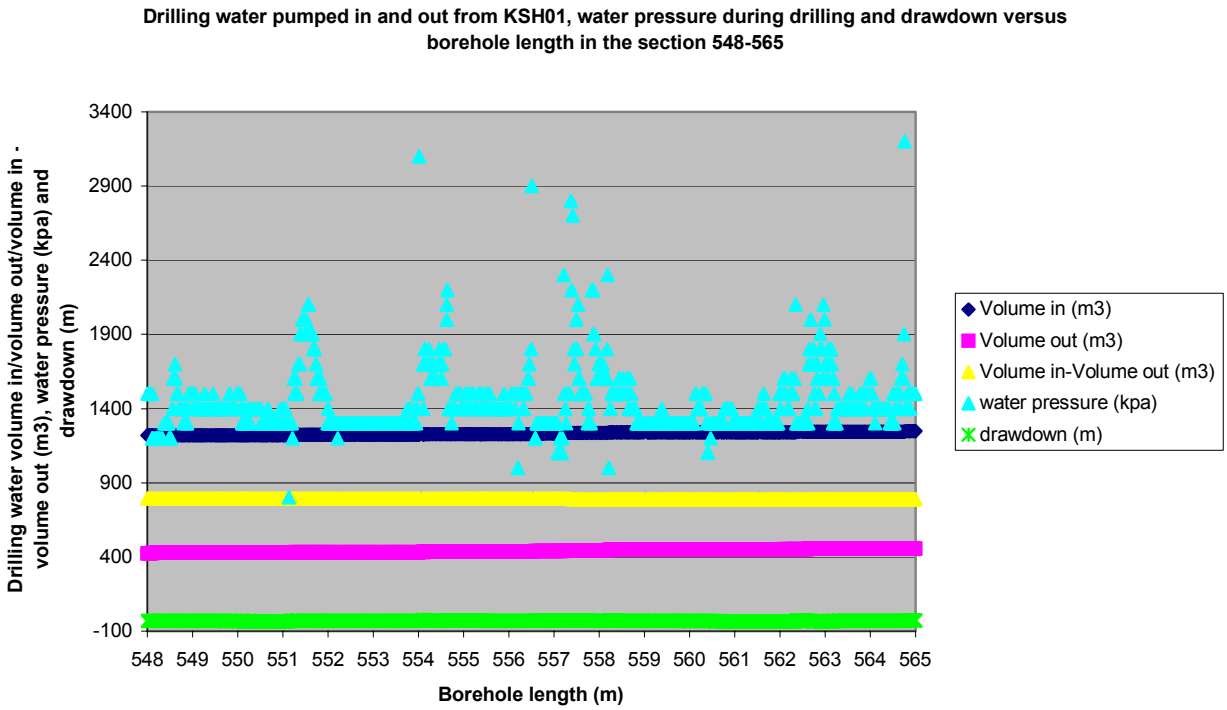

Figure 28: *Accumulated drilling water volume in and out from the borehole, corresponding to section 548-565 m in KSH01. The difference between the drilling water pumped in and out from the borehole is represented in yellow. The water pressure along the borehole during drilling and the drawdown are represented in light blue and green respectively.*

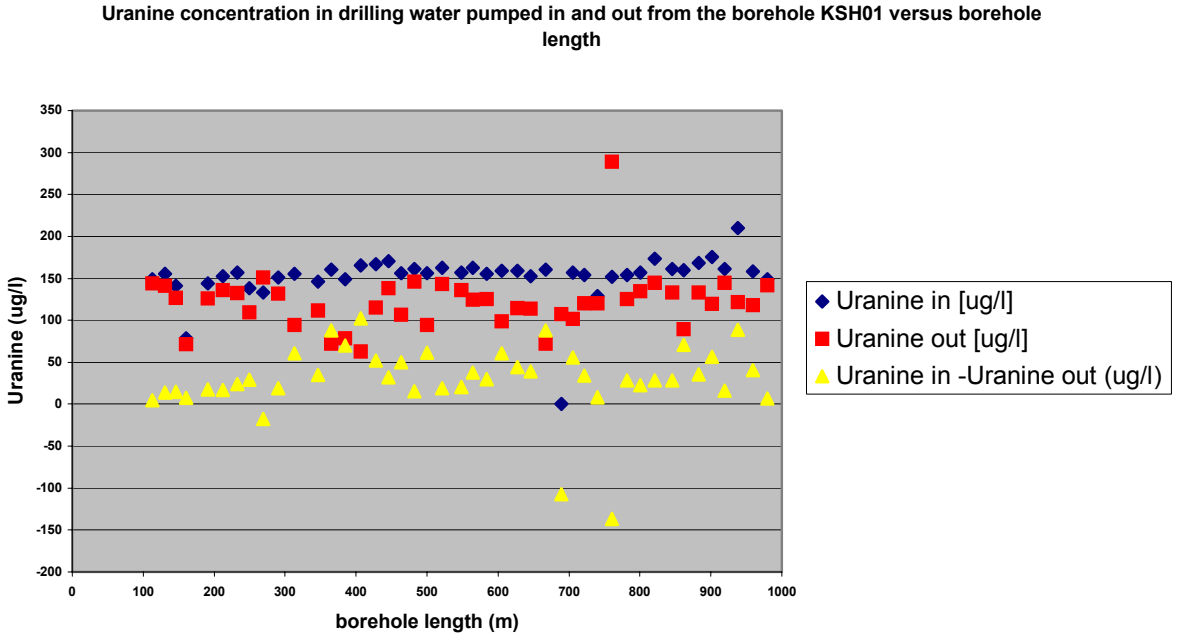

Figure 29*: Average uranine concentration in the drilling water volume pumped in and out and the difference from KSH01 with borehole length.*

6.1 Calculations of hydraulic permeability for individual fracture zone

The DIS calculations shown bellow are made according to the methodology proposed by Gurban and Laaksoharju (2003). In this chapter the calculation of the hydraulic permeability for individual fracture zones are shown.

Calculations of hydraulic permeability for an individual fracture zone by using data from KSH01 and comparison with the DIFF measurements:

- Calculation of the pressure:
    1. from the drill rig data: Δp maximum and Δp average
    2. by composing all the different pressures: h-drawdown+friction losses

- Calculation of the thickness of the section (Δe)

- Calculation of the effective drilling time

- Calculation of the flow in the fracture zone (considered the maximum flow which could penetrate the section)

$$Q = \Delta h \times K \times e$$

- Calculation of the drilling water volume lost in the fracture from the on-line measurements

$$V\ lost = Vol\ in - Vol\ out$$

- Calculation of amount of drilling water remained in the fracture

- Calculation of the hydraulic permeability in the fracture Δ e:
    1. $K = \Delta V / \Delta t / (\Delta h * e)$
    2. Comparison of $K_{calculated}$ with K_{DIFF}

Note: the friction losses along the borehole are very small (around 1 bar per 100m).

By analysing the records from drilling, drilling related activities and DIFF measurements (see figure 30) and by using the above methodology, the following results were obtained for the section investigated in KSH01:

548-565m:

Δpressure max = 2400 kpa
Δpressure average= 1438 kpa
Drawdown average= -31.2m
Drawdown max= -23.5m
The time when the fracture was penetrated by the drilling was Δt= 86810s.
The real time (without stops in the drilling activities) was Δt= 58800s.

The average uranine lost in the fracture is Δuranine= 0.02925mg/l
The maximum uranine lost in the fracture is Δuranine= 0.03778mg/l
The thickness of the section is Δe= 17 m.
The hydraulic conductivity is K= $7*10^{-8}$m/s.
The error margin for the water pressure along borehole is +/-100 kPa.
The drawdown was measured in the borehole relative to the sea level. The sensor was not calibrated. The error margin is +/- 2m.

The calculation of the amount of drilling water volume in the fracture during the drilling event minus the drilling water pumped out from the fracture during the drilling event for this section result in a negative value (-4.7 m^3). Most probably formation water from more conductive upper sections were removed, but this hinders to calculate a water balance for this section based on the drilling water pumped in and out from the borehole. Therefore the drilling water, which contaminated this section will be calculated based only on the DIFF measurements and drilling data as discussed in the next chapter.

6.2 Calculations based on DIFF measurements

By using the hydraulic conductivity K from the DIFF measurements, water pressure during drilling, the drawdown and the fracture thickness the flow of the fracture can be calculated. This result can be compared with the flow calculated above, by using the drilling water volume and the time.

The pressures were calculated with three methods: 1) average of the water pressure during drilling and mean value, 2) the maximum pressure difference between maximum and minimum recorded values and 3) by composing the different pressures during drilling: hydraulic charge, drawdown and friction losses. For example, the maximum value for the water pressure was used in the bellow calculation:

Q = Δh * K * e = (water pressure-drawdown) * K * e = 2.58 * $10^{-4}$$m^3$/s.

The maximum drilling time of this section was 86810s and the maximum drilling water volume which penetrated the fracture was 22.4 m^3.

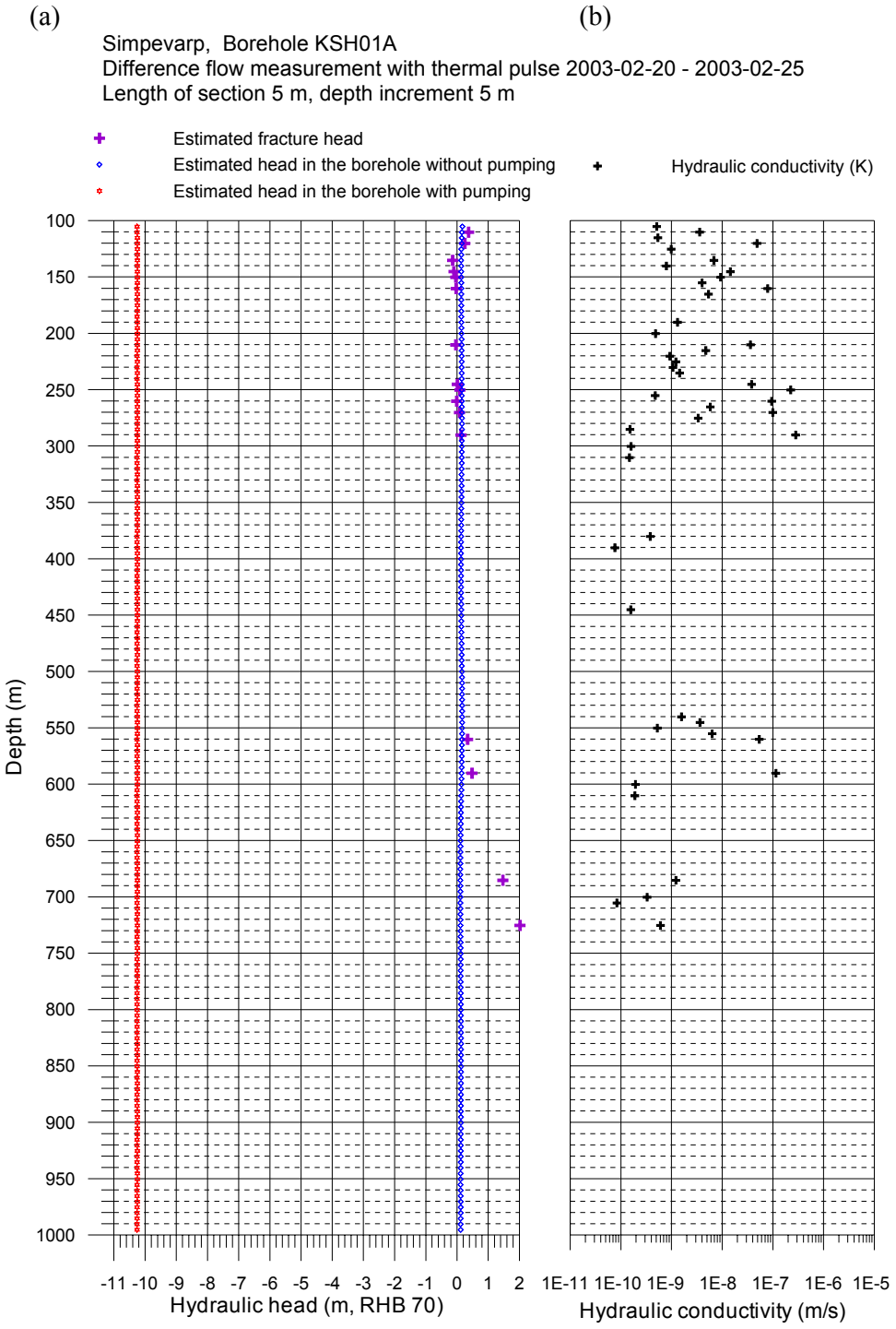

Figure 30. *DIFF measurements along borehole KSH01A (105 to 1000 m). a) groundwater flow rate (mL/h) into and out of the bedrock, and b) hydraulic head and conductivity.*

The above DIFF measurements (Figure 30) indicate that the hydraulic conductivity of the sections 548 - 565 m is $K_{DIFF}= 7*10^{-8}$m/s.

By using the calculation scheme shown above, the DIS calculations show that the section was contaminated with maximum 22.4 m^3 water of which maximum 23.61% consisted of drilling water, during the drilling of this section. The maximum uranine lost in the fracture

during drilling was 0.0378mg/l, which represent 23.61% drilling water. Later drilling activities could have increased the amount of contamination. The results from the sampling show 18.67% remaining drilling water in the first sample at the beginning of the pumping (after pumping 336hours), and 10.74% remaining drilling water in the last sample (see Appendix 5, after pumping 1675 hours). The duration of the pumping (1675 hours) was from 24.06.2003 to 12.09.2003, with an average flow rate 200 ml/min (Pia Wacker et al, 2004, SKB report in print). The volume removed was calculated to be 20 m^3. This can be compared with the maximum 22.4 m^3 volume of water that contaminated the fracture. The average amount of drilling water remaining in the fracture is 2.4 m^3. The sampling shows an amount of 10.74% drilling water after 1675 hours of pumping. The DIS calculations show that the pumping should have continued further in order to remove at least the additional 2.4m^3.

For deep sections the DIS calculations are more difficult to conduct. This is due to the contributions from the upper sections, which may bias the calculations and make the interpretation more difficult.

7. Concluding remarks

This work represents the phase 1.2 of the hydrochemical evaluation and modelling of the Simpevarp 1.2 data. This comprises the explorative analyses (AquaChem), M3 modelling, 3D/2D visualisation and finally DIS (Drilling Impact Study) evaluation.

- M3 modelling helped to summarize and understand the data.
- DIS evaluation can help to judge the representativity of the sampled data. The section 548-565m in KSH01 was investigated and the results compared with the sampled hydrochemical data.
- The visualisation helps to understand the distribution of the data at the site. Two data set were compared: all available data used for M3 modelling, representative and non-representative and data containing only representative samples. The visualisation of both data sets give a general picture of the modelled area. However, the visualisation helps to better understand the importance of the representative samples and their effects on the model.

8. References

Andersson, J., Christiansson, R. and Munier, R., 2001. Djupförvarsteknik: Hantering av osäkerheter vid platsbeskrivande modeller. Tech. Doc. (TD-01-40), SKB, Stockholm, Sweden.

Gurban I and Laaksoharju M, 2003. Drilling Impact Study (DIS); Evaluation of the influences of drilling, in special on the changes on groundwater parameters. SKB report PIR-03-02.

Gurban I, Laaksoharju M, Ledoux E, Made B, Salignac AL, 1998. Indications of uranium transport around the reactor zone at Bagombé (Oklo). SKB Technical Report TR-98-06, Stockholm, Sweden.

Laaksoharju M (editor), Smellie J, Gimeno M, Auqué L, Gomez , Tullborg E-L and Gurban I, 2004. Hydrochemical evaluation of the Simpevarp area, model version 1.1. SKB Report R 04-16, Stockholm, Sweden.

Laaksoharju M, Gurban I, Andersson C, 1999a. Indications of the origin and evolution of the groundwater at Palmottu. The Palmottu NaturalAnalogue Project. SKB Technical Report TR 99-03, Stockholm, Sweden.

Laaksoharju M, Skårman C, Skårman E, 1999b. Multivariate Mixing and Mass-balance (M3) calculations, a new tool for decoding hydrogeochemical information. Applied Geochemistry Vol. 14, #7, 1999, Elsevier Science Ltd., pp861-871.

Laaksoharju M, Tullborg E-L, Wikberg P, Wallin B, Smellie J, 1999c. Hydrogeochemical conditions and evolution at Äspö HRL, Sweden. Applied Geochemistry Vol. 14, #7, 1999, Elsevier Science Ltd., pp835-859.

Laaksoharju M, 1999d. Groundwater Characterisation and Modelling: Problems, Facts and Possibilities. Dissertation TRITA-AMI-PHD 1031; ISSN 1400-1284; ISRN KTH/AMI/PHD 1031-SE; ISBN 91-7170-. Royal Institute of Technology, Stockholm, Sweden. Also as SKB TR-99-42, SKB, Stockholm.

Laaksoharju M, Gurban I, Skårman C, 1998. Summary of the hydrochemical conditions at Aberg, Beberg and Ceberg. SKB Technical Report TR 98-03, Stockholm, Sweden.

Laaksoharju M, Smellie J, Nilsson A-C, Skårman C, 1995a. Groundwater sampling and chemical characterisation of the Laxemar deep borehole KLX02. SKB Technical Report TR 95-05, Stockholm, Sweden.

Laaksoharju M, Skårman C, 1995c. Groundwater sampling and chemical characterisation of the HRL tunnel at Äspö, Sweden. SKB Progress Report PR 25-95-29, Stockholm, Sweden.

Laaksoharju M, Wallin B (eds.), 1997. Evolution of the groundwater chemistry at the Äspö Hard Rock Laboratory. Proceedings of the second Äspö International Geochemistry Workshop, June 6-7, 1995. SKB International Co-operation Report ISRN SKB-ICR-91/04-SE. ISSN 1104-3210 Stockholm, Sweden.

Smellie, J, Laaksoharju, M and Tullborg, E-L (2002) Hydrochemical site descriptive model – a stategy for the model development during site investigation. SKB R-02-49.

Smellie J, Karlsson F, 1996. A reappraisal of some Cigar-Lake issues of importance to performance assessment. SKB Technical Report TR-96-08, Stockholm, Sweden.

Wacker P, Berg C, Bergelin A Oskarshamn site investigation, Complete hydrochemical characterisation in KSH01A, Results from four investigated sections, 156.5-167.0, 245.0-261.6, 586.0-596.7 and 548.0-565.4 metres, SKB report in print.

Appendix 1: Water type classification of the Simpevarp samples by using AquaChem

See the file on the attached CD!

Appendix 2: M3 mixing calculations for Simpevarp 1.2 regional and local model: in dark blue the M3 regional modelling results and in light blue the local M3 modelling results; in green the representative samples

See the file on the attached CD!

Appendix 3: Visualisation of the Cl, TDS and M3 mixing proportions along the core boreholes available for Simpevarp 1.2; in green the representative samples.

See the file on the attached CD!

Appendix 4: Cl, TDS and M3 mixing proportions for the percussion and core boreholes available for Simpevarp 1.2; in green are presented the representative samples.

See the file on the attached CD!

Appendix 5: Drilling water content in the samples from the section 548-565m in KSH01

Idcode	Secup m	Seclow m	Sample no.	Drill_water %
KSH01A	548	565	5271	
KSH01A	548	565	5272	18.67
KSH01A	548	565	5273	
KSH01A	548	565	5274	17.26
KSH01A	548	565	5275	17.46
KSH01A	548	565	5276	15.69
KSH01A	548	565	5277	15.1
KSH01A	548	565	5278	15.39
KSH01A	548	565	5279	13.91
KSH01A	548	565	5280	13.45
KSH01A	548	565	5281	12.92
KSH01A	548	565	5282	12.35
KSH01A	548	565	5283	6 ?
KSH01A	548	565	5284	11.49
KSH01A	548	565	5285	10.93
KSH01A	548	565	5286	11.73
KSH01A	548	565	5287	11.37
KSH01A	548	565	5288	10.74

Appendix 6: Coupled hydrogeological and reactive transport modelling

Contribution to the model version 1.2

Jorge Molinero and Juan Ramón Raposo

Área de Ingeniería del Terreno

Universidade de Santiago de Compostela.

Escola Politécnica Superior. Lugo

November 2004

Contents

1 Introduction

The work presented here constitutes a first attempt for combined hydrogeological and hydrochemical analysis of Simpevarp area. The main objective of this exercise is to develop a framework to integrate available hydrogeological and hydrochemical information, with special emphasis on the consistency assessment between them.

Any reliable coupled hydrogeochemical model requires sound conceptual models of both, hydrogeology and hydrochemistry. This is why a review of previous reports has been done first of all. An executive summary of the background is shown in Chapter 2.

Present time hydrogeological conditions of Laxemar – Simpevarp area consist on a dynamic fresh-groundwater aquifer overlying a deeper and virtually stagnant saline groundwater system. The present work focuses on the coupling between groundwater flow, solute transport and geochemical processes actually taking place within the dynamic aquifer.

Chapter 3 analyze available isotopic and hydrochemical information of fresh-groundwater samples and the consistency with current hydrogeological knowledge. Chapter 4 comprises the description and main results achieved by numerical modelling of groundwater flow, environmental isotopes transport and reactive transport. Finally, the main conclusions and possible future developments are summarized in Chapter 5.

2 Hydrogeological and hydrochemical background

2.1 Hydrogeology

Current knowledge of Simpevarp hydrogeology is based on different sources of information. On one hand, reports of SDM version 0 and 1.1 (SKB, 2002; SKB, 2004) were available for the present work. On the other hand, it is worth noting the great efforts done in order to elaborate a regional hydrogeological model of Laxemar during the last decades, in the framework of the Äspö HRL and other SKB R&D activities. The Simpevarp area is located within (or very close to) the influence of these regional studies. A comprehensive compilation on the geological, hydrogeological and hydrochemical models of the Laxemar area is reported by Rhén et al. (1997a, 1997b). These works provide an excellent overview of the area.

Figure 2-1 illustrates SKB's conceptual approach for hydrogeological modelling of groundwater flow through fractured crystalline bedrocks. From this conceptual point of view there is a division into 3 main hydraulic domains: (1) Hydraulic Soil Domains (HSD) which are used to represent shallowest quaternary deposits; (2) Hydraulic Conductor Domains (HCD) which are used to represent the main deterministic water-conducting fracture zones and; (3) Hydraulic Rock Domains (HRD) which are used to represent the mass of bedrock in between HCD.

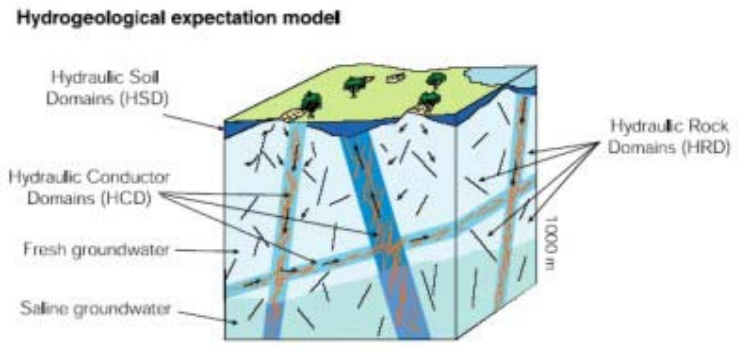

Figure 2-1*. SKB's conceptual approach for hydrogeological modelling of fractured crystalline bedrocks (from SKB, 2002).*

The interpretation of regional fracture network at Simpevarp is displayed in Figure 2-2 (SKB, 2002). According to the current hydrogeological model, all this fracture zones are candidates to become Hydraulic Conductor Domains. According to the information shown by Rhén et al. (1997b), these water-conducting fracture zones have hydraulic conductivity values 3-4 orders of magnitude larger than Rock Mass Domains in between them.

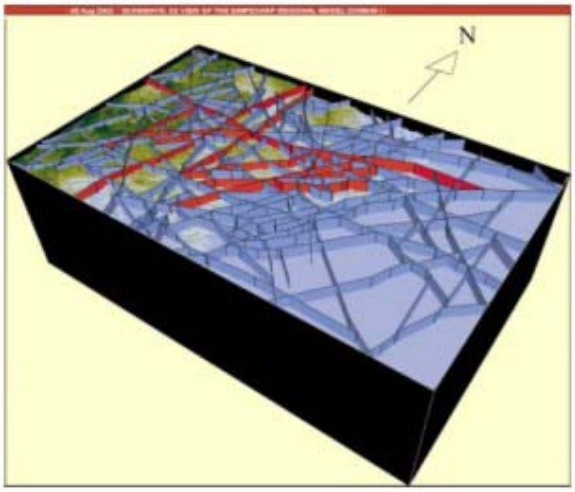

***Figure 2-2**. Schematic 3D visualisation of fracture zones at Simpevarp. The red surface indicate regional fracture zones (probable and certain), and the blue surfaces indicate lineaments (possible fracture zones) (from SKB, 2004).*

In order to deal with the wide variety of flow and transport problems in fractured media, a number of modelling approaches have been developed. Several classifications for these conceptual models can be found in the scientific literature (Carrera et al., 1990; Bear, 1993 and Berkowitz, 1994, among others). Mainly, there are four categories of approaches that can be summarized as: (1) Continuum or Equivalent Porous Media Models (see Bear, 1993); (2) Discrete Fracture Network Models (see Dershowitz et al, 1991 and Berkowitz, 1994); (3) Channel Network Models (see Moreno et al., 1988) and Hybrid or Mixed Models (see Juanes et al., 2002). Nowadays, there is not a total agreement within the scientific community about the most appropriate modelling approach. All of them show advantages and disadvantages, depending on several factors such as the objective and scope of the model, the amount of field information, the modelling scale, the number and complexity of the processes included in the models, etc.

Hydrogeological modelling of Simpevarp is being conducted in parallel by two teams: ConnectFlow and DarcyTools (SKB, 2004), both of them using the Discrete Fracture Network approach. The main objective of these models was to study the paleo-hydrogeological evolution of the area, mainly during the last 10,000 years. Calibration of models has been performed using salinity data and M3 mixing fractions provided by the hydrochemical team. However, in these works (model version 1.1) there is not yet a complete description of the hydrogeological conditions of the site, since they constitute a first step towards a realistic site description.

A visualization of present time hydrogeological conditions of Laxemar area (at regional scale) can be found in Svensson (1997). This work has been taken as the reference regional model for several activities at the Äspö site, such as the modelling activities within the framework of the Äspö Task Force 5 (Rhén and Smellie, 2003). The regional model of Svensson (1997) is based on a heterogeneous continuum approach, accounting

for 3D density driven flow dependent of the groundwater salinity. Figure 2-3 shows a cross-section of the results provided by Svensson (1997).

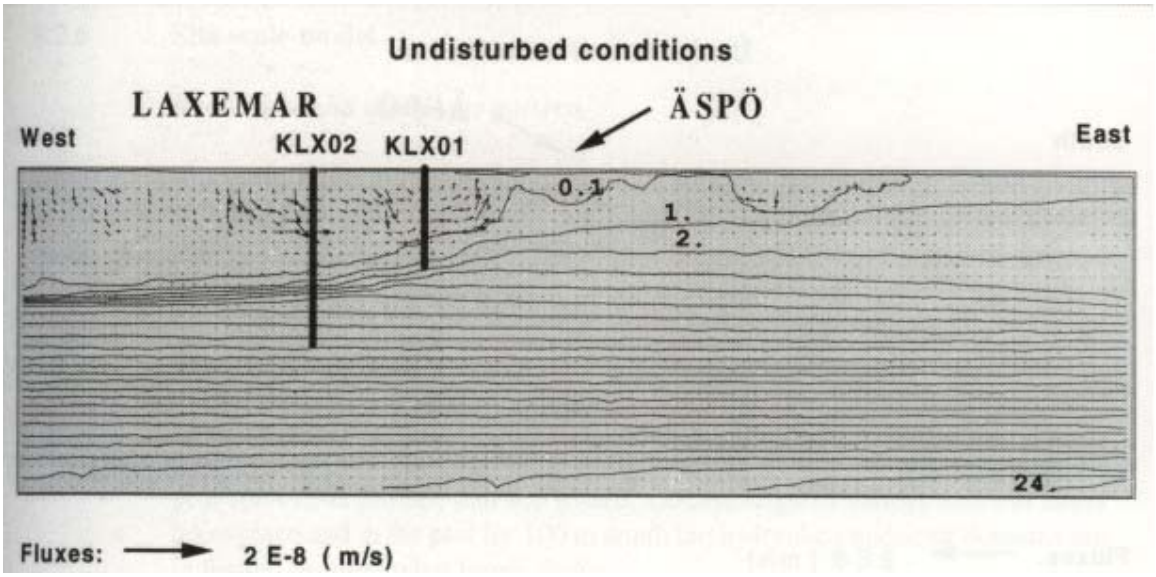

Figure 2-3*.Vertical cross-section (W-E) of the regional-scale groundwater flow model of Laxemar. Vectors indicate the magnitude of computed groundwater fluxes. Iso-lines represent salinity fields (%). (From Svensson, 1997).*

It is well known that coastal aquifers develop a fresh groundwater body with a maximum thickness under recharge zones (usually the water divides located under the highest topographic points). Under natural conditions, the transition zone between fresh and saline water is generally thin and usually idealized as a sharp interface that exhibits parabolic shapes, with the thickness of the fresh water body tending to zero near the coast line or discharge zone (Custodio, 1983).

It can be seen in Figure 2-3 that, according to the regional model, there is fresh water (0.1 % iso-line) down to about 1,000 m at Laxemar (borehole KLX02). One can also see that the discharge of the system is located at the Baltic coastline. Flow vectors as well as the salinity interface show irregular patterns, reflecting the heterogeneity of the media. In general, it can be noticed that present time hydrogeological conditions can be described by a dynamic fresh-water aquifer, recharged by infiltration in the mainland of Laxemar, which discharge in the vicinity of the Baltic sea (estuaries). Downwards there is an almost stagnant and saline groundwater system, which is the result of complex paleo-hydrogeological events (Laaksoharju et al., 1999), and density-driven stratification of salinity.

2.2 Hydrogeochemistry

It is known that different pre- and postglacial events have affected the groundwater composition at the Simpevarp area. However, the effects from the last glaciation and the subsequent land uplift are the most important events which are likely to affect the groundwater composition (Laaksoharju & Wallin. 1997). The latest glacial event (Weichsel) reached its maximum approximately about 18,000 to 20,000 years ago (Ehlers, 1996). The cyclic behaviour in the climate during the Quaternary Period imply that different groundwaters in the basement must have been modified and even replaced several times (Rhén et al., 1997b). Keeping in mind that most probably the events after the last glaciation have a dominant influence on the actual groundwater system, a working hypothesis and a conceptual model for this groundwater system was proposed by Laaksoharju & Wallin (1997) and Laaksoharju et al. (1999a). This conceptual model of the postglacial scenario has been slightly updated recently (SKB, 2002).

A hydrochemical mixing modelling approach, called M3 (Laaksoharju et al., 1999b), has been applied at Simpevarp (Laaksoharju et al., 2004). M3 model assumes that chemical composition of groundwater samples are the result of a theoretical mixing between different end-members. Then, back-analyses of measured and computed groundwater compositions allows one to define deviations from the ideal mixing. Observed deviations from the ideal mixing can be attributed to the occurrence of geochemical processes. This approach has been proved very useful for deciphering hydrochemical signatures produced by the paleo-hydrogeological events in different sites of the the Fennoscandian Shield (Laaksoharju 1999). The application of M3 methodology to groundwater samples of Simpevarp, pointed towards three main water types: (1) one dominated by meteoric water, (2) a second type mainly affected by the marine end-member and, (3) a third type of saline groundwater with clear signatures of glacial influence (Laaksoharju et al., 2004).

Both qualitative and quantitative geochemical modelling were performed within the activities of SDM version 1.1 (Laaksoharju et al., 2004; Smellie and Tullborg, 2004; Gimeno et al., 2004). Based on those modelling results, it has been identified that major processes affecting the local chemistry at Simpevarp waters are: organic matter decomposition, dissolution of calcite, silicates and sulphides (or gypsum), precipitation of some phyllosilicates (all of them with very low mass transfer) and Na-Ca cation exchange. All these heterogeneous processes were clearly identified in the fresh groundwater system. For the brackish-saline waters it was found that calcite is precipitating (instead of dissolving) and dissolution-precipitation of Fe-mineral phases, as well as microbially-mediated reactions, become important controlling sulphate and iron contents and the redox state of this system (Gimeno et al., 2004). Saline waters at Simpevarp have been in contact with the bedrock for a long time, and this is why they are generally at chemical equilibrium with most minerals (Laaksoharju et al., 2004). It is known that deep saline groundwater is virtually stagnant and has an origin related with bedrock interaction (Smellie et al., 1995). Louvat et al. (1999) dated Äspö deep saline groundwater as being 1.5 million years old.

3 Analyses of isotopic and hydrochemical information

3.1 Isotopic information

Isotopic characterization has been performed in a number of water samples at Simpevarp. Analysed environmental isotopes mainly include ^{14}C, ^{13}C, ^{3}H, ^{2}H, and ^{18}O.

^{14}C is the leading tool in estimating the age of paleo-groundwaters. The method is based upon the incorporation of atmospherically derived ^{14}C from the decay of photosynthetically-fixed carbon in soil (Clark & Fritz, 1997). If the ^{14}C gained in the soils remains with the groundwater along a flow path, without subsequent dilution, its decay can be used as straightforward method to derive the age of groundwater. However, it is well known that this is rarely the case, because dilution and loss by geochemical reactions within the aquifers use to affect strongly the ^{14}C activities in groundwater.

Table 3-1 shows age values computed for fresh groundwater at Laxemar and Simpevarp areas, based on measurements of ^{14}C activities in borehole water samples. These values have been taken as they appear in the SICADA database. The values of groundwater age in Table 3-1 correspond to the assumption of no dilution on ^{14}C due to geochemical processes. However, geochemical mass balance modelling identifies calcite dissolution as a geochemical process actually taking place at the fresh groundwater system of Simpevarp (Gimeno et al., 2004). Then, age values shown in Table 3-1 are probably overestimated.

Table 3-1 *Computed age of fresh groundwaters at Laxemar and Simpevarp areas*

Borehole	Sample	Seclow	Secup	center	"Age" (years)	Cl (mg/L)	Comments
HLX10	3904	0.00	200.00	100	4645	6.3	Representative
KLX02	2422	200.00	250.00	225	3255 +- 55	65.8	
KLX02	2421	400.00	450.00	425	2925 +- 70	36.1	Representative
KLX02	2420	600.00	650.00	625	2950 +- 85	35.4	
KLX02	2419	800.00	850.00	825	2870 +- 85	73.2	
KLX02	2418	900.00	950.00	925	2875 +- 80	35.4	
KLX02	2412	1000.00	1050.00	1025	2925 +- 80	83.4	
HSH02	3883	0.00	200.00	100	2832	11.8	
HSH02	3886	0.00	200.00	100	3132	22.6	Representative
HSH03	5858	0.00	200.00	100	3920	462.9	Representative

The dilution factor of ^{14}C in groundwater due to calcite dissolution, q, can be approached by using the measured values of $\delta^{13}C$, as (Clark & Fritz, 1997):

$$q = \frac{\delta^{13}C_{DIC} - \delta^{13}C_{carb}}{\delta^{13}C_{rech} - \delta^{13}C_{carb}}$$

where $\delta^{13}C_{DIC}$ is the measured ^{13}C in groundwater samples, $^{13}C_{rech}$ is the ^{13}C in recharge (infiltrating) water and $\delta^{13}C_{carb}$ is the ^{13}C value of the calcite being dissolved. $\delta^{13}C_{carb}$ is usually close to 0 ‰, and $\delta\ ^{13}C$ in soils is usually close to the value of -23 ‰. However, the value of $\delta\ ^{13}C$ in the recharge water is likely to be different that in the soil due to fractionation and dilution effects during infiltration. In summary, it can be stated that there is relevant uncertainty related with the initial ^{14}C that should be used in the calculations of groundwater age. Vogel (1970) reports initial ^{14}C values for groundwaters in crystalline rocks between 90 and 100 pmC. On the other hand, some authors estimate that initial ^{14}C content in recharge waters of granitic batholiths can be as low as 50 pmC, after interaction with C in soils and overburden horizons (Gascoyne, 2004).

Figure 3-1 shows a plot of ^{13}C versus ^{14}C in different types of waters at Simpevarp. It can be seen that both marine and stream waters have ^{14}C contents around 100 pmC, but they have clearly different values of ^{13}C deviations. ^{13}C contents of marine waters plot close to 0 ‰ while stream waters plot close to -20 ‰ VPDB. Fresh groundwater samples of Simpevarp plot in the middle of the graph, showing a negative correlation of ^{13}C / ^{14}C, which could indicate the occurrence of ^{14}C dilution due to calcite dissolution.

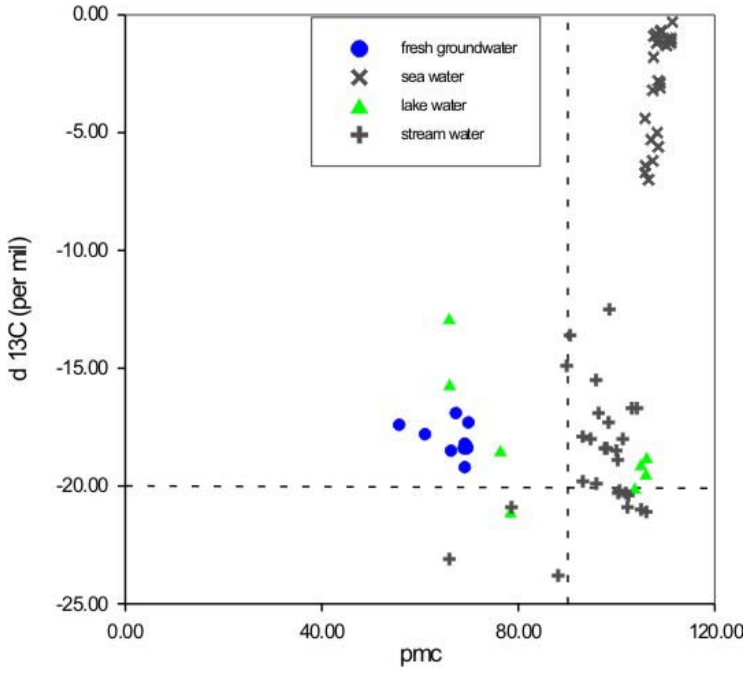

***Figure 3-1**. ^{14}C versus ^{13}C in different types of waters at Simpevarp.*

It is worth noting that some of the lake water samples show carbon signatures which are similar to the stream waters, whereas some others plot close to the groundwaters (Figure

3-1). This could be reflecting two different types of lakes from a hydrogeological point of view: (1) lakes that are mainly recharged by rain and streams and, (2) lakes that constitute discharge areas of the granitic aquifer, thus having similar signatures that groundwater. However, this hypothesis should be tested in future stages of S.I., since there could be a number of possible reasons why the lake water resembles one water type or the other.

Figure 3-2 shows a detailed view of the ^{13}C / ^{14}C relationship in fresh groundwater samples of Simpevarp. The negative correlation becomes apparent in this figure.

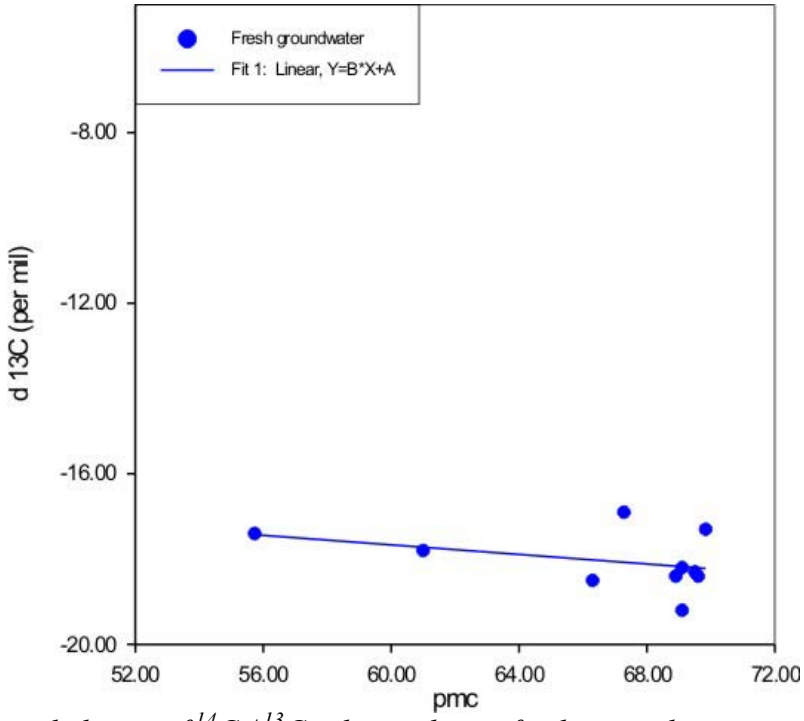

Figure 3-2*.Detailed view of ^{14}C / ^{13}C relationship in fresh groundwater samples of Simpevarp.*

Linear extrapolation of data shown in Figure 3-2 provides an estimation of initial ^{14}C contents in recharge waters of about 85 pmC.

Figure 3-3 shows computed groundwater ages by taking both 100 pmC and 85 pmC as initial value for the recharge water. It can be seen that computed ages are very sensitive to this value. According to (1) geochemical evidences of calcite dissolution, (2) ^{13}C values of fresh groundwater, and (3) previous experiences and published data of other granitic aquifers, it is believed that an initial value of 100 pmC for recharge water in Simpevarp is highly unlikely. Then, looking at Figure 3-3 we think that the age of fresh groundwater at Simpevarp (at a depth of 100 – 200 m) is in the order of magnitude of some decades - hundreds of years, instead of thousands of years initially estimated (see Table 3-1).

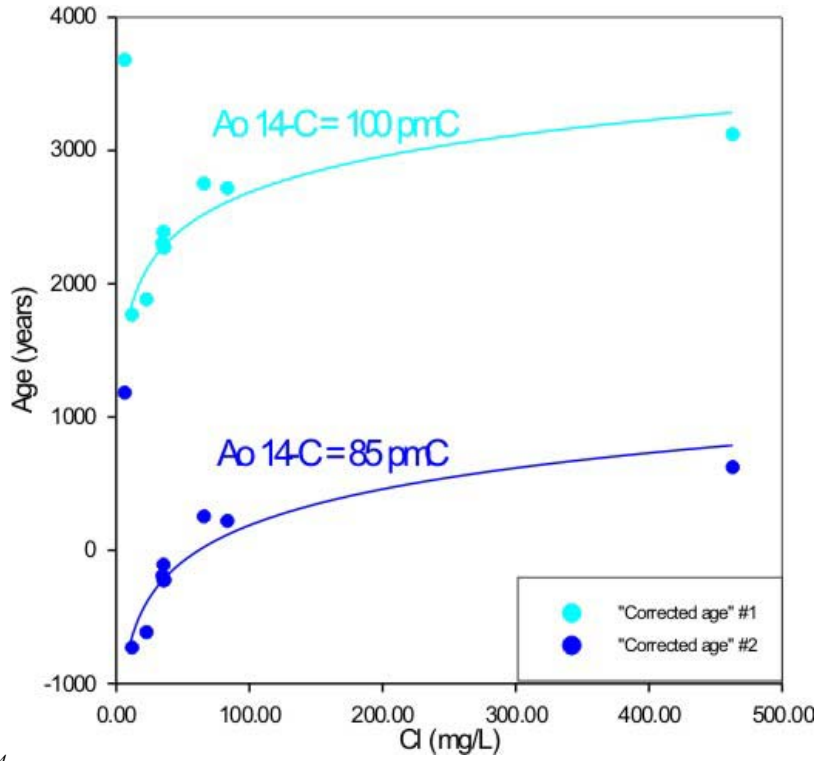

Figure 3-3*.* ^{14}*C-derived ages of fresh groundwater samples of Simpevarp assuming initial values of 100 pmC and 85 pmC.*

Figure 3-4 shows measured values of Tritium in fresh groundwater samples of Simpevarp and Laxemar. PLX samples correspond to very shallow groundwater samples collected in private wells of Laxemar. It can be seen at this figure that some of the groundwater samples plot above 15 TU, which is the average value of recent precipitation in Laxemar. These values indicate an influence of recharge from the 1960s – 1970s in the samples. On the other hand, the rest of groundwater samples have Tritium values between 5 – 15 TU, probably corresponding to a mixture of modern and submodern waters (understanding submoden water as recharged prior to 1952). Then, Tritium contents in groundwaters of Simpevarp are consistent with groundwater ages of decades – hundreds of years.

However, care should be taken looking at Tritium values of Figure 3-4, because available data of Simpevarp and Laxemar area do not correspond to the same sampling dates. Laxemar water samples included in SICADA database were collected a few years ago (in 1993 most of them). Figure 3-5 shows only Tritium values of Simpevarp fresh groundwater samples collected in late 2003.

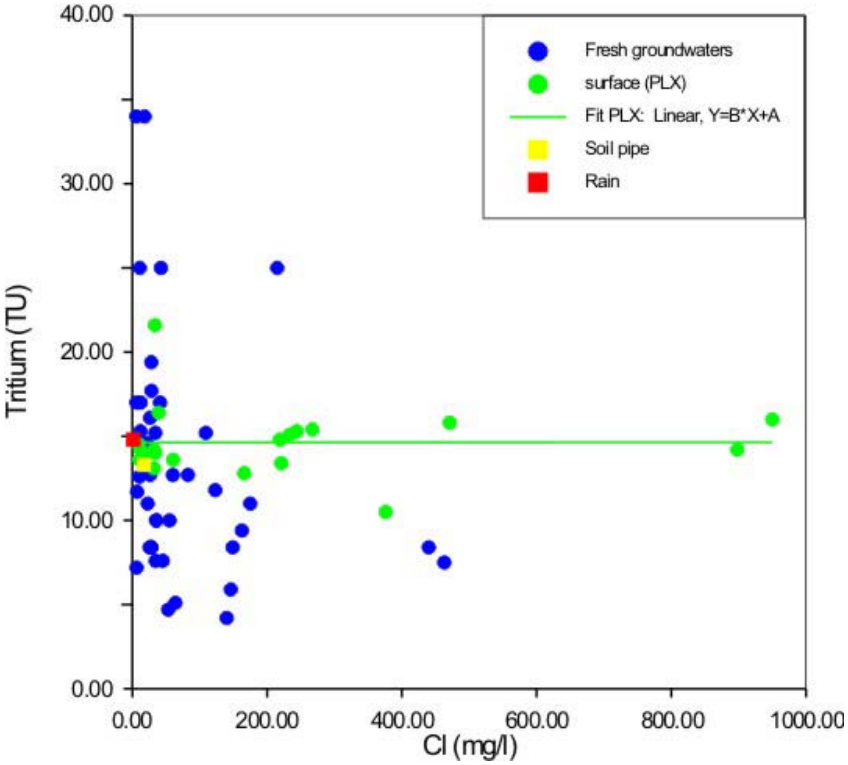

Figure 3-4*.Tritium contents of fresh groundwater samples of Simpevarp and Laxemar.*

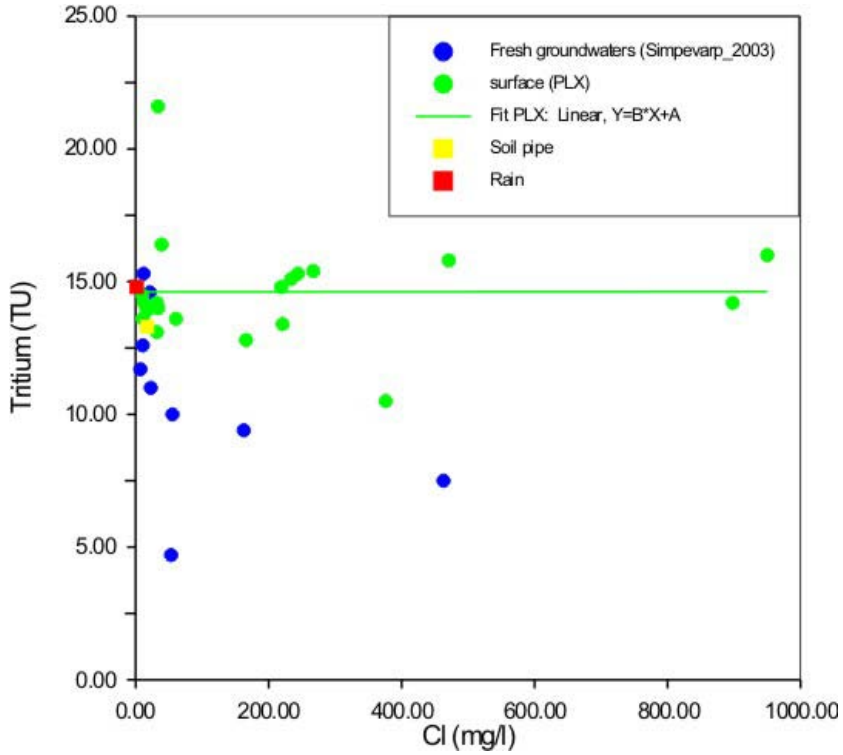

Figure 3-5*.Tritium contents of fresh groundwater samples collected at Simpevarp in 2003.*

It can be seen in Figure 3-5 that there is only one sample with a Tritium value lower than 5 TU, and two samples between 7.5 and 10 TU (clearly affected by mixing with older saline waters). However, the rest of fresh groundwater samples collected at Simpevarp show values in the range of 10 – 15 TU. This observation is relevant for the interpretation of reactive transport model results shown in the next chapter.

3.2 Hydrochemical information

According to the regional hydrogeological model (see Section 2.1; Figure 2.3), groundwater reaches the granitic aquifer by distributed infiltration on the emerged lands, and then flows through the aquifer towards the discharge zones, located mainly in the vicinity of the Baltic coastline (as the Simpevarp area). It is well known that as groundwater moves through aquifers from recharge to discharge areas, its chemistry is altered by the effects of geochemical processes. Then, hydrochemical signatures of groundwater samples should be consistent with the hydrogeological knowledge of Laxemar and Simpevarp areas.

Figure 3.6 shows a Piper diagram containing all fresh groundwater samples (Cl^- < 1000 mg/L) of the Simpevarp and Laxemar areas.

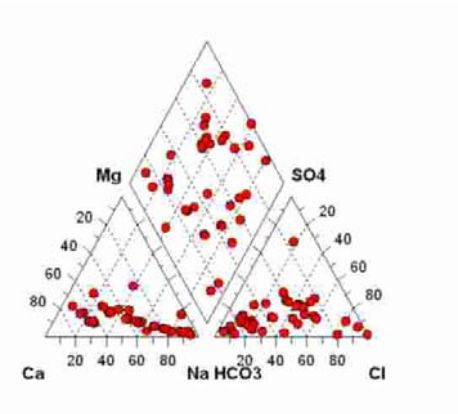

Figure 3-6*.Piper diagram with all fresh groundwater samples of Simpevarp and Laxemar areas.*

One can see in Figure 3-6 that fresh groundwater samples plot along the whole range between chloride – bicarbonate and calcium - sodium hydrochemical facies. However, a separated analysis of fresh groundwater samples (depending on the sampling area) is very useful for the interpretation of the hydrochemical evolution of groundwater within the aquifer. Figure 3-7 shows the individual Piper diagrams for: (1) very shallow groundwater samples of Simpevarp (SSM water samples), (2) inland deeper groundwater of Laxemar (borehole KLX02) and, (3) fresh groundwater samples collected at percussion-drilled boreholes near the Baltic coast, at Simpevarp (HSH boreholes).

According to the hydrogeological conceptual model summarized in Chapter 2, these 3 different types of samples correspond to different hydrogeological "environments". It can be expected that very shallow groundwater samples (SSM) correspond to "recharge water", (i.e., recently infiltrated water). Inland groundwater of Laxemar (KLX02) should correspond to "intermediate transit water" in the fresh-water aquifer, since they are located in the midway between the water divide (the local topographic maximums of Laxemar) and the discharge area (the Baltic coastal areas). Finally, fresh groundwater samples collected at a depth of 100 – 200 m at Simpevarp (HSH) could "conceptually" correspond to discharge waters of the fresh-water granitic aquifer. It is clearly seen at Figure 3-7 that groundwater samples collected at different hydrogeological settings show different hydrochemical facies.

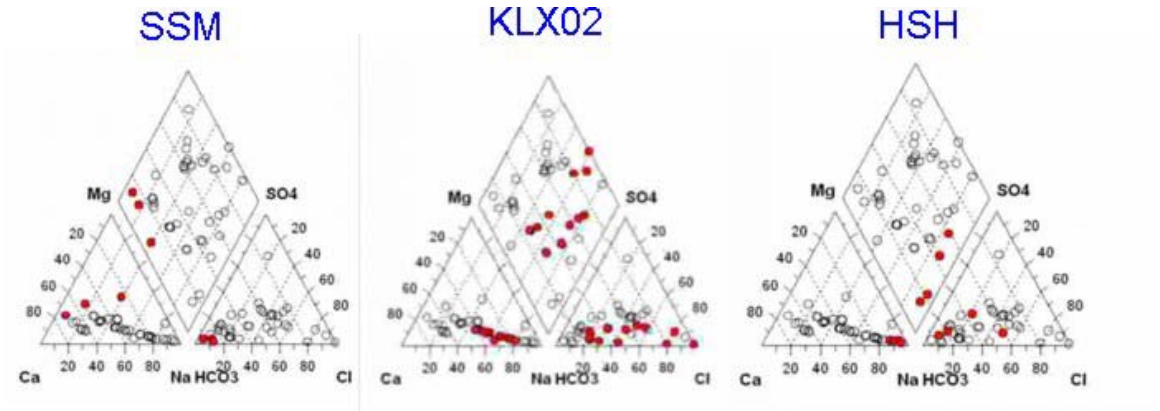

Figure 3-7*.Different Piper diagrams for: (a) recharge groundwater (SSM samples), (b) "intermediate" groundwater (KLX02 samples), and (c) discharge groundwater (HSH samples).*

Groundwater of the fresh granitic aquifer shows a hydrochemical evolution, from recharge waters with Ca-HCO_3 hydrochemical facies to water with Na – HCO_3, Cl facies (Figure 3-7). Water samples of KLX02 borehole at Laxemar show an "intermediate" pattern with Na,Ca - HCO_3, Cl facies.

The cationic evolution from Ca-waters to Na-waters is consistent with Na-Ca exchange processes and silicates weathering occurring along the flow lines in the aquifer, as suggested by expert and explorative analyses (Smellie and Tullborg, 2004), geochemical modelling (Gimeno et al., 2004) and mixing M3 modelling (Gurban & Laaksoharju, 2004).

Figure 3-8 shows computed saturation indexes of calcite for near-surface groundwater of Laxemar (PLX), Simpevarp (SSM) and Bockholmen (HBH). It can be seen that near-surface groundwater samples are quite diluted (with 1 exception) and moderately to highly under-saturated with respect to calcite, as could be expected for recently infiltrated water (i.e. "recharge groundwater").

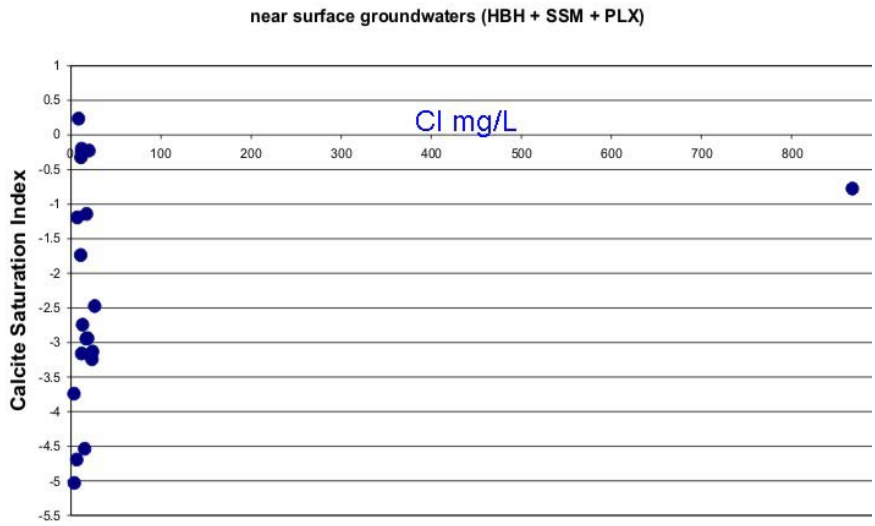

Figure 3-8*.Calcite saturation indexes versus chloride for near surface groundwater samples of Simpevarp (SSM), Laxemar (PLX) and Bockholmen (HBH).*

Figures 3-9 and 3-10 shows computed saturation indexes of calcite for deep inland groundwater of Laxemar (KLX02), and discharge groundwater of Simpevarp (HSH), respectively.

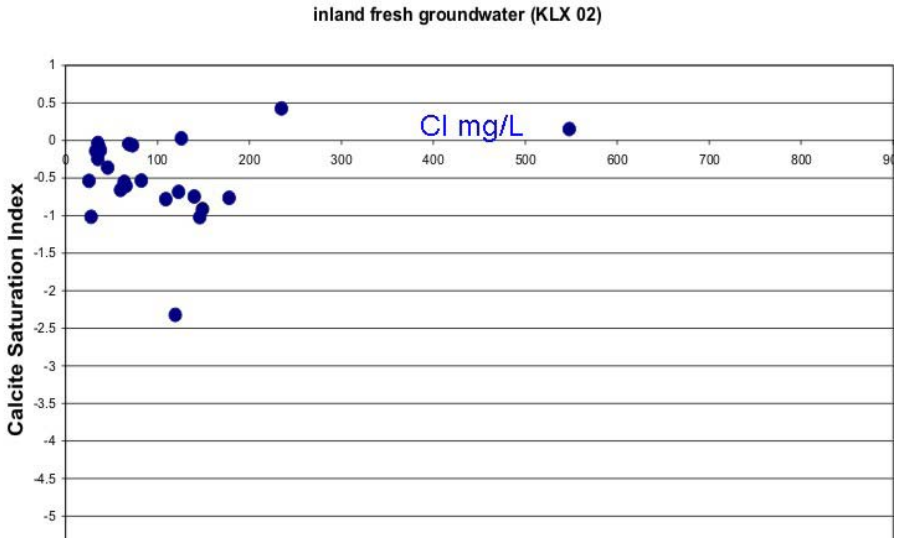

Figure 3-9*.Calcite saturation indexes versus chloride for inland fresh groundwater samples of Laxemar (KLX 02).*

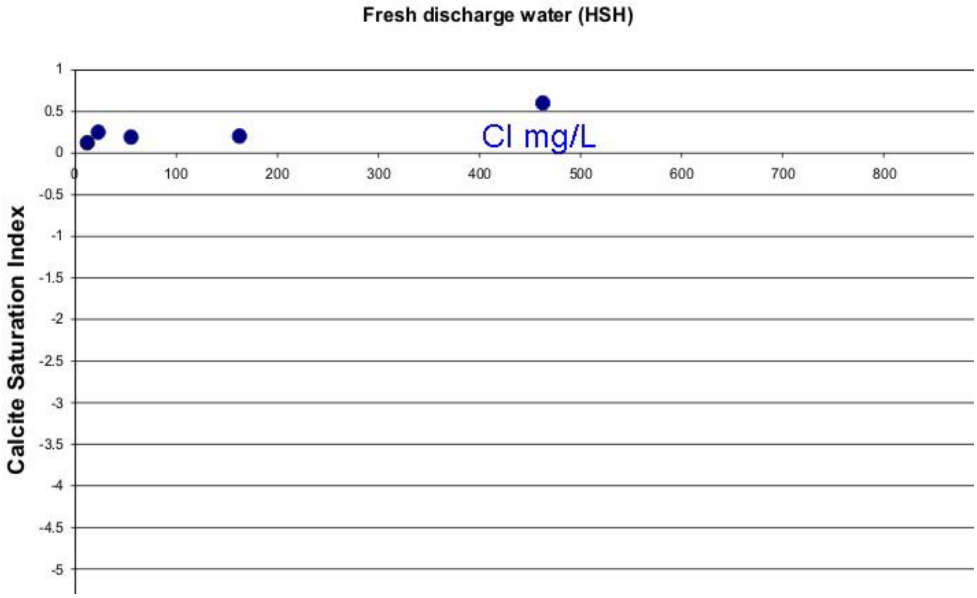

Figure 3-10*.Calcite saturation indexes versus chloride for discharge groundwater samples of Simpevarp (HSH's boreholes).*

It can be noticed that "intermediate" inland groundwater samples are slightly under-saturated or close to saturation with respect to calcite (Figure 3-9), whereas groundwater samples of Simpevarp are all of them saturated (slightly over-saturated) with respect to calcite (Figure 3-10).

The same kind of analyses has been performed with respect to quartz and chalcedony. However, all water samples are found to be saturated (and over-saturated) with respect to these mineral phases, irrespectively to the "hydrogeological location" of the sampling points. These results are not shown here, but the interested reader can see the saturation indexes of Simpevarp water samples in Gimeno et al. (2004; Figure 2.3.B).

It can be concluded that isotopic and hydrochemical analysis of fresh groundwater samples allows one to identify signatures that are consistent with the hydrogeological knowledge of the area. The distributed recharge of the granitic fresh aquifer seems to be confirmed analysing near-surface groundwater samples. Recharge waters have high ^{14}C contents, ^{3}H values close to current precipitation, Ca-HCO_3 hydrochemical facies and are under-saturated with respect to calcite. On the other hand fresh groundwater of Simpevarp at depths of 100 – 200 m, has an average age of decades to one hundred years, ^{3}H values mainly between 10 – 15 TU, Na – HCO_3, Cl hydrochemical facies and are saturated in calcite. According to a "classical" hydrogeologic framework this water could correspond to the aquifer discharge, since samples are located at a certain depth near the Baltic coast. However, with recharge and discharge waters actually found in the same Simpevarp subarea, a reasonable interpretation would also be that there is important vertical water circulation which fits with the hypothesis of local flow cells, instead of the

large scale flow from Simpevarp to Laxemar. It is thought that there is no information enough (yet) as to discard the existence of regional (or larger scale) flow systems under Simpevarp. It is worth noting that local and regional flow systems can be present in the same area, specially in coastal zones. One can expect that recharge zones in coastal areas are only local and discharge zones could be both local and regional.

What is interesting is that inland groundwater samples of Laxemar (very deep water compared to Simpevarp samples) show “intermediate” hydrochemical signatures between near surface water (assumed as to be recharge water) and relatively shallow (< 200 m) Simpevarp water samples.

4 Numerical modelling of groundwater flow and reactive solute transport

4.1 Model geometry and numerical tools

The objective of this model is to develop a quantitative framework to integrate hydrogeological and hydrochemical information. It should be noticed that a reliable coupled model of reactive solute transport requires sound conceptual models of both hydrogeology and hydrochemistry. At the present time, the status of hydrogeological and hydrochemical modelling is still preliminary, with limited amount of data. Available information includes the reports of hydrogeology and hydrochemistry teams, as well as the integrated Site Descriptive Model v 1.1 of Simpevarp. Then, the work described here should be regarded as a first attempt to model groundwater flow and reactive solute transport which will be subjected to further improvement, linked to the availability of new data and conceptual developments along the planned strategy for Site Descriptive Modelling.

At this stage, the regional groundwater model of Laxemar area (Svensson, 1997) is assumed to provide an appropriate representation of natural hydrogeology. The model domain covers a 2D profile (see Figure 2-3) from Laxemar water divide (West) to the Baltic coast (East). Bedrock properties are represented by effective parameters, according to an Equivalent Porous Media Approach.

As was pointed out in Chapter 2, there is a dynamic fresh water body, with distributed recharge input on the emerged lands, and discharge zones located in the vicinity of the Baltic coast. Fresh water aquifer is known to reach depths up to 1000 m at Laxemar. Under the fresh water body, there is an almost stagnant and saline groundwater system, which is the result of complex paleo-hydrogeological events (Laaksoharju et al., 1999a) and subsequent density-driven stratification of salinity. In the present model, the iso-line of 0.1% of salinity has been idealized as an interface to represent the sharp transition between fresh and saline groundwater. Then, this ideal interface constitutes the bottom boundary of the model, and it is assumed to behave as an impervious boundary, since flow rates across it are very small (see Figures 2-3 or 4-1). The West lateral boundary of the model coincides with the local maximum in topography at Laxemar, which is likely to correspond to a groundwater divide. The top boundary is defined mainly by the emerged lands (recharge areas), but a small portion representing the Baltic estuary (discharge areas). Figure 4-1 shows the model domain as well as boundary assumptions used for flow and reactive transport modelling.

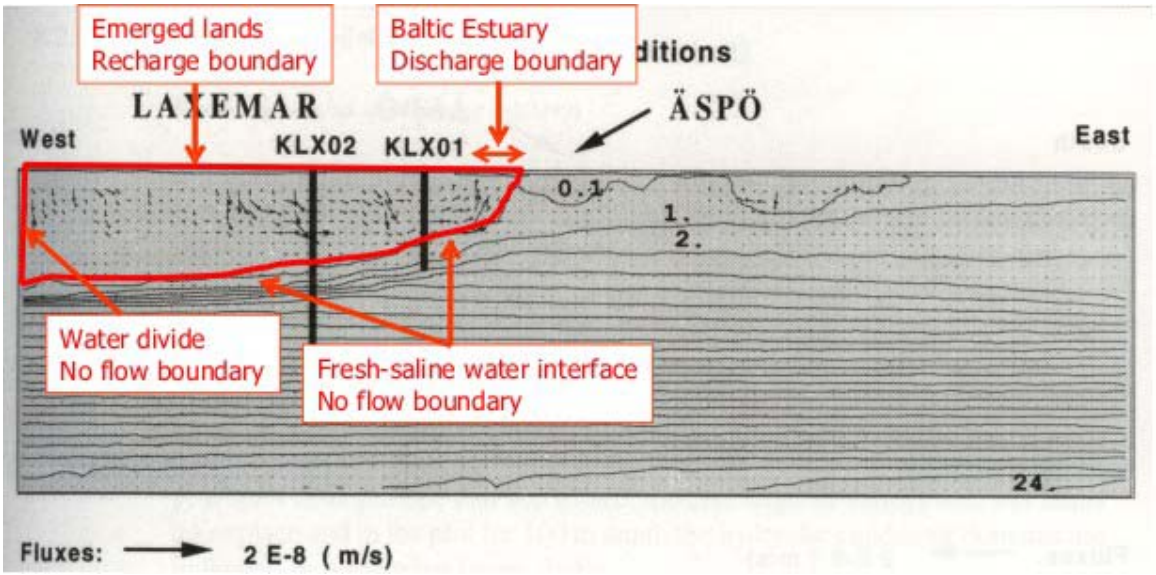

Figure 4-1. *Spatial domain and boundary assumptions used to represent the fresh water aquifer at Laxemar. The geometry has been directly taken from Laxemar Regional Model (Svensson, 1997).*

Looking at Figure 4-1, it is possible to see that the modelled cross section ends just "in front of Äspö". Then, it can be stated that the model is actually located out of the Simpevarp subarea. However, the model domain is a cross-section from the mainland to the Baltic Sea which is "parallel" to the equivalent cross-section through Simpevarp. The implicit simplification of this kind of 2D model approaches means that any point is representative of a given distance to the coast.

Spatial discretisation has been performed by means of a finite element mesh with 1843 nodes and 3456 triangular elements (Figure 4-2).

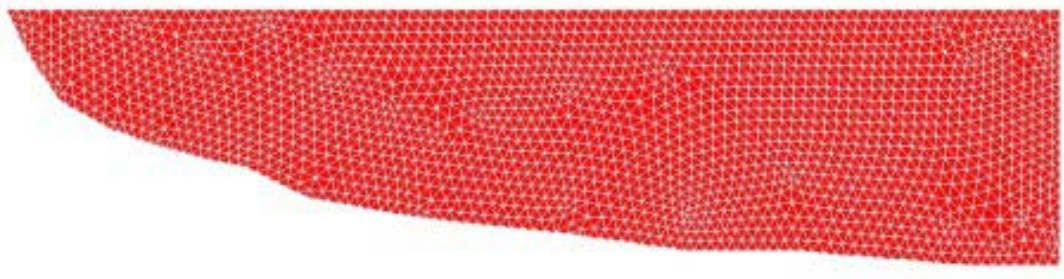

Figure 4-2. *Finite element mesh used for spatial discretization of the fresh water aquifer shown in Figure 4-1.*

The finite element mesh was generated with GEOSTAR, the basic pre and postprocessor of the COSMOS/M finite element package (SRAC, 1998). This program is an interactive CAD like graphic geometric modelling system with a powerful mesh generator for finite elements.

The numerical solver used for flow and reactive transport simulations was CORE^{2D} (Samper et al., 2000). This code solves for variably saturated groundwater flow, heat transport and multi-component reactive solute transport. The coupling of transport and geochemical equations is based on the sequential iteration approach (Xu, 1996; Xu et al., 1999). In this approach the transport and chemical equations are considered as two different subsystems. These subsystems are solved separately in a sequential manner following an iterative procedure. At any given iteration, the chemical sink/source term is assumed known (or taken equal to the value of previous iteration) for the purpose of solving the transport equations. After solving the transport equations, the set of chemical equations is solved in a node basis. Solution of these non linear equations is carried out using Newton-Raphson iterative procedures. After convergence, the chemical source term is updated. The whole iterative process (transport + chemistry) is repeated until overall convergence is attained.

4.2 Groundwater flow

Effective groundwater parameters have been collected from Rhén et al. (1997) and SKB (2004). The average value of hydraulic conductivity at Äspö (measured at packed borehole sections from 50 to 300 m length) was selected.

Preliminary sensitivity analyses showed that the most sensitive parameter for groundwater flow was the value of recharge prescribed on the top boundary. In our model, this value represents the flow rate that actually reaches the granitic bedrock under soils and quaternary sediments. According to the draft hydrogeological model of Simpevarp v 1.1 (SKB, 2004), net precipitation ranges between 150 – 180 mm/year. Surface runoff on Simpevarp – Laxemar areas is estimated to be very small, which means that most of the net precipitation percolates into the quaternary sediments. In the same document it is stated that most of this water flows through the shallow subsurface sediments to the local discharge areas (lakes, streams and estuaries), and only a small fraction of total recharge will reach the uppermost zone of the bedrock, probably less than 10%. This statement is highly consistent with available knowledge of deep recharge at the Äspö area. Banwart et al. (1999) estimated a range from 5 to 30 mm/year for the interpretation of the Redox Zone Experiment. Molinero & Samper (2004) reproduced numerically the groundwater head evolution of the same field experiment using a recharge value of 15 mm/year. At a larger scale, Molinero et al. (2002) proposed a value of 5 mm/year for numerical modelling of the transient drawdown produced by the construction of the Äspö tunnel. Based on this background, a value of 10 mm/year has been adopted for the present numerical model. Table 4.1 list the hydrogeologic parameters used in the base run of the numerical model.

Table 4.1 Main parameters used in the base run of the groundwater flow model

Parameter	Value
Hydraulic conductivity [$m.s^{-1}$]	10^{-7}
Specific storage coeffient [m^{-1}]	10^{-5}
Recharge flow rate [mm/year]	10

Figure 4-3 shows numerically computed groundwater heads and flow rate vectors. It can be seen that a virtual borehole drilled near the Baltic coast (as it is the Simpevarp area) would intercept almost all the ideal flow lines in the system. Then, it can be expected that fresh groundwater samples collected at Simpevarp boreholes correspond to a mixing of waters with different residence times.

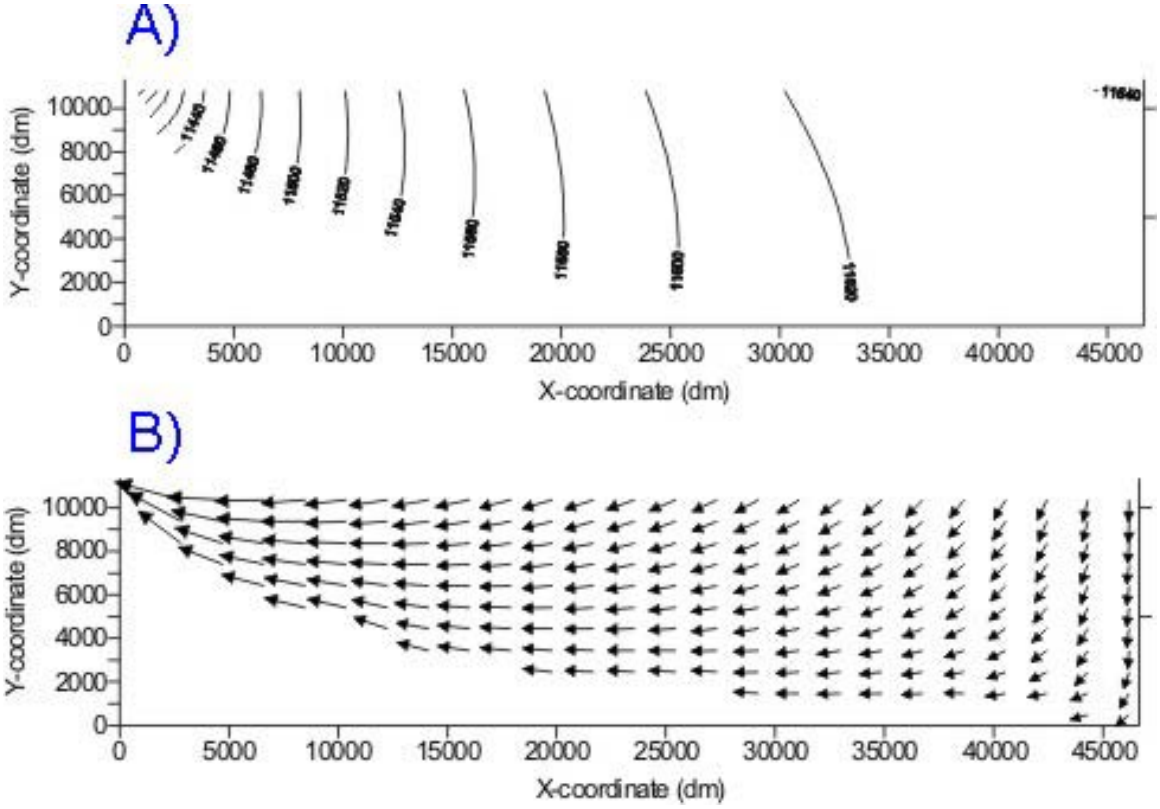

Figure 4-3. *Groundwater flow model results. A) Steady-state groundwater heads (dm). B) Flow rate vectors.*

Computed results are consistent with those reported by Svensson (1997; see figures 2-3 or 4-1). Differences are due to the fact that here a homogeneous domain is considered, while the model of Svensson (1997) accounts for heterogeneity by means of stochastic generation of parameter fields.

4.3 Residence times (groundwater age)

Groundwater age can be a misleading term from a conceptual point of view. Processes such as hydrodynamic dispersion and molecular diffusion produce mixing of waters. Mixing can also be produced by the presence of heterogeneities, pumping or other factors. According to Clark and Fritz (1997) one should not talk about the age of water but about "groundwater mean residence times" or "average groundwater ages". Yet, the term "age" is simpler and has slipped into common usage (Clark and Fritz, 1997). It has been demonstrated that "kinematic age", i.e. the obtained by tracking water along flow paths, is ill-posed in heterogeneous aquifers as well as unable to account for processes producing mixing, which makes it inadequate for comparison with radiometric measurements (Varni & Carrera, 1998). An elegant method to simulate mean groundwater age was proposed by Goode (1996), based on the use of the advection-dispersion transport equation with a distributed zero-order source of unit strength, corresponding to the rate of aging. The governing equation for age is derived from mass-conservation principles. The solution of the transport equation yields the spatial distribution of the mean groundwater age. Interested readers are referred to Goode (1996) and Varny and Carrera (1998).

In our case, mean groundwater age can be computed by simulating a "fictitious" tracer pulse of unit concentration along the inflow boundary (i.e. emerged lands of Simpevarp – Laxemar). The tracer pulse must be "tracked" along the time until reaching a complete flushing. Then, mean groundwater age can be obtained as:

$$A = \frac{\int_0^{\tau} c(t)t\,dt}{\int_0^{\tau} c(t)\,dt} \qquad \text{(Equation 4.1)}$$

where A is "mean groundwater age", c is the concentration of tracer, t is time and τ is the total duration of tracer pulse.

There is not much information about solute transport parameters for Simpevarp – Laxemar areas. The most relevant parameters needed include kinematic porosity and dispersivities. Hydrogeological models of Simpevarp v1.1, used kinematic porosity values ranging from 10^{-3} to 5 x 10^{-3} (see section 5.1.10 of SKB, 2004). A value of 10^{-3} has been adopted for the kinematic porosity of the base run in our numerical model. Longitudinal and transverse dispersivity were set equal to 200 and 100 m, respectively.

Figure 4-4 shows a simulated tracer pulse using the base run of the numerical model for groundwater flow and solute transport.

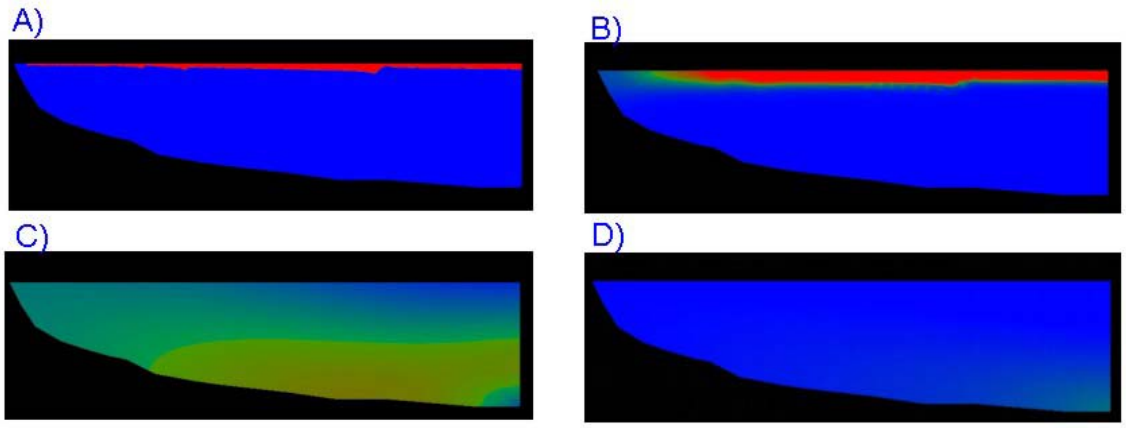

***Figure 4-4**. Simulated tracer pulse at: A) 0 days, B) 55 days, C) 15000 days and D) 55000 days.*

Several sensitivity runs of the model were performed by modifying the values of transport parameters. As expected, kinematic porosity was identified as the most sensitive parameter. After solving the numerical model of the fictitious tracer pulse, Equation 4.1 was solved numerically in order to calculate mean groundwater age, as:

$$A = \frac{\sum_{i=1}^{N_T} c_i^{(n)} T \Delta t_i}{\sum_{i=1}^{N_T} c_i^{(n)} \Delta t_i} \qquad \text{(Equation 4.2)}$$

where N_T is the total number of time steps in the numerical model, Δt_i is the duration of the i^{th} time step, n denotes node (of the finite element mesh) and c denotes tracer concentration.

Figure 4-5 shows computed results of mean groundwater ages using kinematic porosity of 10^{-3} and 10^{-2}.

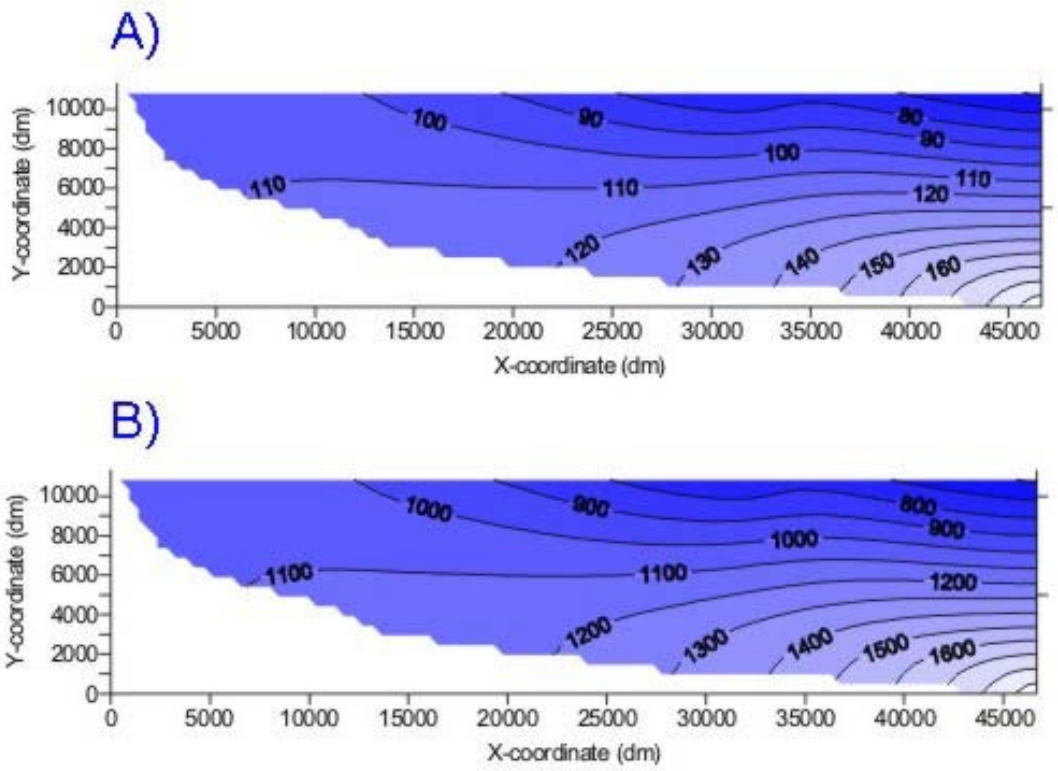

Figure 4-5. *Mean groundwater ages (years) computed by using different values of kinematic porosity. A) $\phi = 0.001$. B) $\phi = 0.01$.*

Looking at Figure 4-5, one can see that using a value of kinematic porosity of 10^{-3} leads to computed "mean groundwater ages" around 100 years at the vicinity of the Baltic boundary. However, using a value of 10^{-2} leads to "mean groundwater ages" around 1000 years.

As already pointed in Chapter 3, groundwater age considerations based on ^{14}C data are largely uncertain at Simpevarp (see also Buckau, 2004). However, qualitative analysis of ^{14}C data indicated that the age of fresh groundwater of Simpevarp is more likely in the order of magnitude of some decades - hundreds of years, in stead of the thousands of years. Then, it can be concluded that an effective kinematic porosity of 10^{-3} (which is the value used by hydrogeologists) is consistent with qualitative ^{14}C data interpretation.

4.4 Tritium transport

Groundwater recharged in the past decades and taking part of an active hydrological cycle is referred to as modern groundwater (Clark & Fritz, 1997). Tritium has become a standard tool for the definition and study of modern groundwater systems. The era of thermonuclear bomb testing in the atmosphere (1951 – 1976), provide the tritium input signal that defines modern water. Due to its natural decay, pre-bomb tritium input cannot

be normally detected. Then, tritium-free groundwater is considered “sub-modern” or old water (Clark & Fritz, 1997).

As it was shown in Chapter 3, all fresh groundwater samples collected at Simpevarp boreholes showed measurable tritium contents. All analysed water samples contained more than 5 TU. In addition, only 2 water samples showed tritium contents lower than 10 TU, and all the rest between 10 and 15 TU. The interpretation of these tritium values is not straightforward. For instance, a water sample with 12 TU could correspond to rain water infiltrated some months ago, or could be the result of mixing between recent (i.e 15 TU), modern (i.e 30 TU) and sub-modern (i.e 0 TU) waters in different proportions. As it was shown in the groundwater flow model, the Simpevarp area is located close to the Baltic coast (close to aquifer discharge) where flow paths tend to converge. Then, Simpevarp boreholes can theoretically intercept different ideal flow lines representing longer and shorter residence times.

Tritium evolution within the Laxemar – Simpevarp aquifer can be simulated as a natural tracer test. The behaviour is not conservative since it is affected by radioactive decay, with a half-life of 12.43 years. Then, the decay constant will be equal to ln2 divided by the half-life. In order to set up a model of groundwater flow and tritium transport, the input function of this environmental tracer is also needed. There is an excellent time series of tritium levels in precipitation measured at Ottawa, Ontario, which has become a classical reference for hydrogeologists. However, such a good time characterization of rain water is not available in other places, such as Sweden. Figure 4-6 shows the Ottawa time series of tritium levels in rain water, as well as discrete values from 4 places in Sweden. All these data have been downloaded from the Isotope Hydrology Information System (the ISOHIS database; http://isohis.iaea.org) provided by the IAEA. It can be seen (Figure 4-6) that, even with relevant latitude difference, the Ottawa time series can be adopted as an appropriate description for atmospheric tritium in Sweden. Figure 4-6 also shows a step-wise function representing a “smoothed” tritium evolution. This step-wise function has been used as the tritium input signal for the numerical model of tritium transport at Laxemar – Simpevarp.

Figure 4-7 shows a sketch of the model domain and the type of boundary condition used to simulate the input of tritium with the recharge (infiltrated) water.

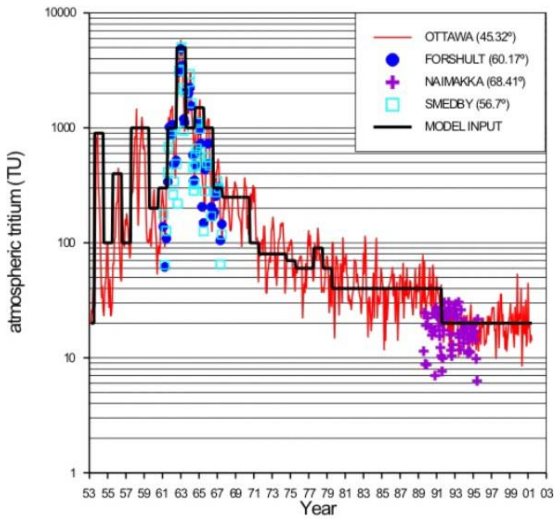

***Figure 4-6**. Evolution of atmospheric tritium at Ottawa and 4 locations in Sweden (data from the ISOHIS database, IAEA, 2001). Step-wise function used as the model input signal is shown in solid black line.*

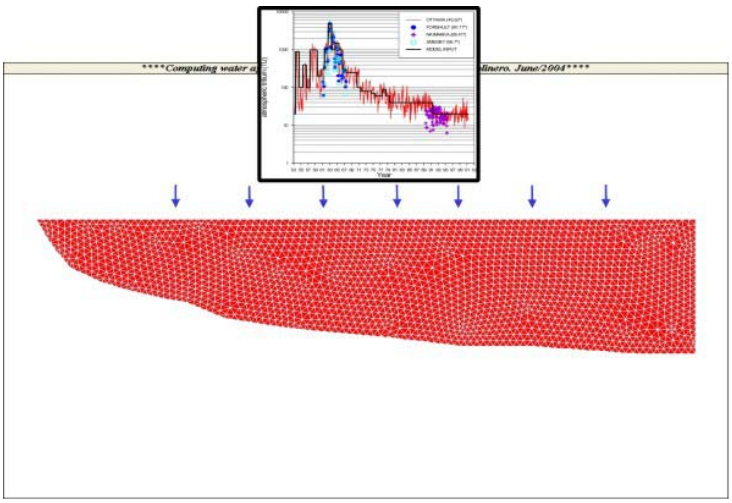

***Figure 4-7**. Sketch of the boundary condition used to represent the input of tritium in the model.*

Initial conditions of tritium contents have been generated by a long-term run of the model, since year 0 to year 1950. Precipitation before 1950 is assumed to have a constant tritium content of 15 TU. Figure 4-8 shows simulated tritium contents in groundwaters at year 1950.

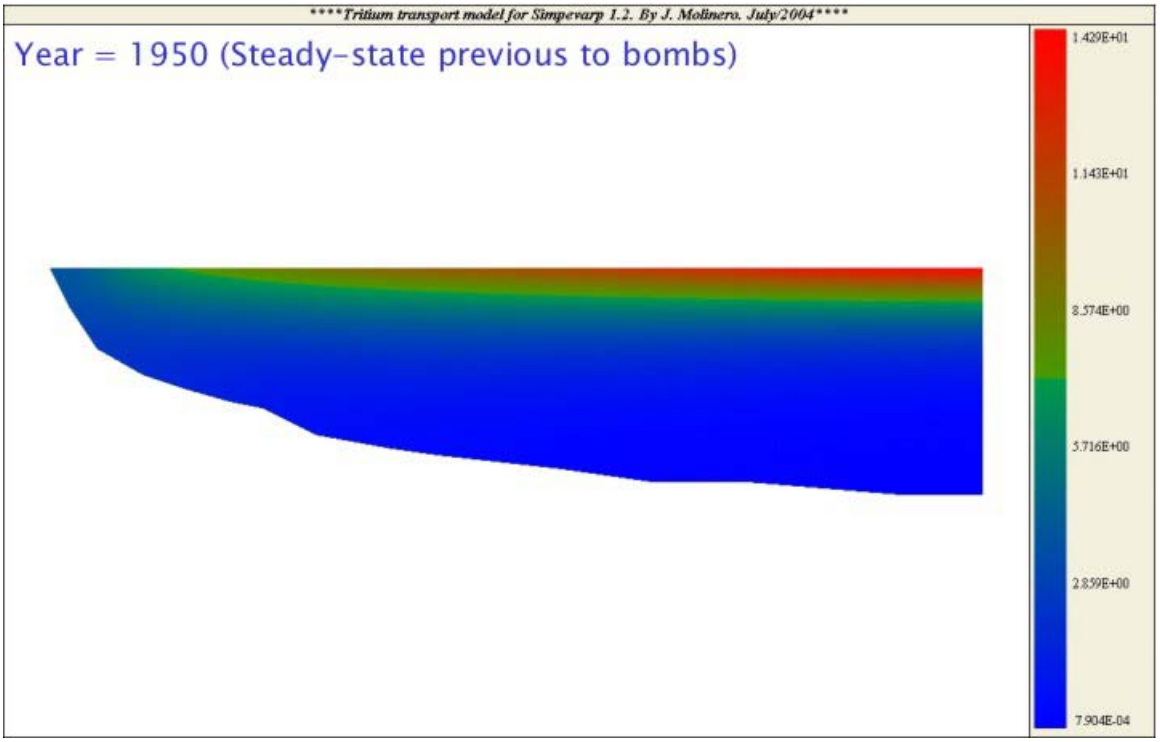

Figure 4-8*.Simulated tritium contents in Laxemar – Simpevarp aquifer at year 1950. It can be seen that maximum tritium contents of near 15 TU are computed at the subsurface levels. Down to 100 – 200 m depth fresh groundwater is tritium free at year 1950.*

Figure 4- 9 shows the simulated tritium contents at year 1980. One can see the difference with respect to the computed situation at 1950. In 1980, after the maximum values of atmospheric tritium due to thermonuclear bombs, larger contents of tritium in groundwater reach almost 150 TU. Moreover, these maximum tritium contents are not located in the subsurface, but about 200 m under the water table at Laxemar area (Figure 4-9). It should be noticed that there is a clear dispersion (mixing) zone between groundwaters infiltrated during the period of 1950's – 1970's and previous "sub-modern" tritium-free groundwater.

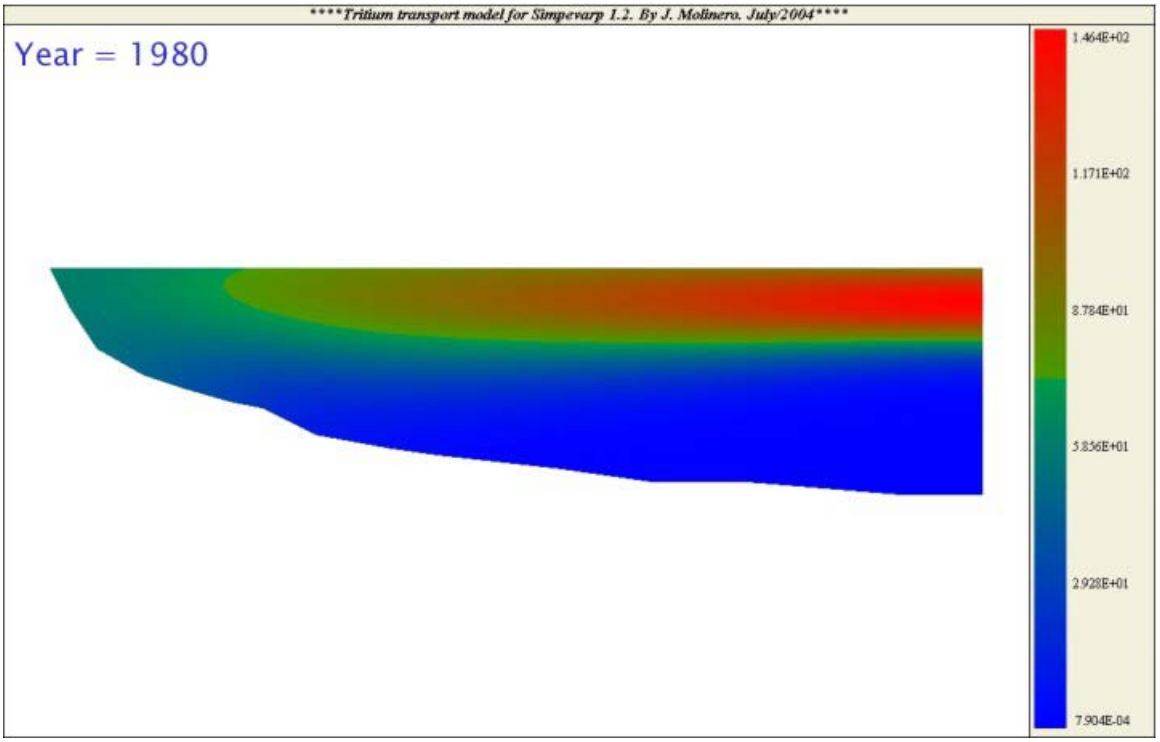

Figure 4-9*. Simulated tritium contents in Laxemar – Simpevarp aquifer at year 1980. It can be seen the advective front with maximum tritium contents of near 150 TU, and the dispersion (mixing) zones.*

Figure 4-10 shows computed tritium contents at year 2004. The advective front of the "modern" water, infiltrated during the 1950's – 1970`s, can bee seen in Laxemar close to the water divide (west boundary; right of the figure), showing maximum tritium contents of 24 TU. Close to the Baltic estuaries (East boundary; at the right-hand side), computed tritium contents range between 10 and 16 TU. The red square in Figure 4-10 indicates, approximately, the equivalent zone of the fresh water samples collected at boreholes in Simpevarp, i.e., the zone corresponding to the discharge of the fresh-water aquifer near to the Baltic coast.

Model results shown in figures 4-8 to 4-10 correspond to the base run of the solute transport model, i.e., by using an effective porosity value of 10^{-3}. Figure 4-11 shows computed tritium contents using a porosity of 10^{-2}. It can be seen in Figure 4-11, that by using a larger porosity value leads to lower computed tritium contents at Simpevarp, ranging from 0 to 7 TU.

It should be reminded that measured tritium contents in Simpevarp fresh groundwater samples are always higher than 5 TU, and mostly in the range between 10 and 15 TU. Then, by using an effective kinematic porosity of 10^{-3} in the transport model leads to consistent results with tritium measurements.

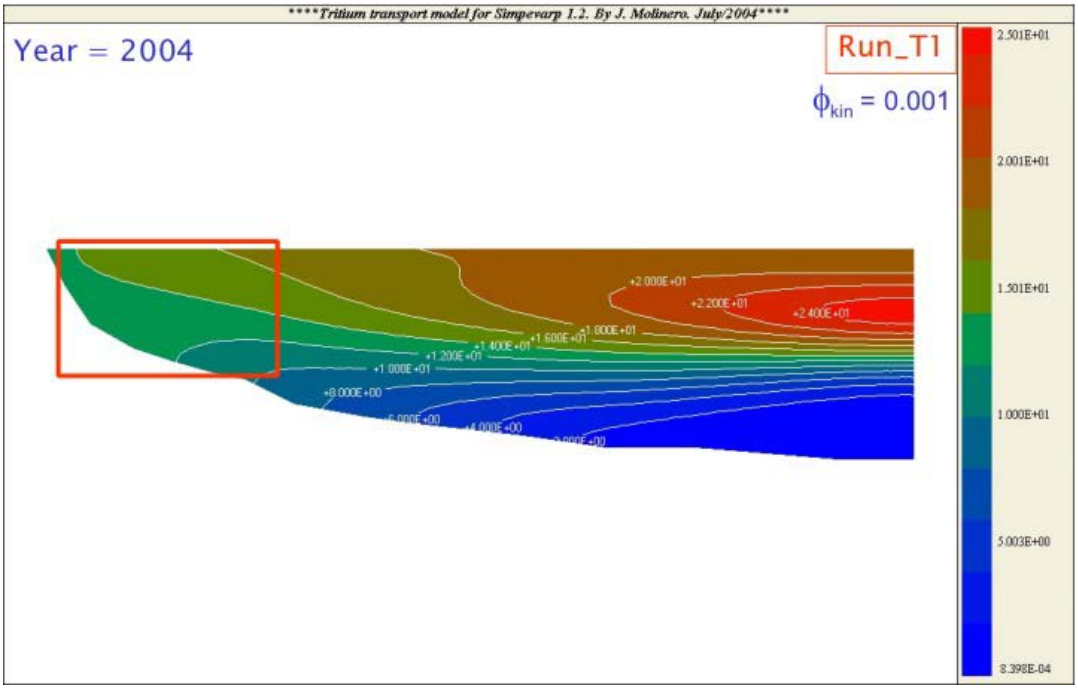

Figure 4-10. *Simulated tritium contents in groundwaters of the Laxemar – Simpevarp aquifer (year 2004), by using a kinematic porosity value of 0.001. Red square represents the equivalent area of fresh groundwaters at Simpevarp.*

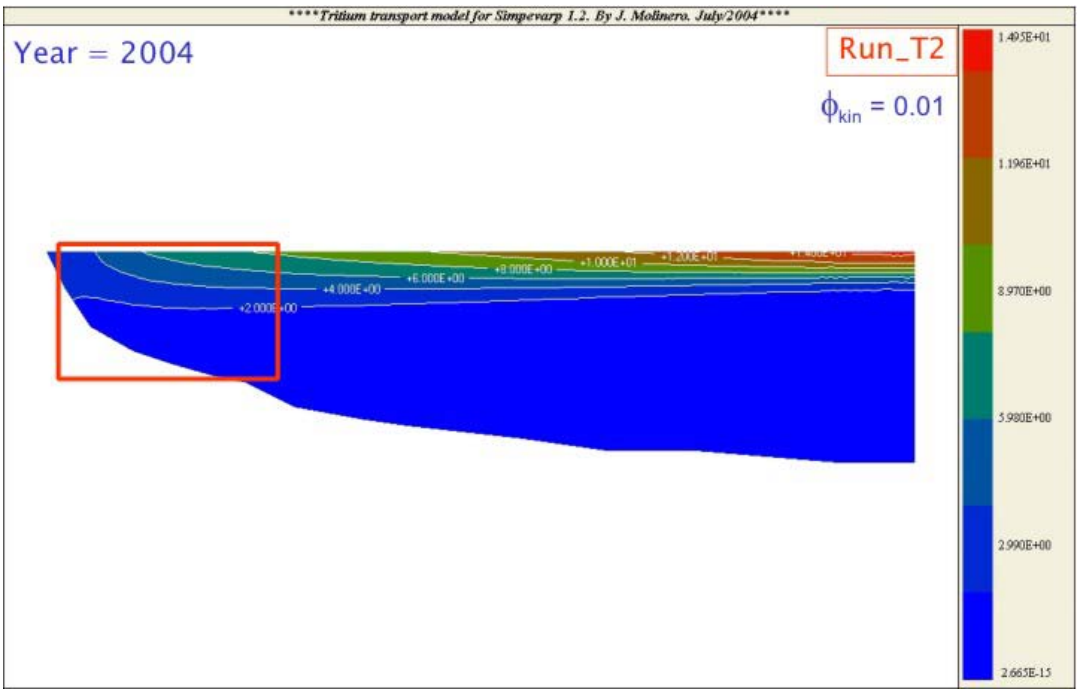

Figure 4-11. *Simulated tritium contents in groundwaters of the Laxemar – Simpevarp aquifer (year 2004), by using a kinematic porosity value of 0.01. Red square represents the equivalent area of fresh groundwaters at Simpevarp.*

Model results suggest that mixing of recent, modern and sub-modern groundwater can be responsible for the tritium contents measured at Simpevarp. This is consistent with hydrochemical analyses (see Chapter 3) and computed mean water age of about 100 years (see section 4.3).

It can also be concluded that the effective porosity is the most sensitive parameter for the transport model. Using the effective porosity value proposed by hydrogeological models, we compute mean water age and tritium contents that are consistent with isotopic information provided by Simpevarp groundwater samples. It is worth noting that current hydrogeological models of Simpevarp (version 1.1) were calibrated using only salinity data (SKB, 2004). Then, model results reported here support hydrogeological models using independent hydrochemical information.

4.5 Calcite dissolution

The occurrence of calcite dissolution has been identified by means of hydrochemical modelling of Simpevarp v1.1 data (Gimeno et al., 2004). Moreover, analyses performed on fresh groundwater samples showed a clear trend from calcite under-saturation in shallow recharge water, towards slight calcite over-saturation in discharge groundwater samples (see figures 3-8, 3-9 and 3-10). Then, according to this experimental evidence, calcite dissolution is expected to take place along flow paths. A coupled model of groundwater flow and reactive transport has been performed in order to corroborate the validity of this assumption.

The same parameters and conditions prescribed on the groundwater flow and solute transport model simulating groundwater age and tritium contents are valid here as well. A set of homogeneous chemical reactions (23) and dissolution-precipitation of calcite are considered herein. Table 4.1 shows the hydrogeochemical processes included in the model.

Initially, the model domain is assumed to contain only saline native groundwater. Then, the numerical model is solved with a fresh water recharge on the top boundary. The chemical nature of fresh water recharge has been set equal to concentrations measured in water sample SSM000002 (very shallow groundwater sample). This chemical boundary condition is undersaturated with respect to calcite, while saline native groundwater is equilibrated with this mineral phase.

As expected, a calcite dissolution front is computed numerically, due to the effect of continuous flushing and replacement of saline water by fresh water flowing from recharge to discharge zones. Figure 4-11 illustrates the computed evolution of the calcite dissolution front at Simpevarp.

Table 4-1 *Hydrogeochemical processes included in the reactive transport model*

Homogeneous reactions	**Log K**
$Ca(H_3SiO_4)_{2(aq)} + 2H^+ \leftrightarrow 2SiO_{2(aq)} + Ca^{2+} + 4H_2O$	15.0530
$CaCl^+ \leftrightarrow Ca^{2+} + Cl^-$	0.6956
$CaCl_{2(aq)} \leftrightarrow Ca^{2+} + 2Cl^-$	0.6436
$CaCO_{3(aq)} + H^+ \leftrightarrow Ca^{2+} + HCO_3^-$	7.0017
$CaH_2SiO_{4\,(aq)} + 2H^+ \leftrightarrow SiO_{2(aq)} + Ca^{2+} + 2H_2O$	18.5620
$CaH_3SiO_4^+ + H^+ \leftrightarrow SiO_{2(aq)} + Ca^{2+} + 2H_2O$	8.7916
$CaHCO_3^+ \leftrightarrow Ca^{2+} + HCO_3^-$	-1.0467
$CaOH^+ + H^+ \leftrightarrow Ca^{2+} + H_2O$	12.8500
$CaSO_{4(aq)} \leftrightarrow Ca^{2+} + SO_4^{2-}$	-2.1111
$CO_{2(aq)} + H_2O \leftrightarrow HCO_3^- + H^+$	-6.3447
$CO_3^{2-} + H^+ \leftrightarrow HCO_3^-$	10.3290
$H_2SiO_4^{2-} + 2H^+ \leftrightarrow SiO_{2(aq)} + H_2O$	22.9120
$H_4(H_2SiO_4)_4^- + 4H^+ \leftrightarrow 4SiO_{2(aq)} + 8H_2O$	35.7460
$H_6(H_2SiO_4)_4^- + 2H^+ \leftrightarrow 4SiO_{2(aq)} + 8H_2O$	13.4460
$HCl_{(aq)} \leftrightarrow H^+ + Cl^-$	0.6700
$HSiO_3^- + H^+ \leftrightarrow SiO_{2(aq)} + H_2O$	9.9525
$HSO_4^- \leftrightarrow H^+ + SO_4^{2-}$	-1.9791
$MgCO_{3(aq)} + H^+ \leftrightarrow Mg^{2+} + HCO_3^-$	7.3499
$MgHCO_3^+ \leftrightarrow Mg^{2+} + HCO_3^-$	-1.0357
$NaCO_3^- + H^+ \leftrightarrow Na^+ + HCO_3^-$	9.8144
$NaHCO_{3(aq)} \leftrightarrow Na^+ + HCO_3^-$	-0.1544
$SrCO_{3(aq)} + H^+ \leftrightarrow Sr^{2+} + HCO_3^-$	7.4635
$OH^- + H^+ \leftrightarrow H_2O$	13.995
Heterogeneous reactions	**Log K**
$CaCO_{3(s)} + H^+ \leftrightarrow HCO_3^- + Ca^{2+}$	1.8487

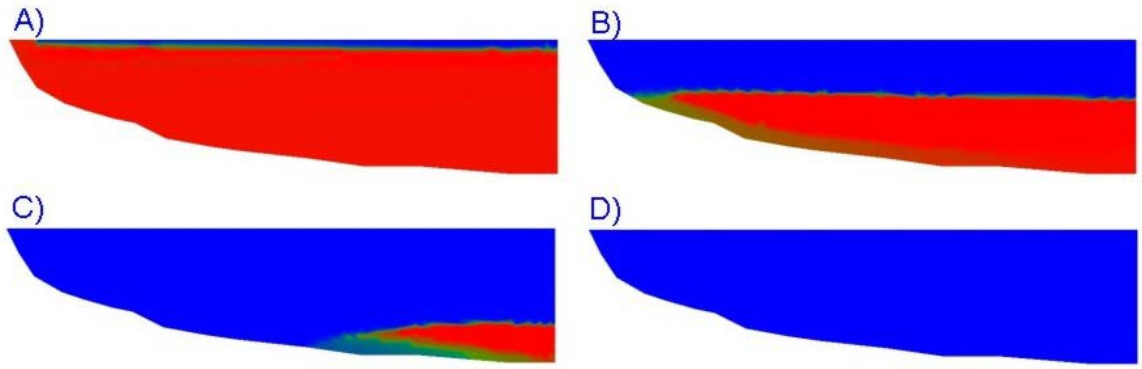

***Figure 4-12**. Simulated calcite dissolution front at: A) 6000 days; B) 56000 days; C)126000 days and D) 256000 days. Blue colour indicates the locations where dissolution of calcite occurs.*

As expected, calcite dissolution affects pH values. Initially, a constant pH of 7.3 is computed over the entire model domain, as a result of the chemical equilibrium of saline water with calcite. Coupled groundwater flow and calcite dissolution by fresh recharge water produces a pH increase. Once the steady-state is reached (i.e., all the saline water is flushed out), a constant pH value of 8.3 is computed for fresh groundwaters of Simpevarp. Figure 4-13 shows computed evolution of pH.

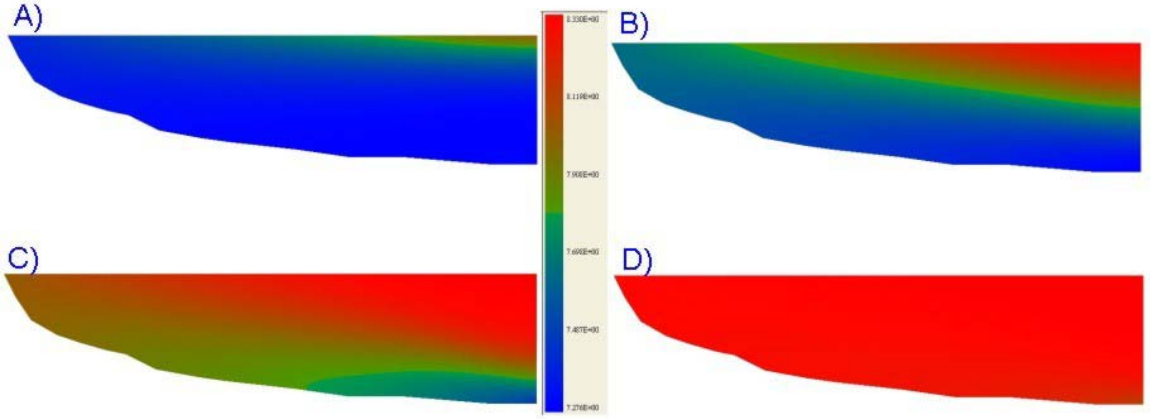

***Figure 4-13**. Computed pH evolution at: A) 6000 days; B) 56000 days; C)126000 days and D) 256000 days. (Blue = 7.3; Red = 8.3).*

Measured pH in Simpevarp fresh groundwater samples ranges from 8.0 to 8.6. Figure 4-14 shows the comparison between measured pH (at boreholes HSH02 and HSH03 and average depth of 100 m) and numerically computed pH. In spite of the consistency of the computed pH, it is still too early to derive definitive conclusions, since there are relevant hydrochemical processes which have not been considered yet.

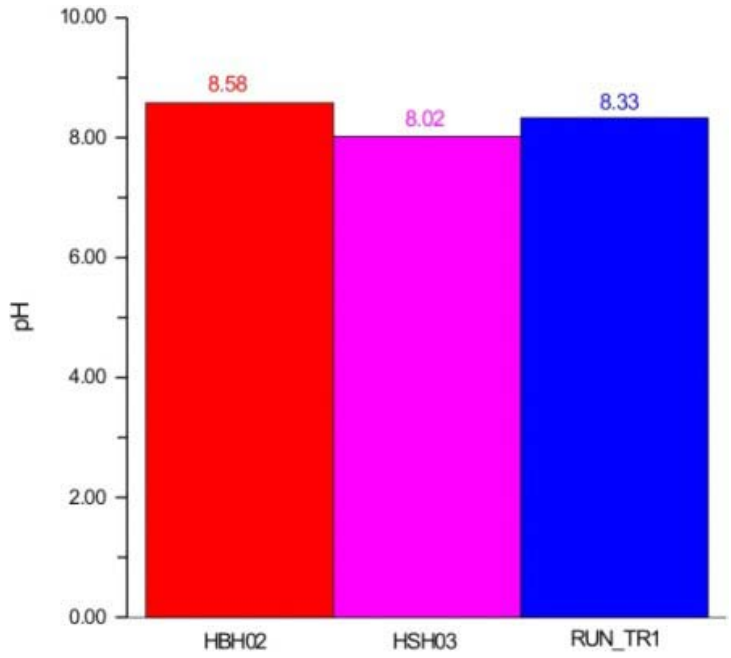

***Figure 4-14**. Measured (HSH02 and HSH03) and numerically computed (RUN_TR1) pH for Simpevarp fresh groundwater.*

Figure 4-15 shows a comparison between measured and computed concentrations of major reactive species in fresh groundwater samples at Simpevarp. It can be seen that the numerical model overestimates iron and calcium concentration, and underestimates silica, sodium, bicarbonate and sulphate concentration.

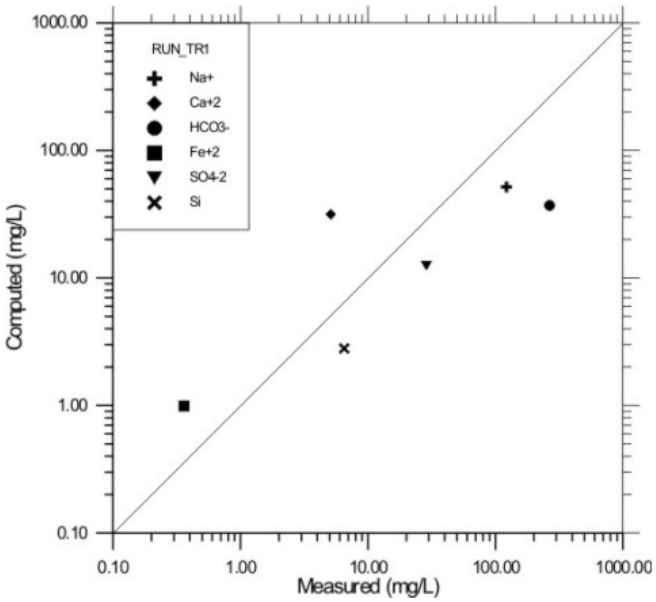

***Figure 4-15**. Measured (HSH02) and numerically computed concentration of major reactive species at Simpervarp fresh groundwaters.*

It can be seen in Figure 4-15 that the computed dissolution of calcite is not able to explain measured concentration of both bicarbonate and calcium. A possible explanation is that measured bicarbonate concentration is higher than the computed ones due to the occurrence of organic matter decomposition. This process has been clearly detected in Äspö groundwater (Banwart, 1999; Banwart et al., 1999). Molinero et al. (2004) performed coupled modelling of reactive transport and microbially-mediated organic matter respiration of the Redox Zone Experiment at Äspö. These authors show the great impact of this process on measured evolution of dissolved bicarbonate.

On the other hand, measured calcium concentration is lower than the computed one, probably because of the occurrence of Na-Ca exchange, which would also imply a decreasing of computed concentrations of Na.

Finally, the numerical underestimation of dissolved silica and sulphate, as well as the overestimation of iron can be attributed to the occurrence of dissolution-precipitation of silicates, pyrite, iron oxides and phyllosilicates. All this processes have been proposed based on hydrochemical model results (Laaksoharju et al., 2004).

Then, the next steps on coupled reactive transport modelling should be directed towards the incorporation of all these geochemical processes. Coupled reactive transport modelling provides an appropriate tool for quantitative testing of these hypotheses.

4.6 Cation exchange

A new run of the groundwater flow and reactive transport model was performed considering Na-Ca exchange. It is known that fracture filling materials contain abundant clay minerals. However, the equivalent value of Cation Exchange Capacity (CEC) of the host rock is difficult to evaluate due to several reasons, such as mineral heterogeneity, lost of clay fractions during sampling, etc. Molinero (2000) and Samper et al. (2003) used coupled reactive transport models to calibrate the effective CEC value of the Redox Fracture Zone by fitting measured evolution of Na and Ca during the Redox Zone Experiment. The best fit was obtained by using a CEC value of 0.6 mol/L (see Molinero 2000 and Samper et al., 2004 for details). Then, a CEC value of 0.6 mol/L was used in the model. The Gaines – Thomas convention was adopted with Na^+ as master species and an exchange coefficient for Ca^{2+} equal to 0.5. Figure 4-16 shows the same comparison between measured and computed concentrations showed before in Figure 4-15.

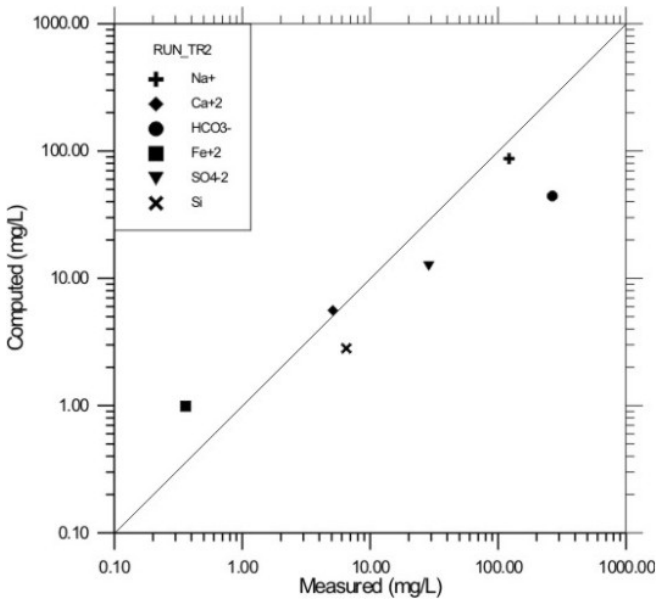

***Figure 4-16**. Measured (HSH02) and numerically computed concentrations of major dissolved species at Simpervarp fresh groundwaters, considering Na-Ca exchange coupled with calcite dissolution.*

One can notice in Figure 4-16 that considering Na-Ca exchange leads to a much better agreement between computed and measured concentrations of dissolved Na^+ and Ca^{2+} (compare figures 4-15 and 4-16). These results provide additional support to the conclusions of hydrochemical models, which identified the relevance of this process at Simpevarp. It is worth noting that used CEC value corresponds to the calibrated value of the Redox Zone Experiment performed at Äspö (Molinero, 2000).

5 Conclusions and future work

Qualitative analysis of environmental isotopes of Simpevarp – Laxemar fresh groundwater samples suggests an average water age from several decades to 100 years.

Tritium activities measured at Simpevarp boreholes are consistent with mixing between recent, modern and sub-modern fresh groundwaters. It is hypothesized that the mixing is produced by the convergence of flow lines discharging on the vicinity of the Baltic coast.

Combined analyses of isotopic and hydrochemical information of fresh groundwater samples, allows one to identify trends which are consistent with the hydrogeological knowledge of the area. The distributed recharge of the granitic fresh aquifer is confirmed through the analysis of shallow groundwater samples. These recharge water shows high ^{14}C contents, ^{3}H values close to actual precipitation, Ca-HCO_3 hydrochemical facies and

are under-saturated with respect to calcite. On the other hand, groundwater samples of Simpevarp (at depths of 100 – 200 m) shows an average age of decades may be one hundred years, ^{3}H values mainly between 10 – 15 TU, Na – HCO_3, Cl hydrochemical facies and they are all saturated in calcite. This water could correspond to the dynamic aquifer discharge. On the halfway from recharge to discharge, deep fresh-groundwater samples of Laxemar show influence of recharge from the 1960's – 1970's and "intermediate" hydrochemical signatures. However this conclusion is based on the presently available set of tritium data, the credibility of which has been partly questioned. A larger set of new and dependable tritium data from the Laxemar area will be used in forthcoming modelling stages.

It has been detected that some lake water shows isotopic signatures very similar to Simpevarp groundwater. This could be reflecting the presence of lakes constituting local discharge areas of the granitic aquifer, but other explanations are possible, so this should be taken just as an indication, may be for further research in those lakes.

Numerical modelling of groundwater flow and solute transport has been performed in order to simulate groundwater age and tritium concentration. As expected, kinematic porosity has been identified as the most sensitive parameter affecting transport model results. Measured activities of environmental isotopes can only be reproduced numerically by using the same porosity values (order of magnitude of 10^{-3}) proposed by hydrogeological models of version 1.1, which were calibrated using salinity data. Then, our model results provide additional support to hydrogeological models by using independent hydrochemical information.

A first attempt to coupled groundwater flow and reactive solute transport modelling has been performed. This model keeps the same parameters and conditions used to simulate groundwater age and tritium transport. The hydrogeochemical part of the model consists on a set of 23 homogeneous reactions (aqueous complexes), calcite dissolution – precipitation and cation exchange. A calcite dissolution front is computed due to the flushing of saline water by fresh recharge (infiltrated) water, in agreement with one of the main processes detected by previous hydrochemical models. However, computed calcite dissolution cannot explain measured concentration of bicarbonate and calcium. By including Ca-Na exchange, computed results are in good agreement with calcium and sodium concentrations measured at Simpevarp. Cation exchange parameters used in the model are exactly the same as the calibrated for the Redox Zone Experiment at Bockholmen.

Measured bicarbonate concentrations are higher than computed ones. A possible explanation could lie on the occurrence of microbially-mediated organic matter decomposition. This process has been clearly detected in Äspö groundwater (Banwart, 1999; Banwart et al., 1999), and successfully modelled by coupled hydro-bio-geochemical approaches (Molinero et al., 2004). The current version of the reactive transport model underestimates dissolved silica and sulphate, as well as overestimates dissolved iron. Most probably this is due to the occurrence of water-rock interaction

processes involving silicates, pyrite, iron oxides and phyllosilicates, as already proposed by the hydrochemical model version 1.1.

Future versions of reactive transport model should incorporate additional geochemical processes, using the same sequential methodology adopted for calcite dissolution and cation exchange. Further versions could also incorporate geological heterogeneity and improvements in the hydrogeologic assumptions made in this version.

6 References

Banwart, S. (1999). Reduction of iron (III) minerals by natural organic matter in groundwater. Geochim. Cosmochim. Acta, 63, 2919 – 2928.

Banwart, S.; Gustafsson, E. & Laaksoharju, M. (1999): Hydrological and reactive processes during rapid recharge to fracture zones. The Äspö large scale redox experiment. App. Geoch. 14, 873-892.

Bear, J. (1993): Modeling flow and contaminant transport in fractured rocks. In: Flow and contaminant transport in fractured media (Bear, J.; Tsang C.-F. & de Marsily, G. Eds.). Chapter 2. Academic Press, Inc. San Diego, California.

Berkowitz, B. (1994): Modelling flow and contaminant transport in fractured media. In: Advances in porous media, chapter 6. M.Y. Corapcioglu (Ed.). Elsevier.

Buckau, G. (2004). Isotope evaluation of Äspö/Ävrö water samples: First iteration. Interim report of the HAG Group.

Carrera, J.; Heredia, J.; Vomvoris, S. & Hufschmied, P. (1990): Fracture flow modeling: application of automatic calibration techniques to a small fractured monzonitic gneiss block. In: Hydrogeology of Low Permeability Environments (Neuman, S.P. & Neretnieks, I. Eds.). Hydrogeology Selected Papers, vol. 2: 115-168. Int. Ass. Hydrog. Verlag Heinz Heise GmbH & Co. Hannover.

Clark, I. & Fritz, P. (1997): Environmental Isotopes in Hydrogeology. Lewis Publishers. Boca Raton, Florida. 328 pp.

Custodio, E. (1983): Relaciones agua dulce-agua salada en las regiones costeras. In: Hidrología Subterránea, Vol. II, Chapter 13. (Custodio, E. & Llamas, M.R.; Eds.) Ediciones Omega, S.A. Barcelona. 1315-1385.

Dershowitz, W.; Geier, J. & Lee, K. (1991): FracMan Discrete Fracture Modeling System- User documentation. Golder Associates Report 903-1368. Golder Associates, Redmond, USA.

Ehlers, J. (1996): Quaternary and glacial geology. John Willey & Sons. New York. 578 pp.

Gimeno, M.J.; Auqué, L. & Gómez, L. (2004): Explorative analyses and mass balance modelling. In: Hydrochemical evaluation of the Simpevarp area, model version 1.1. Appendix 2. SKB R-04-16.

Goode, D.J. (1996): Direct simulation of groundwater age. Water Resources Research, 32 (2): 289-296.

Gurban, I. & Laaksoharju, M. (2004): Explorative análisis, M3 calculations and DIS modelling. In: Hydrochemical evaluation of the Simpevarp area, model version 1.1. Appendix 3. SKB R-04-16.

Juanes, R.; Samper, J. & Molinero, J. (2002). A general and efficient formulation of fractures and boundary conditions in the finite element method. International Journal of Numerical Methods in Engineering, 54: 1751-1774.

Laaksoharju, M. & Wallin, B. (1997): Evolution of the groundwater chemistry at the Äspö Hard Rock Laboratory. Proceedings of the second Äspö International Geochemistry Workshop, June 6-7, 1995. SKB, International Cooperation Report 97-04.

Laaksoharju, M. (1999): Groundwater characterisation and modelling: problems, facts and possibilities. Ph.D. dissertation. Department of Civil and Environmental Engineering. Royal Institute of Technology (KTH). Stockholm.

Laaksoharju, M.; Tullborg, E.-L.; Wikberg, P.; Wallin, B & Smellie, J. (1999a): Hydrogeochemical conditions and evolution at the Äspö HRL, Sweeden. App. Geoch. 14, 835-860.

Laaksoharju, M.; Skarman, C. & Skarman, E. (1999b): Multivariate mixing and mass balance (M3) calculations, a new tool for decoding hydrogeochemical information. App. Geoch. 14, 861-872.

Laaksoharju, M. (Ed.); Smellie, J.; Gimeno, M.J.; Auqué, L.; Gómez, L.; Tullborg, E-L & Gurban, I. (2004): Hydrogeochemical evaluation of the Simpevarp area, model version 1.1. SKB R-04-16.

Louvat, D.; Michelot, J.L. & Aranyossy, J.F. (1999): Origin and residence time of salinity in the Äspö groundwater system. Applied Geochemistry, 14, 917-925.

Molinero, J. (2000): Testing and Validation of Numerical Models of Groundwater Flow, Solute Transport and Chemical Reactions in Fractured Granites. PhD Thesis, Civil Engineering School, University of A Coruña, Spain. (Latter published as ENRESA Publicación Técnica 06/01).

Molinero, J.; Samper, J. & Juanes, R. (2002): Numerical modeling of the transient hydrogeological response produced by tunnel construction in fractured bedrocks. Engineering Geology, 64, 369-386.

Molinero, J. & Samper, J. (2004): Modeling Groundwater Flow and Solute Transport in Fracture Zones: Conceptual and Numerical Models of the Redox Zone Experiment at Äspö (Sweden). Journal of Hydraulic Research, 42, 157 – 172.

Molinero, J.; Samper, J.; Zhang, G. & Yang, C.B. (2004): Biogeochemical reactive transport model of the Redox Zone Experiment of the Äspö Hard Rock Laboratory in Sweden. Nuclear Technology, 148, (to appear in Nov. 2004), in press.

Moreno, L.; Tsang, Y.W.; Tsang, C.F.; Hale, F.V. & Neretnieks, I. (1988): Flow and tracer transport in a single fracture: A stochastic model and its relation to some field observations. Water Resources Research, 24 (12): 2033-2048.

Rhén, I.; Bäckbom, G.; Gustafson, G.; Stanfors, R. & Wikberg, P. (1997b): Results from pre-investigations and detailed site characterization. Summary report. SKB TR 97-03.

Rhén, I.; Gustafson, G.; Stanfors, R. & Wikberg, P. (1997a): Models based on site characterization 1986-1995. SKB TR 97-06.

Samper, J.; Delgado, J.; Juncosa, R. & Montenegro, L. (2000): CORE^{2D} v 2.0: A Code for non-isothermal water flow and reactive solute transport. User's manual.ENRESA Technical report 06/2000.

Samper, J.; Molinero, J.; Zhang, G. & Yang, C-B. (2003): Redox Zone II. Coupled Modeling of Groundwater Flow, Solute Transport, Chemical reactions and Microbial Proceses in the Äspö island. SKB Technical Report TR-03-16

SKB (2002): Simpevarp – site descriptive model version 0. SKB R-02-35.

SKB (2004): Simpevarp – site descriptive model v 1.1 (Draft provided by M. Laaksoharju).

Smellie, J.A.T.; Laaksoharju, M. & Wikberg, P. (1995): Äspö, SE Sweden: a natural groundwater flow model derived from hydrogeochemical observations. Journal of Hydrology, 172. 145-169.

Smellie, J. & Tullborg, E-L (2004): Explorative analysis, expert judgement and modelling. In: Hydrochemical evaluation of the Simpevarp area, model version 1.1. Appendix 1. SKB R-04-16.

SRAC - Structural Research and Analysis Corporation (1998). COSMOS/M. A Complete Finite Element Analysis System. USER'S GUIDE.

Svensson, U. (1997): A regional analysis of groundwater flow and salinity distribution in the Äspö area. SKB TR 97-09.

Varni, M. & Carrera, J. (1998): Simulation of groundwater age distributions. Water Resources Research, 34 (12): 3271-3281.

Xu, T. (1996): Modeling Non-isothermal multi-component reactive solute transport through variably saturated porous media. Ph. D. dissertation. Universidad de A Coruña. A Coruña.

Xu, T.; Samper, J.; Ayora, C.; Manzano, M. & Custodio, E. (1999): Modeling of non-isothermal multi-component reactive transport in field scale porous media flow systems. Journal of Hydrology, 214: 144-164.

Appendix 7: Groundwater data from Simpevarp

For data, please see the attached CD!

Appendix 8: Groundwater data from Nordic sites

For data, please see the attached CD!

Appendix 9: The use of the data in the modelling work

For information, please see the attached CD!